FRONTIERS IN FUNGAL VIRUS RESEARCH

EDITED BY: Sun Liying, Nobuhiro Suzuki, Massimo Turina, Daohong Jiang and Jiatao Xie
PUBLISHED IN: Frontiers in Cellular and Infection Microbiology, Frontiers in Microbiology and Frontiers in Plant Science

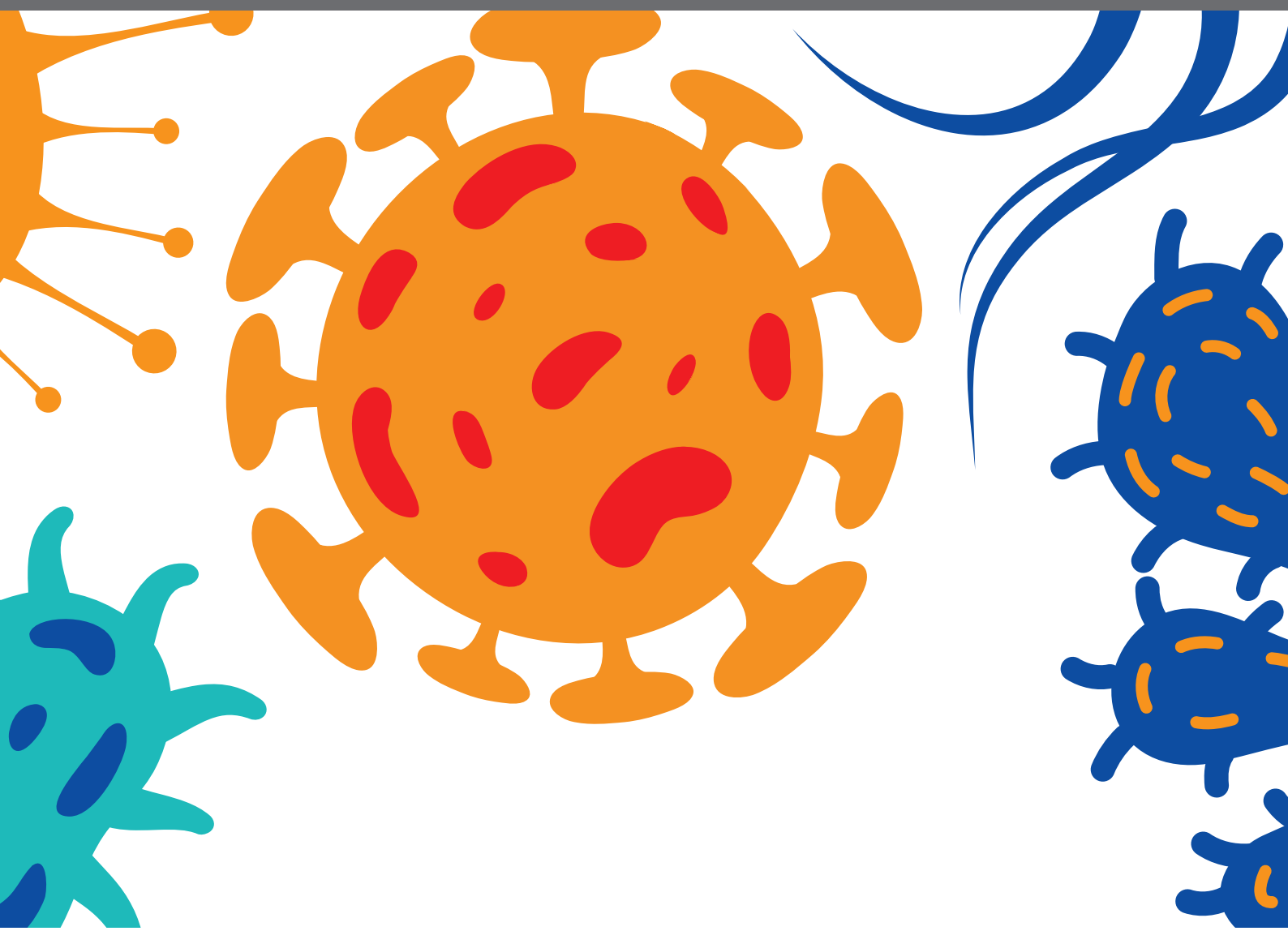

frontiers Research Topics

ISSN 1664-8714
ISBN 978-2-88963-514-6
DOI 10.3389/978-2-88963-514-6

About Frontiers

Frontiers is more than just an open-access publisher of scholarly articles: it is a pioneering approach to the world of academia, radically improving the way scholarly research is managed. The grand vision of Frontiers is a world where all people have an equal opportunity to seek, share and generate knowledge. Frontiers provides immediate and permanent online open access to all its publications, but this alone is not enough to realize our grand goals.

Frontiers Journal Series

The Frontiers Journal Series is a multi-tier and interdisciplinary set of open-access, online journals, promising a paradigm shift from the current review, selection and dissemination processes in academic publishing. All Frontiers journals are driven by researchers for researchers; therefore, they constitute a service to the scholarly community. At the same time, the Frontiers Journal Series operates on a revolutionary invention, the tiered publishing system, initially addressing specific communities of scholars, and gradually climbing up to broader public understanding, thus serving the interests of the lay society, too.

Dedication to Quality

Each Frontiers article is a landmark of the highest quality, thanks to genuinely collaborative interactions between authors and review editors, who include some of the world's best academicians. Research must be certified by peers before entering a stream of knowledge that may eventually reach the public - and shape society; therefore, Frontiers only applies the most rigorous and unbiased reviews.
Frontiers revolutionizes research publishing by freely delivering the most outstanding research, evaluated with no bias from both the academic and social point of view. By applying the most advanced information technologies, Frontiers is catapulting scholarly publishing into a new generation.

What are Frontiers Research Topics?

Frontiers Research Topics are very popular trademarks of the Frontiers Journals Series: they are collections of at least ten articles, all centered on a particular subject. With their unique mix of varied contributions from Original Research to Review Articles, Frontiers Research Topics unify the most influential researchers, the latest key findings and historical advances in a hot research area! Find out more on how to host your own Frontiers Research Topic or contribute to one as an author by contacting the Frontiers Editorial Office: researchtopics@frontiersin.org

FRONTIERS IN FUNGAL VIRUS RESEARCH

Topic Editors:
Sun Liying, Northwest A&F University, China
Nobuhiro Suzuki, Okayama University, Japan
Massimo Turina, Italian National Research Council, Italy
Daohong Jiang, Huazhong Agricultural University, China
Jiatao Xie, Huazhong Agricultural University, China

Citation: Liying, S., Suzuki, N., Turina, M., Jiang, D., Xie, J., eds. (2020). Frontiers in Fungal Virus Research. Lausanne: Frontiers Media SA.
doi: 10.3389/978-2-88963-514-6

Table of Contents

frontiers in Cellular and Infection Microbiology

EDITORIAL
published: 22 January 2020
doi: 10.3389/fcimb.2019.00456

Editorial: Frontiers in Fungal Virus Research

Liying Sun[1], Nobuhiro Suzuki[2], Daohong Jiang[3], Massimo Turina[4] and Jiatao Xie[3]*

[1] State Key Laboratory of Crop Stress Biology for Arid Areas, College of Plant Protection, Northwest Agriculture and Forestry University, Yangling, China, [2] Institute of Plant Science and Resources, Okayama University, Okayama, Japan, [3] The State Key Laboratory of Agricultural Microbiology, Huazhong Agricultural University, Wuhan, China, [4] Institute for Sustainable Plant Protection, Italian National Research Council, Rome, Italy

Keywords: mycovirus, identification, hypovirulence, transmission, host defense, virus-virus interaction

Editorial on the Research Topic

Frontiers in Fungal Virus Research

Compared to animal and plant viruses, fungal viruses have been relatively less studied. However, the recent development of associated methodologies including sequencing technologies has led to the rapid advancement of research on viruses infecting fungi or fungi-like organisms. Fungi can cause human/animal diseases, and they are the major causative agents of crop plant diseases. Fungi harbor highly diverse viruses, many of which constitute distinct virus families/groups that are not present in other organisms. Of note is that there are also some virus taxonomical groups comprising both plant and fungal viruses, suggesting an active and recent horizontal transfer of viruses between the two kingdoms. Therefore, fungal virology is particularly significant for its applicative, fundamental, and evolutionary implications. The Research Topic "Frontiers in Fungal Virus Research" is aimed to present the most recent progresses on different aspects of fungal virology. This topic contains 13 research and two review articles, covering a variety of topics including virus identification, virus-mediated modulation of fungal pathogenicity, virus-virus interactions, and host defense.

In this topic, nine research papers report the characterization of novel fungal viruses from various fungi. Khalifa and MacDiarmid identified a novel totivirus from *Trichoderma koningiopsis*. Another isolate belonging to the same species also was found from *Clonostachys rosea* distinct from *T. koningiopsis*, indicating a very recent natural horizontal transmission of this virus between unrelated fungi. It is interesting to further investigate how this virus is transmitted across different fungal species. Using RNA-seq analysis, Picarelli et al. revealed a high diversity of fungal viruses infecting *Rhizoctonia solani* isolated from *Zoysia japonica* (a cultivated grass) in Brazil. Most of the viruses show low sequence identity with other viruses, which include four large contigs of putative viral RNA that could not be assigned to any existing clade of viruses present in the databases. This suggests that they all belong to possible new viral species. This study provides a sound foundation for further understanding the diversity of fungal viruses. Kartali et al. identified novel totiviruses from *Umbelopsis ramanniana*. This work is particularly interesting and important because it is the first report on fungal viruses infecting this fungal genus, and this fungal species is an oleaginous fungus, a potential oil source for biodiesel production. Wang et al. characterized two novel viruses from *Sclerotinia sclerotiorum* each related to members of the order *Tymovirales* and the genus *Botybirnavirus*. Neither of them confers hypovirulence to the host. Moreover, they detected the accumulation of viral-derived siRNAs in *S. sclerotiorum*, indicating that RNA silencing operates against these viruses in the fungus. Li et al. characterized a novel hypovirulence-inducing hypovirus from *Alternaria alternata* isolated from an apple tree. Moreover, this virus also confers hypovirulence in *Botryosphaeria dothidea*, the causal fungal pathogen of apple white rot. Thus, this virus is a potentially valuable material as a bivalent biocontrol agent against fungal diseases in apple tree. Wang et al. identified a novel virus related to members of the genus *Chrysovirus*,

OPEN ACCESS

Edited and reviewed by:
Joseph Heitman,
Duke University, United States

****Correspondence:***
Liying Sun
sunly_de@126.com

Specialty section:
This article was submitted to Fungal Pathogenesis, a section of the journal Frontiers in Cellular and Infection Microbiology

Received: *25 October 2019*
Accepted: *13 December 2019*
Published: *22 January 2020*

Citation:
Sun L, Suzuki N, Jiang D, Turina M and Xie J (2020) Editorial: Frontiers in Fungal Virus Research. Front. Cell. Infect. Microbiol. 9:456. doi: 10.3389/fcimb.2019.00456

family *Chrysoviridae* from *Penicillium crustosum*, a pathogen of citrus tree. Interestingly, this virus does not affect the growth or morphology of the fungal host but it decreases the fungal resistance against a fungicide. Certainly, this virus is a good molecular tool to study the mechanism of fungal resistance against fungicide. Jiang et al. identified a novel partitivirus from an opportunistic human pathogenic fungus, *Aspergillus flavus*. Infection by this virus causes significantly abnormal colonial and spore morphologies, but does not significantly affect its host virulence. It is important to further explore the presence of viruses in this important human-pathogenic fungus. Using RNA-seq analysis, Zhu et al. characterized viruses that are present in a hypovirulent strain of *Sclerotium rolfsii*. Interestingly, this fungal strain harbors various new viruses belonging to several established virus families and also some novel viruses that could not be assigned to any of the existing families or orders. Chun et al. identified a novel partitivirus from *Trichoderma harzianum*. *Trichoderma* species are known for their ability to inhibit other fungi, and therefore they are used as biocontrol agents for controlling common soil-borne plant pathogens. The important finding in this study is that although the infection by this partitivirus does not affect growth or morphology of its fungal host, it enhances antifungal activities of *T. harzianum* against other fungi, and this is associated with increased activity of antifungal enzyme, β-1,3-glucanase. It is necessary to further analyze how this partitivirus infection regulates the activity of a specific antifungal enzyme. Li et al. present a comprehensive review on fungal viruses infecting members of the fungal genus *Fusarium*. *Fusarium* species are important phytopathogenic fungi that cause damage in a wide variety of host plant species and also produce mycotoxin. Highly diverse viruses are widely present in *Fusarium* spp., and some of them induce hypovirulence in their fungal hosts. This review provides valuable knowledge for understanding virus diversity and prospects for development of biocontrol methods against *Fusarium* spp.

Two papers report studies on the roles of RNA silencing and autophagy pathways in fungal virulence and defense against virus infection in fungi. Neupane et al. revealed that the *Argonaute-like* (*agl*)-2 gene of *S. sclerotiorum* is important for virulence and host tolerance against virus infection. Intriguingly, deletion of *agl-2*, *agl-4*, *Dicer-like* (*dcl*)*-1*, and *dcl-2*, which are key components of RNA silencing, does not affect the production of the most abundant endogenous small RNAs in *S. sclerotiorum*. This suggests the existence of alternative enzymes/pathways for small RNA biogenesis in *S. sclerotiorum*. Autophagy is a highly conserved degradation mechanism of cellular constituents in eukaryotes. Shi et al. observed that infection by a hypovirus in *Cryphonectria parasitica* induces proliferation of autophagic-like vesicles. Furthermore, they demonstrated that *C. parasitica cpatg8*, a gene encoding a homolog of a key autophagy component, *Atg8*, of *Saccharomyces cerevisiae*, is important for fungal virulence and sporulation. Interestingly, *cpatg8* was also shown to play a positive role in hypovirus replication. Recently, autophagy is shown to have both anti- and pro-viral functions in other eukaryotic systems. This is a pioneering study that explores the involvement of autophagy in viral infection in filamentous fungi.

Using GFP-labeled strains of *Fusarium oxysporum*, Torres-Trenas et al. demonstrated that a hyphovirulence-inducing chrysovirus affects the speed and spatial distribution of fungal colonization into plant roots. This is the first study that clearly provides microscopic evidence that a mycovirus can influence the pattern of plant colonization by its fungal host. Kashif et al. examined the reciprocal effects of partitiviruses on the horizontal transmission efficiency through hyphal anastomosis in *Heterobasidion* spp. They observed that two viruses could synergistically enhance the overall transmission rate or antagonistically affect their transmission depending on specific virus combinations. Therefore, the interaction between co-infecting viruses and their host is complex, and the underlying mechanism remains to be elucidated. Thapa and Roossinck discussed determining factors for fungal-virus co-infection. Co-infections of natural fungal isolates by fungal viruses are commonly observed. The authors present interesting perspectives of how suppression of fungal non-self-recognition and RNA silencing, and nutritional/chemical compounds could affect the outcome of virus co-infection in fungi.

Overall, these works contain rich novel information from diverse viruses and fungal species regarding various topics of fungal virology. Indeed, they provide valuable research materials and interesting biological findings that warrant further detailed mechanistic studies. Mycovirus research will contribute to further advances of virology in general as well as lay a solid foundation for research development of control methods of many fungal diseases. Lastly, the editors of this topic greatly appreciate all of the authors and reviewers for their contributions to the collection.

AUTHOR CONTRIBUTIONS

LS, NS, DJ, MT, and JX edited the Research Topic of Frontier in Fungal virus Research and wrote the manuscript.

ACKNOWLEDGMENTS

This work was supported in part by the National Natural Science Foundation of China (31970163), (U1703113) to LS and the National Key Research and Development Program of China (2017YFD0201100), the 111 program (2016KW-069) to LS.

Conflict of Interest: The authors declare that the research was conducted in the absence of any commercial or financial relationships that could be construed as a potential conflict of interest.

frontiers in Plant Science

ORIGINAL RESEARCH
published: 20 November 2018
doi: 10.3389/fpls.2018.01699

Identification of a Novel Partitivirus of *Trichoderma harzianum* NFCF319 and Evidence for the Related Antifungal Activity

*Jeesun Chun[1], Han-Eul Yang[2] and Dae-Hyuk Kim[1,2]**

[1] Institute for Molecular Biology and Genetics, Chonbuk National University, Jeonju, South Korea, [2] Department of Bioactive Material Sciences, Chonbuk National University, Jeonju, South Korea

We have reported 15 agarose gel band patterns of double-stranded RNA (dsRNA) from *Trichoderma* spp. We describe herein that band pattern IX in *Trichoderma harzianum* NFCF319, which appeared to be a single band but consisted of two dsRNAs of similar size, was identified as a novel mycovirus, designated *Trichoderma harzianum* partitivirus 1 (ThPV1). The larger segment (dsRNA1) of the ThPV1 genome comprised 2,289 bp and contained a single open reading frame (ORF) encoding an RNA-dependent RNA polymerase (RdRp). The smaller segment (dsRNA2) consisted of 2,245 bp with a single ORF encoding a capsid protein (CP). Evaluation of the deduced amino acid sequence and phylogenetic analysis indicated that ThPV1 is a new member of the genus *Betapartitivirus* in the family *Partitiviridae*. Curing of virus infection by single-sporing generated 31 virus-free single-spore clones. No significant differences in growth rate, conidia production, or pigmentation were observed between ThPV1-infected and -cured isogenic strains. In addition, comparison of the newly ThPV1-transmitted isolates with their ThPV1-cured parental strain showed no significant difference in colony morphology or pigmentation. However, inhibition of growth in co-cultured *Pleurotus ostreatus* and *Rhizoctonia solani* by *T. harzianum* was increased in ThPV1-containing strains compared with ThPV1-cured isogenic strains. Moreover, β-1,3-glucanase activity was significantly increased in the ThPV1-containing strains. However, no difference in chitinase activity was observed, suggesting that ThPV1 regulates the activity of a specific fungal enzyme.

Keywords: *Trichoderma harzianum*, mycovirus, partitivirus, mycoparasitism, antifungal activity

OPEN ACCESS

Edited by:
Massimo Turina,
Consiglio Nazionale delle Ricerche (CNR), Italy

Reviewed by:
Sotaro Chiba,
Nagoya University, Japan
Jarkko Hantula,
Natural Resources Institute Finland (Luke), Finland

***Correspondence:**
Dae-Hyuk Kim
dhkim@jbnu.ac.kr

Specialty section:
This article was submitted to Virology, a section of the journal Frontiers in Plant Science

Received: *29 July 2018*
Accepted: *31 October 2018*
Published: *20 November 2018*

Citation:
Chun J, Yang H-E and Kim D-H (2018) Identification of a Novel Partitivirus of Trichoderma harzianum NFCF319 and Evidence for the Related Antifungal Activity. Front. Plant Sci. 9:1699. doi: 10.3389/fpls.2018.01699

INTRODUCTION

Mycoviruses, i.e., fungal viruses, are widespread and have been found in all major taxa of filamentous fungi and yeasts (Van Alfen, 1986; Nuss and Koltin, 1990; Wickner, 1992). The majority of characterized mycoviruses have a double-stranded RNA (dsRNA) genome, although others have single-stranded RNA (ssRNA) and DNA genomes. Mycoviruses of seven families, *Chrysoviridae, Endornaviridae, Megabirnaviridae, Quadriviridae, Partitiviridae, Reoviridae*, and *Totiviridae* have dsRNA genomes, while those of six families, *Alphaflexiviridae*, *Barnaviridae*, *Gammaflexiviridae*, *Hypoviridae*, *Narnaviridae*, and *Mymonaviridae* have ssRNA genomes according to a report by the International Committee on the Taxonomy of Viruses (ICTV) in 2016 (Ghabrial et al., 2015).

Using multi-omics techniques, a large number of novel mycoviruses are expected to be discovered and characterized from various fungi. Recently, we reported the presence of a variety of dsRNA elements in many strains of *Trichoderma* spp. causing a green mold disease in shiitake mushroom (*Lentinula edodes*) and confirmed the presence of novel mycoviruses in these *Trichoderma* spp. (Yun et al., 2016). Although infection of fungi by many mycoviruses is asymptomatic or cryptic (Ghabrial, 1998), there are many cases of mycoviruses inducing viral-specific symptoms in the host and reduced fungal virulence, known as hypovirulence, is one of representative examples in phytopathogenic fungi (Nuss, 2005).

Members of the genus *Trichoderma* are fast-growing ubiquitous soil fungi. The evident success of *Trichoderma* species is due to the characteristic mechanisms of *Trichoderma* to survive and proliferate, which include an aggressive ability to inhibit other fungi and production of various enzymes for the degradation of complex carbohydrates (Samuels and Hebbar, 2015). These activities have been exploited for human benefit; indeed, some *Trichoderma* species are used as biocontrol agents, and in the production of commercial enzymes and secondary metabolites, and are endosymbionts for their host plant (Kubicek and Penttila, 1998; Sivasithamparam and Ghisalberti, 1998; Hatvani et al., 2002; Howell, 2003). *T. harzianum* is probably the most commonly cited species and is widely recognized as a potential biocontrol component in controlling common soil-borne plant pathogens (i.e., *Fusarium*, *Pythium*, and *Rhizoctonia*), but is also reported as the causal agent of green mold disease in cultivated mushrooms (Papavizas, 1985; Tokimoto, 1985; Ulhoa and Peberdy, 1992; Seaby, 1998; Kredics et al., 2010). Thus, changes in the beneficial or pathological characteristics of *T. harzianum* impact the industrial application or prevention of this fungus. We have reported the presence of dsRNA in *T. harzianum*; however, the nature and biological function of the dsRNA are unclear.

In this study, we characterized the dsRNA of a novel mycovirus and assessed its biological effects on *T. harzianum*.

MATERIALS AND METHODS

Fungal Strains and Growth Condition

Fungal strains were maintained at 25°C in the dark on PDA. Virus-containing and -cured *T. harzianum* strains were maintained by the hyphal-tipping technique.

Nucleic Acid Extraction and Viral Genome Sequencing

dsRNA extraction and Northern hybridization analysis were performed as described by Park et al. (2008). Purified dsRNA was subjected to cDNA library construction and genome sequencing on the Illumina Hiseq 2000 platform (Macrogen Inc., Seoul, South Korea). The Illumina adapter sequence reads were quality checked by FastQC and trimmed by Trimmomatic (ver. 0.32). Qualified reads were assembled to generate contigs by Trinity and abundance was estimated using RSEM software to calculate the FPKM-values.

Rapid Amplification of cDNA Ends (RACE) Analysis

RNA ligase-mediated rapid amplification of cDNA ends (RLM-RACE) was performed to determine the 5′- and 3′-terminal sequences of dsRNA using an RLM-RACE kit (Ambion, Austin, TX, United States). Purified dsRNA was denatured in dimethylsulfoxide and treated with calf intestine alkaline phosphatase (CIP) and tobacco acid pyrophosphatase (TAP) to remove free 5′ phosphates and cap structures. The 5′ RNA adapter oligonucleotide (5′-GCUGAUGGCGAUGAAUGAACACUGCGUUUGCUGGCUUUGAUGAAA-3′) was ligated to the decapped RNA using T4 RNA ligase. The ligates were subjected to random-primed reverse transcription and the 5′ end of a specific sequence was amplified. The 3′ terminus of dsRNA was ligated to a 3′ RACE adapter oligonucleotide (5′-GCGAGCACAGAATTAATACGACTCACTATAGGT12VN-3′) and subjected to RT-PCR. The resulting cDNA was amplified by PCR to determine the 3′ end sequence.

Sequence Analysis

Phylogenetic trees were constructed by the maximum-likelihood methods (Fitch, 1971) with the software package MEGA7 (Kumar et al., 2016) after performing multiple sequence alignments using CLUSTAL X (ver. 2.1) (Thompson et al., 1997).

Purification of Virus Particles and Transmission Electron Microscopy

Trichoderma harzianum betapartitivirus 1 (ThPV1) particles were purified by the method of Wang et al. (2014) and subjected to sucrose gradient ultracentrifugation. The structure of the virus-like particles was visualized by TEM on an H-7650 instrument installed in the Center for University-Wide Research Facilities (CURF) at Chonbuk National University (Hitachi, Tokyo, Japan) after negative staining with 2% uranyl acetate.

Antifungal Activity Assay

Conidial suspensions (1×10^5 spores/ml) of *T. harzianum* NFCF319 were inoculated in 150 ml of potato dextrose broth (PDB) and incubated in shaking flasks for 2 days at 25°C and 180 rpm. The culture medium was passed through a 0.2 μm membrane filter and tested for each filtrate diluted with PDB containing 10^{-1}, 10^{-2}, and 10^{-3} of the original filtrate. *Pleurotus ostreatus* (ASI No. 2792) and *Rhizoctonia solani* AG-1 (KACC40101) were cultured by placing mycelial plugs in the center of PDA containing each filtrate, and colonial growth was assessed as the mean radial area.

Chitinase and β-1,3-Glucanse Assay

Culture supernatants were harvested and subjected to chitinase assays according to the manufacturer's instructions (Sigma, St. Louis, MO, United States). β-1,3-glucanase assays were

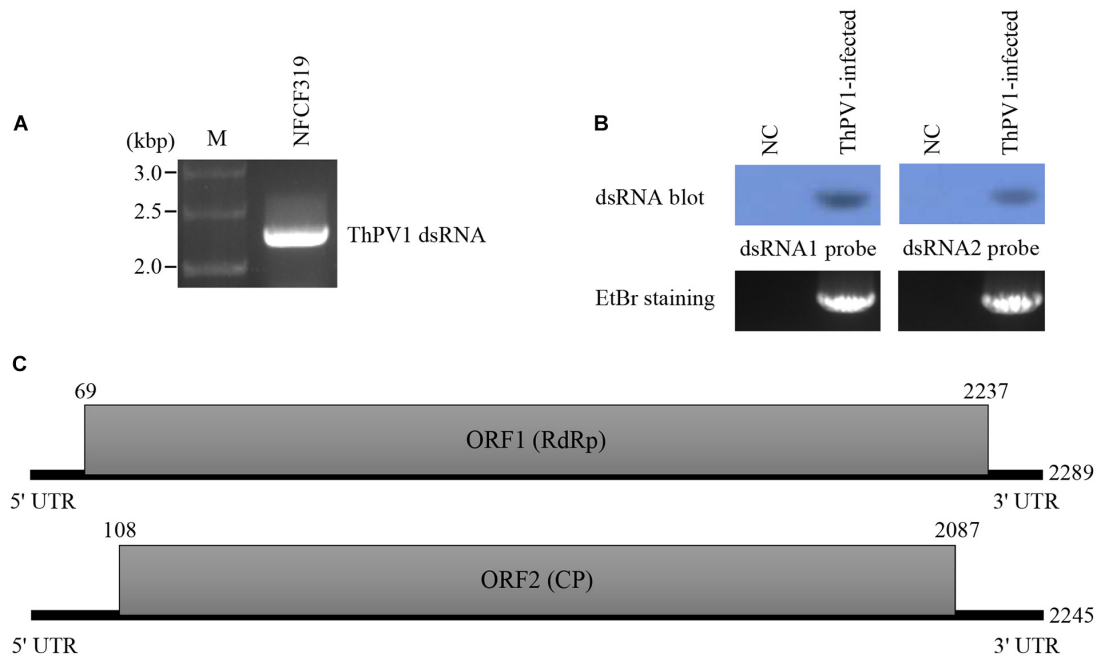

FIGURE 1 | Structure of the *T. harzianum* partitivirus 1 (ThPV1) genomic double-stranded RNAs (dsRNAs). **(A)** Agarose gel electrophoresis of ThPV1 dsRNA. Genomic dsRNA was extracted from virus-infected *T. harzianum* NFCF319. Lane M, DNA size standard. **(B)** Northern blot analysis of ThPV1 dsRNA1 and dsRNA2. RNAs were hybridized with probes for dsRNA1 and dsRNA2. NC: negative control (ThPV1-free). **(C)** Schematic representation of ThPV1 dsRNA segments. Shaded boxes, open reading frames (ORFs) encoding RNA-dependent RNA polymerase (RdRp) and capsid protein (CP). Numbers indicate the total lengths of the ThPV1 genome segments and the positions of the start and stop codons.

performed in 0.05 M sodium citrate buffer (pH 4.5) with β-1,3-glucan for 2 h. The reaction was stopped by heating at 100°C for 5 min, and the amount of reducing sugar liberated was measured using neocuproine. One unit (U) of β-1,3-glucanase activity was defined as the amount of an enzyme that produced 1 μmol of reducing sugar per minute under the assay conditions.

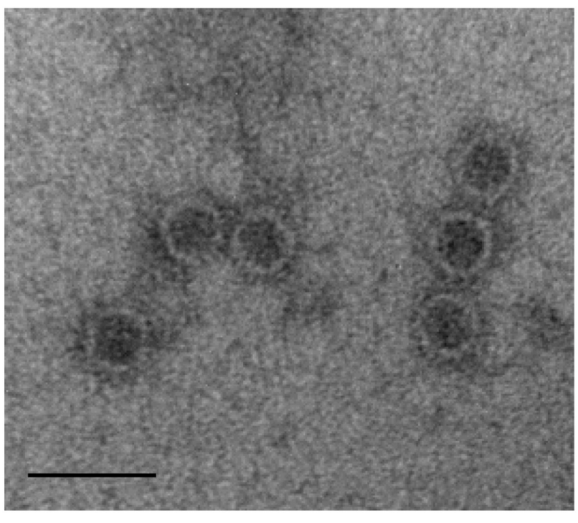

FIGURE 2 | Morphology of ThPV1 particles. Purified virus particles were negative-stained with 2% uranyl acetate and examined by transmission electron microscopy (TEM). Scale bar, 50 nm.

Transformation

Protoplasts were prepared as described previously (Penttilä et al., 1987). Transformation using protoplasts was performed as described previously, with slight modification (Churchill et al., 1990; Kim et al., 2002). Briefly, polyethylene glycol (PEG) 6,000 (Sigma) was used instead of PEG 4,000 when transforming DNA was mixed with protoplasts. The protoplasts were transformed with pDH25, which carried the hygromycin phosphotransferase gene cassette (*hph*) (Cullen et al., 1987). Transformants were selected from agar plates that were supplemented with 150 μg/ml hygromycin B (Calbiochem; Merck, Darmstadt, Germany), passaged three or four times on selective medium, and single-spore isolated as described previously (Kim et al., 2002). PCR and Southern blot analysis were conducted with genomic DNA from the transformants to confirm the hygromycin B resistance gene.

Transmission of dsRNA Virus

Virus transmission was performed as described previously (Kim et al., 2013). Briefly, mycelial plugs of the virus-containing strain were placed on PDA medium adjacent to mycelial plugs of the virus-free hygromycin-B-resistant recipient. After 3 days of co-culture, putatively fused mycelia at the recipient border between each pair of strains were transferred to hygromycin-containing PDA, successively transferred to fresh hygromycin-containing

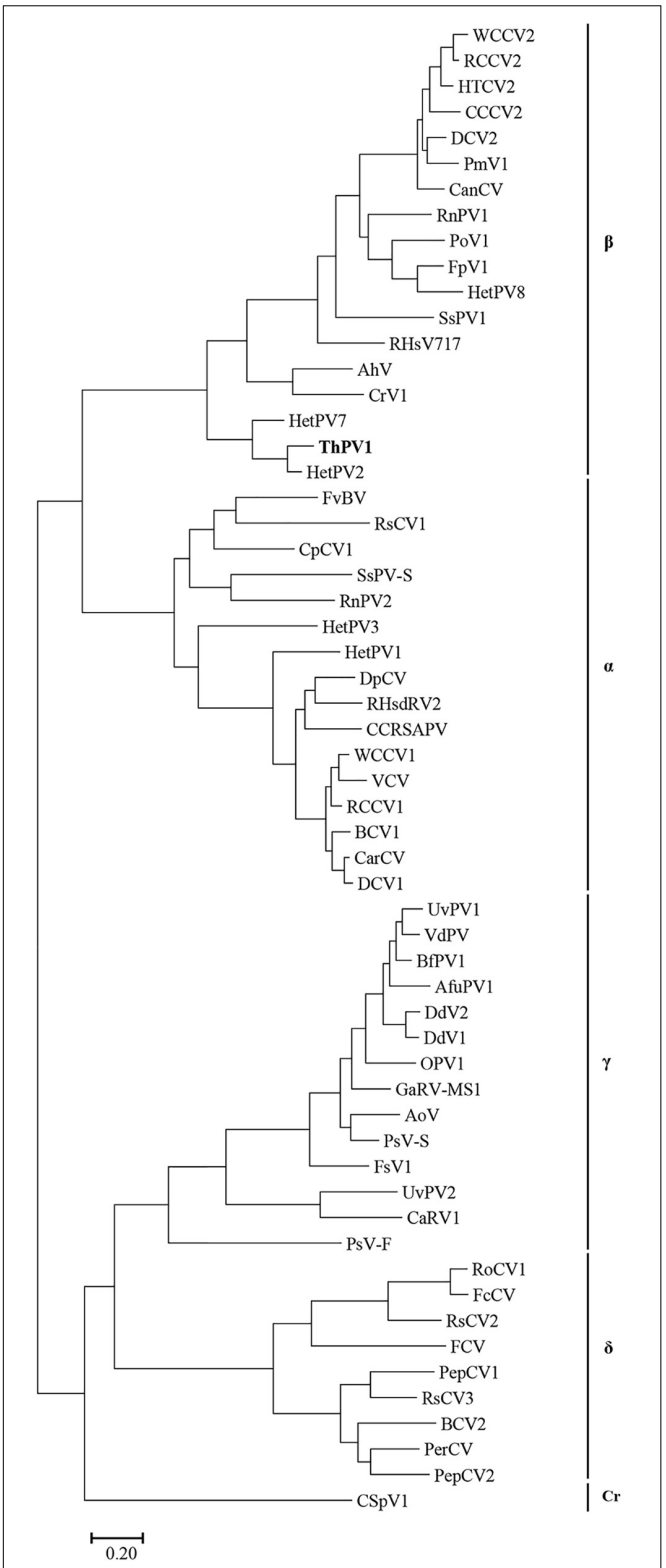

FIGURE 3 | Phylogenetic analysis of ThPV1. Maximum-likelihood (ML) tree based on the RdRp amino acid sequences of *Partitiviridae*. α, *Alphapartitivirus*; β, *Betapartitivirus*; γ, *Gammapartitivirus*; δ, *Deltapartitivirus*; Cr, *Cryspovirus*. See **Supplementary Table S2** for the partitivirus names and their GenBank numbers. Scale bar, number of substitutions per nucleotide site.

medium at least three times, and examined for the presence of virus. Then, the virus-containing mycelial progenies were single-spored to select for the virus-infected recipient transformants. The presence of mycovirus was confirmed by purification of dsRNA from the single-spored isolates.

RESULTS

Sequence Determination and Genome Organization

The dsRNA extracted from the mycelia of *T. harzianum* NFCF319 was resolved by 1% agarose gel electrophoresis, and distinctive bands of approximately 2.3 kb were excised (**Figure 1A**). The gel-purified dsRNAs were subjected to construct an RNA-Seq library followed by sequencing using Illumina HiSeq 2000. A total of 109 assembled reads with significant fragments per kilobase of transcript per million mapped reads (FPKM) values were obtained. A homology search of the assembled reads suggested the presence of contigs with high similarity to the known viral sequences of RNA-dependent RNA polymerase (RdRp) and capsid protein (CP). Based on the sequence analysis, RT-PCR using the corresponding primer pairs (see **Supplementary Table S1**) based on two representative contigs (i.e., one for RdRp and the other for CP) resulted in PCR amplicons of the expected sizes, which were subjected to sequence for verification. Northern blot analysis using the dsRNA extracts and probes (see **Supplementary Table S1**) constructed from PCR amplicons of portions of RdRp and CP revealed a specific hybridization band indicating that the excised dsRNA bands were double bands with similar sizes corresponding each of RdRp and CP. Thus, the analysis of the dsRNA sequences and Northern hybridization indicated that the mycoviral genome is divided into two dsRNA segments (dsRNA1 and dsRNA2) of similar size (**Figure 1B**). Rapid amplification of cDNA ends (RACE) was conducted to determine the full-length of the dsRNAs.

The complete genome sequences indicated that the dsRNA1 segment was of 2,289 bp with a GC content of 45.1%, and dsRNA2 was of 2,245 bp with a GC content of 49.5%. These sequences were deposited in GenBank (accession number MG973751 and MG973752, respectively). Each segment contains a long open reading frame (ORF) and ORF1 and 2 were on the coding strand of dsRNA1 and dsRNA2, respectively. RACE analysis indicated that the 5′ untranslated region (UTR) of the coding strand of dsRNA1 was 68 nt long and the 3′ UTR was 52 nt long. In addition, the coding strand of dsRNA2 contained a 107-nt-long 5′ UTR and 158-nt-long 3′ UTR. The structure of genome organization of dsRNA1 and dsRNA2 are displayed in **Figure 1C**.

The sequence of the 5′-termini of both dsRNA1 and 2 (GAACAAGG) were similar to the known consensus sequence of the betapartitivirus GAWWUWNU (N, any nt; W, A or U) and well-matched those of Heterobasidion partitivirus 2 (HetPV2) (Vainio et al., 2011). In addition, characteristic A-rich regions in the 3′-termini were preserved in both dsRNA1 [31 (A) residue in the 3′-terminal 50 nt] and dsRNA2 [48 (A) residue in the 3′-terminal 50 nt]. Like other fungal partitiviruses showing the

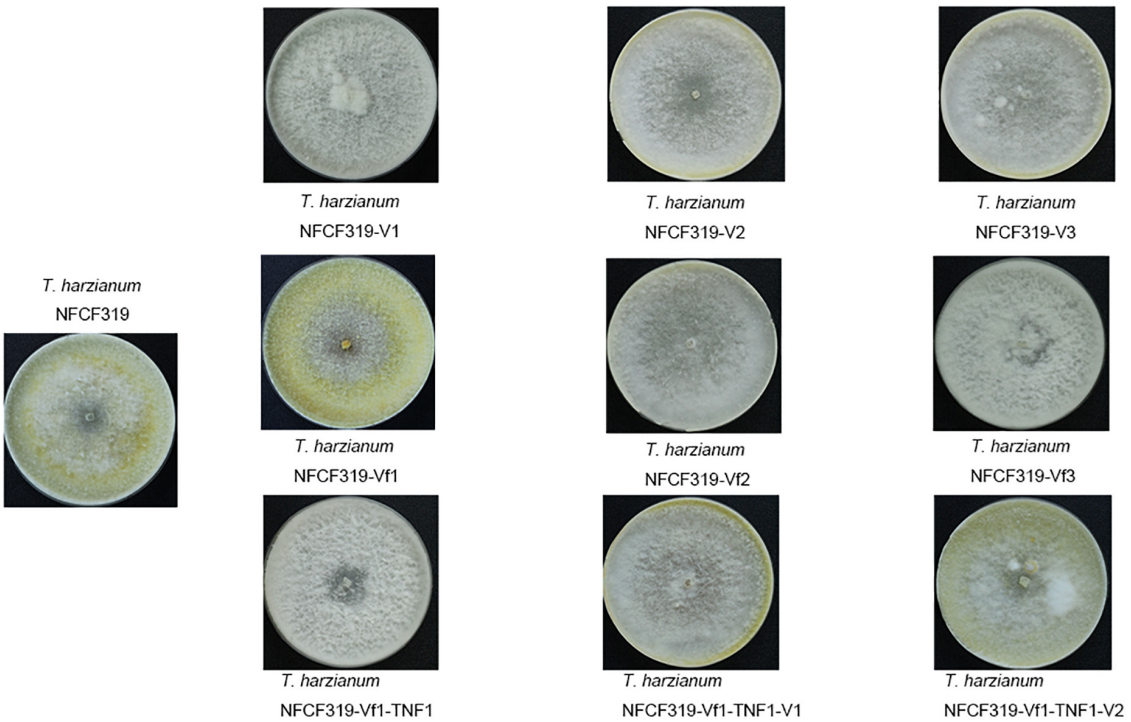

FIGURE 4 | Colony morphology of the original ThPV1-infected (*T. harzianum* NFCF319), three single-spored ThPV1-containing (*T. harzianum* NFCF319-V1, -V2, and -V3), isogenic ThPV1-cured (*T. harzianum* NFCF319-Vf1, -Vf2, and -Vf3), ThPV1-free hygromycin B resistant transformant (*T. harzianum* NFCF319-Vf1-TNF1), and isogenic ThPV1-transmitted (*T. harzianum* NFCF319-Vf1-TNF1-V1 and -V2) isolates.

characteristics of lengths of 5′- and 3′-non-translated region (NTR), longer 3′-NTR than 5′-NTR was found in dsRNA2 and longer 3′-NTR in dsRNA2 than dsRNA1 was found. Therefore, these results indicated that the obtained sequences were of the full-length of dsRNA1 and 2.

Viral particles were visualized by transmission electron microscopy (TEM). The particles were spherical and of diameter 28–30 nm (**Figure 2**).

Phylogenic Analysis of ORF1 and ORF2

The deduced amino acid sequence of ORF1 consisted of 722 amino acids with a predicted molecular mass of 79.4 kDa. Homology search of the deduced amino acid sequence revealed high similarity to the known sequences of RdRp of Heterobasidion partitivirus 2 (HetPV2) [GenBank accession number, HM565953; E-value, 0; AA identity, 589/722 (81%)]. Phylogenetic analysis using the top ranked similar sequences indicated that our RdRp clustered with the genus *Betapartitivirus*, and this was supported by significant bootstrap values. We next used the above sequence information for taxonomic reorganization of the family *Partitiviridae* (Vainio et al., 2015). The extensive analysis showed that our RdRp clustered with HetPV2 and Heterobasidion partitivirus 7 (HetPV7) (**Figure 3**).

ORF2 was deduced to encode a 659-amino acid protein of predicted molecular mass 72.5 kDa. Homology search showed high similarity to the CP of HetPV2 [GenBank accession number, HM565954; E-value 2e − 65; AA identity, 444/655 (68%)]. Phylogenetic analysis of CP indicated that our sequence clustered strongly to those of HetPV2 and HetPV7. Sequence similarity, genome organization, and phylogenetic analysis indicated that the dsRNAs are genome segments of a new member of the genus *Betapartitivirus* in the family *Partitiviridae*. Thus, we named our dsRNA as *Trichoderma harzianum* betapartitivirus 1 (ThPV1). Based on the ICTV species demarcation criteria for the genus *Betapartitivirus* in the family *Partitiviridae* ($\leq$90% and $\leq$80% amino acid identities in the RdRp and CP, respectively), we conclude that ThPV1 represents a novel species.

Characteristics of Mycovirus-Cured and -Containing Strains

Virus-cured isogenic strains were obtained by producing single-spored progenies followed by dsRNA purification. Spores were harvested from 7-day-old culture plates containing actively growing *T. harzianum* NFCF319, and 50 expected colony-forming units (CFUs) were spread on fresh potato dextrose agar (PDA) plate. Of 39 single-spored progenies, ThPV1 dsRNA bands were missing in 31. RT-PCR using gene specific primer pairs did not amplify any band and no hybridization band was observed either, which indicated that ThPV1 was cured in those selected strains. Virus-cured strains were successively sub-cultured weekly and subjected to dsRNA extraction every 4 weeks for 6 months. None of the cured-strains harbored ThPV1 dsRNA, suggesting that they were stable.

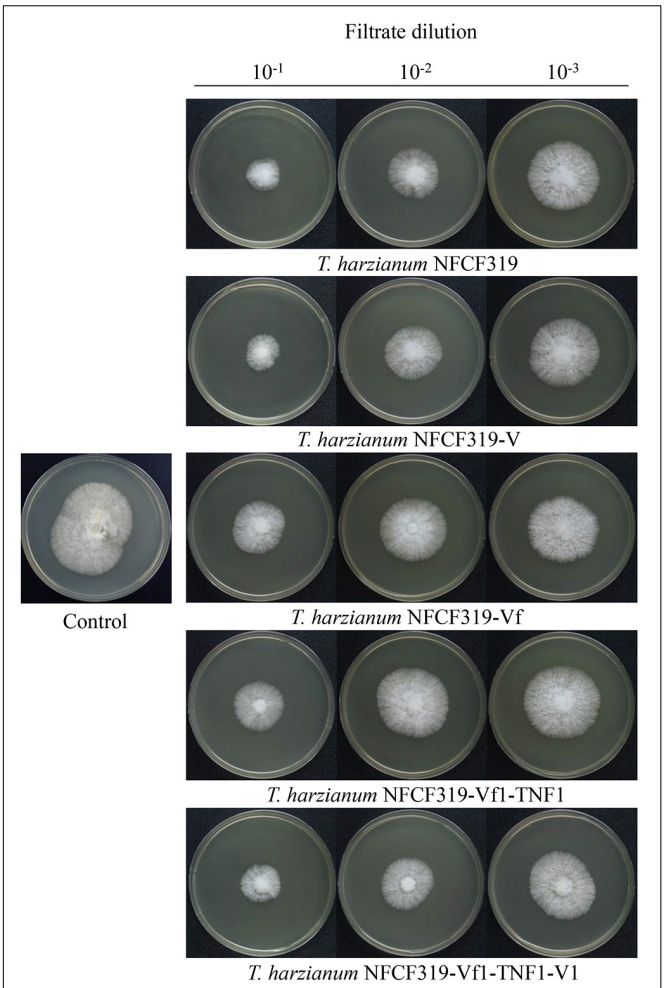

FIGURE 5 | Colony morphology of *P. ostreatus* supplemented with culture filtrates of ThPV1-containing and -free strains. Inhibition of the growth of colonies of *P. ostreatus* with culture filtrate supplementation was compared to without supplementation (control). Numbers at top indicate the dilution factors of the culture filtrates.

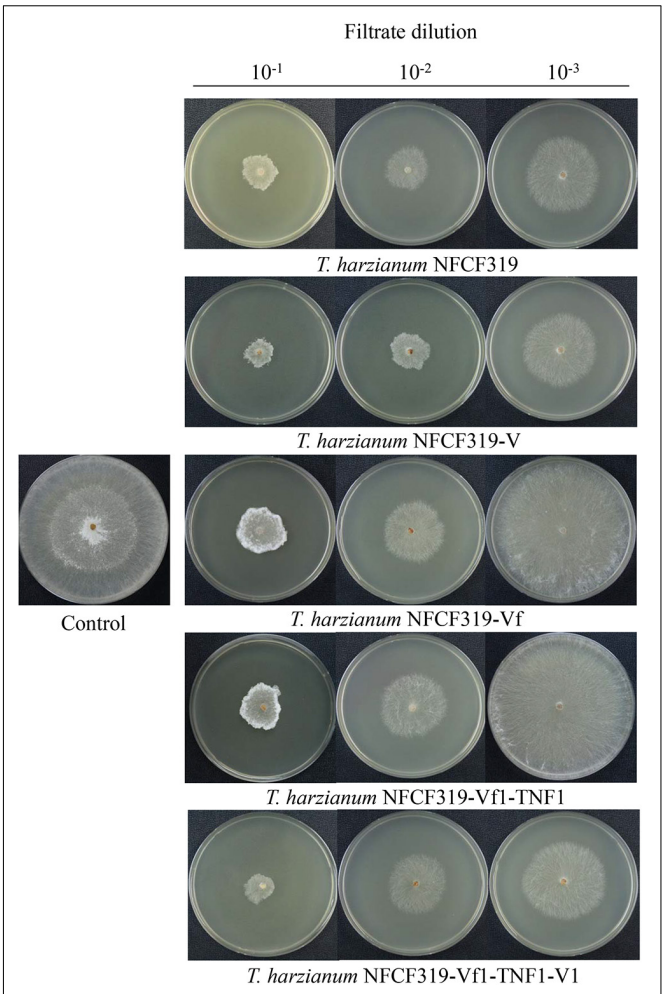

FIGURE 6 | Colony morphology of *R. solani* supplemented with culture filtrates of ThPV1-containing and -free strains. Inhibition of the growth of colonies of *R. solani* with culture filtrate supplementation was compared to without supplementation (control). Numbers at top indicate the dilution factors of the culture filtrates.

To increase the biological replicates, 3 out of 31 cured strains (*T. harzianum* NFCF319-Vf1, -Vf2, and -Vf3), and 3 from 7 vertically transmitted virus-containing clones (*T. harzianum* NFCF319-V1, -V2, and -V3) were randomly selected for further analysis.

No difference in growth rate was observed among the four ThPV1-infected *T. harzianum* isolates, i.e., between the original ThPV1-infected *T. harzianum* NFCF319 strain and its three single-spored virus-containing progenies *T. harzianum* NFCF319-V1, -V2, and -V3. In addition, no significant differences in growth rate or colony morphology were detected between the ThPV1-infected and -cured strains. Although the time of appearance and intensity of the pigmentation varied among individual cultures, a characteristic diffusing yellow pigment developed in all strains during cultivation. In addition, all strains produced similar numbers of gray–green conidia per plate, dispersed in concentric rings (**Figure 4**).

Biological Comparison of Mycovirus-Cured and -Containing Strains

The antagonistic activities of the virus-cured strains against the oyster mushroom, *P. ostreatus*, were measured using culture filtrates of the ThPV1-containg strains (*T. harzianum* NFCF319 and *T. harzianum* NFCF319-V1, -V2, and -V3) and ThPV1-cured strains (*T. harzianum* NFCF319-Vf1, -Vf2, and -Vf3). Significant differences in the growth rate of *P. ostreatus* were observed between medium without and with supplementation with the culture filtrates of *T. harzianum*, regardless of ThPV1 infection. Moreover, significant differences in growth rate were observed between medium supplemented with the culture filtrates of virus-cured and -containing strains. The growth rate was significantly reduced in medium supplemented with culture filtrate of the virus-containing strain (**Figure 5** and

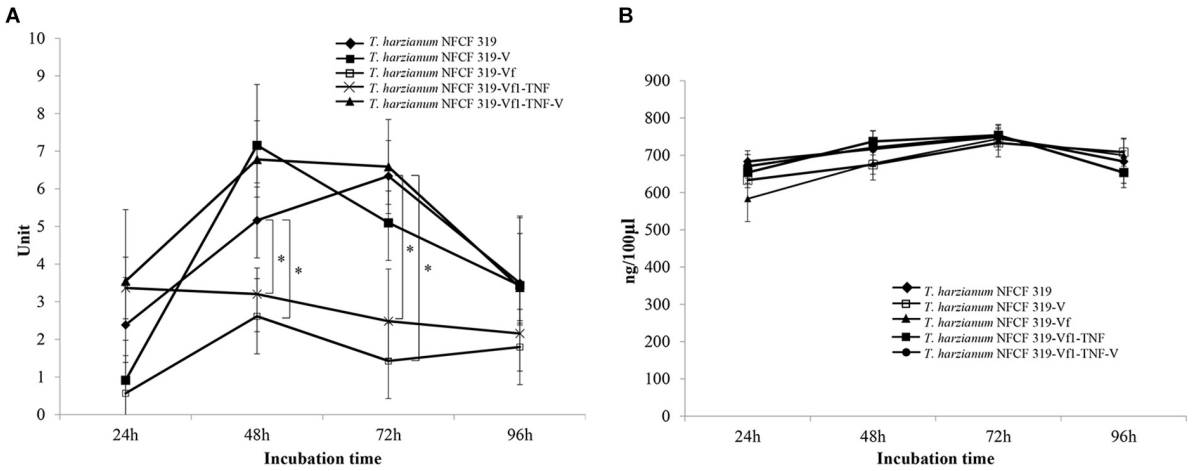

FIGURE 7 | Enzyme activities in culture filtrates of ThPV1-containing and -free strains. The β-1,3-glucanase **(A)** and chitinase **(B)** activities of the original ThPV1-infected (*T. harzianum* NFCF319), mean of three single-spored ThPV1-containing (*T. harzianum* NFCF319-V1, -V2, and -V3), mean of isogenic ThPV1-cured (*T. harzianum* NFCF319-Vf1, -Vf2, and -Vf3) and ThPV1-free hygromycin B resistant transformant (*T. harzianum* NFCF319-Vf1-TNF1), and mean of two isogenic ThPV1-transmitted (*T. harzianum* NFCF319-Vf1-TNF1-V1 and -V2) isolates. The error bars indicate the standard deviations for three repeats per isolate. Student's *t*-test (*$P < 0.05$) was used to analyze the data between the *T. harzianum* NFCF319 and other strains.

Table 1). Colonial growth inhibition was also examined using the plant pathogenic fungus *R. solani* AG-1 (**Figure 6** and **Table 1**). Significant differences in colony growth were observed in supplemented compared with non-supplemented medium. Furthermore, the culture filtrates of the virus-containing strains (*T. harzianum* NFCF319 and *T. harzianum* NFCF319-V1, -V2, and -V3) inhibited the growth of the oyster mushroom and a phytopathogenic fungus more strongly. To examine the effect of the heat-inactivated culture filtrate on fungal growth inhibition, colonial growth inhibition of *R. solani* AG-1 was tested using medium supplemented with the heat-inactivated culture filtrate. Colonial growth was inhibited by supplementation with the heat-inactivated culture filtrate, but the effect was not as intense as it was with the original culture filtrate. Interestingly, heat inactivation altered growth inhibition by the culture filtrates of the virus-containing strains to the level of the virus-cured strains.

The activities of two representative antifungal enzymes, β-1,3-glucanase and chitinase, were analyzed. The enzyme activity of the culture filtrate was monitored at 24 h intervals for 4 days. As shown in **Figure 7**, the time course of the β-1,3-glucanase activity was significantly reduced in the culture filtrate of the virus-cured strains of *T. harzianum* NFCF319 (*T. harzianum* NFCF319-Vf denotes the mean of three replicates of each of the NFCF319-Vf1, -Vf2, and -Vf3 isolates). Interestingly, there was no difference in chitinase activity between the virus-infected and -cured strains.

To validate the viral effect on the antifungal activity, we performed a "plus" experiment, i.e., we artificially transmitted ThPV1 into a virus-cured strain via anastomosis between virus-infected and -cured strains and analyzed the antifungal activity of the resulting virus-infected recipient strains. First, we transformed the cured strain of *T. harzianum* NFCF319-Vf1 using the hygromycin B resistance cassette to differentiate the ThPV1-transmitted progeny from the parental virus-containing *T. harzianum* NFCF319, because all cured strains were isogenic to their parental strain, i.e., the genetic background of all strains was identical, except for the presence or absence of mycovirus. Among 11 transformants showing stable resistance to hygromycin B after successive transfer to selective medium, the transformant *T. harzianum* NFCF319-Vf1-TNF1 was selected randomly and we observed no phenotypic changes from the parental *T. harzianum* NFCF319-Vf1 strain (**Figure 4**). After prolonged paired growth of the viral donor (*T. harzianum* NFCF319) and viral recipient (*T. harzianum* NFCF319-Vf1-TNF1) strains, several hyphae at the recipient border were collected and cultured independently on the selective medium, and the presence of ThPV1 was analyzed. Two independent single-spored virus-transmitted hyphal progenies were obtained. One of each single-spored progeny (*T. harzianum* NFCF319-Vf1-TNF1-V1 and -V2) containing ThPV1 was selected for further analysis (**Figure 4**). As shown in **Figures 5**, **6**, medium supplemented with the culture filtrates of virus-transmitted *T. harzianum* NFCF319-Vf1-TNF1-V resulted in significant differences in the growth inhibition of *P. ostreatus* and *R. solani*. The level of inhibition was similar to that of the original virus-infected *T. harzianum* NFCF319 and significantly greater than those of virus-cured *T. harzianum* NFCF319-Vf and its transformant *T. harzianum* NFCF319-Vf1-TNF. In addition, significant increases in β-1,3-glucanase activity were observed in *T. harzianum* NFCF319-Vf1-TNF1-V compared with the parental virus-cured transformant *T. harzianum* NFCF319-Vf1-TNF (**Figure 7**). The β-1,3-glucanase activity in *T. harzianum* NFCF319-Vf1-TNF1-V was comparable to that of the original virus-infected *T. harzianum* NFCF319 (**Figure 7**). The enzyme activity profiles of β-1,3-glucanase were similar among the virus-containing strains. The enzyme activity of the virus-containing strains reached a peak at 48 or 72 h and then decreased gradually to 96 h. The enzyme activity profiles of β-1,3-glucanase were similar across the virus-cured strains. However, the levels of the

enzyme activity of the virus-cured strains were significantly lower at 48 and 72 h of incubation and remained constant until 96 h. No difference in chitinase activity was observed among all strains tested.

DISCUSSION

The two-segmented dsRNA genome (each with one ORF) and isometric particles of 28–30 nm diameter suggest that ThPV1 belongs to the family *Partitiviridae*. According to the ICTV in 2016, the family *Partitiviridae* comprises the genera *Alphapartitivirus*, *Betapartitivirus*, *Gammapartitivirus*, *Deltapartitivirus*, and *Cryspovirus* (Nibert et al., 2014; Lefkowitz et al., 2017). The sizes of the segments and the molecular masses of the encoded proteins of ThPV1 are within the normal range of the genus *Betapartitivirus*, which are characteristically larger than those of other genera (Nibert et al., 2014). In addition, the high pairwise-identity scores of the amino acid sequences of encoded RdRp (81% to RdRp of HetPV2) and CP (68% to CP of HetPV2) to other known *Partitiviridae* (Nibert et al., 2014), and the clustering of ThPV1 with other members of the genus *Betapartitivirus*, indicates that ThPV1 is a new member of the genus *Betapartitivirus*.

TABLE 1 | Growth inhibition due to the supplementation of culture filtrates.

Dilution rate	Strains	Growth inhibition of *P. ostreatus* (%)	Growth inhibition of *R. solani* (%)
1:10	ThPV1-infected	90.29^{c}	94.78^{c}
	ThPV1-containing	91.33^{c}	95.49^{c}
	Isogenic ThPV1-cured	78.82^{b}	86.87^{b}
	ThPV1-free hygromycin B resistant transformant	81.06^{b}	86.85^{b}
	Isogenic ThPV1-transmitted	91.04^{c}	95.89^{c}
1:100	ThPV1-infected	82.03^{c}	87.01^{c}
	ThPV1-containing	81.64^{c}	87.55^{c}
	Isogenic ThPV1-cured	66.92^{b}	80.98^{b}
	ThPV1-free hygromycin B resistant transformant	66.66^{b}	80.53^{b}
	Isogenic ThPV1-transmitted	81.56^{c}	87.51^{c}
1:1000	ThPV1-infected	66.39^{b}	78.73^{c}
	ThPV1-containing	67.06^{b}	77.08^{c}
	Isogenic ThPV1-cured	66.58^{b}	5.23^{b}
	ThPV1-free hygromycin B resistant transformant	65.58^{b}	5.36^{b}
	Isogenic ThPV1-transmitted	67.05^{b}	76.61^{c}

ThPV1, Trichoderma harzianum partitivirus 1. Growth inhibition by metabolites from the original ThPV1-infected (T. harzianum NFCF319), three single-spored ThPV1-containing (T. harzianum NFCF319-V1, -V2, and -V3), isogenic ThPV1-cured (T. harzianum NFCF319-Vf1, -Vf2, and -Vf3), ThPV1-free hygromycin B resistant transformant (T. harzianum NFCF319-Vf1-TNF1), and isogenic ThPV1-transmitted (T. harzianum NFCF319-Vf1-TNF1-V1 and -V2) isolates. Numbers are the relative inhibition rates (%) compared to without fungal metabolite supplementation. Data were analyzed by ANOVA followed by post hoc Tukey's with the level of significance at $p < 0.05$. The same letters at the top of the relative inhibition rate indicate no significant difference between isolates.

Virus curing by single-spore isolation was successful; i.e., 79.5% of the resulting single-spore colonies were ThPV1-free. In addition, the ThPV1-free proportion was similar (20–84%) among three independent experiments. Therefore, the rate of vertical transmission of ThPV1 to mitotic progenies, conidia, of host fungus was low, although a considerable proportion of conidia showed vertical transmission of ThPV1. Like other mycoviruses, partitiviruses are generally considered to be transmitted vertically during cell division and horizontally during intimate cell-cell contact. Heterobasidion partitiviruses, which are closely related to ThPV1, could be transmitted vertically to basidiospores and conidiospores and horizontally via hyphal contact (Ihrmark et al., 2002, 2004). The mitotic stability measured by inheritance of mycoviruses during asexual conidiation differed depending on the virus–fungus interaction. The mitotic inheritance of ThPV1 during asexual conidiation was less stable than that of Cryphonectria hypovirus 1 (CHV1) in *C. parasitica* (Suzuki et al., 2003; Prospero et al., 2006), and of mycoreovirus 1 (MyRV1) in *C. parasitica* (Sun et al., 2006), but comparable to dsRNAs in the basidiomycetes *H. annosum* (Ihrmark et al., 2002). The low transmission rate of ThPV1 into conidia is exceptional considering that most vertical transmission of dsRNA into asexual spores of ascomycetes occurs at a markedly higher rate. Indeed, the recently characterized Trichoderma atroviride mycovirus 1 (TaMV1) has a very high transmission rate (33/38) (Lee et al., 2017). Therefore, the low transmission rate of ThPV1 into conidia is attributable to the intrinsic characteristics of the virus–fungus (ThPV1–*T. harzianum*) interaction.

Considering their persistent lifestyles and direct cell-to-cell transmission, partitiviruses has few, if any, deleterious effects on host cells (Nibert et al., 2014). However, others have reported negative or positive effects of partitiviruses on their host (Suzuki et al., 2001; Márquez et al., 2007; Jenkins et al., 2008; Kanematsu et al., 2010; Vainio et al., 2010, 2017; Hyder et al., 2013; Xiao et al., 2014; Zheng et al., 2014). ThPV1 did not influence the mycelial growth, colony morphology, pigmentation, or conidiation of its host fungus. However, ThPV1 significantly altered the activities of antifungal enzymes potentiating the biocontrol function of its host fungus *T. harzianum*. It is interesting to see that, regardless of virus-containing or -cured, supplementation of culture filtrates resulted in significantly increased antifungal activities compared to the non-supplementation; furthermore, the heat-treated culture filtrate of the ThPV1-infected strain showed significantly reduced antifungal activities similar to the level of ThPV1-free strain. These results clearly suggested that the antifungal activities were attributable to both heat-stable and -sensitive metabolites. Considering the facts that antifungal

activity was significantly increased by ThPV1, significant increase in the activity of antifungal enzyme of β-1,3-glucanase was observed in the ThPV1-infected strain, and heat treatment reversed the increased antifungal activity of ThPV1-infected strain, the antifungal activity was likely mediated by a hydrolytic enzyme, such as β-1,3-glucanase. ThPV1 modulates the activity of β-1,3-glucanase but not that of chitinase. These results suggest that ThPV1 influences the activity of a specific fungal enzyme, which enhances the mycoparasitism of ThPV1-infected *T. harzianum*. Mycoviruses can exert complex effects on their fungal host, which mediated osmotic stress tolerance (Nerva et al., 2017) and mycotoxin accumulation (Nerva et al., 2018). Thus, whether ThPV1 exerts antagonistic effects on other fungal strains or species should be the subject of further studies.

In addition to the curing experiment including multiple virus-cured and -retained progenies, horizontal viral transmission via hyphal fusion allowed us to verify that the changes in antifungal activities were due to ThPV1. The fact that, compared with the original *T. harzianum* NFCF319 strain, all the viral-transmitted isolates showed similar levels of antifungal activity, such as the growth inhibition of other fungi, indicates that ThPV1 is responsible for the enhanced antifungal activity of the host fungus. Although further work is required, it is important to note the increased β-1,3-glucanase activity is implicated in the hydrolysis of pathogenic fungi during mycoparasitic attack by *T. harzianum* (Qualhato et al., 2013). The antifungal activity was higher in the culture filtrate of ThPV1-infected strains, suggesting that the enhanced β-1,3-glucanase activity influences the potential antifungal activity of ThPV1-infected strains.

To our knowledge, this is the first report of a betapartitivirus in *T. harzianum*. In addition, the mycovirus enhanced the antifungal activity of the host fungus by regulating the activity of a specific antifungal enzyme.

AUTHOR CONTRIBUTIONS

D-HK supervised the experiments. JC and H-EY performed the experiments. D-HK, JC, and H-EY prepared the figures and edited the manuscript. D-HK wrote the manuscript.

FUNDING

This work was supported by the Bio-industry Technology Development Program, Ministry for Food, Agriculture, Forestry and Fisheries, Republic of Korea and in part by the NRF grant by MSIP (2018R1A2A1A05078682). We thank the Institute of Molecular Biology and Genetics at Chonbuk National University for kindly providing the facilities for this research. D-HK was supported by "Research Base Construction Fund Support Program" funded by Chonbuk National University in 2016.

SUPPLEMENTARY MATERIAL

The Supplementary Material for this article can be found online at: https://www.frontiersin.org/articles/10.3389/fpls.2018.01699/full#supplementary-material

REFERENCES

Churchill, A. C. L., Ciuffetti, L. M., Hansen, D. R., Van Etten, H. D., and Van Alfen, N. K. (1990). Transformation of the fungal pathogen *Cryphonectria parasitica* with a variety of heterologous plasmids. *Curr. Genet.* 17, 25–31. doi: 10.1007/BF00313245

Cullen, D., Leong, S. A., Wilson, L. J., and Henner, D. J. (1987). Transformation of *Aspergillus nidulans* with the hygromycin-resistance gene, hph. *Gene* 57, 21–26. doi: 10.1016/0378-1119(87)90172-7

Fitch, W. M. (1971). Toward defining the course of evolution: minimum change for a specific tree topology. *Syst. Zool.* 20, 406–416. doi: 10.2307/2412116

Ghabrial, S. A. (1998). Origin, adaptation and evolutionary pathways of fungal viruses. *Virus Genes* 16, 119–131. doi: 10.1023/A:1007966229595

Ghabrial, S. A., Castón, J. R., Jiang, D., Nibert, M. L., and Suzuki, N. (2015). 50-plus years of fungal viruses. *Virology* 47, 356–368. doi: 10.1016/j.virol.2015.02.034

Hatvani, N., Kredics, L., Antal, Z., and Mécs, I. (2002). Changes in activity of extracellular enzymes in dual cultures of *Lentinula edodes* and mycoparasitic trichoderma strains. *J. Appl. Microbiol.* 92, 415–423. doi: 10.1046/j.1365-2672.2002.01542.x

Howell, C. R. (2003). Mechanisms employed by trichoderma species in the biological control of plant diseases: the history and evolution of current concepts. *Plant Dis.* 87, 4–10. doi: 10.1094/PDIS.2003.87.1.4

Hyder, R., Pennanen, T., Hamberg, L., Vainio, E. J., Piri, T., and Hantula, J. (2013). Two viruses of *Heterobasidion* confer beneficial, cryptic or detrimental effects to their hosts in different situations. *Fungal Ecol.* 6, 387–396. doi: 10.1016/j.funeco.2013.05.005

Ihrmark, K., Johannesson, H., Stenström, E., and Stenlid, J. (2002). Transmission of double-stranded RNA in *Heterobasidion annosum*. *Fungal Genet. Biol.* 36, 147–154. doi: 10.1016/S1087-1845(02)00011-7

Ihrmark, K., Stenström, E., and Stenlid, J. (2004). Double-stranded RNA transmission through basidiospores of *Heterobasidion annosum*. *Mycol. Res.* 108, 149–153. doi: 10.1017/S0953756203008839

Jenkins, M. C., Higgins, J., Abrahante, J. E., Kniel, K. E., O'Brien, C., Trout, J., et al. (2008). Fecundity of *Cryptosporidium parvum* is correlated with intracellular levels of the viral symbiont CPV. *Int. J. Parasitol.* 38, 1051–1055. doi: 10.1016/j.ijpara.2007.11.005

Kanematsu, S., Sasaki, A., Onoue, M., Oikawa, Y., and Ito, T. (2010). Extending the fungal host range of a partitivirus and a mycoreovirus from *Rosellinia necatrix* by inoculation of protoplasts with virus particles. *Phytopathology* 100, 922–930. doi: 10.1094/PHYTO-100-9-0922

Kim, J. M., Jung, J. E., Park, J. A., Park, S. M., Cha, B. J., and Kim, D. H. (2013). Biological function of a novel chrysovirus, CnV1-BS122, in the korean cryphonectria nitschkei BS122 strain. *J. Biosci. Bioeng.* 115, 1–3. doi: 10.1016/j.jbiosc.2012.08.007

Kim, M. J., Choi, J. W., Park, S. M., Cha, B. J., Yang, M. S., and Kim, D. H. (2002). Characterization of a fungal protein kinase from *Cryphonectria parasitica* and its transcriptional upregulation by hypovirus. *Mol. Microbiol.* 45, 933–941. doi: 10.1046/j.1365-2958.2002.03079.x

Kredics, L., García Jimenez, L., Naeimi, S., Czifra, D., Urbán, P., Manczinger, L., et al. (2010). "A challenge to mushroom growers: the green mould disease of cultivated champignons," in *Current Research, Technology and Education Topics in Applied Microbiology and Microbial Biotechnology*, ed. A. Méndez-Vilas (Badajoz: Formatex), 295–305.

Kubicek, C. P., and Penttila, M. E. (1998). "Regulation of production of plant polysaccharide degrading enzymes by Trichoderma," in *Trichoderma and Gliocladium: Enzymes, Biological Control and Commercial Applications*, eds G. E. Harman and C. P. Kubicek (London, UK: Taylor and Francis), 49–71.

Kumar, S., Stecher, G., and Tamura, K. (2016). MEGA7: molecular evolutionary genetics analysis version 7.0 for bigger datasets. *Mol. Biol. Evol.* 33, 1870–1874. doi: 10.1093/molbev/msw054

Lee, S. H., Yun, S. H., Chun, J., and Kim, D. H. (2017). Characterization of a novel dsRNA mycovirus of *Trichoderma atroviride* NFCF028. *Arch. Virol.* 162, 1073–1077. doi: 10.1007/s00705-016-3214-z

Lefkowitz, E. J., Adams, M. J., Davison, A. J., Siddell, S. G., and Simmonds, P. (2017). *Virus Taxonomy: Classification and Nomenclature of Viruses. The Online 10th Report of the ICTV*. Available at: https://talk.ictvonline.org/ictv-reports/ictv_online_report.

Márquez, L. M., Redman, R. S., Rodriguez, R. J., and Roossinck, M. J. (2007). A virus in a fungus in a plant: three-way symbiosis required for thermal tolerance. *Science* 315, 513–515. doi: 10.1126/science.1136237

Nerva, L., Chitarra, W., Siciliano, I., Gaiotti, F., Ciuffo, M., Forgia, M., et al. (2018). Mycoviruses mediate mycotoxin regulation in *Aspergillus ochraceus*. *Environ. Microb.* doi: 10.111/1462-2920.14436 [Epub ahead of print].

Nerva, L., Silvestri, A., Ciuffo, M., Palmano, S., Varese, G. C., and Turina, M. (2017). Transmission of *Penicillium aurantiogriseum* partiti-like virus 1 to a new fungal host (*Cryphonectria parasitica*) confers higher resistance to salinity and reveals adaptive genomic changes. *Environ. Microb.* 19, 4480–4492. doi: 10.111/1462-2920.1389

Nibert, M. L., Ghabrial, S. A., Maiss, E., Lesker, T., Vainio, E. J., Jiang, D., et al. (2014). Taxonomic reorganization of family Partitiviridae and other recent progress in partitivirus research. *Virus Res.* 188, 128–141. doi: 10.1016/j.virusres.2014.04.007

Nuss, D. L. (2005). Hypovirulence: mycoviruses at the fungal-plant interface. *Nat. Rev. Microbiol.* 3, 632–642. doi: 10.1038/nrmicro1206

Nuss, D. L., and Koltin, Y. (1990). Significance of dsRNA genetic elements in plant pathogenic fungi. *Ann. Rev. Phytopathol.* 28, 37–58. doi: 10.1146/annurev.py.28.090190.000345

Papavizas, G. C. (1985). Trichoderma and *Gliocladium*: biology, ecology, and potential for biocontrol. *Ann. Rev. Phytopathol.* 23, 23–54. doi: 10.1146/annurev.py.23.090185.000323

Park, S. M., Kim, J. M., Chung, H. J., Lim, J. Y., Kwon, B. R., Lim, J. G., et al. (2008). Occurrence of diverse dsRNA in a korean population of the chestnut blight fungus, *Cryphonectria parasitica*. *Mycol. Res.* 112, 1220–1226. doi: 10.1016/j.mycres.2008.04.001

Penttilä, M., Nevalainen, H., Rättö, M., Salminen, E., and Knowles, J. (1987). A versatile transformation system for the cellulolytic filamentous fungus *Trichoderma reesei*. *Gene* 61, 155–164. doi: 10.1016/0378-1119(87)90110-7

Prospero, S., Conedera, M., Heiniger, U., and Rigling, D. (2006). Saprophytic activity and sporulation of *Cryphonectria parasitica* on dead chestnut wood in forests with naturally established hypovirulence. *Phytopathology* 96, 1337–1344. doi: 10.1094/PHYTO-96-1337

Qualhato, F. T., Lopes, F. A. C., Steindorff, A. S., Brandão, R. S., Jesuino, R. S. A., and Ulhoa, C. J. (2013). Mycoparasitism studies of trichoderma species against three phytopathogenic fungi: evaluation of antagonism and hydrolytic enzyme production. *Biotechnol. Lett.* 35, 1461–1468. doi: 10.1007/s10529-013-1225-3

Samuels, G. J., and Hebbar, K. P. (2015). *Trichoderma: Identification and Agricultural Applications*. St. Paul, MN: APS Press.

Seaby, D. (1998). "Trichoderma as a weed mould or pathogen in mushroom cultivation," in *Trichoderma and Gliocladium*, eds G. E. Harman and C. P. Kubicek (London, UK: Taylor and Francis), 267–288.

Sivasithamparam, K., and Ghisalberti, E. L. (1998). "Secondary metabolism in Trichoderma and Gliocladium," in *Trichoderma and Gliocladium: Basic Biology, Taxonomy and Genetics*, eds G. E. Harman and C. P. Kubicek (London, UK: Taylor and Francis), 139–191.

Sun, L., Nuss, D. L., and Suzuki, N. (2006). Synergism between a mycoreovirus and a hypovirus mediated by the papain-like protease p29 of the prototypic hypovirus CHV1-EP713. *J. Gen. Virol.* 87, 3704–3714. doi: 10.1099/vir.0.82213-0

Suzuki, A., Kobayashi, F., Abe, M., Uchiumi, T., and Higashi, S. (2001). Cloning and expression of a down-regulated gene (TrEnodDR1) of white clover responded by the nod genes derived from *Rhizobium leguminosarum* bv. trifolii strain 4S. *Gene* 266, 77–84. doi: 10.1016/S0378-1119(01)00377-8

Suzuki, N., Maruyama, K., Moriyama, M., and Nuss, D. L. (2003). Hypovirus papain-like protease p29 functions in trans to enhance viral double-stranded RNA accumulation and vertical transmission. *J. Virol.* 77, 11697–11707. doi: 10.1128/JVI.77.21.11697-11707.2003

Thompson, J. D., Gibson, T. J., Plewniak, F., Jeanmougin, F., and Higgins, D. G. (1997). The CLUSTAL_X windows interface: flexible strategies for multiple sequence alignment aided by quality analysis tools. *Nucleic Acids Res.* 25, 4876–4882. doi: 10.1093/nar/25.24.4876

Tokimoto, K. (1985). Physiological studies on antagonism between *Lentinula edodes* and *Trichoderma* spp. in bedlogs of the former (in Japanese). *Rep. Tottori. Mycol. Inst.* 23, 1–54.

Ulhoa, C. J., and Peberdy, J. F. (1992). Purification and some properties of the extracellular chitinase produced by *Trichoderma harzianum*. *Enzyme Microb. Technol.* 14, 236–240. doi: 10.1016/0141-0229(92)90072-V

Vainio, E. J., Jurvansuu, J., Hyder, R., Kashif, M., Piri, T., Tuomivirta, T., et al. (2017). The partitivirus HetPV13-an1 mediates severe growth debilitation and major alterations in the gene expression of a fungal forest pathogen. *J. Virol.* 92:e01744-17. doi: 10.1128/JVI.01744-17

Vainio, E. J., Keriö, S., and Hantula, J. (2011). Description of a new putative virus infecting the conifer pathogenic fungus *Heterobasidion annosum* P-type partitivirus. *Arch. Virol.* 156, 79–86. doi: 10.1007/s00705-010-0823-9

Vainio, E. J., Korhonen, K., Tuomivirta, T. T., and Hantula, J. (2010). A novel putative partitivirus of the saprotrophic fungus *Heterobasidion* ecrustosum infects pathogenic species of the *Heterobasidion annosum* complex. *Fungal Biol.* 114, 955–965. doi: 10.1016/j.funbio.2010.09.006

Vainio, E. J., Müller, M. M., Korhonen, K., Piri, T., and Hantula, J. (2015). Viruses accumulate in aging infection centers of a fungal forest pathogen. *ISME J.* 9, 497–507. doi: 10.1038/ismej.2014.181

Van Alfen, N. K. (1986). "Hypovirulence of Endothia (Cryphonectria) parasitica and Rhizoctonia solani," in *Fungal Virology*, ed. K. W. Buck (Boca Raton, FL: CRC Press), 143–162.

Wang, L., Jiang, J., Wang, Y., Hong, N., Zhang, F., Xu, W., et al. (2014). Hypovirulence of the phytopathogenic fungus *Botryosphaeria dothidea*: association with a coinfecting chrysovirus and a partitivirus. *J. Virol.* 88, 7517–7527. doi: 10.1128/JVI.00538-14

Wickner, R. B. (1992). Double-stranded and single-stranded RNA viruses of *Saccharomyces cerevisiae*. *Ann. Rev. Microbiol.* 46, 347–375. doi: 10.1146/annurev.mi.46.100192.002023

Xiao, X., Cheng, J., Tang, J., Fu, Y., Jiang, D., Baker, T. S., et al. (2014). A novel partitivirus that confers hypovirulence on plant pathogenic fungi. *J. Virol.* 88, 10120–10133. doi: 10.1128/JVI.01036-14

Yun, S. H., Lee, S. H., So, K. K., Kim, J. M., and Kim, D. H. (2016). Incidence of diverse dsRNA mycoviruses in trichoderma spp. causing green mold disease of shiitake *Lentinula edodes*. *FEMS Microbiol. Lett.* doi: 10.1093/femsle/fnw220 [Epub ahead of print].

Zheng, L., Zhang, M., Chen, Q., Zhu, M., and Zhou, E. (2014). A novel mycovirus closely related to viruses in the genus *Alphapartitivirus* confers hypovirulence in the phytopathogenic fungus *Rhizoctonia solani*. *Virol* 456-457, 220–226. doi: 10.1016/j.virol.2014.03.029

Conflict of Interest Statement: The authors declare that the research was conducted in the absence of any commercial or financial relationships that could be construed as a potential conflict of interest.

frontiers in Plant Science

ORIGINAL RESEARCH
published: 27 November 2018
doi: 10.3389/fpls.2018.01738

Diverse, Novel Mycoviruses From the Virome of a Hypovirulent *Sclerotium rolfsii* Strain

Jun Zi Zhu, Hong Jian Zhu, Bi Da Gao, Qian Zhou and Jie Zhong**

Hunan Provincial Key Laboratory for Biology and Control of Plant Diseases and Insect Pests, Hunan Agricultural University, Changsha, China

Sclerotium rolfsii, which causes southern blight in a wide variety of crops, is a devastating plant pathogen worldwide. Mycoviruses that induce hypovirulence in phytopathogenic fungi are potential biological control resources against fungal plant diseases. However, in *S. rolfsii,* mycoviruses are rarely reported. In a previous study, we found a hypovirulent strain carrying a diverse pattern of dsRNAs. Here, we utilized the RNA_Seq technique to detect viral sequences. Deep sequencing, RT-PCR and Sanger sequencing validation analyses revealed that this strain harbors various new viral species that show affinity to the distinctly established and proposed families *Benyviridae*, *Endornaviridae*, Fusariviridae, *Hypoviridae*, and Fusagraviridae. Moreover, some viral sequences that could not be assigned to any of the existing families or orders were also identified and showed similarities to the *Alphavirus*, *Ourmiavirus*, phlegivirus-like and Curvularia thermal tolerance virus-like groups. In addition, we also conducted deep sequencing analysis of small RNAs in the virus-infecting fugal strain. The results indicated that the Dicer-mediated gene silencing mechanism was present in *S. rolfsii.* This is the first report of viral diversity in a single *S. rolfsii* fungal strain, and the results presented herein might provide insight into the taxonomy and evolution of mycoviruses and be useful for the exploration of mycoviruses as biocontrol agents.

Keywords: Mycovirus, *Sclerotium rolfsii*, virome, deep sequencing, biocontrol

OPEN ACCESS

Edited by:
Jiatao Xie,
Huazhong Agricultural University, China

Reviewed by:
Sotaro Chiba,
Nagoya University, Japan
Shinyi Lee Marzano,
University of Illinois at Urbana-Champaign, United States

***Correspondence:**
Qian Zhou
zhouqian2617@hunau.edu.cn
Jie Zhong
wzzhtx@sina.com

Specialty section:
This article was submitted to Virology, a section of the journal Frontiers in Plant Science

Received: *31 August 2018*
Accepted: *08 November 2018*
Published: *27 November 2018*

Citation:
Zhu JZ, Zhu HJ, Gao BD, Zhou Q and Zhong J (2018) Diverse, Novel Mycoviruses From the Virome of a Hypovirulent Sclerotium rolfsii Strain. Front. Plant Sci. 9:1738. doi: 10.3389/fpls.2018.01738

INTRODUCTION

Mycoviruses are a type of virus that infect and replicate in fungi, infecting all major taxonomic fungal groups (Ghabrial and Suzuki, 2009). Most mycoviruses are associated with latent infections. However, several mycoviruses can obviously cause abnormal symptoms in the host, such as hypovirulence and debilitation, and thus hold great promise for exploitation as biological agents to control fungal diseases. Since Cryphonectria hypovirus 1 (CHV1) was successfully used to control chest blight disease in Europe (Nuss, 1992; Xie and Jiang, 2014; Ghabrial et al., 2015), phytopathologists have been inspired to study mycovirus-mediated hypovirulence in plant pathogenic fungi. Recently, the DNA virus *Sclerotinia sclerotiorum* hypovirulence-associated DNA virus 1 (SsHADV-1) was proven to possess the potential for biologically controlling sclerotinia disease under field conditions (Yu et al., 2010, 2013). Rosellinia necatrix megabirnavirus 1 has the ability to control apple white root rot disease caused by *Rosellinia necatrix* (Chiba et al., 2009; Liu et al., 2016). With the rare exceptions of DNA and negative-sense RNA (-ssRNA) (Liu et al., 2014), mycoviral genomes consist of double-stranded (ds) or positive-sense single-stranded

(+ss) RNA. With the increasing number of mycoviruses identified, some of which have unique molecular and biological properties unlike those of any other known mycoviruses and cannot be assigned into any of the established virus families, mycovirus classification is being refined. Thus, the discovery of novel mycoviruses that have diverse molecular and biological properties will facilitate our understanding of viral ecology and evolution.

The development and application of high-throughput next generation sequencing (NGS) technologies and bioinformatics have greatly enhanced the discovery of new viruses in many organisms, including fungi (Marzano et al., 2016; Zhang et al., 2018). NGS techniques can detect the presence of viral sequences regardless of the sample viral titer and does not require prior knowledge of the genomic sequences of candidate viruses (Mokili et al., 2012; Roossinck, 2015). To date, some examples in deep sequencing of the transcriptome (RNA-seq) (Schoebel et al., 2014; Li et al., 2015; Liu et al., 2016), ribosomal RNA (rRNA)-depleted total RNAs, small interfering RNAs (Marzano et al., 2015; Vainio et al., 2015; Shi et al., 2016; Remnant et al., 2017; Mu et al., 2018), and viral dsRNA (Coetzee et al., 2010; Al Rwahnih et al., 2011; Bartholomäus et al., 2016) have proven the methods to be useful for facilitating the discovery of mycoviruses or other RNA and DNA viruses infecting plants and insects. The NGS data and analysis tools have advanced the virology research in areas of viral evolutionary, ecology, epidemiology, genomic diversity, and interactions between viruses and hosts (Zhang et al., 2018). Because some material needed for deep sequencing library construction can be infected by viruses, we can use transcriptomic data for virus identification and genome assembly *in silico*, which has recently been demonstrated in several studies (Jo et al., 2015, 2016a,b). Usually, RNA viruses with poly (A) tails and polyadenylated RNA viruses that can be collected together with mRNA using oligo d(T) are easily sequenced in transcriptome libraries (Gu et al., 2014). Recently, several recent studies also showed that rRNA depleted RNA libraries were suitable for virus identification lacking poly (A) tails (Jo et al., 2015; Mu et al., 2018). In addition, sequencing of rRNA depleted RNA could reveal an entire micro-organisms in samples collected from environment materials. However, with the increasing of enormous and complicated NGS data, we would be more dependent on the accuracy of sequence assembly and homology searching for discover of new viruses (Zhang et al., 2018).

Sclerotium rolfsii Sacc. [*Athelia rolfsii* (Curzi) Tu Kimbrough] is a soil-borne pathogen that causes southern blight disease in a wide variety of crops (Rivard et al., 2010). *S. rolfsii* infects more than 600 plant species and is thus a serious problem. Moreover, *S. rolfsii* produces sclerotia, which plays a key role in the disease cycle, and has the ability to survive in soil for long periods (Punja, 1985; Xu et al., 2008), thus serving as an important barrier to controlling this disease. Because hypovirulence-associated mycoviruses reportedly have potential for development as biocontrol agents for fungal diseases, screening for mycoviruses possessing biological control potential is significant for the control of southern blight disease.

Previously, we isolated a hypovirulent *S. rolfsii* strain, BLH-1, that contains a series of dsRNAs. Virus-curing and horizontal transmission experiments confirmed that dsRNAs were associated with the hypovirulent traits of BLH-1 (Zhong et al., 2016a). This study aimed to further clarify the species and genomes of all the mycoviruses infecting BLH-1, and to determine the possibility of interactions between the RNA silencing machinery and mycoviruses in *S. rolfsii*. To do this, the following procedures were utilized in this study: transcriptome deep sequencing of the RNA from BLH-1, *de novo* sequence assembly, homology searches against reference viruses in the database, and Sanger sequencing of the RT-PCR amplicons used for virus confirmation.

RESULTS

Transcriptomic Identification of Mycoviruses Infecting the *S. rolfsii* Strain BLH-1

Two high-throughput sequencing libraries were constructed and sequenced on the Illumina MiSeq 2000/2500 platform, producing approximately 3.6 to 4.7 $\times$ 10^7 paired-end reads with lengths of 300 nt. Raw reads were cleaned and *de novo* assembled into contigs using Trinity. All resulting contigs were compared to the *S. rolfsii* reference genome. BLAST searches of the remaining contigs against the NCBI viral database revealed the presence of viral sequences representing partial genomic segments of several distinct mycoviruses. The predicted amino acid sequences of the putative viral genomes showed significant sequence identity with previously described viruses from several distinct lineages, including the families Fusariviridae and *Hypoviridae*, the "alphavirus-like" and "benyvirus-like" viruses and some other unassigned dsRNA mycoviruses. A list of all viruses in the viral database that showed the most BLASTx matches to the assembled provisional viruses generated in this study is shown in **Table 1**. Because most of these assembled viral sequences shared less than 50% amino acid identity with the previously described mycovirus, we suggest that they are novel viruses.

Benyvirus-Like Viral Sequences

A sequence named *Sclerotium rolfsii* beny-like virus 1 (SrBenV1), 7908 nt in length, was predicted to encode proteins showing similarity to the replicases of Benyvirus-like viruses, such as Agaricus bisporus virus 8 (AbV8), beet soil-borne mosaic virus (BsBMV), and Mangifera indica latent virus (MiLV) (**Figure 1**). BsBMV was identified as a member of the genus *Benyvirus* in the family *Benyviridae* that consists of two + ssRNA genomic segments with sizes of 6,883 nt and 4,616 nt, each of which contains one ORF encoding a polyprotein. SrBenV1 was shown to contain a larger ORF1 and a 3′ incomplete ORF2. The predicted amino acid sequence of ORF1 was similar to that of the replicases from viruses in the family *Benyviridae* and most closely related to Agaricus bisporus virus 8 (AQM49930.1) with a 45% identity. ORF2 was incomplete and had no sequence identity to any other sequences in the database. Although benyviruses often have four to five linear positive-sense ssRNAs that are 6.7, 4.6,

TABLE 1 | Assembled viral sequences in the *Sclerotium rolfsii* strain BLH-1.

Name	Accession	Sequence length	Closest relative virus (BLASTx)	Maximum Identity (%)	Genome type	Tentative virus classification	References
Sclerotium rolfsiii beny-like virus 1(SrBenV1)	MH766487	7,865	Agaricus bisporus virus 8	30	+ssRNA	Benyvirus-like	NP_612601.1
Sclerotium rolfsiii alphavirus-like virus 1 (SraLV1)	MH766488	7,550	*Sclerotinia sclerotiorum* RNA virus L	26	+ssRNA	"Alphavirus-like" supergroup	ACE88957.1
Sclerotium rolfsiii alphavirus-like virus 2 (SraLV2)	MH766489	7,591	*Sclerotinia sclerotiorum* RNA virus L	26	+ssRNA	"Alphavirus-like" supergroup	ACE88957.1
Sclerotium rolfsiii alphavirus-like virus 3 (SraLV3)	MH766490	7,888	*Sclerotinia sclerotiorum* RNA virus L	24	+ssRNA	"Alphavirus-like" supergroup	ACE88957.1
Sclerotium rolfsiii fusarivirus 1 (SrFV1)	MH766491	7,301	Agaricus bisporus virus 10	42	+ssRNA	Fusariviridae	YP_009182158.1
Sclerotium rolfsiii fusarivirus 2 (SrFV2)	MH766492	7,281	Agaricus bisporus virus 10	40	+ssRNA	Fusariviridae	YP_009052456.1
Sclerotium rolfsiii hypovirus 1 (SrHV1)	KU885931.1	16,050	*Sclerotinia sclerotiorum* hypovirus 2	57	+ssRNA	Hypoviridae	AHE13861.1
Sclerotium rolfsiii hypovirus 2 (SrHV2)	MH766497	11,010	Ceratobasidium hypovirus A	26	+ssRNA	Hypoviridae	AOX47536.1
Sclerotium rolfsiii hypovirus 3 (SrHV3)	MH766498	10,739	Ceratobasidium hypovirus A	24	+ssRNA	Hypoviridae	AOX47536.1
Sclerotium rolfsiii hypovirus 4 (SrHV4)	MH766499	11,035	Ceratobasidium hypovirus A	25	+ssRNA	Hypoviridae	AOX47536.1
Sclerotium rolfsiii hypovirus 5(SrHV5)	MH766500	10,758	Ceratobasidium hypovirus A	25	+ssRNA	Hypoviridae	AOX47536.1
Sclerotium rolfsiii hypovirus 6 (SrHV6)	MH766501	7,382	Beihai sipunculid worm virus 6	24	+ssRNA	Hypoviridae	YP_009333562.1
Sclerotium rolfsiii hypovirus 7 (SrHV7)	MH766502	10,961	Ceratobasidium hypovirus A	25	+ssRNA	Hypoviridae	AOX47536.1
Sclerotium rolfsiii hypovirus 8 (SrHV8)	MH766503	12,791	Cryphonectria hypovirus 1	26	+ssRNA	Hypoviridae	ATZ76097.1
Sclerotium rolfsiii ourmia-like virus 1 (SrOLV1)	MH766504	443	Magnaporthe oryzae ourmia-like virus	42	+ssRNA	Ourmiavirus	SBQ28480.1
Sclerotium rolfsiii endornavirus 1 (SrEV1)	MH766493	12,081	*Sclerotinia sclerotiorum* endornavirus 2	25	+ssRNA	Endornaviridae	AND83000.1
Sclerotium rolfsii RNA virus 1 (SrRV1)	MH766494	6,720	Rosellinia necatrix fusagravirus 2	34	dsRNA	"Fusagraviridae"	BBB86783.1
Sclerotium rolfsii RNA virus 2 (SrRV2)	MH766495	6,182	Phlebiopsis gigantea mycovirus dsRNA 2	37	dsRNA	"Fusagraviridae"	CAJ34335.2
Sclerotium rolfsii mycovirus dsRNA 1 (SrMYV1)	KU885933.1	10,173	Phlebiopsis gigantea mycovirus dsRNA 1	51	dsRNA	Unclassified	YP_003541123.1
Sclerotium rolfsiii unassigned dsRNA virus 1 (SrURV1)	MH766505	1,910	Heterobasidion RNA virus 6	46	dsRNA	Unclassified	AHA82552.1
Sclerotium rolfsiii unassigned dsRNA virus 1 (SrURV2)	MH766506	1,958	Heterobasidion RNA virus 6	57	dsRNA	Unclassified	AHA82552.1

1.8, 1.4, and 1.3 kb in size, with the first RNA encoding the RdRp (Gilmer et al., 2017), in this study, only the RdRp-encoded RNA1 was identified. Phylogenetic analysis of the SrBenV1 replicase was conducted and revealed that SrBenV1 was clustered in the family *Benyviridae*. These results showed that SrBenV1 belongs to the genome of a new viral species in the family *Benyviridae*. Based on the genome sizes of *Benyviridae* family members, we estimate that the SrBenV1 viral sequence covers approximately more than 90% of RNA1.

Alphavirus-Like Viral Sequences

BLASTx searches of the predicted amino acid sequences of three viral sequences (7,550, 7,591, and 7,888 nt in length) showed similarity to products encoded by alphavirus-like

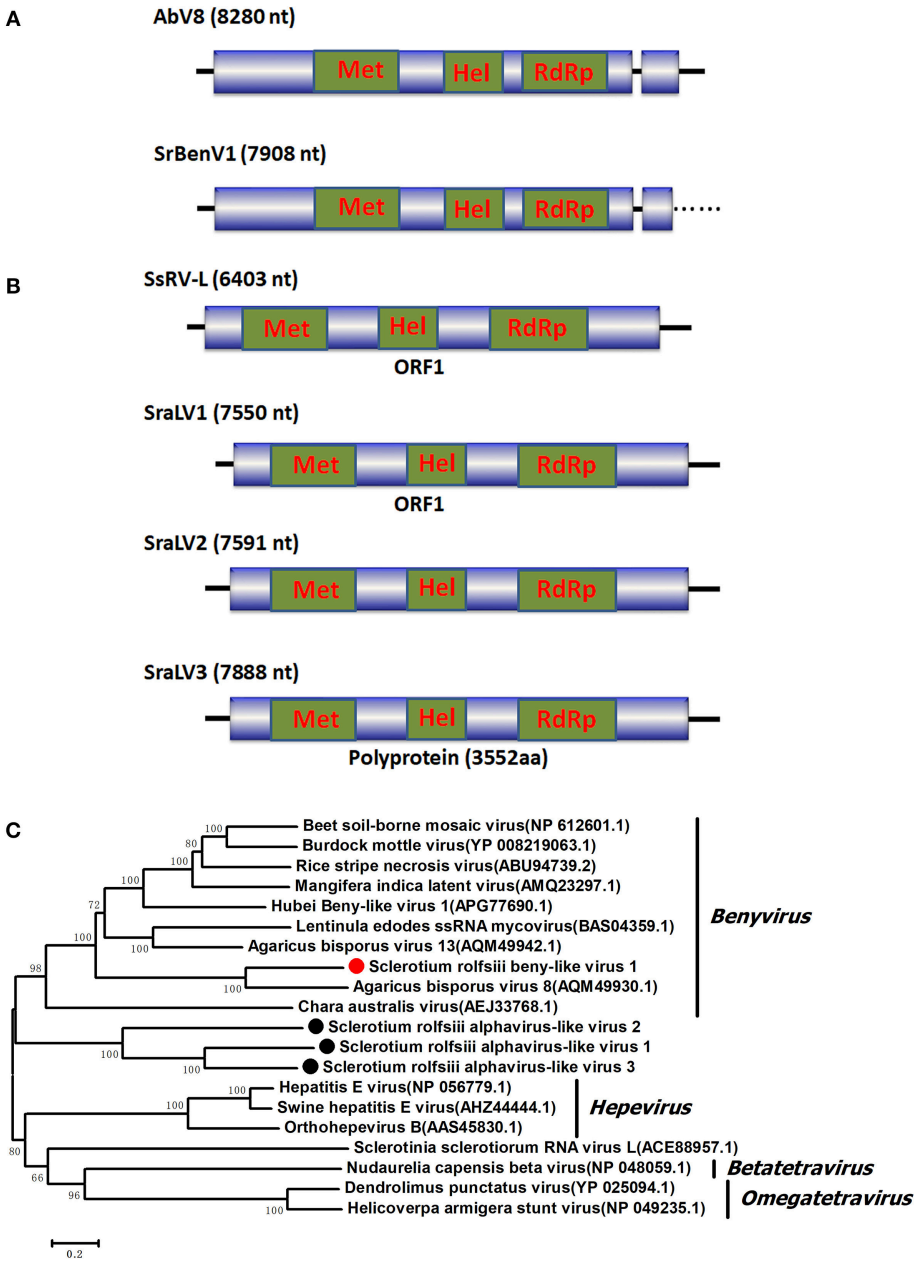

FIGURE 1 | Genomic organization and phylogenetic analysis of the *Benyvirus*-like and Alphavirus-like viral sequences and **(A)** Diagrammatic representations of the predicted genomic organization of SrBenV1 showing the presence of a large 5′ open reading frames (ORF) and a 3′ incomplete ORF, comparisons with those of related AbV8. **(B)** Genome organizations of the *Alphavirus*-like viral sequences, SraLV1, SraLV2, SraLV3, and the AbV8 which related to these containing a single large ORF. **(C)** Phylogenetic analysis of the SrBenV1, SraLV1, SraLV2, and SraLV3 based on amino acid alignments of the replicase encoded protein of the four viruses and other *Benyvirus* and *Alphavirus* viruses related to these. Phylogenetic tree was constructed by Neighbor-Joining algorithm using MEGA6, with a 1000 bootstrap replications. The percentage of bootstrap values supporting the branches in phylogenetic trees were indicated on the nodes. The genetic distance was represented by the scale bar of 0.2 amino acid substitutions per site. The novel virus SrBenV1, SraLV1, SraLV2, and SraLV3 were indicated by red dots. Names and database accession numbers of other related viruses analyzed were indicated in the tree.

+ssRNA viruses, such as *Sclerotinia sclerotiorum* RNA virus L (SsRV-L), bat hepevirus (BHV), and hepatitis E virus (HEV), with identities ranging from 25 to 26%. SsRv-L is a +ssRNA virus with a 6,403 nt genome containing a single ORF that encodes a polyprotein with three domains: viral methyltransferase (pfam0l660), viral_helicase l (pfam0 l443), and RdRP (RdRp_2, pfam00978) (Liu et al., 2009). SsRv-L was most closely related to an HEV belonging to the alphavirus-like supergroup. A conserved domain search revealed that the three viral sequences also contained these three conserved domains, indicating that

they might represent novel +ssRNA mycoviruses belonging to a virus taxonomic unit that is closely related to *Alphavirus*. We named the three virus sequences *Sclerotium rolfsii* alphavirus-like virus 1 (SraLV1), *Sclerotium rolfsii* alphavirus-like virus 2 (SraLV2) and *Sclerotium rolfsii* alphavirus-like virus 3 (SraLV3) (**Figure 1**).

Sequences Related to Fusariviridae

Two RNA sequences showed similarity to members of the family Fusariviridae, the two viral sequences of *Sclerotium rolfsii* fusarivirus 1 (SrFV1, 7301 nt) and *Sclerotium rolfsii* fusarivirus 2 (SrFV2, 7281 nt) (**Figure 2**). Fusariviridae is a new, recently proposed + ssRNA family comprising members that typically have 6 to 8 kbp genomes, with one larger ORF encoding putative polyproteins of replicases and one to three smaller ORFs encoding hypothetical proteins (Zhang et al., 2014). Both SrFV1 and SrFV2 contained two ORFs (ORF1 and ORF2). The ORF1 of each virus encoded polyproteins possessing conserved domains of RdRp (RdRp_1, cd01699) and Hel (helicase, cd00079), with aa identities ranging from 31 to 42%, and corresponded to proteins encoded by members of the Fusariviridae family, including Agaricus bisporus virus 10 (AbV10), Agaricus bisporus virus 11 (AbV11), *Fusarium graminearum* dsRNA mycovirus-1 (FgV1), Pleospora typhicola fusarivirus 1 (PtFV1), and Rosellinia necatrix fusarivirus 1 (RnFV1). Phylogenetic analysis based on ORF1 indicated that consistent with the homology search, SrFV1 and SrFV2 were clustered in the fusarivirus clade. Considering the genome organization and genome sizes, the two viruses likely represent the nearly complete genomes of novel members of the Fusariviridae family.

Sequences Related to *Hypoviridae*

A viral sequence 16,050 bp in length was identified. The predicted amino acid sequences of the viral genome were similar to those of viruses in the family *Hypoviridae*, with *Sclerotinia sclerotiorum* hypovirus 2 (SsHV2) being the best match at 57% identity (**Figure 2**). Viruses in the *Hypoviridae* family consist of +ssRNA genomes that range in size from 9 to 13 kb and contain one or two ORFs (Suzuki et al., 2018). Members of this family are currently grouped into two genera, *Alphahypovirus* and *Betahypovirus* (Yaegashi et al., 2012; Hu et al., 2014; Khalifa and Pearson, 2014). The CHV1 and CHV2 from *C. parasitica* were assigned to the genus *Alphahypovirus*, and their genomes consist of two ORFs. In addition to *Alphahypovirus* and *Betahypovirus*, a third distinct lineage and genus, named *Gamahypovirus,* was recently proposed with SsHV2/5472 and its conspecific SsHV2/SX247 as a prototype (Hu et al., 2014; Khalifa and Pearson, 2014). Based on the genome size and sequence similarity, we suggest that SrHV1 is a new member of the *Gamahypovirus* genus in the family *Hypoviridae*. Seven possible hypovirus-like viral sequences were obtained and showed sequence identities to viruses in the family *Hypoviridae*. Less sequence similarity was observed between these sequences, and these viral sequences might thus be different hypoviruses, designated as Sclerotinia rolfsii hypovirus 2 to Sclerotinia rolfsii hypovirus 8. These viruses were predicted to encode proteins similar to those encoded by Macrophomina phaseolina hypovirus 1 (MpHV1) and CHV1, with identities ranging from 25 to 26%. Hence, diverse infectious hypoviruses belonging to *Gamahypovirus* and *Alphahypovirus* might exist.

Ourmiavirus-Like Viral Sequences

One ourmiavirus-like sequence was identified, which was 443 bp in length and named *Sclerotium rolfsii* ourmia-like virus 1 (SrOLV1). A BLASTx search showed that this virus was similar to ourmiavirus-like mycoviruses, including Magnaporthe oryzae ourmia-like virus (MoOLV) and Rhizoctonia solani ourmia-like virus 1 RNA 1, with identities of 42 and 39%, respectively. Ourmiavirus genomes have three ssRNA segments of 2.8, 1.1, and 0.9 kb, with the largest RNA segment encoding the viral replicase, and the smallest segment encompassing the coat protein (Turina et al., 2017). Although the replicases of mitoviruses and ourmiaviruses are all phylogenetically related, ourmiaviruses are considered to replicate in the cytoplasm instead of mitochondria (Crivelli et al., 2011). A few ourmiavirus-like mycoviruses have previously been discovered from *Sclerotinia sclerotiorum*, *Rhizoctonia solani* (Marzano and Domier, 2016), *Magnaporthe oryzae* (Illana et al., 2017), and *Botrytis* (Donaire et al., 2016). Sequence similarity revealed that the oourmiavirus-like mycovirus SrOLV1 could also infect *S. rolfsii.*

Endornaviridae-Related Sequences

Several RNA sequences showed similarity to members of the family *Endornaviridae*. Viruses in the *Endornaviridae* family have linear ssRNA genomes that range in length from approximately 10 kb to more than 17 kb and contain an ORF encoding a single long polyprotein. The polyprotein encoded by endornavirus often includes conserved domains, such as viral RNA helicases and RdRps (Ghabrial et al., 2015). The gaps between the endornavirus-like sequences were filled by RT-PCR and assembled as an RNA sequence. In addition, the terminal genomic sequences were determined by RLM-RACE. We designated this virus as *Sclerotium rolfsii* endornavirus 1 (SrEV1) (**Figure 3**). The full-length SrEV1 genome was 12081 base, containing a single ORF encoding a 3997 aa polyprotein. Blastp analysis showed that this putative protein showed low sequence identity to the polyprotein of endornavirus, with *Sclerotinia sclerotiorum* endornavirus 2 being the best match at a 25% aa identity. Conserved domain searches revealed that this polyprotein contained the conserved domains of viral methyltransferase (MTR), putative DEXDc, viral helicase (Hel) and RdRp. Consistent with the homology search, phylogenetic analysis based on the conserved RdRp domain suggested that SrEV1 is a new putative species in the family *Endornaviridae*.

Sequences Related to "Fusagraviridae"

Four viral sequences were associated with SsNLV1-like group mycoviruses, such as *Sclerotinia sclerotiorum* dsRNA mycovirus-L (SsNsV-L), Phlebiopsis gigantea mycovirus dsRNA 2 (PgV2), Macrophomina phaseolina dsRNA virus 2, Botrytis cinerea RNA virus 1 and other viruses that could be grouped into the recently proposed family Fusagraviridae (**Figure 4**). The gaps between the contigs were filled by RT-PCR, resulting in the assembly

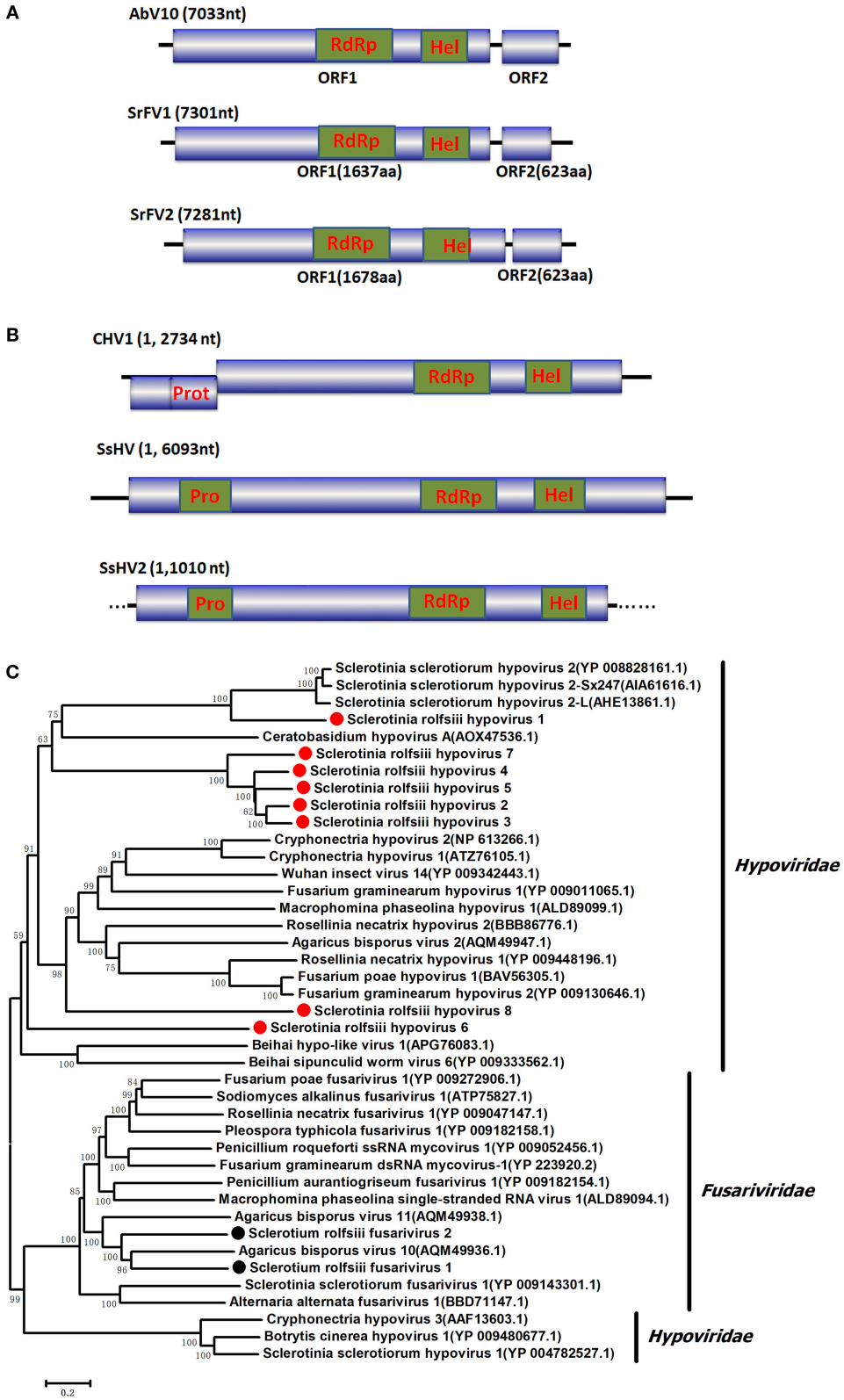

FIGURE 2 | Genome organization and phylogeny of the viruses that similar to members of the *Fusariviriade* and *Hypoviridae* family. **(A)** Comparisons of the genome organizations of SrFV11 and SrFV2 and comparison with that of related virus AbV8 in the *Fusariviriade* family. **(B)** Genome organization of the hypoviruses, exampled as the SrHV1, SrHV2, and CHV1. **(C)** The predicted amino acid sequences of the RdRps were aligned and subjected for phylogenetic tree construction using the method described in **Figure 1**.

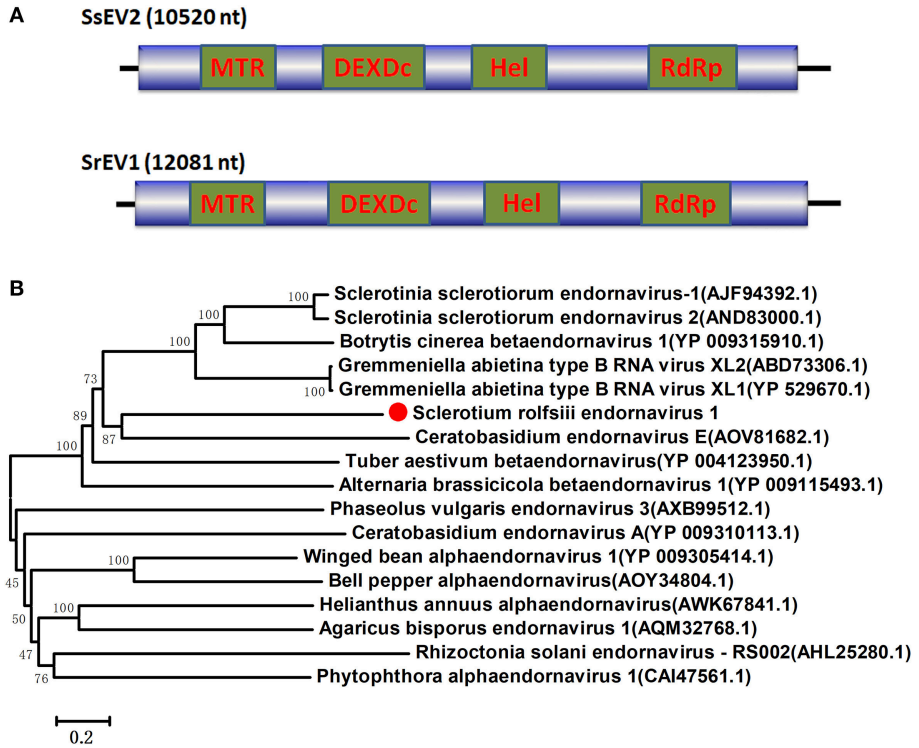

FIGURE 3 | Genome organizations and Neighbor-Joining tree of the novel virus relating to confirmed and proposed members of the *Endornaviridae*. **(A)** Comparisons of the genomic organizations of the novel *Sclerotium rolfsiii* infecting SrEV1 and the identified member SsEV1 of the *Endornaviridae* family. The SrEV1 was completely sequenced and predicted to harbor a single larger ORF containing domains of viral methyltransferase (MTR), putative DEXDc, viral helicase (Hel) and RdRp, which were indicated in the ORF box. **(B)** Phylogenetic tree depicting the relationships of SrEV1 with other *Endornaviuses* were generated using the method described in **Figure 1**.

of two RNA sequences, *Sclerotium rolfsii* RNA virus 1 (SrRV1) and *Sclerotium rolfsii* RNA virus 2 (SrRV2), with lengths of 6,720 bp and 6,182 bp, respectively (dsRNA1 and dsRNA2). BLASTx searches showed that the partially predicted amino acid sequences of the two dsRNAs were similar to those of viruses in the proposed family Fusagraviridae. The sequence of SrRV1 contained two ORFs. The predicted amino acid sequence of SrRV1 ORF2 was similar to that of the RdRps of Rosellinia necatrix fusagravirus 2 at a 35% identity. SrRV2 also contained two ORFs, ORF1 and an incomplete ORF2. The predicted amino acid sequence of SrRV2 ORF2 showed 37% identity to that of the Phlebiopsis gigantea mycovirus dsRNA 2 encoding RdRp (CAJ34335.2). Hence, SrRV1 and SrRV2 likely represent new members of the Fusagraviridae family.

Phlegivirus-Related Sequence

Several RNA sequences showed similarity to unassigned dsRNA mycoviruses, such as Phlebiopsis gigantea mycovirus dsRNA 1 (PgV1), Thelephora terrestris virus 1 (TtV1), and Lentinula edodes mycovirus HKB (Lev-HKB). The gap between the contigs was filled by RT-PCR, and the 5′ terminal sequence was also determined by RACE. All the sequences were assembled as a 10,713 bp RNA sequence, named *Sclerotium rolfsii* mycovirus dsRNA 1 (SrMYV1), as previously described (**Figure 4**). SrMYV1 contained a complete ORF (ORF1) encoding a putative protein with 1634 aa at the 5′-proximal end and an incomplete ORF (ORF2) that encoded 1243 aa at the 3′-proximal end. A BLASTp search showed that ORF1 was 38% identical to the hypothetical protein, and ORF2 was 51% identical to the RpRd of PgV1. PgV1 is an unassigned dsRNA virus with a 11,563 bp genome that contains two major ORFs encoding the hypothetical proteins and RdRp. The organization of the predicted SrRV1 ORFs was similar to that of a Lev-HKB clade including PgV1, TtV1, and Lev-HKB, and the SrRV1 sequence (10,713 bp) might represent a nearly complete genome.

Putative Double-Stranded RNA Viruses

Two viral sequences that showed similarity to Heterobasidion RNA virus 6 (HetRV6) were identified and designated as *Sclerotium rolfsii* unassigned dsRNA virus 1 (SrURV1) and *Sclerotium rolfsii* unassigned dsRNA virus 2 (SrURV2). HetRV6 is an unassigned dsRNA virus composed of a single genomic band of approximately 2 kbp encoding a putative viral RNA polymerase that is distantly related to Curvularia thermal tolerance virus (CThTV) and Fusarium graminearum virus 4 (FgV4) (Vainio et al., 2012). However, the genomes of CThTV and FgV4 contain two dsRNA segments (Márquez et al., 2007; Yu et al., 2009). Both SrURV1 and SrURV2 had incomplete ORFs encoding proteins that were closely related to the RdRp of HeRV6 (46 and 57% identity, respectively). Hence, the two

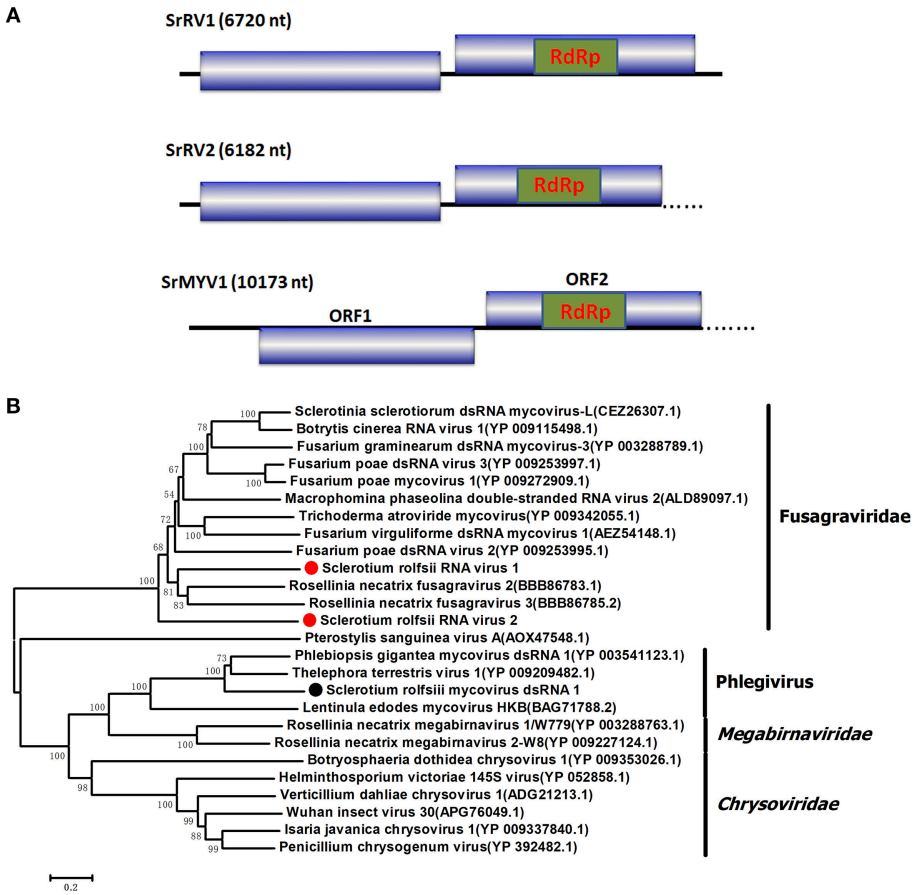

FIGURE 4 | Schematic representation of the genome and phylogenetic analysis of two novel members of the family Fusagraviridae, SrRV1 and SrRV2, and a *Phlegivirus*-related virus, SrMYV1. **(A)** Genome organization of SrRV1, SrRV2, and SrMYV1. The three viruses were all predicted to contain two ORFs, ORF1, and ORF2, with their ORF1 encoded unknown proteins and ORF2 encoded the RdRp. **(B)** phylogenetic analysis illustrating the evolutionary classification of these three viruses was conducted using the **Figure 1** described method.

viruses might represent unassigned viruses related to CThTV-like viruses.

Viral Genome Sequence Validation

We used RT-PCR and Sanger sequencing to confirm the origins of these assembled mycoviral sequences. When PCR amplification was performed using reverse transcription products synthesized from the total RNA of the fungal strain BLH-1 as templates, products of corresponding size were obtained and matched to these viruses (**Figure 5**). However, when we performed PCR using DNA extracted from the fungal strain BLH-1 for all the assembled viral sequences, no products were obtained, indicating that the viral sequences identified were indeed derived from exogenous mycoviruses infecting BLH-1.

Full-Length Genomic Organization of SrHV1

In our previous study, we found that the host fungus BLH-1 was a hypovirulent strain deficient in sclerotium production. As mentioned above, the nearly complete genome of SrHV1 was most closely related to the *S. sclerotiorum*-infecting hypoviruses SsHV2/SX247 and SsHV2/5472 (Hu et al., 2014; Khalifa and Pearson, 2014), which are responsible for the hypovirulence and deficient sclerotium production in the host fungus. Thus, in this study, we further verified and obtained the full-length genomic sequence of SrHV1 by RT-PCR using primers based on the assembled sequences and ligase-mediated terminal amplification method. The sequence was deposited in GenBank under accession number KU885931.1.

The complete genomic sequence of SrHV1 was determined to be 16093 nt long excluding the poly (A) tail at the 3' terminus. In comparison, the nearly complete genome of the high-throughput sequencing-assembled contig of SrHV1 was 16050 nt, indicating 99.61% coverage of the SrHV1 genome. SrHV1 was determined to contain a 13,815 nt long ORF (nt positions 1185 to 14,999) encoding a 513.37 kDa polyprotein of 4604 aa residues that was predicted to contain the domains of a papain-like cysteine protease (Pro), RdRp and helicase (Hel), like reported for SsHV2/5472 and SsHV2/sx247. The 5′-UTR (untranslated region) and 3′-UTR of SrHV1 were 1,184 and 1,094 nt, respectively. The genomic organization of SrHV1 is depicted in **Figure 2B**.

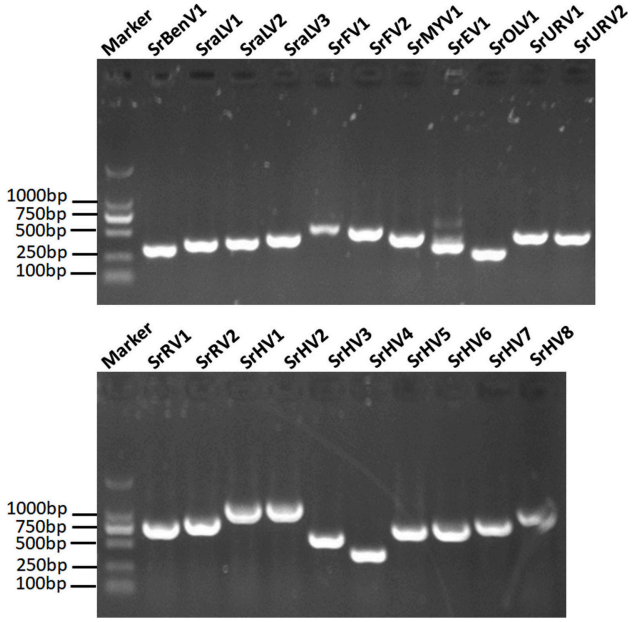

FIGURE 5 | RT-PCR validation of the identified mycoviral sequences. The final assembled viral sequences were confirmed by RT-PCR using the primers that designed based on the obtained viral contigs and the total RNA template extracted from the BLH-1 strain of *S. rolfsii.* The marker was in 2,000 bp Ladder, and the other lanes indicated the abbreviates of these detected viruses which were detailed in the **Table 1**.

Molecular Characterization and Phylogeny of SrHV1

A homology search using the polyprotein aa sequences of SrHV1 showed significant identity with polyproteins encoded by members of the family *Hypoviridae*, with SsHV2 being the best match at 57% (coverage: 63%; E value: 0), followed by CHV2 (accession no. NP_613266.1; coverage: 63%; E value: 4e-52; identity: 23%), CHV1 (accession no. NP_613266.1; coverage: 49%; E value: 1e-53; identity: 23%) and Fusarium graminearum hypovirus 1 (FgHV1) (accession no. YP_009011065.1; coverage: 45%; E value: 1e-34; identity: 23%). Based on its sequence similarity to hypoviruses, we suggest that SrHV1 is a ssRNA mycovirus in the family *Hypoviridae*.

At the N-terminal end of the polyprotein, a putative Pro domain was detected. In this domain, two aa residues, Cys and His, which are necessary for the autoproteolytic activity of the polyprotein and strictly conserved among other reported hypoviruses, and Gly, which is relevant to the potential cleavage site, were observed (Smart et al., 1999; Yuan and Hillman, 2001). An RdRp domain containing the highly conserved aa sequence motifs that are characteristic of hypovirus RdRp domains was detected at aa positions 3101 to 3418. The RdRp of SrHV1 had the highest aa identity (74%) to that of SsHV2 (coverage: 99%; E value: 3e-147). Based on multiple alignments of the RdRp aa sequences of *Hypoviridae* members, a phylogenetic tree was constructed, and SrHV1 clearly clustered with SsHV2-SX-247, forming a branch distinct from members of *Alphahypovirus*. At aa positions 3872 to 4189, downstream from the RdRp domain, a Hel domain was identified. As previously described in other hypoviruses, the Hel domain of SrHV1 also contained three characteristic motifs of the Hel superfamily 2 (Hall and Matson, 1999): GKST, DExH, and QRxGR. The Hel domain of SrHV1 was most closely related to SsHV2, with a 74% aa identity. In addition, the SrHV1 Hel domain also showed aa identities of 27 to 30% to the Hel domains of other *Alphahypovirus* members. Phylogenetic analysis based on the Hel domains revealed that SrHV1 was grouped with SsHV2-SX-247 and SsHV1L, a clade related to but distinctly branched from members in the genera *Alphahypovirus* (**Figure S1**).

Small RNA Profiles of SrHV1 and SrEV1

To survey the presence and mechanism of antiviral immune response in *S. rolfsii* and to confirm that these putative viruses genuinely infect the host fungus, we assessed the presence of antiviral small RNAs in this virus-infected fungal strain. Because SrHV1 might be the candidate causal agent of BLH-1 hypovirulence and its genome has been completely sequenced, we focused on SrHV1. A small RNA library was generated from the *S. rolfsii* strain BLH-1 and subjected to deep-sequencing of small RNAs (sRNA) on the Illumina platform, resulting in 33 million reads.

After filtering according to length, the remaining sRNA reads were mapped to the *S. rolfsii* genome, and the unmapped reads were then aligned against the SrHV1 and SrEV1 genomes. Abundant small RNAs were matched to the target genome. These small RNAs were mainly distributed from 19 to 24 nt, with a peak at 21 nt, and exhibited characteristics typical of Dicer-produced virus derived small interfering RNAs (vsiRNAs), which are produced from dsRNA intermediates upon binding to Dicer (Li et al., 2013) (**Figure 6A**).

Because gene silencing is mediated by argonaute proteins, which bind to small RNAs to induce the degradation of RNAs that complement small RNAs, the composition of the small RNA 5′ nucleotide is preferred by special argonautes (Wilson and Doudna, 2013). We found a clear preference for the U base at the 5′ nucleotide residues of both the SrHV1 and SrEV1 vsiRNAs of all sizes, especially for vsiRNAs of sizes 20-, 21- and 22-nt (**Figure 6B**). The 5′ nucleotide preference of these vsiRNAs was consistent with the high abundance of U bases in the SrHV1 and SrEV1 genome.

When exploring the polar distribution of SrHV1 and SrEV1-derived vsiRNAs, we found that the vsiRNAs in sizes of 21 and 22 nts originated from SrHV1 and SrEV1 were heterogeneously distributed along the sense and antisense strands of the virus genomes. Some regions of hotspots in, which produced more vsiRNAs, were located in the 5′ and middle genome regions of SrHV1 and in the 5′ region for SrEV1 (**Figure 6C**).

Small RNA data indicated that the vsiRNAs were generated from the genomes of SrHV1 and SrEV1 by Dicer, acting on dsRNA replication intermediates, and were bound by argonaute proteins; thus, we can conclude that the two viruses were targeted by the host gene silencing mechanism, an antiviral immune response exhibited by many fungi.

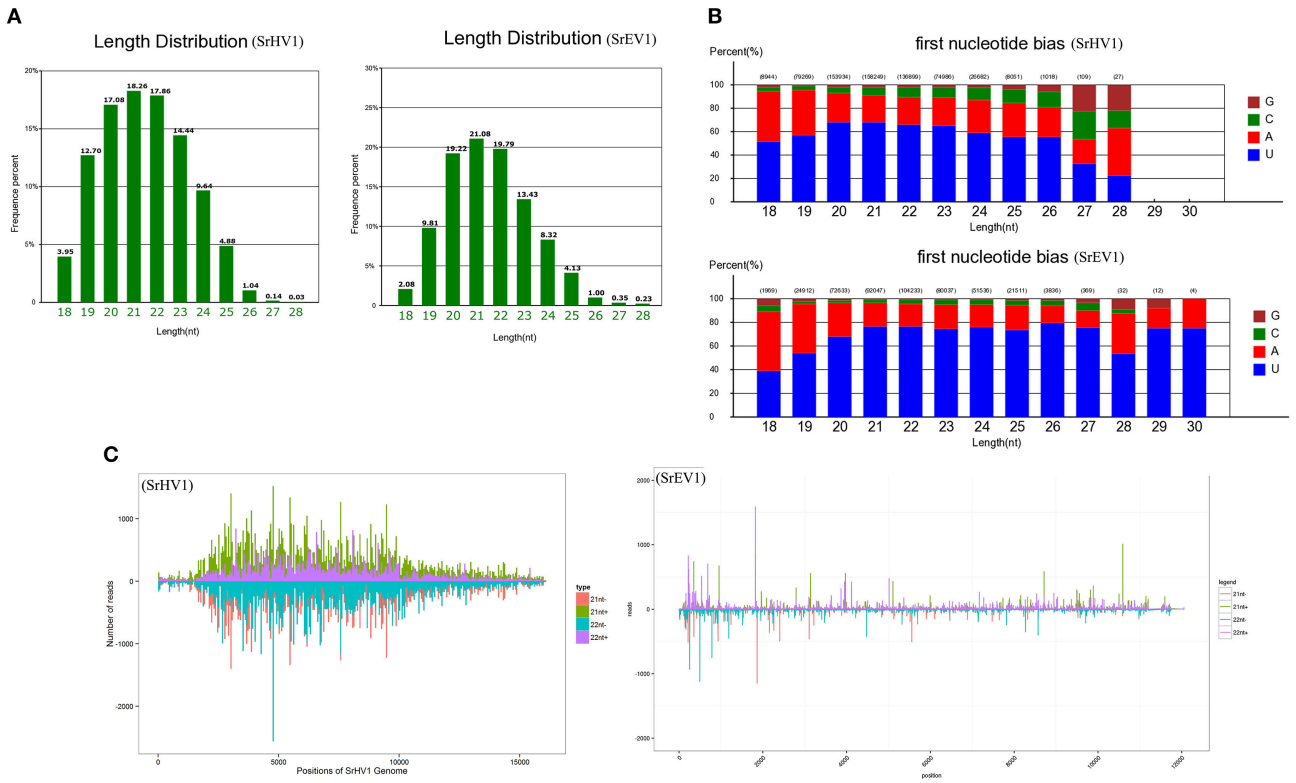

FIGURE 6 | SrHV1 and SrEV1 derived small RNAs analysis. **(A)** Size distribution and abundance of small RNAs matching the SrHV1 and SrEV1 genomes. **(B)** 5′-terminal nucleotide composition among the SrHV1 and SrEV1-derived vsiRNAs. The x-axis represents the length distribution, and the y-axis shows the percentages of nucleotides constitute of G/C/A/U in the 5′-terminal of the vsiRNAs. **(C)** The vsiRNA profiles distribution among the SrHV1 and SrEV1. The vsiRNAs derived from the positive and negative strand of the viral genome were indicated above and below the line, respectively. For SrHV1, the 21-nt vsiRNAs arising from the genomic and antigenomic strands were shown in green and red bars, respectively. The 22-nt vsiRNAs matching the genomic and antigenomic strand were represented by purple and blue, respectively. For SrEV1, the 21-nt and 22-nt vsiRNAs arising from the genomic and antigenomic strands were indicated by green and purple bars, red and blue bars, respectively. The x-axis indicated the length of the SrHV1 and SrEV1 genomes, respectively. While the y-axis in SrHV1 and SrEV1 separately represented numbers of reads matching to the genomic and antigenomic sequences of the two viruses.

DISCUSSION

In this study, we characterized a complex virome from a hypovirulent *S. rolfsii* strain and identified diverse viral segments using high-throughput transcriptome sequencing. Some viruses discovered in our analysis were nearly full-length. These detected viruses might belong to viral species within the families of *Benyviridae*, *Endornaviridae*, Fusariviridae, *Hypoviridae*, and the proposed family "Fusagraviridae" and show similarities to other unclassified LeV-HKB-like and CThTV-like dsRNA viruses and unclassified alphavirus-like and ourmiavirus-like +ssRNA viruses. We conducted RT-PCR, genomic PCR and Sanger sequencing analyses using specific primers based on the obtained fragments to confirm the origins of our viral sequences. Positive amplicons were produced from only RNAs extracted from the *S. rolfsii* strain by RT-PCR but not by genomic PCR, confirming that the viral sequences represented non-integrated RNA virus sequences. To the best of our knowledge, this is the first report of a comprehensive analysis of viral diversity in a hypovirulent *S. rolfsii* strain. Thus, our results represent a step forward in exploring *S. rolfsii* mycoviruses and provide insight into screening the mycovirus potential of *S. rolfsii* controls and understanding the mechanism of *S. rolfsii* hypovirulence.

Among the identified viruses, SrHV1 was the fully cloned putative hypovirus relating to members of the family *Hypoviridae*. SrHV1 shared the highest sequence identity to the previously reported virus SsHV2, which was shown to induce hypovirulence of the plant pathogenic fungus *S. sclerotiorum*. SrHV1 shared the same genomic organization, genome size and phylogenetic grouping as two SsHV2 strains but was distinct from other members of the *Hypoviridae* family. Currently, two genera, *Alphahypovirus* and *Betahypovirus*, which range in size from 9 to 13 kb, are classified within the family *Hypoviridae*. These two genera exhibit several differences in terms of their genome size, organization and gene function, as alphahypoviruses range in genome size from 12.5 to 13 kb and contain two ORFs, whereas betahypoviruses have a smaller genome size of 9.1–10.4 kb and consist of a single large ORF that encodes a polyprotein. A UDP-glucosyltransferase (UGT) domain is present in the proteins encoded by betahypoviruses, while alphahypoviruses lack this domain. Hu et al. (2014) proposed that in addition to *Alphahypovirus* and *Betahypovirus*,

a third genus, Gammahypovirus, should be established to accommodate SsHV2. Here, the identification of SrHV1, which should be classified into the same genus as SsHV2, further validated the rationality to establish a Gammahypovirus genus in the *Hypoviridae* family and indicated the diversity of viruses in the *Hypoviridae* family. It is worth noting that the SsHV2/SX247 alone could likely leads to hypovirulence and complete loss of sclerotia production of the *S. sclerotiorum* host (Hu et al., 2014); thus, we hypothesize that SrHV1 induces hypovirulence in this *S. rolfsii* strain. However, as described in this study, the *S. rolfsii* strain BLH-1 was coinfected by a diverse range of mycoviruses, and we could not exclude the possibility that other mycoviruses also induced host hypovirulence or acted together with SrHV1. To elucidate the cause-and-effect relationships between individual mycoviruses and their hosts and the possible interactions between these coinfected viruses, further research with respect to the construction of full-length infectious cDNA clones and associated experiments is needed.

Studies on mycoviruses using high-throughput sequencing have recently been efficiently applied to the discovery of fungal viruses (Bartholomäus et al., 2016; Marzano and Domier, 2016; Marzano et al., 2016; Deakin et al., 2017; Mu et al., 2018). In contrast to other dsRNA extraction and cloning methods, this approach can provide viral information for a diverse set of viruses belonging to different taxa regardless of their genome types and viral titers. For example, by deep sequencing, 18 phylogenetically distinct RNA viruses and 8 ORFans were identified from the mushroom fruitbodies of *Agaricus bisporus* Deakin et al. (2017). Marzano and Domier (2016) obtained virus contigs from a collection of fungal species from *Colletotrichum truncatum*, *Macrophomina phaseolina*, *Diaporthe longicolla*, *Rhizoctonia solani*, and Sclerotinia sclerotiorum using RNA_Seq analysis. Their analysis also revealed novel types of mycoviruses in the families *Benyviridae*, *Ophioviridae*, and *Virgaviridae*. Recently, deep sequencing was also used to identify the diversity of mycoviruses within a fungal species collected from diverse geographic regions, potentially providing overall knowledge of viral diversity, evolution and ecology on a species scale (Arjona-Lopez et al., 2018; Mu et al., 2018). In addition, when high-throughput sequencing is used for virus detection, the enrichment step, which might bias detection, is not necessary. High-throughput sequencing was used to detect mycoviruses on the phyllosphere and the arbuscular mycorrhizal fungi colonized in the roots (Ezawa et al., 2015; Marzano and Domier, 2016). By deep sequencing extracted dsRNAs, different mycoviral species were shown to coinfect a *Fusarium poae* fungal strain (Osaki et al., 2016), as illustrated in other fungi, such as *Rhizoctonia solani* (Bartholomäus et al., 2016). These studies indicated that the known mycoviruses characterized thus far might represent only the tip of the iceberg of all mycoviruses in nature, and some mycoviruses might have been overlooked by traditional PCR-based detection approaches. Because screening viral sequences principally depends on their homology to known viruses in the database, the recent explosion of viral databases that contain enormous novel viral genome information (Li et al., 2015; Shi et al., 2016) makes isolating and identifying new viruses in a larger host range and geographic distribution more feasible.

Like other eukaryotes, fungi can also use RNA interference (RNAi) as a primary defense against virus infections, as described commonly in *Cryphonectria parasitica* infected by the CHV1 (Nuss, 2011). When the viral genome is targeted by the host RNAi mechanism, an overlapping vsiRNA population derived from the virus can be produced. Like in plant and animal hosts, 21 nt sRNAs represent the primary class size of vsiRNA populations in mycovirus-infected fungi (Yaegashi et al., 2016; Donaire and Ayllón, 2017). For example, the Magnaporthe oryzae virus 2 (MoV2) infection in Magnaporthe oryzae results in the production of 21 nt vsiRNAs (Himeno et al., 2010). In our study, the sizes of most vsiRNAs that mapped to the SrHV1 and SrEV1 genomes ranged from 19 to 24 nt. The 21 nt vsiRNA with 5′ U bias was the most abundant vsiRNA species, which was in accordance with previous reports in fungi and suggested that SrHV1 and SrEV1 are targeted and processed by the host RNAi. The similarities in pattern of vsiRNA composition between our tested SrHV1 and SrEV1 with some other mycoviruses and plant viruses indicated that the biogenesis of vsiRNAs in some RNA silencing pathway, in some case, is conserved among different kingdoms. Of course, different plants might have various siRNA biosynthetic pathways. It has been suggested that DCL4-dependent 21-nt vsiRNA synthesis, is the first antiviral defense in Arabidopsis (Moissiard et al., 2007), whereas DCL2 often acts as a DCL4 surrogate for 22-nt vsiRNA generation (Deleris et al., 2006). The percentage of 21-nt and 22-nt vsiRNAs relies on different virus-plant host associations. Therefore, DCL4 and DCL2 should work redundantly or synergistically for systemic antiviral silencing. In fungi, RNA silencing against mycovirus infection has been fully characterized in some mycovirus/fungus systems such as in the fungus *C. parasitica*, *Colletotrichum higginsianum*, and *Fusarium graminearum* (Segers et al., 2007; Campo et al., 2016; Yu et al., 2018). In the CHV1/*C. parasitica* system, the dicer-like (dcl-2) and argonaute-like genes (agl-2) have been demonstrated to be necessary for antiviral silencing (Segers et al., 2007; Zhang and Nuss, 2008; Sun et al., 2009). However, the presence and contribution of each *S. rolfsii* Dicer protein in the biogenesis of each size class of mycovirus-derived sRNAs is unknown. The virus-derived small RNA from SrHV1 and SrEV1 showed Dicer-mediated siRNA profiles, indicating a gene silencing response of the host against these viruses. In the present study, the 5' nucleotide residues of vsiRNAs derived from SrHV1 and SrEV1 all tended to be U residues instead of A, G or C, indicating that the vsiRNAs with 5′ U might be enriched by sorting into special AGO-containing complexes after dicing. In *Arabidopsis*, different AGO proteins specially recognize the 5′ preference base of vsiRNAs (Mi et al., 2008). As reported in *N. crassa*, argonaute-like proteins (QDE-2) are biased toward associating with sRNAs with 5′ U terminal nucleotides (Lee et al., 2010). We speculate that argonaute-like proteins that are conserved in fungi and plants play a dominant role in the posttranscriptional gene silencing (PTGS) of *S. rolfsii* and other fungi.

The p29 of CHV1, a papain-like protease that shares sequence and functional similarities with the helper-component proteases (HC-Pro) of potyviruses, a symptom determinant, has been shown to act as an RNA silencing suppressor (RSS) in the fungal

host (Segers et al., 2007). Marzano et al. (2015) speculated that SsHV2 also contains a similar symptom determinant because deletions in the SsHV2L and SsHV2/5472 genome regions lead to altered sclerotia production. In our study, SrHV1 was identified as a novel member of the family *Hypoviridae*, like CHV1. In addition, the *S. rolfsii* strain BLH-1 was defective in sclerotia production, and SrHV1 showed an intimate affinity with SsHV2, both of which contain the papain-like proteinases that are closely related to the CHV1-encoded p29. We presume that SrHV1 might also have an RSS that functions to resist host antiviral defenses and determines or participates in host hypovirulence actions, such as growth, virulence, and sclerotia production. However, to validate this hypothesis, additional gene function characterization studies are needed.

MATERIALS AND METHODS

Fungal Isolates, Growth Conditions and RNA Preparation

The fungal strain BLH-1, originally isolated from a southern blight disease-infected *M. cordata* plant in the Hunan province of China, was maintained on potato dextrose agar (PDA) at 27°C. Total RNA was extracted by mycelium harvest using the RNeasy mini kit (Qiagen, Valentia, CA) and quantitatively evaluated using the NanoDrop ND-1000 spectrophotometer (NanoDrop Technologies, USA). High-quality RNAs were subjected to RNA-seq. Sequencing cDNA library was constructed from poly(A) selected total RNA, using the TruSeq^{TM} RNA Sample Prep Kit (Illumina, RS-122-2001).

Bioinformatic Analyses and Virus Genome Identification

Bioinformatics analysis of RNA-seq data was carried out using the CLC Genomic Workbench software package (CLC Bio-Qiagen, Boston, MA). Reads were *de novo* assembled with Trinity (Grabherr et al., 2011). The resulting contigs were compared to the *S. rolfsii* reference genome to subtract the host-derived sequences and then compared against the non-redundant viral reference amino acid sequence database available in NCBI using the BLASTx and tBLASTx programs. Multiple alignments of amino acid sequences were conducted using the ClustalX program (Larkin et al., 2007), and phylogenetic trees were constructed by the neighbor-joining (NJ) method using 1,000 resampling bootstraps in MEGA 6 (Tamura et al., 2013).

Viral Genome Sequence Confirmation

To confirm that the viral sequences were determined from mycoviruses infecting the fungal host rather than from sequences integrated into the host genome, RT-PCR and PCR assays were separately performed using templates of total RNA and DNA extracted from the fungal strain BLH-1 and primers designed based on the *de novo* assembled viral contigs. The amplicons were analyzed by agarose gel electrophoresis and sequenced by Sanger sequencing.

Amplification of cDNA Ends

To completely sequence the genomes of some of the mycoviruses, sequence gaps not covered by the transcriptome sequencing assembly were filled by RT-PCR amplification using designed primers based on the obtained viral sequences flanking the gaps. The 5′ and 3′ terminal sequences were elucidated using a ligase-mediated terminal amplification method as described previously (Zhong et al., 2016b). All of the PCR products were cloned into the pMD18-T vector (TaKaRa) and sequenced, and every base was determined at least three independent times.

Small RNA Deep Sequencing and Analysis

The pooled total RNA from three *S. rolfsii* strain BLH-1 replicates was extracted. The small RNAs were purified from 17% denaturing polyacrylamide gels, ligated with 5′ and 3′ adaptors and then subjected to small RNA library generation and Illumina sequencing.

After the adapter sequences and low-quality reads were removed, the data were subjected to bioinformatics analysis, and sequences 18–30 nt in length were extracted. To identify SrHV1 and SrEV1-derived vsiRNAs, the clean reads were respectively mapped to the SrHV1 and SrEV1 genomes using the BLAST search function. vsiRNA analyses, including the nucleotide size, composition of the 5′ nucleotide and polar distribution, were performed using Perl scripts and Microsoft Excel as previously described (Wang et al., 2016). The data from the raw sRNA reads were deposited in the NCBI Sequence Read Archive under accession number SRR7754484.

AUTHOR CONTRIBUTIONS

JZ and QZ: conceived and designed the experiments; JZZ and JZ: performed the experiments; JZ, BDG, and HJZ: analyzed the data; JZZ: Wrote the paper.

ACKNOWLEDGMENTS

This study is supported by Natural Science Foundation of Hunan Province, China (Grant No. 2018JJ3229) and Youth Foundation of Hunan Educational Committee (Grant no. 17B128). Scientific Research Fund of Hunan Provincial Education Department 14K045.

SUPPLEMENTARY MATERIAL

The Supplementary Material for this article can be found online at: https://www.frontiersin.org/articles/10.3389/fpls.2018.01738/full#supplementary-material

REFERENCES

Al Rwahnih, M., Daubert, S., Urbez-Torres, J. R., Cordero, F., and Rowhani, A. (2011). Deep sequencing evidence from single grapevine plants reveals a virome dominated by mycoviruses. *Arch. Virol.* 156, 397–403. doi: 10.1007/s00705-010-0869-8

Arjona-Lopez, J. M., Telengech, P., Jamal, A., Hisano, S., Kondo, H., Yelin, M. D., et al. (2018). Novel, diverse RNA viruses from Mediterranean isolates of the phytopathogenic fungus, *Rosellinia necatrix*: insights into evolutionary biology of fungal viruses. *Environ. Microbiol.* 20, 1464–1483. doi: 10.1111/1462-2920.14065

Bartholomäus, A., Wibberg, D., Winkler, A., Pühler, A., Schlüter, A., and Varrelmann, M. (2016). Deep sequencing analysis reveals the mycoviral diversity of the virome of an avirulent isolate of *Rhizoctonia solani* AG-2-2 IV. *PLoS ONE* 11:e0165965. doi: 10.1371/journal.pone.0165965

Campo, S., Gilbert, K. B., and Carrington, J. C. (2016). Small RNA-based antiviral defense in the phytopathogenic fungus *Colletotrichum higginsianum*. *PLoS Pathog.* 12:e1005640. doi: 10.1371/journal.ppat.1005640

Chiba, S., Salaipeth, L., Lin, Y. H., Sasaki, A., Kanematsu, S., and Suzuki, N. (2009). A novel bipartite double-stranded RNA mycovirus from the white root rot fungus *Rosellinia necatrix*: molecular and biological characterization, taxonomic considerations, and potential for biological control. *J. Virol.* 83, 12801–12812. doi: 10.1128/JVI.01830-09

Coetzee, B., Freeborough, M. J., Maree, H. J., Celton, J. M., Rees, D. J. G., and Burger, J. T. (2010). Deep sequencing analysis of viruses infecting grapevines: virome of a vineyard. *Virology* 400, 157–163. doi: 10.1016/j.virol.2010.01.023

Crivelli, G., Ciuffo, M., Genre, A., Masenga, V., and Turina, M. (2011). Reverse genetic analysis of Ourmiaviruses reveals the nucleolar localization of the coat protein in *Nicotiana benthamiana* and unusual requirements for virion formation. *J. Virol.* 85, 5091–5104. doi: 10.1128/JVI.02565-10

Deakin, G., Dobbs, E., Bennett, J. M., Jones, I. M., Grogan, H. M., and Burton, K. S. (2017). Multiple viral infections in *Agaricus bisporus*-Characterisation of 18 unique RNA viruses and 8 ORFans identified by deep sequencing. *Sci. Rep.* 7:2469. doi: 10.1038/s41598-017-01592-9

Deleris, A., Gallego-Bartolome, J., Bao, J., Kasschau, K. D., Carrington, J. C., and Voinnet, O. (2006). Hierarchical action and inhibition of plant Dicer-like proteins in antiviral defense. *Science* 313, 68–71. doi: 10.1126/science.1128214

Donaire, L., and Ayllón, M. A. (2017). Deep sequencing of mycovirus-derived small RNAs from *Botrytis* species. *Mol. Plant Pathol.* 18, 1127–1137. doi: 10.1111/mpp.12466

Donaire, L., Rozas, J., and Ayllón, M. A. (2016). Molecular characterization of Botrytis ourmia-like virus, a mycovirus close to the plant pathogenic genus Ourmiavirus. *Virology* 489, 158–164. doi: 10.1016/j.virol.2015.11.027

Ezawa, T., Ikeda, Y., Shimura, H., and Masuta, C. (2015). Detection and characterization of mycoviruses in arbuscular mycorrhizal fungi by deep-sequencing. *Methods Mol. Biol.* 1236, 171–180. doi: 10.1007/978-1-4939-1743-3_13

Ghabrial, S. A., Castón, J. R., Jiang, D., Nibert, M. L., and Suzuki, N. (2015). 50-plus years of fungal viruses. *Virology* 479, 356–368. doi: 10.1016/j.virol.2015.02.034

Ghabrial, S. A., and Suzuki, N. (2009). Viruses of plant pathogenic fungi. *Annu. Rev. Phytopathol.* 47, 353–384. doi: 10.1146/annurev-phyto-080508-081932

Gilmer, D., Ratti, C., and ICTV Report Consortium. (2017). ICTV virus taxonomy profile: *Benyviridae*. *J. Gen. Virol.* 98, 1571–1572. doi: 10.1099/jgv.0.000864

Grabherr, M. G., Haas, B. J., Yassour, M., Levin, J. Z., Thompson, D. A., Amit, I., et al. (2011). Full-length transcriptome assembly from RNA-Seq data without a reference genome. *Nat. Biotechnol.* 29, 644–652. doi: 10.1038/nbt.1883

Gu, Y. H., Tao, X., Lai, X. J., Wang, H. Y., and Zhang, Y. Z. (2014). Exploring the polyadenylated RNA virome of sweet potato through high-throughput sequencing. *PLoS ONE* 9:e98884. doi: 10.1371/journal.pone.0098884

Hall, M. C., and Matson, S. W. (1999). Helicase motifs: the engine that powers DNA unwinding. *Mol. Microbiol.* 34, 867–877. doi: 10.1046/j.1365-2958.1999.01659.x

Himeno, M., Maejima, K., Komatsu, K., Ozeki, J., Hashimoto, M., Kagiwada, S., et al. (2010). Significantly low level of small RNA accumulation derived from an encapsidated mycovirus with dsRNA genome. *Virology* 396, 69–75. doi: 10.1016/j.virol.2009.10.008

Hu, Z., Wu, S., Cheng, J., Fu, Y., Jiang, D., and Xie, J. (2014). Molecular characterization of two positive-strand RNA viruses co-infecting a hypovirulent strain of *Sclerotinia sclerotiorum*. *Virology* 464, 450–459. doi: 10.1016/j.virol.2014.07.007

Illana, A., Marconi, M., Rodríguez-Romero, J., Xu, P., Dalmay, T., Wilkinson, M. D., et al. (2017). Molecular characterization of a novel ssRNA ourmia-like virus from the rice blast fungus *Magnaporthe oryzae*. *Arch. Virol.* 162, 891–895. doi: 10.1007/s00705-016-3144-9

Jo, Y., Choi, H., Cho, J. K., Yoon, J. Y., Choi, S. K., and Cho, W. K. (2015). *In silico* approach to reveal viral populations in grapevine cultivar Tannat using transcriptome data. *Sci. Rep.* 5:15841. doi: 10.1038/srep15841

Jo, Y., Choi, H., Kim, S. M., Kim, S. L., Lee, B. C., and Cho, W. K. (2016a). Integrated analyses using RNA-Seq data reveal viral genomes, single nucleotide variations, the phylogenetic relationship, and recombination for Apple stem grooving virus. *BMC Genomics* 17:579. doi: 10.1186/s12864-016-2994-6

Jo, Y., Choi, H., Yoon, J. Y., Choi, S. K., and Cho, W. K. (2016b). *In silico* identification of Bell pepper endornavirus from pepper transcriptomes and their phylogenetic and recombination analyses. *Gene* 575, 712–717. doi: 10.1016/j.gene.2015.09.051

Khalifa, M. E., and Pearson, M. N. (2014). Characterisation of a novel hypovirus from Sclerotinia sclerotiorum potentially representing a new genus within the *Hypoviridae*. *Virology* 464, 441–449. doi: 10.1016/j.virol.2014.07.005

Larkin, M. A., Blackshields, G., Brown, N. P., Chenna, R., McGettigan, P. A., McWilliam, H., et al. (2007). Clustal W and Clustal X version 2.0. *Bioinformatics* 23, 2947–2948. doi: 10.1093/bioinformatics/btm404

Lee, H. C., Li, L., Gu, W., Xue, Z., Crosthwaite, S. K., Pertsemlidis, A., et al. (2010). Diverse pathways generate microRNA-like RNAs and Dicer-independent small interfering RNAs in fungi. *Mol. Cell.* 38, 803–814. doi: 10.1016/j.molcel.2010.04.005

Li, C. X., Shi, M., Tian, J. H., Lin, X. D., Kang, Y. J., Chen, L. J., et al. (2015). Unprecedented genomic diversity of RNA viruses in arthropods reveals the ancestry of negative-sense RNA viruses. *Elife* 4:e05378. doi: 10.7554/eLife.05378

Li, Y., Lu, J., Han, Y., Fan, X., and Ding, S. W. (2013). RNA interference functions as an antiviral immunity mechanism in mammals. *Science* 342, 231–234. doi: 10.1126/science.1241911

Liu, H., Fu, Y., Jiang, D., Li, G., Xie, J., Peng, Y., et al. (2009). A novel mycovirus that is related to the human pathogen hepatitis E virus and rubi-like viruses. *J. Virol.* 3, 1981–1991. doi: 10.1128/JVI.01897-08

Liu, J. J., Chan, D., Xiang, Y., Williams, H., Li, X. R., Sniezko, R. A., et al. (2016). Characterization of five novel mitoviruses in the white pine blister rust fungus cronartium ribicola. *PLoS ONE* 11:e0154267. doi: 10.1371/journal.pone.0154267

Liu, L., Xie, J., Cheng, J., Fu, Y., Li, G., Yi, X., et al. (2014). Fungal negative-stranded RNA virus that is related to bornaviruses and nyaviruses. *Proc. Natl. Acad. Sci. U.S.A.* 111, 12205–12210. doi: 10.1073/pnas.1401786111

Márquez, L. M., Redman, R. S., Rodriguez, R. J., and Roossinck, M. J. (2007). A virus in a fungus in a plant: three-way symbiosis required for thermal tolerance. *Science* 315, 513–515. doi: 10.1126/science.1136237

Marzano, S. Y., Hobbs, H. A., Nelson, B. D., Hartman, G. L., Eastburn, D. M., McCoppin, N. K., et al. (2015). Transfection of *Sclerotinia sclerotiorum* with *in vitro* transcripts of a naturally occurring interspecific recombinant of *Sclerotinia sclerotiorum* hypovirus 2 significantly reduces virulence of the fungus. *J. Virol.* 89, 5060–5071. doi: 10.1128/JVI.03199-14

Marzano, S. Y. L., and Domier, L. L. (2016). Novel mycoviruses discovered from metatranscriptomics survey of soybean phyllosphere phytobiomes. *Virus Res.* 213, 332–342. doi: 10.1016/j.virusres.2015.11.002

Marzano, S. Y. L., Nelson, B. D., Ajayi-Oyetunde, O., Bradley, C. A., Hughes, T. J., Hartman, G. L., et al. (2016). Identification of diverse mycoviruses through metatranscriptomics characterization of the viromes of five major fungal plant pathogens. *J. Virol.* 90, 6846–6863. doi: 10.1128/JVI.00357-16

Mi, S., Cai, T., Hu, Y., Chen, Y., Hodges, E., Ni, F., et al. (2008). Sorting of small RNAs into *Arabidopsis* argonaute complexes is directed by the 5' terminal nucleotide. *Cell* 133, 116–127. doi: 10.1016/j.cell.2008.02.034

Moissiard, G., Parizotto, E. A., Himber, C., and Voinnet, O. (2007). Transitivity in *Arabidopsis* can be primed, requires the redundant action of the antiviral Dicer-like 4 and Dicer-like 2, and is compromised by viral-encoded suppressor proteins. *RNA* 13, 1268–1278. doi: 10.1261/rna.055012.115

Mokili, J. L., Rohwer, F., and Dutilh, B. E. (2012). Metagenomics and future perspectives in virus discovery. *Curr. Opin. Virol.* 2, 63–77. doi: 10.1016/j.coviro.2011.12.004

Mu, F., Xie, J., Cheng, S., You, M. P., Barbetti, M. J., Jia, J., et al. (2018). Virome characterization of a collection of *Sclerotinia sclerotiorum* from Australia. *Front. Microbiol.* 8:2540. doi: 10.3389/fmicb.2017.02540

Nuss, D. L. (1992). Biological control of chestnut blight: an example of virus-mediated attenuation of fungal pathogenesis. *Microbiol. Rev.* 56, 561–576.

Nuss, D. L. (2011). "Mycoviruses, RNA silencing, and viral RNA recombination," in *Advances in Virus Research Vol. 80* (Academic Press), 25–48. doi: 10.1016/B978-0-12-385987-7.00002-6

Osaki, H., Sasaki, A., Nomiyama, K., and Tomioka, K. (2016). Multiple virus infection in a single strain of *Fusarium poae* shown by deep sequencing. *Virus Genes* 52, 835–847. doi: 10.1007/s11262-016-1379-x

Punja, Z. K. (1985). The biology, ecology, and control of *sclerotium rolfsh*. *Annu. Rev. Phytopathol.* 23, 97–127. doi: 10.1146/annurev.py.23.090185.000525

Remnant, E. J., Shi, M., Buchmann, G., Blacquière, T., Holmes, E. C., Beekman, M., et al. (2017). A diverse range of novel RNA viruses in geographically distinct honey bee populations. *J. Virol.* 91:e158–17. doi: 10.1128/JVI.00158-17

Rivard C. L., O'Connell, S., Peet, M. M., and Louws, F. J. (2010). Grafting tomato with interspecific rootstock to manage diseases caused by *Sclerotium rolfsii* and southern root-knot nematode. *Plant Dis.* 94, 1015–1021. doi: 10.1094/PDIS-94-8-1015

Roossinck, M. J. (2015). Metagenomics of plant and fungal viruses reveals an abundance of persistent lifestyles. *Front. Microbiol.* 5:767. doi: 10.3389/fmicb.2014.00767

Schoebel, C. N., Zoller, S., and Rigling, D. (2014). Detection and genetic characterisation of a novel mycovirus in *Hymenoscyphus fraxineus*, the causal agent of ash dieback. *Infect. Genet. Evol.* 28, 78–86. doi: 10.1016/j.meegid.2014.09.001

Segers, G. C., Zhang, X., Deng, F., Sun, Q., and Nuss, D. L. (2007). Evidence that RNA silencing functions as an antiviral defense mechanism in fungi. *Proc. Natl. Acad. Sci. U.S.A.* 104, 12902–12906. doi: 10.1073/pnas.0702500104

Shi, M., Lin, X. D., Tian, J. H., Chen, L. J., Chen, X., Li, C. X., et al. (2016). Redefining the invertebrate RNA virosphere. *Nature* 540:539. doi: 10.1038/nature20167

Smart, C. D., Yuan, W., Foglia, R., Nuss, D. L., Fulbright, D. W., and Hillman, B. I. (1999). Cryphonectria hypovirus 3, a virus species in the family *Hypoviridae* with a single open reading frame. *Virology* 265, 66–73. doi: 10.1006/viro.1999.0039

Sun, Q., Choi, G. H., and Nuss, D. L. (2009). A single Argonaute gene is required for induction of RNA silencing antiviral defense and promotes viral RNA recombination. *Proc. Natl. Acad. Sci. U.S.A.* 106, 17927–17932. doi: 10.1073/pnas.0907552106

Suzuki, N., Ghabrial, S. A., Kim, K. H., Pearson, M., Marzano, S. Y. L., Yaegashi, H., et al. (2018). ICTV virus taxonomy profile: *hypoviridae*. *J. Gen. Virol.* 99, 615–616. doi: 10.1099/jgv.0.001055

Tamura, K., Stecher, G., Peterson, D., Filipski, A., and Kumar, S. (2013). MEGA6: molecular evolutionary genetics analysis version 6.0. *Mol. Biol. Evol.* 30, 2725–2729. doi: 10.1093/molbev/mst197

Turina, M., Hillman, B. I., Izadpanah, K., Rastgou, M., and Rosa, C. (2017). ICTV virus taxonomy profile: ourmiavirus. *J. Gen. Virol.* 98, 129–130. doi: 10.1099/jgv.0.000725

Vainio, E. J., Hyder, R., Aday, G., Hansen, E., Piri, T., Dogmuş-Lehtijärvi, T., et al. (2012). Population structure of a novel putative mycovirus infecting the conifer root-rot fungus *Heterobasidion annosum sensu lato*. *Virology* 422, 366–376. doi: 10.1016/j.virol.2011.10.032

Vainio, E. J., Jurvansuu, J., Streng, J., Rajamäki, M. L., Hantula, J., and Valkonen, J. P. (2015). Diagnosis and discovery of fungal viruses using deep sequencing of small RNAs. *J. Gen. Virol.* 96, 714–725. doi: 10.1099/jgv.0.000003

Wang, S., Li, P., Zhang, J., Qiu, D., and Guo, L. (2016). Generation of a high resolution map of sRNAs from *Fusarium graminearum* and analysis of responses to viral infection. *Sci. Rep.* 6:26151. doi: 10.1038/srep26151

Wilson, R. C., and Doudna, J. A. (2013). Molecular mechanisms of RNA interference. *Ann. Rev. Biophys.* 42, 217–239. doi: 10.1146/annurev-biophys-083012-130404

Xie, J., and Jiang, D. (2014). New Insights into mycoviruses and exploration for the biological control of crop fungal diseases. *Annu. Rev. Phytopathol.* 52, 45–68. doi: 10.1146/annurev-phyto-102313-050222

Xu, Z., Gleason, M. L., Mueller, D. S., Esker, P. D., Bradley, C. A., Buck, J. W., et al. (2008). Overwintering of *Sclerotium rolfsii* and *S. rolfsii* var. delphinii in different latitudes of the United States. *Plant Dis.* 92, 719–724. doi: 10.1094/PDIS-92-5-0719

Yaegashi, H., Kanematsu, S., and Ito, T. (2012). Molecular characterization of a new hypovirus infecting a phytopathogenic fungus, *Valsa ceratosperma*. *Virus Res.* 165, 143–150. doi: 10.1016/j.virusres.2012.02.008

Yaegashi, H., Shimizu, T., Ito, T., and Kanematsu, S. (2016). Differential inductions of RNA silencing among encapsidated double-stranded RNA mycoviruses in the white root rot fungus *Rosellinia necatrix*. *J. Virol.* 90, 5677–5692. doi: 10.1128/JVI.02951-15

Yu, J., Kwon, S. J., Lee, K. M., Son, M., and Kim, K. H. (2009). Complete nucleotide sequence of double-stranded RNA viruses from *Fusarium graminearum* strain DK3. *Arch. Virol.* 154, 1855–1858. doi: 10.1007/s00705-009-0507-5

Yu, J., Lee, K. M., Cho, W. K., Park, J. Y., and Kim, K. H. (2018). Differential contribution of RNAi components in response to distinct *Fusarium Graminearum* virus infections. *J. Virol.* 92:JVI-01756–17. doi: 10.1128/JVI.01756-17

Yu, X., Li, B., Fu, Y., Jiang, D., Ghabrial, S. A., Li, G., et al. (2010). A geminivirus-related DNA mycovirus that confers hypovirulence to a plant pathogenic fungus. *Proc. Natl. Acad. Sci. U.S.A.* 107, 8387–8392. doi: 10.1073/pnas.0913535107

Yu, X., Li, B., Fu, Y., Xie, J., Cheng, J., Ghabrial, S. A., et al. (2013). Extracellular transmission of a DNA mycovirus and its use as a natural fungicide. *Proc. Natl. Acad. Sci. U.S.A.* 110, 1452–1457. doi: 10.1073/pnas.1213755110

Yuan, W., and Hillman, B. I. (2001). *In vitro* translational analysis of genomic, defective, and satellite RNAs of Cryphonectria hypovirus 3-GH2. *Virology* 281, 117–123. doi: 10.1006/viro.2000.0806

Zhang, R., Liu, S., Chiba, S., Kondo, H., Kanematsu, S., and Suzuki, N. (2014). A novel single-stranded RNA virus isolated from a phytopathogenic filamentous fungus, *Rosellinia necatrix*, with similarity to hypo-like viruses. *Front. Microbiol.* 5:360. doi: 10.3389/fmicb.2014.00360

Zhang, X., and Nuss, D. L. (2008). A host dicer is required for defective viral RNA production and recombinant virus vector RNA instability for a positive sense RNA virus. *Proc. Natl. Acad. Sci. U.S.A.* 105, 16749–16754. doi: 10.1073/pnas.0807225105

Zhang, Y. Z., Shi, M., and Holmes, E. C. (2018). Using metagenomics to characterize an expanding virosphere. *Cell* 172, 1168–1172. doi: 10.1016/j.cell.2018.02.043

Zhong, J., Chen, D., Zhu, H. J., Gao, B. D., and Zhou, Q. (2016a). Hypovirulence of *Sclerotium rolfsii* Caused by Associated RNA Mycovirus. *Front. Microbiol.* 7:1798. doi: 10.3389/fmicb.2016.01798

Zhong, J., Pang, X. D., Zhu, H. J., Gao, B. D., Huang, W. K., and Zhou, Q. (2016b). Molecular characterization of a trisegmented mycovirus from the plant pathogenic fungus *Colletotrichum gloeosporioides*. *Viruses* 8:268. doi: 10.3390/v8100268

Conflict of Interest Statement: The authors declare that the research was conducted in the absence of any commercial or financial relationships that could be construed as a potential conflict of interest.

frontiers in Cellular and Infection Microbiology

ORIGINAL RESEARCH
published: 12 March 2019
doi: 10.3389/fcimb.2019.00051

Mycovirus Fusarium oxysporum f. sp. dianthi Virus 1 Decreases the Colonizing Efficiency of Its Fungal Host

*Almudena Torres-Trenas[1,2], Pilar Prieto[3], M. Carmen Cañizares[2], María Dolores García-Pedrajas[2] and Encarnación Pérez-Artés[1]**

[1] Departamento de Protección de Cultivos, Instituto de Agricultura Sostenible, Consejo Superior de Investigaciones Científicas, Córdoba, Spain, [2] Instituto de Hortofruticultura Subtropical y Mediterránea "La Mayora", Universidad de Málaga, Consejo Superior de Investigaciones Científicas, Málaga, Spain, [3] Departamento de Mejora Genética, Instituto de Agricultura Sostenible, Consejo Superior de Investigaciones Científicas, Córdoba, Spain

OPEN ACCESS

Edited by:
Daohong Jiang, Huazhong Agricultural University, China

Reviewed by:
Todd B. Reynolds, The University of Tennessee, Knoxville, United States
Ying-Lien Chen, National Taiwan University, Taiwan

***Correspondence:**
Encarnación Pérez-Artés
eperezartes@ias.csic.es

Specialty section:
This article was submitted to Fungal Pathogenesis, a section of the journal Frontiers in Cellular and Infection Microbiology

Received: *30 October 2018*
Accepted: *18 February 2019*
Published: *12 March 2019*

Citation:
Torres-Trenas A, Prieto P, Cañizares MC, García-Pedrajas MD and Pérez-Artés E (2019) Mycovirus Fusarium oxysporum f. sp. dianthi Virus 1 Decreases the Colonizing Efficiency of Its Fungal Host. Front. Cell. Infect. Microbiol. 9:51. doi: 10.3389/fcimb.2019.00051

Mycoviruses that induce hypovirulence in phytopathogenic fungi are interesting because their potential use as biological control agents of the plant diseases caused by their fungal hosts. The recently identified chrysovirus Fusarium oxysporum f. sp. dianthi virus 1 (FodV1) has been associated to the induction of hypovirulence in *Fusarium oxysporum* f. sp. dianthi, the forma specialis of *F. oxysporum* that causes vascular wilt in carnation (*Dianthus caryophyllus*). In this work, we have used confocal laser scanner microscopy and two isogenic GFP-labeled strains of *F. oxysporum* f. sp. *dianthi* infected (V^+) and not infected (V^-) with the Fusarium oxysporum f. sp. dianthi virus 1, respectively, to analyze the effect of mycovirus FodV1 on the plant colonization pattern of its fungal host. Results demonstrate that FodV1-viral infection affects the speed and spatial distribution of fungal colonization into the plant. Initial stages of external root colonization were similar for both strains, but the virus-free strain colonized the internal plant tissues faster than the virus-infected strain. In addition, other differences related to the specific zone colonized and the density of colonization were observed between both *F. oxysporum* f. sp. *dianthi* strains. The hyphae of both V^- and V^+ strains progressed up through the xylem vessels but differences in the number of vessels colonized and of hyphae inside them were found. Moreover, as colonization progressed, V^- and V^+ hyphae propagated horizontally reaching the central medulla but, while the virus-free strain V^- densely colonized the interior of the medulla cells, the virus-infected strain V^+ appeared mainly in the intercellular spaces and with a lower density of colonization. Finally, the incidence of FodV1-viral infections in a collection of 221 isolates sampled between 2008 and 2012 in the geographic area where the originally infected isolate was obtained has been also analyzed. The very low (<2%) incidence of viral infections is discussed here. To the best of our knowledge, this work provides the first microscopic evidence about the effect of a hypovirulence-inducing mycovirus on the pattern of plant colonization by its fungal host.

Keywords: *Fusarium oxysporum*, carnation, chrysovirus FodV1, hypovirulence, CLSM microscopy, mycovirus-dissemination

INTRODUCTION

Fungal viruses (mycoviruses) are found infecting the main taxonomic groups of fungi, including phytopathogenic species. Although there are a few recent evidences that extracellular transmission may occur (Yu et al., 2013; Liu et al., 2016; Marzano et al., 2016), mycoviruses are mainly transferred between strains by hyphal anastomosis (horizontal transmission), and during the production of spores (vertical transmission). Most of the viral infections in fungi are cryptic, i.e., no appreciable changes are observed in the phenotype of the host, but in some cases an alteration of particular phenotypic traits occurs as a consequence of the viral infection. Mycoviruses inducing hypovirulence in phytopathogenic species, i.e., that reduce the virulence of the fungus against its host plant, are the most interesting to study, because the possibility of using them as biological control agents of the diseases caused by their fungal hosts (reviewed in: Ghabrial and Suzuki, 2009; Pearson et al., 2009; Xie and Jiang, 2014; Ghabrial et al., 2015). With the exception of a circular single stranded (ss) DNA mycovirus from the plant pathogenic fungus *Sclerotinia sclerotiorum* (Yu et al., 2010), mycoviruses inducing hypovirulence have all single or double-stranded (ds) RNA genomes, and are included in the *Totiviridae, Chrysoviridae, Partitiviridae, Hypoviridae, Narnaviridae,* and *Reoviridae* families.

The species *Fusarium oxysporum* contains important plant-pathogens that cause a wide range of plant diseases, mostly involving a vascular wilt syndrome. Strains of *F. oxysporum* are classified in *formae speciales* on the basis of the host plant affected. *F. oxysporum* f. sp. *dianthi* is the *forma specialis* of *F. oxysporum* that infects carnation (*Dianthus caryophillus*), causing the most devastating carnation disease worldwide (Garibaldi and Gullino, 1987; Baayen, 1988). A few mycoviruses have been described infecting different *F. oxysporum* strains, but none of them could be associated with the induction of hypovirulence in its fungal host (Kilic and Griffin, 1998; Sharzei et al., 2007). Recently, we have described Fusarium oxysporum f. sp. dianthi virus 1 (FodV1), the first hypovirulence-inducing mycovirus described in the species *F. oxysporum*. FodV1 was detected infecting isolate *Fod* 116 of *F. oxysporum* f. sp. *dianthi* (Lemus-Minor et al., 2015). FodV1 consists of four dsRNA segments of 3,555 bp (dsRNA1), 2,809 bp (dsRNA2), 2,794 bp (dsRNA3), and 2,646 bp (dsRNA4), respectively. FodV1 dsRNA1 and dsRNA3 encode a RNA-dependent RNA polymerase (RdRp) and a coat protein, respectively; dsRNA2 and dsRNA4 encode hypothetical proteins with unknown functions (Lemus-Minor et al., 2015). Phylogenetic analysis with the aminoacid sequences identifies FodV1 as a member of the *Chrysoviridae* family, and places it in the same branch as the so-called "chryso-like" mycoviruses, all of them related with the alteration of phenotypic traits in their hosts (Darissa et al., 2012; Lee et al., 2014; Lemus-Minor et al., 2015). The effect of FodV1 on the phenotype of the fungus has been analyzed using two versions of isolate *Fod* 116: the original one infected with a very high titer of the virus ($116V^+$), and another one with a residual titer obtained by single conidia selection ($116V^-$). Results obtained by comparison of both versions evidenced a significant effect of FodV1 on all the phenotypic traits analyzed (Lemus-Minor et al., 2018). Presence of a high titer of FodV1 in isolate *Fod* $116V^+$ modified the morphology and decreased the radial growth of the colony on solid medium, reduced the conidiation in liquid medium, and lowered the virulence against carnation of its fungal host. It has also been demonstrated that FodV1 can be transferred to another isolate in the laboratory by hyphal anastomosis (Lemus-Minor et al., 2019). To prove this, we have used the originally infected strain *Fod* $116V^+$ as a donor, and strain *Fod* 77, a vegetatively compatible virus-free strain that had previously been transformed with a hygromycin resistance gene (*Fod* $77Hyg^R$), as a recipient. Results obtained showed that FodV1 not only was transferred to the recipient isolate, but also accumulated in it at a similarly high level. Comparative analysis of isolates *Fod* $77Hyg^R$ (virus-free) and *Fod* $77Hyg^RV^+$ (virus-infected) proved that FodV1 induces similar phenotypic alterations in the new infected isolate that those described in the original infected isolate *Fod* $116V^+$ (Lemus-Minor et al., 2019).

Previous fungal isolation assays using carnation plants inoculated with V^+ and V^- versions of isolate *Fod* 116 suggested that hypovirulence caused by mycovirus FodV1 could be associated to a delay in the progress of plant colonization by the virus-infected isolate (Lemus-Minor et al., 2018), but this point has not yet been experimentally supported. Using confocal laser scanner microscopy (CLSM) and GFP-labeled strains of *F. oxysporum* f. sp. *dianthi* infected and not infected with the Fusarium oxysporum f. sp. dianthi virus 1 (FodV1), respectively, we have investigated the effect of mycovirus FodV1 on the ability of the fungal isolate to colonize the plant. In addition, as the success in using mycoviruses for the control of phytopathogenic fungi depends on their efficient transmission among isolates in the natural fungal populations, we have analyzed the efficiency of FodV1-viral dispersion by examining the incidence of FodV1 viral-infections in a wide collection of *F. oxysporum* f. sp. *dianthi* isolates from the same geographic area as the original infected isolate $116V^+$.

MATERIALS AND METHODS

Fungal Isolates and Culture Conditions

Mycovirus FodV1 was first identified in isolate *Fod* 116 ($116V^+$), a race 2 strain of *F. oxysporum* f. sp. *dianthi* obtained in 2008 from a diseased carnation plant collected in the carnation growing area of Chipiona (Cádiz province, Spain) (Gómez-Lama Cabanás et al., 2012; Lemus-Minor et al., 2015). To study the prevalence of FodV1-viral infections, a collection of 221 *F. oxysporum* f. sp. *dianthi* isolates obtained between 2008 and 2012 from plants and soils in the geographic area of Cádiz and Seville provinces has been analyzed (**Table 1**). To perform the histologic analyses by CLSM, isogenic virus-free (V^-) and virus-infected (V^+) GFP-labeled strains of isolate *Fod* 77 were obtained (see below). All strains were stored as conidial suspensions at −80°C in glycerol, and propagated in potato dextrose broth (PDB) liquid medium with agitation (125 rpm) at 25°C in the dark.

TABLE 1 | *Fusarium oxysporum* f. sp. *dianthi* isolates analyzed for the presence of FodV1 viral infection.

Isolate (s)[a]	Geographic origin[b]	Source	Year	Race group assignation by PCR pattern[c]
Fod 108, 110, 111, 120, 121	Chipiona(Ca)	Plant	2008	R1t
Fod 112, 113, 114, 117	Chipiona(Ca)	Plant	2008	R2I
Fod 118, 119	Chipiona(Ca)	Plant	2008	R2II
Fod 115	Chipiona(Ca)	Plant	2008	–
Fod 124, 127, 132, 134, 136, 138	Chipiona(Ca)	Plant	2009	R2I
Fod 122, 128, 130, 140, 142	Chipiona(Ca)	Plant	2009	R1t
Fod 183, 185, 187	Chipiona(Ca)	Plant	2010	R2I
Fod 181, 189, 191	Chipiona(Ca)	Plant	2010	R1t
Fod 179, 195,	Chipiona(Ca)	Soil	2010	R2II
Fod 197	Chipiona(Ca)	Soil	2010	R1t
Fod 144, 146, 148, 150, 158, 160, 162, 164	La Colonia(Se)	Plant	2010	R2I
Fod 152, 154	Lebrija(Se)	Plant	2010	R1t
Fod 156	Lebrija(Se)	Plant	2010	R2II
Fod 223, 225, 227, 229, 231, 233, 235, 237, 239, 241, 245, 247, 249, 251, 253	Chipiona(Ca)	Plant	2011	R2I
Fod 200, 201, 203, 205	Chipiona(Ca)	Plant	2011	R1t
Fod 207	Chipiona(Ca)	Soil	2011	R2I
Fod 256, 258, 259, 260, 261, 264, 265, 267, 269, 272, 275, 281	Chipiona(Ca)	Soil	2011	R2II
Fod 270, 280	Chipiona(Ca)	Soil	2011	R1t
Fod 211	Lebrija(Se)	Plant	2011	R2I
Fod 207, 210, 213, 215, 217, 219, 221	Lebrija(Se)	Plant	2011	R2I
Fod 327, 328, 329, 330, 331, 332, 333, 334, 335, 336, 341.1, 357, 358, 359, 360, 361, 364, 368, 373.2, 433, 434, 435, 453	Chipiona(Ca)	Plant	2012	R2I
Fod 365, 452	Chipiona(Ca)	Plant	2012	R2II
Fod 341.2, 342, 343, 344, 345, 346, 347, 348, 349, 350, 351, 363, 366, 367, 371, 372, 373.1, 471	Chipiona(Ca)	Plant	2012	R1t
Fod 337, 338, 339, 340, 369, 370, 375, 437, 438, 439, 442, 443, 444, 445, 446, 451, 469	Chipiona(Ca)	Soil	2012	R2II
Fod 362, 376, 440, 441, 447, 448, 450, 454, 459, 463, 476	Chipiona(Ca)	Soil	2012	R2II
Fod 352, 353, 354, 355, 356, 374, 449, 455, 456, 457, 458, 460, 461, 462, 464, 465, 466, 467, 468, 470, 472, 473, 474, 475, 477, 478, 479, 480, 481, 482, 483, 484, 485, 486, 487	Chipiona(Ca)	Soil	2012	R1t
Fod 383, 384, 385, 386, 387, 388	Lebrija(Se)	Plant	2012	R2I
Fod 377, 378, 379, 380, 381, 382, 391, 392, 393, 394	Lebrija(Se)	Plant	2012	R1t
Fod 400, 402	Lebrija(Se)	Soil	2012	R2I
Fod 389, 390, 395, 403, 404, 405	Lebrija(Se)	Soil	2012	R2II
Fod 396, 397, 398, 399, 401	Lebrija(Se)	Soil	2012	R1t

[a] *Isolates had been previously characterized to race-group by specific-PCR amplifications, as described in Gómez-Lama Cabanás et al. (2012).*
dsRNA from each isolate was purified by cellulose column chromatography and analyzed by RT-PCR using specific primers FodV1f/FodV1r directed to the RdRp sequence of mycovirus FodV1 (Lemus-Minor et al., 2018).
[b] *Ca, Cádiz province; Se, Sevilla province.*
[c] *Race-group assignation by molecular markers. R1t, race 1molecular group type; R2I, race 2 molecular group I; R2II, race 2 molecular group II.*
(–) Unknown data.

dsRNA Extraction and FodV1 Detection

Infection by mycovirus FodV1 was determined in dsRNA extracts. To obtain the dsRNA-enriched extracts, 3 mg of mycelia were ground in liquid nitrogen, suspended in 2 x STE buffer (50 mM Tris-HCl, pH 7.0, 0.1 M NaCl, 1 mM EDTA) and 10% SDS, and the total nucleic acids were extracted with phenol. The extracts were then purified by cellulose column chromatography (Valverde et al., 1990), and visualized by electrophoresis on 1% agarose gels stained with RedSafe Nucleic Acid Staining Solution (iNtRON Biotechnology, Seongnam-si Gyeonggi-do, Korea). Presence of FodV1-dsRNA in the extracts was detected by retrotranscription (RT) followed by a polymerase chain reaction (PCR) using primers directed to the RNA-dependent RNA polymerase (RdRp) sequence of FodV1. Primers FodV1RT (5′-GGGTGGAGACTTGCGATCAT-3′) and FodV1F/FodV1R (5′-GGCCTGCTGACCCCCGACATAG-3′/5′-GACCCGAGGCAGCTGAACCCAATA-3′) were used for the RT and the PCR, respectively. RT reactions were performed

from 2 μL of dsRNA extract using the enzyme NZY M-MuLV reverse transcriptase (NZYTech). PCR amplifications were performed using 2 μL of the cDNA synthesized, and the enzyme GoTaq® DNA polymerase (Promega Corporation, Madison, WI USA).

RT and PCR amplification conditions were as described in Lemus-Minor et al. (2018). The products of the RT-PCR reactions were analyzed by electrophoresis on 1.5% agarose gels, purified from the gel and sequenced, and the sequences were analyzed by homology with the RdRp sequence of FodV1 using the MegAling program (DNASTAR Lasergene 15 software package).

Obtention of a GFP-Expressing Version of Isolate *Fod* 77 and Transference of Mycovirus FodV1

To generate a version of strain *Fod* 77 constitutively expressing a green fluorescent gene (GFP), an *Agrobacterium tumefaciens*-mediated transformation (ATMT) method was used. To obtain a conidial suspension, strain *Fod* 77 was grown in YEPS (1% yeast extract, 2% bactopeptone, 2% sucrose) for 4 days at 25°C under 200 rpm shaking. Conidia were harvested by filtration through sterile Miracloth assembled in funnels and centrifuged at 4,000 × g for 10 min. The conidia concentration was determined using a hemocytometer and diluted to a final concentration of 10^7 conidia/ml. A binary vector containing a *hygR* marker and a green fluorescent protein (GFP) cassette (Sarmiento-Villamil et al., 2018) was generated using a variant of the OSCAR method (Paz et al., 2011; Gold et al., 2017), and introduced into the AGL-1 *Agrobacterium tumefaciens* strain by electroporation. ATMT of the conidial suspension of *Fod* 77 was performed as described by Dobinson et al. (2004) with minor modifications. Transformants were selected on PDA containing hygromycin B (75 μg/ml). To confirm the integration of the selective marker in the genome, a PCR analysis of the transformants was performed with primers Hyg-F (5′-AAAGCC TGAACTCACCGCGACG-3') and Hyg-R (5′-AGCGCGTCT GCTGCTCCATAC-3′), which amplified a 736 bp region of the *hygR* gene.

To generate the mycovirus-infected GFP-tagged strain, FodV1 was transferred from isolate *Fod* $116V^+$ to isolate *Fod* 77-GFP by hyphal anastomosis. For that, mycelial plugs of the mycovirus donor and recipient strains were transferred to a PDA plate, placing them about 1–1.5 cm apart. Plates were then incubated for 10 days at 25°C to allow strains come into contact and exchange genetic material. Mycelial plugs were then taken from different points of the area of contact of both strains, and transferred to fresh PDA plates containing hygromicin B (75 μg/ml) to selectively grow the recipient strain. Selection plates were incubated for 7 days and then flasks with 100 ml of PDB were inoculated with 2–3 fragments of fungal tissue from each plate. After 4 days of growth, mycelium was collected from the liquid cultures by filtration, and ground to fine powder under liquid nitrogen. Samples were then subjected to chromatography on cellulose to detect presence of dsRNA viral molecules as described previously.

Colonization and Virulence Bioassays

One-month cuttings of susceptible carnation cultivar Candela were inoculated by root-deeping in a suspension of conidia (10^6 conidia/ml) of the GFP-tagged isolate *Fod* $77V^+$ or isolate *Fod* $77V^-$. Candela cuttings treated with water (not inoculated) were used as controls. Obtention of fungal inoculum, inoculation of carnation cuttings, and greenhouse conditions, were as described in Gómez-Lama Cabanás et al. (2012). Two bioassays were carried out simultaneously, using 35 plants (replicates) per treatment for each bioassay. A set of 8 plants per treatment were maintained throughout a total period of 40 days to evaluate the progress in the disease severity symptoms. Fusarium wilt symptoms were evaluated every 2 days using a scale of disease from 0 (no symptoms) to 5 (dead plant). Disease severity values were used to calculate the percentage of the standardized area under the disease progress curve (sAUDPC). Analysis of variance (ANOVA) was used to analyze sAUDPC, and significant differences among means for disease severity values with each isolate were determined using the Fisher's least significant difference (LSD $P \leq 0.05$). ANOVA analyses were performed using the GraphPad Prism 6 program.

One week before ending the bioassay, a plant inoculated with each V^- and V^+ *Fod* 77 strain was used to isolate the fungus, as described in Lemus-Minor et al. (2018). Mycelia from representatives of the fungal colonies obtained were analyzed by multiplex PCR (Gómez-Lama Cabanás et al., 2012) to confirm the *forma specialis* and race-group of the fungus, and by cellulose column chromatography to confirm presence or absence of FodV1-dsRNA.

Microscopic Monitoring of Pathogen Progression in Carnation Plants

Plants inoculated with the GFP-labeled isolates *Fod* 77 V^- or *Fod* $77V^+$ were examined using confocal laser scanner microscopy (CLSM) every 24–48 h during 40 days after inoculation. Two plants per treatment were analyzed each time for CLSM analysis. Plants were carefully uprooted from the pots and the roots were dipped in tap water to be slightly washed. During the first week, root samples were taken daily and observed directly under the confocal microscope. From day 8, samples from the root crown and the internodes of the stem were also exhaustively analyzed by confocal microscopy. Around 1 cm long of stem and root crown tissue were sectioned using a Vibratome Series 1000 plus (TAAB Laboratories Equipment Ltd, Aldermarston, UK) under distilled water as described previously (Prieto et al., 2007). If colonization was observed in an internode, serial cuts of the next upper internode were also prepared to stage the colonization progress of the fungal isolate through the vascular bundles. Single confocal optical sections were thoroughly analyzed from all these vibratome sections using an Axioskop 2 MOT microscope (Carl Zeiss, Jena GmbH, Germany), which has a Krypton and an Argon lasers, controlled by LSM5 PASCAL software (Carl Zeiss). Both GFP-tagged *F. oxysporum* f. sp. *dianthi* strains infected and not infected with mycovirus FodV1, respectively, were detected using the 488 nm Argon laser emission light (detection at 500–520 nm). The recorded images were then transferred to Zeiss LSM Image

Browser version 4.0 (Carl Zeiss) for an exhaustive study. Finally, confocal stacks were composed and deeply analyzed to assess colonization of Candela root and stem tissues by *F oxysporum* f. sp. *dianthi* strains. Brightness and contrast were slightly modified in final figures using PhotoShop 10.0 software (Adobe Systems, San Jose, CA, USA).

RESULTS

Tranformation of Isolate *Fod* 77 With the *gfp* Gene and Transference of Mycovirus FodV1

To obtain a *F. oxysporum* f. sp. *dianthi* strain expressing the green fluorescent protein (GFP), a binary vector containing a *hygR* cassette next to a sGFP gene under the control of the *Aspergillus nidulans* Pgdp promoter between the right and left border of the T-DNA (Sarmiento-Villamil et al., 2018) was used. This vector was used for *Agrobacterium tumefaciens*-mediated transformation of parental virus-free isolate *Fod* 77. Three of the transformants obtained following two rounds of selection on PDA plates containing hygromycin B (75 μg/ml) were selected for detailed analysis. The presence of the transgene in the selected transformants was confirmed by performing PCR amplification of a 736 bp amplicon using the primer pair specific for the selectable gene *hyg*, while no amplification was observed in wild type *Fod* 77 isolate (data not shown). Comparison of growth rates and colony morphology on PDA plates of the three transformants and the wild type *Fod* 77 showed no significant differences.

One of the three transformants was selected as virus-free version of the GFP-tagged *Fod* 77, which was named *Fod* 77-GFP. Before transferring mycovirus FodV1 to *Fod* 77-GFP, we performed a pathogenicity test to discard that the integration of the T-DNA carrying the *gfp* gene had any effect on the virulence of the fungal isolate. To do that, we inoculated the wild type strain *Fod* 77 and the GFP expressing strain *Fod* 77-GFP on susceptible carnation cultivars Candela and Pink Bijou, and compared the progress of disease severity symptoms. Results obtained confirmed that *Fod* 77-GFP was as virulent as the parental wild type (**Supplementary Table 1**).

To generate isogenic lines with and without viral infection, the mycovirus FodV1 was transferred from isolate *Fod* 116V^+ to the compatible isolate *Fod* 77-GFP by hyphal anastomosis. FodV1 donor strain *Fod* 116 and recipient strain *Fod* 77-GFP were co-cultivated on PDA plates. All the samples taken from different points of the area in contact between both strains and subcultured on PDA with hygromicin were found to contain the virus. One of these samples was chosen for further work as the FodV1-infected version of the GFP-tagged *Fod* 77.

Mycovirus FodV1 Decreases the Speed and Modifies the Spatial Distribution of the Plant Colonization by Its Fungal Host

A detailed microscopic study of Candela root and stem tissues by CLSM was carried out to reveal the progress of vascular colonization by the GFP-labeled strains *Fod* 77-virus free (V^-) and *Fod* 77-virus infected (V^+). Candela carnation plants were inoculated with both *Fod* 77 strains, respectively, and samples were taken every 24–48 h and used for CLSM analyses. A set of the inoculated carnation plants were maintained throughout the whole bioassay and used to register the progress of external disease severity symptoms.

Weak autofluorescence from cell walls was always observed using CLSM, but did not interfere with detection of the GFP-tagged pathogen, even helping to image plant tissues and cells morphology and avoiding extra tissue staining. No autofluorescent native microorganisms were detected on/in Candela tissues at any time. Observation of intact roots between 1 and 7 days post inoculation (dpi) for both treatments showed that initial stages of carnation root colonization were similar in plants inoculated with the virus-free (V^-) or the virus-infected (V^+) *Fod* 77-GFP isolate. *F. oxysporum* f. sp. *dianti* conidia were readily detected on the root surface just 1 dpi, and most of these conidia had begun to germinate at 2 dpi (**Figures 1A,B**). After 2–4 more days, a hank of hyphae was observed wrapping the root surface. In these early days we were even able to visualize some events of fungal penetration, identifying the formation of apressoria over the surface of the root epidermal cells and haustoria intracellularly (**Figure 1C**). Since penetration of epidermal root cells was detected, cross-sections of the root crown zone were examined every 48 h to detect the presence of hyphal internal colonization.

Root crown sections obtained at 6, 8, 10, and 12 dpi from plants inoculated with either strain *Fod* 77V^+ or *Fod* 77V^- were all free of fungal colonization. Colonization in this zone was first detected at 14 dpi only in crown sections from carnation plants inoculated with the virus-free strain (**Figures 2A,C**). At this same sampling time some hyphae of the V^- strain were already slightly reaching the vascular tissue in the first internode of the stem (**Figures 3A,B**). In contrast, no fungal signals were detected in plants inoculated with the strain carrying the virus (V^+) at this stage (**Figures 3C,D**). In fact, colonization of the root crown of plants inoculated with the strain carrying the virus was firstly detected at 21 dpi (this means 7 days later than with the strain without the virus) (**Figures 2B,D**). In addition, our observations also suggested that, although hyphae of both fungal strains (V^- and V^+) colonized the vascular tissue in the root crown zone, the number of vessels colonized and the hyphae density inside them seemed to be always markedly lower in the plants inoculated with the strain carrying the virus (V^+) (**Figure 2**).

Analysis of stem cross sections at 21 dpi evidenced a rapid progress of the colonization by the virus-free strain, already detecting the hyphae of the fungus in the internode 6 of the carnation plants (**Figures 3E,F**). On the contrary, at this sampling time hyphae of the strain carrying the virus were only observed in one out of four plants sampled and reaching only the first internode (**Figures 3G,H**). It is worthy to mention that, at this sampling time, CLSM observations were consistent with visible symptoms of the carnation plants, which were rated quite differently among both treatments. Thus, plants inoculated with the virus-free strain V^- showed visible symptoms of disease rated as 3 in a 0–5 scale, whereas plants inoculated with the virus-infected strain V^+ were rated 0–1.

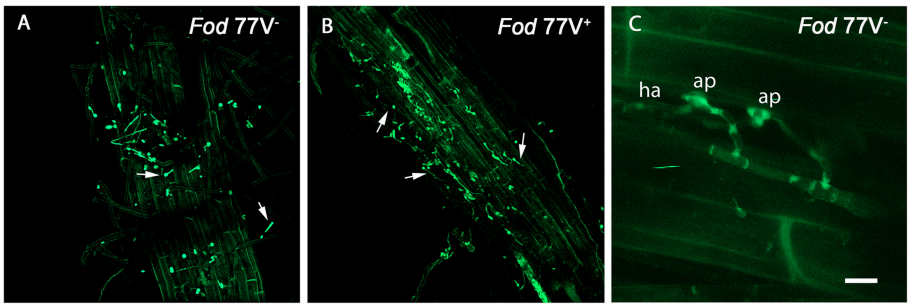

FIGURE 1 | External colonization of carnation roots by the virus-free (V^-) and the virus-infected (V^+) GFP-strains of *Fusarium oxysporum f. sp. dianthi* isolate 77. Images were taken using a confocal laser scanning microscope and intact roots sampled at two **(A,B)** and three **(C)** days after inoculation with the virus-free strain V^- **(A,C)** or the virus-infected strain V^+ **(B)**. **(A,B)** Superficial colonization of adventitious roots by the virus-free **(A)** and the virus-infected **(B)** strains showing single and germinating conidia (arrowed). **(C)** Event of penetration of the root epidermis cells showing the formation of apressoria (ap) on the cell surface, and haustoria (ha) inside the epidermal cell. Scale bar = 50 μm **(A,B)** and 5 μm **(C)**.

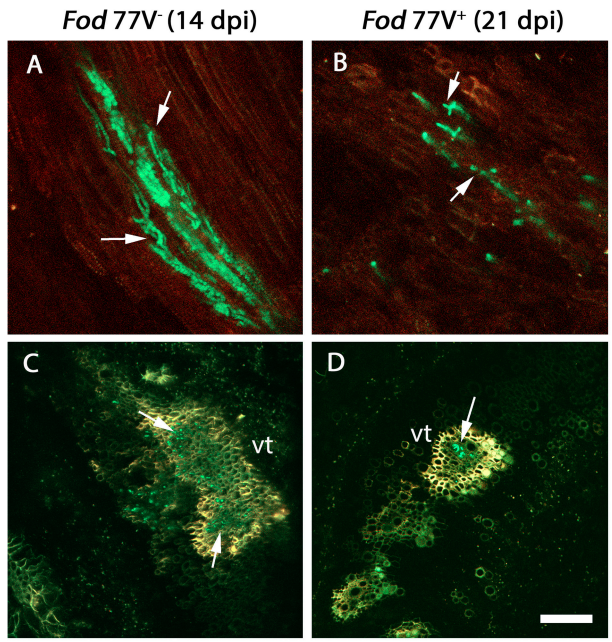

FIGURE 2 | Colonization of the root crown by the virus-free (V^-) and the virus-infected (V^+) GFP- strains of *F. oxysporum* f. sp. *dianthi* isolate 77. **(A)** Longitudinal and **(C)** transversal root crown sections of plants inoculated with the virus-free strain V^- (green) 14 days after inoculation. **(B)** Longitudinal and **(D)** transversal root crown sections of plants inoculated with the virus-infected strain V^+ (green) 21 days after inoculation. Both, the virus free and the virus-infected strain, colonized the plant vascular tissue (arrowed), but the number of vessels colonized as well as the number of hyphae inside them were lower in plants inoculated with the strain carrying the virus. vt, vascular tissue. Scale bar = 50 μm **(A,B)** and 100 μm **(C,D)**.

Successive observation of stem cross-sections of the sampled plants displayed a clear difference in the colonization pattern between *Fod* 77V^- and *Fod* 77V^+ strains. Differences were found related to the rate of progression of the plant colonization by the fungal strains. Cross sections examined at 28 and 35 dpi showed an extensive colonization of the stem including the last internode (internode 11) in plants inoculated with the virus-free strain V^- (**Figures 3I,J,M,N**). On the contrary, plants inoculated with the virus-infected strain V^+ only showed colonization of the vascular tissue up to internode 3 at 28 dpi (**Figures 3K,L**), and up to internode 6 at day 35 (**Figures 3O,P**). In addition to this delay in the colonization progress by the strain carrying the virus, the density of colonization (number of vessels colonized and hyphae inside each vessel) observed at these sampling times seemed to be lower in stem sections of plants inoculated with the virus-infected strain V^+ (**Figures 3I–P**). As colonization progressed, both strains did also invade other plant tissues (medulla) and differences in density between both strains were detected too (**Figure 4**). Moreover, while hyphae of the virus-free strain V^- were easily detected occupying profusely the interior of the medulla cells, hyphae of the virus-infected strain V^+ were preferentially observed in the intercellular spaces of the medulla and rarely were able to invade these cells (**Figure 4**).

At the end of the bioassay (40 dpi), all plants inoculated with the virus-free strain were dead (disease severity = 5) whereas plants inoculated with the virus- infected strain were still alive and maintained disease severity values ≤3. Analysis of the disease severity data obtained during the bioassay evidenced a significant reduction of the sAUDPC when cultivar Candela was inoculated with isolate *Fod* 77V^+ compared to isolate *Fod* 77V^- (**Figure 5**).

Analysis of the mycelia recovered from the inoculated plants confirmed the identity (*F. oxysporum* f. sp. *dianthi* race 2 group I) and presence or absence of viral infection in each inoculated *Fod* 77 strain (**Figure 6**).

Mycovirus FodV1 Has a Low Incidence in the Collection of *F. oxysporum* f. sp. *dianthi* Isolates Analyzed

Micovirus FodV1 was detected infecting isolate *Fod* 116, a race 2 isolate obtained in 2008 from a carnation plant collected in Chipiona (Cádiz, Spain). To determine the incidence of FodV1-dsRNA viral infections, a collection of 221 isolates of *F. oxysporum* f. sp. *dianthi* obtained between years 2008 and 2012 from plants and soils in the same (Cádiz) or adjacent (Sevilla)

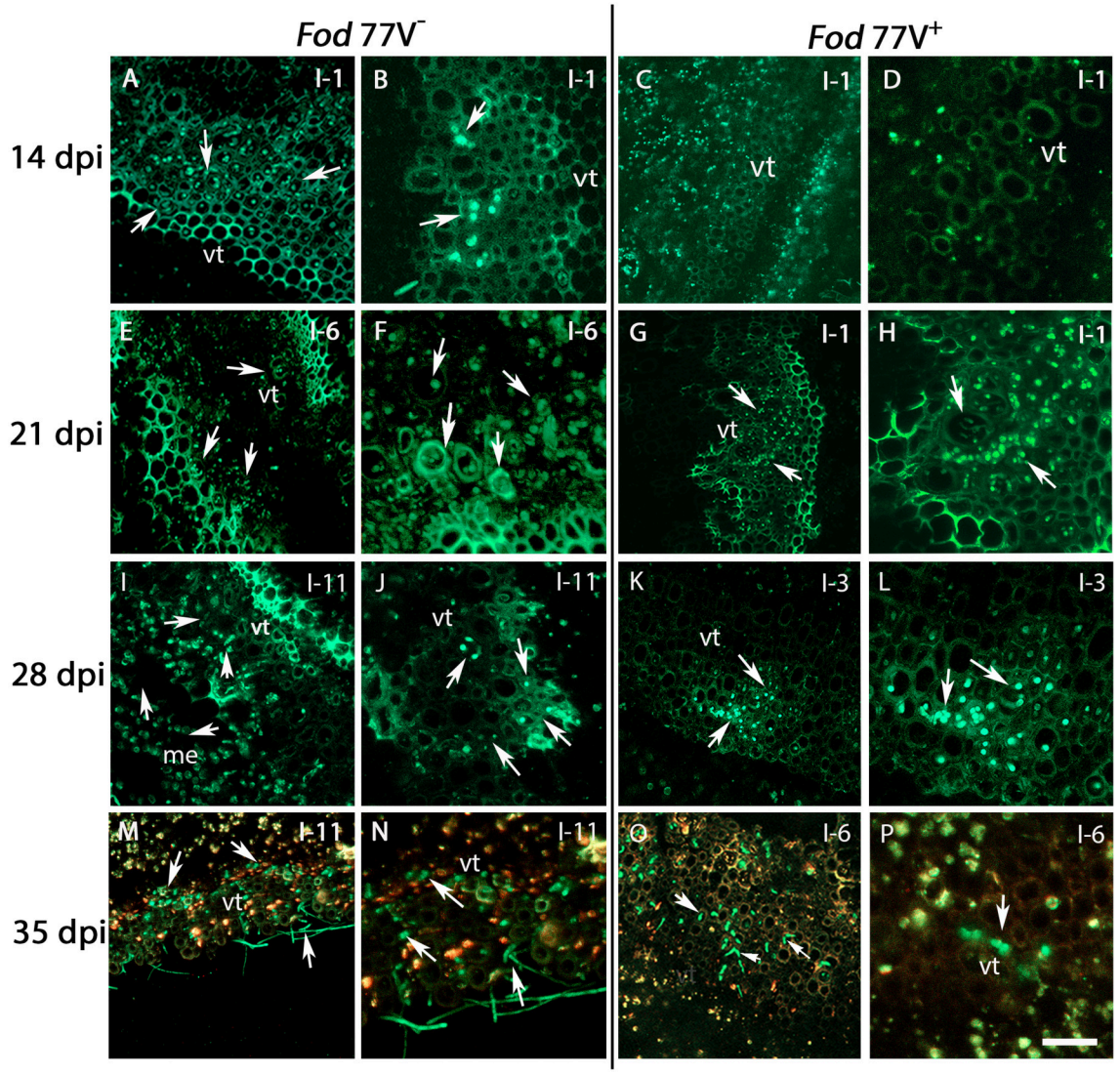

FIGURE 3 | Internal colonization of stem internodes after inoculation of carnation plants with the virus-free (V^-) and the virus-infected (V^+) GFP-strains of *F. oxysporum* f. sp. *dianthi* isolate 77. Transversal sections of the internodes (I) were obtained at 14, 21, 28, and 35 days post inoculation (dpi), and were analyzed by confocal laser scanner microscopy. **(A,B)** Hyphae of the virus-free strain were detected in the vascular tissue of the first internode (I-1) at 14 dpi. **(C,D)** At the same sampling time (14 dpi), hyphae of the virus–infected strain were not detected yet in the same internode. **(E,F)** Stem sections of the sixth internode (I-6) showing the vascular tissue extensively colonized by hyphae of strain V^- at 21 dpi. **(G,H)** At the same time point, hyphae of strain V^+ only reached the first internode (I-1). **(I,J)** Stem sections of plants inoculated with the strain V^- at 28 dpi showing the hyphae reaching the last stem internode (I-11) of the plant. **(K,L)** At the same sampling time (28 dpi), the strain V^+ only reached the vascular tissue of internode 3 (I-3). **(M,N)** Extensive colonization of the vascular tissue up to the last plant internode (I-11) by the virus free strain at 35 dpi. **(O,P)** In contrast, colonization by the V^+ strain did only reach internode 6 (I-6) at the same sampling time (35 dpi). Arrows indicate the presence of hyphae (green). vt, vascular tissue. Scale bar = 50 μm **(A**,**C**,**E**,**G**,**I**,**K**,**M**,**O)**, 20 μm **(B**,**D**,**F**,**H**,**J**,**L**,**N**,**P)**.

geographic area was analyzed (**Table 1**). All the isolates had been previously characterized to race by molecular markers (**Table 1**), and some of them also to vegetative compatibility group (VCG) (Gómez-Lama Cabanás and Pérez-Artés, 2014).

The dsRNA-enriched extracts were obtained by cellulose column chromatography and subjected to RT-PCR amplification using specific primers for the RdRp sequence of FodV1 (**Figure 7**). Direct observation after agarosa gel electrophoresis of the dsRNA extracts indicated presence of FodV1 only in isolate *Fod* 183, an isolate obtained from a carnation plant in 2010 in Chipiona (Cádiz) (**Figure 7A**). Subsequent RT-PCR amplification of the dsRNA extracts showed two additional isolates infected with FodV1: isolate *Fod* 185, obtained from a carnation plant in 2010 in Chipiona, and isolate *Fod* 211, obtained from a carnation plant in 2011 in Lebrija (Sevilla) (**Figure 7B**). All the three new virus-infected isolates were race 2 and belonged to VCG 0021.

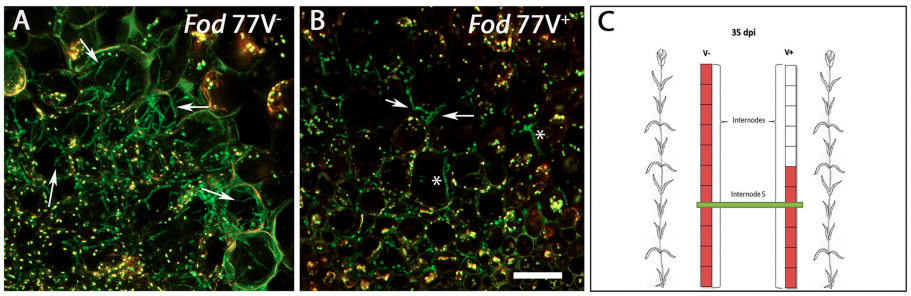

FIGURE 4 | Differences in the colonization pattern of the central medulla in stem sections of plants inoculated with the virus-free (V^-) or the virus-infected (V^+) GFP-strain of *F. oxysporum* f. sp. *dianthi* isolate 77. Images correspond to transversal sections from the same internode (fifth internode) of plants inoculated with the virus-free V^- **(A)** and the virus-infected V^+ **(B)** strains (green), 35 days after inoculation. **(A)** Hyphae of the virus free strain profusely colonizing the interior of the medulla cells. **(B)** Hyphae of the virus-infected strain preferentially located in the intercellular spaces of the medulla cells (arrowed) although some hyphae seem to invade the interior of the cells (asterisks). **(C)** Squematic representation of carnation plants indicating the level of colonization (red) by the virus-free and the virus-infected strains as well as the area shown in panels **A** and **B** corresponding to internode 5 (green). Scale bar represents 50 μm in **(A)** and **(B)**.

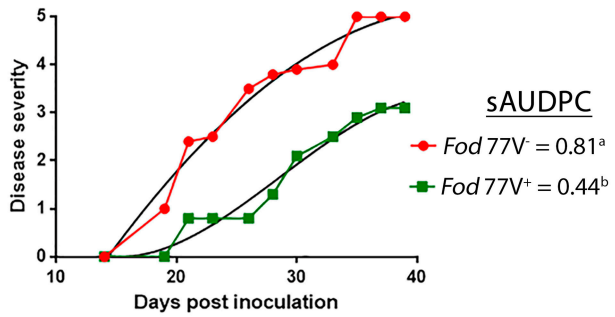

FIGURE 5 | Representative graph of the progress of the disease severity symptoms. Fusarium wilt symptoms were scored for a period of 40 days, using a scale from 0 (no symptoms) to 5 (dead plant), in carnation plants inoculated with the virus-free (V^-) or the virus-infected (V^+) strain of *F. oxysporum* f. sp. *dianthi* isolate 77. Disease severity values were used to calculate the percentage of the standardized area under the disease progress curve (sAUDPC). Values followed by different letters are significantly different according to Fisher's least significant difference (LSD) test ($P \leq 0.05$).

To confirm the identity of the mycovirus detected in isolates *Fod* 183, *Fod* 185 and *Fod* 211, the amplicon obtained by RT-PCR with each isolate was purified from the agarose gel and sequenced. Comparison of these sequences with that of the corresponding fragment of the RdRp sequence of FodV1 showed a 100% homology (**Supplementary Figure 1**).

DISCUSSION

The majority of the studies on the induction of hypovirulence by mycoviruses of phytopathogenic fungi have been focused on the alteration of particular phenotypic traits (reviewed in Ghabrial et al., 2015) or on the modification of the gene expression pattern of the fungal host (Allen and Nuss, 2004; Cho et al., 2012; Lee et al., 2014), but the possible effect of the hypovirulence-inducing mycovirus on the fungal colonization pattern inside the plant has not yet been investigated. In this work, we have analyzed the effect of mycovirus FodV1 on the spatial and temporal dynamics of plant colonization by using confocal laser scanner microscopy. To perform this study, we have used two isogenic GFP-labeled strains of *F. oxysporum* f. sp. *dianthi* isolate 77: the original virus-free strain (V^-), and a FodV1-infected strain obtained in this work (V^+). Both strains were used to inoculate carnation cuttings of susceptible cultivar Candela.

Vascular pathogens are characterized by their ability to colonize the vascular system of the host. Colonization of the xylem vessels leads to a severe decrease in the transport of water and nutrients to the aerial parts of the plant causing its wilting and finally its death. A number of studies have shown that the first stage of plant colonization is common to different *F. oxysporum* strains and hosts, and initiate with the development of a hyphae network over the roots, followed by penetration of the root epidermis (Li et al., 2011; Jiménez-Fernández et al., 2013; Niño-Sánchez et al., 2015; Upasani et al., 2016). In this work, observation of intact roots throughout the first week after inoculation showed no appreciable differences in the root colonization pattern between the virus-free and the virus-infected strains. Conidia of both strains were observed adhered and germinating over the root surface from 1 dpi, and after 2–4 days the roots were covered by a network of hyphae, some of which appeared penetrating the root epidermis. Several works using light or confocal microscopy and other *formae speciales* of *F. oxysporum* revealed the difficulty of finding the specific structures of the fungus at the onset of root cell penetration and the impossibility to photograph them (Lagopodi et al., 2002; Jiménez-Fernández et al., 2013; Niño-Sánchez et al., 2015; Upasani et al., 2016; Pouralibaba et al., 2017). In contrast, in this work we have been able to observe the formation of specific fungal structures such as appressoria over the root surface and haustoria inside the epidermal root cell during the plant cell penetration event using CLSM and the GFP-labeled *F. oxysporum* f. sp. *dianthi* strains.

The architecture of the stem vascular system develops in the crown area, where the primordial ring of xylem vessels is formed. Independently of the strain inoculated (V^- or V^+), root crown sections obtained at 6, 8, 10, and 12 dpi were all free of fungal colonization. This seems to indicate that this period of

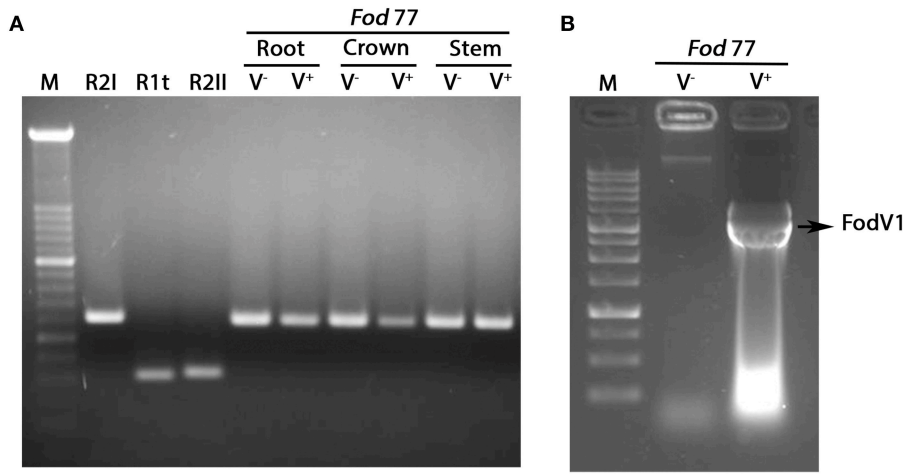

FIGURE 6 | Analysis of the fungal mycelia reisolated from plants inoculated with the virus-free (V^-) and the virus-infected (V^+) strain of *Fusarium oxysporum* f. sp. *dianthi* isolate 77. **(A)** Amplification products obtained in multiplex-PCR reactions using specific primers for the different races-groups described in *F. oxysporum* f. sp. *dianthi* (*Fod*) and DNA from the fungal colonies recovered from root, crown, or stem of carnation plants inoculated with the virus-free strain V^- or the virus-infected strain V^+ of isolate *Fod* 77. Specific primers used and conditions of the multiplex-PCR were as described in Gómez-Lama Cabanás et al. (2012). M, molecular weight marker XIV (Roche Diagnostics). R2I, R1t, and R2II, representative of the respective race-group described in *F. oxysporum* f. sp. *dianthi*. **(B)** Extracts of dsRNA obtained by cellulose column chromatography using mycelia recovered from a carnation plant inoculated with the virus-free (V^-) or the virus-infected (V^+) strain of isolate *Fod* 77. M, 1Kb DNA Ladder (Nippon Genetics).

approximately 1 week from the moment of penetration of the epidermal root cells was necessary for the fungus to reach the central roots and move upward to the crown area.

From 12 dpi, subsequent observations of root crown sections marked the first difference among the virus-free and the virus-infected strains. Colonization of the root crown was first detected in plants inoculated with the virus-free strain at 14 dpi, whereas root crown of plants inoculated with the strain carrying the virus remained free of fungal colonization till 21 dpi. Comparison of crown sections at different times until 28 dpi evidenced that, in addition to the delay in the colonization time, crown of plants inoculated with the virus-infected strain always showed a notably lower density of colonization. This means that, although the hyphae of both V^- and V^+ strains were observed inside the vascular tissue at the root crown zone, the number of vessels colonized and the number of hyphae inside them was lower in the case of V^+-infected plants.

The delay observed in the time of colonization of the root crown area in plants inoculated with strain V^+ compared to plants inoculated with strain V^- was maintained during the colonization of the stem. Hyphae of the virus-free strain were detected colonizing the vessels in the first internode at 14 dpi, while hyphae of the virus-infected strain reached this same zone 6 days later (21 dpi). Once the hyphae of each strain were detected infecting the first internode of the plant, the progress of colonization upwards the stem was faster in plants inoculated with the virus-free strain. Cross stem sections of plants inoculated with strain V^- showed fungal hyphae reaching the last internode (internode 11) at 28 dpi, whereas at the same sampling time hyphae of strain V^+ had colonized only the third lower part of the stem (up to internode 3). Along with this difference in the speed of colonization of the vascular system upwards the stem, some other differences were observed related to the area colonized and the density of colonization reached. The number of vessels colonized and of hyphae inside each of them observed at the different sampling times was always notably lower in stem sections of plants inoculated with the virus-infected strain.

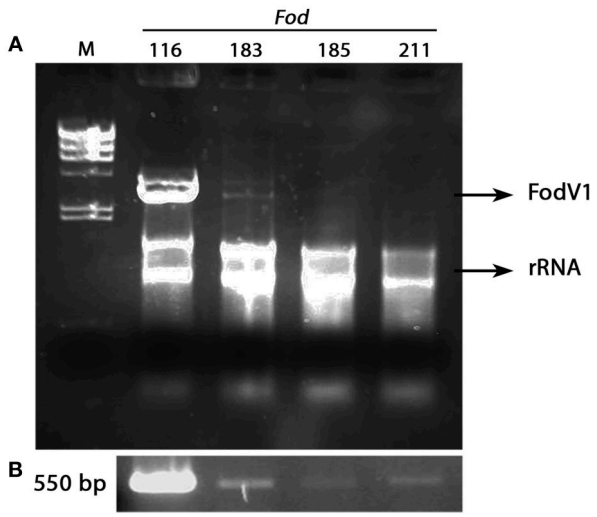

FIGURE 7 | Isolates of *Fusarium oxysporum* f. sp. *dianthi* infected with mycovirus FodV1. **(A)** dsRNA-enriched extracts obtained by cellulose column chromatography from isolates *Fod* 116 (the originally infected isolate), *Fod* 183, *Fod* 185, and *Fod* 211. **(B)** Specific amplicons obtained after RT-PCR of the above dsRNA extracts using specific primers for the RdRp sequence of FodV1. M, molecular weight marker II (Roche Diagnostics) (see also **Supplementary Image to Figure 7**).

At advanced stages of the colonization, differences in the density and location of the hyphae of strains V^- and V^+ were also observed in tissues other than the vascular tissue. As colonization progressed, hyphae of both strains invaded the central area of the stem (medulla), but while hyphae of the virus-free strain V^- were easily detected profusely occupying the interior of the medulla cells, hyphae of the virus-infected strain V^+ were less in number and rarely were able to invade the medulla cells, being preferentially located in the intercellular spaces. This difference in the time and extent of stem colonization correlated with significant differences in the external disease symptoms so that most of the plants inoculated with strain V^- were dead (disease severity = 5) at 35 dpi, whereas plants inoculated with strain V^+ maintained disease severity values $\leq$3 at the end of the bioassay (40 dpi).

The importance of the speed in the colonization of the vascular tissue as determinant of disease severity has been described previously in a study using two strains of *F. oxysporum* f. sp. *phaseoli* differing in virulence (Niño-Sánchez et al., 2015). These authors reported differences on the spatial and temporal dynamic of colonization of a susceptible common bean cultivar infected by a highly virulent (HV) or a weakly virulent (WV) strain. Similar to our results, the main differences between both strains were found in the temporal and spatial dynamic of crown root and hypocotyl colonization, the WV strain being a much slower and less efficient colonizer of the xylem vessels (Niño-Sánchez et al., 2015). Differences in virulence between the HV and WV strains of *F. oxysporum* f. sp. *phaseoli* have been associated to the presence and expression of some transcription factors (Alves-Santos et al., 2002a,b; Ramos et al., 2007). In this work, difference in virulence between the V^- and V^+ strains of *F. oxysporum* f. sp. *dianthi* is associated to the presence of mycovirus FodV1. Therefore, it seems that in these two specific cases, regardless of the endogenous or exogenous cause, the hypovirulence is associated to a delay and restriction in the colonization of the vascular system of the plant.

Previous microscopic analysis related to plant colonization by *F. oxysporum* have been done but focused on particular host-fungus interactions (Czymmek et al., 2007; Nahalkova et al., 2008; Li et al., 2011), compatible (susceptible) or incompatible (resistant) interactions (Zvirin et al., 2010; Jiménez-Fernández et al., 2013; Lü et al., 2013; Pouralibaba et al., 2017), or related to differences in the virulence of the pathogenic strains (Niño-Sánchez et al., 2015). To the best of our knowledge, this work provides the first microscopic evidences on the effect of a hypovirulence-inducing mycovirus on the plant colonization process by its fungal host.

Another aspect analyzed in this study has been that on the incidence of FodV1-viral infections in a collection of *F. oxysporum* f. sp. *dianthi* isolates sampled between 2008 and 2012 in the geographic area where the originally infected isolate *Fod* 116 was obtained. In a previous work, we had demonstrated that FodV1 could be transferred by hyphal anastomosis to another vegetatively compatible isolate in the laboratory (Lemus-Minor et al., 2019). In *F. oxysporum* f. sp. *dianthi,* isolates of race 1 type and of race 2 belong to different VCGs, i.e., VCG 0022 for race 1 type isolates and VCG 0021 for race 2 isolates (Gómez-Lama Cabanás and Pérez-Artés, 2014). The majority of the isolates in the collection analyzed was race 2 and thus belonged to the same 0021 vegetative compatibility group than the virus-infected isolate *Fod* 116. Therefore, in theory, FodV1 should have been able to disperse among compatible hyphae in the fungal population. In spite of that, results obtained in this work demonstrate a very low incidence of FodV1 infections. Mycovirus FodV1 has been detected infecting only another three *F. oxysporum* f. sp. *dianthi* isolates. In addition to the *vic* genes that regulate hyphal anastomosis, the host genetic background has been shown to affect horizontal virus transmission (Cortesi et al., 2001; Choi et al., 2012; Zamora et al., 2015). Although all race 2 isolates are in VCG 0021, we have evidence that some isolates in a same VCG show a reduced compatibility, that is, they can anastomose with a few but not all the isolates in the VCG (Gómez-Lama Cabanás and Pérez-Artés, 2014). The naturally infected isolate *Fod* 116 could be one of those isolates with reduced compatibility, and this fact could have limited the dispersion of the mycovirus. Another factor that could be contributing to the very low dispersion rate of FodV1 is the efficiency in vertical transmission through asexual spores. Previous studies carried out with the original virus-infected isolate *Fod* $116V^+$ and the "in laboratory" virus-infected isolate *Fod* $77V^+$ showed that efficiency in vertical transmission depends on the isolate considered (Lemus-Minor et al., 2019). Thus, while isolate *Fod* $116V^+$ showed a relatively low efficiency (24%), the efficiency of isolate *Fod* $77V^+$ was 100%. This low efficiency of vertical virus-transmission showed by isolate *Fod* $116V^+$ could be contributing to restrict the presence of new virus-infected hyphae of this isolate in the population. In this way, a low density of virus-infected hyphae would decrease the probability of contact between infected and non-infected hyphae and would be limiting the dispersion of the viral infection. This evidence supports the hypothesis that selection of a specific virus-infected isolate could influence transmission and dissemination of hypovirulence (Lee et al., 2014; Lemus-Minor et al., 2019).

Finally, we must take an additional factor into consideration. From the collection analyzed, most (127) of the isolates were obtained from plants with disease symptoms, while 94 isolates were obtained from soil samples. Considering the reduction in the disease severity symptoms associated to the viral infection, this bias in the sampling could also be skewing the data of the prevalence of viral infection in the population. To avoid this inconvenient, it should be necessary to make a more exhaustive analysis with isolates collected exclusively from soil samples.

To the best of our knowledge, this work provides the first microscopic evidence about the effect of a hypovirulence-inducing mycovirus on the plant colonization process, and supplies data that reinforce the idea that the choice of the appropriate isolate is key to achieve an efficient dissemination of a viral infection in a fungal population.

DATA AVAILABILITY

All datasets generated for this study are included in the manuscript and/or the supplementary files.

AUTHOR CONTRIBUTIONS

EP-A, AT-T, and PP conceived and designed the experiments. MC and MG-P obtained the GFP-tagged V^+ and V^- *Fod* strains. PP and AT-T performed the microscopic analysis. EP-A, AT-T, and PP analyzed the data. EP-A and PP wrote the paper.

ACKNOWLEDGMENTS

This research was supported by Grants AGL 2013-48980-R from the Spanish Ministry of Economy and Competitiveness, and AGL 2016-80048-R from the Spanish Ministry of Science and Innovation, co-funded by the European Union (FEDER funds).

We acknowledge support of the publication fee by the CSIC Open Access Publication Support initiative through its Unit of Information Resources for Research (URICI). We thank Antonio Valverde for his valuable technical assistance and Emilio A. Cano (Barberet & Blanc S.A.) for providing carnation cultivars. Authors also want to acknowledge Prof. Antonio Martin for the use of the CLSM facilities.

SUPPLEMENTARY MATERIAL

The Supplementary Material for this article can be found online at: https://www.frontiersin.org/articles/10.3389/fcimb.2019.00051/full#supplementary-material

REFERENCES

Allen, T. D., and Nuss, D. L. (2004). Specific and common alterations in host gene transcript accumulation following infection of the chestnut blight fungus by mild and severe hypoviruses. *J. Virol.* 78, 4145–4155. doi: 10.1128/JVI.78.8.4145-4155.2004

Alves-Santos, F. M., Cordeiro-Rodrigues, L., Sayagués, J. M., Martín-Domínguez, R., García-Benavides, P., Crespo, M. C., et al. (2002b). Pathogenicity and race characterization of *Fusarium oxysporum* f. *sp. phaseoli isolates from Spain and Greece. Plant Pathol.* 51, 605–611. doi: 10.1046/j.1365-3059.2002.00745.x

Alves-Santos, F. M., Ramos, B., García-Sánchez, M. A., Eslava, A. P., and Díaz-Mínguez, J. M. (2002a). A DNA-based procedure for in planta detection of *Fusarium oxysporum* f. *sp. phaseoli. Phytopathology* 92, 237–244. doi: 10.1094/PHYTO.2002.92.3.237

Baayen, R. P. (1988). *Fusarium Wilt of Carnation. Disease Development, Resistance Mechanism of the Host and Taxonomy of the Pathogen*. thesis, University of Utretcht, Holland.

Cho, W. K., Yu, J., Lee, K. M., Son, M., Min, K., Lee, Y. W., et al. (2012). Genome-wide expression profiling shows transcriptional reprogramming in *Fusarium graminearum* by *Fusarium graminearum* virus 1-DK21 infection. *BMC Genomics* 13:173. doi: 10.1186/1471-2164-13-173

Choi, G. H., Dawe, A. L., Churbanov, A., Smith, M. L., Milgroom, M. G., and Nuss, D. L. (2012). Molecular characterization of vegetative incompatibility genes that restrict hypovirus transmission in the chestnut blight fungus *Cryphonectria parasitica*. *Genetics* 190, 113–127. doi: 10.1534/genetics.111.133983

Cortesi, P., McCulloch, C. E., Song, H., Lin, H., and Milgroom, M. G. (2001). Genetic control of horizontal virus transmission in the chestnut blight fungus, *Cryphonectria parasitica*. *Genetics* 159, 107–118.

Czymmek, K. J., Fogg, M., Powell, D. H., Sweigard, J., Park, S. Y., and Kang, S. (2007). *In vivo* time-lapse documentation using confocal and multi-photon microscopy reveals the mechanisms of invasion into the Arabidopsis root vascular system by *Fusarium oxysporum*. *Fungal Genet. Biol.* 44, 1011–1023. doi: 10.1016/j.fgb.2007.01.012

Darissa, O., Adam, G., and Schafer, W. (2012). A dsRNA mycovirus causes hypovirulence of *Fusarium graminearum* to wheat and maize. *Eur. J. Plant Pathol.* 134, 181–189. doi: 10.1007/s10658-012-9977-5

Dobinson, K. F., Grant, S. J., and Kang, S. (2004). Cloning and targeted disruption, via *Agrobacterium tumefaciens*-mediated transformation, of a trypsin protease gene from the vascular wilt fungus *Verticillium dahliae*. *Curr. Genet.* 45, 104–110. doi: 10.1007/s00294-003-0464-6

Garibaldi, A., and Gullino, M. L. (1987). Attempts of biocontrol of Fusarium-wilt of carnation in Italy. *Phytopathology* 77, 1721–1721.

Ghabrial, S. A., Caston, J. R., Jiang, D., Nibert, M. L., and Suzuki, N. (2015). 50-plus years of fungal viruses. *Virology* 479–480, 356–368. doi: 10.1016/j.virol.2015.02.034

Ghabrial, S. A., and Suzuki, N. (2009). Viruses of plant pathogenic fungi. *Annu. Rev. Phytopathol.* 47, 353–384. doi: 10.1146/annurev-phyto-080508-081932

Gold, S. E., Paz, Z., García-Pedrajas, M. D., and Glenn, A. E. (2017). Rapid deletion production in fungi via agrobacterium mediated transformation of OSCAR deletion constructs. *J. Vis. Exp.* e55239. doi: 10.3791/55239

Gómez-Lama Cabanás, C., and Pérez-Artés, E. (2014). New evidence of intra-race diversity in *Fusarium oxysporum* f. sp. *dianthi* populations based on Vegetative Compatibility Groups. *Eur. J. Plant Pathol.* 139, 445–451. doi: 10.1007/s10658-014-0412-y

Gómez-Lama Cabanás, C., Valverde-Corredor, A., and Pérez-Artés, E. (2012). Molecular analysis of Spanish populations of *Fusarium oxysporum f. sp dianthi* demonstrates a high genetic diversity and identifies virulence groups in races 1 and 2 of the pathogen. *Eur. J. Plant Pathol.* 132, 561–576. doi: 10.1007/s10658-011-9901-4

Jiménez-Fernández, D., Landa, B. B., Kang, S., Jiménez-Díaz, R. M., and Navas-Cortes, J. A. (2013). Quantitative and microscopic assessment of compatible and incompatible interactions between chickpea cultivars and *Fusarium oxysporum f.* sp. ciceris races. *PLoS ONE* 8:e61360. doi: 10.1371/journal.pone.0061360

Kilic, O., and Griffin, G. J. (1998). Effect of dsRNA-containing and dsRNA-free hypovirulent isolates of *Fusarium oxysporum* on severity of *Fusarium* seedling disease of soybean in naturally infested soil. *Plant Soil* 201, 125–135. doi: 10.1023/A:1004319614390

Lagopodi, A. L., Ram, A. F., Lamers, G. E., Punt, P. J., Van den Hondel, C. A., Lugtenberg, B. J., et al. (2002). Novel aspects of tomato root colonization and infection by *Fusarium oxysporum f.* sp. radicis-lycopersici revealed by confocal laser scanning microscopic analysis using the green fluorescent protein as a marker. *Mol. Plant Microbe Interact.* 15, 172–179. doi: 10.1094/MPMI.2002.15.2.172

Lee, K. M., Cho, W. K., Yu, J., Son, M., Choi, H., Min, K., et al. (2014). A comparison of transcriptional patterns and mycological phenotypes following infection of *Fusarium graminearum* by four mycoviruses. *PLoS ONE* 9:e100989. doi: 10.1371/journal.pone.0100989

Lemus-Minor, C. G., Canizares, M. C., García-Pedrajas, M. D., and Pérez-Artés, E. (2015). Complete genome sequence of a novel dsRNA mycovirus isolated from the phytopathogenic fungus *Fusarium oxysporum f. sp. dianthi. Arch. Virol.* 160, 2375–2379. doi: 10.1007/s00705-015-2509-9.

Lemus-Minor, C. G., Canizares, M. C., García-Pedrajas, M. D., and Pérez-Artés, E. (2018). *Fusarium oxysporum f. sp. dianthi* virus 1 accumulation is correlated with changes in virulence and other phenotypic traits of its fungal host. *Phytopathology* 108, 957–963. doi: 10.1094/PHYTO-06-17-0200-R

Lemus-Minor, C. G., Cañizares, M. C., García-Pedrajas, M. D., and Pérez-Artés, E. (2019). Horizontal and vertical transmission of the hypovirulence-associated mycovirus *Fusarium oxysporum f. sp. dianthi* virus 1. *Eur. J. Plant Pathol* 153, 645–650. doi: 10.1007/s10658-018-1554-0

Li, C., Chen, S., Zuo, C., Sun, Q., Ye, Q., Yi, G., et al. (2011). The use of GFP-transformed isolates to study infection of banana with *Fusarium oxysporum f.* sp. *cubense* race 4. *Eur. J. Plant Pathol.* 131, 327–340. doi: 10.1007/s10658-011-9811-5

Liu, S., Xie, J., Cheng, J., Li, B., Chen, T., Fu, Y., et al. (2016). Fungal DNA virus infects a mycophagous insect and utilizes it as a transmission vector. *Proc. Natl. Acad. Sci. U.S.A.* 113, 12803–12808. doi: 10.1073/pnas.1608013113

Lü, G., Guo, S., Zhang, H., Geng, L., Martyn, R. D., and Xu, Y. (2013). Colonization of *Fusarium* wilt-resistant and susceptible watermelon roots by a green-fluorescent-protein-tagged isolate of *Fusarium oxysporum* f.sp. niveum. *J. Phytopathol.* 162, 228–237. doi: 10.1111/jph.12174

Marzano, S. L., Nelson, B. D., Ajayi-Oyetunde, O., Bradley, C. A., Hughes, T. J., Hartman, G. L., et al. (2016). Identification of diverse mycoviruses through metatranscriptomics characterization of the viromes of five major fungal plant pathogens. *J. Virol.* 90, 6846–6863. doi: 10.1128/JVI.00357-16.

Nahalkova, J., Fatehi, J., Olivain, C., and Alabouvette, C. (2008). Tomato root colonization by fluorescent-tagged pathogenic and protective strains of *Fusarium oxysporum* in hydroponic culture differs from root colonization in soil. *FEMS Microbiol. Lett.* 286, 152–157. doi: 10.1111/j.1574-6968.2008.01241.x

Niño-Sánchez, J., Tello, V., Casado-Del Castillo, V., Thon, M. R., Benito, E. P., and Díaz-Mínguez, J. M. (2015). Gene expression patterns and dynamics of the colonization of common bean (*Phaseolus vulgaris L.*) by highly virulent and weakly virulent strains of *Fusarium oxysporum*. *Front. Microbiol.* 6:234. doi: 10.3389/fmicb.2015.00234

Paz, Z., García-Pedrajas, M. D., Andrews, D. L., Klosterman, S. J., Baeza-Montanez, L., and Gold, S. E. (2011). One step construction of Agrobacterium-Recombination-ready-plasmids (OSCAR), an efficient and robust tool for ATMT based gene deletion construction in fungi. *Fungal Genet. Biol.* 48, 677–684. doi: 10.1016/j.fgb.2011.02.003.

Pearson, M. N., Beever, R. E., Boine, B., and Arthur, K. (2009). Mycoviruses of filamentous fungi and their relevance to plant pathology. *Mol. Plant Pathol.* 10, 115–128. doi: 10.1111/j.1364-3703.2008.00503.x

Pouralibaba, H. R., Pérez-de-Luque, A., and Rubiales, D. (2017). Histopathology of the infection on resistant and susceptible lentil accessions by two contrasting pathotypes of *Fusarium oxysporum f.* sp. lentis. *Eur. J. Plant Pathol.* 148, 53–63. doi: 10.1007/s10658-016-1068-6

Prieto, P., Moore, G., and Shaw, P. (2007). Fluorescence *in situ* hybridization on vibratome sections of plant tissues. *Nat. Protoc.* 2, 1831–1838. doi: 10.1038/nprot.2007.265

Ramos, B., Alves-Santos, F. M., García-Sánchez, M. A., Martin-Rodrigues, N., Eslava, A. P., and Díaz-Mínguez, J. M. (2007). The gene coding for a new transcription factor (ftf1) of *Fusarium oxysporum* is only expressed during infection of common bean. *Fungal Genet. Biol.* 44, 864–876. doi: 10.1016/j.fgb.2007.03.003

Sarmiento-Villamil, J. L., Prieto, P., Klosterman, S. J., and García-Pedrajas, M. D. (2018). Characterization of two homeodomain transcription factors with critical but distinct roles in virulence in the vascular pathogen *Verticillium dahliae*. *Mol. Plant Pathol.* 19, 986–1004. doi: 10.1111/mpp.12584

Sharzei, A., Banihashemi, Z., and Afsharifar, A. (2007). Detection and characterization of a double-stranded RNA mycovirus in *Fusarium oxysporum f.* sp. melonis. *Iran J. Plant Path.* 43, 9–26.

Upasani, M. L., Gurjar, G. S., Kadoo, N. Y., and Gupta, V. S. (2016). Dynamics of colonization and expression of pathogenicity related genes in *Fusarium oxysporum f.* sp. ciceri during chickpea vascular wilt disease progression. *PLoS ONE* 11:e0156490. doi: 10.1371/journal.pone.0156490.

Valverde, R. A., Nameth, S. T., and Jordan, R. L. (1990). Analysis of double-stranded-RNA for plant-virus diagnosis. *Plant Dis.* 74, 255–258.

Xie, J., and Jiang, D. (2014). New insights into mycoviruses and exploration for the biological control of crop fungal diseases. *Annu. Rev. Phytopathol.* 52, 45–68. doi: 10.1146/annurev-phyto-102313-050222

Yu, X., Li, B., Fu, Y., Jiang, D., Ghabrial, S. A., Li, G., et al. (2010). A geminivirus-related DNA mycovirus that confers hypovirulence to a plant pathogenic fungus. *Proc. Natl. Acad. Sci. U.S.A.* 107, 8387–8392. doi: 10.1073/pnas.0913535107

Yu, X., Li, B., Fu, Y., Xie, J., Cheng, J., Ghabrial, S. A., et al. (2013). Extracellular transmission of a DNA mycovirus and its use as a natural fungicide. *Proc. Natl. Acad. Sci. U.S.A.* 110, 1452–1457. doi: 10.1073/pnas.1213755110

Zamora, P., Martín, A. B., Dueñas, M., San Martín, R., and Diez, J. J. (2015). *Cryphonectria parasitica* isolates of the same vegetative compatibility type display different rates of transfer of CHV1 hypovirus. *Eur. J. Plant Pathol.* 143, 767–777. doi: 10.1007/s10658-015-0727-3

Zvirin, T., Herman, R., Brotman, Y., Denisov, Y., Belausov, E., Freeman, S., et al. (2010). Differential colonization and defence responses of resistant and susceptible melon lines infected by *Fusarium oxysporum* race 1·2. *Plant Pathol.* 59, 576–585. doi: 10.1111/j.1365-3059.2009.02225.x

Conflict of Interest Statement: The authors declare that the research was conducted in the absence of any commercial or financial relationships that could be construed as a potential conflict of interest.

frontiers in Cellular and Infection Microbiology

ORIGINAL RESEARCH
published: 26 March 2019
doi: 10.3389/fcimb.2019.00064

Alphapartitiviruses of *Heterobasidion* Wood Decay Fungi Affect Each Other's Transmission and Host Growth

Muhammad Kashif[1]*, *Jaana Jurvansuu*[2], *Eeva J. Vainio*[1] and *Jarkko Hantula*[1]

[1] Forest Health and Biodiversity, Natural Resources Institute Finland, Helsinki, Finland, [2] Department of Biology, University of Oulu, Oulu, Finland

Heterobasidion spp. root rot fungi are highly destructive forest pathogens of the northern boreal forests, and are known to host a diverse community of partitiviruses. The transmission of these mycoviruses occurs horizontally among host strains via mycelial anastomoses. We revealed using dual cultures that virus transmission rates are affected by pre-existing virus infections among two strains of *H. annosum*. The transmission efficacy of mycovirus HetPV15-pa1 to a pre-infected host was elevated from zero to 50% by the presence of HetPV13-an1, and a double infection of these viruses in the donor resulted in an overall transmission rate of 90% to a partitivirus-free recipient. On contrary, pre-existing virus infections of two closely related strains of HetPV11 hindered each other's transmission, but had unexpectedly dissimilar effects on the transmission of more distantly related viruses. The co-infection of HetPV13-an1 and HetPV15-pa1 significantly reduced host growth, whereas double infections including HetPV11 strains had variable effects. Moreover, the results showed that RdRp transcripts are generally more abundant than capsid protein (CP) transcripts and the four different virus strains express unique transcripts ratios of RdRp and CP. Taken together, the results show that the interplay between co-infecting viruses and their host is extremely complex and highly unpredictable.

Keywords: mycovirus, partitivirus, transmission, transcripts, *Heterobasidion annosum*, growth rate

OPEN ACCESS

Edited by:
Nobuhiro Suzuki,
Okayama University, Japan

Reviewed by:
Sotaro Chiba,
Asian Satellite Campuses Institute,
Nagoya University, Japan
Maria A. Ayllón,
Polytechnic University of Madrid,
Spain

***Correspondence:**
Muhammad Kashif
muhammad.kashif@luke.fi

Specialty section:
This article was submitted to Fungal Pathogenesis, a section of the journal Frontiers in Cellular and Infection Microbiology

Received: *28 November 2018*
Accepted: *01 March 2019*
Published: *26 March 2019*

Citation:
Kashif M, Jurvansuu J, Vainio EJ and Hantula J (2019) Alphapartitiviruses of Heterobasidion Wood Decay Fungi Affect Each Other's Transmission and Host Growth. Front. Cell. Infect. Microbiol. 9:64. doi: 10.3389/fcimb.2019.00064

INTRODUCTION

Fungi are known to host a wide variety of mycoviruses (Vainio and Hantula, 2018). Unlike other viruses, fungal RNA viruses lack extracellular infective particles, and are transmitted only via intramycelial anastomosis contacts and sexual or asexual spores (Ghabrial and Suzuki, 2009; Son et al., 2015; Vainio et al., 2015b). These viruses replicate within their host's cytoplasm or mitochondria and usually cause no visible phenotypic changes, although both adverse and mutualistic effects have been described (Huang and Ghabrial, 1996; Lakshman et al., 1998; Preisig et al., 2000; Ahn and Lee, 2001; Márquez et al., 2007; Yu et al., 2010; Hyder et al., 2013; Xiao et al., 2014; Vainio et al., 2018b). Some mycoviruses are used as biocontrol agents as demonstrated by the highly successful control of the chestnut blight fungus, *Cryphonectria parasitica*, by hypoviruses in Europe (Milgroom and Cortesi, 2004).

Heterobasidion annosum s.lat. species complex includes some of the most devastating infectious agents of conifer forests in the Northern Hemisphere (Garbelotto and Gonthier, 2013). About 15–17% of *Heterobasidion* strains are infected by one or more viruses (Vainio et al., 2013; Kashif et al., 2015; Vainio and Hantula, 2016). The most common species is the taxonomically unclassified Heterobasidion RNA virus 6 (HetRV6) which accounts for 70% of double stranded RNA (dsRNA) infections in *Heterobasidion* isolates of European origin, but also viruses of the families *Partitiviridae* and *Narnaviridae* are known to inhabit *Heterobasidion* mycelia (Ihrmark, 2001; Vainio et al., 2011b, 2012, 2015a). Both partitiviruses and HetRV6 may transmit across vegetatively incompatible or distantly related host isolates of *Heterobasidion* in laboratory and natural forest environments (Ihrmark, 2001; Vainio et al., 2010, 2011a,b, 2013, 2015b). In addition, uncharacterized dsRNA elements have been shown to be present in both basidiospores and conidia (Ihrmark et al., 2002, 2004), but only HetRV6 has been identified in basidiospores (Vainio et al., 2015b).

Most of the mycovirus species in *Heterobasidion* spp. belong to the family *Partitiviridae* with more than 20 species observed in these fungi. Partitiviruses have genomes composed of two segments of dsRNA packed in separate protein capsids and encoding for a putative RNA-dependent RNA polymerase (RdRp) and a capsid protein (CP) (Ihrmark, 2001; Vainio et al., 2010, 2011a,b, 2013; Kashif et al., 2015). The ratio of the RdRp and CP segments and their transcripts in infected mycelia usually deviates from 1:1, and is virus species specific but responds to environmental conditions (Jurvansuu et al., 2014).

Partitiviruses of *Heterobasidion* spp. are mostly cryptic or have only slight effects on their hosts (Vainio et al., 2010, 2012), but Heterobasidion partitivirus 13 strain an1 (HetPV13-an1) originally observed in *H. annosum* causes serious growth debilitation in both *H. annosum* and *H. parviporum* (Vainio et al., 2018b). Also in other fungi, partitiviruses have been shown to cause variable phenotypical changes or hypovirulence (Magae and Sunagawa, 2010; Bhatti et al., 2011; Xiao et al., 2014; Zheng et al., 2014; Zhong et al., 2014; Sasaki et al., 2016).

Multiple virus infections are common among *Heterobasidion* strains (Vainio et al., 2012, 2013, 2015a,b; Kashif et al., 2015; Hyder et al., 2018) as well as other fungi such as *Gremmeniella abietina* (Tuomivirta and Hantula, 2005; Botella et al., 2013), *Rhizoctonia solani* (Lakshman et al., 1998), *Helminthosporium victoriae* (Ghabrial et al., 2013), *Cryphonectria parasitica* (Peever et al., 1997), and *Sclerotinia sclerotiorum* (Marzano et al., 2015). The interactions between co-infecting viruses and their hosts may have a major effect on the ecology of both fungi and their viruses. Such interactions have recently been studied also among few other fungal viruses (Hillman et al., 2018). As one extreme, Zhang et al. (2016) showed mutualistic interactions in two virus strains, where the capsidless positive-sense ssRNA virus yado-kari virus 1 (YkV1) takes over the capsid protein of a dsRNA virus yado-nushi virus 1 (YnV1), and appears thereafter to replicate like a dsRNA virus. Also both a megabirnavirus (Sasaki et al., 2016) and a chrysovirus (Wang et al., 2014) have been shown to confer hypovirulence on their hosts when in coinfection with a partitivirus. In addition, the presence of Rosellinia necatrix mycoreovirus 3 (RnMyRV3) in recipient mycelia restricts horizontal transmission of Rosellinia necatrix partitivirus 1 (RnPV1) and Rosellinia necatrix megabirnavirus 1 (RnMBV1) (Yaegashi et al., 2011).

We tested whether the presence of other viruses in the donor or recipient affects the probability of viral transmission, and whether this effect depends on the taxonomic similarity of the co-infecting viruses in *Heterobasidion annosum*. We also determined the effects of viral co-infections on the host's growth rate and on the ratio of viral RdRp and CP transcripts in the mycelium, and compared the results to those measured from single infections.

MATERIALS AND METHODS

Virus Strains

In order to test the effect of similarity of co-infecting viruses on transmission efficacy, phenotypic outcome of infection, and viral transcript levels, we selected two very closely related Heterobasidion partitivirus 11 strains, HetPV11-au1 and HetPV11-pa1 with 99% RdRp identity at the amino acid level (aa), and two moderately related partitiviruses, HetRV13-an1 and Heterobasidion partitivirus 15 strain pa1 (HetPV15-pa1) sharing 68% (aa) identity, being only distantly related (with 31% aa identity) to the other two viruses (**Supplementary Table 1**). HetPV11-au1 was originally hosted by *H. australe* strain 06111 of the *H. insulare* complex and HetPV11-pa1 by *H. parviporum* 06101 of the *H. annosum* complex. The RdRp encoding genome segments (Genbank accessions HQ541328 and HQ541329) of both strains have been characterized previously (Vainio et al., 2011a). In this study, we characterized the complete sequences of the CP encoding genome segments of both HetPV11 strains in order to determine their identity and screen their transmission between fungal strains.

The fungal strains *H. australe* and *H. parviporum* hosting HetPV11-au1 and HetPV11-pa1 were cultivated on MOS agar plates. The dsRNA was isolated by cellulose affinity chromatography and agarose gel electrophoresis followed by purification (Jurvansuu et al., 2014). Complementary DNA was made by PCR amplification using tagged random hexamer primers (Márquez et al., 2007) and thereafter cloned as previously (Vainio et al., 2011a). Sequence ends were determined by adapter ligation and PCR amplification with specific primers (Lambden et al., 1992). The sequences were compared to other viruses in GenBank using MAFFT alignment and NCBI BlastP.

Preparation of Single Virus Infected Donor and Recipient Fungal Strains

Two heterokaryotic isolates of *Heterobasidion annosum* (03021 and 94233) were used as viral hosts in this investigation (**Table 1**). No viruses have been observed in the original isolate 03021 whereas isolate 94233 was the native host of HetPV13-an1 and hosted also cryptic mitoviruses (Vainio et al., 2015a, 2018b). The 94233-32D strain used in this study had been cured of HetPV13-an1 by thermal treatment (Vainio et al., 2018b).

Virus transmission was examined using *H. annosum* 03021 as a virus donor and *H. annosum* 94233/32D as a recipient. However, the original 94233 isolated from the nature was used

TABLE 1 | Fungal isolates and alphapartitivirus strains and their relevance.

Fungal isolate	Partitivirus infection	Relevant information	Origin	References
H. annosum 94233	HetPV13-an1	Virus causes serious disease on the host	Poland 1994	Kashif et al., 2015; Vainio et al., 2018b
H. annosum 94233/32D	None	94233 cured of HetPV13-an1, normal growth rate	Poland	Vainio et al., 2018b
H. parviporum 95122	HetPV15-pa1	Virus shares 68% RdRp aa identity with HetPV13-an1	Russia 1995	Kashif et al., 2015
H. annosum 03021	None	dsRNA free isolate	Finland 2003	Unpublished, Kari Korhonen, Luke culture collection
H. parviporum 06101	HetPV11-pa1	Cryptic virus sharing 97% RdRp nt identity with HetRV11-au1	Bhutan 2006	Vainio et al., 2011a
H. australe 06111	HetPV11-au1	Cryptic virus sharing 97% RdRp nt identity with HetRV11-pa1	Bhutan 2006	Vainio et al., 2011a

as the HetPV13-an1 hosting recipient. Prior to the experiments, each of the four virus strains were transmitted individually to the donor strain 03021 (not known to host viruses) (Vainio et al., 2011a,b) and to the recipient strain 94233-32D to obtain single infections of all partitiviruses in both strains. These transmissions were done using original or non-native hosts of these viruses (**Supplementary Table 2**) using dual cultures on single malt extract agar (MEA) plates incubated at 20°C for 4–8 weeks until the formation of clear hyphal contacts and a demarcation zone indicating somatic incompatibility between the strains (**Figure 1A**) as described previously (Ihrmark et al., 2002; Vainio et al., 2013). After the incubation, subcultures were established from the recipient side of the plate and the presence of viruses was examined using RT-PCR and host identity as a recipient with a pairing test (see below). However, transfer of HetPV15-pa1 to the recipient was not successful, and therefore 94233 with single HetPV15-pa1 was obtained by screening single hyphal tips of coinfected (HetPV13an1 and HetPV15-pa1) isolates. Double infected strains of *H. annosum* 03021 were generated during the transmission experiments to single infected 94233-32D when HetPV15-infected strains of 03021 (donor) received viruses from 94233 infected by either HetPV11-pa1, HetPV11-au1, or HetPV13-an1 (**Table 2**).

Transmission Frequency Test

In order to test the effects of single viruses hosted by the recipient on the transmission of other viruses we made 20 dual cultures (Vainio et al., 2013) between each of the donors with one of the recipients with one or no partitiviruses on a single MEA plate (**Figure 2A**) resulting in a total of 320 transmission trials. After the incubation, subcultures were established from the recipient side of the plate and the presence of viruses was examined using RT-PCR (see below). In addition, six randomly selected plates from each donor-recipient pair were additionally sampled from the donor side in order to test whether reciprocal virus transmission had occurred.

Similarly, the effect of viruses to each other's transmission in a co-infection situation (two viruses in the same donor) was tested using HetPV15-pa1 in co-infection with either HetPV13-an1, HetPV11-au1, or HetPV11-pa1 in donor 03021, and using 94233-32D as a recipient. This experiment was conducted using 20 replicates.

In all experiments on MEA plates, mycelia was picked from recipient side of the culture using a sterilized Pasteur pipette with a diameter of 5 mm from 3 sampling points, unless the area occupied by the slowly growing recipient strain allowed sampling from only one spot. The three subcultures were then combined, cultured on modified orange serum (MOS) agar covered with a cellophane membrane and analyzed for the transmission of viruses using RT-PCR with both RdRp and CP primers (**Supplementary Table 3**). The significance of the difference between transmissions from hosts with different virus status was tested using Fisher's exact test.

Fungal Strain Confirmation

Single Hyphal Tip Isolation

To get pure cultures of virus infected strains of *H. annosum* 03021 and 94233, three or four independently infected recipient subcultures from all obtained virus-host combinations were selected randomly for single hyphal tip isolations. The hyphal tips were collected under a binocular microscope with a modified Pasteur pipette using 1–3 day old cultures grown on 2% MEA as described by Vainio et al. (2010). The isolated hyphal tips were allowed to recover on MEA plates for 3–5 days before transfer to MOS agar plates covered by cellophane membranes. The mycelium was used to extract RNA for virus screening with RT-PCR and DNA for genetic fingerprinting to confirm the genotype of the recipient host. These purified cultures were then used for transmission, growth rate and RT-qPCR experiments.

Pairing Test and Genotyping (DNA Extraction and Microsatellite Markers)

The genotypes of the recipient strains were investigated using somatic compatibility tests (Stenlid, 1985) to verify their identity. In this experiment, the recipient subcultures were inoculated on a single plate with the original partitivirus-free recipient strain and the donor strain, and hyphal fusion was interpreted as a sign of genetic similarity. Additionally, the genotypes of

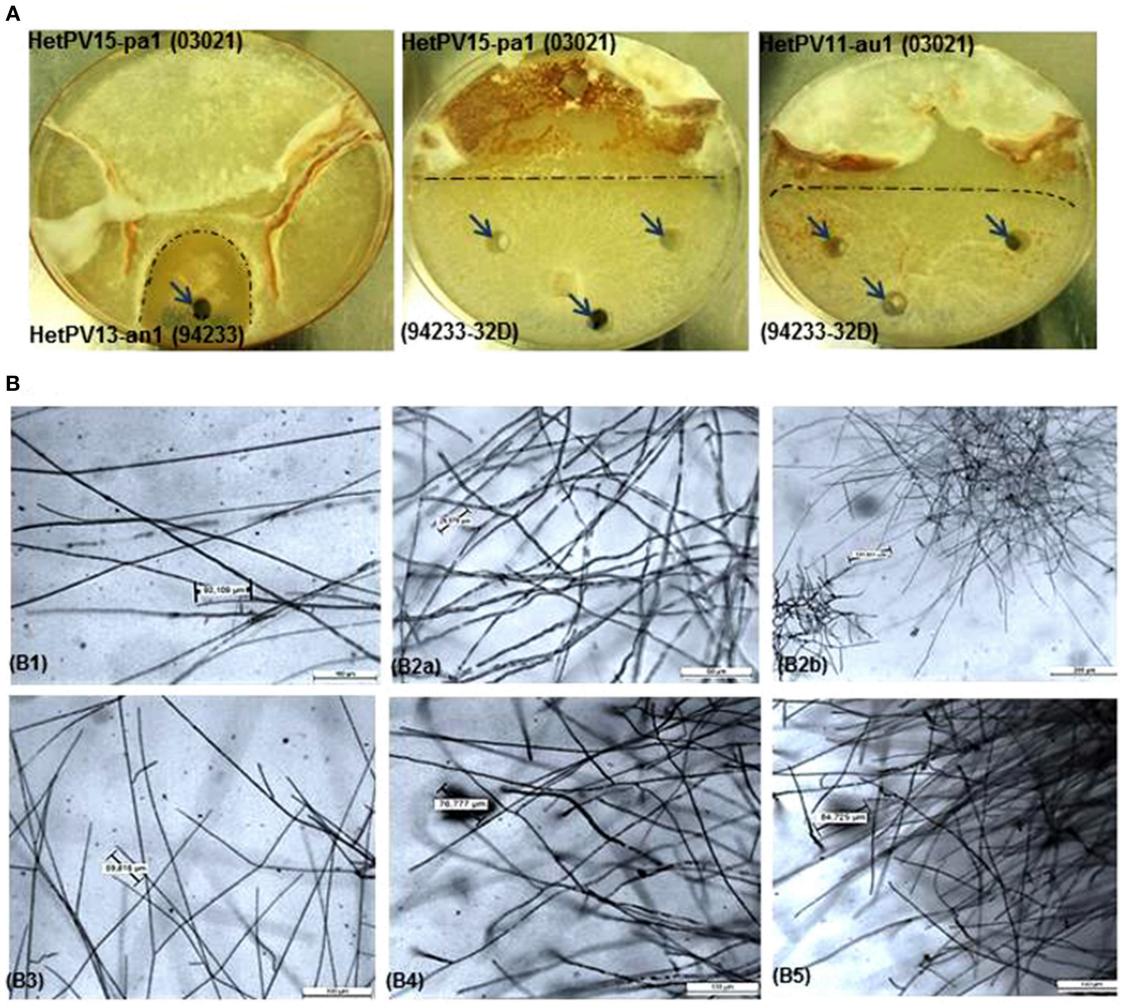

FIGURE 1 | Hyphal phenotype and morphology of *Heterobasidion* strains with or without partitivirus infection, **(A)** Phenotype of dual cultures showing the demarcation area (dark dashed lines) between donor and recipient isolates and sampling spots shown by arrows, **(B)** morphology of fungal cultures under light microscope in different magnifications with eyepiece 10X/20M before and after infection with alphapartitiviruses, (B1) virus-cured 94233 (94233/32D(-)) shows normal less branched growth of hyphae (Objective; 10X/0.40), (B2a) native *H. annosum* 94233 infected with HetPV13-an1 (94233(HetPV13-an1)) displaying extensively branched hyphae (Objective; 20X/0.40) and (B2b) microscopic view of accumulated stunted hyphal growth in native 924233(HetPV13-an1) in lower magnification (5X/0.12). Host morphology (B3) transmission of HetPV13-an1 from the donor (03021) to recipient fungal host (94233) shows the same hyphal appearance (Objective; 10X/0.40) as shown in the native host (94233(HetPV13-an1)), (B4) hyphal growth (Objective; 10X/0.40) in 94233 infected with HetPV15-pa1 (94233(HetPV15)) after having lost HetPV13-an1 during dual culture and (B5) 94233 co-infected by HetPV13-an1 and HetPV15-pa1 exhibiting restricted and debilitated hyphal growth [(Objective; 10X/0.40)] as shown above in B2.

all strains that had received viruses were analyzed using three different Random Amplified Microsatellites (RAMS) markers CT, CGA and CCA (Vainio and Hantula, 1999) which also clarified the cases of weak or unclear demarcation zones in somatic compatibility test.

Growth Rate Measurements

The growth rate experiments were conducted using two strains (derivatives of 94233-32D) from each host/virus combination (either one or two viruses in the host) and partitivirus-free controls (94233-32D and 03021) as well as the original 94233 isolate with a natural infection of HetPV13-an1. The tested virus hosting isolates were obtained from the transmission experiments, and selected based on their apparent growth rates on single plates (as estimated by visual inspection) to cover the range of variation for each host/virus combination. The inoculum size was 0.5 cm in diameter and picked as circular agar plug one centimeter from the edge of the fresh mycelium and placed at the center of a 2% MEA plate. Twelve independent biological replicates were used for each isolate.

The fungal growth was recorded every second day after the mycelial growth was established in 3 days after inoculation. The growth was measured for 7–25 days depending on the growth rates of isolates. The area of fungal growth was

TABLE 2 | The transmission of virus strains were tested in donor strains for their possible reciprocal transmission.

	Reciprocal-transmission Infecting virus in donor 94233 (Transmission efficiency)			
Pre-existing virus in recipient 03021	HetPV13-an1	HetPV15-pa1	HetPV11-pa1	HetPV11-au1
HetPV13-an1		50% (3/6)	50% (3/6)	33% (2/6)
HetPV15-pa1	100% (6/6)		50% (3/6)	50%(3/6)
HetPV11-pa1	50% (3/6)	33% (2/6)		0% (0/6)
HetPV11-au1	50% (3/6)	60% (4/6)	0% (0/6)	

measured by a digital planimeter (Planix 10S, Tamaya) and statistical difference was tested using *t*-test in Microsoft Excel 2010 (**Supplementary Table 4**).

Total RNA Isolation and cDNA Synthesis

Total RNA was extracted from fungal mycelia after one (controls or normally growing virus-infected fungal isolates) or 2 weeks (slowly growing single or co-infected fungal isolates) growth on MOS agar plates (Jurvansuu et al., 2014). In brief, fungal mycelia were collected and homogenized by 1–2 mm quartz sand in TRI Reagent (Molecular Research Center Inc., USA) in the Fast-Prep FP120 homogeniser (JT Baker, Holland). Total RNA was then isolated from the fungal sample by TRI Reagent according to manufacturer's recommendations. RNA pellet was eluted into DEPC treated water (G. Biosciences, USA) and the concentration and purity of the isolated RNA were analyzed by NanoVue (GE healthcare, USA).

Complementary DNA (cDNA) was made from 2 μg of DNase I treated total RNA using RevertAid First Strand cDNA Synthesis Kit (Thermo Scientific, USA) and random hexamer primers (Thermo Scientific, USA) as recommended by the manufacturer.

RT-qPCR Quantification for Virus Transcripts (RdRp and CP)

Half-sample volume of water was added to the cDNAs before using them in quantitative-PCR (qPCR). EvaGreen® dye (Solis BioDyne, Estonia) was used in qPCR on Rotor-GeneQ (Qiagen, USA) according to manufacturer's recommendations. PCR primers were used as follows: RNA polymerase II transcription factor (RNA pol2 TF) was used as a reference gene and specific primers based on RdRp and CP genomic segments of four virus strains including HetPV1-13an1, HetPV15-pa1, HetPV11-pa1, and HetPV11-au1 were used for virus transcripts (**Supplementary Table 3**). The CP and RdRp genes of each virus strain in the purified PCR product were cloned into TOPO-pCR2.1 vector using TOPO® TA Cloning Kit (Invitrogen, USA) according to instructions by the manufacturer. The purified plasmids were then used in absolute quantification as shown by Jurvansuu et al. (2014). The normalization of the viral transcript levels was done using the host RNA pol2 TF as a reference gene (Raffaello and Asiegbu, 2013) and the absolute quantities of RNA transcripts or virus copy number were calculated using a standard curve.

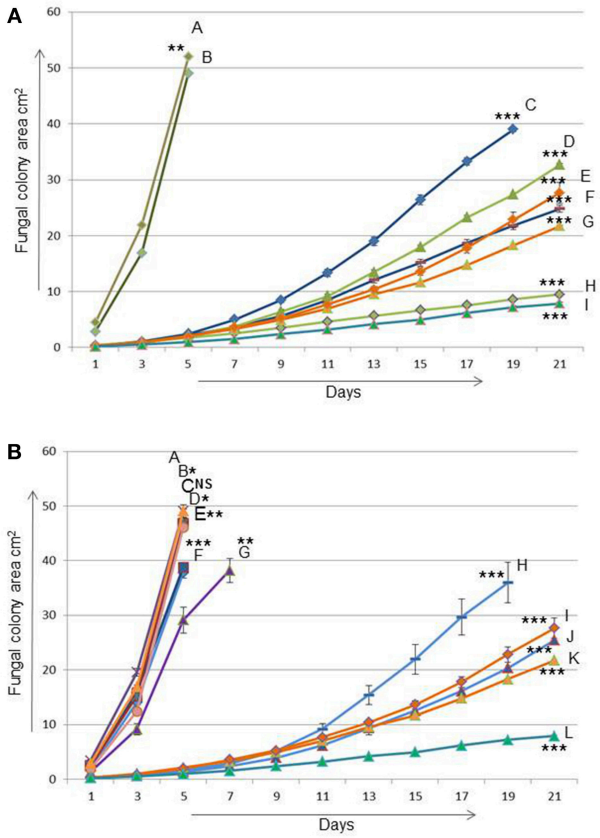

FIGURE 2 | The effect of Heterobasidion partitiviruses in single and coinfection on the growth of their host after transmission from one fungal host (03021) to another (94233) **(A)** A = 03021 is naturally virus-free fungal strain (donor/*H. annosum*), B = 94233/32D is a fungal isolate 94233 (recipient/*H. annosum*) cured of virus HetPV13-an1, C and F = 15pa1 (8 and 6) are two separate fungal isolates (94233) infected by HetPV15-pa1, D and H = 15pa1+13an1 (8 and 6) are two independent isolates (94233) coinfected by HetPV15pa1 and HetPV13-an1, G and E =13an1 (2 and 15) are two separate isolates (94233) where HetPV13-an1 was re-introduced to its native host and I= HetPV13-an1 infection in its native host (94233) **(B)** A= 94233/32D, B and C = 11pa1(1 and 9) isolates are infected by HetPV11-pa1, D and F = 11au1(1 and 7) by HetPV11-au1, E and G = 11au1+13an1(14 and 13) by coinfection of HetPV11-au1 and HetPV13-an1, H and J = 11pa1+13an1(3 and 5) by coinfection of HetPV11-pa1 and HetPV13-an1, I and K = 13an1(15 and 2) by HetPV13-an1 and L = HetPV13-an1 infection in its native host as mentioned above. 94233/32D and 03021 are fungal strains used as recipient and donor in transmission experiments, respectively. The error bars show standard errors of the means of twelve independent biological replicates. The significance of the differences between the mean growth per day of the virus-free/cured and virus infected fungal isolates was calculated with *t*-test and statistically significant differences are shown by asterisks: $^{*}P > 0.05$, $^{**}P < 0.0001$, and $^{***}P < 0.00001$, NS = Non-significant.

RESULTS

Sequence Properties of HetPV11 Capsid Protein

In order to be able to monitor the transmission and transcript levels of the CP-encoding genome segment and to determine the similarity of the genomes of the two different HetPV11 strains, the CP encoding genome segments of both conspecific strains

were characterized (**Supplementary Figure 1**). The genomes of these viruses are composed of two linear dsRNA segments, the larger ones (2,033 and 2,029 bp for HetPV11-pa1 and HetPV11-au1, respectively) of which are coding for putative RdRps (Vainio et al., 2011a). The lengths of the smaller genome segments determined here were 1,818 bp (HetPV11-pa1) or 1,819 bp (HetPV11-au1) including 3′-terminal poly(A) tracts and encoded for a putative CP of 495 aa (nts 124-1611) with a GC content of ca. 52%. The sequences have been deposited to GenBank under the accession numbers MG948857 and MG948858. The CP encoding genome segments of HetPV11-au1 and HetPV11-pa1 share 97.2% nt and 99.8% aa sequence identity. Only one out of the total of 40 single nucleotide polymorphisms located in the CP ORF region results in an amino acid substitution, while the remaining ones are silent. As a comparison, the RdRp encoding genome segments of these virus strains share 97.7% nt sequence identity with 38 sequence polymorphisms in the ORF region causing five aa substitutions (99.2% aa sequence identity) (Vainio et al., 2011a).

The CPs of both HetPV11 strains shared 48% aa sequence identity with Heterobasidion partitivirus 1 (HetPV1-ab1; ADV15442.1), and significantly lower similarity (27% or less) with other viruses such as Diuris pendunculata cryptic virus (27% identity, AFY23215), Rhizoctonia fumigata partitivirus (26%, AJE25831), Amasya cherry disease-associated mycovirus (23%, YP_138536), Ceratobasidium partitivirus CP-b1 (25%, AOX47601), and Cherry chlorotic rusty spot associated partitivirus (23%, CAH03669). The RdRp aa identity between HetPV11 and HetPV1 was ∼75% (Vainio et al., 2011a). These sequence similarities to other viruses were clearly below the species differentiation criteria for the family *Partitiviridae* (≤90% aa sequence identity in the RdRp and ≤80% aa sequence identity in the CP) (Vainio et al., 2018a), confirming that HetPV11 is a distinct species from its closest relative HetPV1 (note that HetPV11 was originally considered to be conspecific with HetPV1, and both viruses were previously named HetRV1; (Vainio et al., 2011a)). Based on ML phylogenetic analyses, the CP and RdRp sequences show similar overall phylogenetic affiliation with other viruses (**Supplementary Figure 1** for CP, RdRp not shown).

Transmission to Pre-Infected and Virus-Free Isolates

The transmission of four alphapartitivirus strains with different taxonomic relatedness in dual cultures resulted in the following findings: HetPV13-an1 had a transmission frequency of 25% to a partitivirus-free host, whereas HetPV11-au1 and HetPV11-pa1 transmitted in 45 and 65% of trials, respectively (**Table 3**). HetPV15-pa1 did not transmit at all to the partitivirus-free recipient even after additional 10 trials done after this experiment.

Transmission efficiency of HetPV15-pa1 was elevated from zero to 50% when the recipient was pre-infected with HetPV13-an1. Interestingly, RT-qPCR showed that HetPV13-an1 had disappeared from four recipients during or after the successful transmission of HetPV15-pa1. The reason for this remains unknown, but it should be noted that we confirmed the presence of HetPV13-an1 in the mycelium in inoculation source plates but not in plates where the transmission trial was conducted. The transmission efficacies of HetPV13-an1, HetPV11-pa1, and HetPV11-au1 to HetPV15-pa1 infected recipient were 40, 50, and 75%, respectively (**Table 3**).

HetPV11-au1 was not transmitted at all to a recipient pre-infected with HetPV11-pa1 and the transmission was poor also vice versa. The transmission efficacy of HetPV11-au1 to recipients pre-infected by HetPV13-an1 and HetPV15-pa1 were 60 and 75%, respectively. HetPV11-pa1 was transmitted to recipients with HetPV13-an1, HetPV15-pa1, and HetPV11-au1 with frequencies of 55, 50, and 15%, respectively (**Table 3**).

Statistical analysis on the differences between transmission rates to virus-free and pre-infected recipients indicated that six out of the 12 viral interactions were affected significantly by pre-infected viruses including transmission of HetPV13-an1 to pre-infected host with HetPV11-au1 ($P = 0.005$), HetPV15-pa1 to the hosts pre-infected with HetPV13-an1 ($P < 0.001$) or HetPV11-au1 ($P < 0.001$), HetPV11-au1 to the hosts with pre-existing viruses HetPV15-pa1 ($P = 0.041$) or HetPV11-pa1 ($P < 0.001$), and HetPV11-pa1 to the host containing HetPV11-au1 infection ($P < 0.001$).

As transmission in dual cultures allows transmission to both directions we also analyzed six isolates from each experiment from the donor side (reciprocal transmission; **Table 2**). Although such a small dataset does not allow meaningful qualitative analysis, the observations confirm that transmission of both HetPV11 strains are hampered by the presence of the other one in the recipient.

Taken together, Heterobasidion partitiviruses in recipient strains have highly variable effects on transmission of new viruses including both enhancement of transmission and mutual exclusion.

TABLE 3 | The transmission efficiencies of alphapartitivirus strains from donor host (*H. annosum* 03021) to recipient fungal isolate (*H. annosum* 94233).

	Virus strains in donor host 03021			
Pre-existing virus in recipient 94233	**HetPV13-an1**	**HetPV15-pa1**	**HetPV11-pa1**	**HetPV11-au1**
Partitivirus free	25% (5/20)	0% (0/20)	65% (13/20)	45% (9/20)
HetPV13-an1		50% (10/20)	55% (11/20)	60% (12/20)
HetPV15-pa1	40% (8/20)		50% (10/20)	75%(15/20)
HetPV11-pa1	25% (5/20)	10% (2/20)		0% (0/20)
HetPV11-au1	70% (14/20)	60% (12/20)	15% (3/20)	

Transmission From a Double Infected Isolate

Transmission of viruses from a double infected donor to a virus-free recipient was tested using three virus combinations. The transmission from a donor with both HetPV15-pa1 and HetPV13-an1 was very efficient with 75% frequency of both viruses and in addition 15% transmission frequency of only HetPV15-an1, thus resulting in a 90% overall transmission rate for HetPV15-pa1. Both changes were statistically significant ($P < 0.001$) compared to transmissions from the single infected strains. No transmission (0/20) was observed from donors with double infections by HetPV15-pa1 and HetPV11-pa1 ($P < 0.001$) or HetPV15-pa1, and HetPV11-au1 ($P < 0.001$) (**Table 4**).

The transmission of both genomic segments RdRp and CP for all the replicates were screened by RT-PCR which consistently showed the transfer of both segments (and thus both particles) of each virus strain. Moreover, pairing tests and genotyping was conducted to confirm the recipient strain of all replicates of successful transmission.

This part of the research, as a whole, showed that HetPV15-pa1 had a significant positive effect on the transmission frequency of HetPV13-an1 and vice versa, whereas coinfecting HetPV15-pa1 prevented completely the transmission of HetPV11 strains.

Growth Rates of Hosts With Single and Double Virus Infections

HetPV13-an1 and HetPV15-pa1 Caused Growth Debilitation

The presence of HetPV13-an1 with or without co-infecting viruses caused an unusual hyphal morphology characterized by dense, stunted, and copiously branched hyphae, whereas the occurrence of other viruses or virus combinations was associated with normal hyphal morphology (**Figure 1B**).

The viral effects on host's growth rate were measured using two independently infected *H. annosum* 94233 strains with 12 parallel measurements for each host/virus combination. *H. annosum* 94233-32D derivatives with single infection of HetPV13-an1 had 87 and 89% reduction in their growth rates (**Figure 2A**). Interestingly, the original isolate 94233 with naturally infected HetPV13-an1 had an even slower growth rate: 96% reduction compared to the cured isolate with no partitiviruses. All these differences were significant (**Supplementary Table 4**).

TABLE 4 | The transmission with co-infected strains in donor host (03021) to partitivirus-free recipient host (94233/32D) (nd = not determined).

Recipient 94233-32D	Virus strains in donor host (03021)		
Viruses transmitted	HetPV15-pa1 +HetPV13an1	HetPV15-pa1 +HetPV11-pa1	HetPV15-pa1 +HetPV11-au1
HetPV15-pa1	90% (18/20)	0% (0/20)	0% (0/20)
HetPV13-an1	75% (15/20)	nd	nd
HetPV11-pa1	nd	0% (0/20)	nd
HetPV11-au1	nd	nd	0% (0/20)

In the case of HetPV15-pa1 the two independently infected *H. annosum* 94233-32D isolates showed 88 and 80% reduced growth rates. In coinfection situation the two double infected (HetPV13-an1 and HetPV15-pa1) strains of 94233-32D had 84 and 95% reduction in their growth rates. The growth rates of these two strains differed significantly from each other and also from the controls and all other isolates (**Figure 2A**).

Variable Growth Effects by Conspecific Virus Strains on Their Fungal Host

Neither of the HetPV11 viruses affected the growth of *H. annosum* 94233-32D as single infections (**Figure 2B**). Also a double infection by HetPV11-au1 and HetPV13-an1 had no or very little effect on its host. However, the 94233-32D strains co-infected by HetPV11-pa1 and HetPV13-an1 showed significant growth debilitation up to 88% with a high range of variation, as half of the twelve individual subcultures displayed irregular growth patterns with slow and fast growing sectors, whereas six subcultures grew slowly but uniformly. In one of the parallel isolates the growth effects were almost as severe as in a single infection of HetPV13-an1 whereas the other one grew almost 7% faster albeit considerably slower than the isogenic control strain 94233-32D (**Figure 2B**). Statistical significance was found only for strains with clear differences in their growth rates (**Supplementary Table 4**).

Taken together the results of growth rate analyses, the presence of co-infecting viruses HetPV13-an1 and HetPV15-pa1 is causing a stable and significant negative effect on their host, whereas the presence of HetPV11 strains has variable phenotypic effects on their hosts when present in combination with HetPV13-an1, and no effects as single infections.

Coinfection of Alphapartitiviruses Affects Transcript Levels of Viral RdRps and CPs

The relative amounts of CP and RdRp viral sequences (copy number of transcripts and genome sequences; designated for simplicity as transcripts from now on) were studied using RT-qPCR for absolute quantification using the same fungal strains as in growth rate experiments. The amounts of transcripts of HetPV15-pa1 remain, on average, almost the same in single and coinfection with HetPV13-an1, although there was variation between the two independently created isolates (**Figure 3A1**). However, the quantity of transcripts of HetPV13-an1 was reduced significantly up to 4.8 and 4.6-fold for RdRp and CP in co-infection with HetPV15-pa1, respectively. Overall, the CP to RdRp transcript ratio of HetPV15-pa1 in two independent isolates was influenced on average by only 10.5% in coinfection. Also the overall change in the ratio between HetPV13-an1 CP and RdRp remained relatively stable (1:4 to 1:6) for single and coinfection (**Figure 3A2**), although the absolute quantities were leveled down (**Figure 3A1**).

Independent double infections by each of the highly similar strains of HetPV11 with HetPV13-an1 showed variable effects when compared with single infections of each of the three virus strains. Comparing the amounts of transcripts in coinfection to single infection, the quantity of viral transcripts for HetPV11-pa1 reduced drastically up to 9.6 and 40 times for CP and

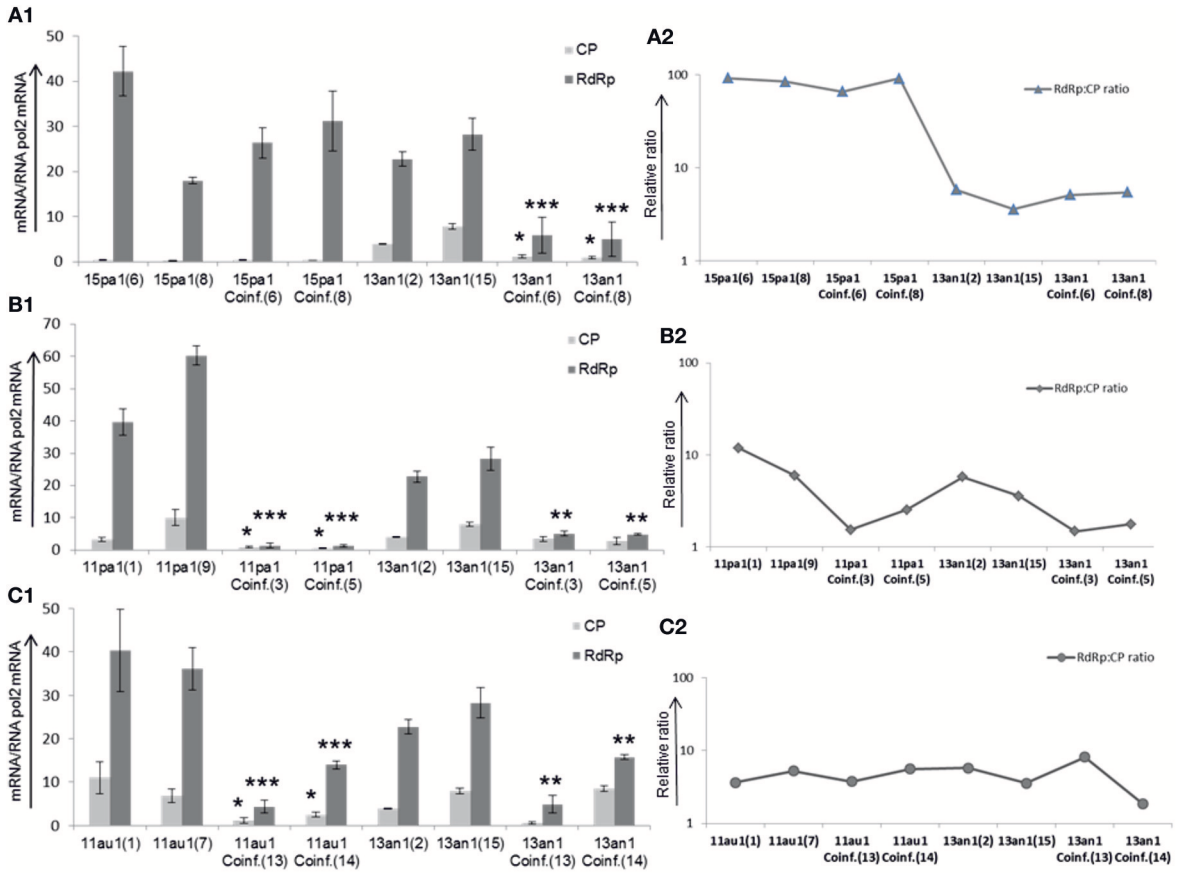

FIGURE 3 | Heterobasidion partitiviruses in coinfection influence the amounts of viral CP and RdRp transcripts in recipient host (94233) **(A1)**. The quantification of viral transcripts was standardized to the amounts of *Heterobasidion* RNA pol2 mRNA. In comparison with HetPV15-pa1, the amounts of HetPV13-an1 transcripts were considerably reduced in coinfection **(A2)**. The relative ratio CP to RdRp of viral transcripts varied to lower or higher extent in each isolate of HetPV15, however the transcripts ratio for HetPV13-an1 remained the same after reduction in coinfection. 15pa1 (6 and 8) are two independent recipient fungal isolates (94233) infected by HetPV15-pa1, 15pa1/13an1Coinf (6 and 8) are two separate isolates coinfected by HetPV15-pa1 and HetPV13-an1 and 13an1 (2 and 15) are two isolates infected by solely HetPV13-an1 **(B1)**. over all amounts of HetPV11-pa1 (shown as 11pa1) transcripts were significantly reduced in coinfection **(B2)**. The relative CP to RdRp transcript ratios of HetPV11 isolates varied followed by considerable reduction whereas that of HetPV13-an1 remained the same after reduction in coinfection **(C1)**. In both isolates the amounts of viral transcripts were significantly affected in coinfection for HetPV11-au1 (shown as 11au1) including variable reduced amounts of HetPV13-an1 in each isolate of coinfection **(C2)**. The relative ratio CP to RdRp of viral transcripts varied to lower or higher extent in each isolate of HetPV11-au1 and HetPV13-an1. The linear scale is used due to variable expression of viral transcripts and log scale for their ratios. The error bars represent standard deviation of at least three separate experiments. The significance of the differences between the mean growth per day of the virus-free/cured and virus infected fungal isolates was calculated with *t*-test and statistically significant differences are shown by asterisks: $*P < 0.05$, $**P < 0.001$, and $***P < 0.0001$.

RdRp, respectively, whereas the CP and RdRp transcript levels of HetPV13-an1 were reduced only by 2 and 5 times, respectively (**Figure 3B1**), only RdRp change being significant. The ratio of CP to RdRp of HetPV11-pa1 changed from 1:5 to 1:13 in the two parallel strains in single viral infection to 1:1.6 and 1:2 in coinfection. The ratio for HetPV13-an1 reduced from 1:3.7 to 1:5 in the two parallel single infected isolates to 1:1.5 and 1:2 in coinfection (**Figure 3B2**).

Conversely, the overall amounts of viral transcripts of HetPV11-au1 were reduced only by 4 times (but significantly) in both viral segments in coinfection, whereas HetPV13-an1 showed 1.3- and 2.5-fold reduction in CP and RdRp transcript quantities in coinfection, only the RdRp change being significant (**Figure 3C1**). No clear direction of change was observed for CP to RdRp ratios of HetPV11-au1 and HetPV13-an1 in single and coinfections (**Figure 3C2**).

Overall, the quantity of viral transcripts of the virus strains was affected by coinfecting viruses except in the case of HetPV15-pa1.

DISCUSSION

In this study, we showed that both conspecific and relatively distantly related alphapartitiviruses affect each other's behavior transmission, phenotypic effects, and viral gene expression in a very complex way. It was expected that the two almost identical viruses (HetPV11-au1 and HetPV11-pa1) mutually hampered each other's transmission between two mycelia of *H. annosum* when present in the recipient (see e.g., Vainio et al., 2015b),

but it was not expected that these two viruses would have very different effects on the transmission of more distantly related viruses: HetPV11-au1 in the recipient enhanced transmission of both HetPV13-an1 and HetPV15-pa1 considerably, whereas HetPV11-pa1 had no significant effect. However, and despite this, neither of the HetPV11 strains affected the transmission of HetPV15-pa1 when present in the same donor mycelium. Increase of transmission by other (co-infecting) viruses was most remarkably seen in HetPV15-pa1, which did not transmit at all without other viruses, but moved very efficiently when HetPV13-an1 co-infected the donor. These viruses have not been found to co-occur naturally, but in our experiments both of them acted as reciprocal helpers as the transmission rate of both viruses increased when they co-infected the donor. As the *Heterobasidion* strain 94233 used in this study was found to host mitoviruses only during the experiments reported here (Vainio et al., 2015a), we did not test their effects on the interactions studied here. Neither did we test the possible effects of host genotype on the virus transmission or phenotypic effects. It should, however, be noted that both mitovirus infection and the host strain may affect the interaction.

Virus transmissions occur frequently among *Heterobasidion* strains in laboratory and in nature, and even between related species (Ihrmark et al., 2002; Vainio et al., 2010, 2013, 2015b, 2017) but no quantitative data has been available on the mutual effects of different viruses transmissions before this study. Here we showed that in the case of HetPV15-pa1 the transmission of a virus occurred either infrequently or not at all between the donor and recipient, but was considerably enhanced by the presence of HetPV13-an1. In regard to HetPV15-pa1, it should also be noted that its transmission rates alone might be higher in nature than on artificial medium as shown previously by Brusini and Robin (2013) for the transmission rates of CHV1 of *C. parasitica*.

It has been shown that mycoviruses may occasionally transmit over fungal species borders (Yaegashi et al., 2013; Yaegashi and Kanematsu, 2016; Vainio et al., 2017; Arjona-Lopez et al., 2018). It has also been well-demonstrated that the transmission rates of fungal viruses depend on their host genome and genetic conservation of the host community (e.g., Biella et al., 2002; Brusini and Robin, 2013). Information from the interactions among other fungal viruses is more restricted, but it has been found that Mushroom bacilliform virus may require a helper-virus, LaFrance isometric virus, for its efficient transmission (Romaine and Schlagnhaufer, 1995). This study adds further evidence for this view by showing that lateral transmission of viruses is strongly affected by other viruses. However, the mechanism(s) of increased transmission rates by co-infecting Heterobasidion viruses remain unsolved, but it has previously been found that Sclerotinia sclerotiorum mycovirus 4 (SsMYRV4) changes the transcription and phenotype of the host fungus so that somatic incompatibility becomes leaky and enhances transmission of other viruses (Wu et al., 2017).

The phenotypic effects of mycovirus double infections on *H. annosum* were highly unexpected. HetPV13-an1 and HetPV15-pa1 caused considerable reduction in the growth rate of their hosts both alone and in coinfection. This is in accordance with previous results showing that these two viruses belong to the same clade among alphapartitiviruses (Kashif et al., 2015) and HetPV13-an1 causes a serious disease on both *H. annosum* and *H. parviporum*, and has a dramatic effect on their gene expression (Vainio et al., 2018b). Furthermore, the double infection by these viruses had a highly negative phenotypic effect (measured here as growth rate) although in some instances, genetically identical fungal strain-virus combinations with dissimilar infection histories (i.e., originating from different transmission trials) had somewhat deviating behavior. This was seen in e.g., the degree of growth rate reduction in strains infected independently by HetPV15-an1, and also between the independent strains with co-infection of HetPV13-an1 and HetPV15-pa1. We also observed considerably different degrees of variation in growth rates between parallel (technical) replicates of strains independently infected by HetPV15-pa1 (i.e., biological replicates). The history of infection expressed itself also as a difference in the growth rates of HetPV13-an1 infections in the original 94233 and 94233-32D strains. Such phenomena have not been reported previously, but these curious findings may point toward the importance of the development of virus-virus-host interactions during the very early infection, when the balance between the viruses and host develops.

Although the presence of HetPV13-an1 with other virus strains usually caused debilitation of its host's growth rate, the coinfection with HetPV11-au1 was an exception as its presence in the mycelium blocked the growth debilitation by HetPV13-an1. This was highly unexpected as the almost identical HetPV11-pa1 had no or a very limited effect. Recalling that the two conspecific HetPV11 strains had also different effects on the transmission of other viruses, they appeared to have a fundamental difference toward co-infecting viruses. It is not known how often highly similar viruses' effects on their hosts differ. In this respect it is, however, interesting that the phenotypic effects of HetPV13-an2 (*H. annosum* S45-8) with 97% nt RdRp/CP similarity to HetPV13-an1 (Kashif et al., 2015; Hyder et al., 2018) did not show similar negative effects on its native host.

The relative amounts of CP and RdRp transcripts were previously shown to vary considerably between different partitiviruses, although each virus had a similar RdRp/CP ratio in different hosts (Jurvansuu et al., 2014). In this study, HetPV13-an1 and HetPV15-pa1 expressed up to 6 and 102 times higher amounts of RdRp than CP transcripts in single infection, respectively, which agrees with the previous study on HetPV13-an1 (Vainio et al., 2015a). No previous information was available on HetPV15-pa1, but the high RdRp/CP ratio in all viruses studied here challenges the previous view that the theoretically expected higher need for CP transcripts (120 proteins in a functional particle compared to one RdRp needed to form a full virus) would usually be reflected in the quantity of transcripts within mycelia (Jurvansuu et al., 2014). It should be noted that the standard curves for qPCR were obtained using cloned cDNA instead of *in vitro* synthesized viral transcripts, which may introduce some bias when comparing the transcript

levels between different genome segments due to possible template discrimination.

In the case of HetPV13-an1, the number of viral transcripts was reduced considerably in mycelia infected by two viruses (instead of one), whereas HetPV15-pa1 had similar amounts of viral transcripts in single and coinfection (with HetPV13-an1) situations. The RdRp/CP ratio, however, remained very similar for both HetPV13-an1 and HetPV15-pa1 as in single infection. Very interestingly, Wu et al. (2010) showed that the replication of Botrytis cinerea mitovirus 1 (BcMV1) is suppressed by another associated RNA virus (BcMV1-S), although it did not influence the debilitation effects on *B. cinerea* caused by BcMV1. Neither did the co-presence of HetPV13-an1 or HetPV15-pa1 affect each other's negative phenotypic effects on the host.

In conclusion, the interactions between partitiviruses of *Heterobasidion* spp. are complicated. Furthermore, especially the effects of HetPV13-an1 and HetPV15-pa1 on each other's transmission frequency and host phenotype makes them highly promising in terms of biocontrol against *Heterobasidion* spp. due to their simultaneous high transmission frequency and negative phenotypic effects.

DATA AVAILABILITY

The datasets generated for this study can be found in NCBI Genbank, MG948857, and MG948858.

AUTHOR CONTRIBUTIONS

MK, EV, and JH conceived and designed the experiments. MK and JJ performed the experiments. MK, JJ, EV, and JH analyzed the data and wrote the paper.

FUNDING

This work was supported by the Academy of Finland (grant numbers 258520 and 309896). Institution Natural Resources Institute Finland provides funds to pay fees for this open access publication.

ACKNOWLEDGMENTS

We are grateful to Juha Puranen, Marja-Leena Santanen, and Tuija Hytönen, and student trainees Ingrid Tobreluts, Krista Tonteri, Ira Lehtonen, Tiia Lehmusmetsä, and Jalal Azam for technical assistance and Minna Rajamäki, Minna Poranen, and Tero Tuomivirta for valuable scientific discussions. We thank Kari Korhonen and Tuula Piri for providing fungal isolates.

SUPPLEMENTARY MATERIAL

The Supplementary Material for this article can be found online at: https://www.frontiersin.org/articles/10.3389/fcimb.2019.00064/full#supplementary-material

REFERENCES

Ahn, I. P., and Lee, Y., H. (2001). A viral double-stranded RNA up regulates the fungal virulence of *Nectria radicicola*. *Mpmi* 14, 496–507. doi: 10.1094/MPMI.2001.14.4.496

Arjona-Lopez, J. M., Telengech, P., Jamal, A., Hisano, S., Kondo, H., Yelin, M. D., et al. (2018). Novel, diverse RNA viruses from mediterranean isolates of the phytopathogenic fungus, *Rosellinia necatrix*: insights into evolutionary biology of fungal viruses. *Environ. Microbiol.* 20, 1464–1483. doi: 10.1111/1462-2920.14065

Bhatti, M. F., Jamal, A., Petrou, M. A., Cairns, T. C., Bignell, E. M., and Coutts, R. H. (2011). The effects of dsRNA mycoviruses on growth and murine virulence of *Aspergillus fumigatus*. *Fungal Genet. Biol.* 48, 1071–1075. doi: 10.1016/j.fgb.2011.07.008

Biella, S., Smith, M. L., Aist, J. R., Cortesi, P., and Milgroom, M. G. (2002). Programmed cell death correlates with virus transmission in a filamentous fungus. *Proc. Biol. Sci.* 269, 2269–2276. doi: 10.1098/rspb.2002.2148

Botella, L., Vainio, E. J., Hantula, J., Diez, J. J., and Jankovsky, L. (2013). Description and prevalence of a putative novel mycovirus within the conifer pathogen *Gremmeniella abietina*. *Arch. Virol.* 160, 1967–1975, doi: 10.1007/s00705-015-2456-5

Brusini, J., and Robin, C. (2013). Mycovirus transmission revisited by *in situ* pairings of vegetatively incompatible isolates of *Cryphonectria parasitica*. *J. Virol. Methods* 187, 435–442. doi: 10.1016/j.jviromet.2012.11.025

Garbelotto, M., and Gonthier, P. (2013). Biology, epidemiology, and control of *Heterobasidion* species worldwide. *Annu. Rev. Phytopathol.* 51, 39–59. doi: 10.1146/annurev-phyto-082712-102225

Ghabrial, S. A., Dunn, S. E., Li, H., Xie, J., and Baker, T. S. (2013). Viruses of *Helminthosporium (cochlioblus) victoriae*. *Adv. Virus Res.* 86, 289–325. doi: 10.1016/B978-0-12-394315-6.00011-8

Ghabrial, S. A., and Suzuki, N. (2009). Viruses of plant pathogenic fungi. *Annu. Rev. Phytopath.* 47, 353–384. doi: 10.1146/annurev-phyto-080508-081932

Hillman, B. I., Annisa, A., and Suzuki, N. (2018). Viruses of plant-interacting fungi. *Adv. Virus Res.* 100, 99–116. doi: 10.1016/bs.aivir.2017.10.003

Huang, S., and Ghabrial, S. A. (1996). Organization and expression of the double-stranded RNA genome of *Helminthosporium victoriae* 190S virus, a totivirus infecting a plant pathogenic filamentous fungus. *Proc. Natl. Acad. Sci. U.S.A.* 93, 12541–12546.

Hyder, R., Pennanen, T., Hamberg, L., Vainio, E. J., Piri, T., and Hantula, J. (2013). Two viruses of *Heterobasidion* confer beneficial, cryptic or detrimental effects to their hosts in different situations. *Fungal Ecol.* 6, 387–396. doi: 10.1016/j.funeco.2013.05.005

Hyder, R., Piri, T., Hantula, J., Nuorteva, H., and Vainio, E. J. (2018). Distribution of viruses inhabiting *Heterobasidion annosum* in a pine-dominated forest plot in southern Finland. *Microb. Ecol.* 75, 622–630. doi: 10.1007/s00248-017-1027-6

Ihrmark, K. (2001). *Double-Stranded RNA Elements in the Root Rot Fungus Heterobasidion annosum*. PhD Dissertation. Swedish University of Agricultural Sciences: Uppsala, Sweden.

Ihrmark, K., Johannesson, H., Stenström, E., and Stenlid, J. (2002). Transmission of double-stranded RNA in *Heterobasidion annosum*. *Fungal. Genet.Biol.* 36, 147–154. doi: 10.1016/S1087-1845(02)00011-7

Ihrmark, K., Stenström, E., and Stenlid, J. (2004). Double-stranded RNA transmission through basidiospores of *Heterobasidion annosum*. *Mycol. Res.* 108, 149–153. doi: 10.1017/S0953756203008839

Jurvansuu, J., Kashif, M., Vaario, L., Vainio, E., and Hantula, J. (2014). Partitiviruses of a fungal forest pathogen have species-specific quantities of genome segments and transcripts. *Virology* 462, 25–33. doi: 10.1016/j.virol.2014.05.021

Kashif, M., Hyder, R., De Vega Perez, D., Hantula, J., and Vainio, E. J. (2015). *Heterobasidion* wood decay fungi host diverse and globally distributed viruses related to *Helicobasidium mompa* partitivirus V70. *Virus Res.* 195, 119–123. doi: 10.1016/j.virusres.2014.09.002

Lakshman, D. K., Jian, J., and Tavantzis, S. M. (1998). A double-stranded RNA element from a hypovirulent strain of *Rhizoctonia solani* occurs in DNA form and is genetically related to the pentafunctional AROM protein of the shikimate pathway. *Proc. Natl. Acad. Sci.U.S.A.* 95, 6425–6429.

Lambden, P. R., Cooke, S. J., Caul, E. O., and Clarke, I. N. (1992). Cloning of non-cultivatable human rotavirus by single primer amplification. *J.Virol.* 66, 1817–1822.

Magae, Y., and Sunagawa, M. (2010). Characterization of a mycovirus associated with the brown discoloration of edible mushroom, *Flammulina velutipes*. *Virol. J.* 7:342. doi: 10.1186/1743-422X-7-342

Márquez, L. M., Redman, R. S., Rodriguez, R. J., and Roossinck, M. J. (2007). A virus in a fungus in a plant: three-way symbiosis required for thermal tolerance. *Science* 315, 513–515. doi: 10.1126/science.1136237

Marzano, S. Y., Hobbs, H. A., Nelson, B. D., Hartman, G. L., Eastburn, D. M., McCoppin, N. K., et al. (2015). Transfection of *Sclerotinia sclerotiorum* with *in vitro* transcripts of a naturally occurring interspecific recombinant of *Sclerotinia sclerotiorum* hypovirus 2 significantly reduces virulence of the fungus. *J.Virol.* 89, 5060–5071. doi: 10.1128/JVI.03199-14

Milgroom, M. G., and Cortesi, P. (2004). Biological control of chestnut blight with hypovirulence: a critical analysis. *Annu. Rev. Phytopathol.* 42, 311–338. doi: 10.1146/annurev.phyto.42.040803.140325

Peever, T. L., Liu, Y. C., and Milgroom, M. G. (1997). Diversity of hypoviruses and other double-stranded RNAs in *Cryphonectria parasitica* in North America. *Phytopathol.* 87, 1026–1033. doi: 10.1094/PHYTO.1997.87.10.1026

Preisig, O., Moleleki, N., Smit, W. A., Wingfield, B. D., and Wingfield, M. J. (2000). A novel RNA mycovirus in a hypovirulent isolate of the plant pathogen *Diaporthe ambigua*. *J. Gen. Virol.* 81, 3107–3114. doi: 10.1099/0022-1317-81-12-3107

Raffaello, T., and Asiegbu, F. (2013). Evaluation of potential reference genes for use in gene expression studies in the conifer pathogen (*Heterobasidion annosum*). *Mol. Biol. Rep.* 40, 4605–4611. doi: 10.1007/s11033-013-2553-z

Romaine, C. P., and Schlagnhaufer, B. (1995). PCR analysis of the viral complex associated with la france disease of *Agaricus bisporus*. *Appl. Environ. Microb.* 61, 2322–2325.

Sasaki, A., Nakamura, H., Suzuki, N., and Kanematsu, S. (2016). Characterization of a new megabirnavirus that confers hypovirulence with the aid of a co-infecting partitivirus to the host fungus, *Rosellinia necatrix*. *Virus Res.* 219, 73–82. doi: S0168-1702(15)30167-2

Son, M., Yu, J., and Kim, K. (2015). Five questions about mycoviruses. *PLoS Pathog.* 11:e1005172. doi: 10.1371/journal.ppat.1005172

Stenlid, J. (1985). Population structure of *Heterobasidion annosum* as determined by somatic incompatibility, sexual incompatibility, and isoenzyme patterns. *Can. J. Bot.* 63, 2268–2273. doi: 10.1139/b85-322

Tuomivirta, T. T., and Hantula, J. (2005). Three unrelated viruses occur in a single isolate of G*remmeniella abietina* var. *abietina type A*. *Virus. Res.* 110, 31–39. doi: S0168-1702(05)00021-3

Vainio, E. J., Chiba, S., Ghabrial, S. A., Maiss, E., Roossinck, M., Sabanadzovic, S., et al. (2018a). ICTV virus taxonomy profile: partitiviridae. *J. Gen. Virol.* 99, 17–18. doi: 10.1099/jgv.0.000985

Vainio, E. J., Hakanp,ää, J., Dai, Y. C., Hansen, E., Korhonen, K., and Hantula, J. (2011a). Species of *Heterobasidion* host a diverse pool of partitiviruses with global distribution and interspecies transmission. *Fungal Biol.* 115, 1234–1243. doi: 10.1016/j.funbio.2011.08.008

Vainio, E. J., and Hantula, J. (1999). Variation of RAMS markers within the intersterility groups of *Heterobasidion annosum* in Europe. *Eur. J. Forest Pathol.* 29, 231–246. doi: 10.1046/j.1439-0329.1999.00148.x

Vainio, E. J., and Hantula, J. (2016). Taxonomy, biogeography and importance of *Heterobasidion* viruses. *Virus Res.* 219, 2–10. doi: 10.1016/j.virusres.2015.10.014

Vainio, E. J., and Hantula, J. (2018). "Fungal viruses," in *Viruses of Microorganisms*, eds Paul Hyman and Stephen T. Abedon (Poole: Caister Academic Press), 193–209.

Vainio, E. J., Hyder, R., Aday, G., Hansen, E., Piri, T., Dogmuş-Lehtijärvi, T., et al. (2012). Population structure of a novel putative mycovirus infecting the conifer root-rot fungus *Heterobasidion annomm* sensu lato. *Virology* 422, 366–376. doi: 10.1016/j.virol.2011.10.032

Vainio, E. J., Jurvansuu, J., Hyder, R., Kashif, M., Piri, T., Tuomivirta, T., et al. (2018b). Heterobasidion partitivirus 13 mediates severe growth debilitation and major alterations in the gene expression of a fungal forest pathogen. *J. Virol.* 92, e01744–17. doi: 10.1128/JVI.01744-17

Vainio, E. J., Jurvansuu, J., Streng, J., Rajamäki, M. L., Hantula, J., and Valkonen, J. P. (2015a). Diagnosis and discovery of fungal viruses using deep sequencing of small RNAs. *J. Gen. Virol.* 96, 714–725. doi: 10.1099/jgv.0.000003

Vainio, E. J., Keriö, S., and Hantula, J. (2011b). Description of a new putative virus infecting the conifer pathogenic fungus *Heterobasidion parviporum* with resemblance to *Heterobasidion annosum* P-type partitivirus. *Arch. Virol.* 156, 79–86. doi: 10.1007/s00705-010-0823-9

Vainio, E. J., Korhonen, K., Tuomivirta, T. T., and Hantula, J. (2010). A novel putative partitivirus of the saprotrophic fungus *Heterobasidion ecrustosum* infects pathogenic species of the *Heterobasidion annosum* complex. *Fungal Biol.* 114, 955–965. doi: 10.1016/j.funbio.2010.09.006

Vainio, E. J., Müller, M. M., Korhonen, K., Piri, T., and Hantula, J. (2015b). Viruses accumulate in aging infection centers of a fungal forest pathogen. *ISME J.* 9, 497–507. doi: 10.1038/ismej.2014.145

Vainio, E. J., Pennanen, T., Rajala, T., and Hantula, J. (2017). Occurrence of similar mycoviruses in pathogenic, saprotrophic and mycorrhizal fungi inhabiting the same forest stand. *FEMS Microbiol. Ecol.* 93. doi: 10.1093/femsec/fix003

Vainio, E. J., Piri, T., and Hantula, J. (2013). Virus community dynamics in the conifer pathogenic fungus *Heterobasidion parviporum* following an artificial introduction of a partitivirus. *Microb. Ecol.* 65, 28–38. doi: 10.1007/s00248-012-0118-7

Wang, L., Jiang, J., Wang, Y., Hong, N., Zhang, F., Xu, W., et al. (2014). Hypovirulence of the phytopathogenic fungus *Botryosphaeria dothidea*: association with a coinfecting chrysovirus and a partitivirus. *J. Virol.* 88, 7517–7527. doi: 10.1128/JVI.00538-14

Wu, M., Zhang, L., Li, G., Jiang, D., and Ghabrial, S. A. (2010). Genome characterization of a debilitation-associated mitovirus infecting the phytopathogenic fungus *Botrytis cinerea*. *Virology* 406, 117–126. doi: 10.1016/j.virol.2010.07.010

Wu, S., Cheng, J., Fu, Y., Chen, T., Jiang, D., Ghabrial, S. A., et al. (2017). Virus-mediated suppression of host non-self recognition facilitates horizontal transmission of heterologous viruses. *PLoS Pathog.* 13:e1006234. doi: 10.1371/journal.ppat.1006234

Xiao, X., Cheng, J., Tang, J., Fu, Y., Jiang, D., Baker, T. S., et al. (2014). A novel partitivirus that confers hypovirulence on plant pathogenic fungi. *J. Virol.* 88, 10120–10133. doi: 10.1128/JVI.01036-14

Yaegashi, H., and Kanematsu, S. (2016). Natural infection of the soil-borne fungus *Rosellinia necatrix* with novel mycoviruses under greenhouse conditions. *Virus Res.* 219, 83–91. doi: 10.1016/j.virusres.2015.11.004

Yaegashi, H., Sawahata, T., Ito, T., and Kanematsu, S. (2011). A novel colony-print immunoassay reveals differential patterns of distribution and horizontal transmission of four unrelated mycoviruses in *Rosellinia necatrix*. *Virology* 409, 280–289. doi: 10.1016/j.virol.2010.10.014

Yaegashi, H., Yoshikawa, N., Ito, T., and Kanematsu, S. (2013). A mycoreovirus suppresses RNA silencing in the white root rot fungus, *Rosellinia necatrix*. *Virology* 444, 409–416. doi: 10.1016/j.virol.2013.07.010

Yu, X., Li, B., Fu, Y., Jiang, D., Ghabrial, S. A., Li, G., et al. (2010). A geminivirus-related DNA mycovirus that confers hypovirulence to a plant pathogenic fungus. *Proc. Natl. Acad.U.S.A.* 107, 8387–8392. doi: 10.1073/pnas.0913535107

Zhang, R., Hisano, S., Tani, A., Kondo, H., Kanematsu, S., and Suzuki, N. (2016). A capsidless ssRNA virus hosted by an unrelated dsRNA virus. *Nat. Microbiol.* 1:15001. doi: 10.1038/nmicrobiol.2015.1

Zheng, L., Zhang, M., Chen, Q., Zhu, M., and Zhou, E. (2014). A novel mycovirus closely related to viruses in the genus alphapartitivirus confers hypovirulence in the phytopathogenic fungus *Rhizoctonia solani*. *Virology* 456, 220–226. doi: 10.1016/j.virol.2014.03.029

Zhong, J., Chen, D., Lei, X. H., Zhu, H. J., Zhu, J. Z., and Da Gao, B. (2014). Detection and characterization of a novel gammapartitivirus in the phytopathogenic fungus *Colletotrichum acutatum* strain HNZJ001. *Virus Res.* 190, 104–109. doi: 10.1016/j.virusres.2014.05.028

Conflict of Interest Statement: MK, EV, and JH are employed by the Natural Resources Institute Finland which has a pending patent application on the combined use of two mycoviruses for biological control based on this work.

The remaining author declares that the research was conducted in the absence of any commercial or financial relationships that could be construed as a potential conflict of interest.

frontiers in Microbiology

ORIGINAL RESEARCH
published: 28 March 2019
doi: 10.3389/fmicb.2019.00626

Molecular Characterization of a Debilitation-Associated Partitivirus Infecting the Pathogenic Fungus *Aspergillus flavus*

Yinhui Jiang[1,2†], Jingxian Wang[3†], Bi Yang[1,2], Qinrong Wang[1,2], Jianjiang Zhou[1,2] and Wenfeng Yu[1,2]*

[1] Key Laboratory of Endemic and Ethnic Diseases, Guizhou Medical University, Ministry of Education, Guiyang, China, [2] Key Laboratory of Medical Molecular Biology, Guizhou Medical University, Guiyang, China, [3] Experiment Center of Stem Cell and Tissue Engineering Research, Guizhou Medical University, Guiyang, China

OPEN ACCESS

Edited by:
Daohong Jiang,
Huazhong Agricultural University, China

Reviewed by:
Massimo Turina,
Italian National Research Council (CNR), Italy
Sotaro Chiba,
Nagoya University, Japan
Huiquan Liu,
Northwest A&F University, China

***Correspondence:**
Yinhui Jiang
jyh5265@163.com

† These authors have contributed equally to this work

Specialty section:
This article was submitted to Virology, a section of the journal Frontiers in Microbiology

Received: *06 January 2019*
Accepted: *12 March 2019*
Published: *28 March 2019*

Citation:
Jiang Y, Wang J, Yang B, Wang Q, Zhou J and Yu W (2019) Molecular Characterization of a Debilitation-Associated Partitivirus Infecting the Pathogenic Fungus Aspergillus flavus. Front. Microbiol. 10:626. doi: 10.3389/fmicb.2019.00626

The opportunistic human pathogenic fungus *Aspergillus flavus* is known to be infected with mycoviruses. In this study, we report a novel mycovirus *A. flavus* partitivirus 1 (AfPV1) that was originally isolated from the abnormal colonial morphology isolate LD-3-8 of *A. flavus*. AfPV1 has spherical virus-like particles about 40 nm in diameter, and three double-stranded RNA (dsRNA) segments (dsRNA1, 2, and 3 with lengths of 1.7, 1.4, and 1.1 kbp, respectively) were packaged in the virions. dsRNA1, dsRNA2, and dsRNA3 each contained a single open reading frame and potentially encoded 62, 42, and 32 kDa proteins, respectively. The dsRNA1 encoded protein shows similarity to the RNA-dependent RNA polymerase (RdRp) of partitiviruses, and the dsRNA2 product has no significant similarity to any other capsid protein (CP) in the GenBank databases, beside some homology with the hypothetical "capsid" protein of a few partitiviruses. The dsRNA3 encodes a protein with no similarity to any protein in the GenBank database. SDS-PAGE and polypeptide mass fingerprint-mass spectrum (PMF-MS) analyses indicated that the CP of the AfPV1 was encoded by dsRNA2. Phylogenetic analysis showed that the AfPV1 and relative viruses were found in an unclassified group inside the *Partitiviridae* family. AfPV1 seems to result in debilitation symptoms, but had no significant effects to murine pathogenicity. These findings provide new insights into the partitiviruses taxonomy and the interactions between viruses and *A. flavus*.

Keywords: *Aspergillus flavus*, dsRNA mycovirus, *Aspergillus flavus* partitivirus 1, unclassified group, debilitation symptoms, murine pathogenicity

INTRODUCTION

Mycoviruses are widespread in almost all major groups of fungi (Ghabrial and Suzuki, 2009; Pearson et al., 2009), and most cause no obvious effects in their hosts, but some do cause obvious symptoms resulting in debilitated virulence, slow growth rate, and poor sporulation (Ghabrial and Suzuki, 2009; Yu et al., 2010; Liu et al., 2014; Xie and Jiang, 2014). Currently recognized

mycoviruses have single-stranded (ss) or double-stranded (ds) RNA, or rarely DNA, as their genetic material (Yu et al., 2010, 2013; Liu et al., 2014). Members of family *Partitiviridae* are classified into four genera, namely *Alphapartitivirus, Betapartitivirus, Gammapartitivirus,* and *Deltapartitivirus* (Vainio et al., 2018). Partitiviruses generally possess two essential dsRNA genome segments (1.3–2.5 kbp in length) containing an open reading frame (ORF), respectively (Nibert et al., 2014). The larger one encodes an RNA dependent RNA polymerase (RdRp) and the smaller one encodes the capsid protein (CP) (Nibert et al., 2014). Partitiviruses are generally encapsidated in isometric particles about 25–40 nm in diameter. Recently, partitivirus capsids were shown to have a so-called "$T = 2$" organization comprising 60 CP dimers arranged on a $T = 1$ icosahedral lattice, as determined by cryo-electron microscopy and three-dimensional (3D) image reconstruction, as well as one determined by X-ray crystallography (Ochoa et al., 2008; Pan et al., 2009; Tang et al., 2010; Xiao et al., 2014). To date, most partitiviruses are typically associated with no obvious effects on their fugal hosts (Nibert et al., 2014). Recently, some interesting reports have clarified about the role of partitivirus in resistance to salinity, regulation of mycotoxin production, and for affecting biocontrol potential in their hosts (Nerva et al., 2017, 2018; Chun et al., 2018).

Aspergillus flavus is an opportunistic pathogen causing aspergillosis diseases in the immunocompromised human population, and the fungus is the second-leading pathogen causing invasive and non-invasive aspergillosis, next to *Aspergillus fumigatus* (Krishnan et al., 2009; Amaike and Keller, 2011). In addition, *A. flavus* produces secondary metabolite aflatoxin, the most toxic, and potent hepatocarcinogenic natural compound (Klich, 2007). Until recent years, the only drugs available to treat aspergillosis are amphotericin B, itraconazole, voriconazole, posaconazole, and caspofungin (Hedayati et al., 2007). But *A. flavus* infections are often complicated by resistance or refractoriness to current antimicrobial agents (Arendrup, 2014; Paul et al., 2015). Therefore, an urgent need exists for new therapeutic strategies to control *A. flavus* infections.

With the increasing discovery of mycoviruses that are able to selectively infect human pathogenic fungi, mycoviruses have shown the significant potential for biological control agents (Van De Sande et al., 2010; Bhatti et al., 2011; Özkan and Coutts, 2015). So it seems possible that some mycovirus conferring hypovirulence could be used as virus control agents for *A. flavus* infection. Mycoviruses in *A. flavus* have been detected, but usually remain latent and seldom induce symptoms (van Diepeningen et al., 2008). Mycoviruses that confer hypovirulence are generally characterized by a reduction in conidiation, pigmentation, and growth rate (Son et al., 2015). In order to obtain the mycoviruses that cause obvious symptoms in *A. flavus*, 417 *A. flavus* isolates collected from patients and patient's room, were tested for mycovirus elements and morphological observation in this study. At last, a novel partitivirus, *A. flavus* partitivirus 1 (AfPV1), causing obvious symptoms on its host morphology was found. The influence of AfPV1 on pathogenicity of *A. flavus* generating virus-infected and virus-free isogenic lines and the unique characteristics of AfPV1 were analyzed and discussed here.

MATERIALS AND METHODS

Fungal Isolates and Growth Conditions

The single-spore isolate *A. flavus* LD-3-8 was isolated from patient's room of Affiliated Hospital of Guizhou Medical University. A virus-free isolate LD-F was obtained from isolate LD-3-8 by single asexual spore isolates. Isolate LD-F1 derived from LD-F, was labeled with a pyrithiamine resistance (*ptr*) gene using PEG-mediated methods. All *A. flavus* isolates were cultured on potato dextrose agar (PDA) plates and Czapek Agar (CZ) plate at 30°C and stored on PDA slants at 4°C.

Extraction and Purification of dsRNA From Mycelia

Mycelial agar plugs of each isolate of *A. flavus* were cultured on sterilized cellophane films placed on PDA plates (9 cm in diameter) at 30°C in the dark for 3–5 days. Mycelia in each plate were harvested and stored at −80°C until use. Extraction and purification of the dsRNAs from mycelia was carried out using CF-11 cellulose (Sigma, St. Louis, MO, United States) column chromatography as previously described (Morris and Dodds, 1979). DsRNA in each extract was analyzed by electrophoresis on an agarose gel (1%, wt/vol), stained with ethidium bromide and viewed on an UV *trans*-illuminator.

cDNA Cloning, Sequencing, and Sequence Analysis

The dsRNA elements (1.7 kb for dsRNA1, 1.4 kb for dsRNA2, and 1.1 kb for dsRNA3) extracted from isolate LD-3-8 of *A. flavus* were separated by agarose gel electrophoresis, and the individual dsRNA bands were cut off for further analysis. cDNA synthesis and molecular cloning of these dsRNAs were performed using the random-primer (5′-CGATCGATCATGATGCAATGCNNNNNN-3′) amplification method, sequencing of the cDNAs, and analysis of the sequences were done using the procedures described in our previous studies (Jiang et al., 2015). The terminal sequences of each dsRNA were cloned using the modified method described previously (Potgieter et al., 2009).

The full-length cDNA sequence for dsRNA1, dsRNA2, or dsRNA3 was obtained from assembling the partial sequences in the different cDNA clones. ORFs in full-length cDNA sequence were searched using DNAMAN 7.0 (Lynnon Biosoft, Quebec, Canada). Amino acid sequences were aligned using Clustal W implemented in MEGA 6.06 (Tamura et al., 2013). The phylogenetic tree was constructed using the Maximum Likelihood method with a Jones-Taylor-Thornton (JTT) with freqs model, and the optimal trees were statistically

evaluated with a bootstrap of 1,000-replicates using MEGA 6.06 (Tamura et al., 2013).

Purification, Observation, and Polypeptide Mass Fingerprint-Mass Spectrum (PMF-MS) Analyses of Virus Particles

The viral particles (VLPs) were isolated from *A. flavus* isolate LD-3-8 using the modified method described previously (Yu et al., 2010). The isolates were cultured at 30°C for 5 days on sterilized cellophane films placed on PDA. Approximately 25 g mycelia were ground in liquid nitrogen and mixed with four volumes of 0.01 M phosphate buffer saline (PBS) (pH 7.4), and then the mixture was gently shaken on ice for 30 min. The mixture was separated with high-speed centrifugation (10,000 × *g* for 30 min). The supernatant was then subjected to ultracentrifugation at 120,000 × *g* for 2 h under 4°C to precipitate the virus particles in the supernatant. The supernatant containing the virus particles was then overlaid on a centrifuge tube containing sucrose density gradient (10–40%) and centrifuged at 70,000 × *g* for 3 h at 4°C. The gradient containing VLPs was diluted with PBS and ultracentrifuged at 120,000 × *g* for 2 h at 4°C. Five separated fractions were individually measured for the presence of the virus particles by dsRNA detection using the agarose gel electrophoresis. The fractions containing virus particles were carefully collected and suspended using 200 μl PBS. The virus particles were observed under transmission electron microscopy (TEM) after staining with 2% (wt/vol) phosphotungstic acid solution (pH 7.4).

The purified virus particles suspension was loaded on a sodium dodecyl sulfate (SDS)-polyacrylamide (12%) gel stained with Coomassie brilliant blue R250. The resulting protein bands on the gel were individually excised and subjected to matrix-assisted laser desorption/ionization-time of flight mass spectrometry (MALDI-TOF-MS) analysis at Sangon Biotech (Shanghai, China). To avoid missing any proteins during virion preparation, purified virus particles suspension was also directly subjected to liquid chromatography-tandem mass spectrometry (LC-MS/MS) analysis at Sangon Biotech (Shanghai, China).

Horizontal Transmission of Mycoviruses AfPV1

A virus-free isolate LD-F was obtained from isolate LD-3-8 by single asexual spore isolates, and then was labeled with a *ptr* gene using PEG-mediated methods as previously described (Chang et al., 2010). The *ptr* isolate (named LD-F1) with no observable differences in biological properties compared to the parental isolate was used in the paired-culture method as previously described (Wu et al., 2007, 2010; Jiang et al., 2015). This method was used to transfer AfPV1 from isolate LD-3-8 (donor) to the virus-free isolate LD-F1 (recipient) on CZ media (Czapek Agar) (**Figure 4A**). After 10 days of paired-culture, three mycelial agar plugs (marked "1," "2," and "3"; **Figure 4A**) from the colony of virus-free isolate LD-F1 were placed onto a fresh CZ plate containing 0.2 μg/ml pyrithiamine at 30°C and subcultured through five serial transfers onto pyrithiamine-amended media to allow only labeled isolates to grow. Finally, mycelial plugs from the new colonies were placed onto fresh PDA and CZ plates without pyrithiamine. AfPV1 was detected as described above. Total RNA of each culture was extracted using the TRIzol reagent (Invitrogen, United States), and was then used for the RT-PCR reaction with a random nonamer primer 5′-d (NNNNNNNNN)-3′. The specific primers (AfPV-det1: 5′-TCAAATACTACACGAAGGACGAAC-3′ and AfPV-det2: 5′-CATAGGCGGAGAAATCCAGAC-3′) were designed for specific detection of AfPV1.

Growth Rate, Sporulation, and Murine Virulence of *A. flavus*

A square agar plug (5 mm wide) from the margin of each colony was inoculated onto the center of PDA and CZ plates (9 cm in diameter), and cultured at 30°C in the dark. The radial growth rate (RGR) was determined for each developing colony (five replicates for each fungal isolate) at 2 days intervals over a week period as follows: RGR (cm/d) = [(D 4−D 2)/2]/2, where D 4 and D 2 represent the diameter of 4 and 2 days old colonies in each plate, respectively.

After 6 days incubation in the dark at 30°C on PDA plates (9 cm in diameter), conidiospores of *A. flavus* were harvested in 2 mL saline buffer, and spore numbers for each colony were estimated using a haemocytometer; the data were transformed to log 10 before analyses. The length of spore chains were measured under microscope.

In order to assess *A. flavus* burden quantitatively, quantitative PCR (qPCR) was tested on total genomic DNA extracted from homogenized whole lungs of mice using a previously described method (Bhatti et al., 2011; Özkan and Coutts, 2015). For analysis of fungal burden in corticosteroid-treated female mice (Kunming mice, aged 6–8 weeks), immunosuppression was induced with subcutaneous injections of cyclophosphamide (200 mg/kg on days −3, −1, and +2). Spores were harvested from *A. flavus* cultured on PDA medium for 6 days at 30°C. On day 0 inocula containing about 1×10^7 conidia were prepared from *A. flavus* isolates in 30 μl of saline buffer. Mice were anesthetized by injection of chloral hydrate and infected by intranasal instillation. In order to prevent bacterial infections, the drinking water was added 100 mg/L cephalosporin. *A. flavus* burden was assessed by qPCR amplification using the specific primers (Aftub-f:CTAGTGAAGTCTGAGTTGATTGTAT and Aftub-r:CCGGAGAGGGGACGACGA) to amplify *A. flavus* β-tubulin (M38265), and the specific primers (Muact-f:GAGACCTTCAACACCCCAGC and Muact-r: ATGTCACG CACGATTTCCC) to amplify the murine actin (NM_007393) as an internal control. Quantification of both gene targets was performed in triplicate, using ten independent infected mice, and saline-injected mice as control. qPCR assay was performed using SYBR green I (TAKARA, Dalian, China). The data of threshold cycle (Ct) were analyzed with unpaired *t*-tests using GraphPad Prism 5.01 (GraphPad Software, La Jolla, CA, United States). In order to confirm this model represent the virulence of the fungus *A. flavus*, microscopic and histological changes of mice

lung tissues were observed after infection using a previously described method (Lan et al., 2018). The whole lungs of infected mice were putted in 10% paraformaldehyde, and then stained with Haema eosin (HE) for histologic examination. In addtion, lung tissues were also homogenized and diluted by sterile water, and the suspends were coated on PDA plus streptomycin and pyrithiamine at 30°C for *A. flavus* detection.

RESULTS

Complete Sequence and Organization of AfPV1 Genome

Three segments (dsRNA1, dsRNA2, and dsRNA3) were detected in single spore isolate LD-3-8 (**Figure 1A**). The full-length cDNA sequences of those segments were obtained by assembling sequences from their respective overlapping cDNA clones. Results showed that dsRNA1 (GenBank Acc No. MK344768) is 1763 bp long with a GC content of 46.2%, dsRNA2 (GenBank Acc No. MK344769) is 1422 bp long with a GC content of 46.7%, and dsRNA3 (GenBank Acc No. MK344770) is 1186 bp long with a GC content of 45.4% (**Figure 1B**). Sequencing analysis indicated that dsRNA1 contains a single ORF from nucleotides (nt) 19 to 1665, which putatively encodes a protein with 547 amino acid (aa) residues and a molecular mass of 63 kDa (**Figure 1B**). The dsRNA2 encodes a single ORF encoding a putative 368-aa protein with a molecular mass of 42 kDa (**Figure 1B**), and dsRNA3 single ORF encodes a putative 280-aa protein with a molecular mass of 32 kDa (**Figure 1B**).

BlastP search indicated that the dsRNA1 product shares highly significant similarities with the RdRp of several viruses in the family *Partitiviridae*, including Botryosphaeria dothidea virus 1 (83% aa sequence identities, GenBank Acc No. AIE47694), *Colletotrichum acutatum* RNA virus 1 (76% aa sequence identities, GenBank Acc No. AGL42312), and *Valsa cypri* partitivirus (85% aa sequence identities, GenBank Acc No. AIS37548) (**Table 1**). No other significant similarity can be found between the putative protein encoded by dsRNA2 and any other CP sequences, except identities of 76 and 59% with the hypothetical proteins encoded by Botryosphaeria dothidea virus 1 and *C. acutatum* RNA virus 1 (**Table 1**). Moreover, no homologous sequences were found when dsRNA3 was queried in the GenBank database. The percent of amino acid identities are listed in **Table 1,** when dsRNA1 and dsRNA2 were queried in the GenBank database by BlastP.

The 5′-untranslated regions (UTRs) of the plus strands of dsRNA1, dsRNA2 and dsRNA3 are 18, 112, and 124 bp long, respectively, and show conserved nucleotides at the 5′ terminus (AAACUUUUGU) (**Figure 1C**). A similar motif (AAACUUUUG/AU/G) is present in the genomes of Botryosphaeria dothidea virus 1. The 3′-UTRs differ in length, and there is little sequence conservation (**Figure 1C**). This is consistent with observations for multi-component RNA viruses, where the 5′ terminal sequences are essential for recognition by the virus RdRp during viral RNA replication. Such conserved sequences near the 5′ termini of partitiviruses are thought to be involved in RdRp recognition for RNA packaging and/or replication (Nibert et al., 2014).

To obtain dsRNA segregation patterns in isolates, we conducted a transmission test of the dsRNAs to asexual conidia spores and other *A. flavus* isolates. In our study, dsRNA1, dsRNA2, and dsRNA3 could not be detected separately and they always appear to coexist in *A. flavus*. Moreover, the three segments appear to coexist in purified VLPs (**Figure 2B**). These results should suggest that the dsRNAs (dsRNA1, dsRNA2, and dsRNA3) belong to the same virus, and this virus is to be assigned to the family *Partitiviridae*. So we named this virus as AfPV1.

Observation and PMF-MS Analyses of Virus Particles

Whether virus particles really exist in the virus preparations, the preparations were subjected to TEM. Spherical VLPs of about 40 nm in diameter were detected under TEM after purification (**Figure 2A**). Three dsRNA segments released from purified VLPs were similar in size to those isolated directly from mycelia of isolate LD-3-8 (**Figure 2B**). The purified VLPs were also examined by SDS-PAGE and Coomassie brilliant blue staining, and a single major band with molecular weight of 42 kDa possibly represents the CP (**Figure 2C**). The band was extracted from a gel and subjected to PMF-MS analysis. Five peptide fragments with ion scores higher than 31 (identity or extensive homology, $p < 0.05$), matched to the deduced amino acid sequence of the protein encoded by dsRNA2 (**Supplementary Table S2**). To avoid missing any proteins during virion preparation, the purified virus particles suspension was also directly subjected to PMF-MS analysis. Seventeen peptide fragments with ion scores higher than 0 (identity or extensive homology, $p < 0.05$), matched to the deduced amino acid sequence of the protein encoded by dsRNA2 (**Supplementary Table S3**). Both PMF-MS results did not match to the deduced amino acid sequence of the protein encoded by dsRNA1 or dsRNA3. The results unequivocally indicated that the CP of the AfPV1 was encoded by dsRNA2, which is similar to the finding for *C. acutatum* RNA virus 1 (Zhong et al., 2014a).

Phylogenetic Analysis of AfPV1

Multiple alignments of RdRp amino acid sequences of the representative viruses in the family *Partitiviridae* were performed and revealed that the RdRp domain of AfPV1 contains six conserved motifs in the putative RdRps of mycoviruses (Bruenn, 1993; **Figure 3A**). To analyze the phylogenetic position of AfPV1, a phylogenetic tree was constructed using deduced amino acid sequences of the RdRp of AfPV1 and other selected dsRNA viruses from the family *Partitiviridae*. These viruses revealed four recognized genera (*Alphapartitivirus, Betapartitivirus, Gammapartitivirus,* and *Deltapartitivirus*) and a new genus (Epsilonpartitivirus) in family of *Partitiviridae* (Nerva et al., 2017; Vainio et al., 2018). This analysis shows that AfPV1 and relative viruses (Botryosphaeria dothidea virus 1, *C. acutatum* RNA virus 1, *V. cypri* partitivirus, *U. virens* partitivirus 2, and *U. virens* partitivirus 3) were found in a unclassified cluster, and this

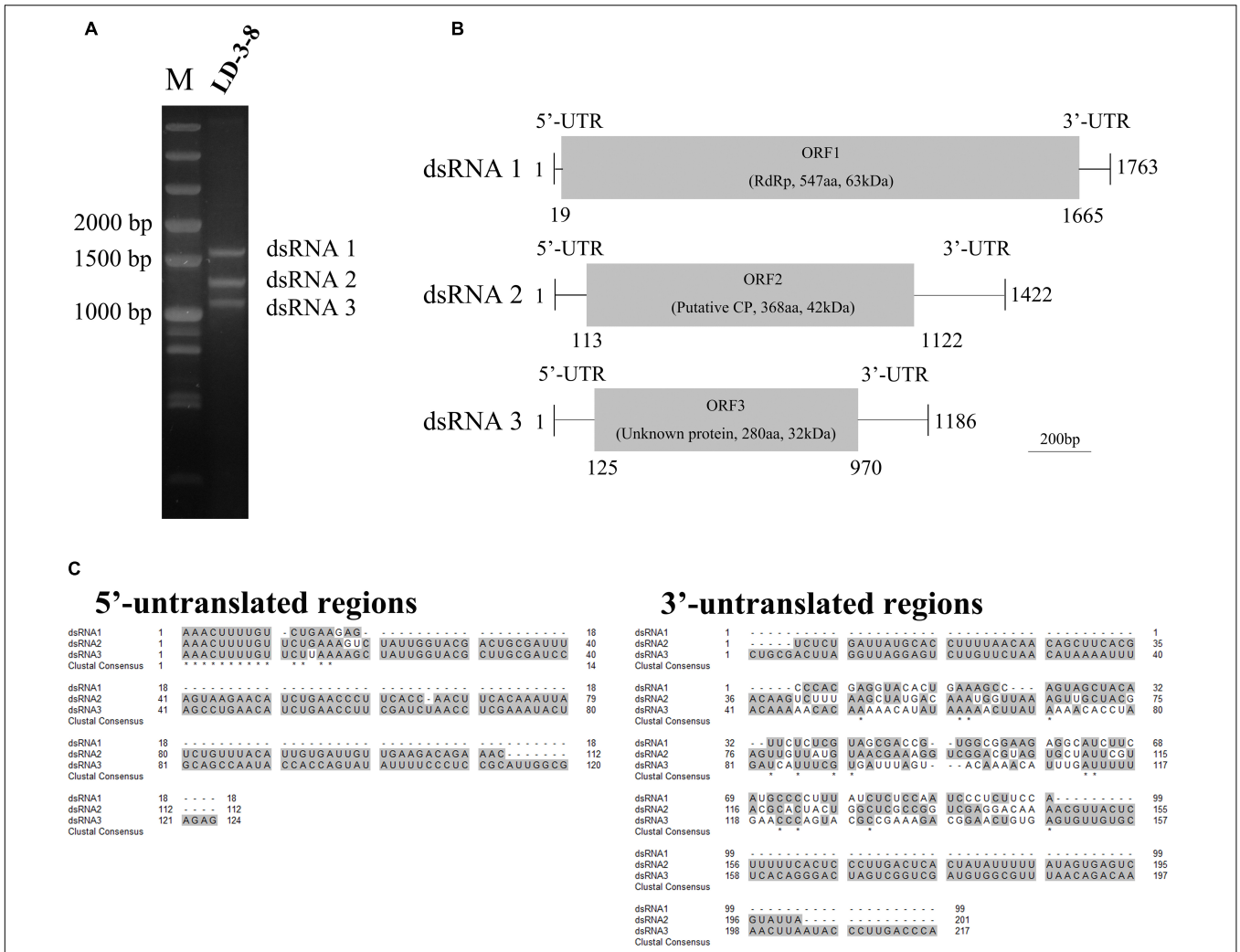

FIGURE 1 | Genomic organization of AfPV1. **(A)** Agarose gel electrophoresis of the dsRNA segments extracted from *Aspergillus flavus* isolate LD-3-8. The molecular sizes are indicated on the left with numbers. **(B)** Genome organization of dsRNA1, dsRNA2, and dsRNA3 indicated by a graphical representation. The dsRNA1 is 1763 bp long and contains an ORF (designated as ORF1), which encodes a putative RdRp with a molecular mass of 63 kDa. The dsRNA2 is 1422 bp long and contains an ORF (designated as ORF2), which encodes a putative coat protein (CP) with a molecular mass of 42 kDa. The dsRNA3 is 1186 bp long and contains an ORF (designated as ORF3), which encodes a protein of unknown function with a molecular mass of 32 kDa. aa, amino acids. **(C)** Identity at the 5′-and 3′-UTR ends of the coding strands of the three genomic segments of AfPV1. Gray shading indicates identical nucleotides in the three segments.

cluster grouped clearly outside of the five genera in *Partitiviridae* family (**Figure 3B**).

Horizontal Transmission and the Effect of AfPV1 in *A. flavus*

Using horizontal transmission methods, the virus-free strain LD-F1 was successfully transfected with AfPV1. Three derivative isolates were obtained from a recipient colony of LD-F1. The mycelia agar plugs were marked "1," "2," and "3" (**Figure 4A**). After subculturing on a CZ plate (0.2 μg/ml pyrithiamine) for 5 generations, the derivative isolates were used for both dsRNA extraction and RT-PCR amplification (**Figure 4B**).

Compared to virus-free isolate LD-F1, the newly AfPV1-infected isolate LD-F1-b displayed debilitation symptoms, including abnormal colonial morphology, slow growth on CZ, and poor sporulation, and that is similar to AfPV1-infected isolate LD-3-8 (**Figures 4C–F**). Moreover, we found that spore chains of these AfPV1-infected isolates (LD-3-8 and LD-F1-b) are shorter, indicating a possible lower sporulation potential (**Figures 4E,F**). Although the AfPV1-infected isolates have caused significantly abnormal colonial morphology (**Figures 4C,D**), the growth rates are not significantly different between AfPV1-infected isolates and virus-free isolates on PDA (**Figure 4F**).

In the murine virulence assays, the lungs tissue of the *A. flavus* (virus-free isolate LD-F1 and AfPV1-infected isolate LD-F1-b) infected mice appeared large numbers of bleeding area compared to saline-injected mice, but no significant differences between LD-F1 and LD-F1-b infected mice (**Supplementary Figure S1**).

TABLE 1 | BlastP analysis of AfPV1 compared to the closest matching sequences in NCBI database, and the percent amino acid identities of putative protein encoded by dsRNA1 and dsRNA2.

Virus	RNA-dependent RNA polymerase (dsRNA1)		hypothetical protein (dsRNA2)	
	Identities	E-value	Identities	E-value
Botryotinia fuckeliana partitivirus 1	450/544 (83%)	0.0	281/370 (76%)	0.0
Colletotrichum acutatum RNA virus 1	409/539 (76%)	0.0	217/370 (59%)	4e-150
Valsa cypri partitivirus	375/440 (85%)	0.0	176/236 (75%)	2e-119
Ustilaginoidea virens partitivirus 3	268/513 (52%)	0.0	96/359 (27%)	2e-22
Ustilaginoidea virens partitivirus 2	264/526 (50%)	2e-174	107/361 (30%)	2e-25
Ophiostoma partitivirus 1	165/515 (32%)	1e-74	N	N
Aspergillus ochraceous virus	187/539 (35%)	8e-74	N	N
Sodiomyces alkalinus partitivirus 2	167/494 (34%)	4e-73	N	N

N means no significant similarity was found via NCBI BlastP analysis. Identity means the identical or similar amino acid residues/total length of the amino acid residues used in sequence comparison analysis. The GenBank accession numbers of the selected viruses are shown in ***Supplementary Table S1****.*

Afer cultured on PDA, *A. flavus* was detected in mice lungs tissue of *A. flavus* (isolate LD-F1 and LD-F1-b) infection, but was not detected in saline-injected mice (**Supplementary Figure S1**). qPCR was performed using the accumulation levels of the *A. flavus*β-tubulin gene as an indication of fungal growth and burden in mice lungs inoculated with virus-free or AfPV1-infected isogenic lines of *A. flavus*. The mice actin gene that was used as an internal control, remained at the same level in all of the qPCR experiments, and there was no β-tubulin gene expression in all saline-injected mice (**Figure 5**). The statistical significance of variances between fungal burdens were calculated using a non-parametric *t*-test. The accumulation levels of β-tubulin were not significantly different between the virus-free and AfPV1-infected isolates ($P = 0.8$; **Figure 5**).

DISCUSSION

Aspergillus flavus is an important fungal pathogen that not only induces diseases in human, animals and plants, but also produces aflatoxins with strong carcinogenic and mutagenic effects (Amaike and Keller, 2011). Nevertheless, mycoviruses are rarely reported in *A. flavus*, only and isolate NRRL 5565 and NRRL 5940 was reported to harbor dsRNA elements (Kotta-Loizou and Coutts, 2017). In this study, we isolated a novel mycovirus (AfPV1) with isometric particles 40 nm in diameter from an abnormal phenotype isolate (LD-3-8) of *A. flavus*. Hypovirulence-associated mycoviruses have shown the significant potential for biological control agents, but the potential of mycoviruses to combat fungal infection in animals and humans is still unknown (Van De Sande et al., 2010;

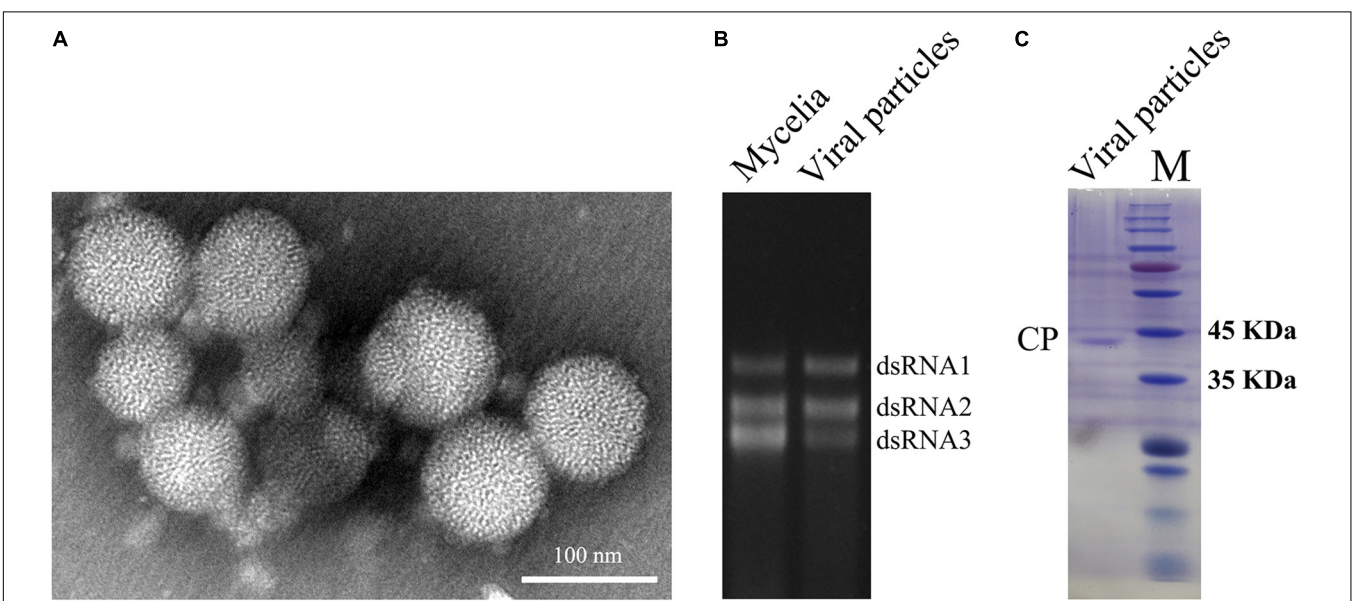

FIGURE 2 | Virus particles of AfPV1. **(A)** TEM observation of the virus particles from *A. flavus* isolate LD-3-8. **(B)** Agarose gel electrophoresed analysis of dsRNA profiles from mycelia and viral particles. **(C)** SDS-PAGE analysis of the purified virus particles showing the 42 kDa protein components. The molecular weight of the protein bands was estimated on the right with numbers.

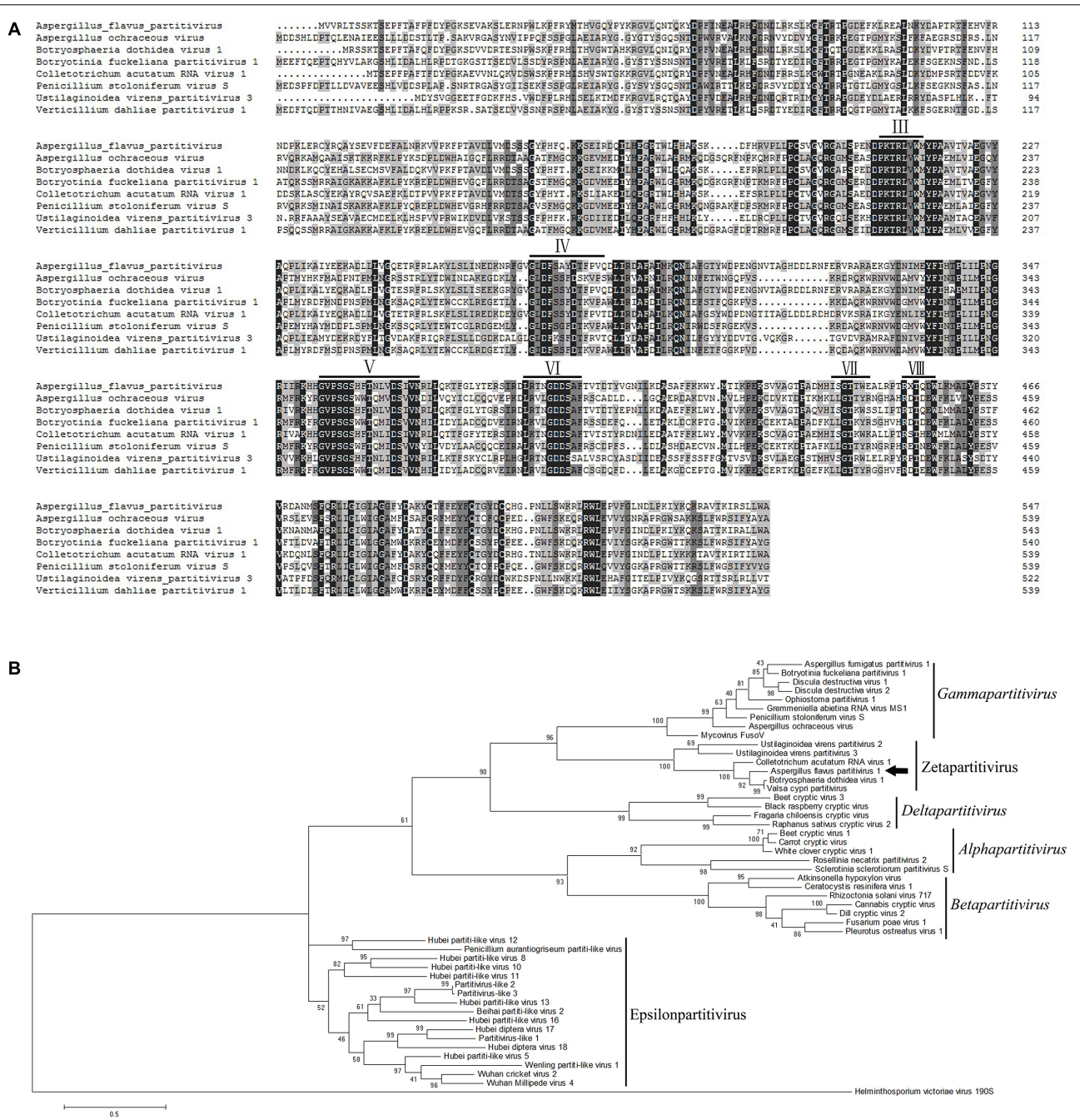

FIGURE 3 | Phylogenetic analysis of AfPV1. **(A)** Amino acid sequence alignment of the core RdRp motifs of AfPV1 and other selected mycoviruses in the family *Partitiviridae*. Similar amino acid residues are shaded in gray. The conserved motifs of RdRp in dsRNA viruses are indicated by numbers (Bruenn, 1993). **(B)** Phylogenetic analysis of the RdRp sequences of AfPV1 and other selected dsRNA mycoviruses in family of *Partitiviridae*. The phylogenic tree was generated based on the Maximum Likelihood method with a 1000-replicate bootstrap search using the program MEGA 6.06, and the bootstrap values are indicated at the branch points. Moreover, the tree was rooted with the RdRp of Helminthosporium victoriae virus 190S, a member of the genus *Totivirus* in the family *Totiviridae*. The arrow indicates the position of AfPV1. The GenBank accession numbers of the selected viruses are shown in **Supplementary Table S1**.

Bhatti et al., 2011; Özkan and Coutts, 2015). Mycoviruses that confer hypovirulence are generally characterized by a reduction in conidiation, pigmentation and growth rate (Son et al., 2015). So we were encouraged by the fact that AfPV1 caused obvious effects on *A. flavus,* such as abnormal colonial morphology, slow growth on CZ, and poor sporulation (**Figure 4**). Nevertheless, we could not detect any significant effect of AfPV1 on its host virulence (**Figure 5**). Histological and microscopic observition of mice lung indicated that the murine model was suitable for testing virulence of *A. flavus* (**Supplementary Figure S1**). The

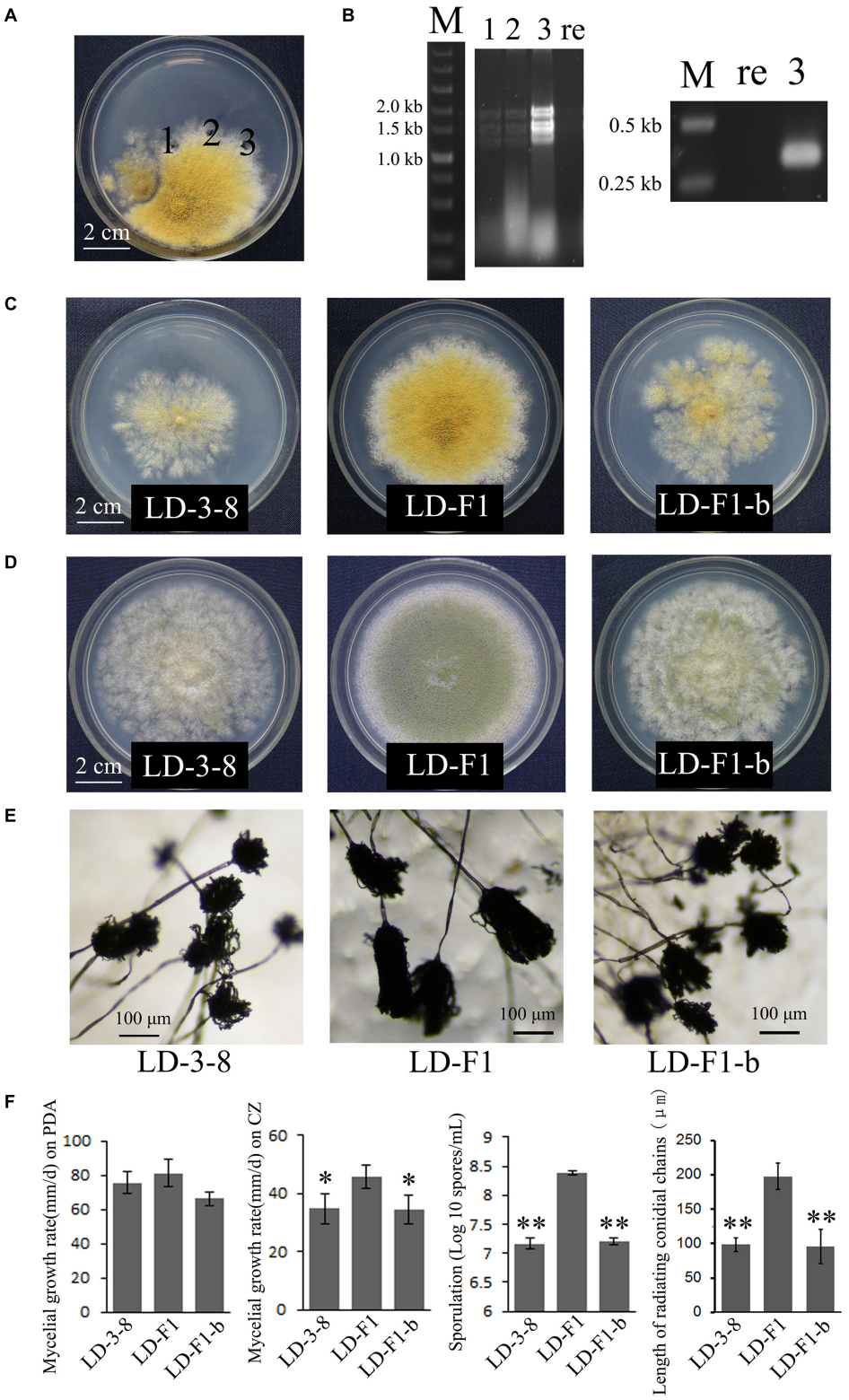

FIGURE 4 | Biological effects of AfPV1 in *A. flavus*. **(A)** Paired-cultures between the donor isolate LD-3-8 (left) and the virus-free recipient isolate LD-F1 (right). Derivative isolates were obtained from the mycelia agar plugs marked "1," "2," and "3". **(B)** Agarose gel electrophoresis of dsRNA extracted from derivative isolates (left) and RT-PCR detection for AfPV1 (right). Lane re is recipient isolate LD-F1; lane 3 is derivative isolate LD-F1-b; lane 1, 2, and 3 in panels **B** correspond to panels **A**. Colony morphology of isolates LD-3-8, LD-F1 and LD-F1-b on CZ **(C)**, and PDA **(D)** for 6 days. **(E)** Conidial heads of isolates LD-3-8, LD-F1, and LD-F1-b.hfill

(Continued)

FIGURE 4 | Continued
(**F**) Comparison of the growth rate, sporulation and length of radiating chains of conidia among isolates LD-3-8, LD-F1, and LD-F1-b. Isolate LD-3-8 was infected with AfPV1, virus-free isolate LD-F1 was obtained from isolate LD-3-8 by single asexual spore isolates, and then was labeled with a pyrithiamine resistance (*ptr*) gene, and isolate LD-F1-b was one of the derivative isolates, which were obtained by transferring AfPV1 from isolate LD-3-8 (donor) to the virus-free isolate LD-F1 (recipient). "*" represented significantly different at the $P < 0.05$ level of confidence and "**" represented significantly different at the $P < 0.01$ level of confidence according to Turkey's multiple comparison test.

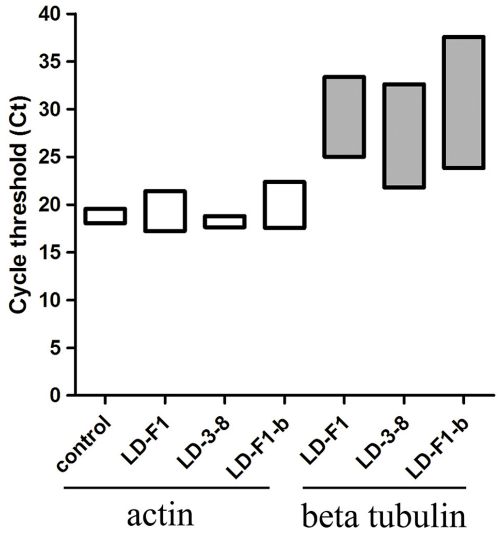

FIGURE 5 | Quantitative PCR (qPCR) showing fungal burden in the mice model. Cycle of threshold (Ct) values are measured for *A. flavus*β-tubulin and mice actin genes from total genomic DNA, extracted from homogenized lung tissue, following infection with isolates LD-F1, LD-3-8, and LD-F1-b. While expression of mice actin gene was measured in the saline-injected mice, no *A. flavus*β-tubulin gene expression was observed.

pathogenicity of aspergilli are tested in both murine and moth infection models (Ford and Friedman, 1967; Bhatti et al., 2011; Özkan and Coutts, 2015; Negri et al., 2017). Both systems have advantages and limitations (Desalermos et al., 2012; Arvanitis et al., 2013). Our tests on the effects of AfPV1 on virulence in *A. flavus* confirmed the utility and reliability of murine model.

Based on nucleotide sequence analysis, AfPV1 is unambiguously identified as a new member of the family *Partitiviridae.* Most partitiviruses generally possess two essential dsRNA genome segments (1.3–2.5 kbp in length), the larger one encodes RNA-dependent RNA polymerase (RdRp) and the smaller one encodes CP (Nibert et al., 2014). Moreover, the presence of one or more additional dsRNA segments is common in *Partitiviridae* family (Nibert et al., 2014). The genome of AfPV1 contains three segments (dsRNA1 with 1.7 kbp, dsRNA2 with 1.4 kbp, and dsRNA3 with 1.2 kbp), and the 5′-untranslated regions (UTRs) of dsRNA1, dsRNA2 and dsRNA3 show high sequence identity with each other, which is a feature of partitiviruses (Nibert et al., 2014).

DsRNA1 encodes the RdRp of AfPV1 and dsRNA2 is considered to encode the CP of AfPV1 which is similar to the finding for *C. acutatum* RNA virus 1 (Zhong et al., 2014a). Moreover, the CP of AfPV1 shows similarity to hypothetical protein encoded by Botryosphaeria dothidea virus 1, *C. acutatum* RNA virus 1, *V. cypri* partitivirus, *U. virens* partitivirus 2, and *U. virens* partitivirus 3 (**Table 1**), but do not have any similarity to partitiviruses in five genera (*Alphapartitivirus, Betapartitivirus, Gammapartitivirus*, *Deltapartitivirus,* and Epsilonpartitivirus). These results indicates the CPs of the viruses in this group may be new CP category in family *Partitiviridae.* AfPV1 and Botryosphaeria dothidea virus 1 contains three segments in each genome, but *C. acutatum* RNA virus 1, *U. virens* partitivirus 2 and *U. virens* partitivirus 3 possesses two segments in each genome, that is the difference in this group (Zhong et al., 2014a,b,c). Recently, new viral sequences associated to invertebrates and fungi were defined as a new genus "Epsilonpartitivirus" in family *Partitiviridae* (Shi et al., 2016; Nerva et al., 2017). The phylogenetic analysis indicates that the AfPV1, Botryosphaeria dothidea virus 1, *C. acutatum* RNA virus 1, *V. cypri* partitivirus, *U. virens* partitivirus 2 and *U. virens* partitivirus 3 are clearly grouped in an unclassified taxon, which is outside the five existing genera in *Partitiviridae* family (**Figure 3B**). Taking these aspects into consideration, we suggest that AfPV1 and relative viruses may group as a new genus named "Zetapartitivirus" according to the nomenclature of genera in *Partitiviridae* family.

Members of the family *Partitiviridae* are usually considered to have latent effect infections of their hosts, such as resistance to salinity, regulation of mycotoxin production or biocontrol potential (Nibert et al., 2014; Nerva et al., 2017, 2018; Chun et al., 2018). However, only few partitiviruses are likely responsible for inducing abnormal phenotypes or virulence reduction in their hosts. Sclerotinia sclerotiorum partitivirus 1 (SsPV1) and Rhizoctonia solani partitivirus 2 (RsPV2) conferred hypovirulence on its natural plant-pathogenic fungal host; Flammulina velutipes browning virus (FvBV) is known to be associated with the cap color of the fruiting bodies of *Flammulina velutipes*; Aspergillus fumigatus partitivirus 1 (AfuPV1) caused abnormal colony phenotypes, slow growth, and production of light pigmentation on its host *A. fumigatus* (Magae and Sunagawa, 2010; Bhatti et al., 2011; Xiao et al., 2014; Zheng et al., 2014). In our study, the AfPV1-infected isolates displayed debilitation symptoms, including abnormal colonial morphology, slow growth on CZ, poor sporulation, and short spore chains. However, there are no significant impact of AfPV1 on the virulence of its host, which is similar to AfuPV1 (Bhatti et al., 2011; Krishnan et al., 2009).

In conclusion, we have isolated and characterized a new partitivirus with 3 genome segments and provided convincing evidence that dsRNA2 encodes a CP, whereas the function of the ORF encoded by dsRNA3 remains unknown. Phylogenetic analysis suggest that AfPV1 belongs to a new genus inside the *Partitiviridae* family for which we propose the name

Zetapartitivirus. Horizontal transmission analysis revealed that AfPV1 infection causes debilitation symptoms but no significant alterations to murine pathogenicity of *A. flavus*.

AUTHOR CONTRIBUTIONS

YJ designed and analyzed the data. JW collected and analyzed the data. BY purified the virus particles. JZ analyzed the mice aspergillosis model. QW and WY gave some advises for the work.

FUNDING

The research was financially supported by National Natural Science Foundation of China (31660012), the Science and Technology Foundation of Guizhou Province [(2019)1277], the Joint Foundation of Collaboration Project between Scientific and Technological Bureau of Guizhou Province and Universities of Guizhou Province [LH(2016)7348], the Joint Foundation of Collaboration Project between Scientific and Technological Bureau of Guiyang City and Guizhou Medical University [(20161001)032], Youth Science and Technology Talent Development Project from Guizhou Provincial Department of Education [KY(2016)146], the Doctoral Cultivating Fund of Guizhou Medical University [J(2014)035], and Program of Scientific and Technological Innovation Team of Guizhou Province [(2017)5652].

ACKNOWLEDGMENTS

We wish to thank the reviewers for their valuable comments.

SUPPLEMENTARY MATERIAL

The Supplementary Material for this article can be found online at: https://www.frontiersin.org/articles/10.3389/fmicb.2019.00626/full#supplementary-material

FIGURE S1 | Histological and microscopic observition of mice lung of control and *A. flavus* (isolate LD-F1 and LD-F1-b) infection. **(A)** Histological changes of mice lungs. **(B)**. Hematoxylin eosin staining analysis of mice lungs. **(C)** Culture detection of *A. flavus* on PDA. Control was saline-injected mice. Bars = 200 μm.

TABLE S1 | NCBI protein database accession numbers of the virus used for phylogenetic analysis.

TABLE S2 | The matrix-assisted laser desorption/ionization-time of flight mass spectrometry (MALDI-TOF-MS) analysis of protein bands on the gel. Ions score is −10 log(*P*), where *P* is the probability that the observed match is a random event. Protein scores are derived from ions scores as a non-probabilistic basis for ranking protein hits. Individual ions scores >31 indicate identity or extensive homology ($p < 0.05$). The overall protein score is 268 ppm means peptide mass tolerance.

TABLE S3 | The liquid chromatography-tandem mass spectrometry analysis of purified virus particles. Ions score is −10 log(*P*), where *P* is the probability that the observed match is a random event. Protein scores are derived from ions scores as a non-probabilistic basis for ranking protein families. Individual ions scores >0 indicate identity or extensive homology ($p < 0.05$). The overall protein score is 1245 ppm means peptide mass tolerance.

REFERENCES

Amaike, S., and Keller, N. P. (2011). *Aspergillus flavus*. *Annu. Rev. Phytopathol.* 49, 107–133. doi: 10.1146/annurev-phyto-072910-095221

Arendrup, M. C. (2014). Update on antifungal resistance in *Aspergillus* and candida. *Clin. Microbiol. Infect.* 6, 42–48. doi: 10.1111/1469-0691.12513

Arvanitis, M., Glavis-Bloom, J., and Mylonakis, E. (2013). Invertebrate models of fungal infection. *Biochim. Biophys. Acta* 1832, 1378–1383. doi: 10.1016/j.bbadis.2013.03.008

Bhatti, M. F., Jamal, A., Petrou, M. A., Cairns, T. C., Bignell, E. M., and Coutts, R. H. (2011). The effects of dsRNA mycoviruses on growth and murine virulence of *Aspergillus fumigatus*. *Fungal Genet. Biol.* 48, 1071–1075. doi: 10.1016/j.fgb.2011.07.008

Bruenn, J. A. (1993). A closely related group of RNA-dependent RNA polymerases from double-stranded RNA viruses. *Nucleic Acids Res.* 21, 5667–5669. doi: 10.1093/nar/21.24.5667

Chang, P. K., Scharfenstein, L. L., Wei, Q., and Bhatnagar, D. (2010). Development and refinement of a high-efficiency gene-targeting system for *Aspergillus flavus*. *J. Microbiol. Methods* 81, 240–246. doi: 10.1016/j.mimet.2010.03.010

Chun, J., Yang, H. E., and Kim, D. H. (2018). Identification of a novel partitivirus of *Trichoderma harzianum* NFCF319 and evidence for the related antifungal activity. *Front. Plant Sci.* 9:1699. doi: 10.3389/fpls.2018.01699

Desalermos, A., Fuchs, B. B., and Mylonakis, E. (2012). Selecting an invertebrate model host for the study of fungal pathogenesis. *PLoS pathog.* 8:e1002451. doi: 10.1371/journal.ppat.1002451

Ford, S., and Friedman, L. (1967). Experimental study of the pathogenicity of *aspergilli* for mice. *J. Bacteriol.* 94, 928–933.

Ghabrial, S. A., and Suzuki, N. (2009). Viruses of plant pathogenic fungi. *Annu.Rev. Phytopathol.* 47, 353–384. doi: 10.1146/annurev-phyto-080508-081932

Hedayati, M. T., Pasqualotto, A. C., Warn, P. A., Bowyer, P., and Denning, D. W. (2007). *Aspergillus flavus*: human pathogen, allergen and mycotoxin producer. *Microbiology* 153, 1677–1692. doi: 10.1099/mic.0.2007/007641-0

Jiang, Y., Zhang, T., Luo, C., Jiang, D., Li, G., Li, Q., et al. (2015). Prevalence and diversity of mycoviruses infecting the plant pathogen *Ustilaginoidea virens*. *Virus Res.* 195, 47–56. doi: 10.1016/j.virusres.2014.08.022

Klich, M. A. (2007). *Aspergillus flavus*: the major producer of aflatoxin. *Mol. Plant Pathol.* 8, 713–722. doi: 10.1111/j.1364-3703.2007.00436.x

Kotta-Loizou, I., and Coutts, R. H. A. (2017). Mycoviruses in *Aspergilli*: a comprehensive review. *Front. Microbiol.* 8:1699. doi: 10.3389/fmicb.2017.01699

Krishnan, S., Manavathu, E. K., and Chandrasekar, P. H. (2009). *Aspergillus flavus*: an emerging non-fumigatus *Aspergillus* species of significance. *Mycoses* 52, 206–222. doi: 10.1111/j.1439-0507.2008.01642.x

Lan, H., Wu, L., Sun, R., Yang, K., Liu, Y., Wu, J., et al. (2018). Investigation of *Aspergillus flavus* in animal virulence. *Toxicon* 145, 40–47. doi: 10.1016/j.toxicon.2018.02.043

Liu, L., Xie, J., Cheng, J., Fu, Y., Li, G., Yi, X., et al. (2014). Fungal negative-stranded RNA virus that is related to bornaviruses and nyaviruses. *Proc. Natl. Acad. Sci. U.S.A.* 111, 12205–12210. doi: 10.1073/pnas.1401786111

Magae, Y., and Sunagawa, M. (2010). Characterization of a mycovirus associated with the brown discoloration of edible mushroom, *Flammulina velutipes*. *Virol. J.* 7:342. doi: 10.1186/1743-422X-7-342

Morris, T., and Dodds, J. (1979). Isolation and analysis of double-stranded RNA from virus-infected plant and fungal tissue. *Phytopathology* 69, 854–858. doi: 10.1094/Phyto-69-854

Negri, C. E., Johnson, A., McEntee, L., Box, H., Whalley, S., Schwartz, J. A., et al. (2017). Pharmacodynamics of the novel antifungal agent F901318 for acute sinopulmonary *aspergillosis* caused by *Aspergillus flavus*. *J. Infect. Dis.* 217, 1118–1127. doi: 10.1093/infdis/jix479

Nerva, L., Chitarra, W., Siciliano, I., Gaiotti, F., Ciuffo, M., Forgia, M., et al. (2018). Mycoviruses mediate mycotoxin regulation in *Aspergillus ochraceus*. *Environ. Microbiol.* doi: 10.1111/1462-2920.14436 [Epub ahead of print].

Nerva, L., Silvestri, A., Ciuffo, M., Palmano, S., Varese, G. C., and Turina, M. (2017). Transmission of *Penicillium aurantiogriseum* partiti-like virus 1 to a new fungal host (*Cryphonectria parasitica*) confers higher resistance to salinity

and reveals adaptive genomic changes. *Environ. Microbiol.* 19, 4480–4492. doi: 10.1111/1462-2920.13894

Nibert, M. L., Ghabrial, S. A., Maiss, E., Lesker, T., Vainio, E. J., Jiang, D., et al. (2014). Taxonomic reorganization of family *Partitiviridae* and other recent progress in partitivirus research. *Virus Res.* 188, 128–141. doi: 10.1016/j.virusres.2014.04.007

Ochoa, W. F., Havens, W. M., Sinkovits, R. S., Nibert, M. L., Ghabrial, S. A., and Baker, T. S. (2008). Partitivirus structure reveals a 120-subunit, helix-rich capsid with distinctive surface arches formed by quasisymmetric coat-protein dimers. *Structure* 16, 776–786. doi: 10.1016/j.str.2008.02.014

Özkan, S., and Coutts, R. H. (2015). *Aspergillus fumigatus* mycovirus causes mild hypervirulent effect on pathogenicity when tested on *Galleria mellonella*. *Fungal Genet. Biol.* 76, 20–26. doi: 10.1016/j.fgb.2015.01.003

Pan, J., Dong, L., Lin, L., Ochoa, W. F., Sinkovits, R. S., Havens, W. M., et al. (2009). Atomic structure reveals the unique capsid organization of a dsRNA virus. *Proc. Natl. Acad. Sci. U.S.A.* 106, 4225–4230. doi: 10.1073/pnas.0812071106

Paul, R. A., Rudramurthy, S. M., Meis, J. F., Mouton, J. W., and Chakrabarti, A. (2015). A novel Y319H substitution in CYP51C associated with azole resistance in *Aspergillus flavus*. *Antimicrob. Agents Chemother.* 59, 6615–6619. doi: 10.1128/AAC.00637-15

Pearson, M. N., Beever, R. E., Boine, B., and Arthur, K. (2009). Mycoviruses of filamentous fungi and their relevance to plant pathology. *Mol. Plant pathol.* 10, 115–128. doi: 10.1111/j.1364-3703.2008.00503.x

Potgieter, A. C., Page, N. A., Liebenberg, J., Wright, I. M., Landt, O., and van Dijk, A. A. (2009). Improved strategies for sequence-independent amplification and sequencing of viral double-stranded RNA genomes. *J. Gen. Virol.* 90, 1423–1432. doi: 10.1099/vir.0.009381-0

Shi, M., Lin, X. D., Tian, J. H., Chen, L. J., Chen, X., Li, C. X., et al. (2016). Redefining the invertebrate RNA virosphere. *Nature* 540, 539–543. doi: 10.1038/nature20167

Son, M., Yu, J., and Kim, K.-H. (2015). Five questions about mycoviruses. *PLoS pathog.* 11:e1005172. doi: 10.1371/journal.ppat.1005172

Tamura, K., Stecher, G., Peterson, D., Filipski, A., and Kumar, S. (2013). MEGA6: molecular evolutionary genetics analysis version 6.0. *Mol. Biol. Evol.* 30, 2725–2729. doi: 10.1093/molbev/mst197

Tang, J., Ochoa, W. F., Li, H., Havens, W. M., Nibert, M. L., Ghabrial, S. A., et al. (2010).). Structure of Fusarium poae virus 1 shows conserved and variable elements of partitivirus capsids and evolutionary relationships to picobirnavirus. *J. Struct. Biol.* 172, 363–371. doi: 10.1016/j.jsb.2010.06.022

Vainio, E. J., Chiba, S., Ghabrial, S. A., Maiss, E., Roossinck, M., Sabanadzovic, S., et al. (2018). ICTV virus taxonomy profile: *Partitiviridae*. *J. Gen. Virol.* 99, 17–18. doi: 10.1099/jgv.0.000985

Van De Sande, W., Lo-Ten-Foe, J., Van Belkum, A., Netea, M., Kullberg, B., and Vonk, A. (2010). Mycoviruses: future therapeutic agents of invasive fungal infections in humans? *Eur. J. Clin. Microbiol. Infect. Dis.* 29, 755–763. doi: 10.1007/s10096-010-0946-7

van Diepeningen, A. D., Varga, J., Hoekstra, R. F., and Debets, A. J. (2008). "Mycoviruses in aspergilli," in *Aspergillus in the Genomic Era*, eds J. Varga and R. A. Samson (Wageningen: Wageningen Academic Publishers), 133–176.

Wu, M., Zhang, L., Li, G., Jiang, D., and Ghabrial, S. A. (2010). Genome characterization of a debilitation-associated mitovirus infecting the phytopathogenic fungus *Botrytis cinerea*. *Virology* 406, 117–126. doi: 10.1016/j.virol.2010.07.010

Wu, M., Zhang, L., Li, G., Jiang, D., Hou, M., and Huang, H.-C. (2007). Hypovirulence and double-stranded RNA in *Botrytis cinerea*. *Phytopathology* 97, 1590–1599. doi: 10.1094/PHYTO-97-12-1590

Xiao, X., Cheng, J., Tang, J., Fu, Y., Jiang, D., Baker, T. S., et al. (2014). A novel partitivirus that confers hypovirulence on plant pathogenic fungi. *J. Virol.* 88, 10120–10133. doi: 10.1128/JVI.01036-14

Xie, J., and Jiang, D. (2014). New insights into mycoviruses and exploration for biological control of crop fungal diseases. *Annu. Rev. Phytopathol.* 52, 45–68. doi: 10.1146/annurev-phyto-102313-050222

Yu, X., Li, B., Fu, Y., Jiang, D., Ghabrial, S. A., Li, G., et al. (2010). A geminivirus-related DNA mycovirus that confers hypovirulence to a plant pathogenic fungus. *Proc. Natl. Acad. Sci. U.S.A.* 107, 8387–8392. doi: 10.1073/pnas.0913535107

Yu, X., Li, B., Fu, Y., Xie, J., Cheng, J., Ghabrial, S. A., et al. (2013). Extracellular transmission of a DNA mycovirus and its use as a natural fungicide. *Proc. Natl. Acad. Sci. U.S.A.* 110, 1452–1457. doi: 10.1073/pnas.1213755110

Zheng, L., Zhang, M., Chen, Q., Zhu, M., and Zhou, E. (2014). A novel mycovirus closely related to viruses in the genus Alphapartitivirus confers hypovirulence in the phytopathogenic fungus *Rhizoctonia solani*. *Virology* 457, 220–226. doi: 10.1016/j.virol.2014.03.029

Zhong, J., Chen, D., Lei, X. H., Zhu, H. J., Zhu, J. Z., and Da Gao, B. (2014a). Detection and characterization of a novel Gammapartitivirus in the phytopathogenic fungus *Colletotrichum acutatum* strain HNZJ001. *Virus Res.* 190, 104–109. doi: 10.1016/j.virusres.2014.05.028

Zhong, J., Lei, X. H., Zhu, J. Z., Song, G., Zhang, Y. D., Chen, Y., et al. (2014b). Detection and sequence analysis of two novel co-infecting double-strand RNA mycoviruses in *Ustilaginoidea virens*. *Arch. Virol.* 159, 3063–3070. doi: 10.1007/s00705-014-2144-x

Zhong, J., Zhu, J. Z., Lei, X. H., Chen, D., Zhu, H. J., and Gao, B. D. (2014c). Complete genome sequence and organization of a novel virus from the rice false smut fungus *Ustilaginoidea virens*. *Virus Genes* 48, 329–333. doi: 10.1007/s11262-013-1022-z

Conflict of Interest Statement: The authors declare that the research was conducted in the absence of any commercial or financial relationships that could be construed as a potential conflict of interest.

frontiers in Cellular and Infection Microbiology

BRIEF RESEARCH REPORT
published: 15 May 2019
doi: 10.3389/fcimb.2019.00156

Molecular Characterization of a Chrysovirus Isolated From the Citrus Pathogen *Penicillium crustosum* and Related Fungicide Resistance Analysis

Shengqiang Wang[1†], *Zhu Yang*[1†], *Tingfu Zhang*[1†], *Na Li*[2], *Qianwen Cao*[1], *Guoqi Li*[1], *Yongze Yuan*[1*] *and Deli Liu*[1*]

[1] Hubei Key Laboratory of Genetic Regulation and Integrative Biology, School of Life Sciences, Central China Normal University, Wuhan, China, [2] College of Life Science and Technology, Honghe University, Mengzi, China

OPEN ACCESS

Edited by:
Daohong Jiang,
Huazhong Agricultural University, China

Reviewed by:
Ying-Lien Chen,
National Taiwan University, Taiwan
Ioly Kotta-Loizou,
Imperial College London, United Kingdom

***Correspondence:**
Yongze Yuan
yuan_yongze@163.com
Deli Liu
ldl@mail.ccnu.edu.cn;
deliliu2013@163.com

[†] These authors have contributed equally to this work

Specialty section:
This article was submitted to Fungal Pathogenesis, a section of the journal Frontiers in Cellular and Infection Microbiology

Received: 29 November 2018
Accepted: 26 April 2019
Published: 15 May 2019

Citation:
Wang S, Yang Z, Zhang T, Li N, Cao Q, Li G, Yuan Y and Liu D (2019) Molecular Characterization of a Chrysovirus Isolated From the Citrus Pathogen Penicillium crustosum and Related Fungicide Resistance Analysis. Front. Cell. Infect. Microbiol. 9:156. doi: 10.3389/fcimb.2019.00156

Penicillium sp. are damaging to a range of foods and fruits including citrus. To date, double-stranded (ds)RNA viruses have been reported in most *Penicillium* species but not in citrus pathogen *P. crustosum*. Here we report a novel dsRNA virus, designated as *Penicillium crustosum* chrysovirus 1 (PcCV1) and isolated from *P. crustosum* strain HS-CQ15. PcCV1 genome comprises four dsRNA segments, referred to as dsRNA1, dsRNA2, dsRNA3, and dsRNA4, which are 3600, 3177, 3078, and 2808 bp in length, respectively. Sequence analysis revealed the presence of four open reading frames (ORFs) in the PcCV1 genome. ORF1 in dsRNA1 encodes a putative RNA-dependent RNA polymerase (RdRp) and ORF2 in dsRNA2 encodes a putative coat protein (CP). The two remaining ORFs, ORF3 in dsRNA3 and ORF4 in dsRNA4, encode proteins of unknown function. Phylogenetic analysis based on RdRp sequences showed that PcCV1 clusters with other members of the genus *Chrysovirus*, family *Chrysoviridae*. Transmission electron microscope (TEM) analysis revealed that the PcCV1 visions are approximately 40 nm in diameter. Regarding biological effects of PcCV1, HS-CQ15 harboring the chrysovirus exhibited no obvious difference in colony morphology under fungicide-free conditions but decreased resistance to demethylation inhibitor (DMI)-fungicide prochloraz, as compared to PcCV1-cured strain. Here we provide the first evidence of a virus present in citrus pathogenic fungus *P. crustosum* and the chrysovirus-induced change in fungicide-resistance of its host fungus.

Keywords: molecular characterization, chrysovirus, citrus, pathogen, *Penicillium crustosum*

INTRODUCTION

Mycoviruses have been widely distributed in fungal hosts including various *Penicillium* species. Mycoviruses with double stranded RNA (dsRNA) genomes can be categorized into seven families, as reviewed by Ghabrial et al. (2015), i.e., *Totiviridae*, *Chrysoviridae*, *Partitiviridae*, *Reoviridae*, *Megabirnaviridae*, *Quadriviridae*, and *Endornaviridae* families. Among these dsRNA mycoviruses,

the members of family *Chrysoviridae* have been early identified in *P. chrysogenum* (Lemke and Ness, 1970; Lemke et al., 1973; Yamashita et al., 1973; Edmondson et al., 1984; Jiang and Ghabrial, 2004), later in *C. nitschkei* (Liu et al., 2007) and rice pathogenic fungus *Magnaporthe oryzae* (Urayama et al., 2010), and recently in filamentous phytopathogenic fungus *Colletotrichum gloeosporioides* (Zhong et al., 2016), *Brassica campestris* var. purpurea (Zhang et al., 2017), entomopathogenic fungus *Isaria javanica* (Herrero, 2017) and *Alternaria* species (Okada et al., 2018). Most of the chrysoviruses reported to date constitute family *Chrysoviridae* that can be classified into two clades, and the members in clade II constitute genus *Chrysovirus* (Liu et al., 2012). However, the evidence on inhabitant of any chrysovirus (even any mycovirus) in host fungus *P. crustosum* is still lacking.

Members of the family *Chrysoviridae* share some common traits regarding their dsRNA genome structures as intensively reviewed before (Ghabrial, 2010; Ghabrial et al., 2015). Usually, a typical chrysovirus genome is comprised of 4 segmented dsRNAs in 2.4∼3.6 kbp full-length, separately encapsidated to form virion particles in ∼40 nm size (Ghabrial et al., 2018). For tetra-segmented genome of chrysovirus, dsRNA1 as the largest segment encodes RNA-dependent RNA polymerase (RdRP), often referred to as P1 in literatures (Jiang and Ghabrial, 2004; Ghabrial et al., 2018), exhibiting 8 conserved motifs found in most dsRNA viruses inhabiting lower eukaryotes (Bruenn, 1993), dsRNA2 encodes the major capsid protein (CP), often referred to as P2 (Jiang and Ghabrial, 2004; Ghabrial et al., 2018), and the rest two dsRNAs (dsRNA3 and dsRNA4) encodes unknown-function proteins, i.e., P3 and P4, respectively (Ghabrial et al., 2018). Sequence-based predictions indicate P3 contains a phytoreovirus S7 domain and has sequence similarity with the RdRP at its N-terminus, and P4 is a putative protease (Liu et al., 2012). Significantly high sequence identity has been observed at both 3′- and 5′-UTRs of chrysovirus genomic dsRNAs, including 5′- and 3′-terminal sequences strictly conserved (Ghabrial, 2010), 40–75 nt region conserved at 5′-UTRs (Ghabrial, 2010; Herrero, 2017), and CCA-repeats in the 30–50 nt stretch at 5′-UTRs (Jiang and Ghabrial, 2004; Urayama et al., 2010; Zhang et al., 2017; Okada et al., 2018). To date, some unusual genome structures composed of 5 or 3 dsRNA segments were documented for chrysoviruses infecting *Fusarium graminearum* (Darissa et al., 2011; Yu et al., 2011), *M. oryzae* (Urayama et al., 2012, 2014), radish *Raphanus sativus* (Li et al., 2013), and *Brassica campestris* (Zhang et al., 2017). These viruses are closely related to recognized chrysoviruses, nevertheless, they are not officially accepted species yet. Now that such great diversity of chrysoviruses that may beyond expected, it would be an interesting issue to identify mycovirus(es) in citrus pathogen *P. crustosum*.

We have reported a number of novel mycoviruses in *P. digitatum* species, including *Penicillium* digitatum virus 1 (PdV1) (a member of the genus Victorivirus in the family Totiviridae) (Niu et al., 2016), *Penicillium* digitatum polymycovirus 1 (PdPmV1, a polymycovirus) and *Penicillium* digitatum narna-like virus 1 (PdNLV1, a narna-like virus) in 2018 (Niu et al., 2018), and *Penicillium* digitatum gammapartitivirus 1 (PdGV1, a partitivirus) in 2018 (Yang et al., 2018). The present report provided the first evidence on a chrysovirus inhabited in *P. crustosum* isolate HS-CQ15, molecularly characterized this mycovirus to the member of *Chrysoviridae* family, referred to as '*Penicillium crustosum* chrysovirus 1' (PcCV1), and effect of PcCV1 infection on the fungal resistance to DMI-fungicide prochloraz was also investigated.

METHOD

The host of PcCV1, *Penicillium* HS-CQ15, was isolated from *Penicillium*-decayed citrus surface (Chongqing, China) and molecularly characterized as *P. crustosum* species, according to internal transcribed spacer (ITS) analysis described before (Gardes and Bruns, 1993; Pandey et al., 2018). HS-CQ15 conidial suspension stored in glycerol at −70°C was initially cultured on potato dextrose agar (PDA) medium at 28°C and 180 rpm for about 7 days, and the resulting mycelium fragments were transferred into potato dextrose broth (PDB) medium for additional 96 h cultivation at the same conditions. The fungal mycelia collected from the PDB cultures was exploited to extract viral dsRNAs, using phenol-chloroform-ethanol method (Sun and Suzuki, 2008; Sotaro et al., 2009). The obtained dsRNA mixture was purified by DNase I and S1 nuclease digestions at RNase-free conditions, separated by 1% (w/v) agarose gel electrophoresis, and finally recovered from individual EB-stained band using Gel Extraction kit (TaKaRa, Dalian, China). The amount of ∼5 μg dsRNA recovered was applied to construct cDNA libraries for Illumina high-throughput sequencing, according to protocols described before (Rwahnih et al., 2011; Niu et al., 2018). Afterwards, reads and contigs assembly, based on reference genome of PcV (Jiang and Ghabrial, 2004), provided sequences with partial length for PcCV1 dsRNAs, i.e., 2437 bp for dsRNA1, 3096 bp for dsRNA2, 2909 for dsRNA3, and 2726 bp for dsRNA4. Thirteen pairs of specific primers (**Table S1**) were designed to full-fill gaps by RT-PCR, generating ORF-included sequences, and then, 4 pairs of adaptor primers (**Table S1**) were designed to PCR-amplify 5′- and 3′-UTRs, finally generating full-length PcCV1 genomic dsRNAs. According to the full-length sequences, specific RNA probes were designed as shown in **Figure 1C** and used for digoxigenin-labeled northern blots, as previously described (Streit et al., 2009; Niu et al., 2018).

Open reading frames (ORFs) in putative viral sequences were identified using the NCBI ORF finder (http://www.ncbi.nlm.nih.gov/gorf/gorf.html) and further confirmed by simulated translation in DNAMAN software package version 6.0 (Lynnon Corporation, Quebec, Canada). The analysis of protein sequence similarity was initially performed using the BLASTp program at NCBI website (http://www.ncbi.nlm.nih.gov/). Multiple sequence alignments were further processed with CLUSTAL_X program (Thompson et al., 1997), and phylogenetic trees were constructed using the neighbor-joining method in MEGA version 6.0 (Tamura et al., 2013), and further confirmed by maximum likelihood approach in the same software.

Viral particles (VPs) were purified and characterized as described previously (Niu et al., 2016, 2018). Approximately

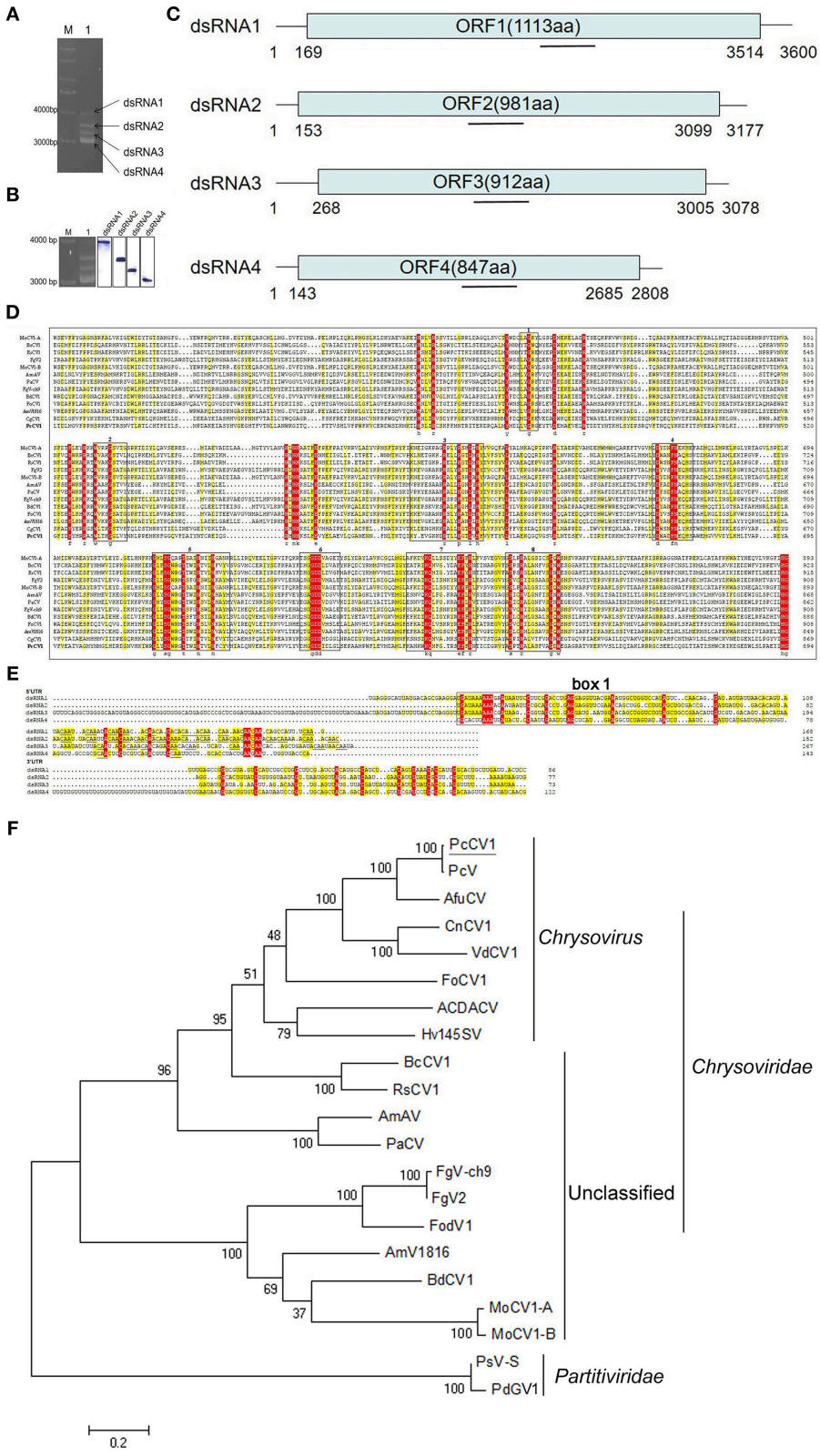

FIGURE 1 | Characterization of PcCV1 genomic organization and phylogenetic analysis. **(A)** Mobility pattern analysis of PcCV1 dsRNAs from *P. crustosum* HS-CQ15 mycelia (lane 1) by agarose gel electrophoresis. Lane M indicates DNA marker DS10000 (TaKaRa, Dalian, China). **(B)** Northern-blot confirmation of PcCV1 genomic

(Continued)

FIGURE 1 | dsRNAs. The left panel is the copy of **(A)**, indicating in-gel positions for dsRNA1 to 4 separated as mentioned above. The full-scan of entire original gels for the RNA blots of PcCV1 genomic dsRNAs is shown in **Figure S3**. **(C)** Schematic representation of PcCV1 genome organization. The boxes represent the ORFs within genomic dsRNAs, and lines depict 5′- and 3′-untranslated regions (UTRs). **(D)** Multiple alignments of RdRps between PcCV1 and other chrysoviriuses. The conserved motifs in the selected RdRp sequences are boxed with numbers 1–8. The names (full and abbreviated) of selected chrysoviriuses as well as GenBank accession numbers of their RdRps are listed in **Table S2**. **(E)** Nucleotide sequence alignments of 5′- and 3′-UTRs of PcCV1 genomic dsRNAs. The identical nucleotides among dsRNA1 to 4 are especially color-shaded. The "box 1" is highlighted in black box, and the "CAA" repeats are highlighted with underlines. **(F)** Phylogenetic analysis of the RdRp sequences for PdGV1. The names (full and abbreviated) of selected chrysoviriuses as well as GenBank accession numbers of their RdRps are listed in **Table S2**.

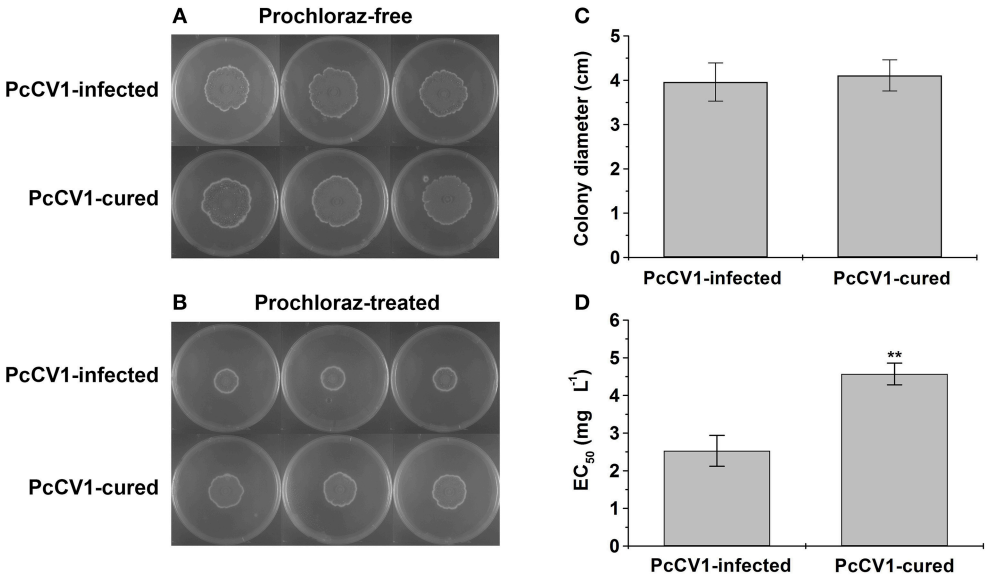

FIGURE 2 | Biological effects of PcCV1-infection on its host fungus. **(A)** Effect of PcCV1-infection on vegetative growth of HS-CQ15. **(B)** Effect of PcCV1-infection on prochloraz (DMI-fungicide) resistance of HS-CQ15. The fungal strains were grown on PDA at 25°C for 7 d and photographed, with or without 5.0 mg L^{-1} prochloraz (final concentration). In panel **(A,B)**, the three plates listed in horizontal line indicate three biological replicates. **(C)** Comparison of colony diameters for HS-CQ15 (PiCV1-infected) and its PiCV1-cured progenies under fungicide-free conditions. **(D)** Comparison of EC_{50} values against prochloraz for HS-CQ15 (PiCV1-infected) and its PiCV1-cured progenies. In panel **(C,D)**, the values are shown as mean ± SD from five independent experiments ($n = 5$) with three biological replicates for each experiment, and SPSS software (version 10.0) was applied to perform statistics analysis (**$P < 0.01$).

100 g (wet weight) mycelia of HS-CQ15 were harvested from PDB cultures, mixed with 400 mL of 50 mM sodium phosphate buffer (pH 7.4), and ground into homogenates for VPs isolation using sucrose density gradient ultracentrifugation. The obtained VPs were suspended with sodium phosphate buffer (pH7.4) for the use of transmission electron microscopy (TEM) and SDS-PAGE analysis.

To investigate biological effects of PcCV1 on its host fungus, we prepared PcCV1-cured HS-CQ15 progenies by ribavirin protocol as described before (Niu et al., 2016, 2018). In detail, the conidia of HS-CQ15 (PcCV1-infected) were incubated in PDB media containing 100 mmol·L^{-1} ribavirin for 12 h to generate virus-free progenies (PcCV1-cured). Five PcCV1-cured strains were selected and independently subjected to the following experiments each containing three biological replicates. The vegetative growth and ability to resist DMI-fungicide for HS-CQ15 and its PcCV1-cured progenies were assessed on fungicide-free PDA media and 5.0 mg L^{-1} (final concentration) prochloraz-containing PDA media, respectively, according to the methods of Niu et al. (2018), and EC_{50} values against prochloraz for the virus-infected and virus-cured strains were also measured. The average of colony diameters in each independent experiment was used for EC_{50} calculation by SPSS software (version 10.0).

RESULTS AND DISCUSSION

Mycovirus PcCV1 was isolated from *P. crustosum* HS-CQ15 and its genomic segments (viral dsRNAs) were extracted and purified by using phenol-chloroform-ethanol method. Four dsRNA bands as PcCV1 genomic segments were designated to dsRNA1, dsRNA2, dsRNA3, and dsRNA4, according to their increasing electrophoresis mobility (**Figure 1A**). The tetra-segmented genome of PcCV1 has been confirmed by northern blotting (**Figure 1B**).

The genome organization of PcCV1 is shown in **Figure 1C**. The sequence of dsRNA1 is 3,600 bp full-length containing a single open reading frame (referred to as ORF1) that encodes a 1,113-amino-acid (aa) protein with putative molecular weight

∼128 kDa. Blastn analysis revealed a high nucleotide sequence similarity (∼82%) between dsRNA1 and RdRp-encoding gene of a classical chrysovirus *Penicillium* chrysogenum virus (PcV), the earliest case of *Penicillium*-hosted chrysovirus (Jiang and Ghabrial, 2004). Blastp analysis also showed a high similarity (∼98%) in aa sequences between ORF1 and PcV RdRp. dsRNA2 with 3,177 bp size contained an ORF (referred to as ORF2) encoding a 981-aa protein (∼108.6 kDa) with ∼96% similarity to capsid protein (CP) of PcV. dsRNA3 and dsRNA4 with 3,078 bp and 2,808 bp full-length, respectively, both contained a single ORF, encoding 912-aa and 847-aa protein with estimated molecular weight ∼101 and ∼95 kDa, respectively. These two relatively smaller proteins exhibited highest similarity to function-unknown proteins encoded by PcV dsRNA3 and dsRNA4, as previously documented (Jiang and Ghabrial, 2004), and also showed considerably high similarity to specific function-unknown proteins reported in other chrysoviruses (Jamal et al., 2010; Cao et al., 2011; Herrero, 2017).

Multiple alignment of the PcCV1 RdRp with other International Committee on Taxonomy of Viruses (ICTV)-registered chrysoviruses belonging to the genus *Chrysovirus* (Jiang and Ghabrial, 2004; Urayama et al., 2010), listed in **Table S2**, showed eight conserved motifs (**Figure 1D**), as early verified to be typical structural traits of RdRps for dsRNA viruses in lower eukaryotes (Bruenn, 1993). Between the two closely related chrysoviruses (PcV and PcCV1), the amino acid sequence identities of their dsRNA-encoding proteins (P1, P2, P3, or P4) were summarized in **Table S3**. Specially, a conserved phytoreovirus S7 domain was observed in the upstream of both P1 (RdRp) and P3 sequences (**Figure S1**). This agreed to the S7 domain reported in other chrysoviruses (Liu et al., 2012). In addition, we found highly conserved sequences at 5′-UTR for the four PcCV1 genomic dsRNAs. As shown in **Figure 1E**, about 60 nt located at or close to 5′-termini exhibited conserved among the present 4 dsRNAs, as named "box 1" in other reported chrysoviruses (Ghabrial, 2010). The second conserved region at PcCV1 5′-UTR, locating downstream from the "box 1," is characterized by a cluster of CAA-repeats (**Figure 1E**), as reported in almost all chrysoviruses (Jiang and Ghabrial, 2004; Urayama et al., 2010; Zhang et al., 2017; Okada et al., 2018). Such CAA-repeats, frequently identified at 5′-UTRs of chrysoviruses, have been functionally associated with translational enhancer elements for tomaviruses (Gallie and Walbot, 1992), thus presumably contributing to control of genome replication and virion assembly of chrysoviruses that facilitated their persistent infections to fungal hosts (Ghabrial et al., 2018). **Figure 1E** indicated ∼13 nt sequence conserved in 3′-UTRs of PcCV1 genomic dsRNAs. The locations of special conserved sequence at 3′-UTRs have been identified in other chrysovirus genomes (Jiang and Ghabrial, 2004; Jamal et al., 2010; Zhong et al., 2016; Herrero, 2017), nevertheless exhibiting sequence diversities among these different chrysoviruses.

The association of PcCV1 with family *Chrysoviridae* was verified by phylogenetic tree analysis (**Figure 1F**), based on aa sequences of RdRps between PcCV1 and ICTV-annotated dsRNA chrysoviruses. PcCV1 (with the closest association with PcV) was also closely clustered with other previously reported members of the genus *Chrysovirus*. Under TEM scanning, the purified virions of PcCV1 were isometric in ∼40 nm diameter (**Figure S2A**) that was consistent with other reported chrysoviruses virions in size (Urayama et al., 2010; Ghabrial et al., 2018), also supporting the evolutionary position of PcCV1. Here, the purified virions were confirmed to be extracted from PcCV1 by gel analysis of genomic dsRNA segments (**Figure S2B**) and SDS-PAGE analysis of CP (**Figure S2C**).

To evaluate biological effects of PcCV1, we compared vegetative growth between PcCV1-infected HS-CQ15 and its virus-cured progenies, as well as fungicide-resistance based on PDA experiments. The colony diameters of PcCV1-infected HS-CQ15 strains were similar to those of PcCV1-cured progenies under fungicide-free conditions (**Figure 2A**), but obviously smaller under prochloraz conditions (**Figure 2B**). These results indicated that PcCV1 had little effect on the vegetative growth but deduced prochloraz resistance of its host fungus. Considering almost no effect of PcCV1 on host growth, as indicated by statistics analysis of colony diameters (**Figure 2C**), the present chrysovirus is not assumed as a hypovirus to decrease HS-CQ15 virulence, and this assumption needs support by citrus-based pathogenicity assessments. Here, we emphasized the PcCV1-induced decrease in prochloraz resistance for its host fungus. As shown in **Figure 2D**, prochloraz EC_{50} value of PcCV1-infected HS-CQ15 was 2.53 ± 0.41 mg L^{-1}, significantly lower than those of PcCV1-cured progenies (4.57 ± 0.29 mg L^{-1}). The similar effects were at first time reported in PdPmV1/PdNLV1-coinfected *P. digitatum* strains (Niu et al., 2018). Now we provided another evidence of mycovirus-induced fungicide-conditioned hypovirulence that would enhance drug efficacy to control citrus pathogen *P. crustosum*.

In conclusion, according to molecular features of genomic dsRNAs, homolog and phylogenetic analysis, and characteristics of their 5′- and 3′-UTRs, this report identified the first mycovirus (PcCV1) found in citrus pathogen *P. crustosum* as a variant of PcV in the *Chrysovirus* genus (*Chrysoviridae* family) and revealed that PcCV1-infection decreased prochloraz-resistance of its host fungus (HS-CQ15).

AUTHOR CONTRIBUTIONS

YY and DL conceived this study, acquired project funding, revised to complete final version of manuscript, and supervised all research activities. SW, ZY, and TZ designed experiments and conducted experimental procedures. QC and GL contributed to data curation and bioinformatics analysis. NL contributed to *P. crustosum* isolation and characterization.

FUNDING

This work was financially supported by the National Natural Science Foundation of China (No.31371893) and Natural Science Fund of Hubei Province (No. 2018CFB676).

ACKNOWLEDGMENTS

We sincerely thank Dr. Huazhong Shi (Texas Tech University, USA) for his helpful language editing.

SUPPLEMENTARY MATERIAL

The Supplementary Material for this article can be found online at: https://www.frontiersin.org/articles/10.3389/fcimb.2019.00156/full#supplementary-material

REFERENCES

Bruenn, J. A. (1993). A closely related group of RNA-dependent RNA polymerases from double-stranded RNA viruses. *Nucleic Acids Res.* 21, 5667–5669.

Cao, Y., Zhu, X., Xiang, Y., Li, D., Yang, J., Mao, Q., et al. (2011). Genomic characterization of a novel dsRNA virus detected in the phytopathogenic fungus *Verticillium dahliae* Kleb. *Virus. Res.* 159, 73–78. doi: 10.1016/j.virusres.2011.04.029

Darissa, O., Willingmann, P., Schäfer, W., and Adam, G. (2011). A novel double-stranded RNA mycovirus from *Fusarium graminearum*: nucleic acid sequence and genomic structure. *Arch. Virol.* 156, 647–658. doi: 10.1007/s00705-010-0904-9

Edmondson, S. P., Lang, D., and Gray, D. M. (1984). Evidence for sequence heterogeneity among the double-stranded RNA segments of *Penicillium chrysogenum* mycovirus. *J. Gen. Virol.* 65, 1591–1599. doi: 10.1099/0022-1317-65-9-1591

Gallie, D. R., and Walbot, V. (1992). Identification of the motifs within the tobacco mosaic virus 5′-leader responsible for enhancing translation. *Nucleic. Acids. Res.* 20, 4631–4638. doi: 10.1093/nar/20.17.4631

Gardes, M., and Bruns, T. D. (1993). ITS primers with enhanced specificity for basidiomycetes-application to the identification of mycorrhizae and rusts. *Mol. Ecol.* 2, 113–118. doi: 10.1111/j.1365-294X.1993.tb00005.x

Ghabrial, S. A. (2010). "Chrysoviruses," in *Desk Encyclopedia of Plant and Fungal Virology,* eds B. W. J. Mahy and M. H. V. Van Regenmortel. (Oxford: Elsevier), 500–509.

Ghabrial, S. A., Castón, J. R., Coutts, R. H., Hillman, B. I., Jiang, D., Kim, D. H., et al. (2018). ICTV Virus Taxonomy Profile: *Chrysoviridae*. *J. Gen. Virol.* 99, 19–20. doi: 10.1099/jgv.0.000994

Ghabrial, S. A., Castón, J. R., Jiang, D., Nibert, M. L., and Suzuki, N. (2015). 50-plus years of fungal viruses. *Virology* 479–480, 356–368. doi: 10.1016/j.virol.2015.02.034

Herrero, N. (2017). Identification and sequence determination of a new chrysovirus infecting the entomopathogenic fungus *Isaria javanica*. *Arch. Virol.* 162, 1113–1117. doi: 10.1007/s00705-016-3194-z

Jamal, A., Bignell, E. M., and Coutts, R. H. A. (2010). Complete nucleotide sequences of four dsRNAs associated with a new chrysovirus infecting *Aspergillus fumigatus. Virus. Res.* 153, 64–70. doi: 10.1016/j.virusres.2010.07.008

Jiang, D., and Ghabrial, S. A. (2004). Molecular characterization of *Penicillium chrysogenum* virus: reconsideration of the taxonomy of the genus *Chrysovirus*. *J. Gen. Virol.* 85, 2111–2121. doi: 10.1099/vir.0.79842-0

Lemke, P. A., Nash, C. H., and Pieper, S. W. (1973). Lytic plaque formation and variation in virus titre among strains of *Penicillium chrysogenum*. *J. Gen. Microbiol.* 76, 265–275. doi: 10.1099/00221287-76-2-265

Lemke, P. A., and Ness, T. M. (1970). Isolation and characterization of a double stranded ribonucleic acid from *Penicillium chrysogenum*. *J. Virol.* 6, 813–819. doi: 10.1099/0022-1317-6-3-437

Li, L., Liu, J., Xu, A., Wang, T., Chen, J., and Zhu, X. (2013). Molecular characterization of a trisegmented chrysovirus isolated from the radish *Raphanus sativus*. *Virus. Res.* 176, 169–178. doi: 10.1016/j.virusres.2013.06.004

Liu, H. Q., Fu, Y. P., Xie, J. T., Cheng, J. S., Ghabrial, S. A., Li, G. Q., et al. (2012). Evolutionary genomics of mycovirus-related dsRNA viruses reveals cross-family horizontal gene transfer and evolution of diverse viral lineages. *BMC Evol. Biol.* 12:91. doi: 10.1186/1471-2148-12-91

Liu, Y., Dynek, J. N., Hillman, B. I., and Milgroom, M. G. (2007). Diversity of viruses in *Cryphonectria parasitic* and *C. nitschkei* in Japan and China, and partiacharacterization of a new chrysovirus species. *Mycol. Res.* 111, 433–442. doi: 10.1016/j.mycres.2006.12.006

Niu, Y., Yuan, Y., Mao, J., Yang, Z., Cao, Q., Zhang, T., et al. (2018). Characterization of two novel mycoviruses from *Penicillium digitatum* and the related fungicide resistance analysis. *Sci. Rep.* 8:5513. doi: 10.1038/s41598-018-23807-3

Niu, Y., Zhang, T., Zhu, Y., Yuan, Y., Wang, S., Liu, J., et al. (2016). Isolation and characterization of a novel mycovirus from *Penicillium digitatum*. *Virology* 494, 15–22. doi: 10.1016/j.virol.2016.04.004

Okada, R., Ichinosea, S., Takeshitaa, K., Urayamaa, S., Fukuharaa, T., Komatsub, K., et al. (2018). Molecular characterization of a novel mycovirus in *Alternaria alternata* manifesting two-sided effects: down-regulation of host growth and upregulation of host plant pathogenicity. *Virology* 519, 23–32. doi: 10.1016/j.virol.2018.03.027

Pandey, B., Naidu, R. A., and Grove, G. G. (2018). Detection and analysis of mycovirus-related RNA viruses from grape powdery mildew fungus *Erysiphe necator*. *Arch. Virol.* 163, 1019–1030. doi: 10.1007/s00705-018-3714-0

Rwahnih, M. A., Daubert, S., Úrbeztorres, J. R., Cordero, F., and Rowhani, A. (2011). Deep sequencing evidence from single grapevine plants reveals a virome dominated by mycoviruses. *Arch. Virol.* 156, 397–403. doi: 10.1007/s00705-010-0869-8

Sotaro, C., Lakha,. S., Lin, Y. H., Sasaki, A., Satoko, K., and Suzuki, N. (2009). A novel bipartite double-stranded RNA mycovirus from the white root rot fungus *Rosellinia necatrix*: molecular and biological characterization, taxonomic considerations, and potential for biological control. *J. Virol.* 24, 12801–12812. doi: 10.1128/JVI.01830-09

Streit, S., Michalski, C. W., Erkan, M., Kleeff, J., and Friess, H. (2009). Northern blot analysis for detection and quantification of RNA in pancreatic cancer cells and tissues. *Nat. Protoc.* 1, 37–43. doi: 10.1038/nprot.2008.216

Sun, L., and Suzuki, N. (2008). Intragenic rearrangements of a mycoreovirus induced by the multifunctional protein p29 encoded by the prototypic hypovirus CHV1-EP713. *RNA* 14, 2557–2571. doi: 10.1261/rna.1125408

Tamura, K., Stecher, G., Peterson, D., Filipski, A., and Kumar, S. (2013). MEGA6: molecular evolutionary genetics analysis version 6.0. *Mol. Biol. Evol.* 30, 2725–2729. doi: 10.1093/molbev/mst197 MBE

Thompson, J. D., Gibson, T. J., Plewniak, F., Jeanmougin, F., and Higgins, D. G. (1997). The CLUSTAL_X windows interface: flexible strategies for multiple sequence alignment aided by quality analysis tools. *Nucleic Acids Res.* 24, 4876–4882. doi: 10.1093/nar/25.24.4876

Urayama, S., Kato, S., Suzuki, Y., Aoki, N., Le, M. T., Arie, T., et al. (2010). Mycoviruses related to chrysovirus affect vegetative growth in the rice blast fungus *Magnaporthe oryzae*. *J. Gen. Virol.* 91, 3085–3094. doi: 10.1099/vir.0.025411-0

Urayama, S., Ohta, T., Onozuka, N., Sakoda, H., Fukuhara, T., Arie, T., et al. (2012). Characterization of *Magnaporthe oryzae* chrysovirus 1 structural proteins and their expression in *Saccharomyces cerevisiae*. *J. Virol.* 86, 8287–8295. doi: 10.1128/JVI.00871-12

Urayama, S., Sakoda, H., Takai, R., Katoh, Y., Le, T., Fukuhara, T., et al. (2014). A dsRNA mycovirus, *Magnaporthe oryzae* chrysovirus 1-B, suppresses vegetative growth and development of the rice blast fungus. *Virology* 448, 265–273. doi: 10.1016/j.virol.2013.10.02

Yamashita, S., Doi, Y., and Yora, K. (1973). Intracellular appearance of *Penicillium chrysogenum* virus. *Virology* 55, 445–452. doi: 10.1016/0042-6822(73)90186-4

Yang, Z., Geng, H., Zheng, Y., Yuan, Y., Wang, M., Mao, J., Zhang, T., et al. (2018). Molecular characterization of a new gammapartitivirus isolated from the citrus-pathogenic fungus *Penicillium digitatum*. *Arch. Virol.* 163, 3185–3189. doi: 10.1007/s00705-018-3951-2

Yu, J., Lee, K. M., Son, M., and Kim, K. H. (2011). Molecular characterization of *Fusarium graminearum* virus 2 isolated from *Fusarium graminearum* strain 98-8-60. *Plant. Pathol. J.* 27, 285–290. doi: 10.5423/PPJ.2011.27.3.285

Zhang, J., Zhao, Z., Hu, R., Guo, L., Zheng, L., Du, Z., et al. (2017). The genome sequence of *Brassica campestris* chrysovirus 1, a novel putative plant-infecting tripartite chrysovirus. *Arch. Virol.* 162, 1107–1111. doi: 10.1007/s00705-016-3196-x

Zhong,. J., Pang, X. D., Zhu, H. J., Gao, B. D., Huang, W. K., and Zhou, Q. (2016). Molecular characterization of a trisegmented mycovirus from the plant pathogenic fungus *Colletotrichum gloeosporioides*. *Viruses* 8:268. doi: 10.3390/v8100268

Conflict of Interest Statement: The authors declare that the research was conducted in the absence of any commercial or financial relationships that could be construed as a potential conflict of interest.

frontiers in Microbiology

ORIGINAL RESEARCH
published: 15 May 2019
doi: 10.3389/fmicb.2019.01076

Identification of a Novel Hypovirulence-Inducing Hypovirus From *Alternaria alternata*

Huan Li[1†], Ruiling Bian[1†], Qian Liu[1], Liu Yang[1], Tianxing Pang[1], Lakha Salaipeth[2], Ida Bagus Andika[3], Hideki Kondo[3] and Liying Sun[1]*

[1] State Key Laboratory of Crop Stress Biology for Arid Areas and College of Plant Protection, Northwest A&F University, Yangling, China, [2] School of Bioresources and Technology, King Mongkut's University of Technology Thonburi, Bangkok, Thailand, [3] Institute of Plant Science and Resources, Okayama University, Kurashiki, Japan

OPEN ACCESS

Edited by:
Robert Czajkowski, University of Gdańsk, Poland

Reviewed by:
Sotaro Chiba, Nagoya University, Japan
Eeva Johanna Vainio, Natural Resources Institute Finland (Luke), Finland

***Correspondence:**
Liying Sun
sunliying@nwafu.edu.cn;
sunly_de@126.com

[†] *These authors have contributed equally to this work*

Specialty section:
This article was submitted to Virology, a section of the journal Frontiers in Microbiology

Received: *14 February 2019*
Accepted: *29 April 2019*
Published: *15 May 2019*

Citation:
Li H, Bian R, Liu Q, Yang L, Pang T, Salaipeth L, Andika IB, Kondo H and Sun L (2019) Identification of a Novel Hypovirulence-Inducing Hypovirus From Alternaria alternata. Front. Microbiol. 10:1076. doi: 10.3389/fmicb.2019.01076

Mycoviruses are wide spread throughout almost all groups of fungi but only a small number of mycoviruses can attenuate the growth and virulence of their fungal hosts. *Alternaria alternata* is an ascomycete fungus that causes leaf spot diseases on various crop plants. In this study, we identified a novel ssRNA mycovirus infecting an *A. alternata* f. sp. *mali* strain isolated from an apple orchard in China. Sequence analyses revealed that this virus is related to hypoviruses, in particular to Wuhan insect virus 14, an unclassified hypovirus identified from insect meta-transcriptomics, as well as other hypoviruses belonging to the genus *Hypovirus*, and therefore this virus is designed as Alternaria alternata hypovirus 1 (AaHV1). The genome of AaHV1 contains a single large open-reading frame encoding a putative polyprotein (∼479 kDa) with a cysteine proteinase-like and replication-associated domains. Curing AaHV1 from the fungal host strain indicated that the virus is responsible for the slow growth and reduced virulence of the host. AaHV1 defective RNA (D-RNA) with internal deletions emerging during fungal subcultures but the presence of D-RNA does not affect AaHV1 accumulation and pathogenicities. Moreover, AaHV1 could replicate and confer hypovirulence in *Botryosphaeria dothidea*, a fungal pathogen of apple white rot disease. This finding could facilitate better understanding of *A. alternata* pathogenicity and is relevant for development of biocontrol methods of fungal diseases.

Keywords: mycovirus, hypovirus, *Alternaria alternata*, apple, leaf blotch disease, hypovirulence, defective RNA

INTRODUCTION

Mycoviruses (fungal viruses) are widely distributed across all major groups of phytopathogenic fungi (Ghabrial and Suzuki, 2009; Pearson et al., 2009). Until recently, most reported mycoviruses were known to have double-stranded RNA (dsRNA) genomes, however, a number of single-strand RNA (ssRNA) mycoviruses have also been discovered (Ghabrial et al., 2015). Mycoviruses

with ssRNA genomes are currently grouped into seven families: *Hypoviridae*, *Narnaviridae*, *Barnaviridae*, *Alphaflexiviridae*, *Gammaflexiviridae*, *Deltaflexiviridae* and *Mymonaviridae*, and one floating genus, *Botybirnavirus* (Amarasinghe et al., 2018; King et al., 2018), but many other mycoviruses have not been classified.

The family *Hypoviridae* contains a sole genus *Hypovirus* with four assigned virus species. Its members (Cryphonectria hypovirus 1–4, CHV1–4) infect a phytopathogenic fungus, *Cryphonectria parasitica*, the causal agent of chestnut blight disease (Suzuki et al., 2018). Hypoviruses are known as capsidless viruses and they have large ssRNA genomes of 9.1–12.7 kb that possess either a single long open-reading frame (ORF) or two ORFs that encode polyproteins with a *cis*-acting papain-like cysteine protease at the N-terminus (Suzuki et al., 2018). In addition, many unclassified hypoviruses (or hypo-like viruses) have recently been discovered from other filamentous fungi, e.g., *Sclerotinia sclerotiorum* (Xie et al., 2011; Hu et al., 2014; Khalifa and Pearson, 2014; Marzano et al., 2015) *Valsa ceratosperma* (Yaegashi et al., 2012), *Fusarium graminearum* (Wang et al., 2013; Li et al., 2015), *Phomopsis longicolla* (Koloniuk et al., 2014), *Macrophomina phaseolina* (Marzano and Domier, 2016), *Botrytis cinerea* (Hao et al., 2018), and *Rosellinia necatrix* (Arjona-Lopez et al., 2018). Recent large-scale meta-transcriptomic analysis also uncovered that the hypo-like viruses are identified from non-fungal eukaryotes (invertebrates) (Shi et al., 2016). Based on phylogenetic analyses and genomic characteristics, CHV1–4 together with several unclassified hypoviruses were proposed to be classified into three genera, namely "Alphahypovirus" (including CHV1 and CHV2), "Betahypovirus" (including CHV3 and CHV4) and "Gammahypovirus" (Yaegashi et al., 2012; Hu et al., 2014; Khalifa and Pearson, 2014).

Mycoviruses are commonly associated with latent infections, while some are able to alter of fungal host phenotypes and/or attenuate the pathogenicity of fungal phytopathogenic hosts (Ghabrial and Suzuki, 2009; Pearson et al., 2009; Xie and Jiang, 2014). Mycovirus-associated hypovirulence has been studied extensively in CHV1-infected *C. parasitica* (Nuss, 2005; Eusebio-Cope et al., 2015; Rigling and Prospero, 2018). In addition, CHV2, CHV3, Botrytis cinerea hypovirus 1, Fusarium graminearum hypovirus 2 and the two strains of Sclerotinia sclerotiorum hypovirus 2 infections have also been associated with the hypovirulence of their fungal hosts (Hillman et al., 1994; Smart et al., 1999; Hu et al., 2014; Khalifa and Pearson, 2014; Li et al., 2015; Hao et al., 2018). In contrast, CHV4 and several other unclassified hypoviruses have no or a limited effect on fungal host virulence (Linder-Basso et al., 2005; Yaegashi et al., 2012; Wang et al., 2013; Koloniuk et al., 2014).

Apple leaf blotch disease caused by *Alternaria alternata* (family Pleosporaceae, class Dothideomycetes), has been a worldwide issue in apple production for decades (Johnson et al., 2000; Abe et al., 2010). *A. alternata* is generally considered a weak and opportunistic pathogen that infects a broad range of plants through various routes, such as wounds. Once infecting the plant, *A. alternata* is able to induce blackish spots on apple leaves in late spring or early summer, causing serious defoliation and declines in fruit quality (Filajdic and Sutton, 1995; Jung, 2007). The conventional use of fungicides to control apple leaf blotch disease is inefficient, therefore biocontrol methods are regarded as potential alternative means to control the disease. To date, several mycoviruses have been identified from *Alternaria* spp., including potential members of the genera *Chrysovirus*, *Partitivirus*, *Victorivirus*, *Botybirnavirus*, *Mitovirus*, and *Endornavirus* (Shang et al., 2015; Komatsu et al., 2016; Chen et al., 2017; Xiang et al., 2017; Okada et al., 2018; Xavier et al., 2018; Shamsi et al., 2019), as well as proposed the genus "Alternavirus," family "Fusariviridae" and an undescribed novel taxon (Aoki et al., 2009; Lin et al., 2015; Zhong et al., 2016). It was reported that certain mycoviruses identified from *A. alternata* appear to impair the colony growth of their host fungus (Aoki et al., 2009; Fuke et al., 2011). Mycoviruses are also associated with the cyclic tetrapeptide tentoxin production in *A. alternata*, which causes chlorosis in seedlings of sensitive plants (Shepherd, 1988). Recently, Alternaria alternata chrysovirus 1 has been described to alter host fungus growth, while it also enhances the pathogenicity of fungal host on plants, most likely through the induction of host-specific toxin production (Okada et al., 2018). However, to date, no mycovirus has been reported to attenuate the pathogenicity of *Alternaria* spp.

In this study, we identified and characterized a novel hypovirulence-inducing hypovirus from *A. alternata* designated as Alternaria alternata hypovirus 1 (AaHV1). We also showed that AaHV1 produces defective RNA (D-RNA) during fungal culture in the laboratory. In addition, we demonstrated that AaHV1 confers hypovirulence in other plant phytogenic fungi.

MATERIALS AND METHODS

Fungal Strains and Plant Materials

A total of 43 *A. alternata* strains were isolated from apple leaves with blotch disease randomly collected from a variety of apple orchards in Yangling County, Shaanxi Province of China in 2016. The *Botryosphaeria dothidea* strain, YL5, and *F. graminearum* strain, PH-1, were gifted from Dr. Zhonghua Ma (Zhejiang University, China) while the *C. parasitica* strain, EP155 (ATCC 3875) (Hillman et al., 1990) was a generous gift from Dr. Donald L. Nuss (University of Maryland). All fungal strains were maintained on potato dextrose agar (PDA) plates in the laboratory. For fungal identification, fungal DNA was isolated using standard phenol-chloroform extraction and ethanol precipitation, then used for polymerase chain reaction (PCR) amplification of the intergenic spacer (ITS) regions of ribosomal RNA gene (ITS1 and ITS2) (White et al., 1990). The amplified ITS sequences were subjected to a BLAST-N search.

All fungal strains were grown on PDA medium for 3–6 days at 24–26°C for morphological observation or on cellophane-covered PDA medium for RNA, DNA and protein extractions. Apple leaves (*Malus domestica* cv. Gala) subjected to pathogenicity tests were provided by Dr. Qingmei Guan (Northwest A&F University, China).

Fungus grew on different stress-inducing mediums for 5 days with the same growth condition as grown on PDA medium. The preparation of Vogel's medium and stress-inducing mediums

with the presence of 1 M NaCl, 1 M Sorbitol, 1% SDS and Congo red in PDA was described previously (Davis and de Serres, 1970; Zheng et al., 2012). All experiments used at least three independent fungal cultures.

Fungal Inoculation

For inoculation of *A. alternata* with apple leaves, mycelia-containing gel plugs (around 0.5 × 1 cm), picked from the edge of a 3-day-old culture colony, were placed on newly grown apple leaves. The petioles of inoculated leaves were wrapped with water-wet cotton for moisturizing. Inoculated apple leaves were kept at 25°C, 70 to 80% humidity and with a photoperiod of 16 h/8 h (day/night). All inoculations were repeated three times.

RNA Extraction, RT-PCR Detection and RNA Blot Analysis

Extraction of ssRNA and dsRNA from fungal mycelia followed the procedure described previously (Sun and Suzuki, 2008). DsRNA-enriched fraction was separated on 8% polyacrylamide gel electrophoresis (PAGE). For RT-PCR detection, first-strand cDNAs were synthesized using ReverTra Ace reverse transcriptase (Toyobo, Osaka, Japan) and amplified using 2 × mixture DNA polymerase (Kangwei, Beijing, China). For Northern blot analysis, Digoxigenin (DIG)-labeled DNA probes specific for genomic viral RNA (N: 180 to 900 nt; M: 7981 to 8603 nt and C: 13486 to 14039 nt, see **Figure 4C**) were utilized. The probes were prepared with the PCR DIG Probe Synthesis Kit (Roche Diagnostics, Penzberg, Germany). Gel electrophoresis and blotting were carried out as described previously (Andika et al., 2005). Hybridization conditions and detection of mRNAs were as described in the DIG Application Manual supplied by Roche. All of the primers used in this study are listed in **Supplementary Table S1**.

For viral dsRNA quantification, total RNA was prepared from *A. alternata* mycelia cultured on PDA covered with cellophane as described by Andika et al. (2017b). The final RNA concentration was adjusted to 0.1 μg/μl and used for agarose gel electrophoresis. The quantification of viral genomic dsRNA as described previously (Suzuki et al., 2003). Total RNA was extracted and subsequently electrophoresed in a 1.4% agarose gel in a 1 × TAE as described before (Sun et al., 2006). RNA bands were visualized with ChampGel 6000, a gel documentation and image analysis system (Beijing Sage Creation Science Co., Beijing, China). Relative amounts of viral genomic RNA were normalized to the amount of host fungal ribosomal RNA (rRNA).

Next-Generation Sequencing and Rapid Amplification of cDNA Ends Analysis

The dsRNA-enriched fraction was used as a template for next-generation sequencing analysis. Preparation of the cDNA library was performed using NEBNext® Ultra™ RNA Library Prep Kit for Illumina (New England Biolabs Inc., Ipswich, MA, United States) and sequenced on the Illumina HiSeq 4000 platform (Illumina, San Diego, CA, United States). Raw reads were cleaned by removing adapter sequences, and low-quality bases (PHRED quality scores ≤ 5) were trimmed by a Trimmomatic package with default parameters so truncated reads smaller than 35 bp were discarded. All clean reads were then assembled through the *de novo* assembly program Trinity[1] with a *K*-mer value = 25. Assembled reads were subjected to BLASTX searches with a cut-off of $E \leq$ 1e-5. To completely sequence the viral genome, RNA ligase-mediated (RLM)-rapid amplification of cDNA ends (RACE) was performed as previously described (Suzuki et al., 2004).

Sequence and Phylogenetic Analyses

Sequence data were analyzed via GENETYX-MAC (Genetyx Co., Tokyo, Japan). Potential stem-loop RNA structures were predicted by employing Mfold version 2.3 (Zuker, 2003) (Web server URL:[2]). The conserved protein domains were predicted by the National Center for Biotechnology Information (NCBI) conserved domain database[3]. Putative transmembrane domains were determined using the TMHMM server version 2.0[4] (Krogh et al., 2001). Multiple sequence alignments were performed using the MAFFT v7 (Katoh and Toh, 2008) or CLC Genomics Workbench v11 (CLC Bio-Qiagen, Aarhus, Denmark). Maximum likelihood (ML) phylogenetic tree construction was carried out as described previously (Kondo et al., 2015). Neighbor joining (NJ) (Saitou and Nei, 1987) tree was constructed based on the amino acid alignments using MAFFT. The trees were visualized with the FigTree 1.3.1[5].

Virus Transmission Assay

Hyphal anastomosis or hyphal fusion was conducted for viral horizontal transmission between fungal strains which are vegetatively compatible. Prior to hyphal fusion, the fungal partners were refreshed in PDA at 3 days. Co-culturing of fungal pairs was in 10-cm PDA plates in close proximity (10 mm) with each other and replicated across three plates. Mycelium blocks were taken randomly from the fungal pair, donor (virus source) side and recipient side (virus-free strain), to evaluate virus transmission. For viral vertical transmission, the assay was carried out to verify the frequencies of virus transmission through asexual spores. Fungal strains infected with the virus were cultured for 4 weeks on the bench top. Asexual spores were liberated in distilled water and spread on 10-cm PDA plates at appropriated dilutions. Single conidial germ lines were transferred to new PDA plates and cultured for 3 days. The number of infected colonies were scored based on visual observation of distinctive virus infection-associated colony morphologies and dsRNA or RT-PCR detection.

Viral RNA Transfection

The polyethyleneglycol (PEG)-mediated transfection described by Sun et al. (2006) was performed. The purified total RNA containing viral RNAs was introduced into the freshly prepared protoplasts (Eusebio-Cope et al., 2009).

[1]http://trinityrnaseq.github.io
[2]http://mfold.rna.albany.edu/
[3]https://blast.ncbi.nlm.nih.gov/Blast.cgi
[4]http://www.cbs.dtu.dk/services/TMHMM/
[5]http://tree.bio.ed.ac.uk/software/

Virulence Assay

The virulence of fungal colonies was assessed on apple leaves. Apple plants were generated from pathogen-free tissue culture and grown in a growth room. Fungi was inoculated on newly developed apple leaves and incubated on a bench top (25–27°C). Lesions were measured at days 5 and 7 post-inoculation. All inoculations were repeated three times.

RESULTS AND DISCUSSION

Isolation of *A. alternata* Strains Carrying Virus-Like dsRNA Elements

In order to study mycoviruses infecting *A. alternata*, 43 field fungal strains were collected from leaves of apple (*M. domestica* cv. Fuji) showing symptoms typical of Alternaria blotch disease (**Supplementary Figure S1A**). The collected fungal strains were isolated by hyphal tip culturing on PDA and re-inoculated to apple leaves to confirm that they are the causative agents of leaf blotch disease (**Supplementary Figure S1A**). Identification by sequencing with the ITS of rRNA with universal fungal primers for the ITS1 and ITS2 regions confirmed those isolates were *A. alternata* f. sp. *mali* (Woudenberg et al., 2015). To examine whether those field strains were carrying RNA mycoviruses, the presence of dsRNA was analyzed. Seventeen out of 43 fungal strains contained at least one dsRNA element but two strains (YL-2B and YL-5D2) lost dsRNA after subsequent subcultures on PDA (**Figure 1A**, **Supplementary Figure S1B**, and **Supplementary Table S2**). This suggest that those strains are infected with mycoviruses.

The phenotypic observation of mycelia growth of dsRNA-containing and dsRNA-free strains on PDA indicated a strain contained a large single dsRNA element (YL-3C strain) while also exhibiting slow growth (**Figures 1A,B**). PAGE analysis of purified dsRNA indicated that the dsRNA band present in YL-3C

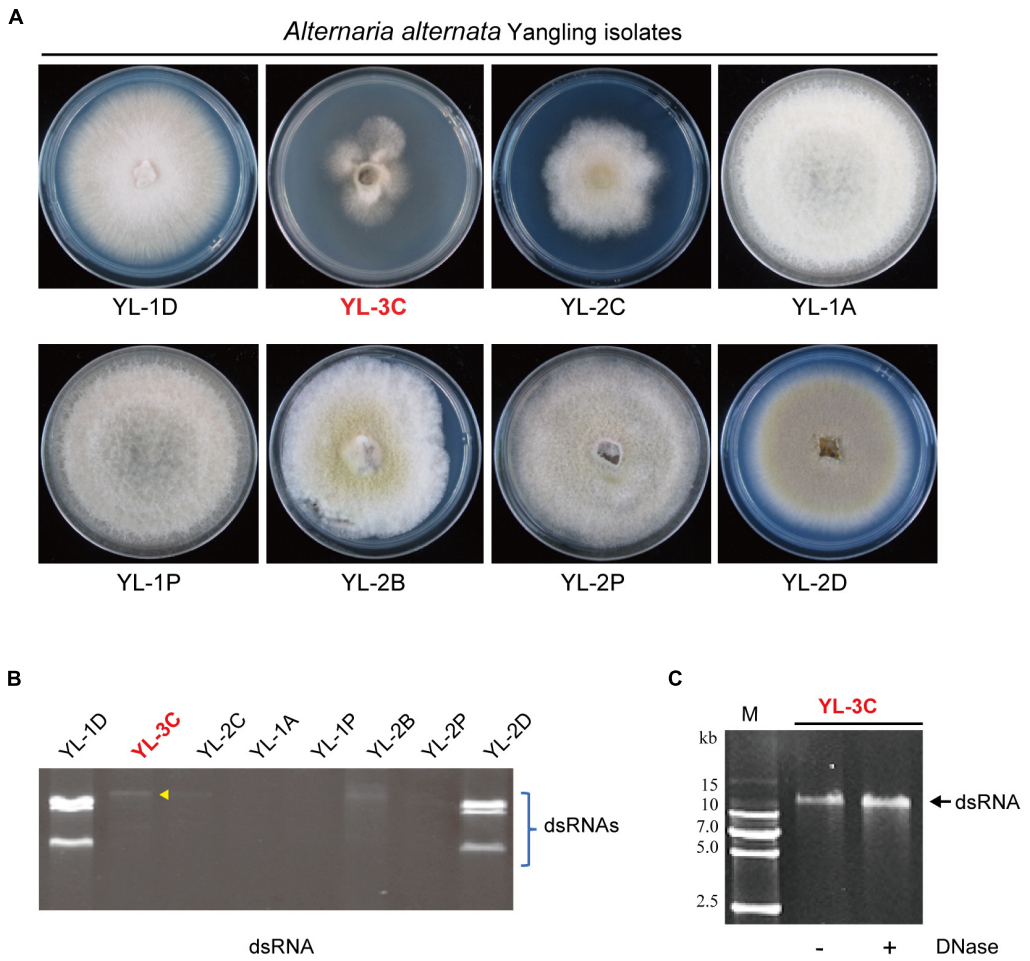

FIGURE 1 | Isolation of *Alternaria alternata* strains carrying mycovirus-like double-stranded RNA (dsRNA) elements. **(A)** Phenotypic growth of *A. alternata* strains (Yangling isolates) on PDA medium. Colonies were grown on PDA for 5 days and photographed. **(B)** DsRNA profiles of the fungal strains shown in **(A)**. The entire gel image was provided in the **Supplementary Figure S1B**. The yellow arrow head shows the position of the band of a putative hypovirus. DsRNA samples were run on agarose gel and stained with EtBr. **(C)** Virus-like dsRNA element isolated from the YL-3C strain. After DNase treatment, the dsRNA sample was run on PAGE and stained. M, DNA size marker (DNA ladder VI, http://www.real-times.com.cn).

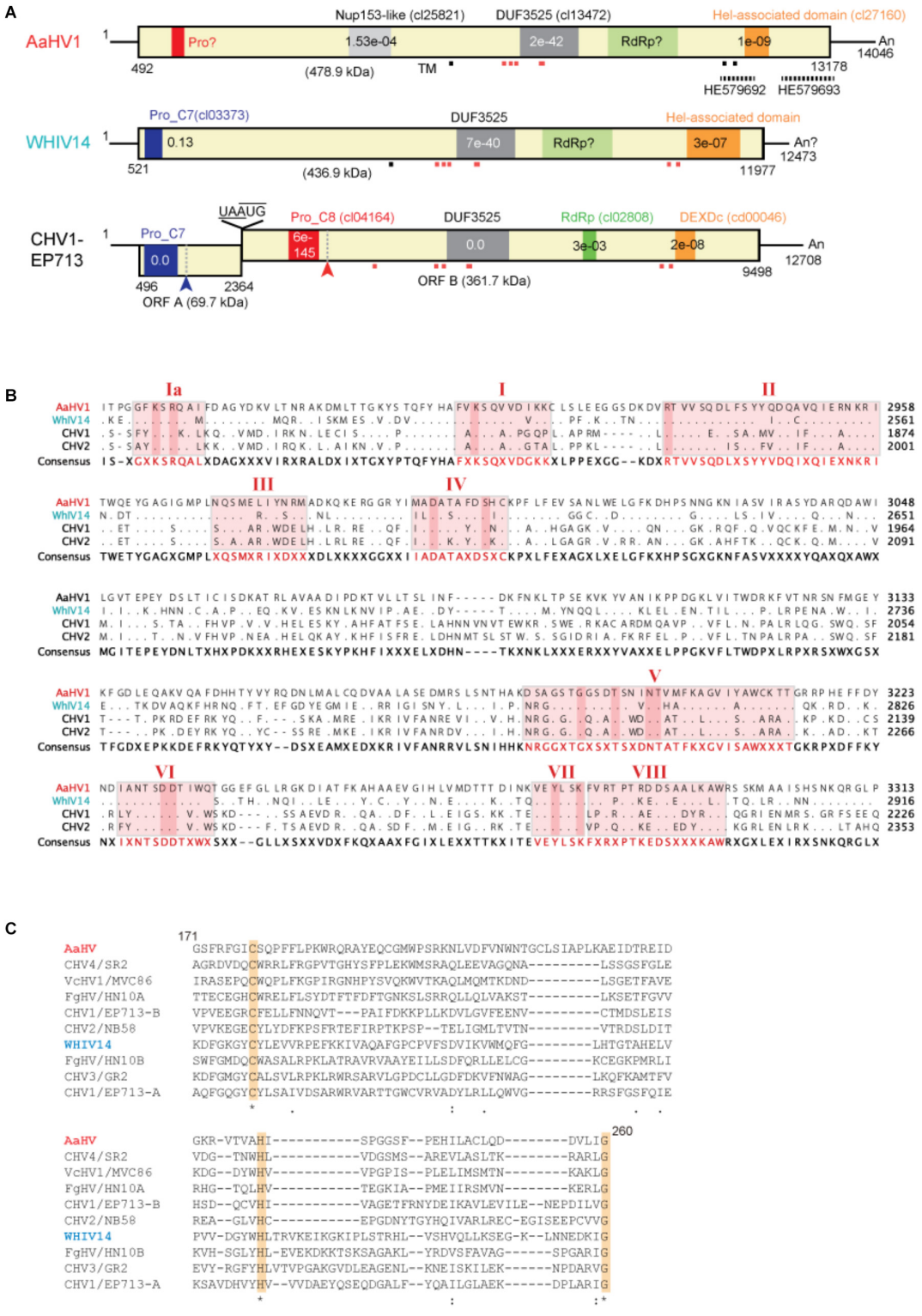

FIGURE 2 | Genomic properties of Alternaria alternata hypovirus 1 (AaHV1). **(A)** Genome organization of AaHV1, Wuhan insect virus 14 (WhlV14) and Cryphonectria hypovirus 1 (CHV1). Dashed lines above HE579692 and HE579693 indicate the corresponding regions of similar virus-like sequences found in *A. alternata* pyrosequencing (Feldman et al., 2012). Small red or gray squares (strong and weak probabilities, respectively) indicate the position of predicted transmembrane domains (TM). **(B)** Amino acid sequence alignment of the region corresponding to RdRp domain. The position of nine core RdRp motifs and conserved residues (Koonin et al., 1991) were highlighted. **(C)** Amino acid sequence alignment of the region corresponding to cysteine protease. Conserved three cysteine protease core residues (cysteine, histidine, and glycine) (Koonin et al., 1991) are highlighted.

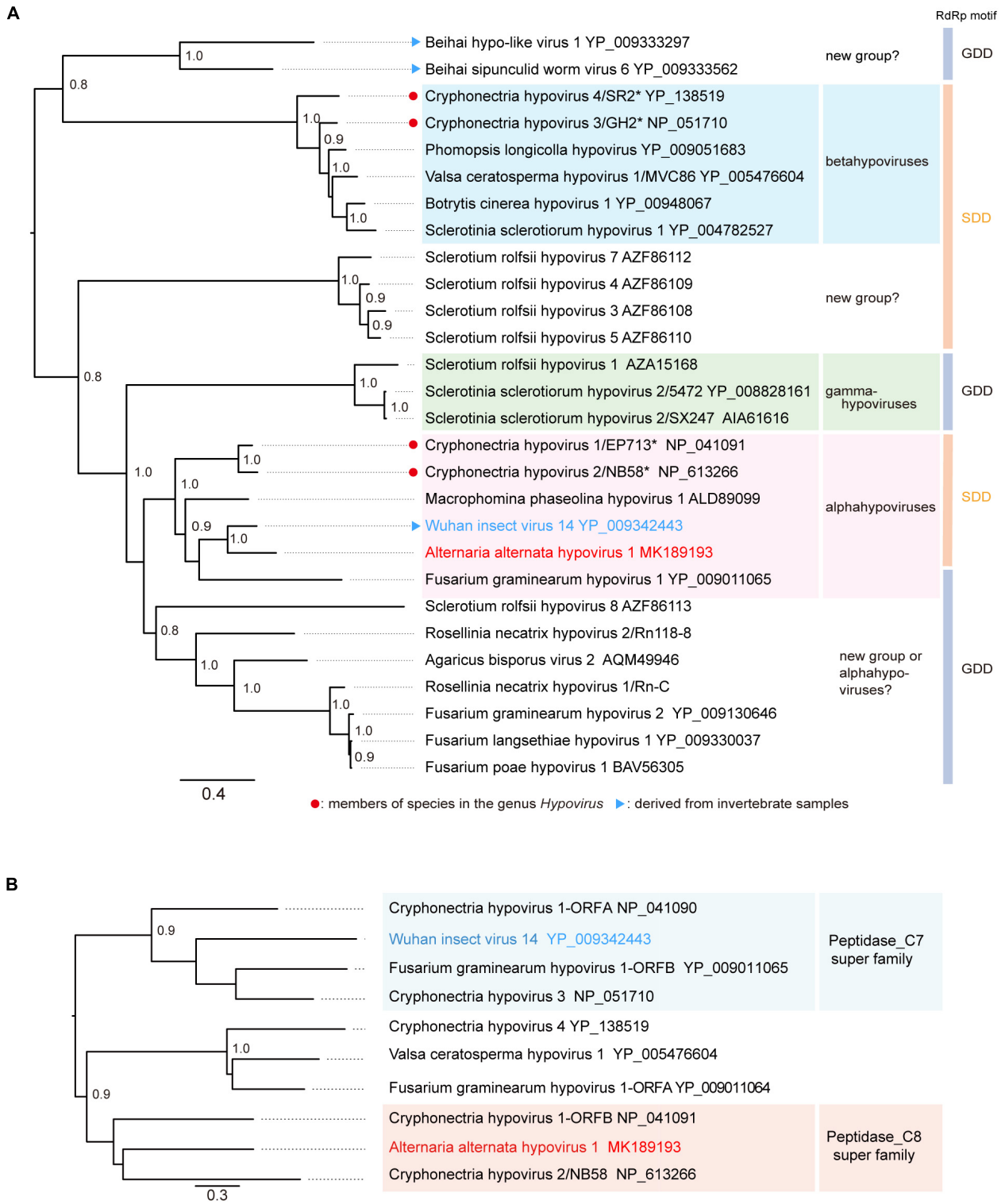

FIGURE 3 | Phylogenetic relationships of AaHIV1 with other hypoviruses. **(A)** An ML phylogenetic tree based on the multiple amino acid sequence alignment of the replicase protein or its candidate protein sequences. Virus names and GenBank/Refseq accession numbers of replicase proteins are shown. The members of species for genus *Hypovirus* were shown with red circles. **(B)** An NJ tree based on cysteine protease or its candidate protein sequences. Numbers at the nodes indicate aLRT or bootstrap values (values less than 0.8 are not displayed).

was around 14 kbp length and resistant against DNase treatment (**Figure 1C**). Thus, it is suggested that the presence of mycoviral-derived dsRNA in YL-3C attenuates the fungal growth.

Identification of a Novel Hypovirus Infecting an *A. alternata* Strain

We determined the complete nucleotide sequence of the dsRNA molecule isolated from YL-3C using high-throughput sequencing and RACE methods. The full-length cDNA was 14,046 nucleotides (nts) in length consisting of a long ORF coding for a polypeptide of 4,228 amino acid (∼479 kDa) with a 5′-untranslated regions (UTR) of 491 nts, a 3′-UTR of 868 nts and an adenine tail (poly A) on the 3′-sequence end (**Figure 2A**). The sequence was submitted to GenBank with the accession number, MK189193. Based on BLAST-P analysis, the large viral-encoded protein has the highest identity (52%, coverage 74%, *E*-value = 0) with polyproteins encoded by Wuhan insect virus 14 (WhIV14), a hypo-like virus identified from insect meta-transcriptomics (Shi et al., 2016). Additionally, this viral protein has a similar identity (39–42%, coverage 50–64%, *E*-value = 0) to those of Macrophomina phaseolina hypovirus 1 (MpHV1) (Marzano et al., 2016), CHV1 (Shapira et al., 1991), Fusarium graminearum hypovirus 1 (FgHV1) (Wang et al., 2013) and CHV2 (Hillman et al., 1994; **Supplementary Figure S2**). Owing to its sequence relatedness to hypo- and hypo-like viruses, this newly identified virus is designated as Alternaria alternata hypovirus 1 (AaHV1). A BLAST-N search showed that AaHV1 has 81–85% identity homology with two hypovirus-like sequence fragments, 957 nts (GenBank accession HE579692) and 626 nts (GenBank accession HE579693), from *A. alternata* pyrosequencing (Feldman et al., 2012) (**Figure 2A**). By RT-PCR, two strains, YL-2C and YL-1E were found to contain AaHV1 RNA (**Supplementary Table S2**). AaHV1 disappeared in YL-2C after subsequent subcultures. YL-1E contains mixed virus infection so it is not further characterized in this study.

NCBI's conserved domain search (Marchler-Bauer et al., 2017) showed that AaHV1-encoded proteins possess three conserved domains, Nucleoporin Nup153-like (accession cl25821), DUF3525 (accession cl13472) and helicase-associated domain (accession cl27160) with low or moderate *E*-values (**Figure 2A**). WhIV14 and CHV1 ORF B proteins also contain DUF3525 and helicase domains but the Nup153-like domain does not exist (**Figure 2A**). Notably, AaHV1 protein contains multiple transmembrane motifs around or within the DUF3525 and helicase domains, similar to the WhIV14 and CHV1 ORF B (**Figure 2A**). Unexpectedly, unlike in CHV1 ORF B protein, the RdRp domain was not detected in AaHV1 and WhIV14 proteins. However, AaHV1 and WhIV14 proteins were aligned with those of CHV1 ORF B and CHV2 ORF B proteins, in particular in the region between the DUF3525 and helicase domains where the presence of nine RdRp core motifs (Ia–VIII) (Koonin et al., 1991) were identified (**Figure 2B**). CHV1, which is the most well-studied hypovirus, processes viral polyproteins with two papain-like cysteine proteases encoded in ORF A and ORF B proteins (Choi et al., 1991; Koonin et al., 1991; Shapira and Nuss, 1991; **Figure 2A**). A papain-like cysteine protease motif was found in the N-terminal region of the WhIV14 protein but not in AaHV1 (**Figure 2A**). Nevertheless, alignment of the N-terminal region (171–260 aa region) of the AaHV1 protein with a papain-like cysteine protease domain regions of proteins encoded by other hypo- and hypo-like viruses uncovered the presence of conserved three cysteine protease core residues (cysteine, histidine and glycine in **Figure 2C**; Koonin et al., 1991), suggesting that AaHV1 encodes polyproteins processed by cysteine protease.

The phylogenetic relationship of AaHV1 with other known hypo- and hypo-like viruses based on complete amino acid sequences of replication-associated proteins were analyzed according to the ML method. The results showed that AaHV1 was clustered with CHV1, CHV2, MpHV1, WhIV14, and FgHV1 (**Figure 3A**), which are the members of the proposed "Alphahypovirus" genus (Yaegashi et al., 2012). This proposed virus group has a conserved SDD tripeptide in RdRP motif IV (see **Figure 2B**), except for FgHV1, which is GDD. In most known (+) ssRNA viruses, the consensus tripeptide is GDD, while for segmented (−) ssRNA viruses and a limited number of (+) ssRNA viruses (coronaviruses), the commonly found consensus sequence is SDD (Poch et al., 1990; Xu et al., 2003). In addition, AaHV1 formed a clade with WhIV14 (**Figure 3A**), suggesting their close evolutionary relatedness. However, when the phylogenetic relationships were analyzed based on the regions corresponding to putative papain-like cysteine protease (**Figure 2C**), AaHV1 and WhIV14 were placed in separated clades, where AaHV1 protease-like domain was placed with CHV1 ORF B protease (p48, peptidase_C8 super family) while WhIV14 protease was found with CHV1 ORF A protease (p29, peptidase_C7 super family) (**Figure 3B**). Thus, although AaHV1 and WhIV14 generally maintain their close evolutionary relationship, they specifically diverge with respect to the type of papain-like cysteine protease. AaHV1 and WhIV14 possibly have different origins of their proteolytic domains owing to potential recombination(s) among ancestral hypoviruses, just as previously reported for modern CHV1 strains (Mlinarec et al., 2018).

The 5′- and 3′-UTRs are important for viral translation, replication and assembly (Newburn and White, 2015). AaHV1 and WhV14 5′-UTRs are not well conserved at nucleotide sequences (**Supplementary Figure S3A**). RNA secondary structure prediction showed the presence of multiple stem loops in the 5′-UTRs of AaHV1 and WhIV14, but the RNA conformations were different between those two viruses (**Supplementary Figure S3B**). Recently, the 5′-UTRs of hypoviruses (CHV1, CHV2, and CHV3) have been demonstrated to have an internal ribosomal entry site (IRES) function (Chiba et al., 2018), therefore it is of interest investigating whether the 5′-UTRs of AaHV1 and other hypo-like viruses, including WhIV14, have similar IRES activity.

Molecular Characterization of AaHV1 Defective RNA

During subcultures of YL-3C isolate in PDA medium, YL-3C cultures were often found to contain an additionally a shorter dsRNA segment (namely YL-3C-D strain) (**Figure 4A**),

suggesting the emergence of viral defective RNA or satellite-like RNA as previously observed for other hypo- or hypo-like viruses (Hillman et al., 2000; Zhang and Nuss, 2008; Xie et al., 2011; Li et al., 2015; Hao et al., 2018). To check this possibility, RNA blot analysis was carried out using three different probes specific for both terminal and middle portions of the AaHV1 genome (**Figure 4C**). The shorter RNA segment was detected through probes specific for both terminal regions but not the probe specific for middle region (**Figure 4B**). This result suggests that the shorter RNA segment is a D-RNA with internal genome deletion. Moreover, the presence of D-RNA does not affect the accumulation level of AaHV1 pertaining to the RNA genome (**Figure 4B**), indicating that the presence of D-RNA does not suppress AaHV1 replication, such as that commonly observed for viral defective interfering. The complete nucleotide sequence of AaHV1 D-RNA was determined. D-RNA has major (6,477 nts) and minor (2 nts) deletions in the central region, and these deletions render a truncated ORF with the addition of a novel 45 aa owing to the frame shift (**Figure 4C**). This result confirms that D-RNA is not a satellite-like RNA, with sequences that are only conserved at the 5′- and 3′-terminal regions and contain unrelated sequences. In the case of CHV1, D-RNA production requires the activity of the dicer-like 2 (DCL2) and argonaute-like 2 (AGL2) proteins, key components of antiviral RNA silencing pathways in filamentous fungus (Zhang and Nuss, 2008; Chiba and Suzuki, 2015). It is interesting to investigate whether RNA silencing is similarly essential for AaHV1 D-RNA production in *A. alternata*.

Effects of AaHV1 Infection on Growth and Pathogenicity of *A. alternata*

AaHV1-free isogenic strain was obtained from YL-3C through single asexual spore isolation (YL-3C/dsF). We observed that AaHV1 was vertically transmitted through conidia with approximately 94–95% efficiency regardless of the presence of AaHV1 D-RNA (**Supplementary Figure S4A**). Moreover, from

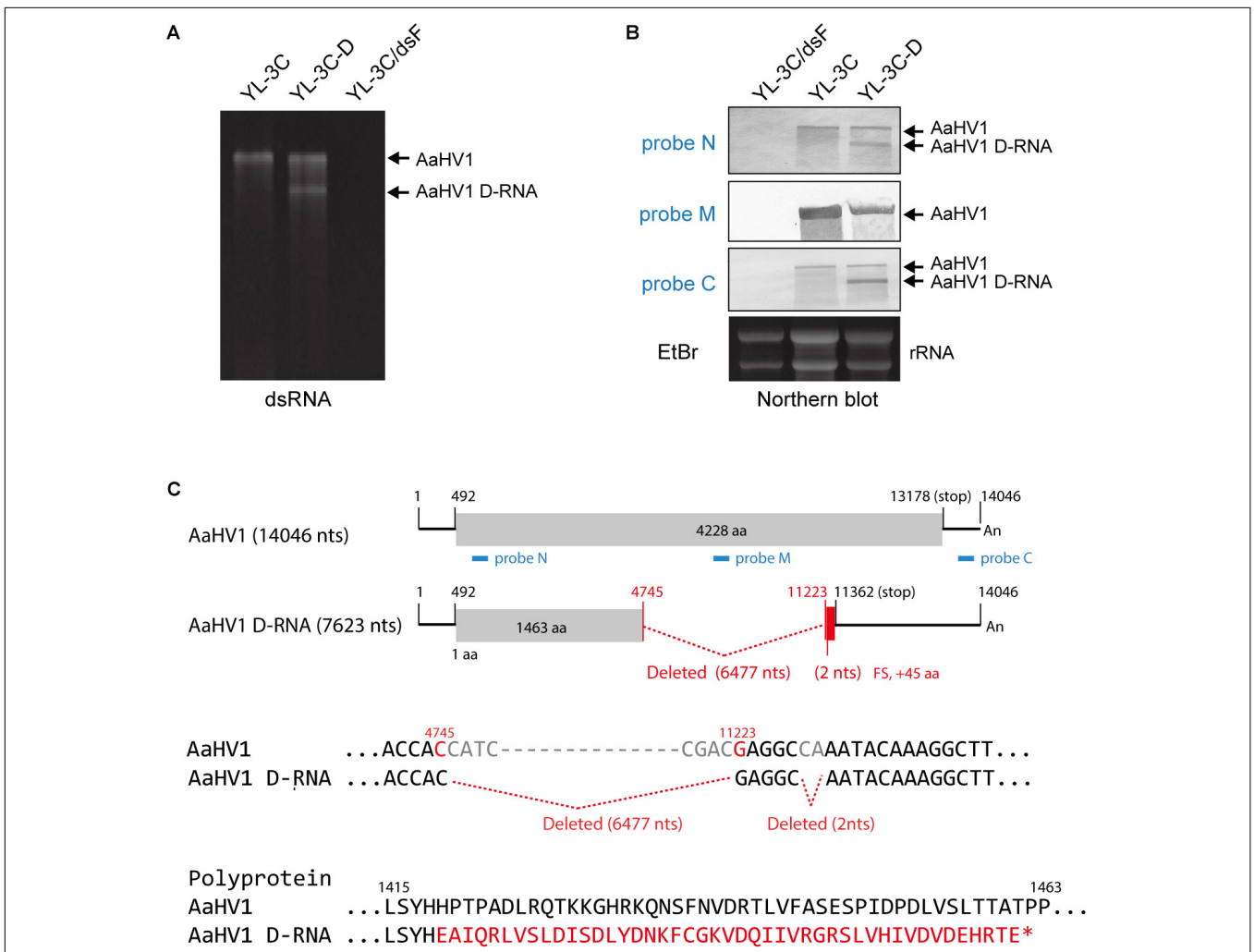

FIGURE 4 | Identification of the defective RNA (D-RNA) of AaHV1. **(A)** DsRNA profiles of YL-3C with D-RNA (YL-3C-D). DsRNA samples were run on PAGE and stained with EtBr. **(B)** RNA blot analysis of YL-3C-D strain carrying AaHV1 D-RNA. The genomic position of the probes used for detection is shown in C (N, M and C, blue lines). **(C)** The sequence of AaHV1 D-RNA. The additional 30 aa owing to the frame shift in D-RNA is shown in red letters.

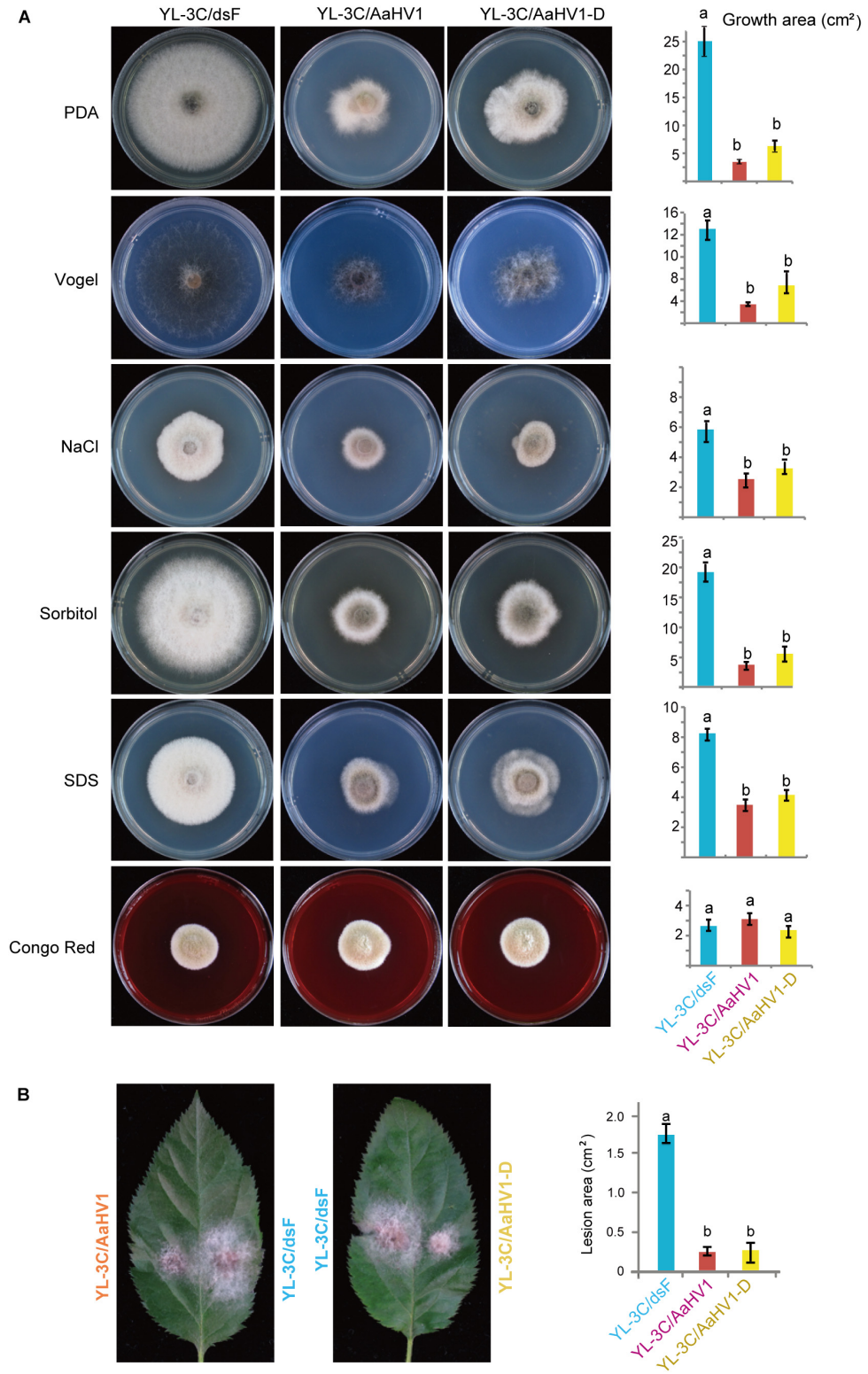

FIGURE 5 | Effects of AaHV1 infection on fungal growth and virulence. **(A)** Phenotypic growth of AaHV1-free and -infected YL-3C strains (YL-3C/dsF, YL-3C, and YL-3C-D) on PDA and stress-inducing mediums. Colonies were grown on PDA for 5 days and photographed. Data are means ± SD (n = 3). Different letters indicate a significant difference at $p < 0.01$ (one-way analysis of variance (ANOVA) using MATLAB anova1 program). **(B)** The colonies of AaHV1-free and -infected YL-3C strains on apple leaves. Colonies were grown on leaves for 5 days and photographed. Data are means ± SD (n = 3). Different letter indicates a significant difference at $p < 0.01$ (one-way ANOVA).

the AaHV1-infected parental strain (YL-3C), roughly 76% of the single spore isolates carried D-RNA (**Supplementary Figure S4A**), indicating the high emergence of D-RNA after vertical transmission through conidia. Both AaHV1 and AaHV1 + D-RNA were then re-introduced to the AaHV1-free isolate (YL-3C/dsF) through hyphal anastomosis to obtain YL-3C/AaHV1 and YL-3C/AaHV1-D (**Supplementary Figure S4B**). AaHV1-infected (YL-3C/AaHV1) and AaHV1 + AaHV1 D-RNA-infected (YL-3C/AaHV1-D) isolates clearly grew slower than AaHV1-free (YL-3C/dsF) isolates on PDA medium (**Figure 5A**). Accordingly, YL-3C/AaHV1 and YL-3C/AaHV1-D developed much smaller colonies than YL-3C/dsF on apple leaves (**Figure 5B**). This observation indicates that AaHV1 confers hypovirulence to the *A. alternata* strain, YL-3C, and the presence of D-RNA does not affect AaHV1's ability to attenuate fungal virulence.

To obtain a general view surrounding what kind of stresses AaHV1 elicits in fungal hosts, we cultured YL-3C/dsF, YL-3C/AaHV1, and YL-3C/AaHV1-D on different stress-inducing mediums. The presence of 1 M NaCl or 1 M Sorbitol in PDA provides hyperosmotic stress conditions for fungal growth, while 1% SDS and Congo red treatment were used to mimic cytoplasmic membrane and cell-wall stresses (Zheng et al., 2012). Vogel's medium was employed for the minimal medium for fungal growth (Davis and de Serres, 1970). Compared to YL-3C/dsF, YL-3C/AaHV1, and YL-3C/AaHV1-D showed obviously reduced mycelia growth across all tested fungal culture conditions except in Congo red treatment, where fungal growth was similar between AaHV1-free and -infected strains, indicating that AaHV1 was not able to induce relevant symptoms under Congo red treatment (**Figure 5A**). This result suggests that cytoplasmic membrane stresses may be connected with AaHV1 symptom induction on fungal hosts.

To investigate AaHV1 pathogenicity in different *A. alternata* host backgrounds, we introduced AaHV1 into a YL-1P strain that contains no detectable dsRNA (**Figure 1A**). Sequencing the ITS1 and ITS2 regions revealed this strain is also *A. alternata* f. sp. *mali*. Co-culture experiments demonstrated that YL-1P and YL-3C isolates belong to different vegetative compatibility groups and thus AaHV1 was not horizontally transmitted to YL-1P by hyphal anastomosis (data not shown). We then introduced AaHV1 to YL-1P by spheroplast transfection with total RNA isolated from YL-3C mycelia. The conidial isolates from AaHV1-transfected YL-1P were re-generated and subjected to four rounds of repeated subculture on PDA plates. It is interesting that all AaHV1 detected in the YL-1P host background did not produce D-RNA (data not shown). This result was consistently confirmed after further subculture (six rounds). As seen in **Figure 6A**, AaHV1 genomic dsRNA accumulated at lower levels in YL-1P than the YL-3C-D strain. RT-PCR with primer sets specific for the 5′ terminal of genomic RNA and the junction sequence in the D-RNA (**Supplementary Table S1**) was employed to further confirm the infection of YL-1P with AaHV1 (**Figure 6A**). D-RNA was only detected in the YL-3C strain, confirming that no D-RNA was accumulated in the YL-1P strain. Low accumulation of AaHV1 in the YL-1P strain may be associated with its genome stability.

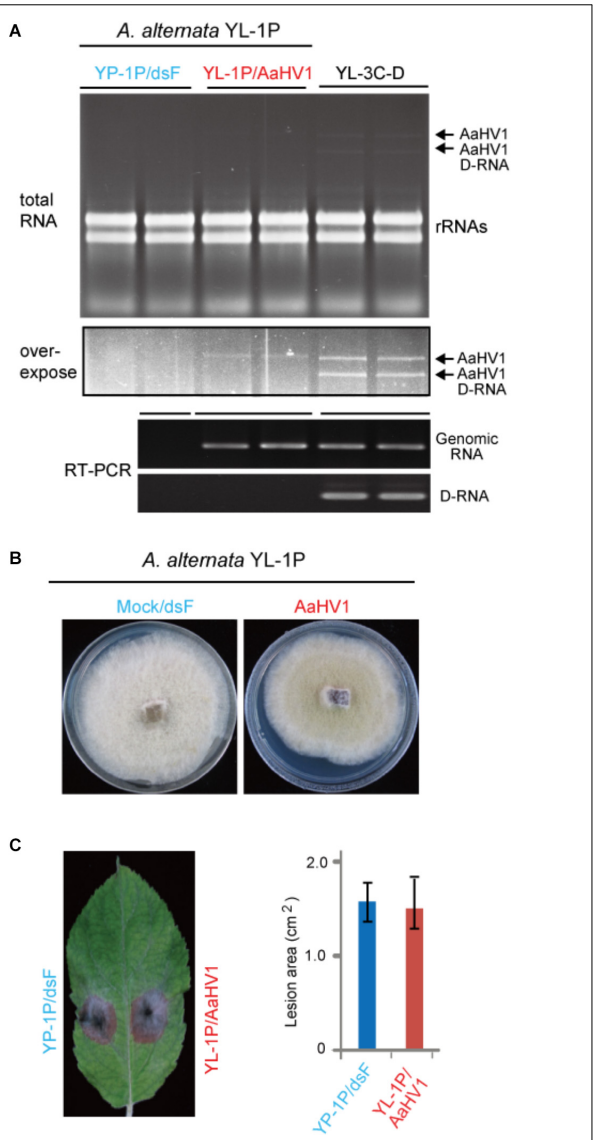

FIGURE 6 | AaHV1 accumulation and pathogenicity in another *A. altenaria* strain YL-1P. **(A)** Relative AaHV1 dsRNA accumulation levels in the YL-1P and YL-3C strains. Total RNA samples were run on agarose gel and stained with EtBr. RT-PCR detection of AaHV1 using genome- and D-RNA-specific primer sets (**Supplementary Table S1**). **(B)** Phenotypic growth of AaHV1-free and -infected YL-1P strains on PDA mediums. Colonies were grown on PDA for 5 days and photographed. **(C)** The colonies of AaHV1-free and -infected YL-1P strains on apple leaves. Colonies were grown on leaves for 5 days and photographed. Data are means ± SD (n = 3).

AaHV1-infected YL-1P grew slightly slower than dsRNA-free YL-1P (**Figure 6B**). Moreover, AaHV1-free and -infected YL-1P strains developed similar size of lesions on apple leaves (**Figure 6C**), indicating that AaHV1 does not confer hypovirulence to the YL-1P strain. These observations suggest that AaHV1 pathogenicity differs among different *A. alternata* f. sp. *mali* strains. Moreover, AaHV1 accumulation is lower in YL-1P than YL-3C strains, suggesting that different *A. alternata* strains have varying defense strengths against virus infection.

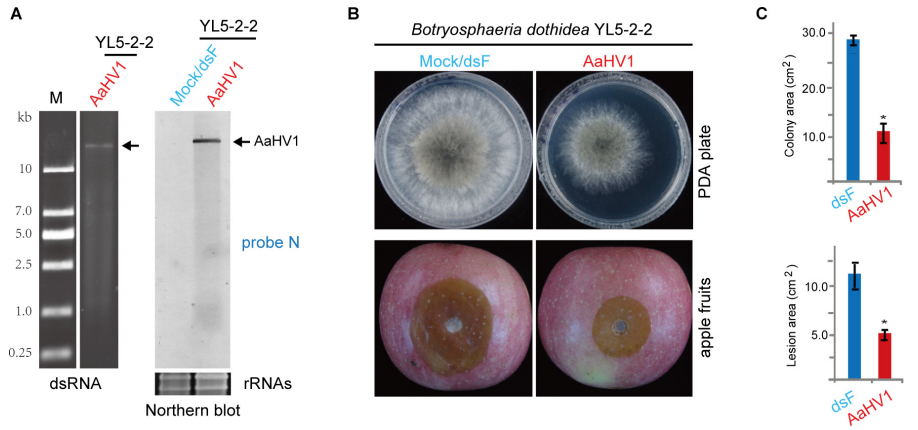

FIGURE 7 | AaHV1 infectivity and pathogenicity in *Botryosphaeria dothidea*. **(A)** AaHV1 RNA in *B. dothidea* YL5 strain (YL5-2-2 isolate) detected by dsRNA isolation and RNA blotting. **(B)** Phenotypic growth and virulence of AaHV1-free and -infected *B. dothidea* strains on PDA medium and apples. Colonies were grown on PDA (for 4 days) and leaves (for 4 days) and photographed. **(C)** The lesion area on apples described in B. Data are means ± SD ($n = 3$). Asterisk indicates $p < 0.01$ (Student's *t*-test).

AaHV1 Infectivity and Pathogenicity in Other Fungal Species

To assess AaHV1 infectivity in other Ascomycota fungal species, AaHV1 was introduced (transfected) to *B. dothidea*, *F. graminearum* and *C. parasitica*, which are the fungal pathogens of apple white rot (or ring rot), wheat head blight and chestnut blight diseases, respectively (Vasilyeva and Kim, 2000; Tang et al., 2012; Rigling and Prospero, 2018). AaHV1 accumulation was detected in *B. dothidea* (family *Botryosphaeriaceae*, belonging the same class Dothideomycetes with *Alternaria* spp.), but not in *F. graminearum* PH-1 (family *Nectriaceae*, class Sordariomycetes) and *C. parasitica* EP155 (family *Cryphonectriaceae*, class Sordariomycetes) (**Figure 7A** and data not shown). It is interesting to note that AaHV1 infection markedly reduced *B. dothidea* growth on PDA medium and apples (**Figures 7B,C**). At present, four RNA mycoviruses are known to infect the *B. dothidea* strains, two of them (a chrysovirus and proposed polymycovirus) are associated with conferring hypovirulence-associated traits to fungal hosts (Wang et al., 2014; Zhai et al., 2015, 2016). Our data indicates that AaHV1 could confer hypovirulence in a heterologous fungal host (unnatural host). This observation also implies that AaHV1 has potential for use as a biocontrol agent for other fungal crop diseases.

CONCLUSION

In this study, we characterized a novel mycovirus related to members of the *Hypoviridae* family from a phytopathogenic fungus, *A. alternata*. Although a number of mycoviruses have been identified from *A. alternata*, this is the first report of a hypovirulence-inducing mycovirus in *A. alternata*. Therefore, the finding with this virus provides a valuable experimental system to study the molecular aspects of virus-fungus interactions and fungal pathogenicity in *A. alternata*. Hypoviruses have a prominent place in mycovirology, in particular owing to long and intensive studies on CHV1 in the fungal host, *C. parasitica* (Nuss, 2005). CHV1 provides the first example of the successful use of a mycovirus as a biocontrol agent (Rigling and Prospero, 2018). In addition, many molecular aspects of mycovirology, including replication, pathogenicity and RNA silencing-associated host immunity, have been elucidated utilizing the CHV1-*C. parasitica* pathosystem (Zhang and Nuss, 2008; Chiba and Suzuki, 2015; Eusebio-Cope et al., 2015; Andika et al., 2017a, 2019). Like CHV1, AaHV1 also confers strong hypovirulence to fungal hosts and possess similar molecular properties. In this regard, AaHV1 is also a prospective research material for further study of the fundamental and applicative aspects of mycovirology.

DATA AVAILABILITY

No datasets were generated or analyzed for this study.

AUTHOR CONTRIBUTIONS

LSu designed the experiments. HL, RB, QL, LY, TP, and LSa performed the experimental work. IBA, HK, and LSu analyzed the data and wrote the manuscript.

FUNDING

This work was supported in part by the National Key Research and Development Program of China (2017YFD0201100), National Natural Science Foundation of China (U1703113), Science Foundation of Shaanxi (2016KW-069) to LSu, and Grants-in-Aid for Scientific Research on Innovative Areas from

the Japanese MEXT (16H06436, 16H06429, and 16K21723) to HK.

ACKNOWLEDGMENTS

We express our deep gratitude to Drs. Zhonghua Ma, Donald L. Nuss, Nobuhiro Suzuki, and Qingmei Guan for providing research materials.

SUPPLEMENTARY MATERIAL

The Supplementary Material for this article can be found online at: https://www.frontiersin.org/articles/10.3389/fmicb.2019.01076/full#supplementary-material

FIGURE S1 | (A) *Alternaria alternata* lesion on apple leaves after isolation and re-inoculation. **(B)** DsRNA profiles of *A. alternata* strains isolated from apple leaves.

FIGURE S2 | BLAST-P result using the AaHV1-encoded protein as a query.

FIGURE S3 | (A) Alignment of 5′-UTR sequences of AaHV1 and WhlV14. The putative start codons are highlighted with red color. **(B)** Predicted RNA secondary structures of 5′-UTR sequences of AaHV1 and WhlV14 (not shown the entire 5′-UTR regions).

FIGURE S4 | (A) Efficiency of vertical transmission of AaHV1 through conidia with or without its D-RNA element (YL-3C-D and YL-3C, respectively). **(B)** Horizontal transmission of AaHV1 and its D-RNA element through hyphal fusion. The dots were the position where mycelia took for sub-culturing.

TABLE S1 | A list of primers used in this study.

TABLE S2 | Detection of AaHV1 in 43 *Alternaria alternata* strains.

REFERENCES

Abe, K., Iwanami, H., Kotoda, N., Moriya, S., and Takahashi, S. (2010). Evaluation of apple genotypes and *Malus* species for resistance to alternaria blotch caused by *Alternaria alternata* apple pathotype using detached-leaf method. *Plant Breed.* 129, 208–218. doi: 10.1111/j.1439-0523.2009.01672.x

Amarasinghe, G. K., Ceballos, N. G., Banyard, A. C., Basler, C. F., Bavari, S., Bennett, A. J., et al. (2018). Taxonomy of the order *Mononegavirales*: update 2018. *Arch. Virol.* 163, 2283–2294. doi: 10.1007/s00705-018-3814-x

Andika, I. B., Jamal, A., Kondo, H., and Suzuki, N. (2017a). SAGA complex mediates the transcriptional up-regulation of antiviral RNA silencing. *Proc. Natl. Acad. Sci. U.S.A.* 114, E3499–E3506. doi: 10.1073/pnas.1701196114

Andika, I. B., Wei, S., Cao, C. M., Salaipeth, L., Kondo, H., and Sun, L. Y. (2017b). Phytopathogenic fungus hosts a plant virus: a naturally occurring cross-kingdom viral infection. *Proc. Natl. Acad. Sci. U.S.A.* 114, 12267–12272. doi: 10.1073/pnas.1714916114

Andika, I. B., Kondo, H., and Suzuki, N. (2019). Dicer functions transcriptionally and posttranscriptionally in a multilayer antiviral defense. *Proc. Natl. Acad. Sci. U.S.A.* 116, 2274–2281. doi: 10.1073/pnas.1812407116

Andika, I. B., Kondo, H., and Tamada, T. (2005). Evidence that RNA silencing-mediated resistance to Beet necrotic yellow vein virus is less effective in roots than in leaves. *Mol. Plant Microbe Interact.* 18, 194–204. doi: 10.1094/mpmi-18-0194

Aoki, N., Moriyama, H., Kodama, M., Arie, T., Teraoka, T., and Fukuhara, T. (2009). A novel mycovirus associated with four double-stranded RNAs affects host fungal growth in *Alternaria alternata*. *Virus Res.* 140, 179–187. doi: 10.1016/j.virusres.2008.12.003

Arjona-Lopez, J. M., Telengech, P., Jamal, A., Hisano, S., Kondo, H., Yelin, M. D., et al. (2018). Novel, diverse RNA viruses from mediterranean isolates of the phytopathogenic fungus, *Rosellinia necatrix*: insights into evolutionary biology of fungal viruses. *Environ. Microbiol.* 20, 1464–1483. doi: 10.1111/1462-2920.14065

Chen, Y., Shang, H. H., Yang, H. Q., Gao, B. D., and Zhong, J. (2017). A mitovirus isolated from the phytopathogenic fungus *Alternaria brassicicola*. *Arch. Virol.* 162, 2869–2874. doi: 10.1007/s00705-017-3371-8

Chiba, S., Jamal, A., and Suzuki, N. (2018). First evidence for internal ribosomal entry sites in diverse fungal virus genomes. *mBio* 9:e2350–17. doi: 10.1128/mBio.02350-17

Chiba, S., and Suzuki, N. (2015). Highly activated RNA silencing via strong induction of dicer by one virus can interfere with the replication of an unrelated virus. *Proc. Natl. Acad. Sci. U.S.A.* 112, E4911–E4918. doi: 10.1073/pnas.1509151112

Choi, G. H., Pawlyk, D. M., and Nuss, D. L. (1991). The autocatalytic protease-p-29 encoded by a hypovirulence-associated virus of the chestnut blight fungus resembles the potyvirus-encoded protease HC-pro. *Virology* 183, 747–752. doi: 10.1016/0042-6822(91)91004-z

Davis, R. H., and de Serres, F. J. (1970). Genetic and microbiological research techniques for *Neurospora crassa*. *Method Enzymol.* 17, 79–143. doi: 10.1016/0076-6879(71)17168-6

Eusebio-Cope, A., Sun, L. Y., Tanaka, T., Chiba, S., Kasahara, S., and Suzuki, N. (2015). The chestnut blight fungus for studies on virus/host and virus/virus interactions: from a natural to a model host. *Virology* 477, 164–175. doi: 10.1016/j.virol.2014.09.024

Eusebio-Cope, A., Suzuki, N., Sadeghi-Garmaroodi, H., and Taga, M. (2009). Cytological and electrophoretic karyotyping of the chestnut blight fungus *Cryphonectria parasitica*. *Fungal Genet. Biol.* 46, 342–351. doi: 10.1016/j.fgb.2009.01.005

Feldman, T. S., Morsy, M. R., and Roossinck, M. J. (2012). Are communities of microbial symbionts more diverse than communities of macrobial hosts? *Fungal Biol.* 116, 465–477. doi: 10.1016/j.funbio.2012.01.005

Filajdic, N., and Sutton, T. B. (1995). Overwintering of alternaria-mali, the causal agent of Alternaria blotch of apple. *Plant Dis.* 79, 695–698. doi: 10.1094/PHYTO.2000.90.9.973

Fuke, K., Takeshita, K., Aoki, N., Fukuhara, T., Egusa, M., Kodama, M., et al. (2011). The presence of double-stranded RNAs in *Alternaria alternata* Japanese pear pathotype is associated with morphological changes. *J. Gen. Plant Pathol.* 77, 248–252. doi: 10.1007/s10327-011-0315-0

Ghabrial, S. A., Caston, J. R., Jiang, D. H., Nibert, M. L., and Suzuki, N. (2015). 50-plus years of fungal viruses. *Virology* 479, 356–368. doi: 10.1016/j.virol.2015.02.034

Ghabrial, S. A., and Suzuki, N. (2009). Viruses of plant pathogenic fungi. *Annu. Rev. Phytopathol.* 47, 353–384. doi: 10.1146/annurev-phyto-080508-081932

Hao, F. M., Ding, T., Wu, M. D., Zhang, J., Yang, L., Chen, W. D., et al. (2018). Two novel hypovirulence-associated mycoviruses in the phytopathogenic fungus *Botrytis cinerea*: molecular characterization and suppression of infection cushion formation. *Viruses* 10:E254. doi: 10.3390/v10050254

Hillman, B. I., Foglia, R., and Yuan, W. (2000). Satellite and defective RNAs of Cryphonectria hypovirus 3-Grand haven 2, a virus species in the family *Hypoviridae* with a single open reading frame. *Virology* 276, 181–189. doi: 10.1006/viro.2000.0548

Hillman, B. I., Halpern, B. T., and Brown, M. P. (1994). A viral dsRNA element of the chestnut blight fungus with a distinct genetic organization. *Virology* 201, 241–250. doi: 10.1006/viro.1994.1289

Hillman, B. I., Shapira, R., and Nuss, D. L. (1990). Hypovirulence-associated suppression of host functions in *Cryphonectria parasitica* can be partially relieved by high light-intensity. *Phytopathology* 80, 950–956.

Hu, Z. J., Wu, S. S., Cheng, J. S., Fu, Y. P., Jiang, D. H., and Xie, J. T. (2014). Molecular characterization of two positive-strand RNA viruses co-infecting a hypovirulent strain of sclerotirtia sclerotiorum. *Virology* 464, 450–459. doi: 10.1016/j.virol.2014.07.007

Johnson, R. D., Johnson, L., Kohmoto, K., Otani, H., Lane, C. R., and Kodama, M. (2000). A polymerase chain reaction-based method to specifically detect *Alternaria alternata* apple pathotype (A. mali), the causal agent of alternaria blotch of apple. *Phytopathology* 90, 973–976. doi: 10.1094/PHYTO.2000.90.9.973

Jung, K. H. (2007). Growth inhibition effect of pyroligneous acid on pathogenic fungus, *Alternaria mali*, the agent of alternaria blotch of apple. *Biotechnol. Bioproc. Eng.* 12, 318–322. doi: 10.1007/bf02931111

Katoh, K., and Toh, H. (2008). Recent developments in the MAFFT multiple sequence alignment program. *Brief. Bioinform.* 9, 286–298. doi: 10.1093/bib/bbn013

Khalifa, M. E., and Pearson, M. N. (2014). Characterisation of a novel hypovirus from *Sclerotinia sclerotiorum* potentially representing a new genus within the *Hypoviridae*. *Virology* 464, 441–449. doi: 10.1016/j.virol.2014.07.005

King, A. M. Q., Lefkowitz, E. J., Mushegian, A. R., Adams, M. J., Dutilh, B. E., Gorbalenya, A. E., et al. (2018). Changes to taxonomy and the international code of virus classification and nomenclature ratified by the international committee on taxonomy of viruses (2018). *Arch. Virol.* 163, 2601–2631. doi: 10.1007/s00705-018-3847-1

Koloniuk, I., El-Habbak, M. H., Petrzik, K., and Ghabrial, S. A. (2014). Complete genome sequence of a novel hypovirus infecting *Phomopsis longicolla*. *Arch. Virol.* 159, 1861–1863. doi: 10.1007/s00705-014-1992-8

Komatsu, K., Katayama, Y., Omatsu, T., Mizutani, T., Fukuhara, T., Kodama, M., et al. (2016). Genome sequence of a novel victorivirus identified in the phytopathogenic fungus *Alternaria arborescens*. *Arch. Virol.* 161, 1701–1704. doi: 10.1007/s00705-016-2796-9

Kondo, H., Chiba, S., and Suzuki, N. (2015). "Detection and analysis of non-retroviral RNA virus-like elements in plant, fungal, and insect genomes," in *Plant Virology Protocols -New Approaches to Detect Viruses and Host Responses*, eds I. Uyeda and C. Masuta (New York, NY: Humana Press. Inc), 73–88. doi: 10.1007/978-1-4939-1743-3_7

Koonin, E. V., Choi, G. H., Nuss, D. L., Shapira, R., and Carrington, J. C. (1991). Evidence for common ancestry of a chestnut blight hypovirulence-associated double-stranded-RNA and a group of positive-strand RNA plant-viruses. *Proc. Natl. Acad. Sci. U.S.A.* 88, 10647–10651. doi: 10.1073/pnas.88.23.10647

Krogh, A., Larsson, B., von Heijne, G., and Sonnhammer, E. L. L. (2001). Predicting transmembrane protein topology with a hidden Markov model: application to complete genomes. *J. Mol. Biol.* 305, 567–580. doi: 10.1006/jmbi.2000.4315

Li, P. F., Zhang, H. L., Chen, X. G., Qiu, D. W., and Guo, L. H. (2015). Molecular characterization of a novel hypovirus from the plant pathogenic fungus *Fusarium graminearum*. *Virology* 481, 151–160. doi: 10.1016/j.virol.2015.02.047

Lin, Y. H., Zhang, H. L., Zhao, C. J., Liu, S. X., and Guo, L. H. (2015). The complete genome sequence of a novel mycovirus from *Alternaria longipes* strain HN28. *Arch. Virol.* 160, 577–580. doi: 10.1007/s00705-014-2218-9

Linder-Basso, D., Dynek, J. N., and Hillman, B. I. (2005). Genome analysis of cryphonectria hypovirus 4, the most common hypovirus species in North America. *Virology* 337, 192–203. doi: 10.1016/j.virol.2005.03.038

Marchler-Bauer, A., Bo, Y., Han, L. Y., He, J. E., Lanczycki, C. J., Lu, S. N., et al. (2017). CDD/SPARCLE: functional classification of proteins via subfamily domain architectures. *Nucleic Acids Res.* 45, D200–D203. doi: 10.1093/nar/gkw1129

Marzano, S. Y. L., and Domier, L. L. (2016). Novel mycoviruses discovered from metatranscriptomics survey of soybean phyllosphere phytobiomes. *Virus Res.* 213, 332–342. doi: 10.1016/j.virusres.2015.11.002

Marzano, S. Y. L., Hobbs, H. A., Nelson, B. D., Hartman, G. L., Eastburn, D. M., McCoppin, N. K., et al. (2015). Transfection of *Sclerotinia sclerotiorum* with *in vitro* transcripts of a naturally occurring interspecific recombinant of Sclerotinia sclerotiorum hypovirus 2 significantly reduces virulence of the fungus. *J. Virol.* 89, 5060–5071. doi: 10.1128/JVI.03199-14

Marzano, S. Y. L., Nelson, B. D., Ajayi-Oyetunde, O., Bradley, C. A., Hughes, T. J., Hartman, G. L., et al. (2016). Identification of diverse mycoviruses through metatranscriptomics characterization of the viromes of five major fungal plant pathogens. *J. Virol.* 90, 6846–6863. doi: 10.1128/JVI.00357-16

Mlinarec, J., Nuskern, L., Jezic, M., Rigling, D., and Curkovic-Perica, M. (2018). Molecular evolution and invasion pattern of Cryphonectria hypovirus 1 in Europe: mutation rate, and selection pressure differ between genome domains. *Virology* 514, 156–164. doi: 10.1016/j.virol.2017.11.011

Newburn, L. R., and White, K. A. (2015). Cis-acting RNA elements in positive-strand RNA plant virus genomes. *Virology* 479, 434–443. doi: 10.1016/j.virol.2015.02.032

Nuss, D. L. (2005). Hypovirulence: mycoviruses at the fungal-plant interface. *Nat. Rev. Microbiol.* 3, 632–642. doi: 10.1038/nrmicro1206

Okada, R., Ichinose, S., Takeshita, K., Urayama, S., Fukuhara, T., Komatsu, K., et al. (2018). Molecular characterization of a novel mycovirus in *Alternaria alternata* manifesting two-sided effects: down-regulation of host growth and up-regulation of host plant pathogenicity. *Virology* 519, 23–32. doi: 10.1016/j.virol.2018.03.027

Pearson, M. N., Beever, R. E., Boine, B., and Arthur, K. (2009). Mycoviruses of filamentous fungi and their relevance to plant pathology. *Mol. Plant Pathol.* 10, 115–128. doi: 10.1111/j.1364-3703.2008.00503.x

Poch, O., Blumberg, B. M., Bougueleret, L., and Tordo, N. (1990). Sequence comparison of five polymerases (L proteins) of unsegmented negative-strand RNA viruses: theoretical assignment of functional domains. *J. Gen. Virol.* 71, 1153–1162. doi: 10.1099/0022-1317-71-5-1153

Rigling, D., and Prospero, S. (2018). Cryphonectria parasitica, the causal agent of chestnut blight: invasion history, population biology and disease control. *Mol. Plant Pathol.* 19, 7–20. doi: 10.1111/mpp.12542

Saitou, N., and Nei, M. (1987). The neighbor-joining method - a new method for reconstructing phylogenetic trees. *Mol. Biol. Evol.* 4, 406–425.

Shamsi, W., Sato, Y., Jamal, A., Shahi, S., Kondo, H., Suzuki, N., et al. (2019). Molecular and biological characterization of a novel botybirnavirus identified from a Pakistani isolate of *Alternaria alternate*. *Virus Res.* 263, 119–128. doi: 10.1016/j.virusres.2019.01.006

Shang, H. H., Zhong, J., Zhang, R. J., Chen, C. Y., Gao, B. D., and Zhu, H. J. (2015). Genome sequence of a novel endornavirus from the phytopathogenic fungus *Alternaria brassicicola*. *Arch. Virol.* 160, 1827–1830. doi: 10.1007/s00705-015-2426-y

Shapira, R., Choi, G. H., and Nuss, D. L. (1991). Virus-like genetic organization and expression strategy for a double-stranded-RNA genetic element associated with biological-control of chestnut blight. *EMBO J.* 10, 731–739. doi: 10.1002/j.1460-2075.1991.tb08004.x

Shapira, R., and Nuss, D. L. (1991). Gene-expression by a hypovirulence-associated virus of the chestnut blight fungus involves 2 papain-like protease activities - essential residues and cleavage site requirements for p48 autoproteolysis. *J. Biol. Chem.* 266, 19419–19425.

Shepherd, H. S. (1988). Viruslike particles in tentoxin-producing strains of alternaria-alternata. *J. Virol.* 62, 3888–3891.

Shi, M., Lin, X. D., Tian, J. H., Chen, L. J., Chen, X., Li, C. X., et al. (2016). Redefining the invertebrate RNA virosphere. *Nature* 7634, 539–543. doi: 10.1038/nature20167

Smart, C. D., Yuan, W., Foglia, R., Nuss, D. L., Fulbright, D. W., and Hillman, B. I. (1999). Cryphonectria hypovirus 3, a virus species in the family hypoviridae with a single open reading frame. *Virology* 265, 66–73. doi: 10.1006/viro.1999.0039

Sun, L. Y., Nuss, D. L., and Suzuki, N. (2006). Synergism between a mycoreovirus and a hypovirus mediated by the papain-like protease p29 of the prototypic hypovirus CHV1-EP713. *J. Gen. Virol.* 87, 3703–3714. doi: 10.1099/vir.0.82213-0

Sun, L. Y., and Suzuki, N. (2008). Intragenic rearrangements of a mycoreovirus induced by the multifunctional protein p29 encoded by the prototypic hypovirus CHV1-EP713. *RNA* 14, 2557–2571. doi: 10.1261/rna.1125408

Suzuki, N., Ghabrial, S. A., Kim, K. H., Pearson, M., Marzano, S. Y. L., Yaegashi, H., et al. (2018). ICTV virus taxonomy profile: *Hypoviridae*. *J. Gen. Virol.* 99, 615–616. doi: 10.1099/jgv.0.001055

Suzuki, N., Maruyama, K., Moriyama, M., and Nuss, D. L. (2003). Hypovirus papain-like protease p29 functions in trans to enhance viral double-stranded RNA accumulation and vertical transmission. *J. Virol.* 77, 11697–11707. doi: 10.1128/jvi.77.21.11697-11707.2003

Suzuki, N., Supyani, S., Maruyama, K., and Hillman, B. I. (2004). Complete genome sequence of mycoreovirus-1/Cp9B21, a member of a novel genus within the family reoviridae, isolated from the chestnut blight fungus *Cryphonectria parasitica*. *J. Gen. Virol.* 85, 3437–3448. doi: 10.1099/vir.0.80293-0

Tang, W., Ding, Z., Zhou, Z. Q., Wang, Y. Z., and Guo, L. Y. (2012). Phylogenetic and pathogenic analyses show that the causal agent of apple ring rot in China is*Botryosphaeria dothidea*. *Plant Dis.* 96, 486–496. doi: 10.1094/PDIS-08-11-0635

Vasilyeva, L., and Kim, W. G. (2000). Valsa mali Miyabe et Yamada, the causal fungus of apple tree canker in east Asia. *Mycobiology* 28, 153–157. doi: 10.1080/12298093.2000.12015742

Wang, L. P., Jiang, J. J., Wang, Y. F., Hong, N., Zhang, F. P., Xu, W. X., et al. (2014). Hypovirulence of the phytopathogenic fungus *Botryosphaeria dothidea*: association with a coinfecting chrysovirus and a partitivirus. *J. Virol.* 88, 7517–7527. doi: 10.1128/JVI.00538-14

Wang, S. C., Kondo, H., Liu, L., Guo, L. H., and Qiu, D. W. (2013). A novel virus in the family hypoviridae from the plant pathogenic fungus *Fusarium graminearum*. *Virus Res.* 174, 69–77. doi: 10.1016/j.virusres.2013.03.002

White, T. J., Bruns, T. S., Lee, S., and Taylor, J. (1990). "Amplification and direct sequencing of fungal ribosomal RNA genes for phylogenetics," in *PCR Protocols: A Guide to Methods and Applications*, eds M. A. Innis, D. H. Gelfand, J. J. Sninsky, and T. J. White (San Diego, CA: Academic Press. Inc), 315–322. doi: 10.1016/b978-0-12-372180-8.50042-1

Woudenberg, J. H. C., Seidl, M. F., Groenewald, J. Z., de Vries, M., Stielow, J. B., Thomma, B., et al. (2015). *Alternaria* section *Alternaria*: species, formae speciales or pathotypes? *Stud. Mycol.* 82, 1–21. doi: 10.1016/j.simyco.2015.07.001

Xavier, A. D., de Barros, A. P. O., Godinho, M. T., Zerbini, F. M., Souza, F. D., Bruckner, F. P., et al. (2018). A novel mycovirus associated to *Alternaria alternata* comprises a distinct lineage in *Partitiviridae*. *Virus Res.* 244, 21–26. doi: 10.1016/j.virusres.2017.10.007

Xiang, J., Fu, M., Hong, N., Zhai, L. F., Xiao, F., and Wang, G. P. (2017). Characterization of a novel botybirnavirus isolated from a phytopathogenic *Alternaria fungus*. *Arch. Virol.* 162, 3907–3911. doi: 10.1007/s00705-017-3543-6

Xie, J. T., and Jiang, D. H. (2014). New insights into mycoviruses and exploration for the biological control of crop fungal diseases. *Annu. Rev. Phytopathol.* 5252, 45–68. doi: 10.1146/annurev-phyto-102313-050222

Xie, J. T., Xiao, X. Q., Fu, Y. P., Liu, H. Q., Cheng, J. S., Ghabrial, S. A., et al. (2011). A novel mycovirus closely related to hypoviruses that infects the plant pathogenic fungus *Sclerotinia sclerotiorum*. *Virology* 418, 49–56. doi: 10.1016/j.virol.2011.07.008

Xu, X., Liu, Y. Q., Weiss, S., Arnold, E., Sarafianos, S. G., and Ding, J. P. (2003). Molecular model of SARS coronavirus polymerase: implications for biochemical functions and drug design. *Nucleic Acids Res.* 31, 7117–7130. doi: 10.1093/nar/gkg916

Yaegashi, H., Kanematsu, S., and Ito, T. (2012). Molecular characterization of a new hypovirus infecting a phytopathogenic fungus, *Valsa ceratosperma*. *Virus Res.* 165, 143–150. doi: 10.1016/j.virusres.2012.02.008

Zhai, L. F., Hong, N., Zhang, M. X., and Wang, G. P. (2015). Complete dsRNA sequence of a novel victorivirus isolated from the pear stem wart fungus *Botryosphaeria dothidea*. *Arch. Virol.* 160, 613–616. doi: 10.1007/s00705-014-2285-y

Zhai, L. F., Xiang, J., Zhang, M. X., Fu, M., Yang, Z. K., Hong, N., et al. (2016). Characterization of a novel double-stranded RNA mycovirus conferring hypovirulence from the phytopathogenic fungus *Botryosphaeria dothidea*. *Virology* 493, 75–85. doi: 10.1016/j.virol.2016.03.012

Zhang, X. M., and Nuss, D. L. (2008). A host dicer is required for defective viral RNA production and recombinant virus vector RNA instability for a positive sense RNA virus. *Proc. Natl. Acad. Sci. U.S.A.* 105, 16749–16754. doi: 10.1073/pnas.0807225105

Zheng, D. W., Zhang, S. J., Zhou, X. Y., Wang, C. F., Xiang, P., Zheng, Q., et al. (2012). The FgHOG1 pathway regulates hyphal growth, stress responses, and plant infection in *Fusarium graminearum*. *PLoS One* 7, e49495. doi: 10.1371/journal.pone.0049495

Zhong, J., Shang, H. H., Zhu, C. X., Zhu, J. Z., Zhu, H. J., Hu, Y., et al. (2016). Characterization of a novel single-stranded RNA virus, closely related to fusariviruses, infecting the plant pathogenic fungus *Alternaria brassicicola*. *Virus Res.* 217, 1–7. doi: 10.1016/j.virusres.2015.11.012

Zuker, M. (2003). Mfold web server for nucleic acid folding and hybridization prediction. *Nucleic Acids Res.* 31, 3406–3415. doi: 10.1093/nar/gkg595

Conflict of Interest Statement: The authors declare that the research was conducted in the absence of any commercial or financial relationships that could be construed as a potential conflict of interest.

frontiers in Cellular and Infection Microbiology

OPINION
published: 24 May 2019
doi: 10.3389/fcimb.2019.00169

Determinants of Coinfection in the Mycoviruses

*Vaskar Thapa and Marilyn J. Roossinck**

Department of Plant Pathology and Environmental Microbiology, Center for Infectious Disease Dynamics, Pennsylvania State University, University Park, PA, United States

Keywords: mixed infections, fungal virus, non-self-recognition, mycovirus transmission, virus symbiosis

INTRODUCTION

Coinfections of mycoviruses are generally common. The coinfecting mycoviruses are not necessarily the result of horizontal virus transmission among homologous fungal hosts compatible for anastomosis, but involve mycoviruses from phylogenetically diverse sources (Herrero and Zabalgogeazcoa, 2011; Osaki et al., 2016; Ran et al., 2016; Hao et al., 2018). An experimental study with different combinations of transmission scenarios among four partitiviruses showed a significant positive influence of one virus (Heterobasidion partitivirus13-an1) on its distantly related coinfecting partner Heterobasidion partitivirus 15-pa1, but no support of coinfection between two related viruses (Heterobasidion partitiviruses 11-au1 and 11-pa1) (Kashif et al., 2019). A more stable coinfection between distantly related species than conspecific strains was also reported among mycoviruses infecting the fungus, *Heterobasidion parviporum* (Vainio et al., 2015). Studies covering large geographical areas indicate that the mycoviruses in coinfections belong to the local fungal community (Ran et al., 2016; Arjona-Lopez et al., 2018). Arjona-Lopez et al. (2018) found a non-overlapping set of coinfecting mycoviruses in isolates of *Rosellinia necatrix* from Japan and the Mediterranean that match with mycoviruses from the respective local fungal pools. In general, transmission of mycoviruses occurs through anastomosis of vegetatively compatible strains of the same species, but phylogenetic evidence implies occasional transmission across vegetatively incompatible strains. The transmissions across vegetatively incompatible fungal hosts are poorly studied except in a few cases (Liu et al., 2003, 2016; Yaegashi et al., 2013a). In addition to transmission across heterologous fungi, interactions among mycoviruses play direct roles in coinfection. The interactions among coinfecting mycoviruses are diverse, ranging from synergistic to neutral to antagonistic. In some cases, mycovirus coinfection induces genome rearrangement of one of the coinfecting partners, likely through recombination (Sun and Suzuki, 2008). A more comprehensive review on the interactions among coinfecting mycoviruses is found in Hillman et al. (2018).

The diversity of coinfecting mycoviruses and the diverse nature of interactions may imply that coinfections occur freely without any constraints. However, in examples from *in vitro* experiments the frequency of coinfection varies with different fungal systems and in many cases is lower than what would be expected from random incidences. For example, in 43 isolates of the ascomycete *Tolypocladium cylindrosporum*, coinfections of mycoviruses were reported in only in about 5% of the population (Herrero and Zabalgogeazcoa, 2011). In contrast, in almost 200 isolates of *Ustilaginoidea virens* examined multiple dsRNA elements were found in large samples, and the coinfection frequency of two common mycoviruses: Ustilaginoidea virens RNA virus 1 (*Totiviridae*) and Ustilaginoidea virens RNA virus 4 (unclassified) was close to 30% (Jiang et al., 2015). In our own study of about 200 North American isolates of *Pseudogymnoascus destructans* a fungus causing a deadly disease in bats, the coinfection incidence of a partitivirus (Thapa et al., 2016) and an unclassified mycovirus is close to 25%, but only in a geographically restricted area (unpublished). Independent segregation of coinfecting mycoviruses in the population has been

OPEN ACCESS

Edited by:
Nobuhiro Suzuki, Okayama University, Japan

Reviewed by:
Sun Liying, Northwest A&F University, China
Shin-Yi Lee Marzano, South Dakota State University, United States
Jarkko Hantula, Natural Resources Institute Finland (Luke), Finland

****Correspondence:***
Marilyn J. Roossinck
mjr25@psu.edu

Specialty section:
This article was submitted to Fungal Pathogenesis, a section of the journal Frontiers in Cellular and Infection Microbiology

Received: *15 February 2019*
Accepted: *06 May 2019*
Published: *24 May 2019*

Citation:
Thapa V and Roossinck MJ (2019) Determinants of Coinfection in the Mycoviruses. Front. Cell. Infect. Microbiol. 9:169. doi: 10.3389/fcimb.2019.00169

described only in a few cases where the interaction is likely neutral, while in other cases one of the partners influences the presence of other. In the coinfection of two unrelated RNA viruses, Yado-nushi virus 1 (YnV1) and Yado-kari virus 1 (YkV1) in *Rosellinia necatrix*, YkV1 is dependent on YnV1. YkV1 does not segregate independently in the population (Zhang et al., 2016). Thus, the coinfection scenarios are likely influenced by the interactions between coinfecting viruses or at the level of mycovirus transmission, particularly during the transmission across vegetatively incompatible fungi or from other factors. Such constraints led us to investigate the determinants of mycovirus coinfections. Here, we discuss some of the determinants for mycovirus coinfection based on the literature available and provide our opinions on coinfection biology.

MYCOVIRUS ASSOCIATED SUPPRESSION OF FUNGAL NON-SELF-RECOGNITION

This is an example of a coinfection system where one of the mycoviruses suppresses its fungal host's non-self-recognition, which facilitates heterologous transmission of mycoviruses. Non-self-recognition or allorecognition is a ubiquitous phenomenon in fungi that enables them to distinguish one from another (Glass and Dementhon, 2006). In fungi, non-self-recognition between two isolates of different mycelial compatibility results in compartmentalization followed by programmed cell death to interrupt fusion between hypha, termed as heterokaryon incompatibility (Glass and Kaneko, 2003). Sclerotinia sclerotiorum mycoreovirus 4 (SsMYRV4), which is associated with hypovirulence in *Sclerotinia sclerotiorum*, was found to suppress non-self-recognition of the fungus and facilitate coinfection through horizontal transmission of mycoviruses across vegetatively incompatible groups (Wu et al., 2017). SsMYRV4 inhibits expression of heterotrimeric G proteins and *het* or *vic* genes involved in vegetative incompatibility (Wu et al., 2017). Further, the infection of SsMYRV4 reduces cellular reactive oxygen species (ROS), which plays a major role in fungal vegetative incompatibility reactions (Brosché et al., 2014). In *S. sclerotiorum*, infection of SsMYRV4 determines the infection ability of other mycoviruses. Involvement of *vic* genes in vegetative incompatibility was also reported in Chestnut blight fungus, *Cryphonectria parasitica* (Choi et al., 2012; Zhang et al., 2014). Cryphonectria hypovirus 1 (CHV1) infection in *C. parasitica* suppresses expression of the pheromone precursor genes, *Mf1/1*, *Mf2/1,* and *Mf2/2*, resulting in disturbance in the fungal sexual cycles. The defect in the sexual cycles likely decreases the allelic diverstity of the *vic* gene, thereby promoting the virus transmission among different strains (Zhang et al., 1998).

INFECTION BY A MYCOVIRUS WITH AN RNA SILENCING SUPPRESSOR

Many fungi use the adaptive immune system of RNA silencing to suppress viruses (Hammond et al., 2008; Yaegashi et al., 2016). Studies showed that mycoviruses like CHV1 and Rosellinia necatrix mycoreovirus 3 infecting *Cryphonectria parasitica* and *Rosellinia necatrix,* respectively, encode RNA silencing suppressor (RSS) proteins that show similarity to plant RSS proteins (Segers et al., 2006; Yaegashi et al., 2013b). The RSS of one mycovirus may help another mycovirus that gets suppressed by the host RNA silencing, to facilitate coinfection (Chiba and Suzuki, 2015). For example, Rosellinia necatrix victorivirus 1 (RnVV1) originally isolated from *R. necatrix* can replicate in *C. parasitica* when coinfected with CHV1, but not in the virus-free *C. parasitica* strain (EP155). Infection in an RNA silencing mutant of *C. parasitica*, dicer-like 2 knockout-*Δdcl-2* has a similar effect (Segers et al., 2006; Chiba et al., 2013). This suggests RnVV1 has very low RNA silencing suppressor activities (Chiba et al., 2013). Similarly, RnVV1 replication is impaired when coinfected with *Mycoreovirus 1* (MyRV1) and CHV1 mutant-*Δp69* in *C. parasitica*. MyRV1 induces silencing genes dicer-like 2 (*dcl2*) and argonaute-like 2 (*agl2*), and CHV1 mutant (*Δp69*) is also impaired in RSS activity (Chiba and Suzuki, 2015). These examples show that a mycovirus can mediate coinfection of another mycovirus through RNA silencing pathways.

NUTRITIONAL/CHEMICAL DETERMINANTS

The roles of chemical compounds that affect the programmed cell death pathways involved in mycelial incompatibility were studied to look at their facilitation of heterologous transmission of mycoviruses. One successful case was the use of a zinc compound *in vitro* that accelerates the transmission of mycoviruses among vegetatively incompatible strains of *R. necatrix* (Ikeda et al., 2013). *Rosellinia necatrix* shows very strong incompatibility with different strains without the formation of anastomosis (Inoue et al., 2011a). Zinc chloride concentrations in the media ranging from 0.5 to 1.5 mM facilitated heterologous transmission of Rosellinia necatrix megabirnavirus 1 and other partitiviruses similar to Rosellinia necatrix partitivirus 3 (Inoue et al., 2011a). How zinc chloride induces anastomosis formation in *R. necatrix* is unknown however, it is inferred that zinc chloride reduces the effects of the hyphal secretion that suppress anastomosis (Inoue et al., 2011a). In the basidiomycete fungus, *Helicobasidium mompa* hyphal incompatibility is inhibited with the supplementation of active charcoal in the media (Inoue et al., 2011b). It is likely that in nature nutrient availability influences the coinfection potential of mycoviruses among fugal hosts through the heterologous anastomosis.

CONCLUSIONS

The determinants of mycovirus coinfections involve multiple factors. One of the constraints that many mycoviruses have to overcome for infection is non-self-recognition. RNA silencing is another major hurdle that influences the success of infection. The roles of nutrients or chemicals or other components of the environment seems to have potential influence in determining infection, but it is a poorly studied field. The biology of coinfection is complex like any other biological phenomena and many factors remained to be explored. On the other hand, it is an important field particularly in manipulating virulence

of pathogenic fungi in which mycoviruses are known to play crucial roles. There are attempts underway to alter the non-self-recognition factors in vegetative incompatible populations for successful transfer of mycovirus related to hypovirulence (Zhang et al., 2016). Similar efforts to modify RNA silencing suppressors may prove more difficult. The idea is to produce desired coinfection interactions to manipulate the fungal host's virulence. The coinfection biology of mycoviruses has an important scope not only academically but also in many practical applications associated with hypovirulence, and deserves further attention.

AUTHOR CONTRIBUTIONS

VT wrote the first draft. MR edited and wrote the final draft.

FUNDING

This work was supported by a grant from the Pennsylvania Game Commission, and by the USDA National Institute of Food and Federal Appropriations under Project PEN04652 and Accession number 1016233.

REFERENCES

Arjona-Lopez, J. M., Telengech, P., Jamal, A., Hisano, S., Kondo, H., Yelin, M. D., et al. (2018). Novel, diverse RNA viruses from Mediterranean isolates of the phytopathogenic fungs, *Rosellinia necatrixI:* insights into evolutionary biology of fungal viruses. *Environ. Microbiol.* 20, 1464–1483. doi: 10.1111/1462-2920.14065

Brosché, M., Blomster, T., Saoljärvi, J., Cui, F., Sipari, N., Leppälä, J., et al. (2014). Transcriptomics and functional genomics of ROS-induced cell death regulation by RADICAL-INDUCED CELL DEATH. *PLoS Genet.* 10:e1004112. doi: 10.1371/journal.pgen.1004112

Chiba, S., Lin, Y. H., Kondo, K., Kanematsu, S., and Suzuki, N. (2013). A novel victorivirus from a phytopathogenic fungus, *Rosellinia necatrix*, is infection as particles and targeted by RNA silencing. *J. Virol.* 87, 6726-6738. doi: 10.1128/JVI.00557-13

Chiba, S., and Suzuki, N. (2015). Highly activated RNA silencing via strong induction of dicer by one virus can interfere with the replication of an unrelated virus. *Proc. Natl. Acad. Sci. U.S.A.* 112, E4911–E4918. doi: 10.1073/pnas.1509151112

Choi, G. H., Dawe, A. L., Churbanov, A., Smith, M. L., Milgroom, M. G., and Nuss, D. L. (2012). Molecular characterization of vegetative incompatibility genes that restrict hypovirus transmission in the chestnut blight fungus *Cryphonectria parasitica*. *Genetics* 190, 113–127. doi: 10.1534/genetics.111.133983

Glass, N. L., and Dementhon, K. (2006). Non-self recognition and programmed cell death in filamentous fungi. *Curr. Opin. Mirobiol.* 9, 553–558. doi: 10.1016/j.mib.2006.09.001

Glass, N. L., and Kaneko, I. (2003). Fatal attractions: nonself recognition and heterokaryon incompatibility in filamentous fungi. *Eukaryot. Cell* 2, 1–8. doi: 10.1128/EC.2.1.1-8.2003

Hammond, T. M., Andrewski, M. D., Roossinck, M. J., and Keller, N. P. (2008). Aspergillus mycoviruses are targets and suppressors of RNA silencing. *Eukaryot. Cell* 7, 350–357. doi: 10.1128/EC.00356-07

Hao, F., Ding, T., Wu, M., Zhang, J., Yang, L., Chen, W., et al. (2018). Two novel hypovirulence-associated mycoviruses in the phytopathogenic fungus *Botrytis cinerea*: molecular characterization and suppression of infection cushion formation. *Viruses* 10:E254. doi: 10.3390/v10050254

Herrero, N., and Zabalgogeazcoa, I. (2011). Mycoviruses infectiing the endophytic and entomopathogenic fungus *Tolypocladium cylindrosporum*. *Vir. Res.* 160, 409–413. doi: 10.1016/j.virusres.2011.06.015

Hillman, B. I., Annisa, A., and Suzuki, N. (2018). "Viruses of plant-interacting fungi," in *Advances in Virus Research,* 100, 99–116. doi: 10.1016/bs.aivir.2017.10.003

Ikeda, K., Inoue, K., Kida, C., Uwamori, T., Sasaki, A., Kanematsu, S., et al. (2013). Potentiation of mycovirus transmission by zinc compounds via attenuation of heterogenic incompatibility in *Rosellinia necatrix*. *Appl. Environ. Microbiol.* 79, 3684–3691. doi: 10.1128/AEM.00426-13

Inoue, K., Kanematsu, S., Park, P., and Ikeda, K. (2011a). Cytological analysis of mycelial incompatibility in *Rosellinia nexatrix*. *Fungal Biol.* 115, 87–95. doi: 10.1016/j.funbio.2010.10.009

Inoue, K., Kanematsu, S., Park, P., and Ikeda, K. (2011b). Cytological analysis of mycelial incompatibility in *Helicobasidium mompa*. *FEMS Microbiol. Lett*. 315, 94–100. doi: 10.1111/j.1574-6968.2010.02174.x

Jiang, Y., Zhang, T., Luo, C., Jiang, D., Li, G., Li, Q., et al. (2015). Prevalence and diversity of mycoviruses infection the plant pathogen *Ustilaginoidea virens*. *Virus Res.* 195, 47–56. doi: 10.1016/j.virusres.2014.08.022

Kashif, M., Jurvansuu, J., Vainio, E. J., and Hantula, J. (2019). Alphapartitiviruses of *Heterobasidion* wood decay fungi affect each other's transmission and host growth. *Front. Cell. Infect. Microbiol.* 9:64. doi: 10.3389/fcimb.2019.00064

Liu, S., Xie, J., Cheng, J., Li, B., Chen, T., Fu, Y., et al. (2016). Fungal DNA virus infects a mycophagous insect and utilizes it as a transmission factor. *Proc. Natl. Acad. Sci. U.S.A.* 113, 12803–12808. doi: 10.1073/pnas.1608013113

Liu, Y. C., Linder-Basso, D., Hillman, B. I., Kaneso, S., and Milgroom, M. G. (2003). Evidence for interspecies transmission of viruses in natural populations of filamentous fungi in the genus *Cryphonectria*. *Mol. Ecol.* 12, 1619-1628. doi: 10.1046/j.1365-294X.2003.01847.x

Osaki, H., Sasaki, A., Nomiyama, K., and Tomioka, K. (2016). Multiple virus infection in a single strain of *Fusarium poae* shown by deep sequencing. *VIrus Genes* 52, 835–847. doi: 10.1007/s11262-016-1379-x

Ran, H., Liu, L., Li, B., Cheng, J., Fu, Y., Jiang, D., et al. (2016). Co-infection of a hypovirulent isolate of *Scherotinia sclerotiorum* with a new botyvirnavirus and a strain of a mitovirus. *Virol. J.* 13:92. doi: 10.1186/s12985-016-0550-2

Segers, G. C., van Wezel, R., Zhang, X., Hong, Y., and Nuss, D. L. (2006). Hypovirus papain-like protease p29 suppresses RNA silencing in the natural fungal host and in a heterologous plant system. *Eukaryot. Cell* 5, 896–904. doi: 10.1128/EC.00373-05

Sun, L., and Suzuki, N. (2008). Intragenic rearrangements of a mycoreovirus induced by the multifunctional protein p29 encoded by the prototypic hypovirus CHV1-EP713. *RNA* 14, 2557–2571. doi: 10.1261/rna.1125408

Thapa, V., Turner, G. G., Hafenstein, S., Overton, B. E., Vanderwolf, K. J., and Roossinck, M. J. (2016). Using a novel partitivirus in *Pseudogymnoascus destructans* to understand the epidemiology of white-nose syndrome. *PLoS Pathog.* 12:e1006076. doi: 10.1371/journal.ppat.1006076

Vainio, E. J., Müller, M. M., Korhonen, K., Piri, T., and Hantula, J. (2015). Viruses accumulate in aging infection centers of a fungal forest pathogen. *Int. Soc. Microb. Ecol. J.* 9, 497–507. doi: 10.1038/ismej.2014.145

Wu, S., Cheng, J., Fu, Y., Chen, T., Jiang, D., Ghabrial, S. A., et al. (2017). VIrus-mediated suppression of host non-self recognition facilitates horizontal transmission of heterologous viruses. *PLoS Pathog.* 13:e1006234. doi: 10.1371/journal.ppat.1006234

Yaegashi, H., Nakamura, H., Sawahata, T., Sasaki, A., Iwanami, Y., Ito, T., et al. (2013a). Appearance of mycovirus-like double-stranded RNAs in the white root rot fungus, *Rosellinia necatrix*, in an apple orchard. *FEMS Microbiol. Ecol.* 83, 49–62. doi: 10.1111/j.1574-6941.2012.01454.x

Yaegashi, H., Shimizu, T., Ito, T., and Kanematsu, S. (2016). Differential inductions of RNA silencing among encapsidated double-stranded RNA mycoviruses in the white root rot fungus *Rosellinia necatrix*. *J. Virol.* 90, 5677–5692. doi: 10.1128/JVI.02951-15

Yaegashi, H., Yoshikawa, N., Ito, T., and Kanematsu, S. (2013b). A mycoreovirus suppresses RNA silencing the white root rot fungus *Rosellinia necatrix*. *Virology* 444, 409–416. doi: 10.1016/j.virol.2013.07.010

Zhang, D. X., Spiering, M. J., Dawe, A. L., and Nuss, D. L. (2014). Vegetative incompatibility loci with dedicated roles in allorecognition restrict mycovirus transmission in chestnut blight fungus. *Genetics* 197, 701–714. doi: 10.1534/genetics.114.164574

Zhang, L., Baasiri, R. A., and Van Alfen, N. K. (1998). Viral repression of fungal pheromone precursor gene expression. *Mol. Cell. Biol.* 18, 953–959. doi: 10.1128/MCB.18.2.953

Zhang, R., Hisano, S., Tani, A., Kondo, H., Kanematsu, S., and Suzuki, N. (2016). A capsidless ssRNA virus hosted by an unrelated dsRNA virus. *Nat. Microbiol.* 1:15001. doi: 10.1038/nmicrobiol.2015.1

Conflict of Interest Statement: The authors declare that the research was conducted in the absence of any commercial or financial relationships that could be construed as a potential conflict of interest.

frontiers in Microbiology

ORIGINAL RESEARCH
published: 02 July 2019
doi: 10.3389/fmicb.2019.01415

Discovery of Two Mycoviruses by High-Throughput Sequencing and Assembly of Mycovirus-Derived Small Silencing RNAs From a Hypovirulent Strain of *Sclerotinia sclerotiorum*

*Qianqian Wang[1,2], Shufen Cheng[1,2], Xueqiong Xiao[2], Jiasen Cheng[1,2], Yanping Fu[2], Tao Chen[2], Daohong Jiang[1,2] and Jiatao Xie[1,2]**

[1] State Key Laboratory of Agricultural Microbiology, Huazhong Agricultural University, Wuhan, China, [2] Hubei Key Laboratory of Plant Pathology, College of Plant Science and Technology, Huazhong Agricultural University, Wuhan, China

OPEN ACCESS

Edited by:
Sead Sabanadzovic,
Mississippi State University,
United States

Reviewed by:
Carmen Hernandez,
Polytechnic University of Valencia,
Spain
Beatriz Navarro,
Istituto per la Protezione Sostenibile
delle Piante, Italy

***Correspondence:**
Jiatao Xie
jiataoxie@mail.hzau.edu.cn

Specialty section:
This article was submitted to
Virology,
a section of the journal
Frontiers in Microbiology

Received: 24 February 2019
Accepted: 05 June 2019
Published: 02 July 2019

Citation:
Wang Q, Cheng S, Xiao X,
Cheng J, Fu Y, Chen T, Jiang D and
Xie J (2019) Discovery of Two
Mycoviruses by High-Throughput
Sequencing and Assembly
of Mycovirus-Derived Small Silencing
RNAs From a Hypovirulent Strain
of Sclerotinia sclerotiorum.
Front. Microbiol. 10:1415.
doi: 10.3389/fmicb.2019.01415

Sclerotinia sclerotiorum, an important phytopathogenic fungus, harbors rich diversity of mycoviruses. Lately, more mycoviruses can be successfully and accurately discovered by deep sequencing, especially those that could not be detected by traditional double-stranded RNA (dsRNA) extraction. Previously, we reported that the hypovirulent *S. sclerotiorum* strain SZ-150 is coinfected by Sclerotinia sclerotiorum hypovirus 1 (SsHV1) and its related satellite RNA. Here, aside from SsHV1, we detected two other mycoviruses, Sclerotinia sclerotiorum botybirnavirus 3 (SsBV3/SZ-150) and Sclerotinia sclerotiorum mycotymovirus 1 (SsMTV1/SZ-150), coinfecting strain SZ-150, by deep sequencing and assembly of mycovirus-derived small RNAs and determined their full-length genomes. The genome of SsBV3/SZ-150 was found to be composed of two linear dsRNA segments, 6,212, and 5,880 bp in size, respectively. Each dsRNA segment of SsBV3/SZ-150 contains a large open reading frame (ORF) encoding RNA-dependent RNA polymerase (RdRp) and a hypothetical protein. The whole genome of SsBV3/SZ-150 shares more than 95% sequence identity with Botrytis porri botybirnavirus 1 (BpBV1) at the nucleotide (nt) or amino acid level. Thus, SsBV3/SZ-150 was assumed to be a strain of BpBV1. The genome of SsMTV1/SZ-150 consists of 6,391 nt excluding the poly(A) tail. SsMTV1/SZ-150 was predicted to contain a large ORF that encodes a putative replication-associated polyprotein (RP) with three conserved domains of viral RNA methyltransferase, viral RNA helicase, and RdRp. Phylogenetic analyses suggest that SsMTV1/SZ-150 is related, albeit distantly, to members of the family *Tymoviridae*. Analysis of the small RNAs derived from SsBV3/SZ-150 and SsMTV1/SZ-150 revealed that small-RNA lengths mainly range from 20 to 24 nt, with a peak at 22 nt, and the most abundant 5′-terminal

nucleotide is uridine, suggesting that the Dicer 2 and Argonaute 1, two key components in the RNA inference pathway, may play important roles in the resistance to mycoviral infection in *S. sclerotiorum*. Neither SsBV3/SZ-150 nor SsMTV1/SZ-150 is a causal agent of hypovirulence in strain SZ-150.

Keywords: *Sclerotinia sclerotiorum*, mycovirus, botybirnavirus, *Tymoviridae*, high-throughput sequencing, small RNA

INTRODUCTION

Mycoviruses (or fungal viruses) are viruses that infect fungi and Oomycete species and depend on their hosts for replication. Since the first mycovirus was reported in 1962 (Hollings, 1962), mycoviruses have been identified in all major taxonomic groups of fungi and have shown remarkable diversity (Ghabrial and Suzuki, 2009; Pearson et al., 2009; Ghabrial et al., 2015). For defense against mycovirus infection, fungi have evolved antiviral defense mechanisms of RNA silencing, which is similar to that of other eukaryote hosts including plants and animals (Torres-Martinez and Ruiz-Vazquez, 2017; Guo et al., 2019). RNA virus infection in fungi induces production of virus-derived small RNAs (vsRNAs) that have specific function in the RNA-silencing process (Wang et al., 2016; Yaegashi et al., 2016; Donaire and Ayllon, 2017; Yu et al., 2018). These vsRNAs share features with host endogenous small interfering RNAs (siRNAs) and can potentially mediate RNA silencing pathways or can regulate viral replication. Therefore, deep sequencing of small RNAs from virus-infected fungi is an efficient strategy to discover and identify mycoviruses, especially latent ones.

Sclerotinia sclerotiorum, a destructive Ascomycota fungus, is capable of attacking more than 400 species of plants, and cause great losses in a wide variety of crops throughout the world (Bolton et al., 2006). Since the first double-stranded RNA (dsRNA) element was found in a hypovirulent *S. sclerotiorum* strain 91 (Boland, 1992), this fungus is increasingly recognized to harbor a great variety of mycoviruses, including dsRNA viruses, single-stranded RNA (ssRNA) viruses, and one single-stranded circular DNA virus. Some of those mycoviruses confer hypovirulence to their hosts and show a great potential for virocontrol (Xie and Jiang, 2014). At present, with development of the high-throughput sequencing technology, novel mycoviruses that are difficult to find by conventional detection methods, such as dsRNA extraction, can be discovered in *S. sclerotiorum* (Marzano et al., 2016; Mu et al., 2017). These discovered *S. sclerotiorum* mycoviruses not only enrich known virus diversity but also supply new knowledge about viral evolution and its coevolution with the host (Jiang et al., 2013; Marzano et al., 2016).

The order *Tymovirales* was first established in 2004 and is currently composed of five families: *Alphaflexiviridae*, *Betaflexiviridae*, *Gammaflexiviridae*, *Deltaflexiviridae*, and *Tymoviridae*[1]. Members of this order possess an ssRNA genome from 5.9 to 9.0 kb in length, which is mostly polyadenylated. The largest protein, i.e., replication-associated polyprotein (RP), with molecular mass approximately 150–250 kDa, is encoded in all the members of the order *Tymovirales*, and the RP protein usually consists of a set of conserved functional domains (King et al., 2011). The members of *Tymovirales* show great diversity in virion morphology. The members of the families *Alphaflexiviridae*, *Betaflexiviridae*, and *Gammaflexiviridae* have virions in the form of flexuous filaments, whereas viruses in the family *Tymoviridae* have non-enveloped isometric particles (Adams et al., 2011b). The viruses belonging to *Tymovirales* also have diverse host ranges. Members of *Betaflexiviridae* and *Tymoviridae* are plant viruses (Adams et al., 2011b), a single member of *Gammaflexiviridae* is reported only from a filamentous fungus (Howitt et al., 2001; Adams et al., 2011b), whereas members of *Alphaflexiviridae* infect both plants and fungi (Adams et al., 2011a).

Botybirnaviruses are a group of bipartite viruses with dsRNA genomes of 5,800–6,500 bp for each segment. The first botybirnavirus, Botrytis porri botybirnavirus 1 (BpBV1), has been discovered in the phytopathogenic fungus *B. porri* and is responsible for hypovirulent traits (Wu et al., 2012). Two botybirnaviruses have been subsequently found in *S. sclerotiorum* (Liu et al., 2015; Ran et al., 2016). The botybirnavirus infection is associated with the hypovirulence of *S. sclerotiorum* as well. Recently, more candidate members of the genus of Botybirnavirus were detected in the fungi of Ascomycota, e.g., fungi of genera *Alternaria* and *Bipolaris* (Xiang et al., 2017; Wang et al., 2018). With the development of sequencing technology, more botybirnavirus-like sequences have also been identified during the metatranscriptomic analysis, e.g., the finding of botybirnavirus-like sequences in the metatranscriptomics survey of soybean phyllosphere phytobiomes (Marzano and Domier, 2016). Therefore, botybirnaviruses may have a wide distribution among different fungal groups.

Previously, we have reported three dsRNA segments, two similarly, sized at 9.5 kbp and a third one of approximately 3.6 kbp. One of the two large dsRNA segments, the replication form of Sclerotinia sclerotiorum hypovirus 1 (SsHV1/SZ-150), has been characterized (Xie et al., 2011). SsHV1/SZ-150 is closely related to CHV3/GH2 and CHV4/SR2 within *Hypoviridae*, whereas the 3.6-kbp dsRNA segment was recognized to be the satellite-like RNA (SatH) of SsHV1/SZ-150. The partial cDNA sequence of the other large dsRNA segment (the genome of the previously named Sclerotinia sclerotiorum RNA virus 1, SsRV1/SZ-150) was determined and putatively assigned to a plant virus (Xie et al., 2011). In the present study, we obtained sRNA from the hypovirulent strain SZ-150 of *S. sclerotiorum* by deep sequencing and discovered two other mycoviruses, Sclerotinia sclerotiorum botybirnavirus 3

[1]https://talk.ictvonline.org/taxonomy

(SsBV3/SZ-150, originally named SsRV1/SZ-150) and Sclerotinia sclerotiorum mycotymovirus 1 (SsMTV1/SZ-150) aside from SsHV1 and SatH. Combined with bioinformatics analysis and rapid amplification of cDNA end (RACE), full-length genomes of these two mycoviruses were determined *via* assembly of myco vsRNAs and were characterized. The assay of biological features on individual strains with different virus combination confirmed that neither SsBV3/SZ-150 nor SsMTV1/SZ-150 is a causal agent of hypovirulence of strain SZ-150.

RESULTS

Assembled Small RNAs and Identification of Two New Mycoviruses

Large-scale sequencing of sRNAs has been used for virus identification in insects, plants, and fungi (Kreuze et al., 2009; Wu et al., 2010; Vainio et al., 2015). To test whether the strain SZ-150 is infected by other new mycoviruses aside form SsHV1/SZ-150 and its SatH, the total RNA from the strain SZ-150 was prepared for deep sequencing of sRNAs. After removing of the adaptors and filtering out low-quality tags, the total number of reads produced by the Illumina sequencer was 12,999,900 [read length ranging from 18 to 30 nucleotides (nts)]. To obtain more information about mycovirus-related sequences, these sRNAs were first matched against the genome sequences of *S. sclerotiorum*, SsHV1/SZ-150 and SatH/SZ-150. The unmatched sRNAs were then assembled into longer contiguous sequences (contigs) before they were used for sequence similarity searches in reference databases. The newly assembled contigs could be subdivided into two groups based on BLASTX against NCBI GenBank database. One group of contigs contained sequences sharing a higher identity (95–100%) with BpBV1/GarlicBc-72, and those contigs were presumed to represent the genome of a putative mycovirus, namely, SsBV3/SZ-150 (accession numbers MK530703 and MK530704) to distinguish it from two botybirnaviruses previously found in *S. sclerotiorum* (Liu et al., 2015; Ran et al., 2016). The second group of sequences revealed that proteins encoded by two contigs shared limited sequence identity (27–39%) with members of the family *Tymoviridae*, suggesting that they represent the genome of a new virus. We tentatively named this virus SsMTV1/SZ-150 (accession number MK530705). Thus, SZ-150 is coinfected with three mycoviruses: two (+)ssRNA viruses (SsHV1 and SsMTV1) and one virus with dsRNA genome (SsBV3), along with a SatH of SsHV1/SZ-150.

Genome Organization and Characterization of SsBV3/SZ-150 and SsMTV1/SZ-150

As a result of a combination of the assembled vsRNA contigs and RACE experiments, the complete genomes of SsBV3/SZ-150 and SsMTV1/SZ-150 were determined. Genomes of both viruses were re-sequenced *via* RT-PCR with specific primers based on the assembled sequence to ensure maximum sequence accuracy (**Supplementary Table S2**).

Characterization of SsBV3/SZ-150

The SsBV3/SZ-150 genome is composed of two linear dsRNA segments (L1-dsRNA and L2-dsRNA) of 6,212 and 5,880 bp in length, respectively (**Figures 1A**, **4C,E**). SsBV3/SZ-150 was subjected to BLAST searches against NCBI GenBank, and results showed that SsBV3/SZ-150 shares 96% sequence identity with Botrytis porri botybirnavirus 1 (BpBV1/GarlicBc-72; Wu et al., 2012). Similar to BpBV1, each dsRNA segment of SsBV3 possesses a large open reading frame (ORF), designated as ORF I (on L1-dsRNA), and ORF II (on L2-dsRNA) (**Figures 1A**, **4C,E**). The protein encoded by the 3′ proximal coding region of ORF I encompasses the RdRp_4 conserved domain sequence and shows sequence similarity (97.58%) to the corresponding region of BpBV1/GarlicBc-72. The hypothetical protein encoded by ORF II shares 97.30% identity with BpBV1/GarlicBc-72. In addition, the proteins encoded by the 5′-proximal region of ORF I and by the entire ORF II lack significant sequence similarity to the proteins of any other known virus groups aside from botybirnaviruses. The phylogenetic analysis confirmed that SsBV3/SZ-150 is most closely related to BpBV1/GarlicBc-72 but distant from two other botybirnaviruses reported from *S. sclerotiorum* (**Figure 1B**). All the above results suggested that SsBV3/SZ-150 and BpBV1/GarlicBc-72 belong to the same species.

Characterization of SsMTV1/SZ-150

The complete genomic sequence of SsMTV1/SZ-150 is 6391 nt in length excluding the 3′-terminal poly (A) tail (**Figures 2A**, **4A**), with a G+C content of 53.3%. This mycovirus contains a 263- and 248-nt-long 5′- and 3′-UTRs, respectively. Sequence analyses revealed that the SsMTV1 genome has a putative single large ORF. This ORF is 5,880 nt long, beginning at AUG (nt positions 264–266) and terminating at UAG (nt positions 6,141–6,143). The ORF codes for a putative RP of 1,958 amino acids residues with a calculated molecular mass of 218.6 kDa. A conserved-motif search revealed that the RP contains three conserved domains (from the N terminus to the C terminus): viral methyltransferase (Mtr), viral RNA helicase (Hel), and RNA-dependent RNA polymerase (RdRP) (**Figures 2A**, **4A**).

Multiple-alignment analysis was conducted based on the full sequence of RP by the methods of pairwise comparisons and the percentage of amino acid sequence identities. The RP of SsMTV1/SZ-150 showed the highest identity (20.3%) with that of turnip yellow mosaic virus (NP_663297) compared to the RP of the representatives of the order *Tymovirales* (**Table 1**). Phylogenetic analyses of the viral RP of SsMTV1/SZ-150 and representatives of the order *Tymovirales* indicated that SsMTV1/SZ-150 is phylogenetically related to members of *Tymoviridae* but belongs to a distinct evolutionary lineage (**Figure 2B**).

Multiple-alignment and phylogenetic analyses were next conducted based on three conserved domains (Mtr, Hel, and RdRp) of RP encoded by SsMTV1/SZ-150 (**Figures 2C–E**). The putative Mtr domain (nt positions 798–1,538) is located near the N-terminal region of the SsMTV1-encoded RP and contains three conserved motifs (I–III; **Supplementary Figure S1**).

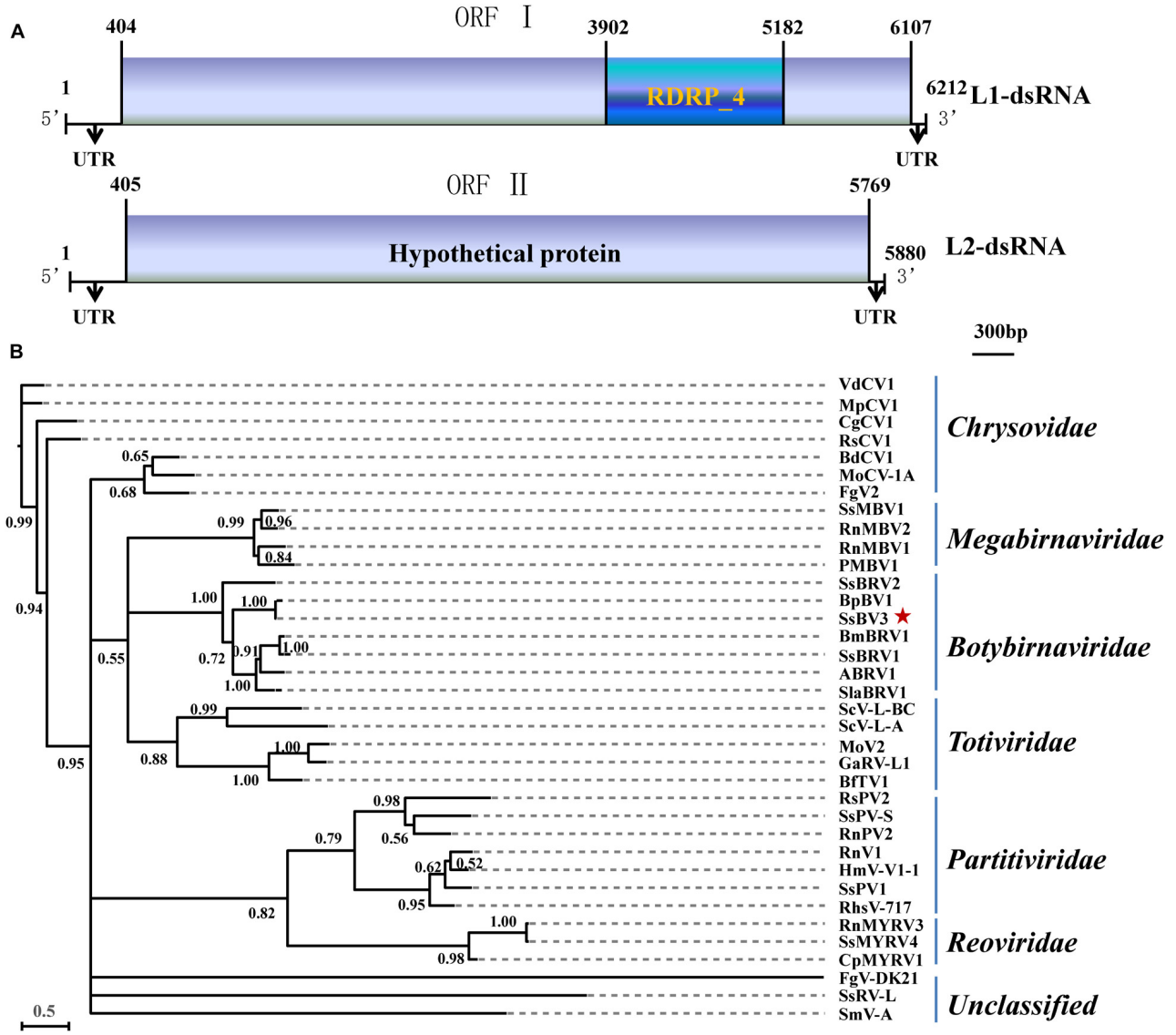

FIGURE 1 | Schematic diagram and phylogenetic analysis of Sclerotinia sclerotiorum botybirnavirus 3 (SsBV3/SZ-150). **(A)** Genomic organization of SsBV3/SZ-150. The 5′- and 3′-UTRs (line) and the ORF (box) are displayed. The blue box indicates a conserved RdRp domain. The scale bar corresponds to a length of 300 bp. **(B)** A Bayesian phylogenetic tree illustrating the relationships of SsBV3/SZ-150 with selected viruses from *Totiviridae*, *Chrysoviridae*, *Partitiviridae*, *Reoviridae*, *Megabirnaviridae*, *Botybirnavirius*, and unassigned viruses, with the model of VT+G+F. The scale bars correspond to 0.5 amino acid substitutions per site, numbers at branch nodes show percentage posterior probabilities. The red star indicates the position of SsBV3/SZ-150. The detailed information on the selected viruses in the phylogenetic tree is shown in **Supplementary Table S1**.

Multiple alignment suggested that this conserved domain shared 34.7% sequence identity with those of watercress white vein virus (AFC95826) and chiltepin yellow mosaic virus (YP_003620401; **Table 1**). The putative Hel domain (nt positions 3,615–4,244) with five conserved motifs (I–V; **Supplementary Figure S1**) shares 36.0 and 35.1% sequence identities with those of grapevine fleck virus (NP_542612) and Fusarium graminearum mycotymovirus 1 (KT360947), respectively (**Table 1**). An RdRP domain, containing six conserved motifs (I–VI; **Supplementary Figure S1**) was detected near the C-terminus of the RP. This domain of SsMTV1 shares highest level of sequence identity (41.3%) with that of turnip yellow mosaic virus (NP_663297; **Table 1**).

Analysis of sRNAs Derived From SsMTV1/SZ-150 and SsBV3/SZ-150

In total, 966,210 virus-derived sRNAs (vsRNAs) of 18–30 nt in length, accounting for 7.43% of all sRNA reads, matched the genome sequence of SsMTV1/SZ-150 (**Table 2**). In addition, 1,077,449 and 794,152 vsRNAs of the same length (accounting for 8.23 and 6.11% of all sRNA reads) matched

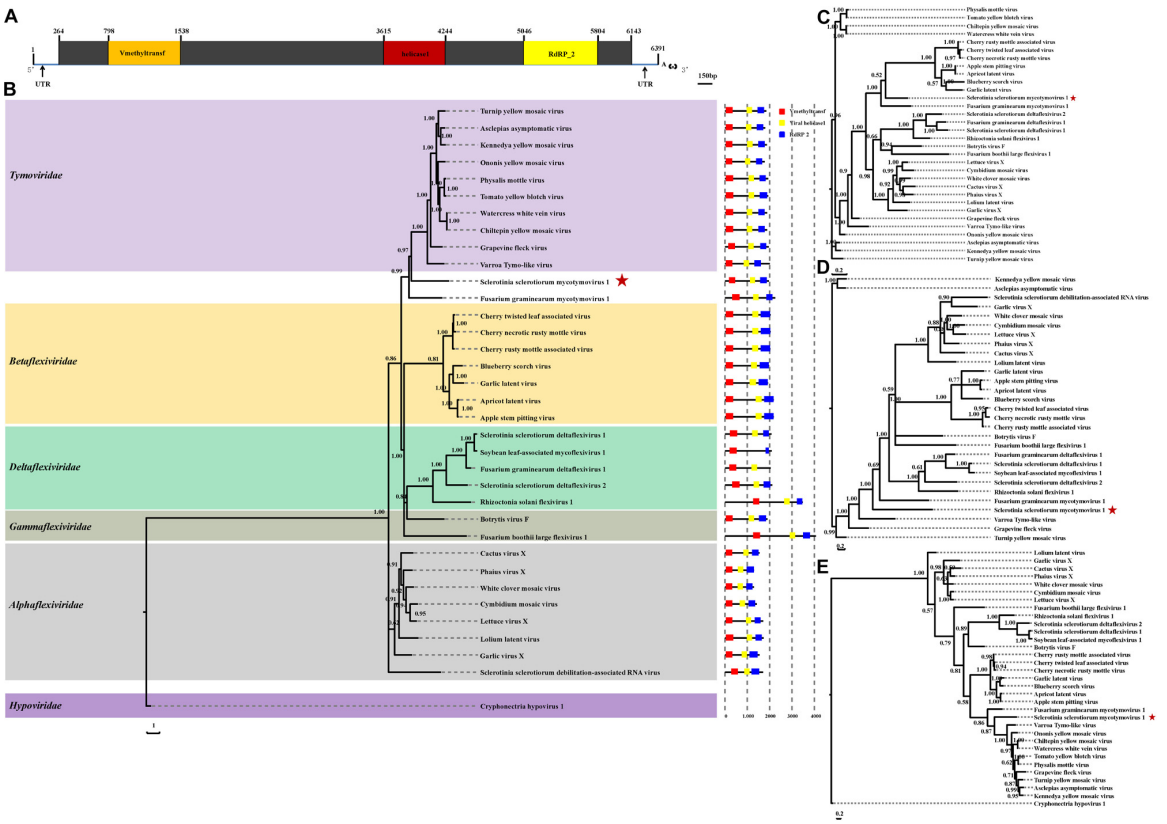

FIGURE 2 | Analyses of identified Sclerotinia sclerotiorum mycotymovirus 1 (SsMTV1/SZ-150) genome. **(A)** Schematic diagrams of the genetic organization of SsMTV1/SZ-150. The ORF (nt positions 264–6,143) encodes a putative viral protein with 1,958 amino acid residues that contains three conserved domains represented by the box: Vmethyltransf (798–1,538 nt), helicase (3,615–4,244 nt), and RNA-dependent RNA polymerase (RdRP_2, 5,046–5,804 nt). 5′-UTR (nt positions 1–263 nt) and 3′-UTR (nt positions 6,144–6,391 nt) are indicated as lines. The scale bar corresponds to a length of 150 bp. Phylogenetic (Bayesian) trees were constructed from the sequences of three conserved domains of the entire RP domain **(B)**, helicase **(C)**, methyltransferase **(D)**, RdRP **(E)**, and the SsMTV1/SZ-150, with the models of VT+I+G+F, RtREV+I+G+F, LG+I+G+F, and LG+I+G+F, respectively. CHV1 (Cryphonectria hypovirus 1) served as an outgroup in the phylogenetic analysis. The scale bar indicates the number of amino acid substitutions per site; numbers at branch nodes show percentage posterior probabilities. The position of SsMTV1/SZ-150 is shown by red asterisks. The detailed information on the selected viruses in the phylogenetic tree is presented in **Table 1**.

the genome sequence of SsBV3-L1-dsRNA/SZ-150 and SsBV3-L2-dsRNA/SZ-150, respectively (**Table 2**). The length of these vsRNAs mainly ranges from 20 to 24 nt, with the 22-nt class being dominant in strain SZ-150. Indeed, the 22-nt class represented approximately 37.3% of the total SsMTV1-derived vsRNAs (**Figure 3A** and **Table 2**) and approximately 27.4 and 27.0% of

TABLE 1 | Percent amino acid sequence identity between the RP polyprotein, methyltransferase (Mtr), helicase (Hel), and RdRp motifs of Sclerotinia sclerotiorum mycotymovirus 1 (SsMTV1/SZ-150) and those of selected viruses of the family *Tymoviridae*.

Virus name	Accession number	RP	Mtr	Hel	RdRp
Physalis mottle virus	NP_619756	297/1,751 (17.0%)	82/280 (29.3%)	55/203 (27.1%)	100/253 (39.5%)
Tomato yellow blotch virus	AEP40395	305/1,660 (18.4%)	61/178 (34.3%)	57/206 (27.7%)	99/253 (39.1%)
Watercress white vein virus	AFC95826	312/1,670 (18.7%)	67/193 (34.7%)	66/217 (30.4%)	101/253 (39.9%)
Chiltepin yellow mosaic virus	YP_003620401	307/1,670 (18.4%)	67/193 (34.7%)	66/217 (30.4%)	99/253 (39.1%)
Ononis yellow mosaic virus	NP_041257	332/1,707 (19.5%)	73/232 (31.5%)	70/204 (34.3%)	102/253 (40.3%)
Turnip yellow mosaic virus	NP_663297	338/1,667 (20.3%)	77/260 (29.6%)	61/204 (29.9%)	105/254 (41.3%)
Asclepias asymptomatic virus	YP_004464924	266/1,743 (15.3%)	78/252 (31.0%)	63/206 (30.6%)	100/253 (39.5%)
Kennedya yellow mosaic virus	NP_044328	286/1,808 (15.8%)	76/256 (29.7%)	63/202 (31.2%)	101/253 (39.9%)
Grapevine fleck virus	NP_542612	330/1,707 (19.3%)	75/249 (30.1%)	73/203 (36.0%)	89/253 (35.2%)
Varro Tymo-like virus	YP_009159826	329/1,641 (20.1%)	75/239 (31.3%)	51/153 (33.3%)	100/254 (39.4%)
Fusarium graminearum mycotymovirus 1	KT360947	324/1,861 (17.4%)	65/229 (28.4%)	73/208 (35.1%)	97/254 (38.2%)

the total SsBV3 vsRNAs (**Figures 3C,E** and **Table 2**). The second most abundant vsRNA species in SsMTV1/SZ-150 was the 23-nt class, accounting for 26.8% of the total vsRNAs (**Figure 3A** and **Table 2**), whereas the number of vsRNAs (21 and 23 species) was essentially equal in SsBV3/SZ-150 (**Figures 3C,E** and **Table 2**). A more specific analysis was performed on the distribution of the vsRNAs derived from the sense and antisense strands of SsMTV1. The results showed that there was an asymmetrical distribution, and the antisense vsRNAs were dominant (nearly 70%; **Figure 3B** and **Table 2**). In contrast to the vsRNAs from SsMTV1/SZ-150, the number of vsRNAs derived from the sense strand was almost equal to that from the antisense strain in SsBV3/SZ-150 (**Figures 3D,F** and **Table 2**).

There was a clear preference for uridine (U) residues (79.2%) in the 5′ terminal nucleotide composition of SsMTV1-derived vsRNAs, while guanidine (G) was the least abundant (4.1%; **Figure 3G**). Similar results were obtained in the analysis of vsRNAs from SsBV3/SZ-150 (**Figures 3H,I**). To determine the distribution of the vsRNAs in genomes of SsMTV1/SZ-150 and SsBV3/SZ-150, vsRNAs reads were then aligned against the genomes of two mycoviruses. As presented in **Figures 4B**,**D**,**F**, vsRNAs were distributed along the whole viral genome, including the coding regions and 5′- or 3′-UTRs; the vsRNAs derived from SsMTV1/SZ-150 were distributed along the genome in a non-random pattern, with the majority derived from the negative strand, and the vsRNAs derived from SsBV3/SZ-150 were uniformly distributed along the positive and negative strands, as described previously. There was one hotspot region, which produced more vsRNAs; they were present on both the positive and negative strands in the 5′ region of genomes of SsMTV1/SZ-150 and SsBV3/SZ-150.

SsBV3/SZ-150 and SsMTV1/SZ-150 Make Only a Limited Contribution to the Hypovirulence of *S. sclerotiorum*

RT-PCR analysis was performed on total-RNA samples from mycelial extracts of the hypovirulent strain SZ-150, from an ascospore progeny derivative SZ-150/A6, and from two protoplast derivatives (SZ-150/R59 and SZ-150/R6) of strain SZ-150. Strain SZ-150/R59 was infected with SsBV3/SZ-150, while SZ-150/R6 was coinfected by three mycoviruses: SsMTV1/SZ-150, SsHV1/SZ-150, and SsBV3/SZ-150 (**Figure 5A**). Strain SZ-150/A6 was virus-free, while we failed to create a strain infected with SsMTV1 alone (**Figure 5A**). To determine the biological effects of SsBV3/SZ-150 and SsMTV1/SZ-150 on hypovirulence of *S. sclerotiorum*, biological features of the four individual strains were assayed. Strain SZ-150 had abnormal colony morphology characterized by a dark pigment, whereas its derivatives SZ-150/A6, SZ-150/R59, and SZ-150/R6 had normal colony morphology with no significant differences on the potato–dextrose–agar (PDA) medium (**Figure 5B**). The growth rate of SZ-150/R59 (15.97 ± 3.34 mm/day) was not significantly different from that of SZ-150/A6 (17.86 ± 2.33 mm/day), but was faster than that of SZ-150/R6 (8.40 ± 1.46 mm/day; **Figure 5D**). Virulence assays were conducted on the detached leaves of rapeseed plants that were kept at 20°C for 48 h post inoculation.

TABLE 2 | The number of vsRNAs derived from Sclerotinia sclerotiorum mycotymovirus 1 (SsMTV1/SZ-150) and Sclerotinia sclerotiorum botybirnavirus 3 (SsBV3/SZ-150).

Virus	Total		20nts		21nts		22nts		23nts		24nts	
	Sense	Anti-sense	Sense	Anti-sense	Sense	Anti-sense	Sense	Anti-sense	Sense	Anti-sense	Sense	Antisense
SsMTV1/SZ-150	295,150	671,063	21,094	46,132	44,906	101,794	93,859	266,997	86,258	172,831	22,404	38,368
SsBV3-L1-dsRNA/SZ-150	596,387	481,062	47,154	48,948	98,526	91,967	164,287	131,221	120,287	72,818	51,181	40,751
SsBV3-L2-dsRNA/SZ-150	447,227	346,925	36,374	38,468	69,877	65,239	123,340	91,039	91,892	56,901	39,443	29,826

Sense indicates the vsRNAs derived from the sense strand of virus. Antisense indicates the vsRNAs derived from the antisense strand of virus.

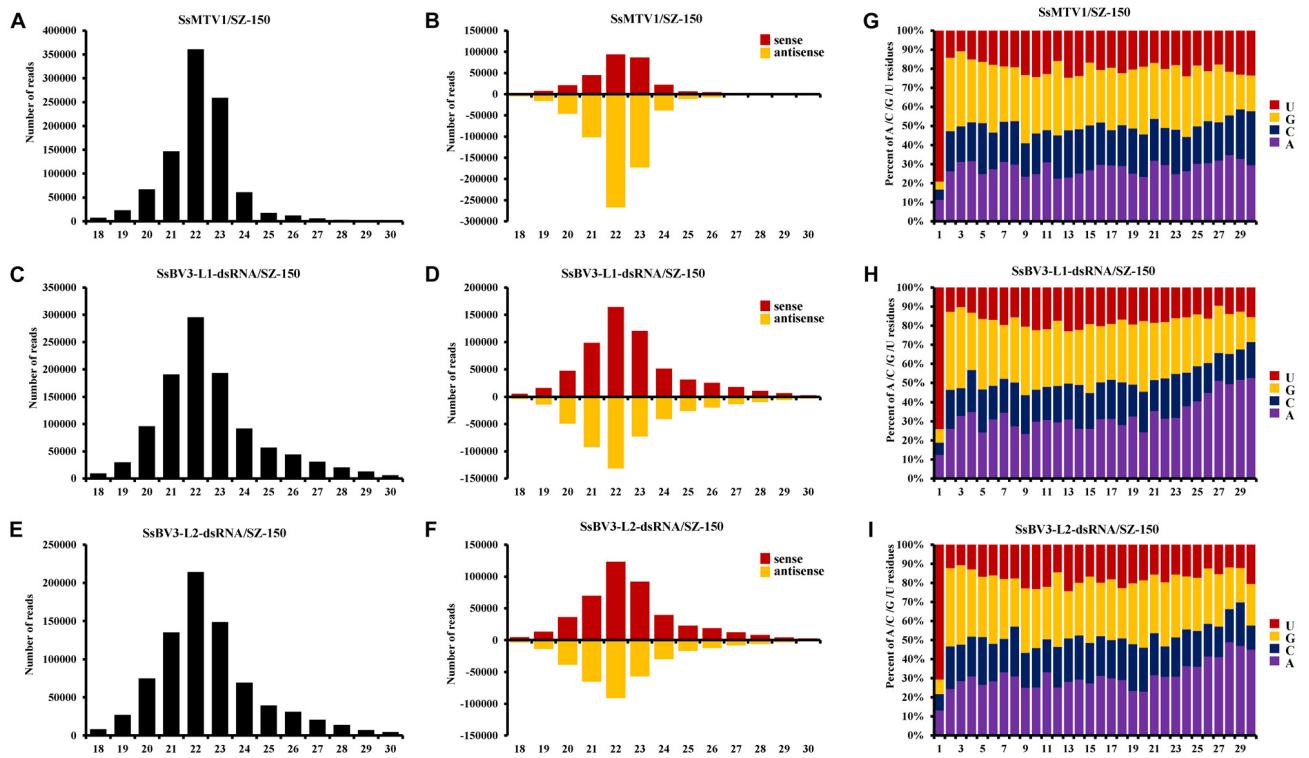

FIGURE 3 | Characterization of vsRNAs from Sclerotinia sclerotiorum mycotymovirus 1 (SsMTV1/SZ-150) and Sclerotinia sclerotiorum botybirnavirus 3 (SsBV3/SZ-150) in mycovirus-infected strain SZ-150. The size distributions of vsRNAs derived from SsMTV1 **(A)**, SsBV3-L1-dsRNA **(C)**, and SsBV3-L2-dsRNA **(E)** in strain SZ-150. The histogram illustrating the number of vsRNA reads; the size distribution of clones 18 to 30 nt. Relative accumulation of vsRNAs from sense and antisense of SsMTV1 **(B)**, SsBV3-L1-dsRNA **(D)**, and SsBV3-L2-dsRNA **(F)** from strain SZ-150. Red and yellow bars indicate sense and antisense vsRNAs, respectively. The identities and the relative frequency of 5′-terminal nucleotide of SsMTV1-derived vsRNAs **(G)**, SsBV3-L1-dsRNA-derived vsRNAs **(H)**, and SsBV3-L2-dsRNA-derived vsRNAs **(I)**. The *y*-axis shows the percentages of 5′-terminal nucleotides consisting of G, C, A, and U in the 18- to 30-nt vsRNAs class, and the *x*-axis represents the length distribution.

Strain SZ-150 failed to infect rapeseed leaves, whereas SZ-150/A6, SZ-150/R59, and SZ-150/R6 induced typical lesions on the leaves (**Figure 5C**). The size of lesion induced by SZ-150/R59 (3.3 ± 0.17 cm) was not significantly different from that induced by strain SZ-150/A6 (3.48 ± 0.26 cm) but was larger than that of strain SZ-150/R6 (1.74 ± 0.21 cm; **Figure 5E**). These results suggest that SsBV3/SZ-150 does not induce phenotypic changes in the host, and SsMTV1/SZ-150 makes only a limited contribution to the hypovirulence.

DISCUSSION

Multiple infection by several mycoviruses is a common phenomenon in the fungi kingdom (Ghabrial and Suzuki, 2008). These viruses are usually detected by conventionally methods, such as dsRNA extraction. Nevertheless, hypovirulence-related mycoviruses receive more attention from researchers, while latent mycoviruses or mycoviruses with a lower copy number of dsRNA formed in a fungal host are often ignored or are difficult to detect by dsRNA extraction.

Previously, our study based on the dsRNA extraction and conventional cloning strategies revealed coinfection by two mycoviruses SsHV1/SZ-150 and SsBV3/SZ-150 (SsRV1/SZ-150 in Xie et al., 2011) in a hypovirulent strain SZ-150 of *S. sclerotiorum*. In the present study, the results of high-throughput sequencing of sRNAs revealed one additional mycovirus (SsMTV1/SZ-150) in the same strain and, combined with RACE, allowed for completion of genome sequences of two mycoviruses (SsMTV1/SZ-150 and SsBV3/SZ-150). High-throughput sequencing is a powerful tool for the discovery of many novel ssRNA mycoviruses, especially (−)ssRNA mycoviruses that have a lower copy number of dsRNA in fungal cells. Several studies have proved the ability of high-throughput sequencing to detect low-copy mycovirus infections, thereby discovering new mycoviruses and evaluating mycovirus diversity in phytopathogenic fungi including *S. sclerotiorum*, *Rhizoctonia solani*, *Rosellinia necatrix*, and *Rhizophagus* spp. (Bartholomaus et al., 2016; Marzano et al., 2016; Yaegashi et al., 2016; Mu et al., 2017).

The genome of SsBV3/SZ-150 shares 97% identity with that of BpBV1/GarlicBc-72 at the amino acid level, thus revealing that SsBV3/SZ-150 should be recognized as an isolate of species Botrytis porri botybirnavirus 1. BpBV1/GarlicBc-72 confers hypovirulence on its natural host *B. porri* (Wu et al., 2012), whereas SsBV3/SZ-150 is associated with a latent infection in

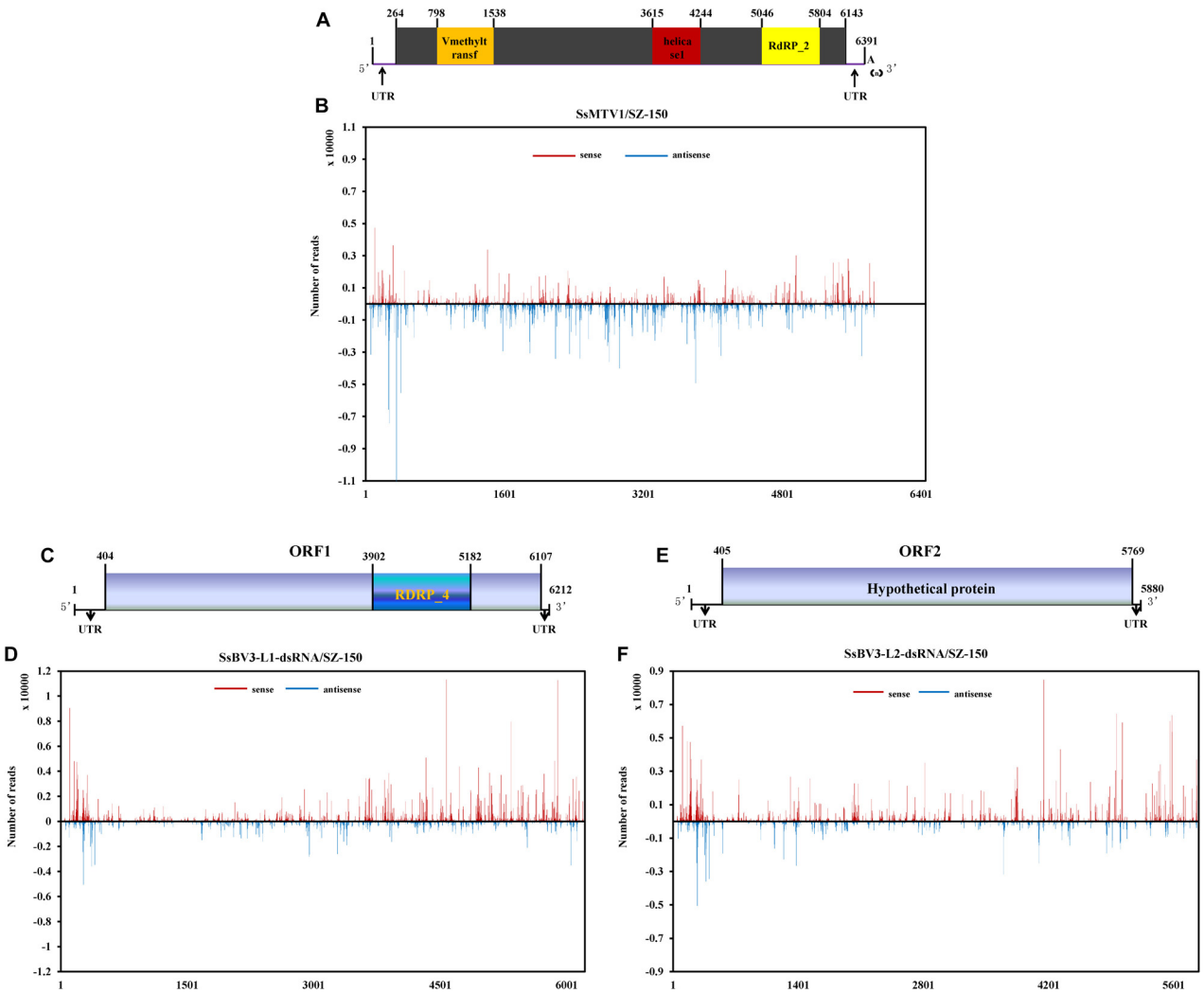

FIGURE 4 | Profiles of vsRNAs along Sclerotinia sclerotiorum mycotymovirus 1 (SsMTV1/SZ-150) and Sclerotinia sclerotiorum botybirnavirus 3 (SsBV3/SZ-150) genomes. The identified vsRNAs were mapped onto the SsMTV1 **(A)**, SsBV3-L1-dsRNA **(C)**, and SsBV3-L2-dsRNA **(E)** genomes. **(B**,**D**,**F)** Distribution of the vsRNAs mapped on the corresponding viral genomes. The *x*-axis shows schematic representations of SsMTV1 and SsBV3 genomic organization. The *y*-axis indicates the numbers of vsRNAs matching the sense strand (red, above the *x*-axis) and antisense strand (blue, below the *x*-axis).

S. sclerotiorum, suggesting that BpBV1 patterns of interaction with *B. porri* and *S. sclerotiorum* are different, even though these two fungi share 83% amino acid identity in the genome (Amselem et al., 2011). Actually, two mycoviruses of SsBV1 and SsBV2 belonging to the genus *Botybirnavirus* have already been characterized from *S. sclerotiorum* (Liu et al., 2015; Ran et al., 2016). SsBV2 infection induces hypovirulence in strains of *S. sclerotiorum* studied. Although infection by SsBV1 alone has no significant effects on culture morphology and virulence of *S. sclerotiorum*, infection by SsBV1 along with its SatH leads to slightly reduced virulence and a slower mycelial growth rate in its host. These combined results imply that the interaction between botybirnavirus and *S. sclerotiorum* is complex. Botybirnaviruses probably have a wide host range. Besides *Botrytis* spp. and *S. sclerotiorum*, botybirnaviruses have also been found in the fungi *Bipolaris maydis* and *Alternaria* spp. (Xiang et al., 2017; Wang et al., 2018). Although the genomes of these two botybirnaviruses have been fully sequenced, the influences on their fungal hosts are still unknown.

Notably, a botybirnavirus, BpBV1, was detected in both *Botrytis squamosa* and *B. cinerea* in addition to *B. porri* and *S. sclerotiorum*. These four phytopathogenic fungi have many similarities in the genome; more importantly, they have similar ecological niches and have opportunities to coinfect the same plants. Similar findings have been reported in other studies. Some viruses detected in *R. necatrix* have the closest relation to viruses infecting *Fusarium* spp., which are sympatric to *R. necatrix* (Arjona-Lopez et al., 2018). Recently, Schoebel et al. (2018) provided evidence that multiple interspecific virus transfers have occurred from *Hymenoscyphus albidus* to *Hymenoscyphus fraxineus* (Schoebel et al., 2018). These data suggest that interspecific transmission, even interfamily transmission, of

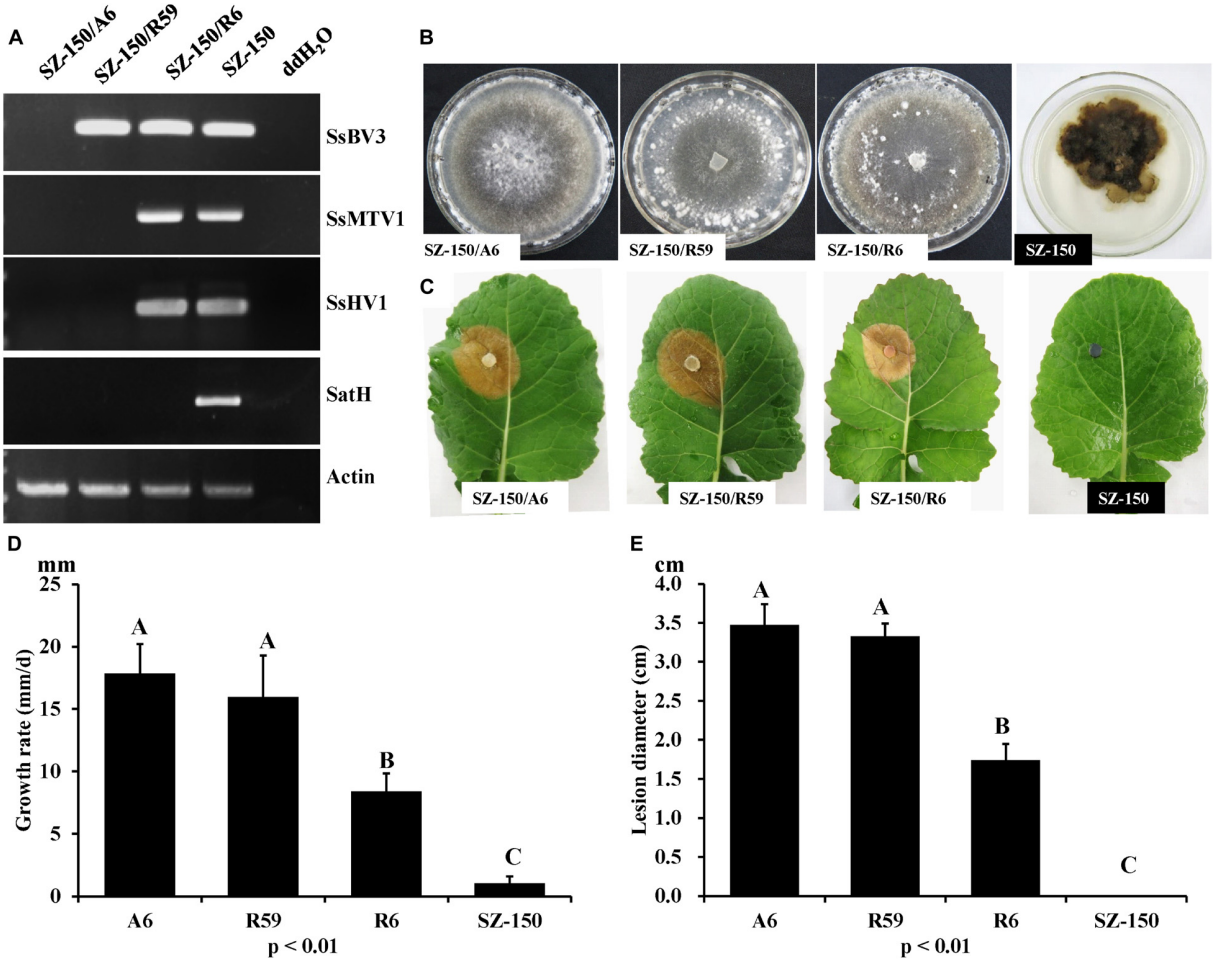

FIGURE 5 | Biological properties of four individual strains: SZ-150/A6, SZ-150/R59, SZ-150/R6, and SZ-150. **(A)** Detection of mycoviruses Sclerotinia sclerotiorum hypovirus 1 (SsHV1/SZ-150) and its related satellite RNA (SatH), Sclerotinia sclerotiorum mycotymovirus 1 (SsMTV1/SZ-150), and Sclerotinia sclerotiorum botybirnavirus 3 (SsBV3/SZ-150) in four strains by RT-PCR. The actin gene served as an internal control. **(B)** Colony morphology and **(D)** growth rate of four individual strains. Four strains were grown on PDA for 15 days at 20°C prior to photography. **(C,E)** Virulence assays of the four strains on the detached leaves of rapeseed plants. Statistical analysis of the growth rate and lesion diameter of the four individual strains was conducted at the $P < 0.01$ level. The error bars indicate the SD from three sample means.

BpBV1, and other mycoviruses may occur under field conditions, although the underlying mechanism is still unclear.

The complete genome sequence of SsMTV1/SZ-150 was determined in this study as well. Phylogenetic analyses of the putative polyprotein strongly suggest that SsMTV1/SZ-150 is related, albeit distantly, to members of the family *Tymoviridae* and forms an independent evolutionary clade. Therefore, SsMTV1/SZ-150 is a novel mycotymo-like virus related to members of *Tymoviridae*. Although most viruses in the order *Tymovirales* infect plants, a few members of this order infecting plant-pathogenic fungi, including *B. cinerea*, *Fusarium boothii*, *Fusarium graminearum*, *R. solani*, and *S. sclerotiorum*, have been characterized (Howitt et al., 2006; Li K. et al., 2016; Li P. et al., 2016; Bartholomaus et al., 2017; Mizutani et al., 2018). Nevertheless, those mycotymo-like viruses were placed into different evolutionary lineages, suggesting that mycotymo-like viruses are more diverse in fungi than previously thought, and have a complex evolutionary relationship with plant viruses within *Tymovirales*.

The genomic RNA of viruses belonging to the family *Tymoviridae* ranges from 6.0 to 7.5 kb in length and is mostly polyadenylated (King et al., 2011) and characterized by a high cytosine content (32–50%). Similar to other members of family *Tymoviridae*, the genomic sequence of SsMTV1/SZ-150 is 6,391 nt in size, excluding the 3′-terminal poly (A) tail. Nevertheless, the genomic sequence of SsMTV1/SZ-150 also contains a high content of cytosines with 30.1%. Consistently with the genomic RNA of Sclerotinia sclerotiorum debilitation-associated RNA virus (Xie et al., 2006), the genome of SsMTV1/SZ-150 has a single ORF encoding a polyprotein but lacks a gene encoding a coat protein (CP). All other recognized members of the order *Tymovirales* contain CP genes regardless of whether they are plant viruses, insect viruses, or two mycoviruses (BotVX and BotV-F).

In the present study, we analyzed the vsRNAs derived from SsMTV1/SZ-150 and SsBV3/SZ-150. vsRNAs from SsMTV1/SZ-150 and SsBV3/SZ-150 have a size from 18 to 30 nt with a peak at 22 nt. vsRNAs are uniformly distributed along the genomes of two viruses, with the majority derived from the negative strand in the case of SsMTV1/SZ-150. In the plant *Arabidopsis thaliana*, different Dicer proteins are responsible for the cleavage of sRNAs of different lengths. Dicer2 is responsible for the cleavage of 22-nt sRNAs (Ruiz-Ferrer and Voinnet, 2009), suggesting that the homolog of DCL2 in *S. sclerotiorum* might be the predominant Dicer ribonuclease involved in the biogenesis of vsRNAs. Some reports indicate that the loading of sRNA onto an AGO-containing effector complex is guided by the 5′-terminal nucleotide of the sRNA in *Arabidopsis* and rice (Mi et al., 2008; Wu et al., 2009). In *Arabidopsis*, AGO1 harbors microRNAs with 5′-terminal U residues (Mi et al., 2008). This finding suggests that most of the vsRNAs are preferentially recruited into AGO1 in *S. sclerotiorum*.

Thus, aside from SsHV1/SZ-150 and its SatH, in this study, we discovered and characterized two other mycoviruses, SsBV3/SZ-150 (belonging to genus *Botybirnavirius*), and SsMTV1/SZ-150 (related to viruses in the order *Tymovirales*), in the hypovirulent strain SZ-150 *via* high-throughput sequencing. The SsMTV1 and SsBV3-vsRNA analyses suggest that the DCL2 and AGO1 are key players in the defense against mycovirus infection in *S. sclerotiorum*.

MATERIALS AND METHODS

Fungal Strains and Culture Conditions

Sclerotinia sclerotiorum strain SZ-150 was originally isolated from a sclerotium collected from a diseased rapeseed (*Brassica napus*) (Xie et al., 2011). SZ-150/R59 and SZ-150/R6 were derived from strain SZ-150 by protoplast isolation and regeneration. SZ-150/A6 was a single-ascospore isolation of strain SZ-150/R59. All fungal strains were grown at 18–22°C on the PDA medium and stored on PDA slants at 4–8°C.

sRNA Sequencing and Bioinformatics Analysis

To prepare total RNA for high-throughput sRNA sequencing, strain SZ-150 was cultured on cellophane membranes overloading PDA plate for 10 days. The harvested mycelium of SZ-150 was ground into a fine powder in liquid nitrogen with a mortar and pestle, and total RNA was extracted with TRIzol RNA extraction kit (Takara Bio, Inc., Japan). The total RNA was stored at −80°C until analysis. Deep sequencing of sRNA was performed on the Illumina HiSeq 2000 platform by the BGI Tech Company (Shenzhen, China). sRNA molecules (≤30 nt) were isolated and purified by polyacrylamide gel electrophoresis (PAGE). The purified sRNA was ligated with an adaptor, and then reverse-transcribed to cDNA, which was then amplified by polymerase chain reaction (PCR) and recovered by PAGE in a 6% gel for deep sequencing. To obtain clean sequences, the raw reads from deep sequencing were processed to remove the adaptor sequences and discard low-quality reads, and then were assembled into contigs in the Velvet software with a k-mer value of 17 excluding the sRNA generated from *S. sclerotiorum*. The assembled contigs were employed in searches in the GenBank database[2] using BLASTN and BLASTX to find similar sequences.

Reads of vsRNAs were mapped to the virus genome using the Bowtie (1.0) software and only those having sequences identical or complementary to the viral genomic sequence (allowing for one mismatch with the reference genomes) were identified as vsRNAs. Then, the sorted and indexed BAM file was processed by viRome[3].

Full-Length cDNA Cloning, Sequencing, Sequence Analysis, and Phylogenetic Analysis

To fill the gap between different contigs, virus-specific primers based on the sequences assembled from sRNAs were designed and used for RT-PCR (**Supplementary Table S2**). The amplicons were purified and then cloned into the pMD18-T vector (Takara, Dalian, China) for sequencing. Finally, we filled the gap between two different contigs. To obtain the complete cDNA sequences of mycovirus genomes, the terminal sequence was determined by RACE-PCR using the SMARTer RACE 5′/3′ Kit (Cat. No. 634858, Clontech) (**Supplementary Table S2**).

Sequence assembly and the basic features (e.g., lengths, G+C content, and ORF identification) of the full-length genome sequence were analyzed using the DNAMAN software. The conserved domains of mycovirus genomes were identified on a motif scan website[4]. The sequences of previously reported mycoviruses and other sequences referenced in this research were downloaded from the NCBI GenBank database[5] and used for multiple-alignment and phylogenetic analyses. Multiple alignment was performed using the Clustal X program. On the basis of the aligned sequences, the best-fit evolution models of SsMTV1 and SsBV3 were obtained using Akaike's information criterion (AIC), and searched using the ProtTest server. BI (Bayesian) trees were constructed with MrBayes-3.2.7, and then the tree files were viewed using FigTree-1.4.0.

Assay of Biological Properties of Mycovirus-Infected and Mycovirus-Free Strains

To determine the contribution of SsMTV1 and SsBV3 to the hypovirulence in strain SZ-150, the presence of viruses in strains SZ-150, SZ-150/A6, SZ-150/R59, and SZ-150/R6 was analyzed *via* RT-PCR using specific primers for SsHV1, SsMTV1, SsBV3, and SatH (**Supplementary Table S2**). Four strains, SZ-150, SZ-150/A6, SZ-150/R59, and SZ-150/R6, were evaluated regarding colony morphology, growth rate, and virulence as previously described (Zhang et al., 2009; Xie et al., 2011). All assays were repeated three times. Experimental data were

[2]http://www.ncbi.nlm.nih.gov/

[3]http://sourceforge.net/projects/virome

[4]http://www.genome.jp/tools/motif/

[5]http://www.ncbi.nlm.nih.gov/genomes

analyzed in SAS 8.0 software. Treatment means were compared by the least significant difference test at *P*n SAS 8.

DATA AVAILABILITY

All datasets generated for this manuscript can be found in GenBank. Accession numbers are listed in the **Supplementary Information**.

AUTHOR CONTRIBUTIONS

QW, DJ, and JX designed the research and wrote the manuscript. QW, SC, and XX executed the experiments. QW, XX, JC, YF, TC, DJ, and JX performed the data and bioinformatics analyses. All authors read and approved the final manuscript.

FUNDING

This research was financially supported by the National Key Research and Development Program of China (2017YFD0201100), the National Natural Science Foundation of China (31571959 and 31722046), the Fund of Fok Ying Tung Education Foundation (151031), and the earmarked fund of China Agriculture Research System (CARS-13).

SUPPLEMENTARY MATERIAL

The Supplementary Material for this article can be found online at: https://www.frontiersin.org/articles/10.3389/fmicb.2019.01415/full#supplementary-material

REFERENCES

Adams, M. J., Candresse, T., Hammond, J., Kreuze, J. F., Martelli, G. P., Namba, S., et al. (2011a). "*Alphaflexiviridae*," in *Virus Taxonomy: Classification and Nomenclature of Viruses: Ninth Report of the International Committee on Taxonomy of Viruses*, eds A. M. Q. King, M. J. Adams, E. B. Carstens, and E. J. Lefkowitz (San Diego, CA: Elsevier), 904–919. doi: 10.1016/b978-0-12-384684-6.00077-x

Adams, M. J., Kreuze, J. F., and Martelli, G. P. (2011b). "*Tymovirales*," in *Virus Taxonomy: Classification and Nomenclature of Viruses: Ninth Report of the International Committee on Taxonomy of Viruses*, eds A. M. Q. King, M. J. Adams, E. B. Carstens, and E. J. Lefkowitz (San Diego, CA: Elsevier), 901–903. doi: 10.1016/b978-0-12-384684-6.00076-8

Amselem, J., Cuomo, C. A., van Kan, J. A., Viaud, M., Benito, E. P., Couloux, A., et al. (2011). Genomic analysis of the necrotrophic fungal pathogens *Sclerotinia sclerotiorum* and *Botrytis cinerea*. *PLoS Genet.* 7:e1002230. doi: 10.1371/journal.pgen.1002230

Arjona-Lopez, J. M., Telengech, P., Jamal, A., Hisano, S., Kondo, H., Yelin, M. D., et al. (2018). Novel, diverse RNA viruses from mediterranean isolates of the phytopathogenic fungus, *Rosellinia necatrix*: insights into evolutionary biology of fungal viruses. *Environ. Microbiol.* 20, 1464–1483. doi: 10.1111/1462-2920.14065

Bartholomaus, A., Wibberg, D., Winkler, A., Puhler, A., Schluter, A., Varrelmann, M., et al. (2016). Deep sequencing analysis reveals the mycoviral diversity of the virome of an avirulent isolate of *Rhizoctonia solani* AG-2-2 IV. *PLoS One* 11:e0165965. doi: 10.1371/journal.pone.0165965

Bartholomaus, A., Wibberg, D., Winkler, A., Puhler, A., Schluter, A., Varrelmann, M., et al. (2017). Identification of a novel mycovirus isolated from *Rhizoctonia solani* (AG 2-2 IV) provides further information about genome plasticity within the order Tymovirales. *Arch. Virol.* 162, 555–559. doi: 10.1007/s00705-016-3085-3

Boland, G. J. (1992). Hypovirulence and double-stranded RNA in *Sclerotinia sclerotiorum*. *Can. J. Plant Pathol.* 14, 10–17. doi: 10.1080/07060669209500900

Bolton, M. D., Thomma, B. P., and Nelson, B. D. (2006). *Sclerotinia sclerotiorum* (Lib). de Bary: biology and molecular traits of a cosmopolitan pathogen. *Mol. Plant Pathol.* 7, 1–16. doi: 10.1111/j.1364-3703.2005.00316.x

Donaire, L., and Ayllon, M. A. (2017). Deep sequencing of mycovirus-derived small RNAs from *Botrytis* species. *Mol. Plant Pathol.* 18, 1127–1137. doi: 10.1111/mpp.12466

Ghabrial, S. A., Caston, J. R., Jiang, D., Nibert, M. L., and Suzuki, N. (2015). 50-plus years of fungal viruses. *Virology* 479, 356–368. doi: 10.1016/j.virol.2015.02.034

Ghabrial, S. A., and Suzuki, N. (2008). "Encyclopedia of virology," in *Fungal viruses*, 3rd Edn, Vol. 2, eds B. W. J. Mahy and M. H. V. Van Regenmortel (Elsevier: Oxford), 284–291.

Ghabrial, S. A., and Suzuki, N. (2009). Viruses of plant pathogenic fungi. *Annu. Rev. Phytopathol.* 47, 353–384. doi: 10.1146/annurev-phyto-080508-081932

Guo, Z., Li, Y., and Ding, S. W. (2019). Small RNA-based antimicrobial immunity. *Nat. Rev. Immunol.* 19, 31–44. doi: 10.1038/s41577-018-0071-x

Hollings, M. (1962). Viruses associated with a die-back disease of cultivated mushroom. *Nature* 196, 962–965. doi: 10.1038/196962a0

Howitt, R. L., Beever, R. E., Pearson, M. N., and Forster, R. L. (2001). Genome characterization of botrytis virus F, aflexuous rod-shaped mycovirus resembling plant 'potex-like' viruses. *J. Gen. Virol.* 82, 67–78. doi: 10.1099/0022-1317-82-1-67

Howitt, R. L., Beever, R. E., Pearson, M. N., and Forster, R. L. (2006). Genome characterization of a flexuous rod-shaped mycovirus, botrytis virus X, reveals high amino acid identity to genes from plant 'potex-like' viruses. *Arch. Virol.* 151, 563–579. doi: 10.1007/s00705-005-0621-y

Jiang, D., Fu, Y., Guoqing, L., and Ghabrial, S. A. (2013). Viruses of the plant pathogenic fungus *Sclerotinia sclerotiorum*. *Adv. Virus Res.* 86, 215–248. doi: 10.1016/b978-0-12-394315-6.00008-8

King, A. M. Q., Adams, M. J., Carstens, E. B., and Lefkowitz, E. J. (2011). *Virus Taxonomy: Classification and Nomenclature of Viruses: Ninth Report of the International Committee on Taxonomy of Viruses*. Elsevier: Amsterdam, 901–952.

Kreuze, J. F., Perez, A., Untiveros, M., Quispe, D., Fuentes, S., Barker, I., et al. (2009). Complete viral genome sequence and discovery of novel viruses by deep sequencing of small RNAs: a generic method for diagnosis, discovery and sequencing of viruses. *Virology* 388, 1–7. doi: 10.1016/j.virol.2009.03.024

Li, K., Zheng, D., Cheng, J., Chen, T., Fu, Y., Jiang, D., et al. (2016). Characterization of a novel *Sclerotinia sclerotiorum* RNA virus as the prototype of a new proposed family within the order *Tymovirales*. *Virus Res.* 219, 92–99. doi: 10.1016/j.virusres.2015.11.019

Li, P., Lin, Y., Zhang, H., Wang, S., Qiu, D., and Guo, L. (2016). Molecular characterization of a novel mycovirus of the family tymoviridae isolated from the plant pathogenic fungus *Fusarium graminearum*. *Virology* 489, 86–94. doi: 10.1016/j.virol.2015.12.004

Liu, L., Wang, Q., Cheng, J., Fu, Y., Jiang, D., and Xie, J. (2015). Molecular characterization of a bipartite double-stranded RNA virus and its satellite-like RNA co-infecting the phytopathogenic fungus *Sclerotinia sclerotiorum*. *Front. Microbiol.* 6:406. doi: 10.3389/fmicb.2015.00406

Marzano, S. L., and Domier, L. L. (2016). Novel mycoviruses discovered from metatranscriptomics survey of soybean phyllosphere phytobiomes. *Virus Res.* 213, 332–342. doi: 10.1016/j.virusres.2015.11.002

Marzano, S. L., Nelson, B. D., Ajayi-Oyetunde, O., Bradley, C. A., Hughes, T. J., Hartman, G. L., et al. (2016). Identification of diverse mycoviruses through metatranscriptomics characterization of the viromes of five major fungal plant pathogens. *J. Virol.* 90, 6846–6863. doi: 10.1128/JVI.00357-16

Mi, S., Cai, T., Hu, Y., Chen, Y., Hodges, E., Ni, F., et al. (2008). Sorting of small RNAs into *Arabidopsis* argonaute complexes is directed by the 5′ terminal nucleotide. *Cell* 133, 116–127. doi: 10.1016/j.cell.2008.02.034

Mizutani, Y., Abraham, A., Uesaka, K., Kondo, H., Suga, H., Suzuki, N., et al. (2018). Novel mitoviruses and a unique Tymo-like virus in hypovirulent and virulent strains of the Fusarium head blight fungus, *Fusarium boothii*. *Viruses* 10:E584. doi: 10.3390/v10110584

Mu, F., Xie, J., Cheng, S., You, M. P., Barbetti, M. J., Jia, J., et al. (2017). Virome characterization of a collection of *S. sclerotiorum* from Australia. *Front. Microbiol.* 8:2540. doi: 10.3389/fmicb.2017.02540

Pearson, M. N., Beever, R. E., Boine, B., and Arthur, K. (2009). Mycoviruses of filamentous fungi and their relevance to plant pathology. *Mol. Plant Pathol.* 10, 115–128. doi: 10.1111/j.1364-3703.2008.00503.x

Ran, H., Liu, L., Li, B., Cheng, J., Fu, Y., Jiang, D., et al. (2016). Co-infection of a hypovirulent isolate of *Sclerotinia sclerotiorum* with a new botybirnavirus and a strain of a mitovirus. *Virol. J.* 13:92. doi: 10.1186/s12985-016-0550-2

Ruiz-Ferrer, V., and Voinnet, O. (2009). Roles of plant small RNAs in biotic stress responses. *Annu. Rev. Plant Biol.* 60, 485–510. doi: 10.1146/annurev.arplant.043008.092111

Schoebel, C. N., Prospero, S., Gross, A., and Rigling, D. (2018). Detection of a conspecific mycovirus in two closely related native and introduced fungal hosts and evidence for interspecific virus transmission. *Viruses* 10:628. doi: 10.3390/v10110628

Torres-Martinez, S., and Ruiz-Vazquez, R. M. (2017). The RNAi universe in fungi: a varied landscape of small RNAs and biological functions. *Annu. Rev. Microbiol.* 71, 371–391. doi: 10.1146/annurev-micro-090816-093352

Vainio, E. J., Jurvansuu, J., Streng, J., Rajamäki, M.-L., Hantula, J., Valkonen, J. P. T., et al. (2015). Diagnosis and discovery of fungal viruses using deep sequencing of small RNAs. *J. Gen. Virol.* 96, 714–725. doi: 10.1099/jgv.0.000003

Wang, H., Li, C., Cai, L., Fang, S., Zheng, L., Yan, F., et al. (2018). The complete genomic sequence of a novel botybirnavirus isolated from a phytopathogenic *Bipolaris maydis*. *Virus Genes* 54, 733–736. doi: 10.1007/s11262-018-1584-x

Wang, S., Li, P., Zhang, J., Qiu, D., and Guo, L. (2016). Generation of a high resolution map of sRNAs from *Fusarium graminearum* and analysis of responses to viral infection. *Sci. Rep.* 6:26151. doi: 10.1038/srep26151

Wu, L., Zhang, Q., Zhou, H., Ni, F., Wu, X., Qi, Y., et al. (2009). Rice microRNA effector complexes and targets. *Plant Cell* 21, 3421–3435. doi: 10.1105/tpc.109.070938

Wu, M., Jin, F., Zhang, J., Yang, L., Jiang, D., and Li, G. (2012). Characterization of a novel bipartite double-stranded RNA mycovirus conferring hypovirulence in the phytopathogenic fungus *Botrytis porri*. *J. Virol.* 86, 6605–6619. doi: 10.1128/JVI.00292-12

Wu, Q., Luo, Y., Lu, R., Lau, N., Lai, E. C., Li, W. X., et al. (2010). Virus discovery by deep sequencing and assembly of virus-derived small silencing RNAs. *Proc. Natl. Acad. Sci. U.S.A.* 107, 1606–1611. doi: 10.1073/pnas.0911353107

Xiang, J., Fu, M., Hong, N., Zhai, L., Xiao, F., and Wang, G. (2017). Characterization of a novel botybirnavirus isolated from a phytopathogenic *Alternaria* fungus. *Arch. Virol.* 162, 3907–3911. doi: 10.1007/s00705-017-3543-6

Xie, J., and Jiang, D. (2014). New insights into mycoviruses and exploration for the biological control of crop fungal diseases. *Annu. Rev. Phytopathol.* 52, 45–68. doi: 10.1146/annurev-phyto-102313-050222

Xie, J., Wei, D., Jiang, D., Fu, Y., Li, G., Ghabrial, S., et al. (2006). Characterization of debilitation-associated mycovirus infecting the plant-pathogenic fungus *Sclerotinia sclerotiorum*. *J. Gen. Virol.* 87(Pt 1), 241–249. doi: 10.1099/vir.0.81522-0

Xie, J., Xiao, X., Fu, Y., Liu, H., Cheng, J., Ghabrial, S. A., et al. (2011). A novel mycovirus closely related to hypoviruses that infects the plant pathogenic fungus *Sclerotinia sclerotiorum*. *Virology* 418, 49–56. doi: 10.1016/j.virol.2011.07.008

Yaegashi, H., Shimizu, T., Ito, T., and Kanematsu, S. (2016). Differential inductions of RNA silencing among encapsidated double-stranded RNA mycoviruses in the white root rot fungus *Rosellinia necatrix*. *J. Virol.* 90, 5677–5692. doi: 10.1128/JVI.02951-15

Yu, J., Lee, K. M., Cho, W. K., Park, J. Y., and Kim, K. H. (2018). Differential contribution of RNA interference components in response to distinct *Fusarium graminearum* virus infections. *J. Virol.* 92:e01756-17. doi: 10.1128/JVI.01756-17

Zhang, L., Fu, Y., Xie, J., Jiang, D., Li, G., Yi, X., et al. (2009). A novel virus that infecting hypovirulent strain XG36-1 of plant fungal pathogen *Sclerotinia sclerotiorum*. *Virol. J.* 6:96. doi: 10.1186/1743-422X-6-96

Conflict of Interest Statement: The authors declare that the research was conducted in the absence of any commercial or financial relationships that could be construed as a potential conflict of interest.

frontiers in Cellular and Infection Microbiology

ORIGINAL RESEARCH
published: 10 July 2019
doi: 10.3389/fcimb.2019.00222

CpATG8, a Homolog of Yeast Autophagy Protein ATG8, Is Required for Pathogenesis and Hypovirus Accumulation in the Chest Blight Fungus

Liming Shi[1], *Jinzi Wang*[1†], *Rui Quan*[1], *Feng Yang*[1], *Jinjie Shang*[1,2*] *and Baoshan Chen*[1*]

[1] State Key Laboratory for Conservation and Utilization of Subtropical Agro-bioresources, College of Life Science and Technology, Guangxi University, Nanning, China, [2] Jiangsu Key Laboratory for Microbes and Functional Genomics, College of Life Sciences, Nanjing Normal University, Nanjing, China

OPEN ACCESS

Edited by:
Daohong Jiang,
Huazhong Agricultural University, China

Reviewed by:
Angie Gelli,
University of California, Davis, United States
Ping Wang,
School of Medicine, Louisiana State University, United States
Zhengyi Wang,
Zhejiang University, China

***Correspondence:**
Jinjie Shang
jinjieshang@njnu.edu.cn
Baoshan Chen
chenyaoj@gxu.edu.cn

†Present Address:
Jinzi Wang,
School of Marine Sciences and Biotechnology, Guangxi University for Nationalities, Nanning, China

Specialty section:
This article was submitted to Fungal Pathogenesis, a section of the journal Frontiers in Cellular and Infection Microbiology

Received: 31 January 2019
Accepted: 11 June 2019
Published: 10 July 2019

Citation:
Shi L, Wang J, Quan R, Yang F, Shang J and Chen B (2019) CpATG8, a Homolog of Yeast Autophagy Protein ATG8, Is Required for Pathogenesis and Hypovirus Accumulation in the Chest Blight Fungus. Front. Cell. Infect. Microbiol. 9:222. doi: 10.3389/fcimb.2019.00222

Autophagy is a degradation system in the cell, involved in the turnover of cellular components, development, differentiation, immune responses, protection against pathogens, and cell death. Autophagy is induced by nutrient starvation, in which cytoplasmic components and organelles are digested *via* vacuoles/lysosomes. In this study, by using electron microscopy, we observed that hypovirus CHV1-EP713 infection of *Cryphonectria parasitica*, the causative agent of chestnut blight disease, caused proliferation of autophagic-like vesicles. This phenomenon could be mimicked by treating the wild-type strain of the fungus EP155 with the autophagy induction drug rapamycin. Some of the hypovirulence-associated traits, including reduced pigmentation and conidiation, were also observed in the rapamycin-treated EP155. Quantitative reverse transcriptase polymerase chain reaction (qRT-PCR) revealed that genes involved in autophagy were up-regulated in expression. Deletion of *cpatg8*, a gene encoding a homolog of ATG8 in *Saccharomyces cerevisiae*, resulted in attenuation of virulence and reduction in sporulation, as well as accumulation of the double-stranded viral RNA. Furthermore, virus-encoded p29 protein was found to co-localize with CpATG8, implying that the viral protein may interfere with the function of CpATG8. Taken together, these findings show that *cpatg8* can be regulated by the hypovirus and is required for virulence and development of the fungus and accumulation of viral dsRNA in chestnut blight fungus.

Keywords: *cpatg8*, autophagy, hypovirus, virulence, chestnut blight fungus

INTRODUCTION

Autophagy is a conserved cellular process of eukaryotic cells that degrades intracellular protein complexes and organelles in the vacuole or lysosome (Klionsky et al., 2016; Liu et al., 2016; Yin et al., 2016). Autophagy has diverse physiological functions in the regulation of energy and nutrient metabolism, organelle quality control, removing misfolded proteins (Yin et al., 2016), and the development of filamentous fungi (Khan et al., 2012; Voigt and Pöggeler, 2013b; Liu et al., 2016). Among many molecular elements, ATG8, a ubiquitin-like protein, is a key element of autophagy pathway (Klionsky et al., 2016). In *Saccharomyces cerevisiae*, it was reported that ATG8

is conjugated to the lipid phosphatidyl ethanolamine (PE) and required for autophagosome formation (Nakatogawa et al., 2007). ATG8 is localized to preautophagosomal structures (PAS), autophagosomes, and autophagic bodies (Suzuki et al., 2001). In filamentous fungi, autophagy has been shown to be involved in virulence, cellular growth, development, and environmental stress (Pollack et al., 2009; Bartoszewska and Kiel, 2011; Klionsky et al., 2016; Liu et al., 2016). In *Fusarium graminearum*, *FgATG8* was found to function in the formation of aerial mycelium and formation of reproductive structures, nutritional use of storage lipid droplets, and infection (Josefsen et al., 2012).

Autophagy could be induced by various abiotic and biotic stresses including pathogen infection (Hayward and Dinesh-Kumar, 2011). In addition, the canonical function of autophagy may play a role in antivirus activities (Dagdas et al., 2016; Clavel et al., 2017; Hafrén et al., 2017; Haxim et al., 2017). However, different animal and plant viruses have developed diversified strategies to evade or hijack the autophagy pathway to promote their own infection or transmission (Dong and Levine, 2013; Chen et al., 2017). Although the role of autophagy in host–virus interactions in animals and plants has been studied to some extent, functions of autophagy in the fungus–virus interface remain to be understood.

Chestnut blight caused by *Cryphonectria parasitica* is a well-known forest disease. Infection with hypoviruses, a group of plus sense RNA viruses, attenuates virulence of this fungus (Dawe and Nuss, 2001). In addition to reducing hypovirulence, traits of phenotype can also be altered in hypovirus-infected *C. parasitica* strains, such as suppressed sporulation, decreased pigmentation, and altered gene expression patterns (Nuss, 2005; Eusebio-Cope et al., 2015). In this report, we observed that both hypovirus CHV1-EP713 infection and treatment with the autophagy-inducing drug rapamycin in the wild-type strain EP155 could cause proliferation of autophagic-like vesicles, and expression of autophagy-related genes was up-regulated following infection by hypovirus CHV1-EP713. Disruption of *cpatg8*, a gene encoding a homolog of *ATG8* in *S. cerevisiae*, caused a profound reduction in fungal virulence, conidiation, and accumulation of the virus.

MATERIALS AND METHODS

Fungal Strains and Growth Conditions

C. parasitica wild-type strain EP155 (ATCC38755), its isogenic strain EP155/CHV1-EP713 harboring hypovirus CHV1-EP713 by transfection, and strain DK80, a *ku80*-deletion mutant of EP155 and highly efficient in gene homologous replacement (Lan et al., 2008; Choi et al., 2012), as well as *cpatg8* deletion strain Δ*cpatg8* were all maintained on potato dextrose agar (PDA) medium (Difco, Detroit, MI) at 24–26°C with a 12 h/12 h light/dark cycle (1,300–1,600 lx), as described previously (Chen et al., 2011). EP complete medium was employed for cultures used for DNA and dsRNA isolation at room temperature with shaking at 200 rpm for 3 days. The transformation of *C. parasitica* was done as described (Chen et al., 2011). Hygromycin (40 μg/ml) or G418 (25 μg/ml) was supplemented into the growth medium for selection of transformants.

TABLE 1 | List of primers used.

Primer name	Sequence 5′-3′	Name of gene
Hyg-F	CTGAAATAAAGGGAGGAAGGG	*hph*
Hyg-R	AGGACACACATTCATCGTAGG	
cpatg8-all-F	CGTGGGGTGACTTTGAGAGTGA	*cpatg8*
cpatg8-all-R	CTTGCCTACGAGGTCACTGGTCA	
cpatg8-LF	TACTTCTTCTGCCTGCCTTTGGG	*cpatg8*
cpatg8-LR	ATATCATCTTCTGTCGACCTGCA GGCCGGTGGTCGGTGAAAGTAGGGT	
cpatg8-RF	TCTTTCTAGAGGATCCCCGGGTACCGAT AGCGGGTGTTCGTTCTTCTGC	*cpatg8*
cpatg8-RR	GTCTCATGTCGCCGGGTACATG	
Δ*cpatg8*-com-F	CGAGAATTCCACTTGGGTACTGCTGGC	*cpatg8*
Δ*cpatg8*-com-R	TATGCGGCCGCGATTGACTCAAAGTCTC	
18S-F	TCTCGAATCGCATGGCCT	18S rRNA
18S-R	TTACCCGTTGTAACCACGGC	
cpatg1-F	TCCACAACCTGTGCCATCCACTTCA	*cpatg1*
cpatg1-R	TTGTCGACCACGACATAGTCACGCT	
cpatg3-F	GGCCTCGGTGCACCCTTGCA	*cpatg3*
cpatg3-R	ATGAACTTGAGGAACACCAC	
cpatg4-F	CGCTCGACAAGAACGTGAGA	*cpatg4*
cpatg4-R	GTATCAGTGTTGGATGGAATG	
cpatg7-F	GCGTCGACAACAGGGAATA	*cpatg7*
cpatg7-R	AGAGACGAAGCGGTCCTCCTC	
cpatg8-F	ATCCAAGTTCAAGGATGAGC	*cpatg8*
cpatg8-R	AGATGGCCTTGTCGGGGGAC	
cpatg18-F	CTCGTCACCGCGTGCGAATCG	*cpatg18*
cpatg18-R	ACCGCTCTGTCTCCGATTTG	
cpatg33-F	ACAACAGTCCCGCAAGGACCGC	*cpatg33*
cpatg33-R	TGCTTCTTGAGGAAGTCCTCG	
p29-F	ATAGCGGCCGCATGGCTCAATTAAG AAAACCC	p29
p29-R	ATAGTTAACTTAGCCAATCCGGGCAA GGGGATC	

Gene Manipulation

Gene cloning, PCR, and Southern analysis were performed according to Sambrook and Russell (2001). Primers used were synthesized by Sangon Biotech Co., Ltd. (Shanghai, China) and listed in **Table 1**.

Construction and Complementation of *cpatg8* Null Mutants

cpatg8 null mutants were constructed by homologous recombination. Briefly, a fragment containing a hygromycin-resistant gene *hph* in place of the *cpatg8* coding region that was flanked with *cpatg8* sequences was generated by PCR. This fragment was introduced into DK80 spheroplasts *via* the PEG-mediated transformation protocol. Putative *cpatg8* disruptants were screened by PCR, selected for nuclear homogeneity by single-spore isolation, and further verified by Southern blot analysis. Confirmed transformants were designated as Δ*cpatg8* strains. A 2.55 kb genomic fragment with *Eco*RI and *Not*I containing the complete *cpatg8* transcript region

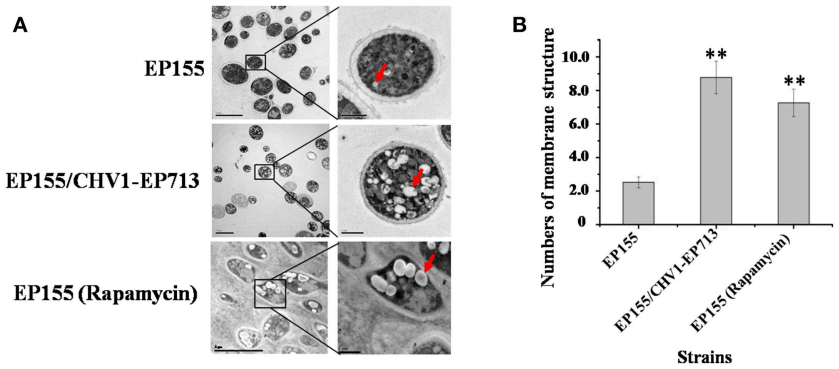

FIGURE 1 | Hypovirus infection and rapamycin treatment resulted in the accumulation of autophagosome-like vesicle. **(A)** Transmission electron micrographs of the hyphae. The hypha morphology of EP155 and EP155/CHV1-EP713 did not show apparent distinction. However, the intracellular structure of EP155/CHV1-EP713 showed much more membrane structures. Arrow indicates autophagosome-like vesicle. **(B)** The quantification of the average number of autophagosome-like vesicles per cell and a minimum of 20 cells were counted. Rapamycin-treated EM graphs (14 days on rapamycin-supplemented PDA plate). ** indicates $P < 0.001$, determined by Student's *t*-test.

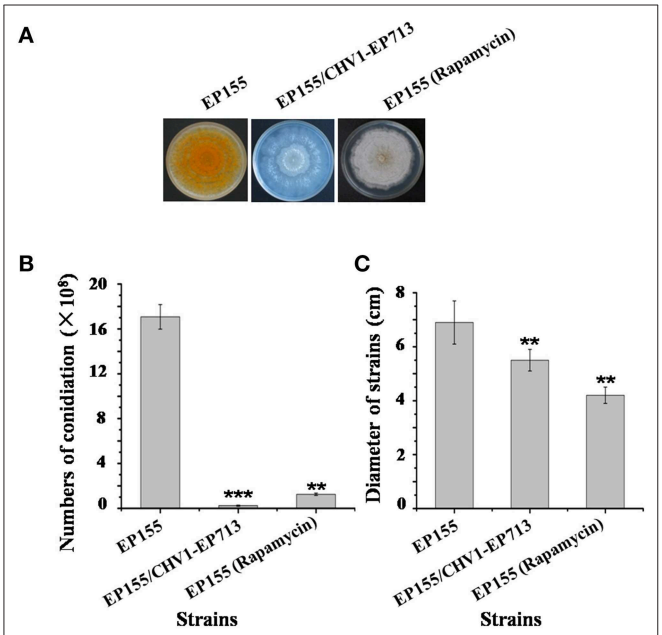

FIGURE 2 | Sporulation level and growth rates of hypovirus infection and rapamycin treatment on *C. parasitica.* **(A)** Phenotypes on PDA. Photo was taken at day 7. **(B)** Sporulation level. Spores were counted on day 14. **(C)** Growth rates of EP155, EP155/CHV1-EP713, and EP155 (rapamycin treatment, 60 nM) Growth rate was measured from cultures grown on PDA for 7 days. Values are means ± S.E.M of three independent experiments. ** indicates $P < 0.01$ and *** indicates $P < 0.001$, determined by Student's *t*-test.

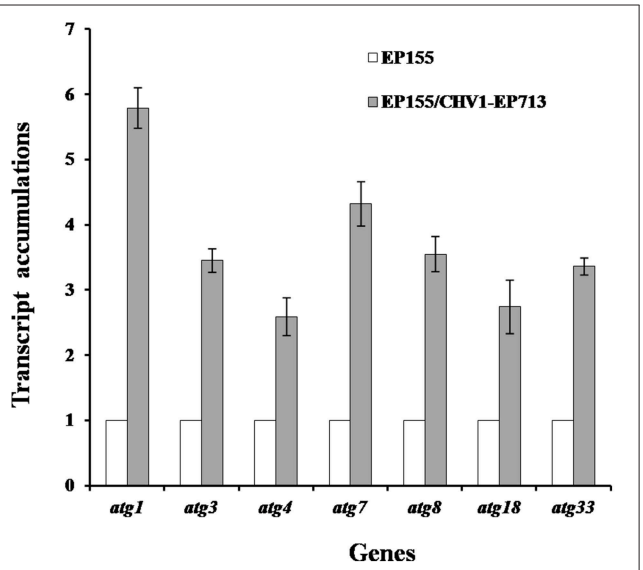

FIGURE 3 | Transcript accumulation levels of autophagy-related genes. The transcript accumulation level for each of the target genes in EP155 was set at 1.0, and the corresponding levels in EP155/CHV1-EP713 were expressed as a percentage of that of EP155. Values were calculated from three biological repeats. Bars indicate mean deviations.

(0.69 kb), promoter region (1.20 kb), and terminator region (0.66 kb) was amplified by PCR and then inserted into the transformation vector pCPXG418 to generate the construct pCPXG418-*cpatg8.* Complemented strains were constructed by transforming Δ*cpatg8* spheroplasts with pCPXG418-*cpatg8* and the complemented transformants were validated by PCR and Southern blot.

Construction of GFP-Labeled CpATG8 and RFP-Labeled p29 Strains

GFP-CpATG8 fusion plasmid (pCPXG418-GFP-*cpatg8*) was constructed as described (Shi et al., 2014). CpATG8 encoding region sequence was amplified and cloned into the pCPXG418-GFP to construct pCPXG418-GFP-*cpatg8.* Likewise, the virus-encoded protein p29 encoding region sequence was amplified by PCR with primer pair *p29*-F/R (**Table 1**) and cloned into the pCPXHY2-RFP to generate the recombinant plasmids pCPXHY2-RFP-p29. Subsequently, these two recombinant plasmids were transformed into the protoplasts of the wild-type

strain EP155, respectively. The expression of GFP and RFP was observed using an Olympus BX51 fluorescence microscope.

Electron Microscopy

For scanning electron microscopy, fungal samples (2 × 4 mm) were prepared after 5 days of cultivation on PDA. Samples were fixed in 2% (v/v) glutaraldehyde in 0.2 M phosphate buffer (pH 6.8) at 4°C for 4–6 h and then washed with the same buffer for 2 h. The samples were dehydrated in a graded acetone series (30, 50, 70, 80, 90, and 100%) with each grade kept for 30 min and three times in 100% acetone. Finally, the fully dehydrated samples were dried in a Critical Point Dryer (HCP-2, Hitachi), mounted on stubs, and then coated with gold about 200 nm in thickness in a Sputter Coater (S-3400N, Hitachi). The coated specimens were observed with a SEM HV (S-3400N, Hitachi) at 10 kV.

For transmission electron microscopy, hyphae cultivated on PDA medium for 7 days were scraped with a clean scalpel and washed three times with sterilized distilled water, fixed with 2.5% glutaraldehyde in 0.1 M phosphate buffer (pH 7.2) at 4°C overnight, rinsed three times with phosphate buffer (50 mM, pH6.8), and post-fixed overnight in 1% osmium tetroxide in 0.1 M cacodylate buffer (pH 7.0) at 4°C for 2 h. After rinsing with phosphate buffer, the samples were dehydrated in a gradient ethanol series and embedded in Epon 812 resin. The ultrathin sections were stained in 2% uranium acetate followed by lead citrate and visualized under a transmission electron microscope (Hitachi, H-7650) operating at 80 kV.

Quantification of Gene Transcripts and Viral dsRNA

The relative accumulation of gene transcripts in the strain DK80 and Δ*cpatg8* was measured using quantitative real-time RT-PCR as previously described (Shi et al., 2014). Total cDNA was synthesized using an amount of 4 μg of RNA with appropriate gene-specific primers (**Table 1**). The real-time PCR was performed in a LightCycler 480 (Roche Applied Science)

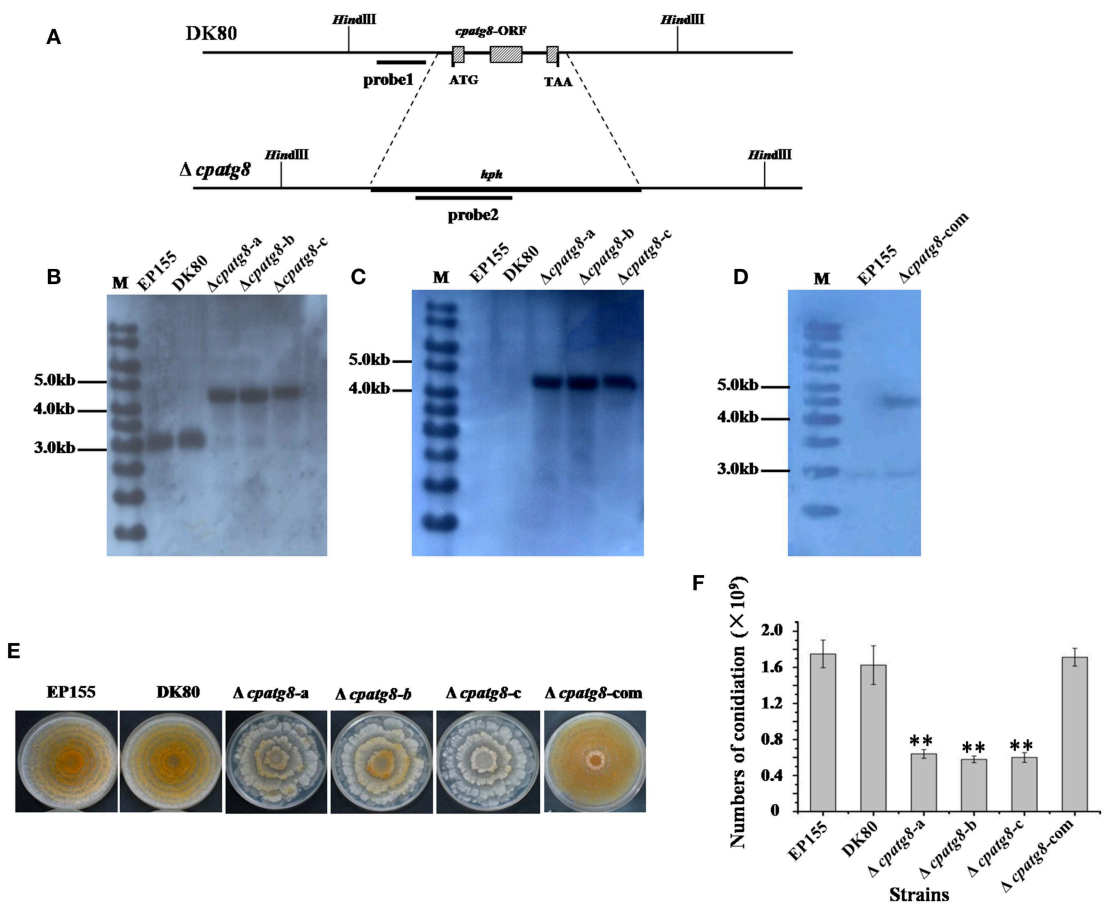

FIGURE 4 | Phenotypes and Southern analysis of *cpatg8* knockout mutants. **(A)** Diagram of *cpatg8* gene replacement strategy; probe fragment on the left arm was used in the Southern blot analysis to distinguish the fragment size of the wild-type strain and *cpatg8* null mutants; Southern analysis of the *cpatg8* null mutants **(B,C)** and complementary strain **(D)**. Fungal total DNAs were digested with *Hind* III and separated on a 0.8% agarose gel by electrophoresis, and blotted using probe 1 **(B)** and probe 2 **(C)**, respectively. Fragment sizes are indicated in the figure margins. **(E)** Mutant colony morphologies on PDA plates. Fungal strains were cultured on the laboratory bench top condition at 24°C, and the photograph was taken on day 14 postinoculation. **(F)** Sporulation level of *cpatg8* knockout mutants. Spores were counted on day 14. Values are means ± S.E.M of three independent experiments. ** indicates $P < 0.01$, determined by Student's *t*-test.

and normalized against that of 18S rRNA. The viral dsRNA accumulation level was examined using the method described previously (Lin et al., 2007). RNA samples stained with ethidium bromide were scanned using a Typhoon 9410 phosphorimager (GE Healthcare Life Sciences). To quantify the relative amount of large and medium dsRNA, the scanned gel image analysis was performed by ImageQuant TL-1D gel analysis software. 18S rRNA was used as the normalization reference.

Virulence Assays

Virulence was tested on dormant stems of Chinese chestnut (*Castanea mollissima*) with five replicates per fungal strain as previously described (Yao et al., 2013). The inoculated stems were kept at room temperature in a plastic bag to maintain moisture for 4 weeks. After incubation for 4 weeks, canker sizes were measured and the results were subjected to statistical analysis using the PROCGLM procedure (SAS, version 8.0). The type I error rate was set at $P < 0.05$.

RESULTS

Hypovirus Infection Promotes Autophagy in *C. parasitica*

Previous studies showed that CHV1-EP713 and virus-encoded protein p29 were presented in vesicles (Dodds, 1980; Jacob-Wilk et al., 2006; Wang et al., 2013). We used an electron microscope to compare the subcellular structure of the wild-type strain EP155 and virus-infected strain EP155/CHV1-EP713 and found that the number of vesicles was increased in the cytoplasm by more than 3-fold following virus infection (**Figure 1**).

Rapamycin can induce autophagy (Klionsky et al., 2016). EP155 treated with rapamycin resulted in a similar increase in vesicle numbers (**Figure 1**). Moreover, rapamycin-induced EP155 exhibited the phenotype similar to that of EP155/CHV-1EP713, including decreased sporulation, growth, and pigment production (**Figure 2**). To understand whether the autophagy pathway could be induced upon CHV1-EP713 infection, qRT-PCR was performed to compare transcripts of autophagy-related genes. Results showed that expression of *cpatg1*, *cpatg3*, *cpatg4*, *cpatg7*, *cpatg8*, *cpatg18*, and *cpatg33* was significantly up-regulated ($P < 0.05$) by 5.79-, 3.45-, 2.59-, 4.32-, 3.55-, 2.74-, and 3.36-fold, respectively (**Figure 3**). Thus, it was concluded that virus infection stimulated autophagy in *C. parasitica*.

cpatg8 Is Essential for Autophagy in *C. parasitica*

The putative *atg8* homolog was inspected against the *C. parasitica* genome database (http://genome.jgi-psf.org/cgi-bin/dispGeneModel?db=Crypa2&id=102797). The coding region of the *cpatg8* gene is composed of three exons with 124 amino acid residues and two introns of 314 bp. The deduced

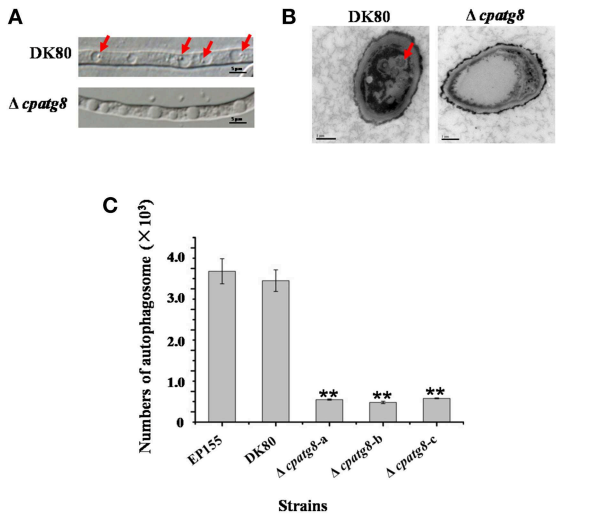

FIGURE 5 | Electron micrographs of the hyphae of strain DK80 and Δ*cpatg8* mutant. **(A)** Autophagy in the aerial hyphae of *C. parasitica*. Autophagic bodies in the vacuoles of the aerial hyphae of the strain DK80 and Δ*cpatg8* mutant grown on plates of PDA were examined using differential interference microscopy. **(B)** Autophagy was blocked in Δ*cpatg8* mutant. Vacuoles in the hyphae of the parental strain DK80 and Δ*cpatg8* mutant were observed using an electron microscope after being cultured in EP liquid media in the presence of 2 mM PMSF for 4 h (bar, 0.5 μm). **(C)** The quantification of the number of autophagic bodies. Arrow indicates autophagic body (bar, 5 μm). Values are means ± S.E.M of three independent experiments. ** indicates $P < 0.01$, determined by Student's *t*-test.

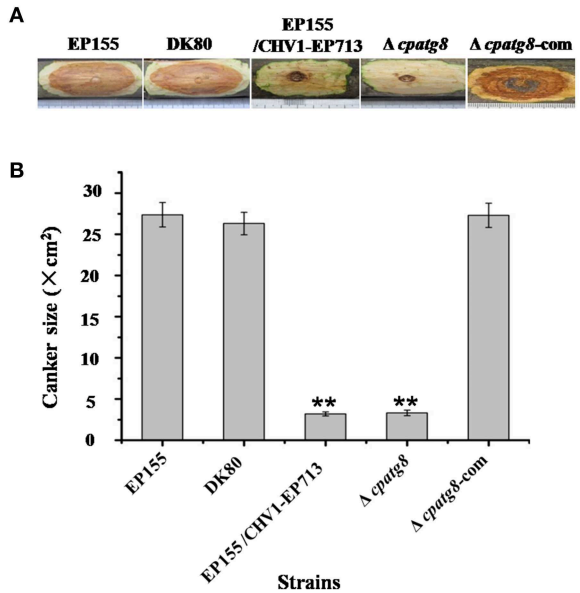

FIGURE 6 | Virulence assay on chestnut stems. **(A)** Cankers induced by the tested strains. The wild-type (EP155), starting (DK80), and hypovirus-infected (DK80/CHV1-EP713) strains and *cpatg8*-deleted (Δ*cpatg8*) and *cpatg8*-complemented (Δ*cpatg8*-com) mutants were inoculated onto Chinese chestnut (*C. mollissima* Blume) stems. The inoculated stems were kept at 24°C and cankers were measured and photographed on day 28 postinoculation. **(B)** Canker size measurements of the tested strains. The assays were with five duplicates for each strain. Values are means ± SEM of three independent experiments. ** indicates $P < 0.01$, determined by Student's *t*-test.

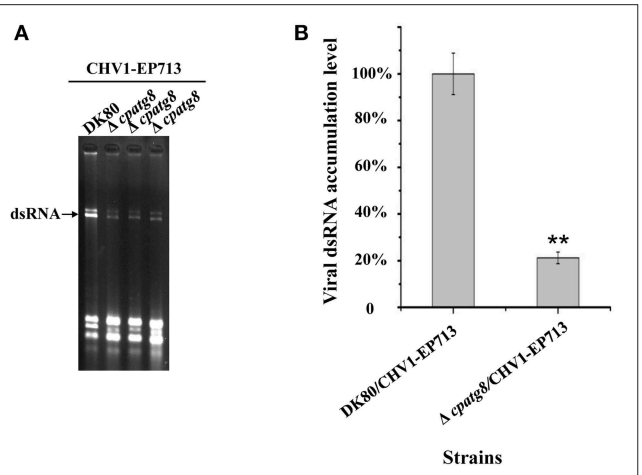

FIGURE 7 | Quantification of viral dsRNA in Δ*cpatg8* mutant transfectants. All transfectants were in the DK80 genetic background. **(A)** Agarose gel electrophoretic analysis of viral dsRNA. Ten micrograms of total RNA from virus-infected hosts was loaded into each lane in a 1.0% agarose gel. Lane 1, DK80/CHV1-EP713; lane 2 to lane 4, Δ*cpatg8* mutant transfectants with CHV1-EP713. The arrow indicates the position of viral dsRNA. **(B)** Semi-quantification of viral dsRNA from different transfectants. The viral dsRNA level of EP155/CHV1-EP713 was set at 100%, and levels of Δ*cpatg8* mutant transfectants were expressed as percentages of that of CHV1-EP713. Values are means ± S.E.M of three independent experiments. ** indicates $P < 0.01$, determined by Student's *t*-test.

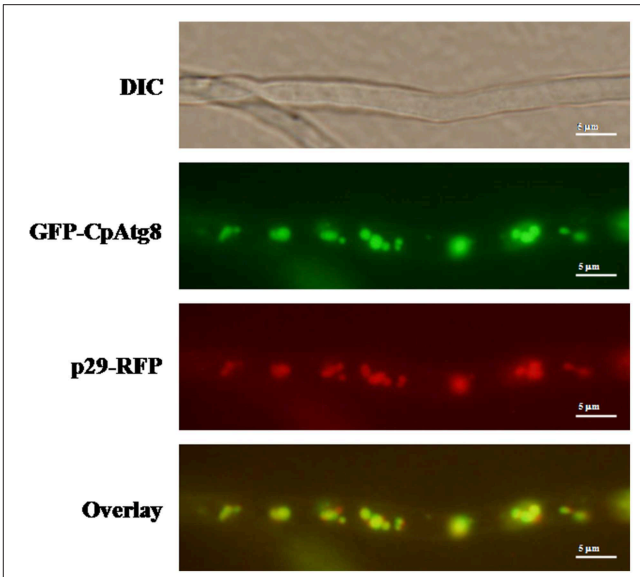

FIGURE 8 | Localization of p29-RFP and GFP-CpATG8 under normal growth conditions. The strain expressing p29-RFP and GFP-CpATG8 was grown on PDA medium. After 7 days, hyphae were observed by DIC and fluorescence microscopy. Scale bars, 5 μm.

CpATG8 protein showed a high level of homology (94–97% amino acid identity) compared to those of *Magnaporthe oryzae*, *Neurospora crassa*, *Pichia pastoris*, and *Aspergillus nidulans*, with *Chaetomium thermophilum* and *M. oryzae* being the highest at 97% and *A. nidulans* being the lowest at 94% (**Figure S1**).

To investigate the functions of the *cpatg8* gene, *cpatg8* disruption mutants were constructed *via* homologous recombination with a hygromycin-B-resistant cassette (**Figure 4A**). Three randomly selected single-spore-derived transformants were screened by PCR and further confirmed by Southern blot analysis (**Figures 4B–D**). The conidiation level of the Δ*cpatg8* was drastically reduced and aerial hyphae were significantly less than those of the parent strain DK80 and wild-type strain EP155 (**Figures 4E,F**). As shown in **Figure 4E**, the day–night growth patterns of Δ*cpatg8* were different from its parental or the wild-type strain. The abnormal phenotype of the mutants could be fully restored by reintroducing a wild-type copy of *cpatg8* (**Figure 4E**), suggesting that *cpatg8* is solely responsible for the altered phenotype.

Using differential interference microscopy and transmission electron microscopy, we examined changes in the process of autophagy stabilized by addition of phenylmethylsulfonylfluoride (PMSF) (Klionsky et al., 2016) in the Δ*cpatg8* mutants and DK80 by differential interference microscopy. Only 8.08 ± 2.35% of the vacuoles had autophagic bodies in the Δ*cpatg8* mutants, whereas it was 79.13 ± 8.21% in DK80, when cultured in EP liquid medium in the presence of 2 mM PMSF for 4 h (**Figures 5A,C**). Autophagic bodies in vacuoles of the strain DK80 were seen by transmission electron microscopy, but not in the *cpatg8* mutant (**Figure 5B**), suggesting that *cpatg8* is a gene essential for autophagy in *C. parasitica*.

Deletion of *cpatg8* Attenuates *C. parasitica* Virulence and Reduces Accumulation of the Hypovirus RNA

EP155 and parental strain DK80 were highly virulent and incited large cankers on chestnut stems, whereas Δ*cpatg8* caused very small cankers, similar to those of EP155/CHV1-EP713. Virulence of the Δ*cpatg8* mutant could be fully restored following reintroduction of the wild-type cpatg8 gene (**Figure 6**).

atg8 is known to be a key gene of autophagy that functions at different stages of the autophagy pathway (Klionsky et al., 2016). To conclusively establish whether autophagy was required for replication of CHV1-EP713, Δ*cpatg8* was paired with hypovirus-infected strain EP155/CHV1-EP713. While the converted Δ*cpatg8* colonies showed viral-infected phenotypes of reduced conidiation and loss of pigmentation, the accumulation level of the viral dsRNA was significantly reduced (**Figure 7**), demonstrating that *cpatg8* plays an important role in CHV1-EP713 replication.

Viral Protein p29 Co-localizes With CpATG8

ATG8 has been used as a marker for autophagy-related structures in a wide range of eukaryotes (Pollack et al., 2009; Voigt and Pöggeler, 2013a; Yin et al., 2016). By co-expression of GFP-CpATG8 and viral p29-RFP in EP155, it was observed that these two proteins co-localized in the vesicles of the cell (**Figure 8**), likely in the autophagosomes.

DISCUSSION

Autophagy is an evolutionarily conserved biological process found in eukaryotic cells involved in recycling processes. Autophagy can be measured by using fluorescent marker-tagged Atg8 and be inhibited by deletion of autophagy-related genes (Veneault-Fourrey et al., 2006; Duan et al., 2013; Sumita et al., 2017; Ren et al., 2018). Consistently, loss of *cpatg8* leads to the inhibited autophagy in *C. parasitica* (**Figure 4**), suggesting that *cpatg8* is essential for autophagy in this fungus.

Disruption of *atg8* has been reported to result in reduced conidiation, impaired aerial mycelial growth, and attenuated virulence in several pathogenic fungi. In the rice blast fungus *M. oryzae*, it was shown that autophagy was necessary for the blast disease (Kershaw and Talbot, 2009). Disruption of *MgATG8* resulted in autophagy-arrested conidial cell death and loss of virulence (Veneault-Fourrey et al., 2006; Liu et al., 2010). In the corn smut fungus *Ustilago maydis*, autophagy was required for pathogenicity (Nadal and Gold, 2010). In *Botrytis cinerea*, *BcATG8* is essential for autophagy to regulate fungal development and pathogenesis, and deletion of *BcATG8* blocked autophagy and significantly impaired aerial hyphal growth, reproductive development, and virulence (Ren et al., 2018). In this regard, our current study was in accordance with the previous findings that ATG8 is required for conidiation and virulence.

Induction of autophagy and exploitation of components of autophagy pathway in favor of viral replication and spread have been reported for many RNA and DNA viruses. For example, HIV blocks the formation of mature autolysosomes in macrophages and exploits the autophagic component during early stages in replication (Kyei et al., 2009). Poliovirus uses autophagy components for genome replication, while dengue and Zika viruses use autophagy components for post-replication processes (Abernathy et al., 2019). In our study, accumulation of autophagosome-like vesicle was found in both CHV1-EP713-infected and rapamycin-treated strains (**Figure 1**), and genes involved in autophagy were up-regulated in hypovirus-infected strain (**Figure 3**), suggesting that hypovirus may induce and exploit autophagy for its genome replication. Reduced accumulation of hypoviral dsRNA in cpatg8 null mutant (**Figure 7**) further supports this assumption. As a matter of fact, it has been reported that hypovirus infection induces proliferation of the vesicle in *C. parasitica* (Dodds, 1980; Wang et al., 2013) and hypovirus dsRNA and viral encoded p29 had been found to co-fractionate with a trans-Golgi network-derived membrane (Jacob-Wilk et al., 2006), implying that the hypovirus may be trafficked by the vesicles.

The hypovirus-encoded p29 is a multifunctional protein involved in virus replication, suppression of host RNA interference system, post-transcription modification, sporulation, host symptom development, and virulence (Choi et al., 1991; Suzuki et al., 2003; Andika et al., 2019). Our studies also showed hypovirus CHV1-EP713 protein p29-RFP co-localized with GFP-CpATG8. Whether p29 is involved in the process of autophagosome fusion with lysosomes remains to be determined.

AUTHOR CONTRIBUTIONS

LS carried out the experiment and helped to drafted the manuscript. JW participated in the culture of fungal strains, data analysis, and helped to draft the manuscript. RQ and FY participated in the culture of fungal strains and data analysis. JS designed and supervised the experiment and drafted the manuscript. BC designed and supervised the experiment and revised the manuscript.

FUNDING

This work was supported in part by grants from the National Natural Science Foundation of China (30960018 and 31170137) and the Natural Science Foundation of Guangxi Province (2012GXNSFAA053044).

SUPPLEMENTARY MATERIAL

The Supplementary Material for this article can be found online at: https://www.frontiersin.org/articles/10.3389/fcimb.2019.00222/full#supplementary-material

REFERENCES

Abernathy, E., Mateo, R., Majzoub, K., van Buuren, N., Bird, S. W., Carette, J. E., et al. (2019). Differential and convergent utilization of autophagy components by positive-strand RNA viruses. *PLoS Biol.* 17:e2006926. doi: 10.1371/journal.pbio.2006926

Andika, I. B., Kondo, H., and Suzuki, N. (2019). Dicer functions transcriptionally and posttranscriptionally in a multilayer antiviral defense. *Proc. Natl. Acad. Sci. U S A.* 116, 2274–2281. doi: 10.1073/pnas.1812407116

Bartoszewska, M., and Kiel, J. A. (2011). The role of macroautophagy in development of filamentous fungi. *Antioxid. Redox Signal.* 14, 2271–2287. doi: 10.1089/ars.2010.3528

Chen, M. M., Jiang, M., Shang, J., Lan, X., Yang, F., Huang, J., et al. (2011). CYP1, a hypovirus-regulated cyclophilin, is required for virulence in the chestnut blight fungus. *Mol. Plant Pathol.* 12, 239–246. doi: 10.1111/j.1364-3703.2010.00665.x

Chen, Y., Chen, Q., Li, M., Mao, Q., Chen, H., Wu, W., et al. (2017). Autophagy pathway induced by a plant virus facilitates viral spread and transmission by its insect vector. *PLoS Pathog.* 13:e1006727. doi: 10.1371/journal.ppat.1006727

Choi, G. H., Dawe, A. L., Churbanov, A., Smith, M. L., Milgroom, M. G., and Nuss, D. L. (2012). Molecular characterization of vegetative incompatibility genes that restrict hypovirus transmission in the chestnut blight fungus *Cryphonectria parasitica*. *Genetics* 190, 113–127. doi: 10.1534/genetics.111.133983

Choi, G. H., Pawlyk, D. M., and Nuss, D. L. (1991). The autocatalytic protease p29 encoded by a hypovirulence-associated virus of the chestnut blight fungus resembles the potyvirus-encoded protease HC-Pro. *Virology* 183, 747–752. doi: 10.1016/0042-6822(91)91004-Z

Clavel, M., Michaeli, S., and Genschik, P. (2017). Autophagy: a double-edged sword to fight plant viruses. *Trends Plant Sci.* 22, 646–648. doi: 10.1016/j.tplants.2017.06.007

Dagdas, Y. F., Belhaj, K., Maqbool, A., Chaparro-Garcia, A., Pandey, P., Petre, B., et al. (2016). An effector of the Irish potato famine pathogen antagonizes a host autophagy cargo receptor. *Elife* 5:e10856. doi: 10.7554/eLife.10856

Dawe, A. L., and Nuss, D. L. (2001). Hypoviruses and chestnut blight: exploiting viruses to understand and modulate fungal pathogenesis. *Annu. Rev. Genet.* 35, 1–29. doi: 10.1146/annurev.genet.35.102401.085929

Dodds, J. A. (1980). Association of type 1 viral-like dsRNA with club-shaped particles in hypovirulent strains of *Endothia parasitica*. *Virology* 107, 1–12. doi: 10.1016/0042-6822(80)90267-6

Dong, X., and Levine, B. (2013). Autophagy and viruses: adversaries or allies? *J. Innate Immun*. 5, 480–493. doi: 10.1159/000346388

Duan, Z., Chen, Y., Huang, W., Shang, Y., Chen, P., and Wang, C. (2013). Linkage of autophagy to fungal development, lipid storage and virulence in *Metarhizium robertsii*. *Autophagy* 9, 538–549. doi: 10.4161/auto.23575

Eusebio-Cope, A., Sun, L., Tanaka, T., Chiba, S., Kasahara, S., and Suzuki, N. (2015). The chestnut blight fungus for studies on virus/host and virus/virus interactions: from a natural to a model host. *Virology* 477, 164–175. doi: 10.1016/j.virol.2014.09.024

Hafrén, A., Macia, J. L., Love, A. J., Milner, J. J., Drucker, M., and Hofius, D. (2017). Selective autophagy limits cauliflower mosaic virus infection by NBR1-mediated targeting of viral capsid protein and particles. *Proc. Natl. Acad. Sci. U S A*. 114, E2026–E2035. doi: 10.1073/pnas.1610687114

Haxim, Y., Ismayil, A., Jia, Q., Wang, Y., Zheng, X., Chen, T., et al. (2017). Autophagy functions as an antiviral mechanism against geminiviruses in plants. *Elife* 6:e23897. doi: 10.7554/eLife.23897

Hayward, A. P., and Dinesh-Kumar, S. P. (2011). What can plant autophagy do for an innate immune response? *Annu. Rev. Phytopathol*. 49, 557–576. doi: 10.1146/annurev-phyto-072910-095333

Jacob-Wilk, D., Turina, M., and Van Alfen, N. K. (2006). Mycovirus cryphonectria hypovirus 1 elements cofractionate with trans-Golgi network membranes of the fungal host *Cryphonectria parasitica*. *J. Virol*. 80, 6588–6596. doi: 10.1128/JVI.02519-05

Josefsen, L., Droce, A., Sondergaard, T. E., Sørensen, J. L., Bormann, J., Schäfer, W., et al. (2012). Autophagy provides nutrients for nonassimilating fungal structures and is necessary for plant colonization but not for infection in the necrotrophic plant pathogen *Fusarium graminearum*. *Autophagy* 8, 326–337. doi: 10.4161/auto.18705

Kershaw, M. J., and Talbot, N. J. (2009). Genome-wide functional analysis reveals that infection-associated fungal autophagy is necessary for rice blast disease. *Proc. Natl. Acad. Sci. U S A*. 106, 15967–15972. doi: 10.1073/pnas.0901477106

Khan, I. A., Lu, J. P., Liu, X. H., Rehman, A., and Lin, F. C. (2012). Multifunction of autophagy-related genes in filamentous fungi. *Microbiol. Res*. 167, 339–345. doi: 10.1016/j.micres.2012.01.004

Klionsky, D. J., Abdelmohsen, K., Abe, A., Abedin, MJ., Abeliovich, H., Acevedo Arozena, A., et al. (2016). Guidelines for the use and interpretation of assays for monitoring autophagy (3rd edition). *Autophagy* 12, 1–222. doi: 10.1080/15548627.2015.1100356

Kyei, G. B., Dinkins, C., Davis, A. S., Roberts, E., Singh, S. B., Dong, C., et al. (2009). Autophagy pathway intersects with HIV-1 biosynthesis and regulates viral yields in macrophages. *J. Cell Biol*. 186, 255–268. doi: 10.1083/jcb.200903070

Lan, X., Yao, Z., Zhou, Y., Shang, J., Lin, H., Nuss, D. L., et al. (2008). Deletion of the cpku80 gene in the chestnut blight fungus, *Cryphonectria parasitica*, enhances gene disruption efficiency. *Curr. Genet*. 53, 59–66. doi: 10.1007/s00294-007-0162-x

Lin, H., Lan, X., Liao, H., Parsley, T. B., Nuss, D. L., and Chen, B. (2007). Genome sequence, full-length infectious cDNA clone, and mapping of viral double-stranded RNA accumulation determinant of hypovirus CHV1-EP721. *J. Virol*. 81, 1813–1820. doi: 10.1128/JVI.01625-06

Liu, T. B., Liu, X. H., Lu, J. P., Zhang, L., Min, H., and Lin, F. C. (2010). The cysteine protease MoAtg4 interacts with MoAtg8 and is required for differentiation and pathogenesis in *Magnaporthe oryzae*. *Autophagy* 6, 74–85. doi: 10.4161/auto.6.1.10438

Liu, X. H., Xu, F., Snyder, J. H., Shi, H. B., Lu, J. P., and Lin, F. C. (2016). Autophagy in plant pathogenic fungi. *Semin. Cell Dev. Biol*. 57, 128–137. doi: 10.1016/j.semcdb.2016.03.022

Nadal, M., and Gold, S. E. (2010). The autophagy genes ATG8 and ATG1 affect morphogenesis and pathogenicity in Ustilago maydis. *Mol. Plant Pathol*. 11, 463–478. doi: 10.1111/j.1364-3703.2010.00620.x

Nakatogawa, H., Ichimura, Y., and Ohsumi, Y. (2007). Atg8, a ubiquitin-like protein required for autophagosome formation, mediates membrane tethering and hemifusion. *Cell* 130, 165–178. doi: 10.1016/j.cell.2007.05.021

Nuss, D. L. (2005). Hypovirulence: mycoviruses at the fungal-plant interface. *Nat. Rev. Microbiol*. 3, 632–642. doi: 10.1038/nrmicro1206

Pollack, J. K., Harris, S. D., and Marten, M. R. (2009). Autophagy in filamentous fungi. *Fungal Genet. Biol*. 46, 1–8. doi: 10.1016/j.fgb.2008.10.010

Ren, W., Liu, N., Sang, C., Shi, D., Zhou, M., Chen, C., et al. (2018). The autophagy gene BcATG8 regulates the vegetative differentiation and pathogenicity of *Botrytis cinerea*. *Appl. Environ. Microbiol*. 84:e02455-17. doi: 10.1128/AEM.02455-17

Sambrook, J., and Russell, D. W. (2001). *Molecular Cloning: A Laboratory Manual*. New York, NY: Cold Spring Harbor press.

Shi, L., Li, R., Liao, S., Bai, L., Lu, Q., and Chen, B. (2014). Prb1, a subtilisin-like protease, is required for virulence and phenotypical traits in the chestnut blight fungus. *FEMS Microbiol. Lett*. 359, 26–33. doi: 10.1111/1574-6968.12547

Sumita, T., Izumitsu, K., and Tanaka, C. (2017). Characterization of the autophagy-related gene BmATG8 in *Bipolaris maydis*. *Fungal Biol*. 121, 785–797. doi: 10.1016/j.funbio.2017.05.008

Suzuki, K., Kirisako, T., Kamada, Y., Mizushima, N., Noda, T., and Ohsumi, Y. (2001). The pre-autophagosomal structure organized by concerted functions of APG genes is essential for autophagosome formation. *EMBO J*. 20, 5971–5981. doi: 10.1093/emboj/20.21.5971

Suzuki, N., Maruyama, K., Moriyama, M., and Nuss, D. L. (2003). Hypovirus papain-like protease p29 functions in trans to enhance viral double-stranded RNA accumulation and vertical transmission. *J. Virol*. 77, 11697–11707. doi: 10.1128/JVI.77.21.11697-11707.2003

Veneault-Fourrey, C., Barooah, M., Egan, M., Wakley, G., and Talbot, N. J. (2006). Autophagic fungal cell death is necessary for infection by the rice blast fungus. *Science* 312, 580–583. doi: 10.1126/science.1124550

Voigt, O., and Pöggeler, S. (2013a). Autophagy genes Smatg8 and Smatg4 are required for fruiting-body development, vegetative growth and ascospore germination in the filamentous ascomycete *Sordaria macrospora*. *Autophagy* 9, 33–49. doi: 10.4161/auto.22398

Voigt, O., and Pöggeler, S. (2013b). Self-eating to grow and kill: autophagy in filamentous ascomycetes. *Appl. Microbiol. Biotechnol*. 97, 9277–9290. doi: 10.1007/s00253-013-5221-2

Wang, J., Wang, F., Feng, Y., Mi, K., Chen, Q., Shang, J., et al. (2013). Comparative vesicle proteomics reveals selective regulation of protein expression in chestnut blight fungus by a hypovirus. *J. Proteomics* 78, 221–230. doi: 10.1016/j.jprot.2012.08.013

Yao, Z., Zou, C., Zhou, H., Wang, J., Lu, L., Li, Y., et al. (2013). Delta(1)-pyrroline-5-carboxylate/glutamate biogenesis is required for fungal virulence and sporulation. *PLoS ONE* 8:e73483. doi: 10.1371/journal.pone.0073483

Yin, Z., Pascual, C., and Klionsky, D. J. (2016). Autophagy: machinery and regulation. *Microb. Cell* 3, 588–596. doi: 10.15698/mic2016.12.546

Conflict of Interest Statement: The authors declare that the research was conducted in the absence of any commercial or financial relationships that could be construed as a potential conflict of interest.

frontiers in Cellular and Infection Microbiology

ORIGINAL RESEARCH
published: 11 July 2019
doi: 10.3389/fcimb.2019.00249

Detection and Molecular Characterization of Novel dsRNA Viruses Related to the *Totiviridae* Family in *Umbelopsis ramanniana*

*Tünde Kartali[1], Ildikó Nyilasi[1], Boglárka Szabó[1], Sándor Kocsubé[1], Roland Patai[2], Tamás F. Polgár[2], Gábor Nagy[3], Csaba Vágvölgyi[1] and Tamás Papp[1,3]**

[1] Department of Microbiology, Faculty of Science and Informatics, University of Szeged, Szeged, Hungary, [2] Biological Research Centre of the Hungarian Academy of Sciences, Institute of Biophysics, Szeged, Hungary, [3] MTA-SZTE Fungal Pathogenicity Mechanisms Research Group, Department of Microbiology, University of Szeged, Hungarian Academy of Sciences, Szeged, Hungary

OPEN ACCESS

Edited by:
Daohong Jiang,
Huazhong Agricultural University, China

Reviewed by:
Hiromitsu Moriyama,
Tokyo University of Agriculture and Technology, Japan
Jie Zhong,
Hunan Agricultural University, China

***Correspondence:**
Tamás Papp
pappt@bio.u-szeged.hu

Specialty section:
This article was submitted to Fungal Pathogenesis, a section of the journal Frontiers in Cellular and Infection Microbiology

Received: 27 February 2019
Accepted: 26 June 2019
Published: 11 July 2019

Citation:
Kartali T, Nyilasi I, Szabó B, Kocsubé S, Patai R, Polgár TF, Nagy G, Vágvölgyi C and Papp T (2019) Detection and Molecular Characterization of Novel dsRNA Viruses Related to the Totiviridae Family in Umbelopsis ramanniana. Front. Cell. Infect. Microbiol. 9:249. doi: 10.3389/fcimb.2019.00249

Umbelopsis ramanniana is an oleaginous fungus belonging to the Mucoromycotina subphylum. Our group had previously detected four double-stranded RNA (dsRNA) bands in the *U. ramanniana* NRRL 1296 strain by gel electrophoresis. Here we describe the molecular characterization of its dsRNA elements as well as the discovery of four novel dsRNA viruses: Umbelopsis ramanniana virus 1 (UrV1), Umbelopsis ramanniana virus 2 (UrV2), Umbelopsis ramanniana virus 3 (UrV3), and Umbelopsis ramanniana virus 4 (UrV4). Full genomes of UrV1, UrV3, and UrV4 were determined using the full-length amplification of cDNAs (FLAC) technique; they contain two open reading frames (ORF), which putatively encode the coat protein (CP) and the RNA dependent RNA polymerase (RdRp), respectively. In case of UrV2, a partial ORF encoding a partial RdRp gene could be determined. Based on the phylogeny inferred from the RdRp sequences, UrV1 and UrV4 belong to the genus *Totivirus*, while UrV2 may belong to the genus *Victorivirus.* UrV3 nested to a novel, unclassified group of *Totiviridae*, which is related to the genus *Totivirus*. Hybridization analysis revealed that the dsRNA molecules of UrV1 and UrV4 correspond to the same 5.0-kbp electrophoretic band, whilst the probe for the UrV3 hybridized to the largest, 5.3-kbp and the 3.0-kbp bands of the dsRNA pattern of *U. ramanniana*. Interestingly, the probe for the UrV2 sequence did not hybridized to any dsRNA bands, but it could be amplified from the isolated 3.0-kbp fragment. By transmission electron microscopy, two different isometric virus particles with about 50 and 35 nm in diameter were detected in *U. ramanniana* NRRL 1296 indicating that this strain harbor multiple viruses. Beside *U. ramanniana*, dsRNA elements were also detected in other *Umbelopsis* isolates with different patterns consisting of 2 to 4 discrete and different sized (0.7–5.3-kbp) dsRNA molecules. Based on a hybridization analysis with UrV1 CP and RdRp probes, the bands with the size of around 5.0-kbp, which were present in all tested *Umbelopsis* strains, are presumed as possible full mycovirus genomes.

Keywords: mycovirus, dsRNA, virus particle, *Totivirus*, *Victorivirus*, *Chrysoviridae*, Mucoromycotina

INTRODUCTION

Mycovirus research has achieved a significant advance in the last decades and viruses have been described in all major fungal phyla (Ghabrial et al., 2015; Son et al., 2015). Vast majority of the known mycoviruses have linear dsRNA genome but linear positive- and negative-sense single-stranded RNA (ssRNA) and circular ssDNA genomes has also been described from fungi (Hillman and Cai, 2013; Ghabrial et al., 2015). Mycoviruses with dsRNA genomes are currently classified into the families *Chryso-*, *Endorna-*, *Megabirna-*, *Quadri-*, *Partiti-*, *Reo-*, and *Totiviridae* (Ghabrial et al., 2015). Among them, *Totiviridae* is the most characterized group (Ghabrial, 1998; King et al., 2011). Members of this family have isometric virions, which contain a non-segmented, linear, uncapped dsRNA molecule (King et al., 2011). The size of the genome is between 4.6 and 7.0-kbp and consists of two, usually overlapping ORFs encoding the coat protein (CP) and the RNA dependent RNA polymerase (RdRp) (King et al., 2011). Within the *Totiviridae*, the genera *Giardiavirus*, *Leishmaniavirus*, *Trichomonasvirus*, *Totivirus,* and *Victorivirus* are discerned. Fungal viruses are generally found in the latter two genera (Ghabrial et al., 2015). The family *Chrysoviridae* is related to the *Totiviridae* and contains viruses with segmented genomes. The *Chrysoviridae* genome typically consists of four linear dsRNA segments (with 2.4–3.6-kbp in size) encoding the CP, the RdRp, and two proteins with an unknown function (Ghabrial, 2008).

Although presence of most mycoviruses proved to be asymptomatic in their hosts, an increasing number of data indicates that it can causes smaller or greater changes in the phenotype of their fungal host (Ghabrial, 1998; Ghabrial and Suzuki, 2009; Ghabrial et al., 2015). In some cases, presence of the mycoviruses can reduce or enhance the virulence of the fungal host causing hypo- or hypervirulence, respectively (Nuss, 2005; Ghabrial et al., 2015).

Basal fungi, especially the different groups of the former Zygomycota have remained among the least explored organisms in respect of virus harboring. According to the recently accepted taxonomy, majority of the most common species generally known as zygomycetes fungi belong to the subphylum Mucoromycotina (Spatafora et al., 2016). There is only sporadic information about mycoviruses in this group. DsRNA elements and isometric, non-enveloped virus-like particles (VLPs) about 30–40 nm in diameter were earlier detected in five *Mucor* and three *Rhizopus* species without further molecular studies or sequence information (Vágvölgyi et al., 1998; Papp et al., 2001). Recently, Vainio et al. (2017) detected the presence of viral RNA sequences in various zygomycetes strains from a forest habitat identified only as *Mucor*/Mucorales, *Mortierella*/*Umbelopsis,* and "other zygomycetes" and reported a bunya-type virus in Mucorales spp. named as Mucorales RNA virus 1 (MucRV1). In addition, a geminivirus-like ssDNA virus was described and characterized in *Mucor racemosus* (Hafez et al., 2013).

Umbelopsis species are oleaginous fungi, which are widespread in soil and frequently isolated from the rhizosphere (Takeda et al., 2014; Spatafora et al., 2016). They constitute the monogeneric family *Umbelopsidaceae* in the order Umbelopsidales, which forms Mucoromycotina, together with Mucorales and Endogonales (Spatafora et al., 2016). Several members of the genus were previously described or referred as *Mucor*, *Micromucor,* or *Mortierella* species (Meyer and Gams, 2003). Although no mycoviruses have hitherto been observed in the representatives of this genus, Vágvölgyi et al. (1993, 1998) had earlier reported the detection of four or five dsRNA bands in the *Umbelopsis ramanniana* (*Mucor ramannianus*) strain NRRL 1296 by gel electrophoresis. In the present study, detection of virus particles in this strain as well as sequencing and characterization of its dsRNA elements were carried out. A screening to detect the UrV1 or related viral sequences in other *Umbelopsis* isolates representing various species was also performed.

MATERIALS AND METHODS

Fungal Strains and Cultivation

Twenty-four strains representing 11 *Umbelopsis* species (see **Supplementary Table S1**) were tested for the presence of dsRNA molecules. The strains were maintained on malt extract agar slants (0.5% malt extract, 0.5% yeast extract, 1% glucose, 2% agar) at 4°C. Mycelia for virus particle and dsRNA purification were grown in yeast extract-glucose broth (1% glucose, 0.5% yeast extract) at 25°C for 3 days.

Isolation of dsRNA Molecules

To screen for the presence of dsRNA elements, a variation of the lithium chloride-based total nucleic acid extraction method of Leach et al. (1986) was used. Frozen mycelia (300 mg) were powdered under liquid nitrogen in a mortar and incubated in 700 µl ice-cold LETS buffer (0.1 M LiCl, 10 mM EDTA, 10 mM Tris-HCl, 0.5% SDS, pH 8.0) and 70 µl 10% SDS for 2 min at room temperature with continuous vortexing. The samples were then centrifuged at 17,000 × *g* for 15 min at 4°C. The supernatant was purified with phenol:chloroform:isoamyl alcohol (25:24:1) extraction twice and one extraction was done by chloroform:isoamyl alcohol (24:1). Then, nucleic acids were precipitated from the upper phase with two volumes of 96% ethanol and 10% sodium-acetate overnight at -70°C. After centrifugation of the samples at 17,000 × *g* for 20 min at 4°C, nucleic acids were washed with 75% ethanol and dried under vacuum, then resuspended in 100 µl AccuGene molecular biology water (Lonza).

CF-11 cellulose chromatography was used to purify dsRNA elements from total nucleic acid extracts purified with LETS buffer extraction. The purification was done according to the method of Morris and Dodds (1979) with minor modifications. After supplementing 100 µl of total nucleic acid extracts with 3 ml 16% ethanolic STE buffer (0.1 M NaCl, 0.05 M TrisHCl, 0.001 M EDTA, pH 8.0), 0.2 g CF-11 cellulose (Sigma-Aldrich) was added to the samples. These mixtures were carried up to a home-made column, which contained 0.2 g CF-11 cellulose and was previously washed with 5 ml 16% ethanol and 2% β-mercaptoethanol containing STE buffer. The samples were then percolated on the cellulose columns. The columns were washed with 5 ml 16% ethanol containing STE buffer for four

times, then dsRNA molecules were eluted from the cellulose column with 2 ml STE buffer. After ethanolic precipitation and centrifugation (17,000 × *g*, 20 min, 4°C), the samples were dried under vacuum and resuspended in 100 μl AccuGene molecular biology water (Lonza).

All dsRNA samples were separated by electrophoresis on 0.8% agarose/TAE (40 mM Tris/acetic acid, 1 mM EDTA, pH 7.6) horizontal gels. Nucleic acids were visualized by UV fluorescence after ethidium bromide (0.5 μg/ml) staining. The relative sizes of the dsRNA molecules were estimated using GeneRuler 1-kb DNA ladder (Thermo Scientific) as size standards. The nature of the detected dsRNA elements was confirmed by their resistance to DNase I (Thermo Scientific) and S1 nuclease (Thermo Scientific) digestions, which were carried out according to the recommendations of the manufacturers'.

Purification and Examination of the Virus Particles

Virus particles were purified from frozen mycelium according to the method of Lot et al. (1972). After the disruption of the mycelium under liquid nitrogen in a mortar with pestle, it was extracted with 25 ml citrate buffer (0.5 M trisodium citrate, 1 mM disodium EDTA, pH 6.5), 40 μl chloroform and 120 μl sodium thioglycolate. This solution was centrifuged (9,000 rpm, 30 min, 4°C) and the aqueous phase was supplemented with 10% polyethylene glycol 6,000 (VWR) and 0.5 M sodium chloride and then incubated for overnight at 4°C. After a centrifugation (10,000 rpm, 30 min, 4°C), the pellets were resuspended in 10 ml borate buffer (5 mM boric acid, 1.475 mM sodium tetraborate, 0.5 mM EDTA) and 300 μl Triton X-100 (Sigma-Aldrich) and incubated for 30 min at room temperature. After a subsequent centrifugation (12,000 rpm, 15 min, 4°C), the virus particles were recovered by pelleting them from the supernatant with an ultracentrifugation at 78,000 × *g* for 10 h at 4°C. Finally, the pellet was resuspended in 120 μl borate buffer.

Purified virus particles were analyzed with transmission electron microscopy. Samples were evaluated under a JEM-1400 Flash transmission electron microscope (JEOL) to identify the morphological characteristics of the particles. To obtain the negatively stained samples, 10 μl of the virus particle extract was mounted on a formvar-coated 150-mesh copper grid (Electron Microscopy Sciences). After 5 min, the excessive fluid was blotted away with the edge of a filter paper and the samples were contrasted with 10 μl 2% uranyl acetate (Electron Microscopy Sciences) in 50% ethanol for 5 min (3 times). After the removal of the excessive staining solution, samples were dried under a Petri dish for 2 h before the electron microscopic evaluation. Negatively stained samples were systematically screened at 30,000 × magnification to localize the presence of the virus particles on the grid. Afterwards, the particles were recorded at 40,000–60,000 × magnification with a 16 MP Matataki Flash scientific complementary metal–oxide–semiconductor (sCMOS) camera (JEOL).

cDNA Synthesis and Sequencing of the dsRNA Molecules

For the synthesis and amplification of cDNAs from the dsRNA templates the "Full-length amplification of cDNAs" (FLAC) technique (Maan et al., 2007) was used. Purification of the dsRNA fragments was performed with the RNaid kit (MP Biomedicals). Ligation of the PC3-T7 loop primer (5'-p-GGATCCCGGGAATTCGGTAATACGACTCACTATATTTTT ATAGTGAGTCGTATTA-OH-3'; Potgieter et al., 2009) to the purified dsRNA fragments, the denaturation of the primer-ligated dsRNAs and cDNA synthesis reaction were performed as described by Darissa et al. (2010). Amplification of the cDNA was performed using 1.25 μM PC2 primer (5'-CCGAATTCCCGGGATCC-3'; Potgieter et al., 2009) and 2.5 units of the Phusion High-Fidelity DNA Polymerase (Thermo Scientific). The PCR was incubated in a MJ Mini 48-Well Personal Thermal Cycler (Bio-Rad) at 72°C for 2 min and 98°C for 1 min, followed by 35 cycles of 98°C for 10 s, 66°C for 30 s and 72°C for 4 min, and a final elongation at 72°C for 10 min. PCR products were purified from the agarose gel with the Zymoclean Large Fragment DNA Recovery Kit (Zymo Research). Purified products were then cloned into the pJET1.2/Blunt vector (CloneJET PCR Cloning Kit, Thermo Scientific). Sequences of the inserts were determined by the LGC Genomics (Germany). The sequences were then subjected to BLAST searches (http://blast.ncbi.nlm.nih.gov/Blast.cgi) in the nucleic acid and protein databases of the National Center for Biotechnology Information (NCBI). The identified sequences were deposited to European Nucleotide Archive (ENA; accession numbers: LR216267-LR216269 and LR595925-LR595928). All sequences are also presented in **Supplementary Data S1**.

Hybridization Studies

For hybridization, dsRNAs and control plasmids were separated by electrophoresis on 1.0% agarose/TAE (40 mM Tris/acetic acid, 1 mM EDTA, pH 7.6) horizontal gels. The relative sizes of the dsRNA molecules were estimated using DIG-labeled DNA Molecular Weight Marker VII (Roche) as size standards. After gel electrophoresis, gel was divided, since dsRNA and DNA samples were denatured under different conditions. Accordingly, dsRNAs were denatured in 0.05 M sodium hydroxide and 0.15 M sodium chloride buffer for 30 min and neutralized in 1 M Tris-hydrochloride and 1.5 M sodium chloride buffer (pH 7.5) for 2 × 20 min as described by Hong et al. (1998). DNA samples (i.e., the control plasmids) were denatured in 0.5 M sodium hydroxide and 1.5 M sodium chloride buffer and neutralized in 0.5 M Tris and 1.5 M sodium chloride buffer (pH 7.5). Gel slides were blotted onto a positively-charged nylon membrane (Amersham Hybond-N+, GE Healthcare) with 2 × SSC buffer. Samples were allowed to dry at room temperature and immobilized with UV-crosslinking. Blots were hybridized with the UrV1 CP and RdRp, UrV2 RdRp, UrV3 RdRp, UrV4 CP, and UrV4 RdRp gene probes in hybridization buffer (0.9 M sodium chloride, 1% SDS, 10% dextran sulfate) containing 5 μg/ml salmon sperm DNA (Invitrogen). Probes were prepared by PCR from DNA

TABLE 1 | The dsRNA patterns of the mycovirus-harboring *Umbelopsis* isolates.

Species name	Collection number	Substrate/ Origin	dsRNA size (kb)
Umbelopsis ramanniana	NRRL 1296	–/Wisconsin, USA	5.3; 5.0; 3.0; 2.8
Umbelopsis gibberispora	CBS 109328	*Fagus crenata*/Japan	5.0; 4.0; 0.7
Umbelopsis angularis	CBS 603.68	Soil/Baarn, Netherlands	5.0; 4.0
Umbelopsis dimorpha	CBS 110039	Soil/New Zealand	5.0; 4.0; 2.8
Umbelopsis versiformis	CBS 473.74	Soil/Victoria, Australia	5.0; 0.9

templates in the presence of digoxigenin-UTP (DIG DNA Labeling Mix, Roche) using DreamTaq polymerase (Thermo Scientific). Primers used to amplify the probes are listed in the **Supplementary Table S2**. Hybridization was followed by immunological detection using alkaline phosphatase-conjugated anti-digoxigenin antibody (Roche). Reactions for detection were carried out according to the manufacturer's instructions (Roche).

Sequence and Phylogenetic Analysis

Representative sequences of the families *Totiviridae*, *Chrysoviridae,* and *Partitiviridae* were obtained from the viruSite (http://www.virusite.org/index.php; Stano et al., 2016). The corresponding accession numbers are indicated on the tree. The dataset was supplemented by homologous hits of *U. ramanniana* RdRp sequences derived from BLAST (https://blast.ncbi.nlm.nih.gov/Blast.cgi) search. Multiple sequence alignment was carried out by MAFFT v7.312 using the E-INS-i option (Katoh and Standley, 2013) (for the alignment see **Supplementary Data S2**). Maximum Likelihood (ML) analysis was conducted by RAxML v8.121 (Stamatakis, 2014) using the WAG model with GAMMA rate heterogeneity and statistical support of the results was obtained by 500 thorough bootstrap replicates. Alternatively, phylogeny was also reconstructed with the Neighbor Joining (NJ) method using 500 bootstrap replicates. Sequences of the whole ITS region of *Umbelopsis* isolates were aligned using MAFFT v7.312 with the E-INS-i iterative refinement method. NCBI accession numbers for the involved sequences are available in the **Supplementary Table S1**. The ITS region of *Mortierella polycephala* (NCBI accession no.: HQ630335) was used as an outgroup to root the tree. ML tree was constructed by using RAxML v8.121 with 1,000 bootstrap replicates under the GTR model with gamma distributed rate heterogeneity. To determine the conserved motifs in the RdRp amino acid sequences, the alignment was performed using the Clustal Omega program at the website of the European Bioinformatics Institute (EMBL-EBI; https://www.ebi.ac.uk/Tools/msa/clustalo/). The alignment is presented in **Supplementary Data S3**. Putative proteins were predicted and analyzed using the tools of the Expasy Bioinformatics Resource Portal (https://www.expasy.org/). The HPknotter program (http://genome.cs.nthu.edu.tw/HPKNOTTER/; Huang et al., 2005) was used to predict possible RNA H-type pseudoknots. Molecular weights of the identified proteins were predicted with the Protein Molecular Weight program (https://www.bioinformatics.org/sms/prot_mw.html).

RESULTS

Screening for the Presence of dsRNA Elements in *Umbelopsis* Strains

Twenty-four fungal isolates representing 11 species were screened and dsRNA molecules were detected in five strains belonging to the species *Umbelopsis angularis*, *Umbelopsis dimorpha*, *Umbelopsis gibberispora*, *U. ramanniana,* and *Umbelopsis versiformis* (**Table 1** and **Figures 1A,C**). All strains contained different dsRNA patterns consisting of 2–4 discrete bands with estimated sizes ranging from 0.7 to 5.3-kbp (**Table 1** and **Figures 1A,C**). Although all patterns proved to be different, each of them included a band with a similar size (∼5.0-kbp).

The dsRNA harboring feature was compared with the phylogeny of the examined *Umbelopsis* strains inferred from their ITS sequence data (**Figure 2**). The location of the dsRNA harboring species in the phylogenetic tree and the similarity of the dsRNA patterns raise the question whether some of the dsRNA molecules would be related or of the same origin.

Sequence Analysis of the dsRNA Elements in the *U. ramanniana* NRRL 1296 Strain

In the extracts of this fungus, four dsRNA fragments with the estimated sizes of 5.3, 5.0, 3.0, and 2.8-kbp could be detected by gel electrophoresis (**Figure 3A**). From the total dsRNA extract, cDNA was generated by using the FLAC technique and the resulted clones were sequenced in both directions. Four clones contained fragments corresponding to possible dsRNA/mycovirus genomes. One of them carried a fragment determined to be 4,637-nt in length. It contained two open reading frames (ORF1 and ORF2) in different frames, with a 236-nt spacer in between. Genome organization is presented in **Figure 3B**. ORF1 (from 30 to 2,093-nt; EMBL accession number: LR216267) encodes a putative, 687-aa coat protein (CP) while ORF2 (from 2,330 to 4,600-nt; EMBL accession number: LR216268) was predicted to encode a putative, 756-aa RNA-dependent RNA polymerase (RdRp). The predicted molecular weights of the proteins were found to be 77.64 and 87.13-kDa for the CP and the RdRp, respectively. BLASTp homology search with the corresponding fragment sequence in the NCBI GenBank revealed a high degree of identity with the CP and RdRp of viruses in the *Totiviridae* family; best matches are presented in **Table 2**. The highest similarity was found to the Wuhan insect virus 26 and 27 for both the CP and the RdRp. We suggest that this dsRNA segment corresponds to a genomic component of a novel mycovirus in the *Totiviridae* family, and we have tentatively named it as Umbelopsis ramanniana virus 1 (UrV1).

Another clone contained a 2,454-nt fragment with a partial ORF (from 1 to 2,336-nt; EMBL accession number: LR216269) encoding a partial putative RdRp protein (**Figure 3B**). Within the sequence the RdRp_4 (pfam: 02123) could be identified (nt 177–1,583) and the putative active site (nt 1,098–1,380) could

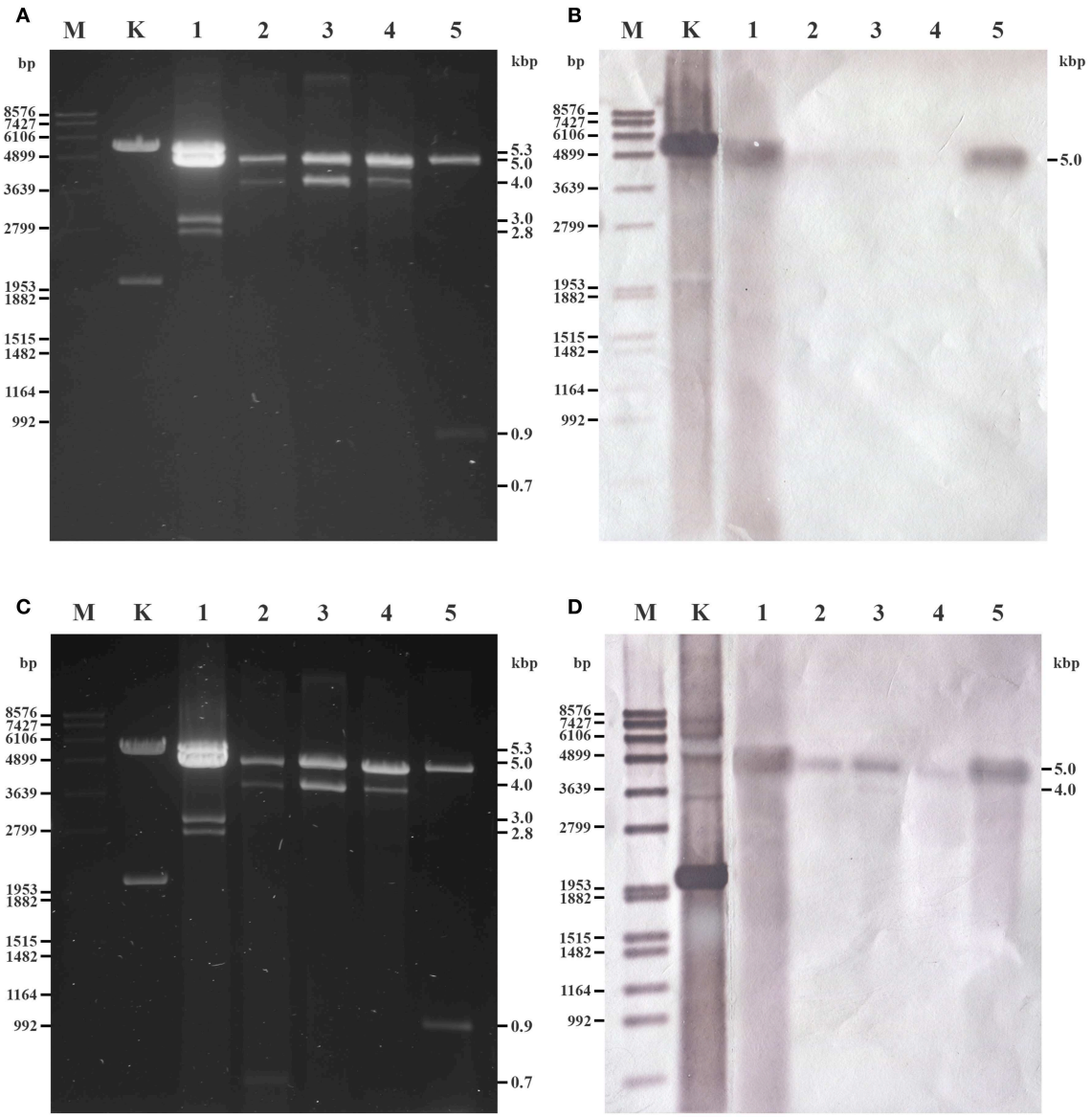

FIGURE 1 | Gel electrophoretic pattern and Northern blotting of dsRNA fragments purified from the mycovirus-harboring *Umbelopsis* strains. **(A,C)** Agarose gel electrophoresis of *Umbelopsis* dsRNA fragments. Lane M, DIG-labeled DNA Molecular Weight Marker VII (Roche); Lane K, KpnI digested control plasmid containing the PCR amplicon of the UrV1 genome; Lane 1, *U. ramanniana* NRRL 1296; Lane 2, *U. gibberispora* CBS 109328; Lane 3, *U. angularis* CBS 603.68; Lane 4, *U. dimorpha* CBS 110039; Lane 5, *U. versiformis* CBS 473.74. Right numbers indicate the sizes (kbp) of the detected dsRNA fragments. **(B,D)** Northern blot analysis of *Umbelopsis* dsRNA fragments hybridized with UrV1 CP and UrV1 RdRp probes, respectively. UrV1 CP probes gave strong hybridization signal with the 5.0-kbp fragments of *U. ramanniana* (Lane 1) and *U. versiformis* (Lane 5) and weakly hybridized to the 5.0-kbp fragments of *U. gibberispora* (Lane 2) and *U. angularis* (Lane 3). UrV1 RdRp probes gave hybridization signal with the 5.0-kbp fragments of all strains and hybridized weakly to the 4.0-kbp dsRNA fragment of *U. angularis*. In case of the KpnI digested control plasmid, the 5.5-kbp bands gave strong hybridization signal with the UrV1 CP, and the 2.0-kbp bands gave strong hybridization signal with the UrV1 RdRp probe.

also be predicted. BLASTp search also indicated high similarity to members of the *Totiviridae*, with the best match to the RdRp of the Thelebolus microsporus totivirus 1. Details of the five best matches are presented in **Table 2**. Accordingly, we can assume that this sequence corresponds to a partial genomic dsRNA for a novel mycovirus belonging to the family *Totiviridae*, which has been named as Umbelopsis ramanniana virus 2 (UrV2).

The third clone carried a 4,987-nt fragment containing two open reading frames (ORF1 and ORF2) in different frames and with a 98-nt spacer in between (**Figure 3B**). ORF1 (from 45 to 2,582-nt; EMBL accession number: LR595925) encodes an 845-aa hypothetical protein with a 92.04-kDa predicted molecular weight. Homology searches carried out with the nucleotide and amino acid sequences of this ORF using the BLASTx and

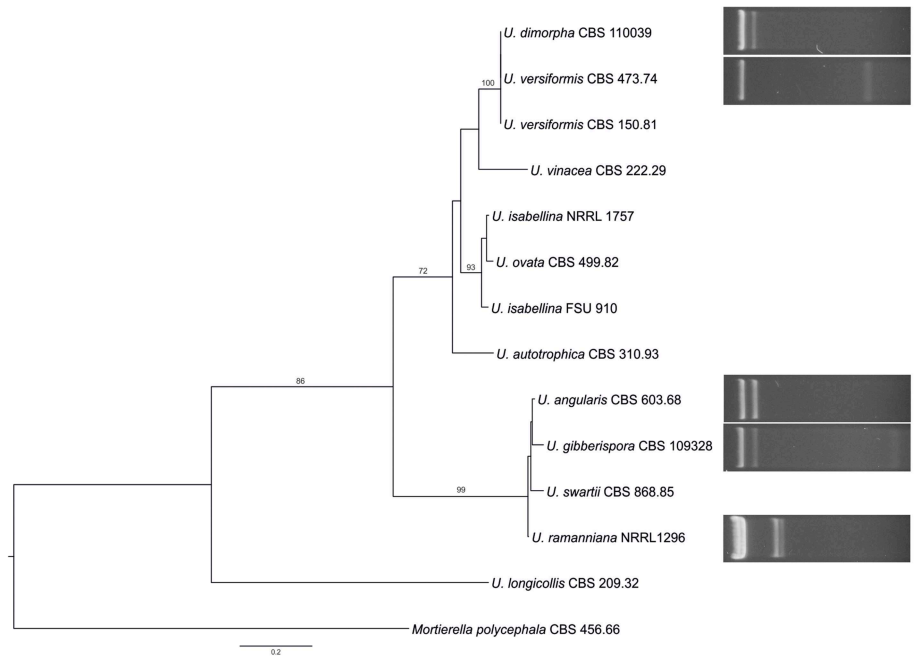

FIGURE 2 | Comparison of the phylogeny of the tested *Umbelopsis* species inferred from the ITS region with the mycovirus-harboring feature. The presented tree was constructed by the Maximum Likelihood method using the RAxML program. Bootstrap values (%) indicated on branches were obtained with 1,000 replicates. *Mortierella polycephala* CBS 456.66 was used as the outgroup. The list of the investigated *Umbelopsis* strains and the accession number of the applied sequences can be seen in **Supplementary Table S1**.

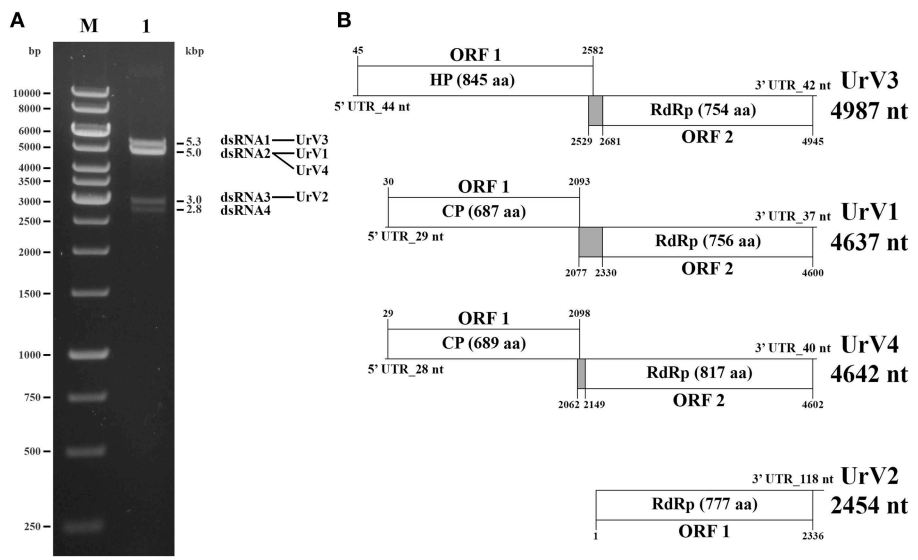

FIGURE 3 | Gel electrophoretic pattern and genomic organization of *U. ramanniana* NRRL 1296 dsRNA fragments. **(A)** Agarose gel electrophoresis of dsRNA fragments purified from the mycovirus-harboring *U. ramanniana* NRRL 1296 strain. Lane M, GeneRuler 1-kb DNA Ladder (Thermo Scientific); Lane 1, *U. ramanniana* NRRL 1296. The sizes (kbp) of the detected dsRNA fragments and the corresponding virus genomes are indicated as well. **(B)** Genomic organization of the four detected dsRNA genomes showing putative open reading frames (ORFs). The first codons of the possible pseudoknot sequences are also marked. The gray boxes indicate the probable beginning of the fusion protein and the spacer region. HP, hypothetical protein; CP, coat protein; RdRp, RNA dependent RNA polymerase.

tBLASTn tool of NCBI, respectively, found no similarity with any sequences in the GenBank. ORF2 (from 2,681 to 4,945-nt; EMBL accession number: LR595926) was predicted to encode a putative, 754-aa RdRp protein with an 85.47-kDa predicted molecular weight. This protein showed the highest degree of identity with the Beihai barnacle virus 15 hypothetical protein 2.

TABLE 2 | Amino acid sequence identities of the UrV1 CP, UrV1 RdRp, UrV2 RdRp, URV3 ORF1, UrV3 RdRp, UrV4 CP, and UrV4 RdRp with similar databank sequences deduced by BLAST search.

Virus	Virus name	Accession number	Identity (%)	E-Value	Query coverage (%)
UrV1 CP	Wuhan insect virus 26 hypothetical protein 1	YP 009342427.1	44.26	5e-162	78
	Wuhan insect virus 27 hypothetical protein 1	YP 009342433.1	37.12	7e-151	95
	Red clover powdery mildew-associated totivirus 4 CP	BAT62483.1	33.18	4e-123	96
	Xanthophyllomyces dendrorhous virus L1B CP	YP 009507834.1	31.79	2e-111	100
	Hortaea werneckii totivirus 1 CP	AZT88646.1	30.67	5e-109	94
UrV1 RdRp	Wuhan insect virus 26 hypothetical protein 2	YP 009342428.1	57.14	0	99
	Wuhan insect virus 27 hypothetical protein 2	YP 009342434.1	48.93	0	99
	Delisea pulchra totivirus IndA RdRp	AMB17470.1	48.10	0	92
	Xanthophyllomyces dendrorhous virus L1B RdRp	YP 009507835.1	42.93	0	98
	Xanthophyllomyces dendrorhous virus L1A RdRp	YP 007697651.1	41.11	0	97
UrV2 RdRp	Thelebolus microsporus totivirus 1 RdRp	AZT88643.1	50.78	0	98
	Tolypocladium ophioglossoides totivirus 1 RdRp	AZT88645.1	46.89	0	99
	Ustilaginoidea virens RNA virus 5 RdRp	YP 009182167.1	46.73	0	99
	Helicobasidium mompa totivirus 1–17 RdRp	NP 898833.1	42.24	0	97
	Beauveria bassiana victorivirus NZL/1980 RdRp	YP 009032633.1	43.22	0	98
UrV3 ORF1	No significant similarity found				
UrV3 RdRp	Beihai barnacle virus 15 hypothetical protein 2	YP 009333150.1	31.05	1e-65	80
	Diatom colony associated dsRNA virus 17 genome type B RdRp	YP 009551502.1	30.12	3e-63	85
	Diatom colony associated dsRNA virus 17 genome type A RdRp	YP 009551504.1	29.62	8e-63	85
	Hubei toti-like virus 5 hypothetical protein	YP 009336942.1	27.80	1e-44	77
	Hubei toti-like virus 6 hypothetical protein 2	APG75978.1	33.26	1e-43	57
UrV4 CP	Wuhan insect virus 26 hypothetical protein 1	YP 009342427.1	43.17	3e-150	78
	Wuhan insect virus 27 hypothetical protein 1	YP 009342433.1	38.02	2e-148	94
	Red clover powdery mildew-associated totivirus 4 CP	BAT62483.1	31.89	9e-112	96
	Hortaea werneckii totivirus 1 CP	AZT88646.1	32.01	1e-107	91
	Xanthophyllomyces dendrorhous virus L1A CP	YP 007697650.1	31.44	6e-107	96
UrV4 RdRp	Wuhan insect virus 26 hypothetical protein 2	YP 009342428.1	56.62	0	96
	Wuhan insect virus 27 hypothetical protein 2	YP 009342434.1	47.76	0	95
	Delisea pulchra totivirus IndA RdRp	AMB17470.1	45.34	0	85
	Hortaea werneckii totivirus 1 RdRp	AZT88647.1	43.28	0	94
	Xanthophyllomyces dendrorhous virus L1A RdRp	YP 007697651.1	42.04	0	91

Details of the five best matches given by the BLASTp query with the corresponding amino acid sequence are presented in **Table 2**. As this sequence may correspond to a genomic dsRNA for a novel mycovirus, it has been named as Umbelopsis ramanniana virus 3 (UrV3).

The fourth clone carried a fragment determined to be 4,642-nt in length. It contained two open reading frames (ORF1 and ORF2): ORF1 (from 29 to 2,098-nt; EMBL accession number: LR595927) encodes a putative, 689-aa CP, while ORF2 (from 2,149 to 4,602-nt; EMBL accession number: LR595928) was predicted to encode a putative, 817-aa RdRp (**Figure 3B**). The predicted molecular weights of the proteins were found to be 77.12 and 93.17-kDa for the CP and the RdRp, respectively. The two genes are in different frames and a 50-nt spacer can be found between them. BLASTp homology search with the corresponding fragment sequence in the NCBI GenBank revealed a high degree of identity with the CP and RdRp of viruses in the *Totiviridae* family; best matches are presented in **Table 2**. As in case of the sequence of UrV1, the highest similarity was found to the Wuhan insect virus 26 and 27 for both the CP and the RdRp. We suggest that this dsRNA segment corresponds to a genomic component of a novel mycovirus in the *Totiviridae* family, and we have tentatively named it as Umbelopsis ramanniana virus 4 (UrV4).

EMBOSS Needle pairwise alignment tool at the EMBL-EBI site (https://www.ebi.ac.uk/Tools/psa/emboss_needle/) found 48.7 and 60.2% sequence identity of CP and RdRp proteins of UrV1 and Urv4, respectively. In case of the other sequences, lower level of similarity/homology was detected (13.3–21.0%) as it shown in **Supplementary Table S3**.

UrV1, UrV3, and UrV4 contain a spacer region between their two ORFs, which are in the same frame as ORF2 (**Figure 3B**). Using the HPknotter program, a putative H-type pseudoknot, which may be involved in translation re-initiation (Li et al., 2011), could be predicted for each genome (from 2,077 to 2,099-nt for UrV1, from 2,529 to 2,560-nt for UrV3 and from 2,062 to 2,081-nt for UrV4) suggesting that an ORF1-ORF2 fusion protein may be produced by a −1 ribosomal frameshift in each case.

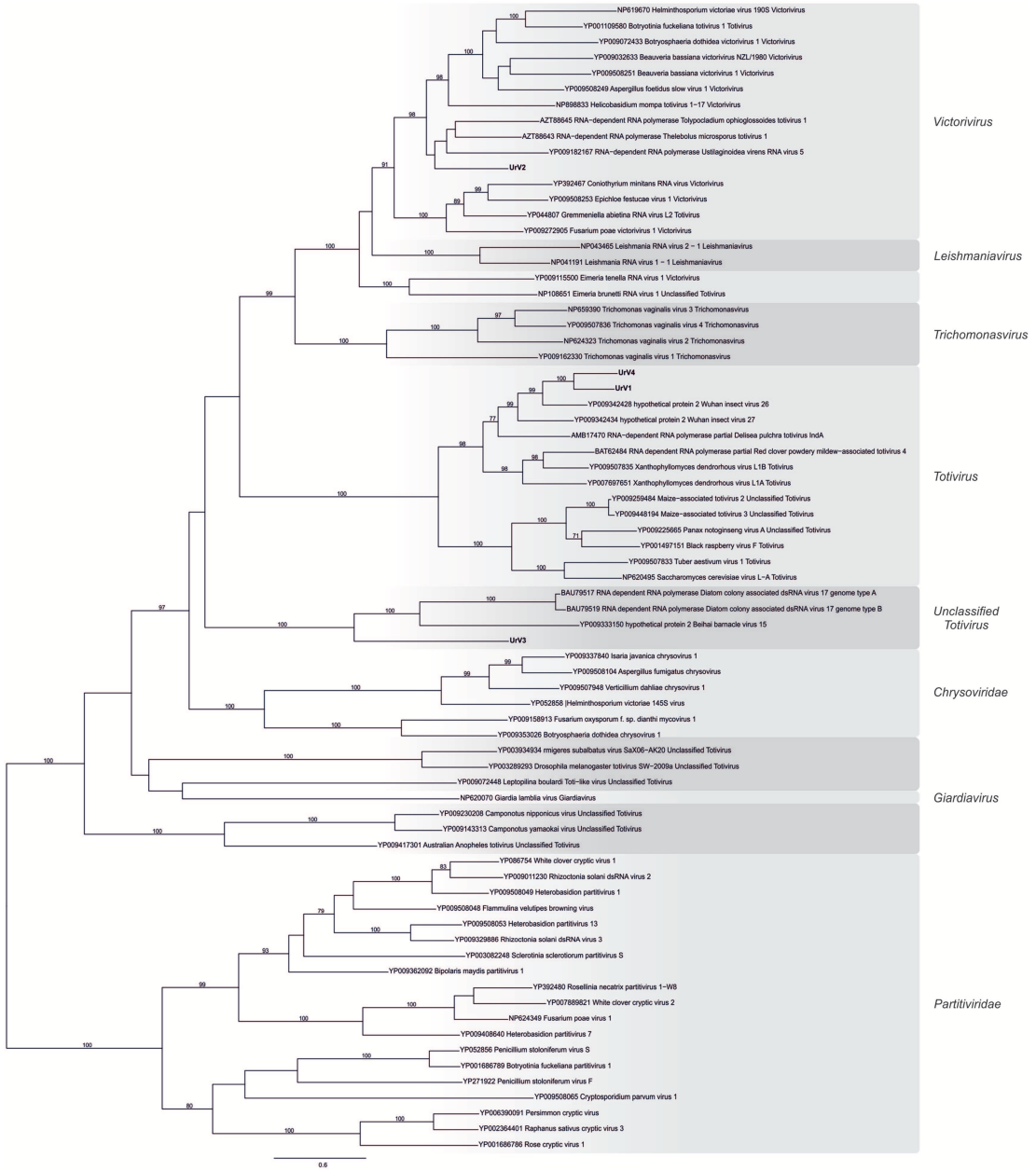

FIGURE 4 | Phylogenetic analysis of UrV1, UrV2, UrV3, and UrV4 RdRps. The presented phylogenetic tree was constructed based on the RdRp amino acid sequences from representative members of the family *Totiviridae*, *Chrysoviridae,* and *Partitiviridae*. Results indicate that UrV1 and UrV4 are members of the genus *Totivirus*, UrV2 belongs to the genus *Victorivirus,* and UrV3 forms a clade with unclassified dsRNA viruses. The phylogenetic tree was constructed using Maximum Likelihood method using the RAxML program. Bootstrap values (%) indicated on branches were obtained with 500 replicates. The genetic distance was represented by the scale bar of 0.8 amino acid substitutions per nucleotide site. The novel *Umbelopsis* mycoviruses are indicated with bold letters.

Phylogenetic Analysis of the *U. ramanniana* Viruses

Based on RdRp amino acid sequences from representative members of the family *Totiviridae*, *Chrysoviridae,* and *Partitiviridae*, a phylogenetic analysis was performed using the ML method (**Figure 4**). In this phylogeny, UrV1 and UrV4 is seated in the clade containing viruses from the genus *Totivirus*, while UrV2 is part of the clade representing the genus *Victorivirus*. UrV3 together with some unclassified dsRNA viruses forms well-defined and yet unclassified clade, which is related to the genus *Totivirus*. We gave the same result with alternatively performed NJ analysis (**Supplementary Figure S1**).

Besides the universally conserved GDD motif (Bruenn, 1993), multiple alignment of the viral RdRps isolated from *U. ramanniana* and those of other similar mycoviruses revealed the eight conserved domains specific to the *Totiviridae* family

FIGURE 5 | Multiple amino acid sequence alignment of the conserved RdRp motifs of the novel UrV1, UrV2, UrV3, UrV4, and other related mycoviruses. Numbers at the top indicate the eight conserved domains characteristic to the *Totiviridae* family (Bruenn, 1993). Residues found in all sequences are shaded in yellow. Sequence lengths between the motifs are indicated with the number of amino acids in parentheses. Abbreviations of the virus names and accession numbers of the aligned sequences are the following: BBV15, Beihai barnacle virus 15 (YP_009333150); DCADV17, Diatom colony associated dsRNA virus 17 genome type A (BAU79517); HVV190S, Helminthosporium victoriae virus 190S (AAB94791); UVRV5, Ustilaginoidea virens RNA virus 5 (YP_009182167); SCVL-A, Saccharomyces cerevisiae virus L-A (NP_620495); WIV26, Wuhan insect virus 26 (YP_009342428).

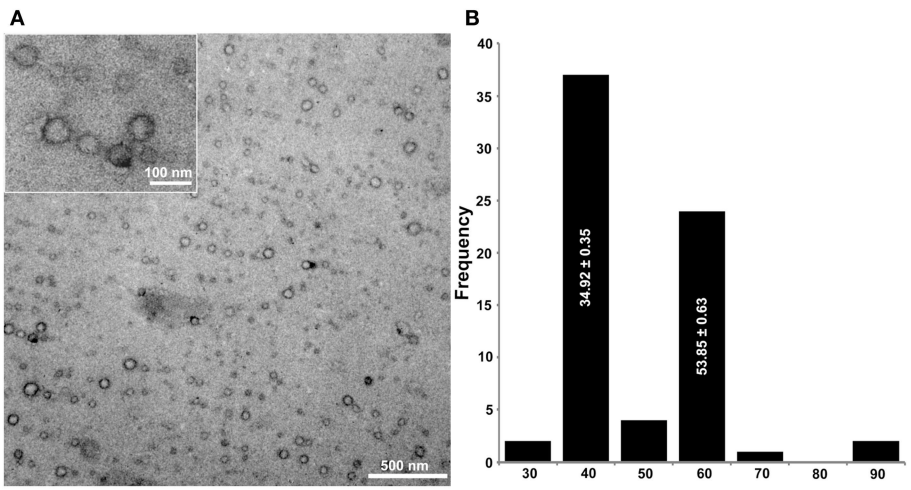

FIGURE 6 | Morphology of virus particles detected in *U. ramanniana* NRRL 1296 strain **(A)** and the histogram of the particle size distribution measured by electron microscopy ($n = 70$) **(B)**. The virus particles were recovered by ultracentrifugation at 78,000 × *g* for 10 h at 4°C. Purified virus particles were negatively stained with 2% uranyl acetate in 50% ethanol for 5 min (3 times) and examined under a JEM-1400 Flash transmission electron microscope. Two different isometric virus particles could be discerned in the samples. The sizes of particles are estimated to be about 50 and 35 nm in diameter. In **(A)**, magnification in the large and small pictures are 40,000× and 60,000×, respectively.

RdRps (Bruenn, 1993; Routhier and Bruenn, 1998; Campo et al., 2016) (**Figure 5**). Furthermore, group-specific sequence patterns observed within these conserved domains reinforce the result of the phylogenetic analysis that UrV1 and UrV4 belong to the genus *Totivirus*, while UrV2 and UrV3 are members of the genus *Victorivirus* and an unclassified *Totiviridae*-related group, respectively.

Detection of Virus Particles in *U. ramanniana*

Transmission electron microscopy revealed the presence of isometric virus particles in the purified extracts of *U. ramanniana* NRRL 1296. **Figures 6A,B** shows that particles with at least two different sizes (i.e., with about 50 or 35 nm in diameter) could be discerned in the samples.

Hybridization Analysis of the dsRNA Patterns

Probes designed for the CP and the RdRp genes of UrV1 and UrV4 hybridized to the second largest band (5.0-kbp) of the dsRNA electrophoretic pattern of *U. ramanniana* NRRL 1296 (**Figures 7A–D,I–L**) indicating that this band represents two molecules with highly similar sizes, which correspond to the UrV1 and UrV4 dsRNA genomes. The probe designed

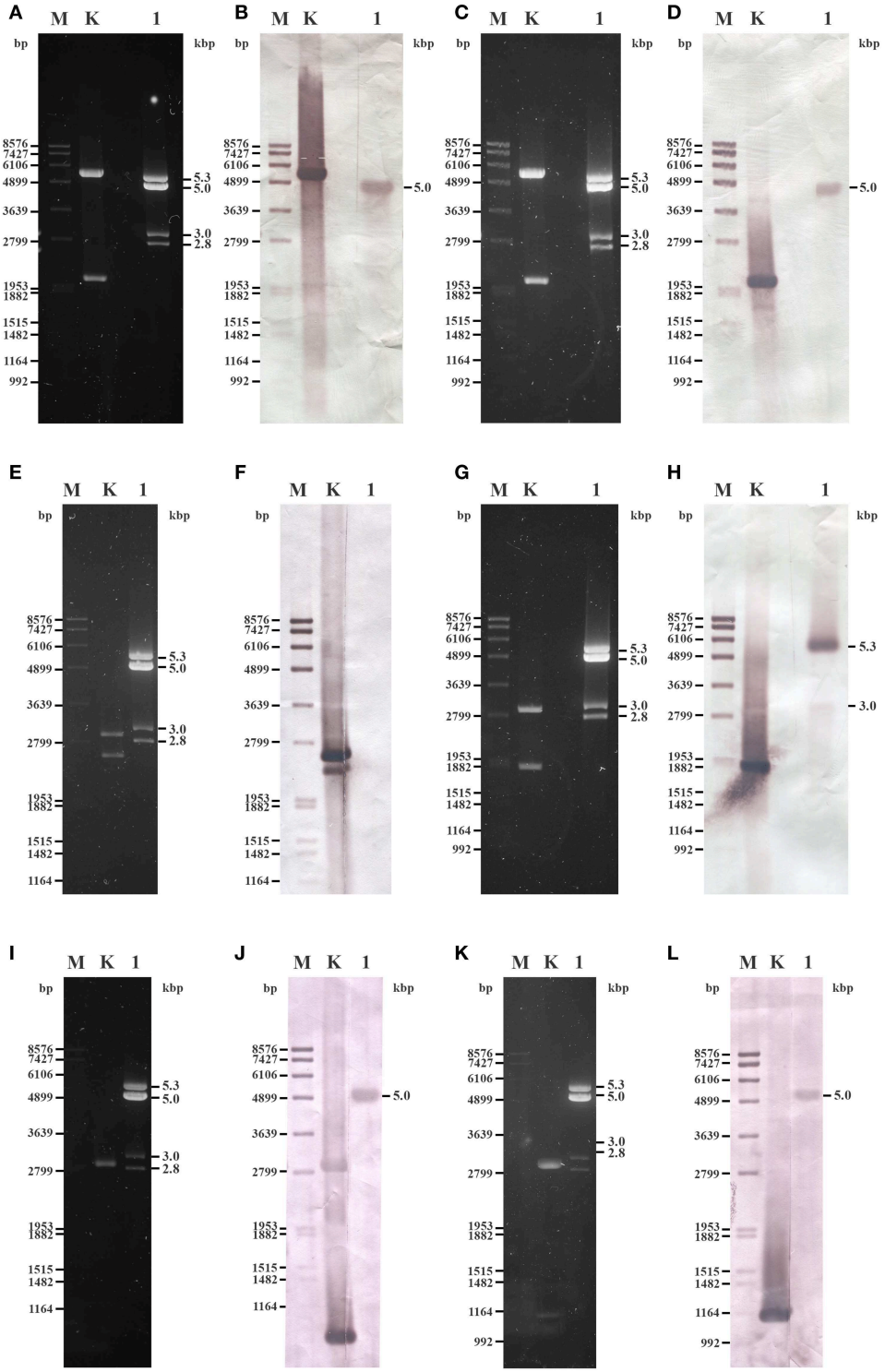

FIGURE 7 | Northern blot analysis of dsRNA fragments purified from the mycovirus-harboring *Umbelopsis ramanniana* NRRL 1296 strain with probes designed by the UrV1, UrV2, UrV3, and UrV4 sequences. **(A,C,E,G,I,K)** Agarose gel electrophoresis of *U. ramanniana* NRRL 1296 dsRNA fragments. Lane M, DIG-labeled DNA Molecular Weight Marker VII (Roche); Lane K, control plasmid containing the corresponding PCR amplicon of virus genomes; Lane 1, *U. ramanniana* NRRL 1296. Right numbers indicate the sizes (kbp) of the detected dsRNA fragments. **(B,D,F,H,J,L)** Northern blot analysis of *U. ramanniana* NRRL 1296 dsRNA fragments hybridized with UrV1 CP, UrV1 RdRp, UrV2 RdRp, UrV3 RdRp, UrV4 CP, and UrV4 RdRp probes, respectively. In **(B,D)**, UrV1 CP and UrV1 RdRp probes both gave strong hybridization signal with the 5.0-kbp fragments of *U. ramanniana* NRRL 1296. In the case of the control plasmid, which contains the PCR amplicon of the UrV1

(Continued)

FIGURE 7 | genome, the 5.5-kbp band gave strong hybridization signal with the UrV1 CP, and the 2.0-kbp band gave strong hybridization signal with the UrV1 RdRp probe. In panel **(F)**, UrV2 RdRp probe gave no hybridization signal to any dsRNA fragments, however the 2.4-kbp band of the BglII digested control plasmid, which contains the PCR amplicon of the UrV2 genome gave strong hybridization signal. In **(H)**, UrV3 RdRp probe hybridized to the largest, 5.3-kbp and the 3.0-kbp dsRNA bands of the pattern. In case of the ClaI-SpeI double digested control plasmid, which contains the PCR amplicon of the UrV3 genome, the 1.7-kbp band gave strong hybridization signal with the UrV3 RdRp probe. In **(J,L)**, UrV4 CP and UrV4 RdRp probes also gave strong hybridization signal with the 5.0-kbp fragments. In the case of the control plasmids, the ClaI-SpeI double digested control plasmid, which contains the PCR amplicon of the UrV4 CP genome, the 0.85-kbp band gave strong hybridization signal with the UrV4 CP probe. The 1.0-kbp band of the BglII digested control plasmid, which contains the PCR amplicon of the UrV4 RdRp genome gave hybridization signal with the UrV4 RdRp probe.

for the UrV2 sequence gave no signal to any dsRNA bands (**Figures 7E,F**), while the probe based on the sequence of the UrV3 fragment hybridized to the largest, 5.3-kbp and the 3.0-kbp dsRNA bands of the pattern (**Figures 7G,H**).

Although hybridization experiments to match the dsRNA electrophoretic bands with the UrV2 sequence, which was determined after amplification using the FLAC method from the total dsRNA extract, have remained unsuccessful, this fragment could be amplified from the isolated 3.0-kbp dsRNA band using both the FLAC adaptor and UrV2-specific primers (see **Supplementary Table S2**) as well. This result also suggests that this 3.0-kbp dsRNA band can be a mixture of dsRNA molecules.

As a band with a size similar to that of the band corresponding to the dsRNA of UrV1 and UrV4 was present in the dsRNA patterns of the other four dsRNA harboring *Umbelopsis* strains, the probes corresponding to the UrV1 CP and RdRp genes were also used to examine these dsRNA patterns. Both probes hybridized to the bands with the size of around 5.0-kbp in case of all tested *Umbelopsis* strains, except that UrV1 CP probe gave no hybridization signal with the fragments of *U. dimorpha*. It might be attributed to the presence of sequence variation in the 5.0-kbp segment of *U. dimorpha*, which will affect the binding specificity of the UrV1 CP and RdRp probes. Similar to that of UrV1, the RdRp probe of UrV4 also could hybridize to the dsRNA extracts of all four *Umbelopsis* strains (**Supplementary Figure S2**). At the same time, probes corresponding to the RdRp sequences of UrV2 and UrV3 did not give any signal with the dsRNAs of these strains (**Supplementary Figure S2**). Based on this result, we can suggest that the detected bands in *Umbelopsis* strains also can be possible full mycovirus genomes similar to those of UrV1 and UrV4 (**Figures 1A–D**). The probe corresponding to the UrV1 CP did not give any signal for other bands of these strains, while the probe of the UrV1 RdRp hybridized also to the smaller, 4.0-kbp dsRNA fragment of *U. angularis* suggesting that this fragment may also contain an RdRp sequence.

DISCUSSION

In this study, we screened for the presence of dsRNA molecules in a collection of 24 *Umbelopsis* isolates representing 11 species and found dsRNA elements in strains of five different species. Moreover, discovery of four independent viral genomes and genome fragments corresponding to four novel mycoviruses in *U. ramanniana* was also reported.

We found dsRNA elements in the 46 and 21% of the tested *Umbelopsis* species and strains, respectively. This prevalence is much higher frequencies than that observed previously testing 121 *Mucor* isolates, which represented 17 species (i.e., 29 and 4%, respectively) (Vágvölgyi et al., 1998). In another study, 19% of the tested *Rhizopus* isolates harbored dsRNAs and these isolates represented three of the four involved species (Papp et al., 2001).

The dsRNA pattern of the *U. ramanniana* NRRL 1296 was reported earlier (Vágvölgyi et al., 1993, 1998). Vágvölgyi et al. (1993) originally detected a pattern consisting of four dsRNA molecules but later, they also reported the presence of a fifth, 2.5-kbp dsRNA fragment (Vágvölgyi et al., 1998). In our study, we could reconstruct only the earlier reported pattern with the same four bands. Maybe that fifth fragment would represent a defective dsRNA element, which can frequently be present in dsRNA mycoviruses (Son et al., 2015).

Efforts to determine the dsRNA molecules of this fungus resulted in four sequences, among which three encode a CP (or potential CP) and an RdRp protein and the one corresponds to a partial RdRp coding gene. Considering that the four sequences represent different novel dsRNA viruses, they were named as UrV1, UrV2, UrV3, and UrV4. All four dsRNAs found to be related to viral sequences belonging to the *Totiviridae* family. Isometric virus particles with different sizes were also detected in *U. ramanniana* NRRL 1296 indicating that this strain harbor multiple viruses. Mixed infections have also been found in other fungi, such as in case of the entomopathogenic *Beauveria bassiana* (Herrero et al., 2012).

The phylogeny inferred from the RdRp sequences placed UrV1 and UrV4 into the genus *Totivirus* together with Wuhan insect virus 26 and 27 (Shi et al., 2016), which also proved to be the most similar to the UrV1 and UrV4 sequences by the BLAST search of the NCBI GenBank (**Table 2** and **Figure 4**). Within the *Totivirus* clade, they form a sub-clade together with the Delisea pulchra totivirus IndA (KT455453; Lachnit et al., 2016). Hybridization analysis revealed that the 5.0-kbp band of the dsRNA pattern obtained from *U. ramanniana* NRRL 1296 corresponds to the genomes of UrV1 and UrV4. This size agrees with the typical genome sizes of the totiviruses (King et al., 2011; Ghabrial et al., 2015). A band with a similar size was found in all tested strains. Moreover, the probes, which correspond to the CP and RdRp sequences of UrV1 and UrV4, could hybridize to them indicating that they can represent similar mycovirus genomes possibly belonging to the genus *Totivirus*. In case of *U. versiformis*, both UrV1 probes gave a hybridization signal as strong as those given with the corresponding dsRNA molecule of *U. ramanniana* NRRL 1296 suggesting that this fungus may harbor a highly similar dsRNA/mycovirus (**Figures 1A–D**).

The sequence of UrV2 proved to be the most related to Thelebolus microsporus totivirus 1 and Tolypocladium

ophioglossoides totivirus 1, which were recently identified by a survey of transcriptomic datasets of Pezizomycotina fungi and determined as members of the genus *Victorivirus* (Gilbert et al., 2019). Indeed, these viruses together with Ustilaginoidea virens RNA virus 5, of which RdRp sequence is also very similar to that of UrV2, form a sub-clade within the *Victorivirus* genus in the phylogenetic tree of RdRp sequences (**Figure 4**). Hybridization analysis could not match the UrV2 sequence to any dsRNA bands of *U. ramanniana* NRRL 1296 but its 2,454-nt fragment could be amplified from the isolated 3.0-kbp dsRNA band of the same pattern. These results suggest that UrV2 can represent a partial genome and/or a defective sequence, which is present in a very low amount in the fungal cells.

In case of UrV3, the RdRp probe hybridized to the largest fragment of the dsRNA pattern of *U. ramanniana*. It also gave a hybridization signal to one of the smaller bands, which may indicate that the latter could be a defective dsRNA originated from the genome of UrV3 (**Figures 7G–H**). The UrV3 sequence had the largest degree of identity with Beihai barnacle virus 15 identified by the analysis of invertebrate transcriptomes as a Toti-Chryso-like virus (Shi et al., 2016) and the RdRps of Diatom colony associated dsRNA virus 17 genome types A and B, which were discovered as not assigned dsRNA viruses by metagenomic methods in a diatom colony (Urayama et al., 2016). UrV3 together with the abovementioned three viruses formed a clade, which proved to be paraphyletic with the *Totivirus* and the *Chrysoviridae* clades (**Figure 4**). Viruses in the *Chrysoviridae* have segmented genomes typically consisting of four dsRNA segments, which are among 2.4 and 3.6-kbp in size (King et al., 2011), although unusual chrysoviruses with three or five segments have also been reported (Li et al., 2013; Ghabrial et al., 2015). *Totiviridae* contains viruses with non-segmented genomes with various sizes ranging from 4.6 to 7.0-kbp (Ghabrial et al., 2015). Despite this profound difference in their genome organizations, phylogenetic analyses have demonstrated their close relationship and similarity (King et al., 2011; Chen et al., 2016). Based on the hybridization analysis, it can be suggested that UrV3 has a non-segmented genome. The other members of its clade have also monosegmented genomes, with the sizes of 5.9-kbp for Diatom colony associated dsRNA virus 17 genome types A and B (Urayama et al., 2016) and 7.4-kbp for Beihai barnacle virus 15 (Shi et al., 2016). Considering their phylogenetic position and genome structure, it can be suggested that these viruses represent a novel, *Totivirus*-related group of dsRNA mycoviruses.

In conclusion, we detected dsRNA elements in various *Umbelopsis* species and identified four novel *Totiviridae* related viruses in *U. ramanniana*. Our results suggest that UrV1 and UrV4 are members of the genus *Totivirus*, UrV2 belongs to the genus *Victorivirus*, and UrV3 may belong to a novel group of mycoviruses in the *Totiviridae* family.

DATA AVAILABILITY

The datasets generated for this study can be found in European Nucleotide Archive, LR216267-LR216269, LR595925-LR595928.

AUTHOR CONTRIBUTIONS

TP and IN contributed to the design and implementation of the research, analyzed the results, and drafted the manuscript. TK and BS performed the experimental work. SK performed the phylogenetic analysis. RP and TFP carried out the electron microscopic examinations. CV and GN contributed to analyze the results and helped in drafting the manuscript.

FUNDING

This study was supported by the Lendület Grant of the Hungarian Academy of Sciences (LP2016-8/2016) and the Hungary grant 20391-3/2018/FEKUSTRAT of the Ministry of Human Capacities. Infrastructural background for the electron microscopic evaluation was partially supported by the Ministry for National Economy of Hungary through the GINOP-2.3.3-15-2016-00001 program. SK was supported by the grant PD116609.

SUPPLEMENTARY MATERIAL

The Supplementary Material for this article can be found online at: https://www.frontiersin.org/articles/10.3389/fcimb.2019.00249/full#supplementary-material

REFERENCES

Bruenn, J. A. (1993). A closely related group of RNA-dependent RNA polymerases from double-stranded RNA viruses. *Nucl. Acids Res.* 21, 5667–5669. doi: 10.1093/nar/21.24.5667

Campo, S., Gilbert, K. B., and Carrington, J. C. (2016). Small RNA-based antiviral defense in the phytopathogenic fungus *Colletotrichum higginsianum*. *PLoS Pathog.* 12:e1005640. doi: 10.1371/journal.ppat.1005640

Chen, S., Cao, L., Huang, Q., Qian, Y., and Zhou, X. (2016). The complete genome sequence of a novel maize-associated totivirus. *Arch. Virol.* 161, 487–490. doi: 10.1007/s00705-015-2657-y

Darissa, O., Willingmann, P., and Adam, G. (2010). Optimized approaches for the sequence determination of double-stranded RNA templates. *J. Virol. Methods* 169, 397–403. doi: 10.1016/j.jviromet.2010.08.013

Ghabrial, S. A. (1998). Origin, adaptation and evolutionary pathways of fungal viruses. *Virus Genes* 16, 119–131. doi: 10.1023/A:1007966229595

Ghabrial, S. A. (2008). "Chrysoviruses. 3rd ed," in *Encyclopedia of Virology*, Vol. 2, eds B. W. J. Mahy, M. H. V. Van Regenmortel (Oxford, Elsevier), 284–291.

Ghabrial, S. A., Castón, J. R., Jiang, D., Nibert, M. L., and Suzuki, N. (2015). 50-plus years of fungal viruses. *Virology* 479–480, 356–368. doi: 10.1016/j.virol.2015.02.034

Ghabrial, S. A., and Suzuki, N. (2009). Viruses of plant pathogenic fungi. *Annu. Rev. Phytopathol.* 47, 353–384. doi: 10.1146/annurev-phyto-080508-081932

Gilbert, K., Holcomb, E. E., Allscheid, R. L., and Carrington, J. (2019). Discovery of new mycoviral genomes within publicly available fungal transcriptomic datasets. *BioRxiv* 510404. doi: 10.1101/510404

Hafez, E. E., Aseel, D. G., and Mostafa, S. (2013). Two novel mycoviruses related to Geminivirus isolated from the soil-borne fungi *Macrophomina phaseolina* (Tassi) Goid. and *Mucor racemosus* Bull. *Biotechnol. Biotechnol. Equip.* 27, 4222–4226. doi: 10.5504/BBEQ.2013.0086

Herrero, N., Dueñas, E., Quesada-Moraga, E., and Zabalgogeazcoa, I. (2012). Prevalence and diversity of viruses in the entomopathogenic fungus *Beauveria*

bassiana. *Appl. Environ. Microbiol*. 78, 8523–8530. doi: 10.1128/AEM.01954-12

Hillman, B. I., and Cai, G. (2013). The family narnaviridae: simplest of RNA viruses. *Adv. Virus Res*. 86, 149–176. doi: 10.1016/B978-0-12-394315-6.00006-4

Hong, Y., Cole, T. E., Brasier, C. M., and Buck, K. W. (1998). Novel structures of two virus-like RNA elements from a diseased isolate of the Dutch elm disease fungus, *Ophiostoma novo-ulmi*. *Virology* 242, 80–89. doi: 10.1006/viro.1997.8999

Huang, C. H., Lu, C. L., and Chiu, H. T. (2005). A heuristic approach for detecting RNA H-type pseudoknots. *Bioinformatics* 21, 3501–3508. doi: 10.1093/bioinformatics/bti568

Katoh, K., and Standley, D. M. (2013). MAFFT multiple sequence alignment software version 7: improvements in performance and usability. *Mol. Biol. Evol*. 30, 772–780. doi: 10.1093/molbev/mst010

King, A. M. Q., Adams, M. J., Carstens, E. B., and Lefkowitz, E. J. (2011). *Virus Taxonomy*. Ninth Report of the International Committee on Taxonomy of Viruses. Elsevier.

Lachnit, T., Thomas, T., and Steinberg, P. (2016). Expanding our understanding of the seaweed holobiont: RNA viruses of the red alga *Delisea pulchra*. *Front. Microbiol*. 6:1489. doi: 10.3389/fmicb.2015.01489

Leach, J., Finkelstein, D. B., and Rambosek, J. A. (1986). Rapid miniprep of DNA from filamentous fungi. *Fungal Genet. Rep*. 33:9. doi: 10.4148/1941-4765.1585

Li, H., Havens, W. M., Nibert, M. L., and Ghabrial, S. A. (2011). RNA sequence determinants of a coupled termination-reinitiation strategy for downstream open reading frame translation in *Helminthosporium victoriae* virus 190S and other victoriviruses (Family *Totiviridae*). *J. Virol*. 85, 7343–7352. doi: 10.1128/JVI.00364-11

Li, L., Liu, J., Xu, A., Wang, T., Chen, J., and Zhu, X. (2013). Molecular characterization of a trisegmented chrysovirus isolated from the radish *Raphanus sativus*. *Virus Res*. 176, 169–178. doi: 10.1016/j.virusres.2013.06.004

Lot, H., Marrou, J., Quiot, J. B., and Esvan, C. (1972). Contribution a l'etude du virus de la mosaique du concombre (CMV). II. Methode de purification rapide du virus. *Ann. Phytopathol*. 4, 25–38.

Maan, S., Rao, S., Maan, N. S., Anthony, S. J., Attoui, H., Samuel, A. R., et al. (2007). Rapid cDNA synthesis and sequencing techniques for the genetic study of bluetongue and other dsRNA viruses. *J. Virol. Methods* 143, 132–139. doi: 10.1016/j.jviromet.2007.02.016

Meyer, W., and Gams, W. (2003). Delimitation of *Umbelopsis* (*Mucorales*, *Umbelopsidaceae* fam. nov.*)* based on ITS sequence and RFLP data. *Mycol. Res*. 107, 339–350. doi: 10.1017/S0953756203007226

Morris, T. J., and Dodds, J. A. (1979). Isolation and analysis of double-stranded RNA from virus-infected plant and fungal tissue. *Phytopathology* 69, 854–858.

Nuss, D. L. (2005). Hypovirulence: mycoviruses at the fungal-plant interface. *Nature Rev. Microbiol*. 3, 632–642. doi: 10.1038/nrmicro1206

Papp, T., Nyilasi, I., Fekete, C., Ferenczy, L., and Vágvölgyi, C. (2001). Presence of double-stranded RNA and virus-like particles in *Rhizopus* isolates. *Can. J. Microbiol*. 47, 443–447. doi: 10.1139/w01-020

Potgieter, A. C., Page, N. A., Liebenberg, J., Wright, I. M., Landt, O., and van Dijk, A. A. (2009). Improved strategies for sequence-independent amplification and sequencing of viral double-stranded RNA genomes. *J. Gen. Virol*. 90, 1423–1432. doi: 10.1099/vir.0.009381-0

Routhier, E., and Bruenn, J. A. (1998). Functions of conserved motifs in the RNA-dependent RNA polymerase of a yeast double-stranded RNA virus. *J. Virol*. 72, 4427–4429.

Shi, M., Lin, X. D., Tian, J. H., Chen, L. J., Chen, X., Li, C. X., et al. (2016). Redefining the invertebrate RNA virosphere. *Nature* 540, 539–543. doi: 10.1038/nature20167

Son, M., Yu, J., and Kim, K. H. (2015). Five questions about mycoviruses. *PLoS Pathog*. 11:e1005172. doi: 10.1371/journal.ppat.1005172

Spatafora, J. W., Chang, Y., Benny, G. L., Lazarus, K., Smith, M. E., Berbee, M. L., et al. (2016). A phylum-level phylogenetic classification of zygomycete fungi based on genome-scale data. *Mycologia* 108, 1028–1046. doi: 10.3852/16-042

Stamatakis, A. (2014). RAxML version 8: a tool for phylogenetic analysis and post-analysis of large phylogenies. *Bioinformatics* 30, 1312–1313. doi: 10.1093/bioinformatics/btu033

Stano, M., Beke, G., and Klucar, L. (2016). viruSITE - integrated database for viral genomics. *Database* 2016:baw162. doi: 10.1093/database/baw162

Takeda, I., Tamano, K., Yamane, N., Ishii, T., Miura, A., Umemura, M., et al. (2014). Genome sequence of the Mucoromycotina fungus *Umbelopsis isabellina*, an effective producer of lipids. *Genome Announc*. 2:e00071-14. doi: 10.1128/genomeA.00071-14

Urayama, S., Takaki, Y., and Nunoura, T. (2016). FLDS: a comprehensive dsRNA sequencing method for intracellular RNA virus surveillance. *Microbes Environ*. 31, 33–40. doi: 10.1264/jsme2.ME15171

Vágvölgyi, C., Magyar, K., Papp, T., Vastag, M., Ferenczy, L., Hornok, L., et al. (1998). Detection of double-stranded RNA molecules and virus-like particles in different *Mucor* species. *Ant. Van Leeuwenhoek* 73, 207–210. doi: 10.1023/A:1000515905099

Vágvölgyi, C., Varga, J., and Ferenczy, L. (1993). Detection of double-stranded RNA in *Mucor ramannianus*. *Fungal Genet. Rep*. 40:79. doi: 10.4148/1941-4765.1422

Vainio, E. J., Pennanen, T., Rajala, T., and Hantula, J. (2017). Occurrence of similar mycoviruses in pathogenic, saprotrophic and mycorrhizal fungi inhabiting the same forest stand. *FEMS Microbiol. Ecol*. 93:fix003. doi: 10.1093/femsec/fix003

Conflict of Interest Statement: The authors declare that the research was conducted in the absence of any commercial or financial relationships that could be construed as a potential conflict of interest.

frontiers in Cellular and Infection Microbiology

ORIGINAL RESEARCH
published: 12 July 2019
doi: 10.3389/fcimb.2019.00244

Extreme Diversity of Mycoviruses Present in Isolates of *Rhizoctonia solani* AG2-2 LP From *Zoysia japonica* From Brazil

Maria Aurea S. C. Picarelli[1†], *Marco Forgia*[2,3†], *Eliana B. Rivas*[4], *Luca Nerva*[3,5], *Marco Chiapello*[3], *Massimo Turina*[3] *and Addolorata Colariccio*[1*]

[1] Plant Virology Laboratory, Instituto Biológico, São Paulo, Brazil, [2] Department of Life Science and System Biology, University of Turin, Turin, Italy, [3] Institute for Sustainable Plant Protection, CNR, Turin, Italy, [4] Phytopathological Diagnostic Laboratory, Instituto Biológico, São Paulo, Brazil, [5] Council for Agricultural Research and Economics—Research Centre for Viticulture and Enology CREA-VE, Conegliano, Italy

OPEN ACCESS

Edited by:
Dee Carter,
University of Sydney, Australia

Reviewed by:
James A. Fraser,
University of Queensland, Australia
Yen-Ping Hsueh,
Academia Sinica, Taiwan
Jessie Uehling,
University of California, Berkeley,
United States

***Correspondence:**
Addolorata Colariccio
colariccio@biologico.sp.gov.br

[†]These authors have contributed equally to this work

Specialty section:
This article was submitted to Fungal Pathogenesis, a section of the journal Frontiers in Cellular and Infection Microbiology

Received: 28 February 2019
Accepted: 21 June 2019
Published: 12 July 2019

Citation:
Picarelli MASC, Forgia M, Rivas EB, Nerva L, Chiapello M, Turina M and Colariccio A (2019) Extreme Diversity of Mycoviruses Present in Isolates of Rhizoctonia solani AG2-2 LP From Zoysia japonica From Brazil. Front. Cell. Infect. Microbiol. 9:244. doi: 10.3389/fcimb.2019.00244

Zoysia japonica, in Brazil, is commonly infected by *Rhizoctonia solani* (*R. solani*) in humid and cool weather conditions. Eight isolates of *R. solani*, previously identified as belonging to the AG2-2 LP anastomosis group, isolated from samples from large path symptoms, were collected from three counties in São Paulo state (Brazil) and investigated for the presence of mycoviruses. After detection of double-strand RNA (dsRNA) in all samples, RNA_Seq analysis of ribosomal RNA-depleted total RNA from *in vitro* cultivated mycelia was performed. Forty-seven partial or complete viral unique RNA dependent-RNA polymerase (RdRp) sequences were obtained with a high prevalence of positive sense ssRNA viruses. Sequences were sufficiently different from the first match in BLAST searches suggesting that they all qualify as possible new viral species, except for one sequence showing an almost complete match with Rhizoctonia solani dsRNA virus 2, an alphapartitivirus. Surprisingly four large contigs of putative viral RNA could not be assigned to any existing clade of viruses present in the databases, but no DNA was detected corresponding to these fragments confirming their viral replicative nature. This is the first report on the occurrence of mycoviruses in *R. solani* AG2-2 LP in South America.

Keywords: mycoviruses, *Rhizoctonia solani*, grass, multiple infection, viral diversity, phylogenetic analysis, virus taxonomy

INTRODUCTION

Zoysia japonica (*Z. japonica*) Steud, especially from the cultivar "Esmeralda", comprises 81% of the cultivated grasses in Brazil (Zanon, 2015). In 2015, the sod production of cultivated grasses reached 24,000 hectares (Antoniolli, 2015), which is an increase of 40% between 2010 and 2015 (Zanon, 2015). Nevertheless, it is very susceptible to the large patch disease caused by the fungus *Rhizoctonia solani* (*R. solani*) AG 2-2 LP, considered the most important disease of zoysia grass worldwide. Disease control is difficult, and practices employed in management are hardly effective, also, because fungicides are not approved on public areas, or home gardens. Considering these obstacles, biological control agents are desirable alternatives for disease management thanks to their environmental safety.

Since the first report in the 1960s, mycoviruses were searched for and found in many classes of phytopathogenic fungi, mostly because some mycoviruses can reduce the capacity of fungi to cause disease and may have the potential application as biological control agents. More recently, mycoviruses were also shown to be important for their environmental role and for modulating intra and inter-species interactions (Drinnenberg et al., 2011; Nerva et al., 2017, 2018a; Chun et al., 2018), possibly mediated by complex tripartite symbiotic relationships (Marquez et al., 2007). Not all the viruses associated with fungal pathogens affect virulence, but some can indeed cause hypovirulence, as is the case of the classic model system Cryphonectria hypovirus 1, infecting *Cryphonectria parasitica* (Nuss, 2005; Turina and Rostagno, 2007), or the association between Rhizoctonia solani partitivirus 2 (RsPV2) and *R. solani* AG-1 IA causing hypovirulence on rice (Zheng et al., 2014).

The presence of double-stranded RNAs (dsRNAs) is evidence of a mycovirus infection, which have been reported in many phytopathogenic fungi species and in different anastomosis groups from various hosts of *R. solani* (Strauss et al., 2000; Bharathan et al., 2005; Das et al., 2016; Zheng et al., 2018). More recently, ssDNA viruses were also shown to infect phytopathogenic fungi (Yu et al., 2010).

Nowadays, most approaches used to characterize fungal viruses rely on Next-Generation Sequencing (NGS) of total RNA depleted of ribosomal RNA or sequencing of small RNA (Vainio et al., 2015; Marzano and Domier, 2016; Marzano et al., 2016; Donaire and Ayllon, 2017). We directly compared the two methods in previous work and found that NGS of total RNA provides a more complete characterization of fungal associated viruses (Nerva et al., 2016).

Mycoviruses in single and mixed infections have been previously detected in *R. solani*: Rhizoctonia solani virus 717 (*Betapartitivirus*), Rhizoctonia solani RNA virus HN008, Rhizoctonia solani dsRNA virus 1, Rhizoctonia solani partitivirus 2, and Rhizoctonia solani flexivirus 1 (unclassified virus) (Zhong et al., 2015; Bartholomäus et al., 2016; Zheng et al., 2018). Moreover, recently, a plant virus—cucumber mosaic virus—was shown to accumulate and replicate in *R. solani* (Andika et al., 2017). Further NGS characterization of *R. solani*-associated viromes were performed on samples from USA (Marzano et al., 2016) and from samples from Germany (Bartholomäus et al., 2016).

In a preliminary screen, we detected the presence of dsRNAs in eight asymptomatic Brazilian *R. solani* AG2-2 LP isolates, a pathogen of *Z. japonica,* from three counties of São Paulo state (Picarelli, 2015). All the dsRNA electrophoretic patterns showed 3–6 bands with different sizes, all >2 kbp, and a fragment >8 kbp (Picarelli, 2015). These complex electrophoretic patterns could be due to the presence of segmented viral genomes, mixed infections, or defective dsRNAs. In this study, we aimed to characterize the virome associated with *R. solani*, isolated from *Z. japonica* grass that were positive in a preliminary dsRNA screen, to gather the first information about the diversity and the spread of mycoviruses in *R. solani* in different Brazilian regions. Although none of the isolates under scrutiny were hypovirulent, such a library of mycoviruses could be the basis for a targeted virus-induced gene silencing (VIGS) approach.

MATERIALS AND METHODS

Fungal Isolates Origin and Growth Conditions

Z. japonica sheaths, showing large patch symptoms, were collected in three municipalities of São Paulo State, Brazil: Cotia (isolates IBRS07, IBRS15, IBRS16, and IBRS19), São Paulo (isolates IBRS04, IBRS22, and IBRS23), and Ilhabela (isolate IBRS11) (**Supplementary Figure 1**, online). All *R. solani* samples were collected from diseased patches of zoysia grass lawns showing the same characteristics. The eight *R. solani* AG2-2 LP isolates were maintained on potato dextrose agar medium at 25°C, for a 12 h photoperiod (Picarelli, 2015). Long-term conservation of the fungal isolates was obtained by growing the fungi on paper strips stored at −80°C or lyophilised mycelia after growth on potato dextrose broth and stored at −20°C.

RNA Extraction, DNA Extraction, and cDNA Synthesis

Total RNA was extracted from 0.1 g of lyophilised fungal mycelium using the Spectrum™ Plant Total RNA Kit (Sigma-Aldrich, Darmstadt, Germany), according to the manufacturer's instructions. Copy DNA (cDNA) synthesis was performed using the High-Capacity cDNA Reverse Transcription Kit (Thermo Fisher Scientific, Waltham, MA, USA) as described in the kit's manual. DNA extraction was performed by breaking 50 mg of lyophilised mycelia in a bead beater, using 0.5 mm diameter glass beads, in a 2 mL Eppendorf tube with 700 μL of phenol and 700 μL of 2x STE-2%SDS. After centrifugation, the supernatant was collected and washed twice with chloroform-isoamyl alcohol, 24:1. The supernatant was then precipitated with 2 volumes of 100% ethanol and 0.1 volumes of 3 M sodium acetate, pH 5.2. The pellet was resuspended in 50 μL of H_2O, quantified with a Nanodrop 2000 (Thermo Fisher Scientific, Waltham, USA) and diluted to 10 ng/μL for PCR applications.

Library Preparations and Bioinformatic Analysis

Ribosomal RNA depletion, library preparations and Illumina sequencing were performed by Macrogen (Seoul, Republic of Korea); the assembly and virus identification steps were performed as previously described (Nerva et al., 2018b), where we have specified the details of commands and scripts used for each bioinformatics analysis step. Briefly, reads from RNA-Seq were assembled *de novo* using Trinity version 2.3.2 (Haas et al., 2013). Trinity assembly was then BLASTed against a custom viral database (https://osf.io/c9x2p/) to identify contigs of viral origin. The number of reads covering the viral genomes was obtained by mapping the reads from each sequenced library on reference sequences with Burrows-Wheeler Aligner (BWA) and Samtools (Li and Durbin, 2009; Li et al., 2009). The mapping

TABLE 1 | List of viruses discovered in *Rhizoctonia solani* isolates from São Paulo State (Brazil).

Virus name		NCBI ID	Abbreviation	Segment length (bp)	No. of reads	BLASTx first hit	Ident	Query cover
Rhizoctonia solani endornavirus 4		MK393902	RsEV4	20,215	23,587	Endornavirus-like virus	35.16	23
Rhizoctonia solani endornavirus 5		MK393903	RsEV5	16,227	6,414	Rhizoctonia cerealis alphaendornavirus 1	47.31	36
Rhizoctonia solani endornavirus 6		MK393904	RsEV6	15,273	4,441	Morchella importuna endornavirus 2	45.18	49
Rhizoctonia solani endornavirus 7		MK393905	RsEV7	14,325	73,559	Rhizoctonia solani endornavirus 2	30.69	83
Rhizoctonia solani partitivirus 8	RNA1	MK532273	RsPV8	1,958	2,239	Rhizoctonia oryzae-sativae partitivirus 1	53.19	90
	RNA2	MK532274		778	178	Heterobasidion partitivirus 20	42.35	74
Rhizoctonia solani partitivirus 6	RNA1	MK507781	RsPV6	2,401	5,189	Fusarium poae partitivirus 2	50.96	90
	RNA2	MK507782		2,310	11,867	Rosellinia necatrix partitivirus 8	58.08	84
Rhizoctonia solani partitivirus 7	RNA1	MK507783	RsPV7	1,912	10,488	Trichoderma atroviride partitivirus 1	68.08	95
	RNA2	MK507784		1,867	3,218	Trichoderma atroviride partitivirus 1	31.69	86
Rhizoctonia solani dsRNA virus 2	RNA1	MK400668	RsdsRNA2	1,942	32,967	Rhizoctonia solani dsRNA virus 2	99.36	96
	RNA2	MK400669		1,727	16,114	Rhizoctonia solani dsRNA virus 2	98.77	84
Rhizoctonia solani bipartite-like virus 1	RNA1	MK492913	RsBLV1	1,827	279	Ceratobasidium mycovirus-like	71.50	69
	RNA2	MK492914		1,888	331	Ceratobasidium mycovirus-like	61.60	41
Rhizoctonia solani dsRNA virus 6		MK507788	RsdsRNA6	11,847	5,257	Rhizoctonia fumigata mycovirus	30.95	20
Rhizoctonia solani dsRNA virus 7		MK507789	RsdsRNA7	3,523	1,839	Rhizoctonia fumigata mycovirus	31.70	78
Rhizoctonia solani dsRNA virus 8		MK507790	RsdsRNA8	2,905	1,370	Rhizoctonia fumigata mycovirus	30.83	85
Rhizoctonia solani dsRNA virus 9		MK507791	RsdsRNA9	2,162	445	Rhizoctonia fumigata mycovirus	35.48	70
Rhizoctonia solani dsRNA virus 10		MK532272	RsdsRNA10	9,416	3,945	Sclerotium rolfsii mycovirus dsRNA 1	37.37	37
Rhizoctonia solani beny-like virus 1		MK507778	RsBeLV1	11,666	11,135	Sclerotium rolfsii beny-like virus 1	36.35	39
Rhizoctonia solani bunya/phlebo-like virus 1		MK507779	RsBPLV1	7,804	25,865	Barns Ness serrated wrack bunya/phlebo-like virus 1	30.56	60
Rhizoctonia solani flexi-like virus 1		MK507787	RsFLV1	2,982	1,848	Rhizoctonia solani flexivirus 2	70.50	27
Rhizoctonia solani alphavirus-like 1		MK507793	RsALV1	2,414	949	Rhizoctonia solani RNA virus 3	82.14	38
Rhizoctonia solani alphavirus-like 2		MK507792	RsALV2	3,396	509	Rhizoctonia solani RNA virus 1	69.38	27
Rhizoctonia solani alphavirus-like 3		MK507786	RsALV3	6,752	924	Rhizoctonia solani RNA virus 3	83.12	13
Rhizoctonia solani mitovirus 21		MK372892	RsMV21	4,100	20,0,8721	Rhizoctonia solani mitovirus 13	51.13	66
Rhizoctonia solani mitovirus 22		MK490928	RsMV22	2,177	27,09274	dsRNA viral RdRp (mitochondrion) [Thanatephorus cucumeris]	80.15	73
Rhizoctonia solani mitovirus 23		MK375261	RsMV23	2,792	16,946	Ceratobasidium mitovirus A	61.98	83
Rhizoctonia solani mitovirus 24		MK372893	RsMV24	2,149	7,52995	Macrophomina phaseolina mitovirus 2	85.48	75
Rhizoctonia solani mitovirus 25		MK372894	RsMV25	3,767	24,180	Macrophomina phaseolina mitovirus 3	38.49	43
Rhizoctonia solani mitovirus 26		MK372895	RsMV26	2,580	94,168	Rhizoctonia cerealis mitovirus	46.15	90
Rhizoctonia solani mitovirus 27		MK372896	RsMV27	3,176	11,379	Rhizoctonia cerealis mitovirus	50.42	77
Rhizoctonia solani mitovirus 28		MK372897	RsMV28	2,640	2,693	Rhizoctonia mitovirus 1	39.85	76
Rhizoctonia solani mitovirus 29		MK372898	RsMV29	2,904	56,286	Binucleate Rhizoctonia mitovirus K1	42.14	79
Rhizoctonia solani mitovirus 30		MK372899	RsMV30	2,760	3,461	Binucleate Rhizoctonia mitovirus K1	42.74	80
Rhizoctonia solani mitovirus 31		MK372900	RsMV31	3,820	16,05182	Rhizoctonia solani mitovirus 7	52.80	69
Rhizoctonia solani mitovirus 32		MK372901	RsMV32	3,409	14,32655	Rhizoctonia solani mitovirus 7	42.81	73
Rhizoctonia solani mitovirus 33		MK372902	RsMV33	2,733	50,5184	Rhizoctonia solani mitovirus 7	37.97	69
Rhizoctonia solani mitovirus 34		MK372903	RsMV34	3,389	10,356	Rhizoctonia solani mitovirus 11	44.00	71
Rhizoctonia solani mitovirus 35		MK490929	RsMV35	3,772	24,59926	Rhizoctonia solani mitovirus 13	43.70	67
Rhizoctonia solani mitovirus 36		MK490930	RsMV36	2,562	9,58130	Rhizoctonia solani mitovirus 13	54.90	71
Rhizoctonia solani mitovirus 37		MK372904	RsMV37	3,597	3,79328	Rhizoctonia solani mitovirus 15	51.06	69
Rhizoctonia solani mitovirus 38		MK372905	RsMV38	3,197	24,67420	dsRNA viral RdRp (mitochondrion) [Thanatephorus cucumeris]	45.42	66
Rhizoctonia solani ourmia-like virus 2		MK372906	RsOLV2	4,104	22,042	Rhizoctonia solani ourmia-like virus 1 RNA 1	78.18	44

(Continued)

TABLE 1 | Continued

Virus name	NCBI ID	Abbreviation	Segment length (bp)	No. of reads	BLASTx first hit	Ident	Query cover
Rhizoctonia solani ourmia-like virus 3	MK372907	RsOLV3	3,223	3,795	Rhizoctonia solani ourmia-like virus 1 RNA 1	76.59	57
Rhizoctonia solani ourmia-like virus 4	MK372909	RsOLV4	4,557	5,471	Rhizoctonia solani ourmia-like virus 1 RNA 1	48.96	34
Rhizoctonia solani ourmia-like virus 5	MK372908	RsOLV5	5,234	3,868	Agaricus bisporus virus 15	25.89	29
Rhizoctonia solani fusarivirus 1	MK558257	RsFV1	10,776	2,788	Rosellinia necatrix fusarivirus 2	40.00	25
Rhizoctonia solani fusarivirus 2	MK558256	RsFV2	10,710	36,543	Rosellinia necatrix fusarivirus 2	40.57	25
Rhizoctonia solani fusarivirus 3	MK558258	RsFV3	5,959	8,858	Fusarium graminearum dsRNA mycovirus-1	38.09	57
Rhizoctonia solani hypovirus 1	MK558259	RsHV1	18,371	86,930	Sclerotium rolfsii hypovirus 1	27.35	32
Rhizoctonia solani hypovirus 2	MK558260	RsHV2	9,606	4,582	Sclerotium rolfsii hypovirus 1	27.16	24
Rhizoctonia solani hypovirus 3	MK558255	RsHV3	5,518	1,553	Agaricus bisporus virus 2	28.49	18
Rhizoctonia solani putative virus 1	MK507780	RsPuV1	6,311	56,781	Lily symptomless virus	24.91	9
Rhizoctonia solani putative virus 2	MK507785	RsPuV2	7,137	18,568	Sanxia atyid shrimp virus 1	22.73	9
Rhizoctonia solani putative virus 3	MK532275	RsPuV3	7,214	3,662	Guarapuava tymovirus-like 1	31.91	9
Rhizoctonia solani putative virus 4	MK507793	RsPuV4	7,833	7,495	Gayfeather mild mottle virus	25.28	9

For each virus the NCBI code is reported together with the abbreviation used in the paper, segment length, number of reads mapping the segment, and first hit obtained from BLASTx analysis with query cover and identity percentages.

step was performed as explained in detail previously (Nerva et al., 2018b) with only one exception: the bwa mem algorithm was used for the alignment instead of bwa aln. Mapping results were displayed using Tablet (Milne et al., 2013). Viral contigs displaying incomplete open reading frames (ORFs) and cut reads on the 5′ or 3′ ends were analyzed using MITObim (Hahn et al., 2013) to attempt extending the incomplete 5′ and 3′ ends. After one iteration, the eventually extended sequences were used as a query for a BLAST search against the trinity assembly to find contigs overlapping the extended region. Identified contigs were assembled using the CAP3 sequence assembly program (Huang and Madan, 1999).

Quantitative RT-PCR Analysis

Primers for qRT-PCR were designed using Primer 3 (Untergasser et al., 2012), with the amplicon size between 70 and 120 bp. To associate specific RNA samples to each specific contig, qRT-PCR analysis were performed using a CFX Connect™ Real-Time PCR Detection System (Biorad, Hercules, USA). The PCR reaction was performed in 10 μL using the iTaq™ Universal SYBR® Green Supermix (Biorad, Hercules, USA). A melting curve analysis was performed at the end of the qRT-PCR protocol to check for unspecific PCR products. All the oligonucleotides used in the qRT-PCR protocol are reported in **Supplementary Table 1**, online.

ORF Prediction and Phylogenetic Analyses

ORF predictions were performed using the ORF finder tool from NCBI, and predictions were made selecting the "standard" genetic code for all viral contigs, except the one closely related to mitoviruses, generally hosted in the mitochondria. These contigs were analyzed selecting the "Mold, protozoan and coelenterate mitochondrial" genetic code. The putative function of the predicted protein was established by BLAST analysis, looking at the function of the closest proteins in the NCBI database. The predicted protein sequences were analyzed through a BLASTP search using the domain finder option to evaluate the presence of any conserved domain in the sequence (such as the viral polymerase GDD conserved domain). Phylogenetic analyses were performed by aligning the viral RNA dependent-RNA polymerase (RdRp) proteins with MUSCLE implemented in MEGA6 (Tamura et al., 2013). Alignments were exported in FASTA format and submitted to the IQ-TREE web server (Trifinopoulos et al., 2016) to produce Maximum likelihood phylogenetic trees (Lam-Tung et al., 2015). The best substitution model was estimated automatically by IQ-TREE with ModelFinder (Kalyaanamoorthy et al., 2017) and ultrafast bootstrap analysis (Diep Thi et al., 2018) in which 1000 replicates were performed. For each tree, each specific model is indicated in the figure legend.

Amplification and Cloning of Fragments From the Viral Genomes

To confirm the sequence of regions of interest in the assembled contigs, fragments from some of the viral genomes were amplified by designing PCR primers based on the *in silico* assembly and performing PCR reactions on cDNA produced as described above (**Supplementary Table 2**, online). Using electrophoresis, amplified bands were separated on an agarose gel. Cut bands were cleaned using Zymoclean Gel DNA Recovery Kit (Zymo Research, Irvine, USA), inserted in the pGEMT vector using pGEM®-T Easy Vector Systems (Promega, Madison, USA) and transformed in chemically competent *E. coli* DH5α (Mix & Go! E. coli Transformation kit, Zymo Research, Irvine, USA). Colonies that were positive for the insertion were selected for Sanger sequencing (Biofab S.r.l., Rome, Italy).

TABLE 2 | List of Ct (threshold cycles) obtained from qRT-PCR analysis for each viral genome segment in every fungal isolate investigated.

Viral contig		*Rhizoctonia solani* isolates							
		IBRS22	**IBRS23**	**IBRS04**	**IBRS07**	**IBRS11**	**IBRS15**	**IBRS16**	**IBRS19**
RsEV4					27			26	28
RsEV5		28	31	25	28			30	
RsEV6									27.8
RsEV7		25	24	22	24	24	24	23	24
RsPV6	RNA1		22						
	RNA2		19.4						
RsPV7	RNA1		24						
			27						
RsPV8	RNA1							23	
	RNA2							27	
RsdsRNA2	RNA1	24	29	22	27			29	24
	RNA2	29	30	21	26			25	23
RsBLV1	RNA1					28			
	RNA2					28.5			
RsdsRNA6		31	27	27.5	27.5			33	
RsdsRNA7			30	32	30			30	
RsdsRNA8			31	32	33			34	
RsdsRNA9			29	32				30	
RsdsRNA10		30	29		30	29		29	28
RsBeLV1									22
RsBPLV1			20.48						
RsFLV1					30				31
RsALV1									28.5
RsALV2			30			30			30
RsALV3			29						
RsMV21			15.5						
RsMV22			18		18	16			30
RsMV23					14.5				
RsMV24		26	24	29	25	23	25.5	26	24
RsMV25				26					
RsMV26				25					
RsMV27				27					
RsMV28									21
RsMV29		24.5	22.5	28	22	21	21.5	22.5	22.5
RsMV30									21.3
RsMV31					14				
RsMV32			15						
RsMV33				25					
RsMV34				29					
RsMV35				27	29				17
RsMV36			18						
RsMV37			22	28	23	23			
RsMV38			17		16		34		
RsOLV2			20			16		26	21
RsOLV3					24				28
RsOLV4		30.5	25		25			30.5	27
RsOLV5					24.44				
RsFV1							26		

(Continued)

TABLE 2 | Continued

Viral contig	*Rhizoctonia solani* isolates							
	IBRS22	IBRS23	IBRS04	IBRS07	IBRS11	IBRS15	IBRS16	IBRS19
RsFV2	26.5	25		25.5	24		26	26.5
RsFV3		29	29	29				28
RsHV1							33	19
RsHV2							23	
RsHV3							24.55	
RsPuV1	23	22	28	21.5		21	22	
RsPuV2							24	20
RsPuV3	29	26	34	25.5			26.5	26
RsPuV4				22				

Empty boxes have been left where no specific amplification curve was detected.

RESULTS AND DISCUSSION

A single sequencing run of the eight pooled *R. solani* isolates under scrutiny produced 167,355,298 total reads deposited in the SRA archive linked to BioProject PRJNA524447. After the Trinity run, a total of 89,779 contigs were assembled. A BLAST search of a custom prepared viral database identified a total of 56 putative viral contigs (**Table 1**). Among those, 44 contained the typical conserved motifs of a viral RdRp, which is essential for the replication of RNA viruses and often displays three conserved amino acids (GDD) that are crucial for the catalytic activity. Two are partial viral genomes, where the RdRp domain is probably located in the missing part, and one is a contig where the RdRp domain cannot be detected by search engines, but the protein sequence shows a similarity with the typical GDD RdRp domain from proteins belonging to the family *Hypoviridae*. Therefore, we identified at least 47 distinct viruses (**Table 1**). There were five contigs encoding Coat Protein (CP) of bipartite viruses, and finally four putative viral contigs, encoding for proteins of unknown function (ORFans). We then checked the association of each contig with each of the eight isolates using qRT-PCR specific for each fragment; the results are displayed in **Table 2**. The number of virus contigs/isolate varies from isolate IBRS15 containing 6 viral contigs to isolate IBRS23 containing 30 viral contigs.

A quantitative estimation of the abundance of each contig can also be inferred by the number of mapped reads on each segment (**Table 1**).

The retrieved contigs showing homology with RdRps fell in 6 from the 16 clades that accommodate the overall viral diversity of RNA viruses of invertebrates (Shi et al., 2016).

Narna-Levi Related Sequences

From the RNAseq assembly, we identified 22 sequences encoding for proteins showing high similarity with viruses from the Narna-levi clade (Shi et al., 2016). All these sequences encode for one ORF producing the putative RdRp; however, at least four of them were not complete. Since the RdRp domain was still detectable in the partial sequences, we included them in our phylogenetic analysis (**Figures 1**, **2**). The predicted protein alignment and phylogenetic analysis showed that 18 sequences appeared to be part of the genus *Mitovirus*, while the 4 remaining were strongly related to ourmia-like viruses, but not included in the currently recognized *Narnavirus* genus. Thus, sequences were named as Rhizoctonia solani mitovirus 21 to 38 and Rhizoctonia solani ourmia-like virus 2 to 5, since previous work had already identified Rhizoctonia solani mitoviruses and ourmia-like viruses (Lakshman et al., 1998; Bartholomäus et al., 2016; Marzano et al., 2016). The amino acid sequence identity against the first hit in a BLAST search ranged from 80% (in the case of RsMV22 and a dsRNA viral element discovered in the same species) to 25.89% (in the case of RsOLV5 and Agaricus bisporus virus 15). From the phylogenetic tree (**Figure 1**), it is possible to observe that the mitoviruses detected in *R. solani* gather in four distinct sub-clades. Furthermore, we confirmed the necessity to revise the overall taxonomy of Levi-Narna viruses: the putative order Narnavirales should be established with a number of families, including the *Narnaviridae* (with the current *Narnavirus* genus) and the proposed/putative Mitoviridae (the current *Mitovirus* genus). The proposed new family Mitoviridae should be subdivided into a number of genera, including plant and fungal mitoviruses (Nibert et al., 2018; Nerva et al., 2019). The fact that most *R. solani* mitoviruses fall in the same three clades is probably due to the fact that mitoviruses are located and replicate in the host mitochondria and interspecific transmission does not easily occur in nature. Nevertheless, at least four clades mixed with viruses from ascomycetes and basidiomycetes occur, suggesting that some horizontal transfer can still occur. Further pairwise comparison among the distinct viral contigs from the Trinity assembly showed that RsMV 21 and 36 and RsMV 28 and 30 were almost completely identical (98 and 100% at the nucleotide (nt) level, respectively, for the two pairs in the conserved regions), but RsMV28 had a 120-nt deletion in position 504 of the genome. Rhizoctonia solani mitovirus 22 encodes for an RdRp showing 80% identity with the ORF characterized from a dsRNA element isolated from a hypovirulent strain of *R. solani* in 1998 (Lakshman et al., 1998). Since this sequence is still annotated in the NCBI database, as

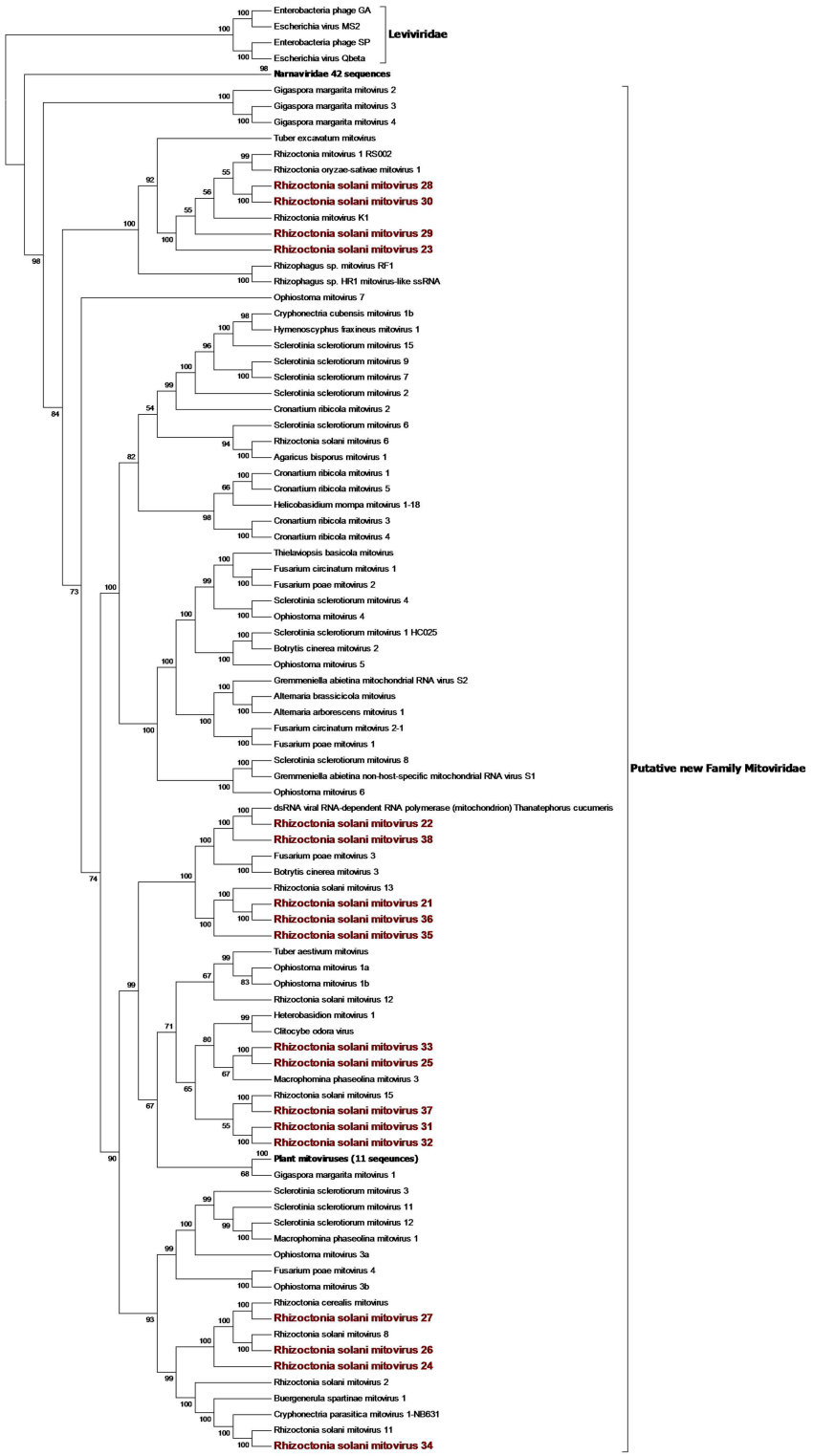

FIGURE 1 | Phylogenetic analysis of positive sense RNA viruses related to the genus *Mitovirus*. 142 sequences have been used to produce an alignment starting from viruses belonging to the family *Narnaviridae*, *Botourmiaviridae,* and *Leviviridae* as outgroup; the phylogenetic tree was built using the maximum likelihood method, the best choice for the substitution model according to ModelFinder was PMB+F+I+G4. Ultrafast bootstrap analysis was performed with 1,000 replicates, and branches displaying values below 50 were collapsed. Viruses discovered in this work are in bold red ink; 42 sequences belonging to the *Narnaviridae* family have been compressed in one branch. A list of accession numbers of the sequences used for this analysis can be found in **Supplementary Table 3**, online. Detailed information about softwares used for the analysis can be found in the material and methods section.

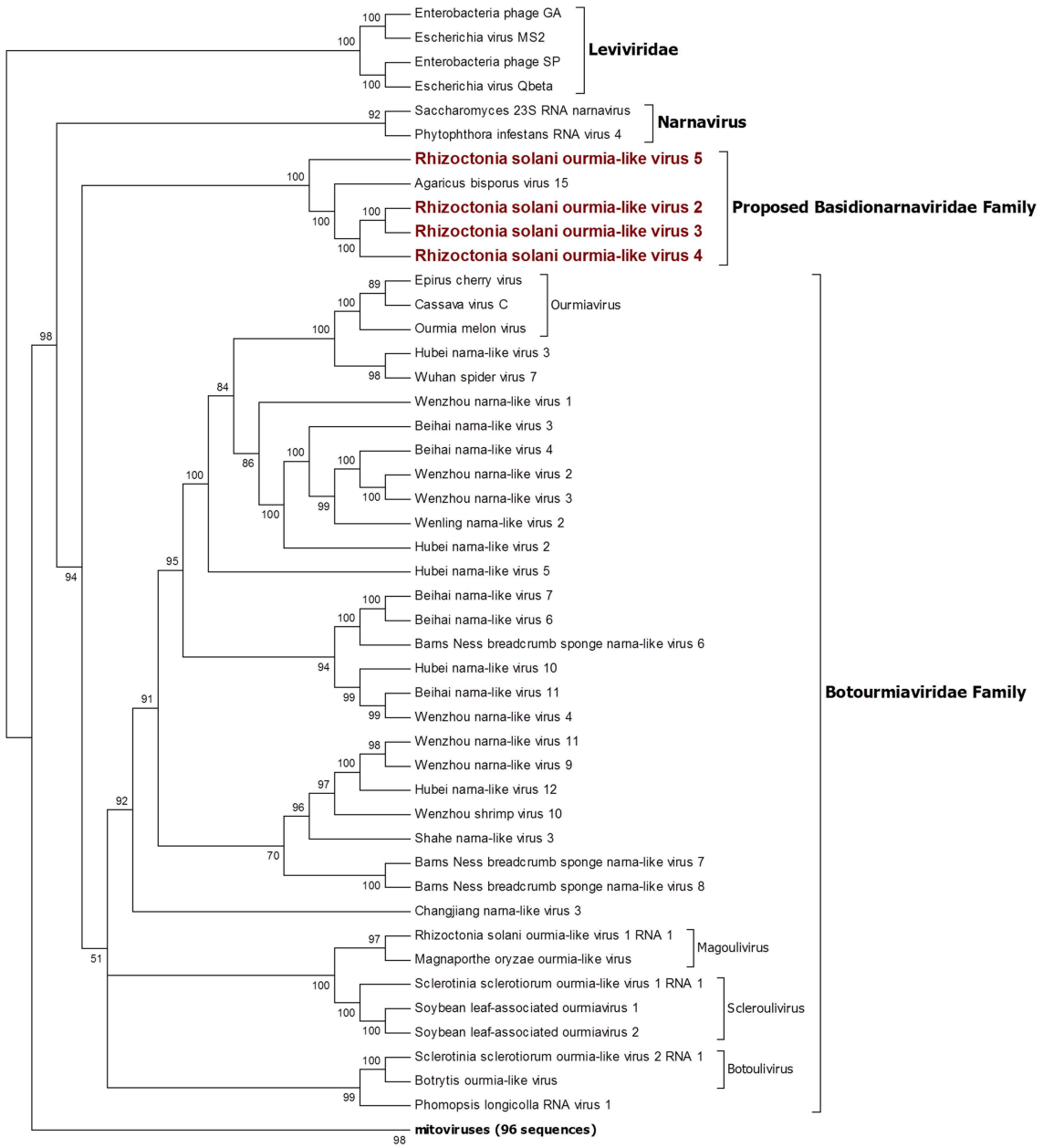

FIGURE 2 | Phylogenetic analysis of positive sense RNA viruses related to the genus *Botourmiaviridae*. 142 sequences have been used to produce an alignment starting from viruses belonging to the family *Narnaviridae*, *Botourmiaviridae,* and *Leviviridae* as outgroup; phylogenetic tree was built using the maximum likelihood method the best choice for the substitution model according to ModelFinder was PMB+F+I+G4. Ultrafast bootstrap analysis was performed with 1,000 replicates, and branches displaying values below 50 were collapsed. Viruses discovered in this work are in bold red ink; 96 sequences belonging to the genus *Mitovirus* have been compressed in one branch. A list of accession numbers of the sequences used for this analysis can be found in **Supplementary Table 3**, online. Detailed information about softwares used for the analysis can be found in the material and methods section.

a viral dsRNA element located in the fungal mitochondria, we decided to submit our sequence assigning it to a viral name. In previous work, the presence of ectopic DNA fragments derived from mitoviruses, infecting a fungal host (*Gigaspora margarita*), was detected but their function is still uncharacterised (Turina et al., 2018), contrary to analogous cDNA fragments found in insects and involved in anti-viral defense (Goic et al., 2016). Furthermore, RsMV22 is closely related to the viral dsRNA element isolated by Lakshman and co-authors in 1998, where a DNA stage was reported. To search for indications of mitovirus-derived DNA sequences in our samples, we analyzed DNAs extracted from the eight *R. solani* isolates by qPCR using the same primers used for the detection of the viruses (by qRT-PCR) after the bioinformatic analysis. No evidence of amplification

was observed (data not shown). We designed primers for PCR amplification of around 300 base pair fragments on the genome of RsMV22, RsMV21, and RsMV24. Also, in this case, we were able to amplify and clone the fragments in *E. coli* using the cDNA template and confirming the sequence, while no amplification was observed using extracted DNA as template. A 300 bp fragment was amplified and also cloned for RsOLV5, demonstrating the presence of the viral sequence only in the cDNA and not in the genomic DNA. Overall, we could not provide evidence of the existence of DNA fragments corresponding to the *R. solani* mitovirus in the isolates we tested.

The four viruses named Rhizoctonia solani ourmia-like virus 2 to 5 were grouped together with the fungal ourmia-like viruses, with Agaricus bisporus virus 15 as the closest hit in a BLAST search (**Figure 2**). Putative RdRp produced by RsOLV 2 and RsOLV 3 showed a 77% identity between them, and therefore, they are likely different isolates of the same species. A recent proposal grouped fungal ourmiaviruses together with plant ourmiaviruses in a new family called *Botourmiaviridae*; inside this family, three different genera containing fungal ourmiaviruses are established: *Botoulivirus*, *Magoulivirus,* and *Scleroulivirus* (**Figure 2**). Our phylogenetic analysis shows that the new species identified in our study are part of a distinct clade containing also Agaricus bisporus virus 15, which appears to be basal to the proposed *Botourmiaviridae* family, therefore, posing the ground for a new virus family for which we propose the name Basidionarnaviridae, since currently it contains members infecting basidiomycetes.

Hepe-Virga Group

Our bioinformatics pipeline unveiled four contigs encoding a single ORF showing similarity with viruses belonging to the *Endornaviridae* family. Phylogenetic analysis (**Figure 3**) on the predicted proteins shows that viral contigs are grouped together with viruses from the genus *Alphaendornavirus*, thus, we renamed the sequences as Rhizoctonia solani endornavirus 4 to 7. All the proteins predicted from the viral contigs show an RdRp domain, and proteins encoded from RsEV4, RsEV6, and RsEV7 also showed a helicase domain. A methyl-transferase domain was detected only in RsEV5 protein. In general, our endornavirus phylogenetic tree showed differences with the current taxonomic organization of this family, that we think requires an update to recognize new genera inside the family. *Endornavirus* RsEV4, RsEV6, and RsEV7 constitute a new clade that could possibly turn into a new genus, for which we propose the name Gammaendornavirus (**Figure 3**).

A single 11.666-nt-long contig was identified as a new virus; an ORF prediction and BLAST analysis showed similarities with other characterized beny-like mycoviruses. Thus, the contig was named Rhizoctonia solani beny-like virus 1 (**Figure 4**). PCR with specific primers for RsBLV1 allowed us to amplify a 274 bp fragment from cDNA obtained from the infected isolates, while no specific amplification was observed on DNA extracted from the same isolate. Similarly to the still unpublished Sclerotium rolfsii beny-like virus 1, RsBLV1 encodes for one single ORF producing a 3,584-amino acid-long protein showing a viral helicase domain and an RdRp domain. Other beny-like mycoviruses like Agaricus bisporus virus 8 and 13 show three ORFs that were not detected in RsBLV1.

Four contigs showed high similarity with viruses encoding ORFs with an RdRp domain belonging to the alphavirus supergroup (Wolf et al., 2018). Among these, a 2,982-nt-long contig encodes for an ORF displaying an RdRp domain and a viral helicase domain. BLAST and phylogenetic analysis show that the closest viruses to this contig is Rhizoctonia solani flexivirus 2, and these two viruses probably belong to the newly characterized genus *Deltaflexivirus* (**Figure 5**). Viruses belonging to the genus *Deltaflexivirus* are supposed to encode small proteins in the 3-terminal part of the genome region and are usually around 8 kbp-long; all these characteristics were not observed in our contig or in the Rhizoctonia solani flexivirus 2 (Bartholomäus et al., 2016), but we cannot exclude that these two genomes are indeed partial. Taken together these considerations, we decided to name this virus Rhizoctonia solani flexi-like virus 1. The three remaining contigs belonged to viruses that we named Rhizoctonia solani alphavirus-like 1 to 3; RsAVL1 and RsAVL2 encode for uncomplete ORFs encoding RdRp, while the protein predicted from RsAVL3 seems to be a complete RdRp. Phylogenetic analysis (**Figure 5**) showed that these viruses are grouped together with three very small partial viral genomes discovered in *Rhizoctonia solani* (Rhizoctonia solani RNA virus 1 to 3) that have high homology with our sequences (Bartholomäus et al., 2016). Together with Sclerotinia sclerotiorum RNA virus L, these viruses form a distinct clade for which we propose a new family called Mycoalphaviridae. PCR amplification of overlapping fragments of around 800 bp from RsALV 3 confirmed the absence of the viral contig in the DNA of the host fungal isolate, confirming the viral nature of this segment.

Hypo Related Sequences

Six contigs showed a relationship to the *Hypoviridae* family (**Figure 6**). Among those, three contigs were closely related to the genus *Hypovirus*, while the remaining three were more similar to the still unclassified viruses generally called fusarivirus in a number of publications; identity percentages resulting from BLASTx analysis showed levels between 28.5 and 40.5% compared to the first hit. No other clearly correlated Rhizoctonia solani hypoviruses and fusariviruses were found in the literature. Thus, we named these contigs Rhizoctonia solani hypovirus 1 to 3 and Rhizoctonia solani fusarivirus 1 to 3. RsHV1 had an 18,371-bp-long genome. The ORF prediction showed just one large putative protein of 5,344 amino acids where only one helicase domain can be detected. RdRp domains could not be observed and no GDD amino acid triplet, the hallmark of most viral RdRps, was found in the protein sequence. Nevertheless, from the BLAST analysis, it was clear that the RsHV1 protein had homology with the region encoding for the GDD domain in other hypoviruses like Sclerotinia sclerotiorum hypovirus 2 (for which an RdRp domain was annotated), even though such domain is not detected by common domain searching software, such as CDD sparkle and ExPASy-PROSITE (Sigrist et al., 2013; Marchler-Bauer et al., 2017). According to the International Committee

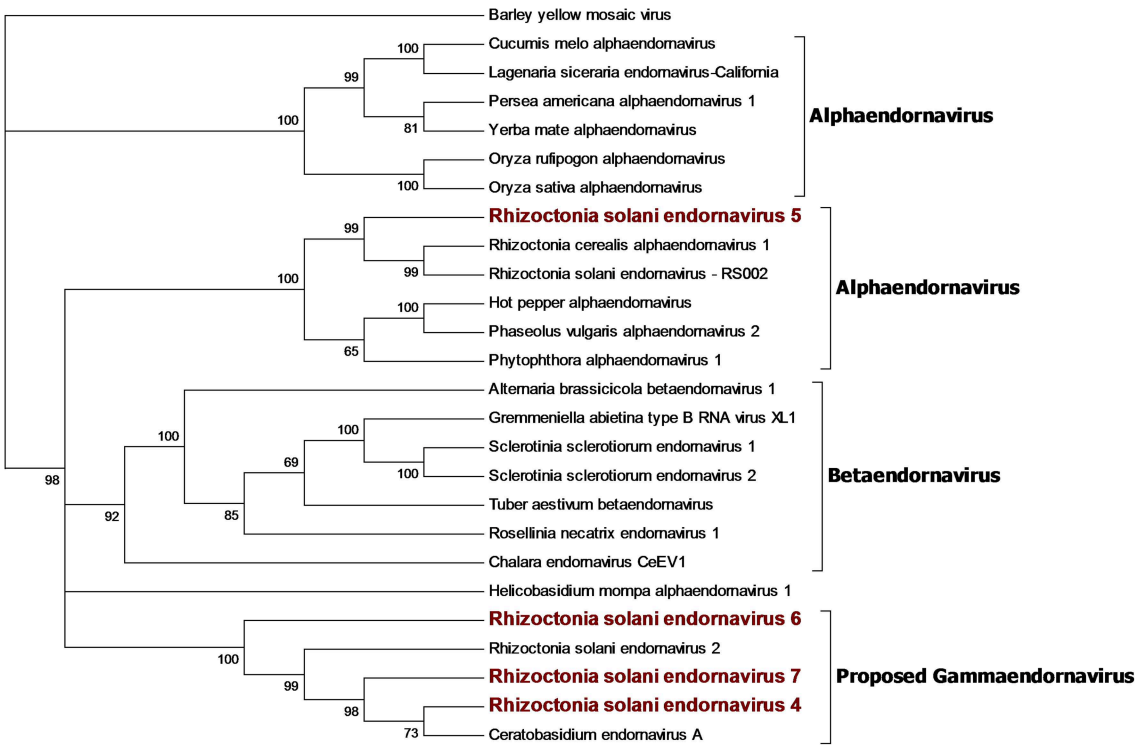

FIGURE 3 | Phylogenetic analysis of viruses belonging to the family *Endornaviridae*. Twenty six viral sequences were used to build the alignment. A phylogenetic tree was built using the maximum likelihood method and the best substitution model selected by ModelFinder was VT+F+I+G4. Ultrafast bootstrap analysis was performed with 1,000 replicates and branches displaying values below 50 were collapsed. Viruses discovered in this work are outlined in bold red. Barley yellow mosaic virus, belonging to the family *Potyviridae*, was used as outgroup. A list of accession numbers of the sequences used for this analysis can be found in **Supplementary Table 4**, online. Detailed information about softwares used for the analysis can be found in the material and methods section.

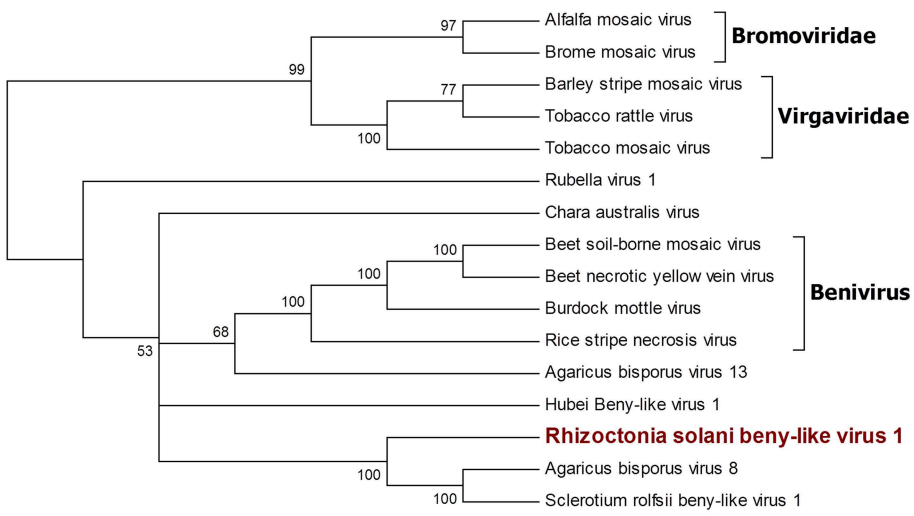

FIGURE 4 | Phylogenetic analysis of viruses belonging to the family *Benyviridae*. Sixteen viral sequences were aligned and a phylogenetic tree was derived using the maximum likelihood method. The best substitution model selected by ModelFinder was VT+F+I+G4. Ultrafast bootstrap analysis was performed with 1,000 replicates, and branches displaying values below 50 were collapsed. Viruses discovered in this work are outlined in bold red. *Bromoviridae* and *Virgaviridae* were used as outgroups. A list of accession numbers of the sequences used for this analysis can be found in **Supplementary Table 4**, online. Detailed information about softwares used for the analysis can be found in the material and methods section.

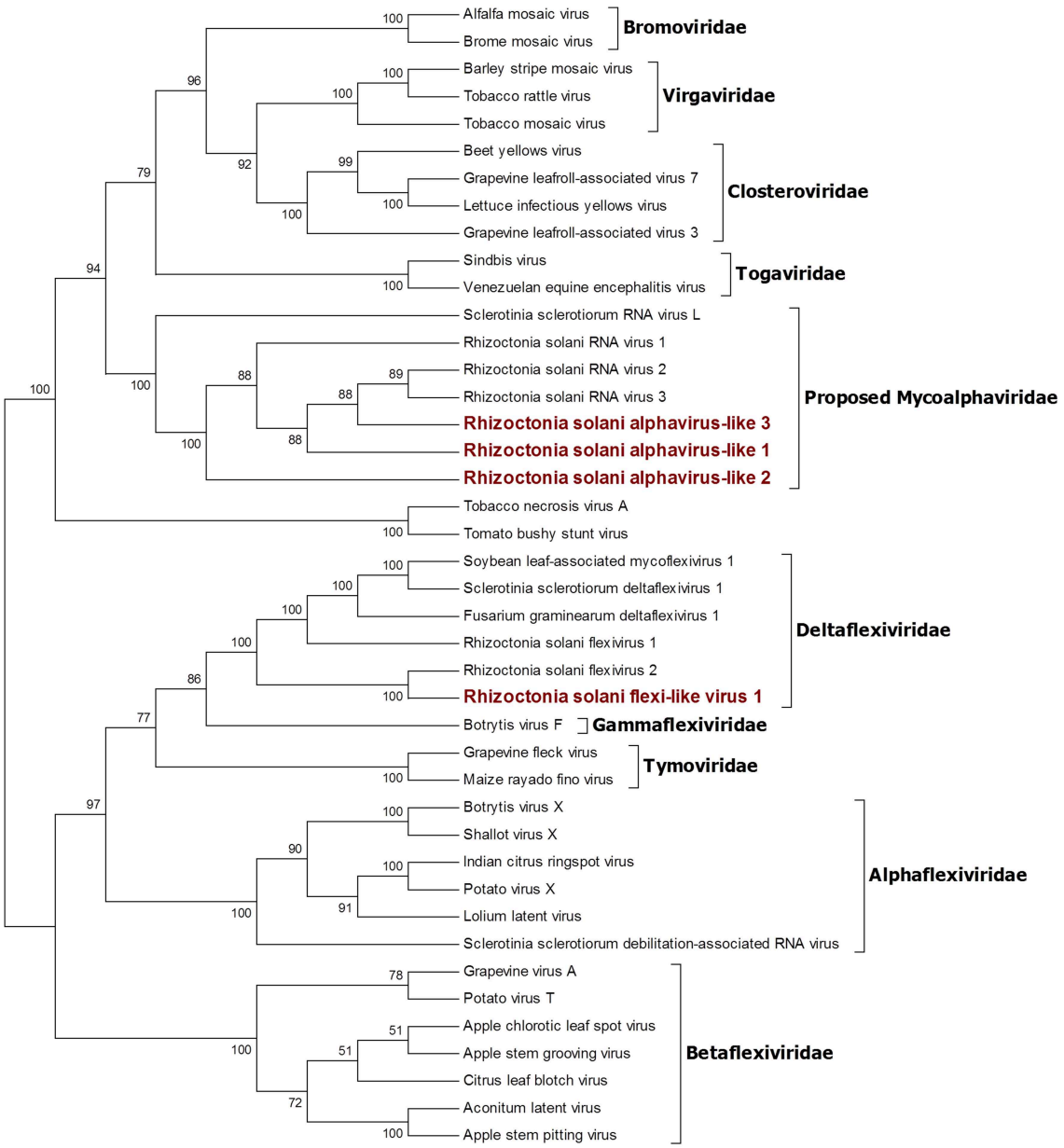

FIGURE 5 | Phylogenetic analysis of viruses related to the Alphavirus supergroup. Forty two sequences were aligned and a phylogenetic tree was built using the maximum likelihood method. The best substitution model selected by ModelFinder was VT+F+I+G4 and ultrafast bootstrap analysis was performed with 1,000 replicates. Branches displaying values below 50 were collapsed. Viruses discovered in this work are outlined in bold red ink. A list of accession numbers of the sequences used for this analysis can be found in **Supplementary Table 4**, online. Detailed information about softwares used for the analysis can be found in the material and methods section.

on Taxonomy of Viruses—ICTV description, hypoviruses have a genome dimension of 9.1–12.7 kb. On the contrary, RsHV1 has one of the longest genomes known so far for a putative hypovirus. RsHV2 is a 9,606-bp contig encoding for two ORFs, but the 3′ proximal-ORF appears to be incomplete. Both ORFs did not show any conserved motif, although the protein amino acid sequence BLASTs with viruses belonging to the genus *Hypovirus*. RsHV3 is 5,518-bp-long with an ORF prediction which underlined two putative proteins of which the 3'proximal ORF was likely an incomplete protein displaying a viral helicase domain. No RdRp domain could be detected in this case, and no conserved domains were observed on the 5' distal ORF. Alignments performed to produce a phylogenetic tree showed that RsHV1 and RsHV3 could be aligned on the helicase domain, and that the phylogenetic tree resulting from the analysis show a clade containing RsHV1, RsHV2,

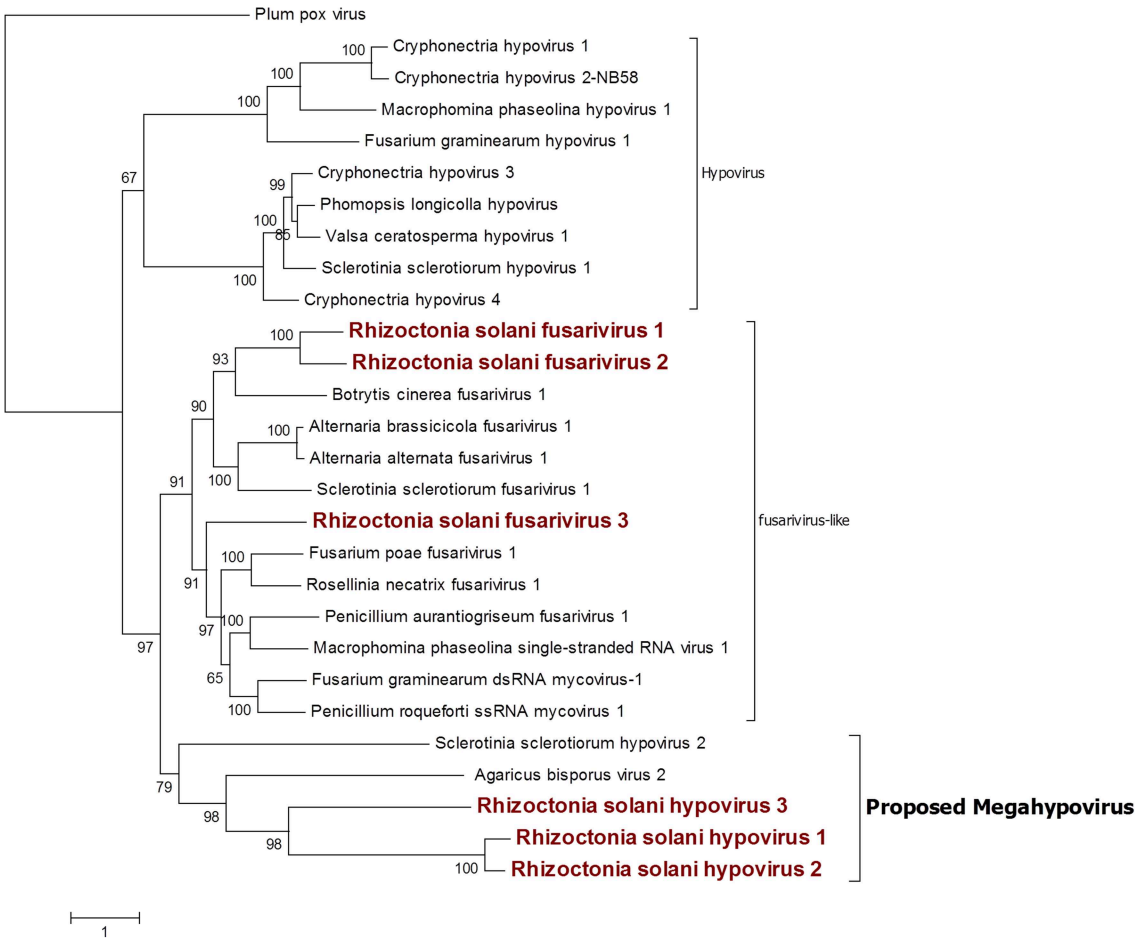

FIGURE 6 | Phylogenetic analysis of viruses related to the family *Hypoviridae*. Twenty eight sequences were used to build an alignment and to derive a phylogenetic tree using the maximum likelihood method. The best substitution model selected by ModelFinder was VT+F+G4 and an ultrafast bootstrap analysis was performed with 1,000 replicates. Viruses discovered in this work are outlined in bold red. Plum pox virus, belonging to the family *Potyviridae*, was used as outgroup. A list of accession numbers of the sequences used for this analysis can be found in **Supplementary Table 5**, online. Detailed information about softwares used for the analysis can be found in the material and methods section.

RsHV3 related to a hypovirus from *Agaricus bisporus* (Agaricus bisporus virus 2) and Sclerotinia sclerotiorum hypovirus 2. These viruses are included in a statistically well supported clade that separates them from the current characterized fusariviruses and the members of the genus *Hypovirus* (**Figure 6**). For this reason, we propose here the name of a new genus (Megahypovirus) for the large size of the genomes of the two complete sequences so far characterized in this group (SsHV2 and RsHV1). The presence of RsHV3 was confirmed through RT-PCR amplification; we were able to amplify and clone a fragment of the expected size just in the cDNA produced from the infected fungal isolate, and nothing was observed in the DNA extracted from the same fungus—confirming its viral nature and that the transcript was not derived from an endogenised viral fragment.

Among the three fusariviruses discovered (**Figure 6**), RsFV1 was the longest one, as it had a 10,776-bp genome and the ORF prediction displayed four putative proteins. ORF 2 and 4 were the smallest: ORF 2 encoded a putative protein of 525 amino acids and ORF 4 encoded a putative protein of 578 amino acids. BLAST analysis and domain prediction could not find any convincing hit or conserved domain for both ORFs. ORF 1 was 731 amino acids long and it had a viral helicase domain, while the RdRp domain was found in ORF 3, together with another helicase domain. The same genome organization was observed for RsFV2, a 10,710-bp contig showing a PolyA site at the 3′ of the sequence and encoding for four putative proteins. In this virus, ORF 2 and 4 (472 and 718 amino acids, respectively) were short ORFs with no significant homology with other viral proteins. ORF1 had a viral helicase domain and ORF 3 had a helicase and an RdRp domain. Finally, RsFV3 was a 5959-bp contig encoding for just one protein. The predicted protein sequence showed helicase and RdRp domains as observed for the other two fusarivirus and a PolyA site at the 3′ end. As previously described, fusariviruses often encoded two ORFs, with the 5′-ORF encoding for the RdRp. The new viruses that we discovered

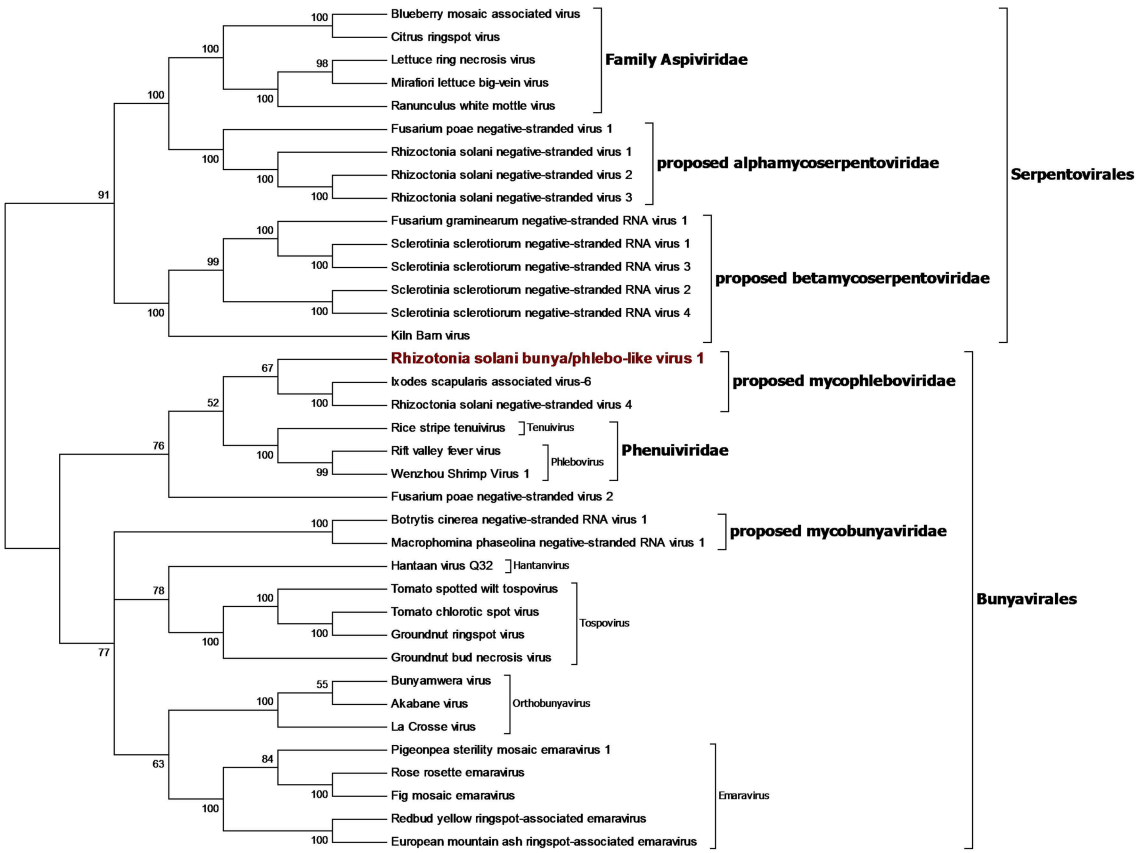

FIGURE 7 | Phylogenetic analysis of viruses related to the orders *Bunyavirales* and *Serpentovirales*. Thirty seven sequences were aligned and the best substitution model selected by ModelFinder was VT+F+G4 and implemented in a maximum likelihood method to derive the Phylogenetic tree. Ultrafast bootstrap analysis was performed with 1,000 replicates and branches displaying values below 50 were collapsed. The Virus discovered in this work is outlined in red. A list of accession numbers of the sequences used for this analysis can be found in **Supplementary Table 6**, online. Detailed information about software used for the analysis can be found in the material and methods section.

in this work presented some different characteristics that are peculiar for this group of viruses (four ORFs in RsFV1 and RsFV2). We decided to further investigate the ORF prediction of RsFV1 and RsFV2 by designing PCR primers and amplifying sequences overlapping the regions of discontinuity between the four ORFs to verify possible mistakes in the sequence. Cloned fragments were sequenced and compared to the viral genomes proving that the reference sequence assembled from Trinity was identical to the one amplified through PCR. Thus, the four proteins predicted cannot be due to an error in the RNAseq assembly. Phylogenetic analysis confirmed BLAST analysis and placed our three fusariviruses together with others already characterized in the same clade. We propose that currently recognized fusariviruses, based on their sequence length and genome organization, be subdivided into at least two further genera (**Figure 6**).

Bunya-Arena Like Sequences

We identified a contig encoding for a protein showing the RdRp domain from bunyaviruses and we named this contig Rhizoctonia solani bunya/phlebo-like virus 1. RsBPLV1 is 7,804 bp long and the putative RdRp is 2513 amino acids long. BLASTp analysis on the RdRp showed 30.59% identity with the closest virus in the database. Phylogenetic analysis previously carried out showed that the fungal negative single-strand RNA viruses belong to three orders: the order *Mononegavirales* and family *Mymonaviridae* (Liu et al., 2014), the order *Serpentovirales* which likely includes two families that we propose to name Alphamycoserpentoviridae and Betamycoserpentoviridae, and the order *Bunyavirales* that includes other mycoviruses. RsBPLV1 was clearly in this order, in our analysis (**Figure 7**). Nevertheless, two distinct new families that include mycoviruses can be proposed inside this order: for the one that includes RsBPLV1 we propose the name Mycophleboviridae, whereas for the other well supported clade, we propose the name Mycobunyaviridae.

Partiti-Picobirna Sequence Group

Contigs coding for proteins showing high homology with partitivirus RdRps were detected in our samples (**Figure 8**). From the initial BLAST analysis, Four contigs encoding for partitivirus RdRp and three contigs encoding for partitivirus coat proteins

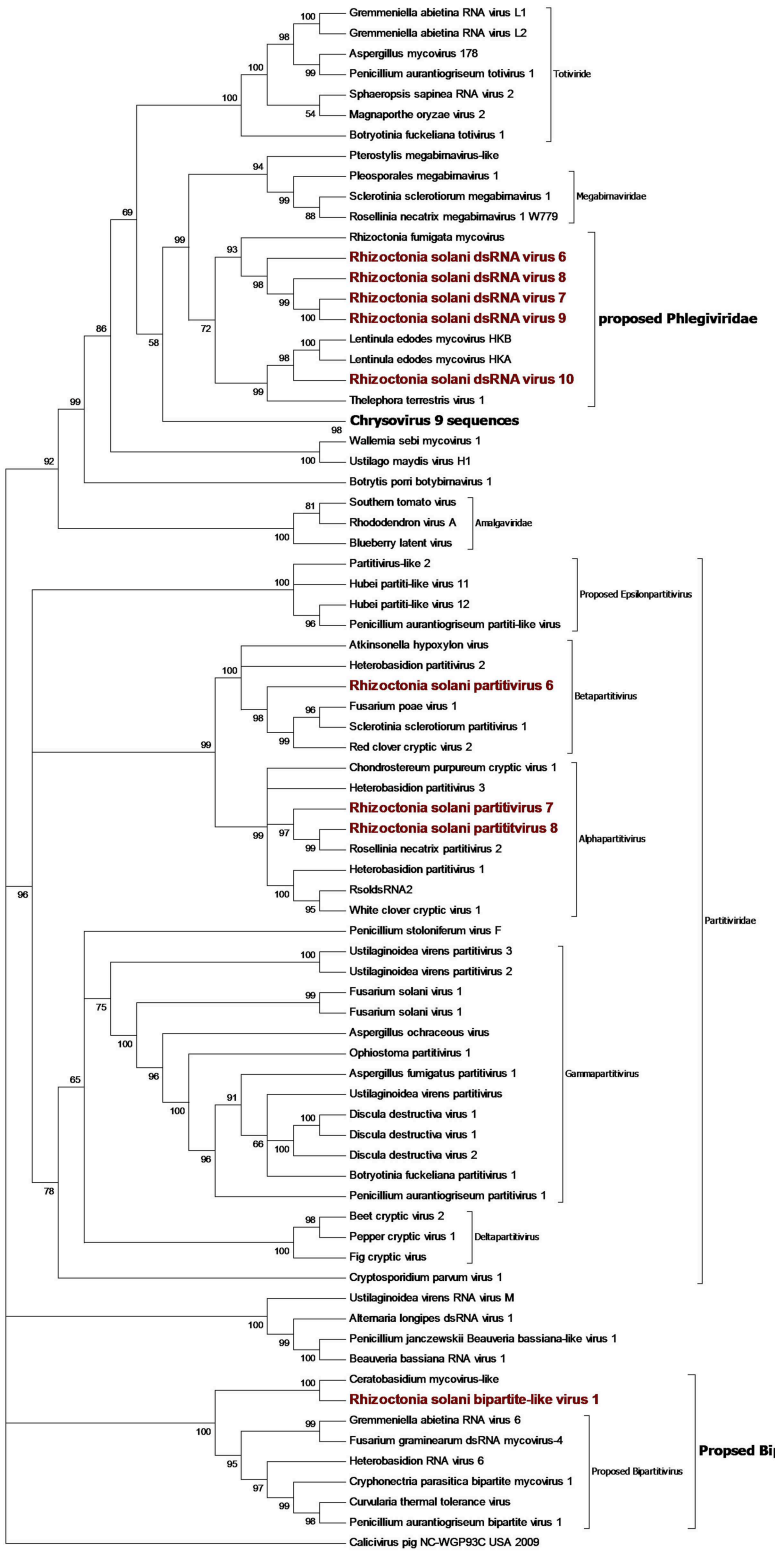

FIGURE 8 | Phylogenetic analysis of dsRNA viruses. Eighty four sequences were used to build an alignment. Phylogenetic tree was built using the maximum likelihood method, the best substitution model selected by ModelFinder was Blosum62+F+G4 and ultrafast bootstrap analysis was performed with 1,000 replicates, branches displaying values below 50 were collapsed. Viruses discovered in this work are underlined in red. A list of accession numbers of the sequences used for this analysis can be found in **Supplementary Table 7**, online. Detailed information about software used for the analysis can be found in the material and methods section.

were retrieved. Among these seven contigs, one encoding for an RdRp and one encoding for a coat protein were easily matched as part of the same virus since they showed almost complete identity with an already characterized virus belonging to the genus *Alphapartitivirus* called Rhizoctonia solani dsRNA virus 2. Indeed, these contigs were always detected in the same fungal isolates through qRT-PCR, confirming that these two segments belonged to the same virus. The remaining contigs were submitted to the NCBI database as Rhizoctonia solani partitivirus 6 to 8. RsPV7 and RsPV8 RdRps were part of the genus *Alphapartitiviruses*, while RsPV6 belonged to the group hosting viruses from the genus *Betapartitivirus* (**Figure 8**). A correct correlation between RdRp and coat protein of RsPV6 and RsPV7 have been complicated by the fact that the two viruses were found in the same fungal isolate in our collection. Thus, we grouped together the two RNAs attributed to RsPV7 because the RdRp protein and the coat protein produced from the two segments had as a first BLAST hit the same two proteins from a single viral species called Trichoderma atroviride partitivirus 1 (**Table 1**). No RNA2 producing coat protein was detected initially for RsPV8, but we tried to look for the missing genome segment by a direct TBLASTn search on the RNAseq assembly using as a query the coat protein sequence from the virus whose RdRp is more similar to RsPV8 RdRp. We were able to find a short contig producing a protein that showed homology with partitivirus coat proteins, however, the coverage of this contig is low and attempts to extend the sequence with MITObim were not successful. Nevertheless, qRT-PCR analysis confirmed the presence of the contig only in the fungal isolate hosting the RsPV8 RNA1 fragment. Taken together, we submitted to Genbank the contig as RsPV8's partial RNA2.

Two short contigs of 1827 and 1888 bp were found as part of the same viral genome, where the 1827-bp contig encoded a single incomplete ORF producing a protein showing homology with RdRp from viruses with a bipartite genome related to a partitivirus that we have previously described (Nerva et al., 2016), and provisionally named bipartite viruses. The 1888-bp segment codes for a hypothetical protein, showing homology with the same virus group. Phylogenetic analysis (**Figure 8**) placed this virus basal to the virus group already proposed in literature as bipartite (Nerva et al., 2016), thus, we decided to rename this virus *R. solani* bipartite-like virus 1.

Toti-Chryso

Five contigs encoded for putative RdRp with similarities to viruses belonging to the Toti-Chryso group (**Figure 8**). These contigs were renamed Rhizoctonia solani dsRNA virus 6 to 10, and phylogenetic analysis grouped these viruses together in a clade containing unclassified viruses related to the genus *Megabirnavirus*. This clade has already been proposed to form a new genus called Phlegivirus by previous work (Petrzik et al., 2016). Here, we show that such taxon comprises two genera, and therefore, we propose the family Phlegiviridae to include both of them (**Figure 8**). Rhizoctonia solani dsRNA 6 and 10 showed two ORFs; the first was a protein of unknown function, and the second ORF encoded for the RdRp. The RsdsRNA6 genome was 11,847 bp long: the first ORF was 2,300 amino acids long and the RdRp was a smaller protein of 1,125 amino acids. RsdsRNA 10 was 9,416 nt-long. The first ORF was 1,636 amino acids long, while the predicted RdRp was a 1,475-amino acid protein. No clear conclusion about genome organization of RsdsRNA 7 to 9 could be drawn since all three genomic segments encoded for a single ORF, the putative RdRps. Furthermore, RsdsRNA 9 ORF was partial, while for the other two ORFs, a stop codon could be detected. Since these three contigs were much shorter compared to the closest viruses according to the phylogenetic analysis, we can assume that they are probably incomplete. So far, attempts to extend the viral contigs were unsuccessful. PCR amplification of a target fragment from RsdsRNA10 gave positive results only when using the cDNA of the infected isolate as a template, while no PCR amplification was observed from total DNA, once again suggesting that the RNA was not derived from transcription of endogenised viral fragments.

ORFans Fragments

Four fragments resulting from our bioinformatic pipeline were detected as viral but could not be located in any known taxonomical group, and no evidence of an RdRp domain was detected in these sequences. We called these contigs Rhizoctonia solani putative virus 1 to 4. RsPuV 1 was a 6,311-bp-long sequence, and the ORF encoded showed a conserved viral helicase domain, which has similarities with viruses from different groups like *Tymovirus* and *Endornaviruses*. Rhizoctonia solani putative virus 2 was 7,137 bp long, and in this case, the 2,083-amino acid long protein only had a conserved viral helicase motif. Rhizoctonia solani putative virus 3 had a 7,713-bp sequence, encoding for a 2,011-amino acid long uncomplete protein, showing a viral methyl transferase domain. BLAST analysis showed little homology with viruses from the genus *Tymovirus*. Rhizoctonia solani putative virus 4 had a 7,833-bp sequence coding for an ORF resulting in a putative 2,414-amino acid protein with a viral helicase domain. In each of these sequences, the homology with other viruses is always located on the small part of the protein showing the conserved domain (helicase and methyltransferase); thus, it is hard to hypothesize a specific taxonomic placement for these viral sequences. Indications that these fragments are of viral origin also comes from the fact that no DNA was detected corresponding to these fragments using DNA as template for PCR amplification (**Supplementary Figure 2**, online). We confirmed the presence of these putative virus RNA fragments through RT-PCR using cDNA as a template, which resulted in bands of the expected size. We cannot exclude that some of these viral fragments are part of a multipartite virus that has escaped our detection or are associated with one of the viruses we have described in this paper.

CONCLUSIONS

In the present study we reported sequences corresponding to mostly new viral species belonging to the positive sense ssRNA genome virus groups (*Mitovirus*, *Botourmiaviridae*, *Hypovirus*, *Endornavirus*, Hepe-Virga-like), and to dsRNA virus groups such as the *Alphapartitivirus* and *Gammapartitivirus*. Furthermore,

a single negative strand virus in the *Bunyavirales* was also characterized in our collection.

The number of viral species infecting each *R. solani* isolates ranged from 6 (IBRS 15) to 27 (IBRS23). The mitoviruses RsMV24 and RsMV29, and the endornavirus RsEV7, were the most prevalent viruses since they occurred in all the isolates. However, some mycoviruses were detected in only one isolate of *R. solani*: RsMV21, RsMV23, RsMV25, RsMV26, RsMV27, RsMV28, RsMV30, RsMV31, RsMV36, RsEV6, RsPV6, RsPV7, RsPV8, RsBPLV1, RsBLV1, RsBeLV1, RsALV3, RsOLV5, RsPuV4, RsFV1, RsHV2, and RsHV3.

Successful uses of mycoviruses have already been reported for the biological control of *C. parasitica* (Nuss, 1992) in natural conditions. Some promising hypovirulent strains were also detected for *Ophiostoma novo-ulmi* (Hong et al., 1999), *Fusarium graminearum* (Chu et al., 2002), *Botrytis cinerea* (Wu et al., 2007), and *Rosellinea necatrix* (Chiba et al., 2009).

The ability of fungi to cause disease in the host plant seems to not be affected by the wide diversity of the viral species detected in the same *Rhizoctonia* isolates, since all the isolates induced the same kind of symptoms in the *Z. japonica* host. Indeed, in greenhouse tests, the isolates IBRS11, IBRS19, and IBRS23 were the most pathogenic, while the isolate IBRS15 was the least pathogenic (Picarelli et al., in review). We could not correlate virus distribution to the geographical distribution of the isolates (**Supplementary Figure 1**, online), and it is surprising that the comprehensive characterization of the three viromes associated with *R. solani* so far have only a minimal overlap of identical sequences (Bartholomäus et al., 2016; Marzano et al., 2016). Nevertheless, some new taxonomical groups that include mostly *R. solani* viruses were common to the various studies as was the case of some subclades in the *Mitovirus* genus, the proposed Gammaendornavirus genus, the proposed Mycoalphaviridae family and the proposed Phlegiviridae family. Our study helps to define two completely new clades of mycoviruses, the proposed genus Megahypovirus and the family Basidiourmiaviridae.

DATA AVAILABILITY

The datasets generated for this study can be found in GenBank, MK393902, MK393903, MK393904, MK393905, MK532273, MK532274, MK507781, MK507782, MK507783, MK507784, MK400668, MK400669, MK492913, MK492914, MK507788, MK507789, MK507790, MK507791, MK532272, MK507778, MK507779, MK507787, MK507793, MK507792, MK507786, MK372892, MK490928, MK375261, MK372893, MK372894, MK372895, MK372896, MK372897, MK372898, MK372899, MK372900, MK372901, MK372902, MK372903, MK490929, MK490930, MK372904, MK372905, MK372906, MK372907, MK372909, MK372908, MK507780, MK507785, MK532275, MK507793, MK558257, MK558256, MK558258, MK558259, MK558260, MK558255, and Bioproject PRJNA524447.

AUTHOR CONTRIBUTIONS

MP collected the samples, characterized the fungal isolates, checked their virulence, and extracted dsRNA. MF extracted the total RNA, carried out all the virus annotation, carried out RT-PCR and PCR, mapped reads on the genome, carried out the phylogenetic analysis, and wrote the manuscript. ER curated virus nomenclature and classification, and carried out some phylogenetic analyses and edited the manuscript. LN carried out the initial bionformatic virome characterization. MC extended the genome segments with MitoBIM. MT edited the manuscript and supervised LN, MC, and MF. AC supervised MP, planned the experiments and edited the manuscript and deposited sequences in the databases with ER.

SUPPLEMENTARY MATERIAL

The Supplementary Material for this article can be found online at: https://www.frontiersin.org/articles/10.3389/fcimb.2019.00244/full#supplementary-material

REFERENCES

Andika, I. B., Wei, S., Cao, C., Salaipeth, L., Kondo, H., and Sun, L. (2017). Phytopathogenic fungus hosts a plant virus: a naturally occurring cross-kingdom viral infection. *Proc. Natl. Acad. Sci. U.S.A.* 114, 12267–12272. doi: 10.1073/pnas.1714916114

Antoniolli, D. (2015). "Produção, regularização e conquistas do mercado de gramas cultivadas no Brasil," in *Tópicos atuais em gramados IV, VII SIGRA – Simpósio sobre Gramados. FCA/UNESP.* eds C.M.D'A. Mateus, R.L. Villas Bôas, T. F. Andrade, M.R. Oliveira, C. Backes, A.J.M. Santos, and L.J.G. Godoy (Botucatu: Editora Fepaf), 9–22.

Bartholomäus, A., Wibberg, D., Winkler, A., Pühler, A., Schlüter, A., and Varrelmann, M. (2016). Deep sequencing analysis reveals the mycoviral diversity of the virome of an avirulent isolate of *Rhizoctonia solani* AG-2-2 IV. *PLoS ONE* 11:e0165965. doi: 10.1371/journal.pone.0165965

Bharathan, N., Saso, H., Gudipati, L., Bharathan, S., and Whited, K. (2005). Double-stranded RNA: distribution and analysis among isolates of *Rhizoctonia solani* AG-2 to−13. *Plant Pathol.* 54, 196–203. doi: 10.1111/j.1365-3059.2005.01159.x

Chiba, S., Salaipeth, L., and Lin, Y. H. (2009). A novel bipartite double-stranded RNA mycovirus from the white root rot fungus *Rosellinia necatrix*: molecular and biological characterization, taxonomic considerations, and potential for biological control. *J. Virol.* 3, 12801–12812. doi: 10.1128/JVI.01830-09

Chu, Y. M., Jeon, J. J., Yea, S. J., Kim, Y. H., Yun, S. H., Lee, Y. W., et al. (2002). Double-stranded RNA mycovirus from *Fusarium graminearum*. *Appl. Environ. Microbiol.* 68, 2529–2534. doi: 10.1128/AEM.68.5.2529-2534.2002

Chun, J., Yang, H.-E., and Kim, D.-H. (2018). Identification of a novel *Partitivirus* of *Trichoderma harzianum* NFCF319 and evidence for the related antifungal activity. *Front. Plant Sci.* 9:1699. doi: 10.3389/fpls.2018.01699

Das, S., Fallon, R. E., Stewart, A., and Pitman, A. R. (2016). Novel mitoviruses in *Rhizoctonia solani* AG-3PT infecting potato. *Fungal Biol.* 120, 338–350. doi: 10.1016/j.funbio.2015.11.002

Diep Thi, H., Chernomor, O., von Haeseler, A., Minh, B. Q., and Le Sy, V. (2018). UFBoot2: improving the ultrafast bootstrap approximation. *Mol. Biol. Evol.* 35, 518–522. doi: 10.1093/molbev/msx281

Donaire, L., and Ayllon, M. A. (2017). Deep sequencing of mycovirus-derived small RNAs from *Botrytis* species. *Mol. Plant Pathol.* 18, 1127–1137. doi: 10.1111/mpp.12466

Drinnenberg, I. A., Fink, G. R., and Bartel, D. P. (2011). Compatibility with killer explains the rise of RNAi-deficient fungi. *Science* 333, 1592–1592. doi: 10.1126/science.1209575

Goic, B., Stapleford, K. A., Frangeul, L., Doucet, A. J., Gausson, V., Blanc, H., et al. (2016). Virus-derived DNA drives mosquito vector tolerance to arboviral infection. *Nat. Commun.* 7:12410. doi: 10.1038/ncomms12410

Haas, B. J., Papanicolaou, A., Yassour, M., Grabherr, M., Blood, P. D., Bowden, J., et al. (2013). *De novo* transcript sequence reconstruction from RNA-Seq: reference generation and analysis with Trinity. *Nat. Protoc.* 8, 1094–1515. doi: 10.1038/nprot.2013.084

Hahn, C. L., Bachmann, B., and Chevreux, B. (2013). Reconstructing mitochondrial genomes directly from genomic next-generation sequencing reads-a baiting and iterative mapping approach. *Nucleic Acids Res.* 41:e129. doi: 10.1093/nar/gkt371

Hong, Y. G., Dover, S. L., Cole, T. E., Brasier, C. M., and Buck, K. W. (1999). Multiple mitochondrial viruses in an isolate of the Dutch elm disease fungus *Ophiostoma novo-ulmi*. *Virology* 258, 118–127. doi: 10.1006/viro.1999.9691

Huang, X. Q., and Madan, A. (1999). CAP3: a DNA sequence assembly program. *Genome Res.* 9, 868–877. doi: 10.1101/gr.9.9.868

Kalyaanamoorthy, S., Bui Quang, M., Wong, T. K. F., von Haeseler, A., and Jermiin, L. S. (2017). ModelFinder: fast model selection for accurate phylogenetic estimates. *Nat. Methods* 14, 587–589. doi: 10.1038/nmeth.4285

Lakshman, D. K., Jian, J. H., and Tavantzis, S. M. (1998). A double-stranded RNA element from a hypovirulent strain of *Rhizoctonia solani* occurs in DNA form and is genetically related to the pentafunctional AROM protein of the shikimate pathway. *Proc. Natl. Acad. Sci. U.S.A.* 95, 6425–6429. doi: 10.1073/pnas.95.11.6425

Lam-Tung, N., Schmidt, H. A., von Haeseler, A., and Bui Quang, M. (2015). IQ-TREE: a fast and effective stochastic algorithm for estimating maximum-likelihood phylogenies. *Mol. Biol. Evol.* 32, 268–274. doi: 10.1093/molbev/msu300

Li, H., and Durbin, R. (2009). Fast and accurate short read alignment with Burrows-Wheeler transform. *Bioinformatics* 25, 1754–1760. doi: 10.1093/bioinformatics/btp324

Li, H., Handsaker, B., Wysoker, A., Fennell, T., Ruan, J., Homer, N., et al. (2009). Genome project data the sequence alignment/map format and SAMtools. *Bioinformatics* 25, 2078–2079. doi: 10.1093/bioinformatics/btp352

Liu, L., Xie, J., Cheng, J., Fu, Y., Li, G., Yi, X., et al. (2014). Fungal negative-stranded RNA virus that is related to bornaviruses and nyaviruses. *Proc. Natl. Acad. Sci. U.S.A.* 111, 12205–12210. doi: 10.1073/pnas.1401786111

Marchler-Bauer, A., Bo, Y., Han, L., He, J., Lanczycki, C. J., Lu, S., et al. (2017). CDD/SPARCLE: functional classification of proteins via subfamily domain architectures. *Nucleic Acids Res.* 45, D200–D203. doi: 10.1093/nar/gkw1129

Marquez, L. M., Redman, R. S., Rodriguez, R. J., and Roossinck, M. J. (2007). A virus in a fungus in a plant: three-way symbiosis required for thermal tolerance. *Science* 315, 513–515. doi: 10.1126/science.1136237

Marzano, S.-Y., Nelson, B. D., Ajayi-Oyetunde, O., Bradley, C. A., Hughes, T. J., Hartman, G. L., et al. (2016). Identification of diverse mycoviruses through metatranscriptomics characterization of the viromes of five major fungal plant pathogens. *J. Virol.* 90, 6846–6863. doi: 10.1128/JVI.00357-16

Marzano, S.-Y. L., and Domier, L. L. (2016). Novel mycoviruses discovered from metatranscriptomics survey of soybean phyllosphere phytobiomes. *Virus Res.* 213, 332–342. doi: 10.1016/j.virusres.2015.11.002

Milne, I., Stephen, G., Bayer, M., Cock, P. J., Pritchard, L., Cardle, L., et al. (2013). Using Tablet for visual exploration of second-generation sequencing data. *Brief. Bioinform.* 14, 193–202. doi: 10.1093/bib/bbs012

Nerva, L., A., Silvestri, M., Ciuffo, S., Palmano, G. C., and Varese, G. C., Turina, M. (2017). Transmission of *Penicillium aurantiogriseum* partiti-like virus 1 to a new fungal host (*Cryphonectria parasitica*) confers higher resistance to salinity and reveals adaptive genomic changes. *Environ. Microbiol.* 19, 4480–4492. doi: 10.1111/1462-2920.13894

Nerva, L., Varese, G. C., and Turina, M. (2018b). Different approaches to discover mycovirus associated to marine organisms. *Methods Mol. Biol.* 1746, 97–114. doi: 10.1007/978-1-4939-7683-6_8

Nerva, L. G., Vigani, D., Di Silvestre, M., Ciuffo, M., Forgia, W., Chitarra, W., et al. (2019). Biological and molecular characterization of *Chenopodium quinoa* mitovirus 1 reveals a distinct sRNA response compared to cytoplasmic RNA viruses. *JVI.* 93, e01998–18. doi: 10.1128/JVI.01998-18

Nerva, L. M., Ciuffo, M., Vallino, P., Margaria, G. C., Varese, G. C., Gnavi, G., et al. (2016). Multiple approaches for the detection and characterization of viral and plasmid symbionts from a collection of marine fungi. *Virus Res.* 219, 22–38. doi: 10.1016/j.virusres.2015.10.028

Nerva, L. W., Chitarra, I., Siciliano, F., Gaiotti, M., Ciuffo, M., Forgia, M., et al. (2018a). Mycoviruses mediate mycotoxin regulation in *Aspergillus ochraceus*. *Environ. Microbiol.* 21, 1957–1968. doi: 10.1111/1462-2920.14436

Nibert, M. L., Vong, M., Fugate, K. K., Debat, H. J. (2018). Evidence for contemporary plant mitoviruses. *Virology* 518, 14–24. doi: 10.1016/j.virol.2018.02.005

Nuss, D. L. (1992). Biological control of chestnut blight: an example of virus-mediated attenuation of fungal pathogenesis. *Microbiol.* 56, 561–576.

Nuss, D. L. (2005). Hypovirulence: mycoviruses at the fungal-plant interface. *Nat. Rev. Microbiol.* 3, 632–642. doi: 10.1038/nrmicro1206

Petrzik, K., Sarkisova, T., Starý, J., Koloniuk, I., Hrabáková, L., and Kubešová, O. (2016). Molecular characterization of a new monopartite dsRNA mycovirus from mycorrhizal *Thelephora terrestris* (Ehrh.) and its detection in soil oribatid mites (Acari: Oribatida). *Virology* 489, 12–19. doi: 10.1016/j.virol.2015.11.009

Picarelli, M. A. S. C. (2015). *Estudo de micovirus em Rhizoctonia solani como estratégia para controle biológico de rizoctoniose em gramados* (dissertation). São Paulo (SP): Instituto Biológico. Available at: http://www.biologico.agricultura.sp.gov.br/pos/uploads/files/pdf/2015/aurea.pdf (accessed November 24, 2018).

Shi, M., Lin, X.-D., Tian, J.-H., Chen, L.-J., Chen, X., Li, C.-X., et al. (2016). Redefining the invertebrate RNA virosphere. *Nature* 540, 539–543. doi: 10.1038/nature20167

Sigrist, C. J. A., Castro, E., de, Cerutti, L., Cuche, B. A., Hulo, N., Bridge, A., et al. (2013). New and continuing developments at PROSITE. *Nucleic Acids Res.* 41, E344–E347. doi: 10.1093/nar/gks1067

Strauss, E. E., Lakshman, D. K., and Tavantzis, S. M. (2000). Molecular characterization of the genome of a partitivirus from the basidiomycete *Rhizoctonia solani*. *J. Gen. Virol.* 81, 549–555. doi: 10.1099/0022-1317-81-2-549

Tamura, K., Stecher, G., Peterson, D., Filipski, A., and Kumar, S. (2013). MEGA6: molecular evolutionary genetics analysis version 6.0. *Mol. Biol. Evol.* 30, 2725–2729. doi: 10.1093/molbev/mst197

Trifinopoulos, J., Lam-Tung, N., von Haeseler, A., and Minh, B. Q. (2016). W-IQ-TREE: a fast online phylogenetic tool for maximum likelihood analysis. *Nucleic Acids Res.* 44, W232–W235. doi: 10.1093/nar/gkw256

Turina, M., Ghignone, S., Astolfi, N., Silvestri, A., Bonfante, P., and Lanfranco, L. (2018). The virome of the *Arbuscular mycorrhizal* fungus *Gigaspora margarita* reveals the first report of DNA fragments corresponding to replicating non-retroviral RNA viruses in Fungi. *Environ. Microbiol.* 20:2012–2025. doi: 10.1111/1462-2920.14060

Turina, M., and Rostagno, L. (2007). Virus-induced hypovirulence in Cryphonectria parasitica: still an unresolved conundrum. *J. Plant Pathol.* 89, 165–178.

Untergasser, A., Cutcutache, I., Koressaar, T., Ye, J., Fairclothm, B. C., Remm, M., et al. (2012). Primer3-new capabilities and interface. *Nucleic Acid Res.* 40:e115. doi: 10.1093/nar/gks596

Vainio, E. J., Jurvansuu, J., Streng, J., Rajamaki, M. L., Hantula, J., and Valkonen, J. P. T. (2015). Diagnosis and discovery of fungal viruses using deep

sequencing of small RNAs. *J. Gen. Virol.* 96, 714–725. doi: 10.1099/jgv.0.000003

Wolf, Y. I., Kazlauskas, D., Iranzo, J., Lucia-Sanz, A., Kuhn, J. H., Krupovic, M., et al. (2018). Origins and evolution of the global RNA virome. *Mbio* 9:e02329–18. doi: 10.1128/mBio.02329-18

Wu, M. D., Zhang, L., Li, G. Q., Jiang, D. H., Hou, M. S., and Huang, H. C. (2007). Hypovirulence and double-stranded RNA in *Botrytis cinerea*. *Phytopathology* 97, 1590–1599. doi: 10.1094/PHYTO-97-12-1590

Yu, X., Li, B., Fu, Y., Jiang, D., Ghabrial, S. A., Li, G., et al. (2010). A geminivirus-related DNA mycovirus that confers hypovirulence to a plant pathogenic fungus. *Proc. Natl. Acad. Sci. U.S.A.* 107, 8387–8392. doi: 10.1073/pnas.0913535107

Zanon, M. E. (2015). *Desenvolvimento de grama "Esmeralda," grama bermudas "Tifway 410" e "Celebration" submetidas a aplicação de reguladores de crescimento* (Ph.D. thesis). Brazil: Universidade Estadual Paulista/UNESP, Jaboticabal.

Zheng, L., Liu, C., Zhang, M., Yang, M., and Zhou, E. (2018). Diversity of dsRNA viruses intecting rice sheat blight. *Rice Sci.* 25, 57–60. doi: 10.1016/j.rsci.2017.09.002

Zheng, L., Zhang, M., Chen, Q., Zhu, M., and Zhou, E. (2014). A novel mycovirus closely related to viruses in the genus *Alphapartitivirus* confers hypovirulence in the phytopathogenic fungus *Rhizoctonia solani*. *Virology* 456/457, 220–226. doi: 10.1016/j.virol.2014.03.029

Zhong, J., Chen, C. Y., and Gao, B. D. (2015). Genome sequence of a novel mycovirus of *Rhizoctonia solani*, a plant pathogenic fungus. *Virus Gene* 51, 167–170. doi: 10.1007/s11262-015-1219-4

Conflict of Interest Statement: The authors declare that the research was conducted in the absence of any commercial or financial relationships that could be construed as a potential conflict of interest.

frontiers in Cellular and Infection Microbiology

REVIEW
published: 18 July 2019
doi: 10.3389/fcimb.2019.00257

Mycoviruses in *Fusarium* Species: An Update

Pengfei Li†, *Pallab Bhattacharjee*†, *Shuangchao Wang, Lihang Zhang, Irfan Ahmed and Lihua Guo**

State Key Laboratory for Biology of Plant Diseases and Insect Pests, Institute of Plant Protection, Chinese Academy of Agricultural Sciences, Beijing, China

OPEN ACCESS

Edited by:
Daohong Jiang, Huazhong Agricultural University, China

Reviewed by:
Mingde Wu, Huazhong Agricultural University, China
Maria A. Ayllón, Polytechnic University of Madrid, Spain

***Correspondence:**
Lihua Guo
guolihua72@yahoo.com

†*These authors have contributed equally to this work*

Specialty section:
This article was submitted to Fungal Pathogenesis, a section of the journal Frontiers in Cellular and Infection Microbiology

Received: *28 February 2019*
Accepted: *03 July 2019*
Published: *18 July 2019*

Citation:
Li P, Bhattacharjee P, Wang S, Zhang L, Ahmed I and Guo L (2019) Mycoviruses in Fusarium Species: An Update. Front. Cell. Infect. Microbiol. 9:257. doi: 10.3389/fcimb.2019.00257

Fusarium is an important genus of plant pathogenic fungi, and is widely distributed in soil and associated with plants worldwide. The diversity of mycoviruses in *Fusarium* is increasing continuously due to the development and extensive use of state-of-the-art RNA deep sequencing techniques. To date, fully-sequenced mycoviruses have been reported in 13 *Fusarium* species: *Fusarium asiaticum*, *F. boothii*, *F. circinatum*, *F. coeruleum*, *F. globosum*, *F. graminearum*, *F. incarnatum*, *F. langsethiae*, *F. oxysporum*, *F. poae*, *F. pseudograminearum*, *F. solani,* and *F. virguliforme*. Most *Fusarium* mycoviruses establish latent infections, but some mycoviruses such as Fusarium graminearum virus 1 (FgV1), Fusarium graminearum virus-ch9 (FgV-ch9), Fusarium graminearum hypovirus 2 (FgHV2), and *Fusarium oxysporum* f. sp. dianthi mycovirus 1 (FodV1) cause hypovirulence. Rapid advances in various omics technologies used to elucidate genes or biological processes can facilitate an improved understanding of mycovirus-host interactions. The review aims to illuminate the recent advances in studies of mycoviruses in *Fusarium*, including those related to diversity, molecular mechanisms of virus-host interaction. We also discuss the induction and suppression of RNA silencing including the role of RNAi components as an antiviral defense response.

Keywords: *Fusarium*, mycovirus, mycovirus diversity, hypovirulence, mycovirus-host interactions, RNAi component

INTRODUCTION

According to the tenth report of the International Committee for Taxonomy of Viruses (ICTV), fungal viruses or mycoviruses have been classified into seven linear dsRNA virus families and one linear dsRNA virus genus (*Chrysoviridae*, *Endornaviridae*, *Megabirnaviridae*, *Quadriviridae*, *Partitiviridae*, *Reoviridae*, *Totiviridae*, and *Botybirnavirus*, respectively), six linear positive-sense ssRNA virus families (*Alphaflexiviridae*, *Barnaviridae*, *Deltaflexiviridae*, *Gammaflexiviridae*, *Hypoviridae*, and *Narnaviridae*), one linear negative-sense ssRNA virus family (*Mymonaviridae*), two reverse transcribing linear ssRNA virus families (*Metaviridae* and *Pseudoviridae*), and one circular ssDNA virus family (*Genomoviridae*) (Lefkowitz et al., 2018). No dsDNA mycoviruses have been isolated from fungi.

Mycoviruses are generally transmitted vertically via spores and horizontally via anastomosis, with one exception, Sclerotinia gemycircularvirus 1 (formerly named Sclerotinia sclerotiorum hypovirulence-associated DNA virus 1), which can extracellularly infect fungi (Yu et al., 2013). Although many mycoviruses show latent infections, some cause phenotypic alterations that reduce or increase the virulence of the host (hypo- or hypervirulence) (Nuss, 2005; Pearson et al., 2010; Jiang et al., 2013; Ghabrial et al., 2015). Fungal viruses causing hypovirulence attract much attention as potential candidates for the biological control of phytopathogenic fungal diseases and provide an opportunity to understand the interactions between mycoviruses and plant-pathogenic fungal hosts (Nuss, 2005; Xie and Jiang, 2014; Ghabrial et al., 2015). Because most viruses lack an extracellular replication phase, researchers have developed many transformation and transfection techniques using cDNA infectious clones (Choi and Nuss, 1992; Chen et al., 1993; Zhang et al., 2016), dsRNA (Stanway and Buck, 1984; Kanhayuwa et al., 2015), *in vitro*-transcribed RNA transcripts (Chen et al., 1994; Chen and Nuss, 1999; Moleleki et al., 2003; Lin et al., 2007; Marzano et al., 2015), and purified virions (Hillman et al., 2004; Sasaki et al., 2007). These techniques have accelerated the identification of host and/or viral factor(s) involved in the interactions between mycoviruses and their hosts (Son et al., 2015). These methods can also be used to extend the experimental host ranges of some mycoviruses, without the restriction of fungal vegetative incompatibility (Son et al., 2015).

Fusarium is a widely dispersed filamentous phytopathogenic fungus genus of the phylum *Ascomycota*, which causes serious damage to many field, ornamental, forest, and horticultural crops (Sharma et al., 2018). Many *Fusarium* species also produce mycotoxins such as trichothecenes and fumonisins that cause health problems in humans and livestock, and some of the greatest economic impacts are associated with deoxynivalenol (DON) and its derivatives (Munkvold, 2017). Many species of *Fusarium* also act as hosts for mycoviruses. Although many mycoviruses have been reported from different species of *Fusarium*, only a few isolates have a hypovirulent effect on their host, which is one of the major challenges to using mycoviruses efficiently as a biocontrol agent against *Fusarium* species. This review discusses recent advances in research related to mycoviruses infecting *Fusarium* species.

DIVERSE VIRUSES IN *FUSARIUM*

Due to the advancement and widespread use of next generation sequencing (NGS) techniques, knowledge of the diversity of known mycoviruses has rapidly increased in the past few years. To date, complete genome sequences are available for 29 mycoviruses, which have been identified from different species of *Fusarium* (**Table 1**), including 17 dsRNA viruses from six established or provisionally designated families (*Crysoviridae*, *Megabirnaviridae*, *Partitiviridae*, *Totiviridae*, Alternaviridae, Fusagraviridae) and one unassigned dsRNA group, 11 (+)ssRNA viruses from five established or provisionally designated families (*Deltaflexiviridae*, *Hypoviridae*, *Narnaviridae*, Fusariviridae, and Tymoviridae) and one unassigned (+)ssRNA group, and one (−)ssRNA virus from the family *Mymonaviridae*.

Double-Stranded RNA Mycoviruses

Family *Crysoviridae*

Three members of the family *Crysoviridae* have been isolated from *Fusarium*, Fusarium graminearum virus-ch9 (FgV-ch9) from *F. graminearum* strain China 9 (Darissa et al., 2011, 2012), Fusarium graminearum virus 2 (FgV2) from *F. graminearum* strain 98-8-60 (Chu et al., 2004; Yu et al., 2011), and *Fusarium oxysporum* f. sp. dianthi mycovirus 1 (FodV1) from *F. oxysporum* f. sp. dianthi strain 116 (Lemus-Minor et al., 2015). The genome of FgV-ch9 consists of five dsRNAs, denoted as dsRNA1 to dsRNA5, 3,581, 2,850, 2,830, 2,746, and 2,423 bp in size, respectively, each containing a single open reading frame (ORF). These five dsRNAs are encapsidated separately in unequal amounts. Among those five dsRNAs, dsRNA1 encodes the viral RNA-dependent RNA polymerase (RdRp), 127 kDa in size, dsRNA2, and dsRNA3 encode two structural proteins, 94 and 93 kDa, resptectively. FgV-ch9 dsRNA4 and dsRNA5 encode polypeptides of unknown function, 91 and 79 kDa in size, respectively. The FgV2 genome also consists of five dsRNA segments referred to as dsRNA1 to dsRNA5, 3,580, 3,000, 2,982, 2,748, and 2,414 bp in size, respectively, each containing a single ORF flanked by conserved 5′ and 3′ untranslated regions (UTRs). FgV2 dsRNA1 encodes the viral RdRp, which is 127 kDa in size, while the other four dsRNAs encode proteins of unknown function (Yu et al., 2011). The FodV1 genome contains four dsRNA segments, 3,555, 2,809, 2,794, and 2,646 bp in length, respectively. Each of these segments contains a single ORF. FodV1 dsRNA1 and dsRNA3 encode an RdRp and a coat protein (CP), respectively, while dsRNA2 and dsRNA4 encode hypothetical proteins (named P2 and P4) with unknown functions (Lemus-Minor et al., 2015).

Family *Megabirnaviridae*

A member of the family *Megabirnaviridae* has been isolated from *Fusarium pseudograminearum* strain FC136-2A and is designated Fusarium pseudograminearum megabirnavirus 1 (FpgMBV1) (Zhang et al., 2018). The genome of FpgMBV1 consists of two dsRNA segments, L1-dsRNA (8,951 bp), and L2-dsRNA (5,337 bp), each containing two ORFs. L1-dsRNA encodes a CP of 131 kDa and an RdRp of 126 kDa, while L2-dsRNA encodes two proteins of 97 kDa and 31 kDa with unknown functions.

Family *Partitiviridae*

Three members of the family *Partitiviridae* have been isolated from *Fusarium*, Fusarium solani virus 1 (FsV1; synonym, FusoV) from *Fusarium solani* f. sp. *rohiniae* strain SUF704 (Nogawa et al., 1996), Fusarium poae virus 1 (FpV1; synonym, FuPO-1) from *Fusarium poae* strain A-11 (Compel et al., 1999), and Fusarium solani partitivirus 2 (FsPV2) from *Fusarium solani* f. sp. *pisi* (Osaki et al., 2015). The FsV1 genome consists of two dsRNAs, 1,645 and 1,445 bp in size, each containing one ORF. The large dsRNA encodes the viral RdRp, 60 kDa in size, while the small dsRNA encodes the CP, 44 kDa in size (Nogawa et al., 1996). The

TABLE 1 | Fully-sequenced *Fusarium*-infecting mycoviruses.

Genome type	Mycovirus	Established or proposed family	Host	RNA segment	Size of nucleotides	Accession no.	References
dsRNA	FgV-ch9	*Chrysoviridae*	*F. graminearum* strain China 9	RNA1	3,581	HQ228213	Darissa et al., 2011, 2012
				RNA2	2,850	HQ228214	
				RNA3	2,830	HQ228215	
				RNA4	2,746	HQ228216	
				RNA5	2,423	HQ228217	
	FgV2	*Chrysoviridae*	*F. graminearum* strain 98-8-60	RNA1	3,580	HQ343295	Chu et al., 2004; Yu et al., 2011
				RNA2	3,000	HQ343296	
				RNA3	2,982	HQ343297	
				RNA4	2,748	HQ343298	
				RNA5	2,414	HQ343299	
	FodV1	*Chrysoviridae*	*F. oxysporum* f. sp. *dianthi* strain 116	RNA1	3,555	KP876629	Lemus-Minor et al., 2015
				RNA2	2,809	KP876630	
				RNA3	2,794	KP876631	
				RNA4	2,646	KP876632	
	FpgMBV1	*Megabirnaviridae*	*F. pseudograminearum* strain FC136-2A	RNA1	8,951	MH057692	Zhang et al., 2018
				RNA2	5,337	MH057693	
	FsV1	*Partitiviridae*	*F. solani* f. sp. robiniae strain SUF704	RNA1	1,645	NC_003885	Nogawa et al., 1996
				RNA2	1,445	NC_003886	
	FpV1	*Partitiviridae*	*F. poae* strain A-11	RNA1	2,185	NC_003883	Compel et al., 1999
				RNA2	2,203	NC_003884	
	FsPV2	*Partitiviridae*	*F. solani* f.sp. pisi	RNA1	1,950	LC006130	Osaki et al., 2015
	FaVV1	*Totiviridae*	*F. asiaticum* strain F16176	RNA1	5,281	MH615042	Li et al., 2019
	FgAV1	Alternaviridae	*F. graminearum* strain AH11	RNA1	3,524	MG254901	He et al., 2018
				RNA2	2,470	MG254902	
				RNA3	2,460	MG697236	
	FiAV1	Alternaviridae	*F. incarnatum* strain LY003-07	RNA1	3,548	MH899114	Zhang et al., 2019
				RNA2	2,514	MH899115	
				RNA3	2,498	MH899116	
	FpV2	Fusagraviridae	*F. poae* strain SX63	RNA1	9,518	KU728180	Wang et al., 2016a
	FpV3	Fusagraviridae	*F. poae* strain SX63	RNA1	9,419	KU728181	Wang et al., 2016a
	FvV1	Fusagraviridae	*F. virguliforme*	RNA1	9,402	JN671444	Marvelli et al., 2014
	FvV2	Fusagraviridae	*F. virguliforme*	RNA1	9,327	JN671443	Marvelli et al., 2014
	FgV3	Fusagraviridae	*F. graminearum* strain DK3	RNA1	9,098	NC_013469	Yu et al., 2009
	FgV4	Unassigned	*F. graminearum* strain DK3	RNA1	2,383	NC_013470	Yu et al., 2009
				RNA2	1,739	NC_013471	
	FgV5	Unassigned	*F. graminearum* strain HN1	RNA1	2,030	KX380787	Wang et al., 2017

(Continued)

TABLE 1 | Continued

Genome type	Mycovirus	Established or proposed family	Host	RNA segment	Size of nucleotides	Accession no.	References
				RNA2	1,740	KX380788	
(+)ssRNA	FgDFV1	*Deltaflexiviridae*	*F. graminearum* strain BJ59	RNA1	8,246	KX015962	Chen et al., 2016
	FgHV1	*Hypoviridae*	*F. graminearum* strain HN10	RNA1	13,023	KC330231	Wang et al., 2013
	FgHV2	*Hypoviridae*	*F. graminearum* strain JS16	RNA1	12,800	KP208178	Li et al., 2015
	FlHV1	*Hypoviridae*	*F. langsethiae* strain AH32	RNA1	12,839	KY120321	Li et al., 2017
	FcMV1	*Narnaviridae*	*F. circinatum* strain FcCa070	RNA1	2,419	KF803546	Martínez-Álvarez et al., 2014
	FcoMV1	*Narnaviridae*	*F. coeruleum* (MAFF No. 235976)	RNA1	2,423	LC006129	Osaki et al., 2015
	FgMV1	*Narnaviridae*	*F. globosum* (MAFF No. 237511)	RNA1	2,414	LC006128	Osaki et al., 2015
	FbMV1	*Narnaviridae*	*F. boothii* strain Ep-BL13	RNA1	2,802	LC425112	Mizutani et al., 2018
		Narnaviridae	*F. boothii* strain Ep-BL14	RNA1	2,801	LC425113	
		Narnaviridae	*F. boothii* strain Ep-N28	RNA1	2,802	LC425114	
	FgV1	Fusariviridae	*F. graminearum* strain DK21	RNA1	6,624	NC_006937	Chu et al., 2002; Kwon et al., 2007
	FgMTV1	Tymoviridae	*F. graminearum* strain SX64	RNA1	7,863	KT360947	Li et al., 2016
	FbLFV1	Unassigned	*F. boothii* strain Ep-BL13	RNA1	12,579	LC425115	Mizutani et al., 2018
(−)ssRNA	FgNSRV-1	*Mymonaviridae*	*F. graminearum* strain HN1	RNA1	9,072	MF276904	Wang et al., 2018

FpV1 genome consists of two dsRNAs, 2,185 and 2,203 bp in size. The two dsRNAs encode the viral RdRp and CP, 70 and 74 kDa in size, respectively (Compel et al., 1999). FsPV2 dsRNA1 (1,950 bp) in *F. solani* f. sp. *pisi* contains an ORF encoding an RdRp, 72 kDa in size. Sequence and phylogenetic analysis of the viral RdRps show that FsPV2 belongs to the genus *Alphapartitivirus*, family *Partitiviridae*. In general, partitiviruses possess two essential dsRNA genome segments: dsRNA1 (encoding the RdRp), and dsRNA2 (encoding the CP). However, the attempt to clone dsRNA2 of FsPV2 has failed (Osaki et al., 2015).

Family *Totiviridae*

A member of the genus *Victorivirus*, family *Totiviridae*, has been isolated from *Fusarium asiaticum* strain F16176 and is designated Fusarium asiaticum victorivirus 1 (FaVV1) (Li et al., 2019). The genome of FaVV1 consists of a single, linear dsRNA of 5,281 bp that contains two ORFs. ORF1 is predicted to encode a CP with a molecular mass of 79 kDa. ORF2 is predicted to encode an RdRp with a molecular mass of 92 kDa. Interestingly, the CP and RdRp of FaVV1 are most similar (77 and 75% identical, respectively) to those of Rosellinia necatrix victorivirus 1 (RnVV1), which infects the white root rot pathogen fungus *Rosellinia necatrix*. Both ORFs overlap with each other at a pentanucleotide "UAAUG," and the overlapping pentanucleotide is one of the features of the genus *Victorivirus* (Li et al., 2019).

Family Alternaviridae

Two members of the newly proposed family Alternaviridae have been isolated from *Fusarium*, Fusarium graminearum alternavirus 1 (FgAV1) from *F. graminearum* strain AH11 (He et al., 2018), Fusarium incarnatum alternavirus 1 (FiAV1) from *F. incarnatum* strain LY003-07 (Zhang et al., 2019). The genome of FgAV1 possesses three dsRNA segments, dsRNA1 (3,524 bp), dsRNA2 (2,470 bp), and dsRNA3 (2,460 bp), each coding an ORF. FgAV1 dsRNA1 encodes an RdRp, 126 kDa in size, while dsRNA2 and dsRNA3 encode polypeptides of unknown function, 84 and 81 kDa in size, respectively. The RdRp of FgAV1 is most similar to Fusarium poae alternavirus 1 (FpAV1), with 98% (ORF1), 99% (ORF2), and 98% (ORF3) aa sequence identities (He et al., 2018), while the terminal sequences of FpAV1 have not been determined (Osaki et al., 2016). Compared to the genomic composition (4 dsRNA segments) of three other members of

this family, namely, Alternaria alternata virus 1 (AaV1) (Aoki et al., 2009), Aspergillus mycovirus 341 (AMV) (Hammond et al., 2008), and Aspergillus foetidus mycovirus (AfMV) (Kozlakidis et al., 2013), FgAV1/AH11 and FpAV1 both lack the fourth segment. The genome of FiAV1 also consists of three dsRNA segments, dsRNA1 (3,548 bp), dsRNA2 (2,514 bp), and dsRNA3 (2,498 bp), each encoding a single ORF. FiAV1 dsRNA1 encodes an RdRp of 127 kDa, while dsRNA2 and dsRNA3 encode proteins with unknown functions (Zhang et al., 2019).

Family Fusagraviridae

Five members of the newly proposed family Fusagraviridae (Wang et al., 2016a) have been isolated from *Fusarium*, Fusarium poae dsRNA virus 2 (FpV2), and Fusarium poae dsRNA virus 3 (FpV3) isolated from the same *Fusarium poae* strain SX63 (Wang et al., 2016a), Fusarium virguliforme dsRNA mycovirus 1 (FvV1) and Fusarium virguliforme dsRNA mycovirus 2 (FvV2) isolated from *Fusarium virguliforme* (Marvelli et al., 2014), and Fusarium graminearum virus 3 (FgV3) isolated from *F. graminearum* strain DK3 (Yu et al., 2009). The respective genomes of FpV2 and FpV3 consist of a single dsRNA, 9,518 and 9,419 bp, respectively. Each contains two ORFs (ORF1 and ORF2), and encode a protein of unknown function and an RdRp, respectively (Wang et al., 2016a). A phytoreo_S7 domain is found downstream of the RdRp domain of the ORF2-coded proteins of both FpV2 and FpV3. The same shifty heptamer motif (GGAAAAC) is found immediately before the stop codon UAG of ORF1 in both FpV2 and FpV3, which could mediate programmed −1 ribosomal frameshifting (−1 PRF). The respective genomes of both FvV1 and FvV2 consist of a dsRNA, 9,402 and 9,327 bp, respectively, and contain two ORFs (ORF1 and ORF2) that overlap by 25 nt. The 25-nt overlap between ORFs 1 and 2 contain a slippery sequence (AAAAAAC) that is a−1 frameshift signal. ORF2 encodes an RdRp, while the function of ORF1 is unclear (Marvelli et al., 2014). The FgV3 genome also has a dsRNA (9,098 bp), and possesses two ORFs. ORF1 encodes a protein of unknown function, while ORF2 encodes an RdRp. A phytoreovirus S7 protein domain is also found downstream of the RdRp domain of ORF2 (Yu et al., 2009).

Unassigned dsRNA Mycoviruses in *Fusarium*

Fusarium graminearum virus 4 (FgV4) has been isolated from *F. graminearum* strain DK3 (Yu et al., 2009). The FgV4 genome consists of two dsRNAs, 2,383 and 1,739 bp, respectively. FgV4 dsRNA1 contains a single ORF encoding the viral RdRp, while FgV4 dsRNA2 contains two putative ORFs coding for products of unknown function. Fusarium graminearum dsRNA virus 5 (FgV5) has been isolated from *Fusarium graminearum* strain HN1 (Wang et al., 2017). The FgV5 genome comprises two dsRNAs (dsRNA1 and dsRNA2), 2,030 and 1,740 bp, respectively. FgV5 dsRNA1 contains an ORF encoding an RdRp, 70 kDa. FgV5 dsRNA2 contains two ORFs (ORF2 and ORF3) that code for products of unknown function. Phylogenetic analysis indicates that FgV4 and FgV5 belong to a taxonomically unassigned dsRNA mycovirus group that is related to the families *Amalgaviridae* and *Partitiviridae* (Wang et al., 2017).

Positive-Sense, Single-Stranded RNA Mycoviruses

Family *Deltaflexiviridae*

A member of the family *Deltaflexiviridae* has been isolated from *F. graminearum* strain BJ59 and is designated as Fusarium graminearum deltaflexivirus 1 (FgDFV1) (Chen et al., 2016). The FgDFV1 genome harbors a linear, positive-sense ssRNA, 8,246 nt in length excluding the poly (A) tails, and contains five putative ORFs. The largest ORF (ORF1) encodes a replication-associated polyprotein (RP) of 227 kDa, containing three conserved domains including viral RdRp, Hel, and Mtr. The four smaller ORFs (ORFs 2–5) encode four proteins of unknown function, 12, 13, 18, and 17 kDa, respectively.

Family *Hypoviridae*

Three members of the family *Hypoviridae* have been isolated from *Fusarium*, Fusarium graminearum hypovirus 1 (FgHV1) from *Fusarium graminearum* strain HN10 (Wang et al., 2013), FgHV2 from *Fusarium graminearum* strain JS16 (Li et al., 2015), and Fusarium langsethiae hypovirus 1 (FlHV1) from *Fusarium langsethiae* strain AH32 (Li et al., 2017). The FgHV1 genome consists of a linear, positive-sense ssRNA of 13,023 nt containing two ORFs (ORF A and ORF B). The 5′ proximal ORF A encodes a papain-like proteinase (p20), which is closely related to the Cryphonectria hypovirus 1 (CHV1)-encoded RNA silencing suppressor (RSS; p29) (Wang et al., 2016c). The 3′ proximal ORF B encodes a large polyprotein of 421 kDa with three conserved domains including papain-like protease (Pro), RdRp, and RNA helicase (Hel) (Wang et al., 2013). The FgHV2 genome consists of a linear, positive-sense ssRNA of 12,800 nt in size, containing a single ORF. The ORF encodes a large polyprotein of 446 kDa with three conserved domains, Pro, RdRp, and Hel, and a novel domain with homologous bacterial SMC (structural maintenance of chromosomes) chromosome segregation proteins (Li et al., 2015). The genome of FIHV1 contains a linear, positive-sense ssRNA, 12,839 nt in size, encoding a single ORF. The ORF encodes a polyprotein of 447 kDa, containing three conserved domains, Pro, RdRp, and Hel, which is a common feature of the family *Hypoviridae*.

Family *Narnaviridae*

Four members of the genus *Mitovirus* (family *Narnaviridae*) have been isolated from *Fusarium*, Fusarium circinatum mitovirus 1 (FcMV1) from *Fusarium circinatum* strain FcCa070 (Martínez-Álvarez et al., 2014), Fusarium coeruleum mitovirus 1 (FcoMV1) and Fusarium globosum mitovirus 1 (FgMV1) from *Fusarium coeruleum* (MAFF No. 235976) and *Fusarium globosum* (MAFF No. 237511), respectively (Osaki et al., 2015), and Fusarium boothii mitovirus 1 (FbMV1) from three different strains of *Fusarium boothii*: Ep-BL13, Ep-BL14, and Ep-N28 (Mizutani et al., 2018). The FcMV1 genome consists of a linear, positive-sense ssRNA of 2,419 nt, containing a single ORF that encodes an RdRp of 85 kDa. The genomes of FcoMV1 and FgMV1 consist of linear, positive-sense ssRNA, 2,423 and 2,414 nt, respectively, each containing a single ORF encoding an RdRp (86 and 84 kDa, respectively). FbMV1 genomes in strains Ep-BL13 and

Ep-N28 are 2,802 nt in length and the genome in strain Ep-BL14 is 2,801 nt in length. These three virus strains share 98% nucleotide identity and each contains a single ORF encoding an RdRp.

Family Fusariviridae

A member of the newly proposed family, Fusariviridae has been isolated from *F. graminearum* strain DK21 (Chu et al., 2002; Zhang et al., 2014) and is designated Fusarium graminearum virus 1 strain DK21 (FgV1-DK21) (Yu et al., 2009). The genome of FgV1 consists of a linear, positive-sense ssRNA of 6,621 nt in length excluding the 3′-terminal poly (A) tail and contains four ORFs. The four ORFs (1-4) encode proteins with molecular masses of 174, 16.7, 6.2, 48.4 kDa, respectively, among which ORF1 encodes an RdRp, while the products of ORFs 2–4 reveal no obvious similarities to other viral sequences in the NCBI protein database (Kwon et al., 2007).

Family *Tymoviridae*

A member of the newly proposed genus Mycotymovirus, family *Tymoviridae* has been isolated from *F. graminearum* strain SX64 and is designated Fusarium graminearum mycotymovirus 1 (FgMTV1) (Li et al., 2016). The FgMTV1 genome consists of a linear, positive-sense ssRNA of 7,863 nt excluding the poly (A) tails, and contains four ORFs. ORF1 encodes a RP of 249 kDa, containing four conserved domains, viral RNA methyltransferase (Mtr), tymovirus endopeptidase (Pro), RdRp, and Hel. These four conserved domains are the common features of members of the family *Tymoviridae* (Martelli et al., 2002). ORFs 2–4 encode three hypothetical proteins of unknown function, 14, 13, and 19 kDa, respectively. FgMTV1 is the first tymo-like mycovirus isolated from a plant pathogenic fungus (Li et al., 2016).

Unassigned (+)ssRNA Mycoviruses in *Fusarium*

Fusarium boothii large flexivirus 1 (FbLFV1) has been isolated from *Fusarium boothii* strain Ep-BL13 (Mizutani et al., 2018). The FbLFV1 genome consists of a linear, positive-sense ssRNA of 12,579 nt, and encompasses a single large ORF encoding a replicase of 444 kDa, containing three conserved domains, Mtr, Hel, and RdRp. There are also two regions of unknown function in the polypeptide with similarity to a PHA03247 domain found in herpesviruses (large dsDNA viruses). Sequence and phylogenetic analyses show that FbLFV1 belongs to a novel virus species that may form an independent genus, or even a novel family, in the order *Tymovirale*s (Mizutani et al., 2018).

Negative-Sense, Single-Stranded RNA Mycoviruses

Family *Mymonaviridae*

A member of the family *Mymonaviridae* has been isolated from *Fusarium graminearum* strain HN1 and is designated Fusarium graminearum negative-stranded RNA virus 1 (FgNSRV-1) (Wang et al., 2018). The genome of FgNSRV-1 harbors a linear, negative-sense ssRNA of 9,072 nt, and contains five discontinuous but linear ORFs (ORF I-V), encoding five proteins (termed P I–P V) with molecular masses ranging from 6 to 221 kDa. Among the five FgNSRV-1 proteins, P II and P IV are related to the putative nucleoprotein N and large protein L of Sclerotinia sclerotiorum negative-stranded RNA virus 1 (SsNSRV-1) and SsNSRV-3 (Liu et al., 2014; Lee Marzano et al., 2016). The 3′ and 5′-ends of FgNSRV-1 RNA have perfect complementarity of the first six residues (3′-UCCUGC—GCAGGA-5′), which is a common feature among mononegaviruses (Chen et al., 2016).

EFFECT OF VIRUSES ON *FUSARIUM*

Due to recent technological advances, a number of virus/fungal host systems can be established by curing viruses along with artificial introduction (Kondo et al., 2013; Suzuki, 2017). The vegetative growth, development, and physiological properties of host fungi are highly influenced by the harmful, beneficial, or neutral (little or no) effects of fungal viruses (Kondo et al., 2013). In this review, we mainly focus on the interplay between mycoviruses and *Fusarium* spp.

Mitigation of fungal virulence or "hypovirulence" is a good example of the harmful effect of several viruses on their host fungi. Therefore, fungal viruses could act as a potential candidate for the biological control of fungi (Hillman et al., 2018). The most studied example of reduced fungal virulence is CHV1/*C. parasitica* (Dawe and Nuss, 2013). In the case of *Fusarium* spp., four mycoviruses have harmful effects on fungal phenotypes. FgHV2, a novel hypovirus of the newly proposed genus Alphahypovirus, is associated with hypovirulence phenotypes, including reduced mycelial growth rate, conidia production, and DON concentration. In the virulence assay, the virus-free strain spreads more quickly from the inoculation sites to nearby spikelets than the virus-carrying strain JS16 (Li et al., 2015). FgV1, a member of the novel family Fusariviridae, has been reported to reduce the virulence of *F. graminearum*, delay mycelial growth, increase pigmentation, and reduce the production of mycotoxin (Chu et al., 2002). FgV-ch9, a member of the family *Crysoviridae*, is associated with hypovirulence of *F. graminearum* at high and medium viral dsRNA levels, including reduced mycelial growth rate and conidiation capacity, abnormal colony morphology, disorganized cytoplasm, and reduced virulence in wheat and maize plants (Darissa et al., 2012). FodV1, a member of the family *Chrysoviridae*, causes significant phenotypic alterations in the vegetative growth and virulence of the fungal host (Lemus-Minor et al., 2018).

In most cases, mycovirus infection causes little or no symptoms in the host (Ghabrial and Suzuki, 2009). For example, FgV3 and FgV4 infections do not cause any phenotypic change in the host *F. graminearum* (Lee et al., 2014). FgHV1 infection has mild or no effects on the fungal phenotypes of *F. graminearum* including morphology, mycelial growth, conidiation, and virulence or toxin production (Wang et al., 2013). FsV1 and FpV1 are also not associated with phenotypic changes in their hosts *F. solani* and *F. poa*e (Nogawa et al., 1996; Compel et al., 1999). Another two mycoviruses, FpV2 and FpV3, isolated from the same strain of *Fusarium poae*, do not show any deleterious effect on their host fungus (Wang et al., 2016a).

GENE REGULATIONS ASSOCIATED WITH *FUSARIUM* VIRUS INFECTION

The proteome and transcriptome analysis of virus-infected fungi will help to elucidate the proteins and genes regulated by mycovirus infection that are involved in growth, development, and stress responses and direct further studies on the interactions between pathogenic fungi and viruses. The differential expression of *F. graminearum* proteins caused by FgV1 infection was investigated by two-dimensional electrophoresis with mass spectrometry (Kwon et al., 2009). Seven proteins, including sporulation-specific gene SPS2, triose phosphate isomerase, nucleoside diphosphate kinase, and woronin body major protein precursor, were induced or significantly upregulated by FgV1 infection. The significant decrease or down regulation of 16 proteins, including enolase, saccharopine dehydrogenase, flavohemoglobin, mannitol dehydrogenase, and malate dehydrogenase, caused by FgV1 infection was also identified. However, the number of proteins identified was insufficient to obtain a comprehensive understanding of the host response (Kwon et al., 2009; Cho et al., 2013). Therefore, genome-wide expression analyses were carried out using a 3′-tiling microarray in FgV1-infected *F. graminearum*. Genes associated with protein synthesis (such as ribosome assembly, nucleolus, and ribosomal RNA processing) and genes required for transcription and signal transduction (such as fungal-specific transcription factors and cAMP signaling), were significantly up-regulated in fungal host cells, which seems to be related to virus replication. In contrast, significant down-regulation of genes required for metabolism (such as carboxylic acids, aromatic amino acids, nitrogen compounds, and polyamines) and transporting systems in a fungal host containing the virus appears to be related to the host defense mechanism and fungal virulence (Cho et al., 2012, 2013). Furthermore, a comprehensive genome-wide gene expression analysis elucidated completely distinct expression patterns of *F. graminearum* transcriptomes in response to infections by two hypovirulent mycoviruses (FgV1 and FgV2) and two non hypovirulent mycoviruses (FgV3 and FgV4), respectively. Interestingly, changes in the host transcriptome caused by different mycoviruses are not always correlated with observed host phenotypes. The fungal host transcriptome was more affected by FgV1 and FgV4 infections than by FgV2 and FgV3 infections. In addition, 12 differentially expressed genes were identified in response to all four mycovirus infections, but functions of most of these genes are still unknown (Lee et al., 2014). In the FgHV1-infected *F. graminearum* strain, enriched genes related to redox regulation are differentially expressed. It has been demonstrated that FgHV1-encoded p20 could induce H_2O_2 accumulation and a hypersensitive response in *Nicotiana benthamiana* leaves (Wang et al., 2016c).

Subsequently, the hexagonal peroxisome protein FgHex1 was screened using transcriptional and proteomic analyses. By generating *FgHEX1* gene deletion and overexpression mutants, it was indicated that the *FgHEX1* gene plays a direct role in the asexual reproduction and virulence of *F. graminearum* and facilitates viral RNA accumulation in the FgV1-infected host fungus (Son et al., 2013). To investigate the molecular mechanism underlying the production of *FgHEX1* and the replication of FgV1 viral RNA, electrophoretic mobility shift assays (EMSA) was conducted with recombinant FgHex1 protein and RNA sequences derived from various regions of FgV1 genomic RNA. These analyses demonstrated that the FgHex1 functions in the synthesis of both strands of FgV1 RNA and therefore in FgV1 replication probably by specifically binding the FgV1 genomic RNA. This is the first report about the regulation of viral RNA replication by a fungal cellular protein that can directly bind to viral genomic RNA (Son et al., 2016). Otherwise, another host gene, the putative 3′(2′),5′-bisphosphate nucleotidase gene, *FgHal2*, in *F. graminearum* is down-regulated following FgV1 infection. The possible function(s) of *FgHal2* was investigated in *F. graminearum* using gene deletion and gene over-expression mutants. It was found that deletion of *FgHal2* reduced conidiation, mycelial growth, and the production of secondary metabolites. Moreover, deletion of *FgHal2* decreased viral RNA accumulation and the vertical transmission of FgV1 via conidia. Together, these results indicate that *F. graminearum* can down-regulate one of its major multifunctional genes, *FgHal2*, in response to FgV1 infection (Yu et al., 2015). Recently, an mRNA binding protein (named virus response 1, *vr1*) was identified to be involved in symptom expression in *F. graminearum*. Downregulation of *vr1* in the virus FgV-ch9 infected fungus and *vr1* deletion evoke virus-infection like symptoms while constitutive expression overrules the cytopathic effects of the virus infection. Intriguingly, the presence of a specific viral structural protein P3 is sufficient to trigger the fungal response, i.e., *vr1* downregulation, and symptom development similar to virus infection. Hence, *vr1* represents a fundamental host factor for the expression of virus-related symptoms and helps to understand the underlying mechanism of hypovirulence. The advancements in understanding fungal infection and response may aid biological pest control approaches using mycoviruses or viral proteins to prevent future *Fusarium* epidemics (Bormann et al., 2018).

RNAI IN *FUSARIUM* RESPONDING TO VIRAL INFECTION

RNA silencing or RNA interference (RNAi) functions as an antiviral defense mechanism in eukaryotic organisms. The core elements of the cross-kingdom RNA silencing defense response consists of conserved ribonucleases: members of the Dicer-like (DCL) and Argonaute-like (AGO) protein families. Dicer nucleases recognize viral double-stranded and structured RNAs and use the associated RNase III-type activity to process these RNAs into small RNAs of 21–24 nts in length, termed virus-derived small (vs.) RNAs. The vsRNAs are then incorporated into an effector complex termed the RNA-induced silencing complex (RISC) with the aid of an Argonaute family protein. One strand of the vsRNA is degraded and the remaining guide strand targets the effector complex to the cognate viral RNA, which is then cleaved by the Argonaute-associated RNAse H-like activity. Subsequently, the antiviral RNA silencing response is further amplified by host RNA-dependent RNA polymerases

(RdRPs) (Ding, 2010; Nuss, 2011). To combat RNA silencing-based antiviral defense, viruses of plants, insects, mammals, and fungi encode proteins, designated viral suppressors of RNA silencing (VSR), that employ a variety of mechanisms to suppress RNA silencing pathways. RNA silencing and viruses against host RNA silencing have been well-characterized in the *Cryphonectria parasitica*-hypovirus system (Ding, 2010; Nuss, 2011). More encouragingly, the roles of core components of the RNAi pathway have been also been gradually revealed in *F. graminearum*.

F. graminearum contains genes encoding two dicer proteins (FgDicer1 and FgDicer2), two Argonaute proteins (FgAgo1 and FgAgo2), and five RdRp proteins (FgRdRp1 to 5). Chen et al. showed that RNAi machinery was not involved in growth, abiotic stress and pathogenesis in *F. graminearum*. In addition, it was demonstrated that the hairpin RNA (hpRNA) can efficiently silence the expression level of target gene and the argonaute protein FgAgo1 and dicer protein FgDicer2 played a critical role in the hpRNA mediated gene silencing process (Chen et al., 2015). FgDicer2 was also involved in small RNA (sRNA, 17–40 nt) transcription and micro-like-RNA (milRNA) generation in this fungus (Chen et al., 2015). Strikingly, a recent study showed that FgDicer2 is the primary DCL component for defense against viroids in *F. graminearum* (Wei et al., 2019). Furthermore, a combined analysis of functional genetics and deep sequencing of small non-coding RNA (sRNA), mRNA, and the degradome indicate that the sex-specifically induced exonic small interference RNA (exsiRNA)-mediated RNA interference (RNAi) mechanism has an important role in fine-tuning the transcriptome during ascospore formation in *F. graminearum*. It is FgDicer1 and FgAgo2 that primarily mediate the sex-specific RNAi pathway. Each fungal species appears to have evolved RNAi-based gene regulation for specific developmental stages or stress responses. This study provides new insights into the regulatory role of sRNAs in fungi and other lower eukaryotes (Son et al., 2017).

To preliminarily elucidate the RNA silencing mechanism of the *F. graminearum*/hypovirus system, the properties of sRNAs in FgHV1 and FgHV2 were analyzed by using HiSeq deep sequencing in *F. graminearum*. The length distributions of *F. graminearum* sRNAs were altered by hypoviral infection. Potential milRNA candidates were differentially expressed between the hypovirus-free and hypovirus-infected library types. The 1,831,081 and 3,254,758 total reads generated from the FgHV1 and FgHV2 genomes in *F. graminearum* yielded the first high-resolution sRNA maps of fungal viruses. In particular, FgDicer1 and FgRdRp5 were predicted targets of FgHV1- and FgHV2-derived siRNAs, possibly revealing a novel anti-RNA silencing strategy employed by mycoviruses (Wang et al., 2016b). To investigate the contributions of RNAi components to the antiviral response against Fusarium graminearum viruses (FgV1, 2, and 3), reverse genetics and virus-derived small RNA profiling were used. FgV1–3 infection differentially induces the gene expression of RNAi components in *F. graminearum*. *FgDICER2* and *FgAGO1* transcripts accumulated at lower levels following FgV1 infection than following FgV2 or FgV3 infection. *FgAGO1* can efficiently robust RNAi response against FgV1 infection, but the functions of two dicer genes, i.e., *FgDICER1* and *FgDICER2*, might be partially redundant in response to FgV 1–3 infections. These results show that *F. graminearum* developed more complex and robust RNA silencing system against mycoviruses (Yu et al., 2018).

CONCLUSION AND PROSPECTS

The characterization of the viruses isolated from *Fusarium* mentioned above has enhanced our understanding of the great diversity of mycoviruses. Most *Fusarium* mycoviruses have double-stranded or single-stranded, positive- or negative-sense RNA genomes. No DNA viruses have been isolated from *Fusarium* species. Additionally, purified virions of *Fusarium* mycoviruses can be obtained in large quantities and of high quality and can serve as good material for structural analysis, which will promote a better understanding of mycovirus assembly, function, evolution, and its uses in nanotechnological applications (Ghabrial et al., 2015; De Ruiter et al., 2019).

Fungal viruses causing hypovirulence can be used as potential biocontrol agents of phytopathogenic fungal diseases, which are always restricted by fungal vegetative incompatibility (Son et al., 2015). Recent studies have demonstrated that some mycoviruses can be transmitted between vegetatively incompatible strains, particularly SsHADV-1, Sclerotinia sclerotiorum partitivirus 1 (SsPV1), Sclerotinia sclerotiorum mycoreovirus 4 (SsMYRV4), and Sclerotinia sclerotiorum deltaflexivirus 2 (SsDFV2) (Yu et al., 2013; Xiao et al., 2014; Wu et al., 2017; Hamid et al., 2018). In addition, these mycoviruses can cause hypovirulence. Their hypovirulent properties suggest that SsHADV-1, SsPV1, SsMYRV4, and SsDFV2, have potential for controlling plant disease in the field. Therefore, further research is required to clarify whether the transmission of *Fusarium* mycoviruses can occur and their corresponding transmission efficiency between vegetative-incompatible individuals or interspecific fungi.

Fusarium graminearum has emerged as a good model system for studying mycovirus–host interactions, similar to three other host-virus interaction systems: *C. parasitica*–mycovirus, *S. sclerotiorum*–mycovirus, and *R. necatrix*–mycovirus. There are some advantages of using *F. graminearum*–mycovirus for such studies. For example, the genome of the *F. graminearum* strain PH-1 is sequenced and is available publicly, allowing RNA-seq-based, genome-wide expression analysis and modification of targeted gene disruptions. Additionally, protoplasts of *F. graminearum* are easy to prepare and store and are competent in genetics transformation systems with DNA. Infectious cDNA clones have been successfully used in a few fungal species, including *C. parasitica*, *Diaporthe ambigua*, and *Sclerotinia sclerotiorum* (Choi and Nuss, 1992; Chen et al., 1993, 1994; Chen and Nuss, 1999; Moleleki et al., 2003; Lin et al., 2007; Marzano et al., 2015; Zhang et al., 2016), but not so far in *F. graminearum*. The

construction of infectious cDNA clones can be used to explore the properties of mycoviruses and employ mycoviruses as vectors to introduce genes deleterious to the fungal host (Pearson and Bailey, 2013).

Future studies should focus on systematically identifying viral and host factors important for the interactions between mycoviruses and their hosts, especially crucial determinants responsible for the phenotypic changes (including hypovirulence) and reduction of *Fusarium* mycotoxin production caused by mycovirus infection.

AUTHOR CONTRIBUTIONS

SW, LZ, and IA performed the literature search and prepared the manuscript table. LG drafted and revised the manuscript. PL and PB contributed equally to writing the manuscript. All authors revised and agree with the final manuscript version.

FUNDING

This work was supported by the National Key R&D Program of China (2018YFD0200500) to LG.

REFERENCES

Aoki, N., Moriyama, H., Kodama, M., Arie, T., Teraoka, T., and Fukuhara, T. (2009). A novel mycovirus associated with four double-stranded RNAs affects host fungal growth in *Alternaria alternata*. *Virus Res.* 140, 179–187. doi: 10.1016/j.virusres.2008.12.003

Bormann, J., Heinze, C., Blum, C., Mentges, M., Brockmann, A., Alder, A., et al. (2018). Expression of a structural protein of the mycovirus FgV-ch9 negatively affects the transcript level of a novel symptom alleviation factor and causes virus infection-like symptoms in *Fusarium graminearum*. *J. Virol.* 92, e00326–e00318. doi: 10.1128/JVI.00326-18

Chen, B., Choi, G. H., and Nuss, D. L. (1993). Mitotic stability and nuclear inheritance of integrated viral cDNA in engineered hypovirulent strains of the chestnut blight fungus. *EMBO J.* 12, 2991–2998. doi: 10.1002/j.1460-2075.1993.tb05967.x

Chen, B., Choi, G. H., and Nuss, D. L. (1994). Attenuation of fungal virulence by synthetic infectious hypovirus transcripts. *Science.* 264, 1762–1764. doi: 10.1126/science.8209256

Chen, B., and Nuss, D. L. (1999). Infectious cDNA clone of hypovirus CHV1-Euro7: a comparative virology approach to investigate virus-mediated hypovirulence of the chestnut blight fungus *Cryphonectria parasitica*. *J. Virol.* 73, 985–992.

Chen, X., He, H., Yang, X., Zeng, H., Qiu, D., and Guo, L. (2016). The complete genome sequence of a novel Fusarium graminearum RNA virus in a new proposed family within the order *Tymovirales*. *Arch. Virol.* 161, 2899–2903. doi: 10.1007/s00705-016-2961-1

Chen, Y., Gao, Q. X., Huang, M. M., Liu, Y., Liu, Z. Y., Liu, X., et al. (2015). Characterization of RNA silencing components in the plant pathogenic fungus *Fusarium graminearum*. *Sci. Rep.* 5:13. doi: 10.1038/srep12500

Cho, W. K., Lee, K. M., Yu, J., Son, M., and Kim, K. H. (2013). Insight into mycoviruses infecting *Fusarium* species. *Adv. Virus Res.* 86, 273–288. doi: 10.1016/B978-0-12-394315-6.00010-6

Cho, W. K., Yu, J., Lee, K. M., Son, M., Min, K., Lee, Y. W., et al. (2012). Genome-wide expression profiling shows transcriptional reprogramming in *Fusarium graminearum* by Fusarium graminearum virus 1-DK21 infection. *BMC Genomics* 13:173. doi: 10.1186/1471-2164-13-173

Choi, G. H., and Nuss, D. L. (1992). Hypovirulence of chestnut blight fungus conferred by an infectious viral cDNA. *Science.* 257, 800–803. doi: 10.1126/science.1496400

Chu, Y. M., Jeon, J. J., Yea, S. J., Kim, Y. H., Yun, S. H., Lee, Y. W., et al. (2002). Double-stranded RNA mycovirus from *Fusarium graminearum*. *Appl. Environ. Microbiol.* 68, 2529–2534. doi: 10.1128/AEM.68.5.2529-2534.2002

Chu, Y. M., Lim, W. S., Yea, S. J., Cho, J. D., Lee, Y. W., and Kim, K. H. (2004). Complexity of dsRNA mycovirus isolated from *Fusarium graminearum*. *Virus Genes.* 28, 135–143. doi: 10.1023/B:VIRU.0000012270.67302.35

Compel, P., Papp, I., Bibo, M., Fekete, C., and Hornok, L. (1999). Genetic interrelationships and genome organization of double-stranded RNA elements of *Fusarium poae*. *Virus Genes* 18, 49–56. doi: 10.1023/A:1008069318838

Darissa, O., Adam, G., and Schäfer, W. (2012). A dsRNA mycovirus causes hypovirulence of *Fusarium graminearum* to wheat and maize. *Eur. J. Plant Pathol.* 134, 181–189. doi: 10.1007/s10658-012-9977-5

Darissa, O., Willingmann, P., Schafer, W., and Adam, G. (2011). A novel double-stranded RNA mycovirus from *Fusarium graminearum*: nucleic acid sequence and genomic structure. *Arch. Virol.* 156, 647–658. doi: 10.1007/s00705-010-0904-9

Dawe, A. L., and Nuss, D. L. (2013). Hypovirus molecular biology: from Koch's postulates to host self-recognition genes that restrict virus transmission. *Adv. Virus Res.* 86, 109–147. doi: 10.1016/B978-0-12-394315-6.00005-2

De Ruiter, M. V., Klem, R., Luque, D., Cornelissen, J. J. L. M., and Castón, J. R. (2019). Structural nanotechnology: three-dimensional cryo-EM and its use in the development of nanoplatforms for *in vitro* catalysis. *Nanoscale* 11, 4130–4146. doi: 10.1039/C8NR09204D

Ding, S. (2010). RNA-based antiviral immunity. *Nat. Rev. Immunol.* 10, 632–644. doi: 10.1038/nri2824

Ghabrial, S. A., Castón, J. R., Jiang, D., Nibert, M. L., and Suzuki, N. (2015). 50-plus years of fungal viruses. *Virology* 479–480, 356–368. doi: 10.1016/j.virol.2015.02.034

Ghabrial, S. A., and Suzuki, N. (2009). Viruses of plant pathogenic fungi. *Annu. Rev. Phytopathol.* 47, 353–384. doi: 10.1146/annurev-phyto-080508-081932

Hamid, M. R., Xie, J., Wu, S., Maria, S. K., Zheng, D., Assane, H. A., et al. (2018). A novel deltaflexivirus that infects the plant fungal pathogen, *Sclerotinia sclerotiorum*, can be transmitted among host vegetative incompatible strains. *Viruses* 10:E295. doi: 10.3390/v10060295

Hammond, T. M., Andrewski, M. D., Roossinck, M. J., and Keller, N. P. (2008). *Aspergillus* mycoviruses are targets and suppressors of RNA silencing. *Eukaryot. Cell* 7, 350–357. doi: 10.1128/EC.00356-07

He, H., Chen, X., Li, P., Qiu, D., and Guo, L. (2018). Complete genome sequence of a Fusarium graminearum double-stranded RNA virus in a newly proposed family, Alternaviridae. *Genome Announc.* 6, e00064–e00018. doi: 10.1128/genomeA.00064-18

Hillman, B. I., Annisa, A., and Suzuki, N. (2018). Viruses of plant-interacting fungi. *Adv. Virus Res.* 100, 99–116. doi: 10.1016/bs.aivir.2017.10.003

Hillman, B. I., Supyani, S., Hideki, K., and Nobuhiro, S. (2004). A reovirus of the fungus *Cryphonectria parasitica* that is infectious as particles and related to the coltivirus genus of animal pathogens. *J. Virol.* 78, 892–898. doi: 10.1128/JVI.78.2.892-898.2004

Jiang, D., Fu, Y., Li, G., and Ghabrial, S. A. (2013). Viruses of the plant pathogenic fungus *Sclerotinia sclerotiorum*. *Adv. Virus Res.* 86, 215–248. doi: 10.1016/B978-0-12-394315-6.00008-8

Kanhayuwa, L., Kotta Loizou, I., Ozkan, S., Gunning, A. P., and Coutts, R. H. A. (2015). A novel mycovirus from *Aspergillus fumigatus* contains four unique dsRNAs as its genome and is infectious as dsRNA. *Proc. Natl. Acad. Sci. U.S.A.* 112, 9100–9105. doi: 10.1073/pnas.1419225112

Kondo, H., Kanematsu, S., and Suzuki, N. (2013). Viruses of the white root rot fungus, *Rosellinia necatrix*. *Adv. Virus Res.* 86, 177–214. doi: 10.1016/B978-0-12-394315-6.00007-6

Kozlakidis, Z., Herrero, N., Ozkan, S., Kanhayuwa, L., Jamal, A., Bhatti, M. F., et al. (2013). Sequence determination of a quadripartite dsRNA virus isolated from *Aspergillus foetidus*. *Arch. Virol.* 158, 267–272. doi: 10.1007/s00705-012-1362-3

Kwon, S. J., Cho, S. Y., Lee, K. M., Yu, J., Son, M., and Kim, K. H. (2009). Proteomic analysis of fungal host factors differentially expressed by *Fusarium graminearum* infected with Fusarium graminearum virus-DK21. *Virus Res.* 144, 96–106. doi: 10.1016/j.virusres.2009.04.004

Kwon, S. J., Lim, W. S., Park, S. H., Park, M. R., and Kim, K. H. (2007). Molecular characterization of a dsRNA mycovirus, Fusarium graminearum Virus-DK21, which is phylogenetically related to hypoviruses but has a genome organization and gene expression strategy resembling those of plant potex-like viruses. *Mol. Cells* 28, 73–74. doi: 10.1007/s10059-009-0112-1

Lee Marzano, S. Y., Nelson, B. D., Ajayi-Oyetunde, O., Bradley, C. A., Hughes, T. J., Hartman, G. L., et al. (2016). Identification of diverse mycoviruses through metatranscriptomics characterization of the viromes of five major fungal plant pathogens. *J. Virol.* 90, 6846–6863. doi: 10.1128/JVI.00357-16

Lee, K. M., Cho, W. K., Yu, J., Son, M., Choi, H., Min, K., et al. (2014). A comparison of transcriptional patterns and mycological phenotypes following infection of *Fusarium graminearum* by four mycoviruses. *PLoS ONE* 9:e100989. doi: 10.1371/journal.pone.0100989

Lefkowitz, E. J., Dempsey, D. M., Hendrickson, R. C., Orton, R. J., Siddell, S. G., and Smith, D. B. (2018). Virus taxonomy: the database of the International Committee on Taxonomy of Viruses (ICTV). *Nucleic Acids Res.* 46, D708–D717. doi: 10.1093/nar/gkx932

Lemus-Minor, C. G., Canizares, M. C., Garcia-Pedrajas, M. D., and Perez-Artes, E. (2015). Complete genome sequence of a novel dsRNA mycovirus isolated from the phytopathogenic fungus *Fusarium oxysporum* f. sp. dianthi. *Arch. Virol.* 160, 2375–2379. doi: 10.1007/s00705-015-2509-9

Lemus-Minor, C. G., Cañizares-Nolasco, C., Mdd, G. P., and Pérez-Artés, E. (2018). *Fusarium oxysporum* f. sp. dianthi virus 1 accumulation is correlated with changes in virulence and other phenotypic traits of its fungal host. *Phytopathology* 108, 957–963. doi: 10.1094/PHYTO-06-17-0200-R

Li, P., Chen, X., He, H., Qiu, D., and Guo, L. (2017). Complete genome sequence of a novel hypovirus from the phytopathogenic fungus *Fusarium langsethiae*. *Genome Announc.* 5, e01722–e01716. doi: 10.1128/genomeA.01722-16

Li, P., Lin, Y., Zhang, H., Wang, S., Qiu, D., and Guo, L. (2016). Molecular characterization of a novel mycovirus of the family *Tymoviridae* isolated from the plant pathogenic fungus *Fusarium graminearum*. *Virology* 489, 86–94. doi: 10.1016/j.virol.2015.12.004

Li, P., Zhang, H., Chen, X., Qiu, D., and Guo, L. (2015). Molecular characterization of a novel hypovirus from the plant pathogenic fungus *Fusarium graminearum*. *Virology* 481, 151–160. doi: 10.1016/j.virol.2015.02.047

Li, W., Xia, Y., Zhang, H., Zhang, X., and Chen, H. (2019). A Victorivirus from *Fusarium asiaticum*, the pathogen of *Fusarium* head blight in China. *Arch. Virol.* 164, 313–316. doi: 10.1007/s00705-018-4038-9

Lin, H., Lan, X., Liao, H., Parsley TB, Nuss DL, Chen B. (2007). Genome sequence, full-length infectious cDNA clone, and mapping of viral double-stranded RNA accumulation determinant of hypovirus CHV1-EP721. *J. Virol.* 81, 1813–1820. doi: 10.1128/JVI.01625-06

Liu, L., Xie, J., Cheng, J., Fu, Y., Li, G., Yi, X., et al. (2014). Fungal negative-stranded RNA virus that is related to bornaviruses and nyaviruses. *Proc. Natl. Acad. Sci. U.S.A.* 111, 12205–12210. doi: 10.1073/pnas.1401786111

Martelli, G. P., Sabanadzovic, S., Sabanadzovic, A. G., Edwards, M. C., and Dreher, T. (2002). The family *Tymoviridae*. *Arch. Virol.* 147, 1837–1846. doi: 10.1007/s007050200045

Martínez-Álvarez, P., Vainio, E. J., Botella, L., Hantula, J., and Diez, J. J. (2014). Three mitovirus strains infecting a single isolate of *Fusarium circinatum* are the first putative members of the family *Narnaviridae* detected in a fungus of the genus *Fusarium*. *Arch. Virol.* 159, 2153–2155. doi: 10.1007/s00705-014-2012-8

Marvelli, R. A., Hobbs, H. A., Li, S., Mccoppin, N. K., Domier, L. L., Hartman, G. L., et al. (2014). Identification of novel double-stranded RNA mycoviruses of *Fusarium virguliforme* and evidence of their effects on virulence. *Arch. Virol.* 159, 349–352. doi: 10.1007/s00705-013-1760-1

Marzano, S.-Y. L., Hobbs, H. A., Nelson, B. D., Hartman, G. L., Eastburn, D. M., Mccoppin, N. K., et al. (2015). Transfection of *Sclerotinia sclerotiorum* with *in vitro* transcripts of a naturally occurring interspecific recombinant of *Sclerotinia sclerotiorum* hypovirus 2 significantly reduces virulence of the fungus. *J Virol.* 89, 5060–5071. doi: 10.1128/JVI.03199-14

Mizutani, Y., Abraham, A., Uesaka, K., Kondo, H., Suga, H., Suzuki, N., et al. (2018). Novel mitoviruses and a unique tymo-like virus in hypovirulent and virulent strains of the *Fusarium* head blight fungus, *Fusarium boothii*. *Viruses* 10:E584. doi: 10.3390/v10110584

Moleleki, N., Van Heerden, S. W., Wingfield, M. J., Wingfield, B. D., and Preisig, O. (2003). Transfection of *Diaporthe perjuncta* with Diaporthe RNA virus. *Appl. Environ. Microbiol.* 69, 3952–3956. doi: 10.1128/AEM.69.7.3952-3956.2003

Munkvold, G. P. (2017). *Fusarium* species and their associated mycotoxins. *Methods Mol. Biol.* 1542, 51–106. doi: 10.1007/978-1-4939-6707-0_4

Nogawa, M., Kageyama, T., Nakatani, A. G., Shimosaka, M., and Okazaki, M. (1996). Cloning and characterization of mycovirus double-stranded RNA from the plant pathogenic fungus, *Fusarium solani* f. sp. robiniae. *Biosci. Biotechnol. Biochem.* 60, 784–788. doi: 10.1271/bbb.60.784

Nuss, D. L. (2005). Hypovirulence: mycoviruses at the fungal-plant interface. *Nat. Rev. Microbiol.* 3, 632–642. doi: 10.1038/nrmicro1206

Nuss, D. L. (2011). Mycoviruses, RNA silencing, and viral RNA recombination. *Adv. Virus Res.* 80, 25–48. doi: 10.1016/B978-0-12-385987-7.00002-6

Osaki, H., Sasaki, A., Nomiyama, K., Sekiguchi, H., Tomioka, K., and Takehara, T. (2015). Isolation and characterization of two mitoviruses and a putative alphapartitivirus from *Fusarium* spp. *Virus Genes* 50, 466–473. doi: 10.1007/s11262-015-1182-0

Osaki, H., Sasaki, A., Nomiyama, K., and Tomioka, K. (2016). Multiple virus infection in a single strain of *Fusarium poae* shown by deep sequencing. *Virus Genes* 52, 835–847. doi: 10.1007/s11262-016-1379-x

Pearson, M. N., and Bailey, A. M. (2013). Viruses of *Botrytis*. *Adv. Virus Res.* 86, 249–272. doi: 10.1016/B978-0-12-394315-6.00009-X

Pearson, M. N., Beever, R. E., Boine, B., and Arthur, K. (2010). Mycoviruses of filamentous fungi and their relevance to plant pathology. *Mol. Plant Pathol.* 10, 115–128. doi: 10.1111/j.1364-3703.2008.00503.x

Sasaki, A., Kanematsu, S., Onoue, M., Oikawa, Y., Nakamura, H., and Yoshida, K. (2007). Artificial infection of *Rosellinia necatrix* with purified viral particles of a member of the genus *Mycoreovirus* reveals its uneven distribution in single colonies. *Phytopathology* 97, 278–286. doi: 10.1094/PHYTO-97-3-0278

Sharma, M., Guleria, S., Singh, K., Chauhan, A., and Kulshrestha, S. (2018). Mycovirus associated hypovirulence, a potential method for biological control of *Fusarium* species. *Virusdisease* 29, 134–140. doi: 10.1007/s13337-018-0438-4

Son, H., Park, A. R., Lim, J. Y., Shin, C., and Lee, Y. W. (2017). Genome-wide exonic small interference RNA-mediated gene silencing regulates sexual reproduction in the homothallic fungus *Fusarium graminearum*. *PLoS Genet.* 13:e1006595. doi: 10.1371/journal.pgen.1006595

Son, M., Choi, H., and Kim, K. H. (2016). Specific binding of *Fusarium graminearum* Hex1 protein to untranslated regions of the genomic RNA of Fusarium graminearum virus 1 correlates with increased accumulation of both strands of viral RNA. *Virology* 489, 202–211. doi: 10.1016/j.virol.12015.12.013

Son, M., Lee, K.-M., Yu, J., Kang, M., Park, J.-M., Kwon, S.-J., et al. (2013). The HEX1 gene of *Fusarium graminearum* is required for fungal asexual reproduction and pathogenesis and for efficient viral RNA accumulation of Fusarium graminearum virus 1. *J. Virol.* 87, 10356–10367. doi: 10.1128/JVI.01026-13

Son, M., Yu, J., and Kim, K. H. (2015). Five questions about mycoviruses. *PLoS Pathog.* 11:e1005172. doi: 10.1371/journal.ppat.1005172

Stanway, C. A., and Buck, K. W. (1984). Infection of protoplasts of the wheat take-all fungus, *Gaeumannomyces graminis* var. tritici, with double-stranded RNA viruses. *J. Gen. Virol.* 65, 2061–2065. doi: 10.1099/0022-1317-65-11-2061

Suzuki, N. (2017). Frontiers in fungal virology. *J. Gen. Plant Pathol.* 83, 419–423. doi: 10.1007/s10327-017-0740-9

Wang, L., He, H., Wang, S., Chen, X., Qiu, D., Kondo, H., et al. (2018). Evidence for a novel negative-stranded RNA mycovirus isolated from the plant pathogenic fungus *Fusarium graminearum*. *Virology* 518, 232–240. doi: 10.1016/j.virol.2018.03.008

Wang, L., Wang, S., Yang, X., Zeng, H., Qiu, D., and Guo, L. (2017). The complete genome sequence of a double-stranded RNA mycovirus from *Fusarium graminearum* strain HN1. *Arch. Virol.* 162, 2119–2124. doi: 10.1007/s00705-017-3317-1

Wang, L., Zhang, J., Zhang, H., Qiu, D., and Guo, L. (2016a). Two novel relative double-stranded RNA mycoviruses infecting *Fusarium poae* strain SX63. *Int. J. Mol. Sci.* 17:E641. doi: 10.3390/ijms17050641

Wang, S., Kondo, H., Liu, L., Guo, L., and Qiu, D. (2013). A novel virus in the family *Hypoviridae* from the plant pathogenic fungus *Fusarium graminearum*. *Virus Res.* 174, 69–77. doi: 10.1016/j.virusres.2013.03.002

Wang, S., Li, P., Zhang, J., Qiu, D., and Guo, L. (2016b). Generation of a high resolution map of sRNAs from *Fusarium graminearum* and analysis of responses to viral infection. *Sci. Rep.* 6:26151. doi: 10.1038/srep26151

Wang, S., Zhang, J., Li, P., Qiu, D., and Guo, L. (2016c). Transcriptome-based discovery of *Fusarium graminearum* stress responses to FgHV1 infection. *Int. J. Mol. Sci.* 17:E1922. doi: 10.3390/ijms17111922

Wei, S., Bian, R., Andika, I. B., Niu, E., Liu, Q., Kondo, H., et al. (2019). Symptomatic plant viroid infections in phytopathogenic fungi. *Proc. Natl. Acad. Sci. U.S.A.* 116, 13042–13050. doi: 10.1073/pnas.1900762116

Wu, S., Cheng, J., Fu, Y., Chen, T., Jiang, D., Ghabrial, S. A., et al. (2017). Virus-mediated suppression of host non-self recognition facilitates horizontal transmission of heterologous viruses. *PLoS Pathog.* 13:e1006234. doi: 10.1371/journal.ppat.1006234

Xiao, X., Cheng, J., Tang, J., Fu, Y., Jiang, D., Baker, T. S., et al. (2014). A novel partitivirus that confers hypovirulence on plant pathogenic fungi. *J. Virol.* 88, 10120–10133. doi: 10.1128/JVI.01036-14

Xie, J., and Jiang, D. (2014). New insights into mycoviruses and exploration for the biological control of crop fungal diseases. *Annu. Rev. Phytopathol.* 52, 45–68. doi: 10.1146/annurev-phyto-102313-050222

Yu, J., Kwon, S. J., Lee, K. M., Son, M., and Kim, K. H. (2009). Complete nucleotide sequence of double-stranded RNA viruses from *Fusarium graminearum* strain DK3. *Arch. Virol.* 154, 1855–1858. doi: 10.1007/s00705-009-0507-5

Yu, J., Lee, K. M., Cho, W. K., Park, J. Y., and Kim, K. H. (2018). Differential contribution of RNA interference components in response to distinct Fusarium graminearum virus infections. *J. Virol.* 92, e01756–e01717. doi: 10.1128/JVI.01756-17

Yu, J., Lee, K. M., Son, M., and Kim, K. H. (2015). Effects of the deletion and over-expression of *Fusarium graminearum* gene FgHal2 on host response to mycovirus Fusarium graminearum virus 1. *Mol. Plant Pathol.* 16, 641–652. doi: 10.1111/mpp.12221

Yu, J.-S., Lee, K.-M., Son, M.-I., and Kim, K.-H. (2011). Molecular characterization of Fusarium graminearum virus 2 Isolated from *Fusarium graminearum* strain 98-8-60. *Plant Pathol. J.* 27, 285–290. doi: 10.5423/PPJ.2011.27.3.285

Yu, X., Li, B., Fu, Y., Xie, J., Cheng, J., Ghabrial, S. A., et al. (2013). Extracellular transmission of a DNA mycovirus and its use as a natural fungicide. *Proc. Natl. Acad. Sci. U.S.A.* 110, 1452–1457. doi: 10.1073/pnas.1213755110

Zhang, R., Hisano, S., Tani, A., Kondo, H., Kanematsu, S., and Suzuki, N. (2016). A capsidless ssRNA virus hosted by an unrelated dsRNA virus. *Nat. Microbiol.* 1:15001. doi: 10.1038/nmicrobiol.2015.1

Zhang, R., Liu, S., Chiba, S., Kondo, H., Kanematsu, S., and Suzuki, N. (2014). A novel single-stranded RNA virus isolated from a phytopathogenic filamentous fungus, *Rosellinia necatrix*, with similarity to hypo-like viruses. *Front. Microbiol.* 5:360. doi: 10.3389/fmicb.2014.00360

Zhang, X., Gao, F., Zhang, F., Xie, Y., Zhou, L., Yuan, H., et al. (2018). The complete genomic sequence of a novel megabirnavirus from *Fusarium pseudograminearum*, the causal agent of wheat crown rot. *Arch. Virol.* 163, 3173–3175. doi: 10.1007/s00705-018-3970-z

Zhang, X., Xie, Y., Zhang, F., Sun, H., Zhai, Y., Zhang, S., et al. (2019). Complete genome sequence of an alternavirus from the phytopathogenic fungus *Fusarium incarnatum*. *Arch. Virol.* 164, 923–925. doi: 10.1007/s00705-018-04128-2

Conflict of Interest Statement: The authors declare that the research was conducted in the absence of any commercial or financial relationships that could be construed as a potential conflict of interest.

frontiers in Plant Science

ORIGINAL RESEARCH
published: 30 July 2019
doi: 10.3389/fpls.2019.00976

Roles of Argonautes and Dicers on *Sclerotinia sclerotiorum* Antiviral RNA Silencing

Achal Neupane[1†], Chenchen Feng[2†], Pauline K. Mochama[1†], Huma Saleem[1] and Shin-Yi Lee Marzano[1,2]*

[1] Department of Biology and Microbiology, South Dakota State University, Brookings, SD, United States, [2] Department of Agronomy, Horticulture and Plant Science, South Dakota State University, Brookings, SD, United States

RNA silencing or RNA interference (RNAi) is an essential mechanism in animals, fungi, and plants that functions in gene regulation and defense against foreign nucleic acids. In fungi, RNA silencing has been shown to function primarily in defense against invasive nucleic acids. We previously determined that mycoviruses are triggers and targets of RNA silencing in *Sclerotinia sclerotiorum*. However, recent progresses in RNAi or dsRNA-based pest control requires more detailed characterization of the RNA silencing pathways in *S. sclerotiorum* to investigate the utility of dsRNA-based strategy for white mold control. This study elucidates the roles of argonaute enzymes, *agl*-2 and *agl*-4, in small RNA metabolism in *S. sclerotiorum*. Gene disruption mutants of *agl*-2 and *agl*-4 were compared for changes in phenotype, virulence, viral susceptibility, and small RNA profiles. The Δ*agl*-2 mutant but not the Δ*agl*-4 mutant had significantly slower growth and virulence prior to virus infection. Similarly, the Δ*agl*-2 mutant but not the Δ*agl*-4 mutant, showed greater debilitation under virus infection compared to uninfected strains. The responses were confirmed in complementation studies and revealed the antiviral role of *agl*-2. Gene disruption mutants of *agl*-2, *agl*-4, Dicer-like (*dcl*)-1, and *dcl*-2 did not change the stability of the most abundant endogenous small RNAs, which suggests the existence of alternative enzymes/pathways for small RNA biogenesis in *S. sclerotiorum.* Furthermore, *in vitro* synthesized dsRNA targeting *agl*-2 showed a significantly reduced average lesion diameter ($P < 0.05$) on canola leaves with *agl*-2 down-regulated compared to controls. This is the first report describing the effectiveness of RNA pesticides targeting *S. sclerotiorum* RNA silencing pathway for the control of the economically important pathogen.

Keywords: RNA pesticide, argonautes, dicers, mycovirus, *Sclerotinia sclerotiorum*, RNA silencing, tRNA halves

OPEN ACCESS

Edited by:
Daohong Jiang, Huazhong Agricultural University, China

Reviewed by:
Attila Molnar, The University of Edinburgh, United Kingdom
Carmen Hernandez, Polytechnic University of Valencia, Spain

***Correspondence:**
Shin-Yi Lee Marzano
shinyi.marzano@sdstate.edu; sylee1110@yahoo.com

[†] These authors have contributed equally to this work

Specialty section:
This article was submitted to Virology, a section of the journal Frontiers in Plant Science

Received: *01 February 2019*
Accepted: *11 July 2019*
Published: *30 July 2019*

Citation:
Neupane A, Feng C, Mochama PK, Saleem H and Lee Marzano S-Y (2019) Roles of Argonautes and Dicers on Sclerotinia sclerotiorum Antiviral RNA Silencing. Front. Plant Sci. 10:976. doi: 10.3389/fpls.2019.00976

INTRODUCTION

RNA silencing is a transcriptional and post-transcriptional suppression of gene expression. One of the roles that RNA silencing plays has long been identified as an adaptive defense mechanism against foreign nucleic acids, including viruses in animals, fungi, and plants (Waterhouse et al., 2001; Baulcombe, 2004, 2005). Unlike in animals and plants, the evolved RNA silencing in fungi to date has demonstrated that it is almost dispensable for endogenous gene

regulation because gene disruption mutants often grow just fine. Instead, only when the mutants of RNA silencing genes are under virus infection, the antiviral role of those genes play then become evident (Segers et al., 2007; Zhang et al., 2014; Yu et al., 2018). However, studies of *Neurospora crassa* and other filamentous fungi have revealed diverse small RNA biogenesis pathways, suggesting that fungi adapt RNAi silencing pathways for several cellular processes with some of the RNA silencing genes playing dual roles (reviewed in Dang et al., 2011). On the other hand, fungal RNA silencing genes can also have redundant functions, such as antiviral, processing of dsRNA or transgenes (Catalanotto et al., 2004; Wang et al., 2016; Yu et al., 2018).

Sclerotinia sclerotiorum is a devastating plant fungal pathogen that causes up to 100% yield losses in crop production affecting a wide array of crops (Heffer Link and Johnson, 2007). Recent studies demonstrated that cross-kingdom RNA silencing can be blocked to control *Botrytis cinerea* which is closely related to *S. sclerotiorum* (Amselem et al., 2011). The virulence of *B. cinerea* can be greatly suppressed by silencing both *B. cinerea* Dicers at the same time (Wang et al., 2016). A similar observation was made in *S. sclerotiorum* following simultaneous disruption of both its Dicers to result in reduced pathogenicity (Mochama et al., 2018). Therefore, RNA silencing pathway has great potential to be manipulated to control fungal pathogens. As *S. sclerotiorum* has two predicted Argonautes (GenBank accession numbers Ss1G_00334 and Ss1G_11723), it is intriguing whether corresponding argonaute genes affect *S. sclerotiorum* virulence and whether it could add to the tool box of disease control with other novel strategies.

The Argonaute protein family constitutes four domains, N-terminal domain, Mid domain, and RNA-binding domains known as PAZ domains, and slicer domains known as PIWI domains (Poulsen et al., 2013). Argonaute proteins stabilize small dsRNA molecules produced by Dicer proteins to form RNA-induced silencing complexes (RISC) which are involved in post-transcriptional gene silencing or RNA-induced transcriptional silencing complexes involved in transcriptional gene silencing including chromatin modification in animals, plants, and insects (Irvine et al., 2006). When small dsRNA molecules produced by Dicers are incorporated into these effector complexes, one strand of the RNA molecule is removed and the remaining strand guides the complex to complementary RNA sequences which are subsequently cleaved by the Argonaute RNase H-like activity (Qihong et al., 2009).

Argonaute homologs have been identified in various fungi and they differ in function and number. The basal fungus, *Mucor circinelloides*, has three argonaute genes while *Cryphonectria parasitica* has four argonaute genes and *Colletotrichum higginsianum* has two (Qihong et al., 2009; Trieu et al., 2015; Campo et al., 2016). QDE-2 is a fungal argonaute homolog in *N. crassa* involved in quelling-the silencing of repetitive sequences such as transgenes (Fulci and Macino, 2007). In *N. crassa*, a separate silencing pathway called meiotic silencing of unpaired DNA (MSUD) has been characterized, and *N. crassa* RNA silencing components not involved in quelling have been shown to be involved in this pathway (Fulci and Macino, 2007). Similarly, in other fungi, not all components of the RNA silencing machinery are involved in RNA silencing mediated viral defense mechanisms. In *Fusarium graminearum*, only one of two argonaute genes, FgAgo1, is important in RNA silencing of viral nucleic acids (Yu et al., 2018) while in *C. parasitica* only *agl*-2 is required for antiviral RNA silencing, and in *C. higginsianum*, *agl*-1 but not *agl*-2 is essential for antiviral RNA silencing (Qihong et al., 2009; Trieu et al., 2015; Campo et al., 2016). The primary functions of the other gene homologs have not been fully characterized. As *S. sclerotiorum* are predicted to have two argonaute genes, *agl*-2 and *agl*-4, it presents a potential strategy to impede the proper small RNA processing after characterizing the roles of argonautes in *S. sclerotiorum*.

The goals of this study were to determine the function of argonaute genes in endogenous small RNA processing and defending virus infection in *S. sclerotiorum*, and as a proof of concept, to demonstrate a control strategy from silencing a specific argonaute gene. To achieve them, we made gene displacement mutants of argonaute genes in this study and transfected *S. sclerotiorum* with a RNA virus (SsHV2-L) and

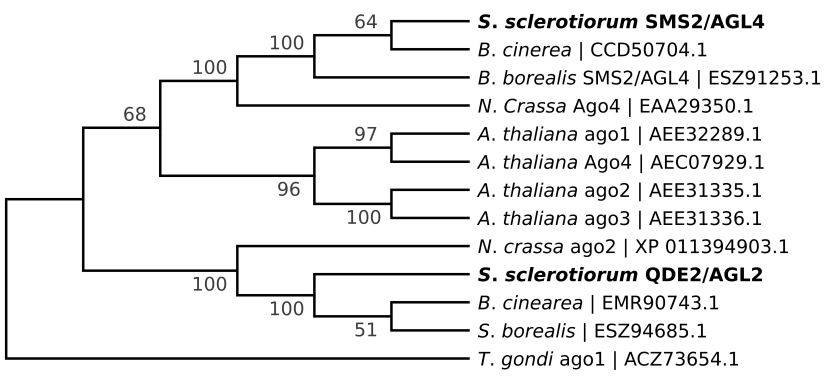

FIGURE 1 | Phylogenetic analysis (Maximum Likelihood tree) of *agl*-2 and *agl*-4 genes depicting the relationships between the protein sequences from *S. sclerotiorum* (in bold), along with their orthologs in *B. cinerea*, *S. borealis*, *N. crassa* and *Arabidopsis thaliana*. The *Toxoplasma gondii agl*-1 amino acid sequence was used as an outgroup. Bootstrap consensus was calculated based on 100 bootstrap replicates using Mega 7.0 (Kumar et al., 2016).

compared the changes in morphology and pathogenicity. Gene displacement mutants revealed that only *agl*-2 is important in vegetative growth, as well as antiviral defense, whereas the biological function of *agl-4* remains unknown. We further established the application of dsRNA externally targeting *agl*-2 as an RNA pesticide to slow the infection in a dose-dependent manner.

MATERIALS AND METHODS

Fungal Culture Strains and Conditions

The wild type strain, DK3, of *S. sclerotiorum* was grown on potato dextrose agar (PDA) (Sigma) at 20–22Δ. The gene displaced mutants of Δ*agl*-2 and Δ*agl*-4 strains were grown on PDA amended with hygromycin B (Alfa Aesar) at 100 μg/mL as selection. Dicer mutants were produced in our previous study (Mochama et al., 2018).

Gene Disruption of *agl*-2 and *agl*-4

Sclerotinia sclerotiorum argonaute-like genes were predicted based on homology to those identified in *N. crassa* (Laurie et al., 2012). Published sequences of Ss1G_00334 and Ss1G_11723 in the GenBank (NCBI) are the putative argonaute genes coding for QDE-2/AGO-2 and SMS-2/AGO-4 in *N. crassa*, respectively (**Figure 1**). Argonaute genes were displaced by the hygromycin phosphotransferase gene (*hph*) using the split-marker homologous recombination cassettes as described before (Mochama et al., 2018). To generate the Δ*agl*-2 gene displacement mutant, a 1.5 kb 5′ flanking arm of *agl*-2 was PCR-amplified by primers F1-AGO2 and F2-AGO2 and a 1.5 kb 3′ flanking arm of *agl*-2 was PCR-amplified by primers F3-AGO2 and F4-AGO2. The *hph* gene was amplified from pCSN43 (Fungal Genetics Stock Center) using primers PtrpC – HY and YG – TrpC to give two amplicons (1.2 and 1.3 kb) each containing part of the *hph* marker gene with an overlap (**Table 1**). The 5′-flank of the Δ*agl*-2 gene was then connected to the partial *hph* amplicon containing P*trp*C and the 3' flank was connected to the *hph* amplicon containing T*trp*C using the overlap extension PCR method. Eventually, an *agl*-2 gene deletion construct that included 1 kb of identical sequence to the 5′ flanking arm of the gene and 812 bp of the 3′ flanking arm sequence was derived. A similar procedure was used to generate the *agl*-4 deletion construct with 805 bp of sequence identical to the 5′ flanking arm and 1.1 kb of the 3′ flanking arm of *agl*-4.

Fungal Transformation

PEG-mediated transformation method was used to transfer the gene deletion cassettes into *S. Sclerotiorum* DK3 protoplasts as described before (Mochama et al., 2018). Fungal DNA was extracted from mycelia and PCR-amplified by the use of primers-F1, F4, F1, HYR, YG2, and F4 to ascertain that argonaute genes were each displaced by the *hph* gene, confirmed by Sanger sequencing. Because *S. sclerotiorum* does not produce conidia, repeated hyphal tipping and nested PCR were necessary to derive a monokaryotic line of each targeted gene disruption to avoid mixed results from heterokaryotic mutants.

Complementation

To complement *agl*-2, protoplasts from the Δ*agl*-2 strain was transformed with a bialaphos plasmid (pBARKS-1) cloned to express the full *agl*-2 gene flanked by 2.8 kb of 5′-upstream and 1.5 kb of 3′-downstream sequences to include the corresponding promoter and terminator. The *agl*-2 gene and flanking arms were amplified from the DNA extract of DK3 using primers F1-COMP-AGO2 and F4-COMP-AGO2 (**Table 1**) and inserted into the *Not*I and *BamHI* sites of pBARK-1 downstream to PTrpC and bialaphos resistance gene, *bla*1. Protoplasts and PEG-mediated transformation were the same as described earlier, except that the regeneration media was now supplemented with bialaphos at 10 μg/mL for selection. Multiple transformants were selected and hyphal-tipped several times to fresh PDA

TABLE 1 | Primer used in this study.

Primer Name	Sequence	Note
F1-AGO2	TGGTGAATTGTGAGTT GAATGGTG	*agl*-2 KO
F2-AGO2	ACCCAATTCGCCCTATAGT GAGTCGTGCTGCTGGA TCAAAAGACAT	*agl*-2 KO
F3-AGO2	AAGCCTACAGGACACACA TTCATCGTAGGTACCT GGTCATACCTTCCGCAT	*agl*-2 KO
F4-AGO2	CAGGTCCAAGTCCT GTCCAC	*agl*-2 KO
YG-F	CGTTGCAAGACCTGC CTGAA	Both KO
PtrpC-F	ACGACTCACTATAGGG CGAATTGGGT	Both KO
TtrpC-R	TACCTACGATGAATGTGTG TCCTGTAGGCTT	Both KO
HY-R	GGATGCCTCCGCTCGA AGTA	Both KO
F1-AGO2-nested	GTTTGCAACAATC GCAGGTG	*agl*-2 KO
F4-AGO2-nested	TCTCCAACCAG CTACCGATG	*agl*-2 KO
F1-AGO4	TTTGGTCCAGG CCTTGGTTT	*agl*-4 KO
F1-AGO4-nested	TTTTCACAACGG GTTTGGGC	*agl*-4 KO
F2-AGO4	ACCCAATTCGCCCTATAGT GAGTCGTGAGCCATTAGCTTGG ATATTCGCA	*agl*-4 KO
F3-AGO4	AAGCCTACAGGACACA CATTCATCGTAGGTAAGTGCCT TCATATCATAATCCTCC	*agl*-4 KO
F4-AGO4	AAGGTTCGTCGGTT GGTAGT	*agl*-4 KO
F4-AGO4-nested	CCCTACTTGTCCC ACGTGAT	*agl*-4 KO
F1-COMP-AGO2	ATAATAGCGGCCGCCGGA TAAACTGCCTCTTCGC	*agl*-2 Complementation
F4-COMP-AGO2	TTTTACTGGATCCTCCT GTCCACAATCCCACAA	*agl*-2 Complementation
Ss-Ago2-T7p-1898F	TAATACGACTCACTATAG GGAGATGAATCTACA AGCCGTGCTG	dsRNA synthesis targeting *agl*-2
Ss-Ago2-T7p-2065R	TAATACGACTCACTATAGG GAGATGAGAGGTA GCCGCTTCATT	dsRNA synthesis targeting *agl*-2
Ss-Ago4-T7p-F	TAATACGACTCACTATAGGGAGA TTTGGTTGCAAAATCGATCA	dsRNA synthesis targeting *agl*-4
Ss-Ago4-T7p-R	TAATACGACTCACTATAGGGA GATTGCTTGCTTTGTTGACCAG	dsRNA synthesis targeting *agl*-4

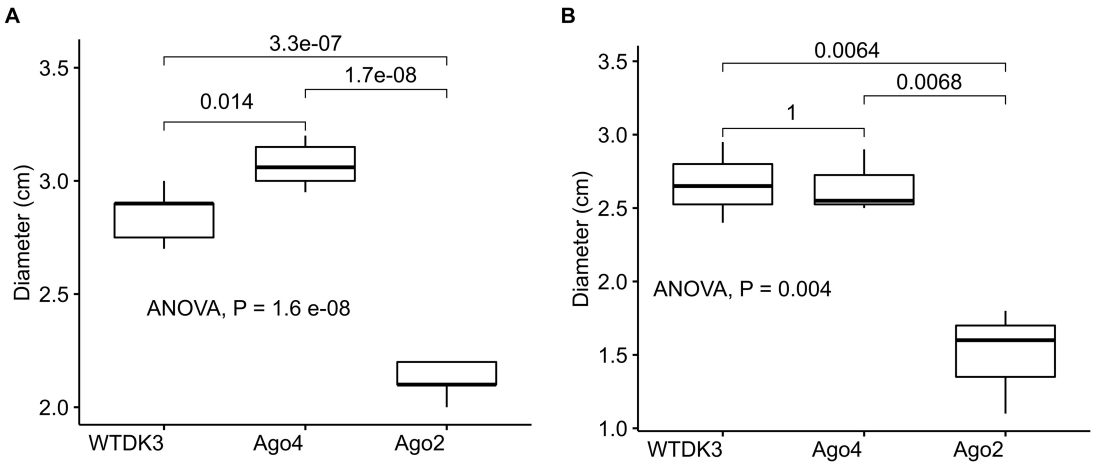

FIGURE 2 | Average hyphal diameter of *S. sclerotiorum* wild type and argonaute gene disruption mutants (Δ*agl*-2 and Δ*agl*-4) grown **(A)** on PDA for 1 dpi, and **(B)** on detached canola leaves 2 dpi.

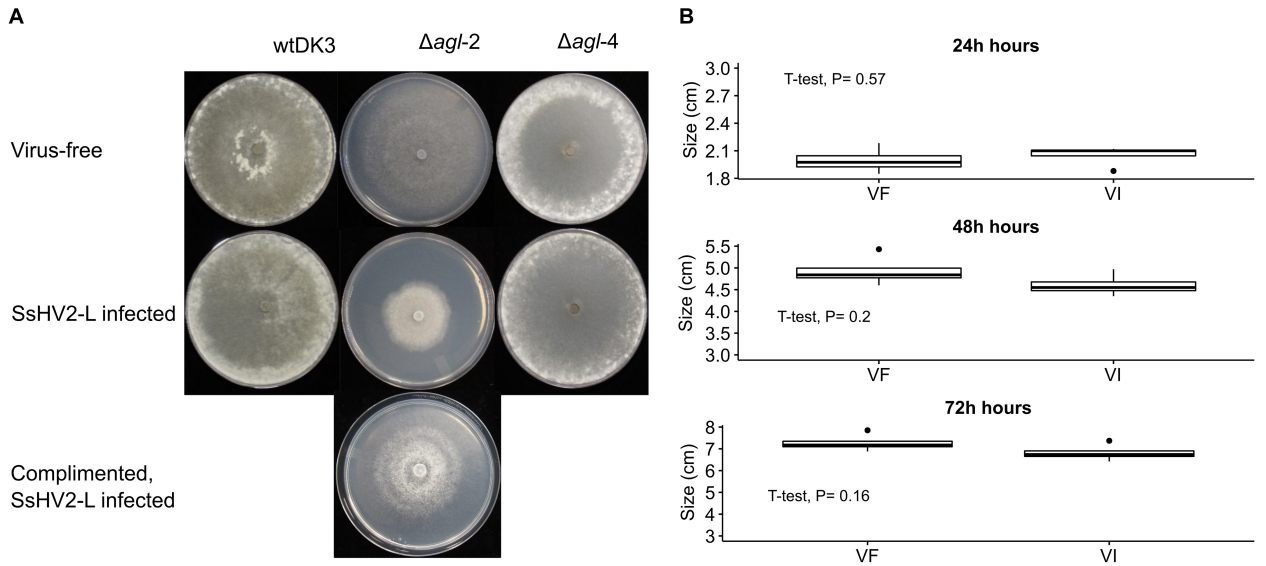

FIGURE 3 | Colony morphology of virus-free and virus-infected gene deletion mutants. (Top row) Virus-free DK3, Δ*agl*-2 and Δ*agl*-4. (Bottom row) wild-type and mutant strains infected with hypovirus SsHV2-L. Cultures were grown for **(A)** 4 days on PDA. The virus-infected *agl*-2 mutant displays significantly slower growth and altered colony morphology. **(B)** Comparison of the complemented strains with and without virus infection ($P > 0.05$).

plates amended with bialaphos. PCR amplification using *agl*-2 specific primers confirmed the ectopic integration of the gene, and then four transformants were compared for the morphology on PDA between the virus-free and SsHV2-L virus-infected complemented strains.

Phenotypic Characterization of Gene Deletion Mutants

At least five replications each of DK3, Δ*agl*-2, and Δ*agl*-4 cultures with or without SsHV2 infections were compared for the phenotypes. Hyphal diameter was measured daily as described before (Mochama et al., 2018). A 5-mm plug was placed on a freshly cut canola leaf. More than three replicates of the leaves were inoculated on moist paper towels in covered petri dishes kept on a lab bench at room temperature. Hyphal area was measured daily at 24, 48, and 72 h post-inoculation.

In vitro dsRNA Synthesis, Inoculation, and Confirmation of Silencing by RT-qPCR

PCR amplification of the *agl*-2 target was performed using gene-specific primers with T7 promoter sequence added on both the forward primer and the reverse primer. Primers Ss-Ago2-T7p-1898F and Ss-Ago2-T7p-2065R were used

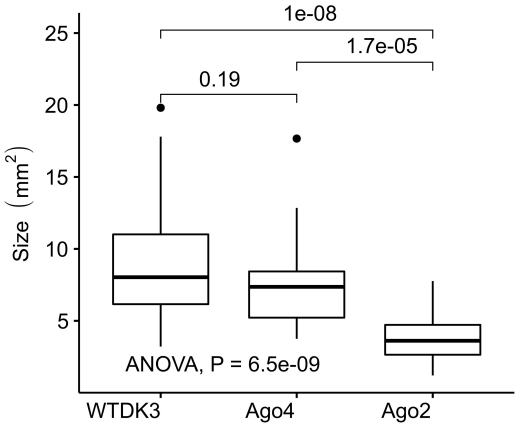

FIGURE 4 | Comparison of sclerotial morphology in wild-type DK3 and mutant strains, Δ*agl*-2 and Δ*agl*-4. The Δ*agl*-2 mutant produces smaller sclerotia on average.

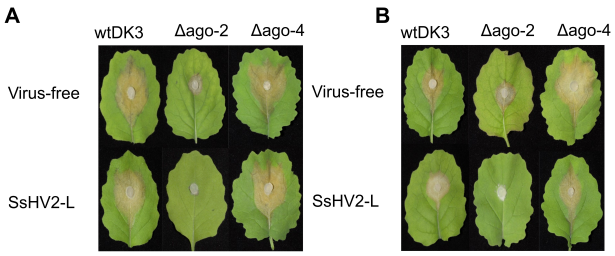

FIGURE 5 | Virulence assays on detached canola. Plugs were taken from the edge of actively growing DK3, Δ*agl*-2, and Δ*agl*-4 cultures and inoculated onto detached leaves. Lesion size was measured **(A)** 2 dpi, **(B)** 3 dpi.

(**Table 1**). dsRNAs were synthesized using MEGAscript T7 Transcription kit (Invitrogen) following the manufacturer's procedure. To compare the suppressing effect of dsRNA on fungal pathogenicity, a 2 days actively growing plug in 3-mm diameter taken from the margin of a colony of *S. sclerotiorum* DK3 was placed on each canola leaf. Six replications each of different doses of abovementioned dsRNA at 200, 400, and 800 ng was pipetted to surround an agar plug in the volume of 20 μl, taking reference from the dosage of 800 ng/20 μl published by Wang et al. (2016). As controls, the same volume of water, as well as dsRNA targeting *agl*-4 were pipetted to surround the agar plug on canola leaves. dsRNA targeting *agl*-4 was produced the same way as that targeting *agl*-2 but with primers Ss-Ago4-T7p-F and Ss-Ago4-T7p-R. The lesion was measured length wise and at right angle across again to obtain an average for a representative diameter 2 days post-inoculation. The data was statistically analyzed using paired *t*-test; and using one-way ANOVA (for three or more samples), and when significant effect was determined, Tukey's HSD test was performed to compare all pairs of means.

Only the lesions from 200 and 400 ng/20 μl were cut out to extract for total RNA using RNeasy Plant Mini Kit (Qiagen) since 800 ng/20 μl treatment does not produce lesions. RT-qPCR was performed to confirm the silencing of *agl*-2 gene in a dose-response manner using Luna Universal One-Step RT-qPCR Kit (NEB) following the manufacturer's protocol. The comparative CT method (ΔΔCT method) was used to analyze the data. The expression levels of *agl*-2 and an endogenous control (actin) were evaluated with three biological replicates and four technical replicates each. The statistical significance of observed fold-difference was analyzed by ANOVA and Tukey's test for pair-wise means separation.

Small RNA Libraries Preparation and Analysis of the Sequencing Results

MirVana miRNA Isolation kit (Thermo Fisher Scientific) was used to extract small RNAs from 4-day-old mycelia. NEBNext small RNA Library Kit (NEB, Ipswich, MA, United States) was used to construct the libraries for sequencing. The libraries were barcoded, pooled in a single lane for 50-nt single-end reads sequencing on an HiSeq4000 at the Roy J. Carver Biotechnology Center, UIUC. Three replicates of samples from SsHV2-L virus-infected DK3 as well as four replicates (two virus-infected and two virus-free mutants) each of Δ*dcl*-1, Δ*dcl*-2, Δ*agl*-2, and Δ*agl*-4 samples were sequenced. Adaptors were trimmed by BBMap tools (Bushnell, 2014). ShortStack (Axtell, 2013) was used to identify loci producing sRNAs by clustering. The number of reads aligned to *S. sclerotiorum* and SsHV2-L genomes were computed using bowtie (Langmead et al., 2009), and further downstream analysis were performed using in-house Perl and R scripts. tRNA encoding genes were predicted by tRNAscan-SE (Lowe and Chan, 2016).

RESULTS

Disruption Mutants of Argonaute-Like Genes Were Generated

Argonaute-like genes were disrupted directly from wild-type strain DK3 using the same approach as described before (Mochama et al., 2018). Disruption was screened by PCR amplification using F1 and F4 primers and DNA extracts from multiple transformants as the templates to rule out ectopic integration of the *hph* gene. Sanger sequencing of the PCR amplicons confirmed the integration. Once a monokaryotic mutation was obtained by hyphal-tipping and confirmed by PCR that the target genes were completely deleted, further characterizations of the mutants were carried out.

Effect of Argonaute-Like Genes Disruption on Phenotype

The colony morphology including the growth rate and the size of the sclerotia of the argonaute mutants and the wild-type strain DK3 on PDA were compared. Single mutant Δ*agl*-4 and DK3 exhibited similar growth rates, whereas the Δ*agl*-2 gene displacement mutant exhibited significantly slower growth at 24 h measured by the diameters of hyphal growth

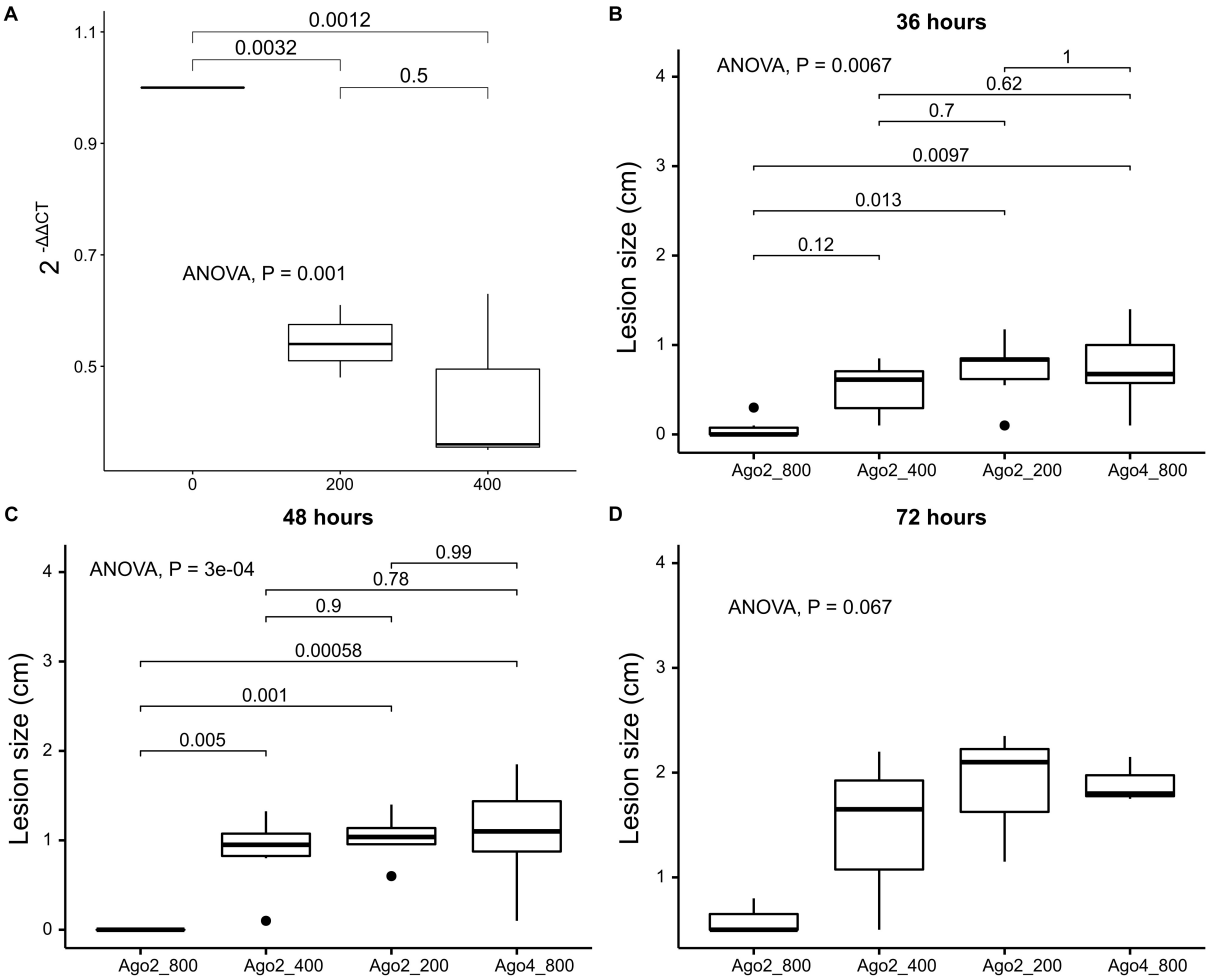

FIGURE 6 | Effects of external RNA pesticide on inhibiting *S. sclerotiorum* from causing lesions on canola leaves comparing dsRNA targeting *agl*-2 at 800 ng/20 μl, 400 ng/20 μl, 200 ng/20 μl, dsRNA targeting *agl*-4 at 800 ng/20 μl as control (from left to right), confirmed by **(A)** RT-qPCR with reduced expression levels of *agl*-2 at 200 and 400 ng, and lesion comparison at **(B)** 36, **(C)** 48, and **(D)** 72 h post-inoculation.

($P < 0.05$) (**Figure 2A**). As shown in **Figure 3**, at 4 days post-inoculation (dpi) (**Figure 3A**), no change in growth rate was observed in Δ*agl*-4, whereas Δ*agl*-2 mutant shows a slower growth and a reduction in the size of sclerotia produced (**Figure 4**). After multiple times of hyphal-tipping, four *agl*-2 complemented transformants were assayed. The complemented strains exhibited a reversal of phenotype in antiviral defense (**Figure 3B**).

Effects of Argonaute-Like Gene Disruptions on *S. sclerotiorum* Pathogenicity

The virulence of *S. sclerotiorum* argonaute mutants was evaluated by inoculating detached leaves with agar plugs of mycelia. Lesion size data was collected at 1, 2, and 3 dpi showed that no difference in the lesion size produced by the mutant Δ*agl*-4, but a significantly smaller lesion produced by Δ*agl*-2 mutant compared to those produced by DK3 (**Figures 2B**, **5**) ($P < 0.05$).

Effects of Argonaute Gene on Antiviral Defense

To examine the effect of viral infection on strains containing null-mutations of *agl*-2 and *agl*-4, mutants were transfected through hyphal fusion with SsHV2-L infected mycelia. As shown in **Figure 3**, no significant differences were observed in growth and morphology in the *agl*-4 mutant infected with the mycovirus compared to virus-infected DK3, whereas the *agl*-2 mutant showed a significantly debilitated growth (**Figures 3**, **5**) ($P < 0.05$).

In vitro Synthesized dsRNA Targeting *agl*-2 Shows Reduced Virulence of *S. sclerotiorum*

Once we determined that *agl*-2 plays an important role in endogenous small RNA processing, exemplified by a debilitated growth even without virus infection, the *agl*-2 was then targeted using *in vitro* synthesized dsRNA constructs in order to disrupt

the fungal small RNA processing. RT-qPCR confirmed that *agl*-2 was silenced at the level of 800 ng in 20 µl volume but not at the lower doses of 200 or 400 ng (**Figure 6A**). As shown in **Figures 6B–D**, strains in which *in vitro* 800 ng of dsRNA was applied externally to target *agl*-2 exhibited a slower spread on canola leaves up to 3 days post-infection compared to lower doses at 200 and 400 ng applied or the targeting of *agl*-4 by the corresponding dsRNA (**Supplementary Material**).

Profiles of sRNAs in Distinct *S. sclerotiorum* Strains

The raw sequence reads were uploaded to NCBI SRA database under accessions SRR8844548 (WT-1), SRR8844549 (WT-2), SRR8785208 (WT-3), SRR8785205 (Δdcl1-1), SRR8785204 (Δdcl1-2), SAMN12129781 (Δdcl1-VF1), SAMN12129782 (Δdcl1-VF2), SRR8785203 (Δdcl2-1), SRR8785202 (Δdcl2-2), SAMN12129783 (Δdcl2-VF1), SAMN12129784 (Δdcl2-VF2), SRR8785201 (Δagl2-1), SRR8785200 (Δagl2-2), SAMN12129777 (Δagl2-VF1), SAMN12129778 (Δagl2-VF2), SRR8785199 (Δagl4-1), SRR8785198 (Δagl4-2), SAMN12129779 (Δagl4-VF1), and SAMN12129780 (Δagl4-VF2). **Table 2** summarized the numbers of aligned small RNA sequence reads from the mutants and the WT sample that passed the ShortStack filtering parameters to allow the clustered reads for downstream analysis.

A major portion of endogenous small RNAs were found to represent the same small RNAs identified from our previous study (Lee Marzano et al., 2018), predominantly tRNA halves (tRFs): tRF5-Glu(GAA), 5′-TCCGAATTAGTGTAGGGGTTAACATAACTC-3′, and tRF5-Asp(GAC), 5′-TCTTTGATGGTCTAACGGTCATGATTTCC-3′, derived from tRNAs delivering glutamic acid and aspartic acid at 1.1 and 1.3% of total filtered reads in average, respectively. Homologs of the abovementioned two tRFs range in size from 29 to 35 bases with a major peak at 33 nt as TCTTTGATGGTCTAACGGTCATGATTTCCGTCC (**Figures 7A–D**) (underlined are the bases when expanding the size of small RNAs up to 34 nt long). tRF5-Glu(GAA) is predicted to be produced from SS1G_14562 and SS1G_14600 on chromosomes 7 and 4, respectively, whereas tRF5-Asp(GAC) is produced from SS1G_14527 on chromosome 14. The clustering result showed that these two small RNAs were mapped solely to intergenic regions. The BLASTn search (Altschul et al., 1990) indicates their homology to specific loci on chromosomes 4, 7, 14, and 16 for tRF5-Glu(GAA), and on chromosomes 1, 5, 11, 12, and 14 for tRF5-Asp(GAC). These small RNAs and their homologs are derived from mature tRNAs and contribute to the major peak at 29 or 33 nt. Compared to the wild type (**Figure 7A**), the productions of the two species were not affected by either single dicer mutations (**Figures 7B,C**), nor double dicer mutations (**Figure 7D**) (Mochama et al., 2018), and the stability of these small RNAs were not drastically affected by argonaute mutations (**Figures 7E,F**). Therefore, the reanalyzed data of double dicer mutant (previously published in Mochama et al., 2018) revealed that the production of these tRFs were not produced by either dicer.

DISCUSSION

Studies conducted on a number of fungal species have uncovered robust RNA silencing mechanisms with important roles in fungal antiviral defense. Similarly, this study elucidates the RNA silencing mechanisms in *S. sclerotiorum* and establishes

TABLE 2 | Numbers of aligning small RNA sequence reads from hypovirus-transfected wild type and mutants of *Sclerotinia sclerotiorum*.

	Read counts	Percent of aligned reads					
Samples	**Filtered read**	**IGR (% of tRNA derived small RNA)**	**CDS**	**Retrotransposons**	**Mitochondria**	**rRNA**	**Other**
Ago2_SsHV2L_1	6510462	46.4 (42.7%)	10.6	3.3	5.7	5.6	28.5
Ago2_SsHV2L_2	6599083	46.7 (46.73%)	9.3	2.9	5.6	5.8	29.7
Ago2_VF_1	5895665	48.4 (31.46%)	12.7	4.4	5.6	4.3	24.6
Ago2_VF_2	5646987	49.1 (32.7%)	13.5	4.8	5.2	3.9	23.5
Ago4_SsHV2L_1	15140898	58.1 (68.9%)	5.9	2.2	2.8	1.9	29.1
Ago4_SsHV2L_2	8083962	49.4 (56.8%)	8.2	3.0	4.5	8.0	26.9
Ago4_VF_1	18251848	80.1 (78.6%)	3.9	0.5	1.6	4.2	9.7
Ago4_VF_2	13039613	83.0 (80.6%)	3.5	0.5	1.8	2.8	8.4
Dcl1_SsHV2L_1	6932872	32.9 (77.6%)	2.2	0.2	1.7	24.9	38.1
Dcl1_SsHV2L_2	7040569	52.5 (62.7%)	5.3	2.3	2.6	9.2	28.1
Dcl1_VF1	9213301	50.4 (57.8%)	6.3	1.5	4.5	8.0	29.4
Dcl1_VF2	9087471	32.7 (28.6%)	5.6	0.9	4.2	19.8	36.8
Dcl2_SsHV2L_1	14427517	43.6 (62.5%)	5.6	2.3	4.6	4.9	38.9
Dcl2_SsHV2L_2	11097593	43.2 (59.2%)	6.7	3.0	4.2	5.5	37.3
Dcl2_VF1	17041328	40.6 (35.4%)	9.8	3.4	4.7	6.7	34.7
Dcl2_VF2	13619703	50.0 (59.2%)	5.6	1.8	4.7	7.2	30.8
WTDK3_SsHV2L_1	15565013	63.7 (76.0%)	5.1	1.7	3.1	3.4	23
WTDK3_SsHV2L_2	14313982	39.2 (41.4%)	9.4	4.4	2.8	1.2	43
WTDK3_SsHV2L_3	14553278	40.8 (25.4%)	11.6	4.5	8.5	2.8	31.8

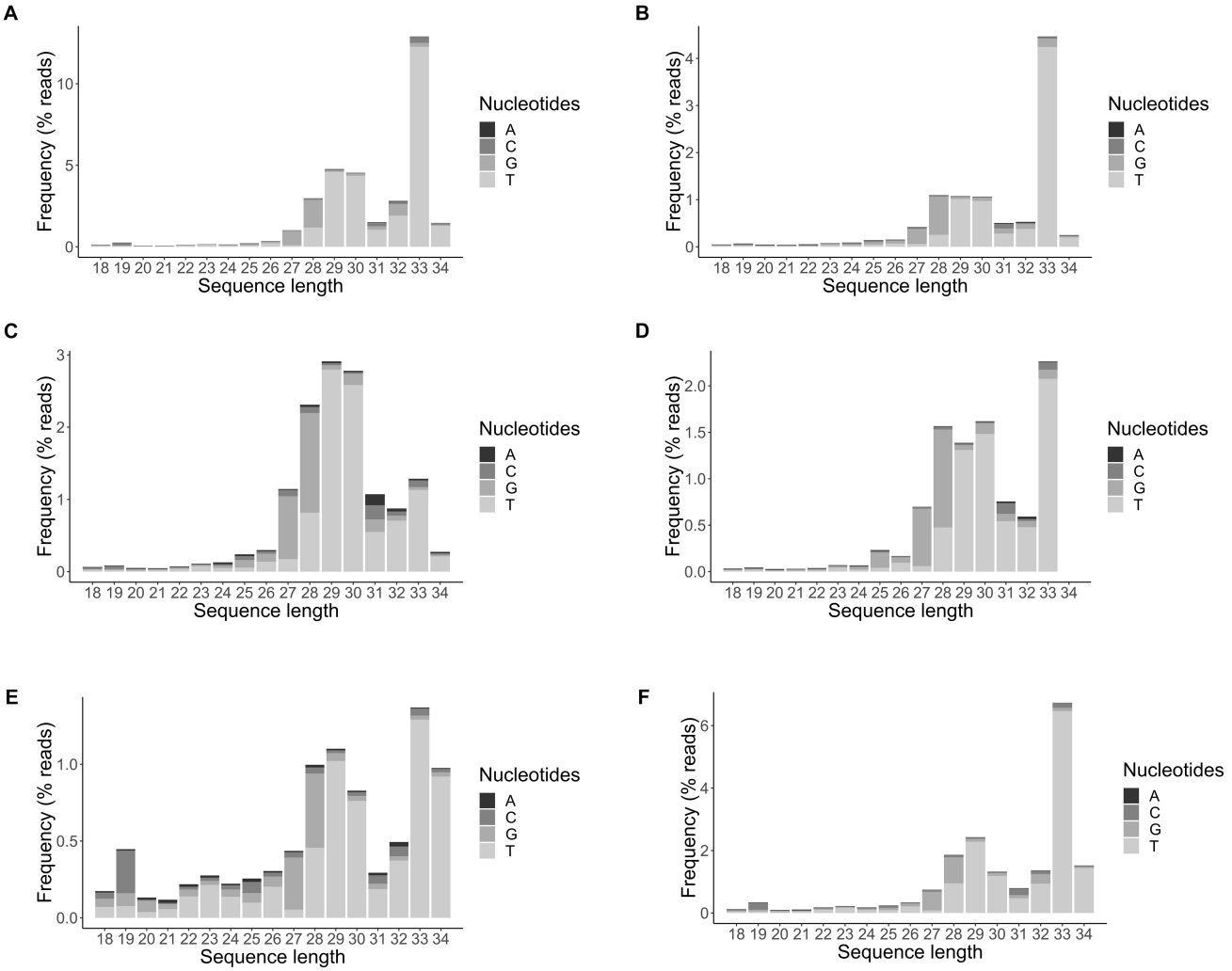

FIGURE 7 | tRNA-derived small RNAs profiled for their size distribution in panel **(A)** wild type strain DK3, **(B)** Δ*dcl*-1, **(C)** Δ*dcl*-2, **(D)** Δ*dcl*-1/*dcl*-2, **(E)** Δ*agl*-2, **(F)** Δ*agl*-4.

the significant roles played by Argonaute-like genes in this devastating plant pathogenic fungus. Primarily, these findings clearly demonstrate that while the wild-type strain displayed reduced virulence following SsHV2-L virus infection (Marzano et al., 2015), RNA-silencing-deficient mutants [specifically Δ*agl*-2 mutant in this study, and previously reported Δ*dcl*-1/*dcl*-2 double mutant (Mochama et al., 2018)] displayed an even more significantly debilitated growth and reduced virulence under virus infection.

The slower growth of Δ*agl*-2 without virus infection also suggested that *agl*-2 contributes to cellular gene regulation through the prevention of RISC formation with endogenous small RNAs. Specifically, we found that the deletion of *agl*-2 gene but not *agl*-4 resulted in compromised growth and virulence prior to virus infection, suggesting the contributions made by *agl*-2 to physiological and developmental processes. The *agl*-2 mutant exhibited slower growth, smaller sclerotia, and reduced virulence. Therefore, the changes observed in the *agl*-2 mutant may be attributed to a significant reduction in small RNA loading and stabilization of endogenous small RNAs. As expected, size distribution of small RNAs is not greatly affected upon the deletions of *agl*-2 or *agl*-4 genes when the Dicers are functional.

The great debilitation observed in the Δ*agl*-2 mutant caused by virus infection was not detected in the virus-infected Δ*agl*-4. This suggests that the AGL-2 protein is solely responsible for incorporating vsiRNAs into the RISC complex as part of the viral RNA silencing mechanism leading to the silencing of viral RNA. Argonaute proteins have been shown to associate with vsiRNAs in plants to target complementary viral mRNAs and in some cases host genes as well (Mengji et al., 2014; Carbonell and Carrington, 2015). miRNA-like molecules with possible gene regulation functions have been found to associate with fungal Argonaute proteins like the QDE-2 protein in *N. crassa* (Lee et al., 2010). Our study suggests that AGL-2 protein in *S. sclerotiorum* may also contribute to endogenous gene regulation. While AGL-4

protein's function remains unknown, it is likely to play important roles including miRNA degradation (Sheu-Gruttadauria et al., 2019). Moreover, as single argonaute mutants do not have drastic changes in small RNA stability, this suggests possible functional redundancy in the two Argonautes.

Single gene disruption mutants of *dcl*-1, *dcl*-2, *agl*-2, *agl*-4, and double dicer mutants of *dcl*-1/*dcl*-2 did not alter the accumulation of tRFs, which suggests the existence of alternative enzymes or pathways for the biogenesis of this class of small RNA in *S. sclerotiorum*. Other endonuclease exist in *S. sclerotiorum*, such as RNaseL-like endonuclease that share similarities with yeast Ire1p proteins which are said to be involved in fungal mRNA splicing (Dong et al., 2001). Another endonuclease, Rny1 in yeast, is a ribonuclease T2-like precursor, and disruption of Rny1 lead to usually large cells that are temperature-sensitive for growth in yeast (MacIntosh et al., 2001). Also, the sizes of small RNA for tRFs were much larger than the dicer-processed ∼22 nt ones, supporting the speculation of different endonuclease(s) in action. Therefore, generating Rny1 and RNase L mutants to assess any disruption in the fungal growth and development and most importantly quantify the changes in the levels of tRFs will answer the pending questions brought up by this study. Moreover, the biological function of this under-characterized class of small RNA in this major pathogen of all dicots demands further study. Questions such as whether tRFs are induced by virus infection or simply a stress response, whether they target the IGRs as Blastn results suggested, or whether tRFs can be manipulated to debilitate *S. sclerotiorum* remain to be answered in the future.

The results derived from this study pave the way for the development of new control strategies that exploit RNA silencing mechanisms. The external RNA pesticide developed suggests the occurrence of external uptake of RNA in *S. sclerotiorum*. Furthermore, host-induced gene silencing (HIGS), virus-induced gene silencing (VIGS) approaches or heterologous expression of dsRNA sprays (spray-induced gene silencing) targeting *agl*-2 in *S. sclerotiorum* are expected to be effective in reducing the virulence, adding to the tool box of disease control.

AUTHOR CONTRIBUTIONS

AN, PM, and S-YLM conceived and designed the experiments and wrote the manuscript. PM, CF, and HS performed the experiments. AN analyzed the small RNA data.

FUNDING

This study was supported in part by National Sclerotinia Initiative Grant SA1800330 (to S-YLM) and SDSU startup from USDA Hatch fundSD00H606-16 project number with accession number 1009451.

SUPPLEMENTARY MATERIAL

The Supplementary Material for this article can be found online at: https://www.frontiersin.org/articles/10.3389/fpls.2019.00976/full#supplementary-material

REFERENCES

Altschul, S. F., Gish, W., Miller, W., Myers, E. W., and Lipman, D. J. (1990). Basic local alignment search tool. *J. Mol. Biol.* 215, 403–410. doi: 10.1016/S0022-2836(05)80360-2

Amselem, J., Cuomo, C. A., van Kan, J. A., Viaud, M., Benito, E. P., Couloux, A., et al. (2011). Genomic analysis of the necrotrophic fungal pathogens *Sclerotinia sclerotiorum* and *Botrytis cinerea*. *PLoS Genet.* 7:e1002230. doi: 10.1371/journal.pgen.1002230

Axtell, M. J. (2013). ShortStack: comprehensive annotation and quantification of small RNA genes. *Rna* 19, 740–751. doi: 10.1261/rna.035279.112

Baulcombe, D. (2004). RNA silencing in plants. *Nature* 431, 356–363.

Baulcombe, D. (2005). RNA silencing. *Trends Biochem. Sci.* 30, 290–293.

Bushnell, B. (2014). *Bbmap: a Fast, Accurate, Splice-Aware Aligner*. Berkeley, CA: Lawrence Berkeley National Laboratory (LBNL).

Campo, S., Gilbert, K. B., and Carrington, J. C. (2016). Small RNA-based antiviral defense in the phytopathogenic fungus *Colletotrichum higginsianum*. *PLoS Pathog.* 12:e1005640. doi: 10.1371/journal.ppat.1005640

Carbonell, A., and Carrington, J. C. (2015). Antiviral roles of plant Argonautes. *Curr. Opin. Plant Biol.* 27, 111–117. doi: 10.1016/j.pbi.2015.06.013

Catalanotto, C., Pallotta, M., ReFalo, P., Sachs, M. S., Vayssie, L., Macino, G., et al. (2004). Redundancy of the two dicer genes in transgene-induced posttranscriptional gene silencing in *Neurospora crassa*. *Mol. Cell. Biol.* 24, 2536–2545. doi: 10.1128/mcb.24.6.2536-2545.2004

Dang, Y., Yang, Q., Xue, Z., and Liu, Y. (2011). RNA interference in fungi: pathways, functions, and applications. *Eukary. Cell* 10, 1148–1155. doi: 10.1128/EC.05109-11

Dong, B., Niwa, M., Walter, P., and Silverman, R. H. (2001). Basis for regulated RNA cleavage by functional analysis of RNase L and Ire1p. *Rna* 7, 361–373. doi: 10.1017/s1355838201002230

Fulci, V., and Macino, G. (2007). Quelling: post-transcriptional gene silencing guided by small RNAs in *Neurospora crassa*. *Curr. Opin. Microbiol.* 10, 199–203. doi: 10.1016/j.mib.2007.03.016

Heffer Link, V., and Johnson, K. (2007). White mold. *Plant Health Instruct.* doi: 10.1094/PHI-I-2007-0809-01

Irvine, D. V., Zaratiegui, M., Tolia, N. H., Goto, D. B., Chitwood, D. H., Vaughn, M. W., et al. (2006). Argonaute slicing is required for heterochromatic silencing and spreading. *Science* 313, 1134–1137. doi: 10.1126/science.1128813

Kumar, S., Stecher, G., and Tamura, K. (2016). MEGA7: molecular evolutionary genetics analysis version 7.0 for bigger datasets. *Mol. Biol. Evol.* 33, 1870–1874. doi: 10.1093/molbev/msw054

Langmead, B., Trapnell, C., Pop, M., and Salzberg, S. L. (2009). Ultrafast and memory-efficient alignment of short DNA sequences to the human genome. *Genome Biol.* 10:R25. doi: 10.1186/gb-2009-10-3-r25

Laurie, J. D., Ali, S., Linning, R., Mannhaupt, G., Wong, P., Güldener, U., et al. (2012). Genome comparison of barley and maize smut fungi reveals targeted loss of RNA silencing components and species-specific presence of transposable elements. *Plant Cell* 24, 1733–1745. doi: 10.1105/tpc.112.097261

Lee, H.-C., Li, L., Gu, W., Xue, Z., Crosthwaite, S. K., Pertsemlidis, A., et al. (2010). Diverse pathways generate microRNA-like RNAs and dicer-independent small interfering RNAs in fungi. *Mol. Cell* 38, 803–814. doi: 10.1016/j.molcel.2010.04.005

Lee Marzano, S. Y., Neupane, A., and Domier, L. (2018). Transcriptional and small RNA responses of the white mold fungus *Sclerotinia sclerotiorum* to infection by a virulence-attenuating hypovirus. *Viruses* 10:E713. doi: 10.3390/v10120713

Lowe, T. M., and Chan, P. P. (2016). tRNAscan-SE On-line: integrating search and context for analysis of transfer RNA genes. *Nucleic Acids Res.* 44, W54–W57. doi: 10.1093/nar/gkw413

MacIntosh, G. C., Bariola, P. A., Newbigin, E., and Green, P. J. (2001). Characterization of Rny1, the *Saccharomyces cerevisiae* member of the T2

RNase family of RNases: unexpected functions for ancient enzymes? *Proc. Natl. Acad. Sci.* 98, 1018–1023. doi: 10.1073/pnas.98.3.1018

Marzano, S.-Y., Hobbs, H. A., Nelson, B. D., Hartman, G. L., Eastburn, D. M., McCoppin, N. K., et al. (2015). Transfection of *Sclerotinia sclerotiorum* with in vitro transcripts of a naturally occurring interspecific recombinant of *Sclerotinia sclerotiorum* hypovirus 2 significantly reduces virulence of the fungus. *J. Virol.* 89, 5060–5071. doi: 10.1128/jvi.03199-14

Mengji, C., Du, P., Wang, X., Yu, Y.-Q., Qiu, Y.-H., Li, W., et al. (2014). Virus infection triggers widespread silencing of host genes by a distinct class of endogenous siRNAs in *Arabidopsis*. *Proc. Natl. Acad. Sci. U.S.A.* 111:14613. doi: 10.1073/pnas.1407131111

Mochama, P., Jadhav, P., Neupane, A., and Marzano, S.-Y. L. (2018). Mycoviruses as triggers and targets of RNA silencing in white mold fungus *Sclerotinia sclerotiorum*. *Viruses* 10:E214. doi: 10.3390/v10040214

Poulsen, C., Vaucheret, H., and Brodersen, P. (2013). Lessons on RNA silencing mechanisms in plants from eukaryotic argonaute structures. *Plant Cell* 25, 22–37. doi: 10.1105/tpc.112.105643

Qihong, S., Gil, H. C., and Donald, L. N. (2009). A single argonaute gene is required for induction of RNA silencing antiviral defense and promotes viral RNA recombination. *Proc. Natl. Acad. Sci. U.S.A.* 106:17927. doi: 10.1073/pnas.0907552106

Segers, G. C., Zhang, X., Deng, F., Sun, Q., and Nuss, D. L. (2007). Evidence that RNA silencing functions as an antiviral defense mechanism in fungi. *Proc. Natl. Acad. Sci. U.S.A.* 104, 12902–12906. doi: 10.1073/pnas.0702500104

Sheu-Gruttadauria, J., Pawlica, P., Klum, S. M., Wang, S., Yario, T. A., Oakdale, N. T. S., et al. (2019). *Structural Basis for Target-Directed MicroRNA Degradation*. Available at SSRN: https://ssrn.com/abstract=3318944. (accesed January 24, 2019).

Trieu, T. A., Calo, S., Nicolás, F. E., Vila, A., Moxon, S., Dalmay, T., et al. (2015). A non-canonical RNA silencing pathway promotes mRNA degradation in basal fungi (An RdRP-dependent degradation mechanism of mRNA). *PLoS Genet.* 11:e1005168. doi: 10.1371/journal.pgen.1005168

Wang, M., Weiberg, A., Lin, F.-M., Thomma, B. P. H. J., Huang, H.-D., Jin, H., et al. (2016). Bidirectional cross-kingdom RNAi and fungal uptake of external RNAs confer plant protection. *Nat. Plants* 2:16151. doi: 10.1038/nplants.2016.151

Waterhouse, P. M., Wang, M. B., and Lough, T. (2001). Gene silencing as an adaptive defence against viruses. *Nature* 411, 834–842. doi: 10.1038/35081168

Yu, J., Lee, K.-M., Cho, W. K., Park, J. Y., and Kim, K.-H. (2018). Differential contribution of RNA interference components in response to distinct fusarium graminearum virus infections. *J. Virol.* 92, e1756–e1717. doi: 10.1128/JVI.01756-17

Zhang, D.-X., Spiering, M. J., and Nuss, D. L. (2014). Characterizing the roles of Cryphonectria parasitica RNA-dependent RNA polymerase-like genes in antiviral defense, viral recombination and transposon transcript accumulation. *PLoS One* 9:e108653. doi: 10.1371/journal.pone.0108653

Conflict of Interest Statement: The authors declare that the research was conducted in the absence of any commercial or financial relationships that could be construed as a potential conflict of interest.

frontiers in Microbiology

ORIGINAL RESEARCH
published: 11 October 2019
doi: 10.3389/fmicb.2019.02318

A Novel Totivirus Naturally Occurring in Two Different Fungal Genera

Mahmoud E. Khalifa[1,2]* *and Robin M. MacDiarmid*[1,3]

[1] The New Zealand Institute for Plant and Food Research Limited, Auckland, New Zealand, [2] Botany and Microbiology Department, Faculty of Science, Damietta University, Damietta, Egypt, [3] School of Biological Sciences, The University of Auckland, Auckland, New Zealand

Mycoviruses are widely distributed across different phyla of the fungal kingdom. Viruses that share significant sequence similarities have been reported in different fungi, suggesting descent from a common ancestor. In this study, two fungal genera isolated from the same sample, *Trichoderma koningiopsis* isolate Mg10 and *Clonostachys rosea* isolate Mg06, were reported to have identical double-stranded RNA (dsRNA) profiles that consist of two virus-like, dsRNA elements (dsRNA-L and dsRNA-S). The complete sequence and genome organization of dsRNA-L from isolate Mg10 was determined. It is 4712 nucleotides (nt) long and contains two non-overlapping open reading frames (ORFs) that code for proteins with similarities to totiviruses. Consequently the virus was given the proposed name Trichoderma koningiopsis totivirus 1 (TkTV1/Mg10). The TkTV1/Mg10 genome structure resembles that of yeast totiviruses in which the region preceding the stop codon of ORF1 contains the elements required for -1 ribosomal frameshifting which may induce the expression of an ORF1–ORF2 (CP-RdRp) fusion protein. Sequence analyses of viral dsRNA-L from *C. rosea* isolate Mg06 revealed that it is nearly identical with that of TkTV1/Mg10. This relatedness was confirmed by northern blot hybridization and indicates very recent natural horizontal transmission of this virus between unrelated fungi. TkTV1 purified isometric virions were ∼38–40 nm in diameter and were able to transfect *T. koningiopsis* and *C. rosea* protoplasts. This is another report of a mycovirus present naturally in two taxonomically distinct fungi.

Keywords: ***Totivirus*, mycovirus, dsRNA, *Trichoderma*, *Clonostachys***

OPEN ACCESS

Edited by:
Nobuhiro Suzuki,
Okayama University, Japan

Reviewed by:
Jie Zhong,
Hunan Agricultural University, China
Mingde Wu,
Huazhong Agricultural University, China
Hideki Kondo,
Okayama University, Japan

***Correspondence:**
Mahmoud E. Khalifa
Mahmoud.khalifa@du.edu.eg;
mkha201@aucklanduni.ac.nz

Specialty section:
This article was submitted to Virology, a section of the journal Frontiers in Microbiology

Received: *28 June 2019*
Accepted: *23 September 2019*
Published: *11 October 2019*

Citation:
Khalifa ME and MacDiarmid RM (2019) A Novel Totivirus Naturally Occurring in Two Different Fungal Genera. Front. Microbiol. 10:2318. doi: 10.3389/fmicb.2019.02318

INTRODUCTION

Mycoviruses, viruses that infect fungi, are widely distributed and have been reported in several fungal groups (Pearson et al., 2009). Mycoviruses mostly induce symptomless infections but several examples have been reported to induce notable effects on their hosts including reduced or enhanced virulence (Nuss and Koltin, 1990; Ghabrial, 1994; Lau et al., 2018). Three genome types, double-stranded RNA (dsRNA), single-stranded RNA (ssRNA), and single-stranded DNA (ssDNA), have been reported for mycoviruses; dsRNA genomes are the most frequently reported.

One of the dsRNA virus families is the *Totiviridae* which accommodates members with non-enveloped isometric virions harboring a single linear dsRNA genome of 4.6–7.0 kbp in size. The genome consists of two overlapping open reading frames (ORFs) coding for a coat protein (CP or Gag) and an RNA-dependent RNA polymerase (RdRp or Pol) that could be expressed as a gag-pol fusion protein (Dinman et al., 1991; Ghabrial, 2008). Ghabrial and Suzuki (2009) have summarized at least three RdRP-expression strategies in *Totiviridae* members including: (a) as a CP/RdRP fusion protein by utilizing a ribosomal frameshifting mechanism; (b) as a CP/RdRp fusion protein, that is later released by proteolysis, without the involvement of ribosomal frameshifting; and (c) as a separate protein by utilizing a stop/restart mechanism. The family is currently classified into five genera: *Totivirus*, *Victorivirus*, *Giardiavirus*, *Trichomonasvirus*, and *Leishmaniavirus*. Only the *Totivirus* and *Victorivirus* genera have species that infect fungi; the remaining three genera include members that infect protozoa (Goodman et al., 2011; Wickner et al., 2012).

Members of the *Totivirus* genus are characterized by virions that are 40 nm in diameter, containing the linear dsRNA genome typical of their family (4.6–6.7 kbp). Some members are considered as helper viruses by providing capsids required for the separate encapsidation of associated satellite dsRNAs encoding killer proteins (Wickner et al., 2012). Novel *Totivirus* species are defined based on biological and molecular criteria. Viruses found in distinct hosts are different species, and viruses that share less than 50% of amino acid (aa) sequence identity are also considered different species (Wickner et al., 2012).

Trichoderma koningiopsis and *Clonostachys rosea* are both ascomycetes with biological control potential against several pathogens. *T. koningiopsis* and *C. rosea* are classified within the same order *Hypocreales* but belong to *Bionectriaceae* and *Hypocreaceae* families, respectively (Karlsson et al., 2015). *T. koningiopsis* is common and a cosmopolitan species that is known to have the ability to control several fungal pathogens, including *Thielaviopsis basicola* and *Fusarium verticillioides* (Samuels et al., 2006). Similarly, *C. rosea* is a mycoparasite that is commonly found in soil and considered a highly efficient antagonistic fungus against a wide range of pathogenic fungi, including *Botrytis cinerea* (Sutton et al., 1997; Wu et al., 2014). Poorly characterized dsRNAs have been previously reported in two isolates of *T. koningiopsis* (Yun et al., 2016) and nothing is yet known about the association of *C. rosea* with mycoviruses. In this study, we report the molecular characteristics of a novel totivirus naturally occurring in two different fungal hosts, *T. koningiopsis* and *C. rosea*.

MATERIALS AND METHODS

Fungal Isolates and Culturing Conditions

Trichoderma koningiopsis (isolate Mg10) and *C. rosea* (isolate Mg06) were isolated in 2016 from a single soil sample obtained from Mamaku, Rotorua using a standard isolation method (Warcup, 1950). Pure fungal cultures were obtained by single spore isolation and maintained and subcultured onto potato dextrose agar (PDA) plates (**Figure 1A**). Their identities were confirmed by amplifying and sequencing the non-coding internal transcribed spacer (ITS) regions using the primer pair ITS4/ITS5 (White et al., 1990). *T. koningiopsis* isolate TkF-T-11 and *C. rosea* isolate CrF-T-13 were produced by polyethylene glycol (PEG)-mediated mycovirus transfection of dsRNA-free isolates TkF and CrF of *T. koningiopsis* and *C. rosea*, respectively.

Viral dsRNA and Fungal Total RNA Extraction

Viral dsRNA was extracted and purified from 400 mg of fungal mycelium using a method modified from that described by Valverde et al. (1990), as previously detailed by Khalifa and Pearson (2014). DsRNAs were resolved on 1% (w/v) agarose gel, in 1× TAE buffer (40 mM Tris, 20 mM glacial acetic acid, and 1 mM EDTA; pH 7.2) pre-stained with SYBR safe, and visualized and photographed under UV using a GelDoc (Bio-Rad). The dsRNA nature of the bands was confirmed by DNase and RNase treatments as described by Howitt et al. (1995). Total RNA was extracted from 100 mg of fungal mycelium, grown on cellophane over PDA medium for 5 days, using the Spectrum Plant Total RNA Kit (Sigma) as described by the manufacturer.

Reverse Transcription-PCR and Sequencing

Purified dsRNAs were used as templates for RT-PCR using a protocol based on that of Roossinck et al. (2010) as described by Khalifa and Pearson (2013). RT-PCR products were purified using an Agencourt AMPure XP PCR purification kit (Beckman Coulter) and sequenced by Macrogen Inc. (Seoul, South Korea) using an Illumina HiSeq2000 platform. For sequence confirmation using Sanger sequencing, five pairs of dsRNA-L specific primers were designed and used to amplify overlapping fragments of dsRNA-L using a protocol described by Khalifa and Pearson (2013). The terminal sequences were amplified and sequenced as previously described by Khalifa and Pearson (2013). T4LC primer (5′-AAAGAGCCAGCAAACGACGGG-3′) was used as an adapter together with one of the specific primers 5′-ATTTTTGTCCGTGATGGG-3′ and 5′-TGTACTAGCATCGACGCC-3′ for the RT-PCR amplification of the 5′ and 3′ terminal sequences, respectively. RT-PCR products were cloned and sequenced by Macrogen Inc. (Seoul, South Korea). Bands corresponding to dsRNA-S from isolates Mg10 and Mg06 were excised separately and dsRNAs extracted using a gel extraction kit (AxyPrep). RT-PCR was performed and cDNAs partially sequenced to determine the identity of dsRNA-S as described by Khalifa and Pearson (2013).

Northern Blot Analysis

A sequence-specific digoxigenin (DIG)-labeled probe was amplified using a PCR labeling kit (Roche), following the manufacturer's protocol, with a primer pair of the following sequences: 5′-GTAAAGTAGGAGCCGTCC-3′ and 5′-TGTAAGAAGTACCAGTTCCC-3′. Northern blot hybridization and probe-RNA hybrid detection were performed as previously described by Khalifa and Pearson (2014).

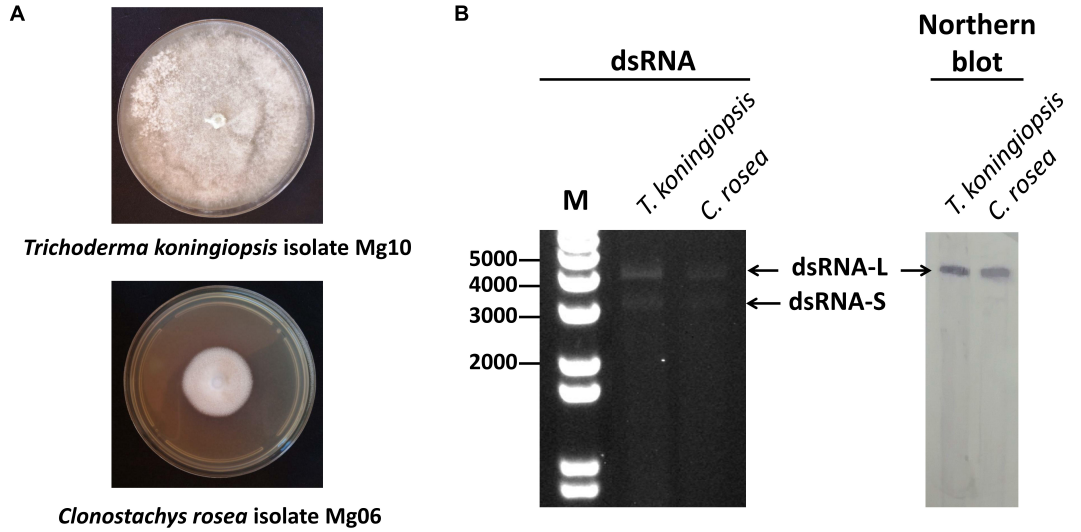

FIGURE 1 | (A) Colony morphology of *Trichoderma koningiopsis* isolate Mg10 and *Clonostachys rosea* isolate Mg06 on potato dextrose agar (PDA). **(B)** The dsRNA profile (dsRNA-L and dsRNA-S) of *T. koningiopsis* isolate Mg10 and *C. rosea* isolate Mg06 on 1% (w/v) agarose gel (left panel) and northern hybridization detection of Trichoderma koningiopsis totivirus 1 (TkTV1/Mg10) represented by dsRNA-L in both fungal isolates (right panel) using DNA probes. M: 1 Kb Plus DNA Ladder (Invitrogen).

Bioinformatics, Sequence and Phylogenetic Analyses

Illumina reads with quality scores of less than Q20 were filtered out using The Galaxy Project server (Goecks et al., 2010), and low quality terminal sequence regions in the remaining reads were trimmed based on the FastQC report[1]. The remaining reads were assembled *de novo* using Geneious R8.1 (Kearse et al., 2012) set to medium sensitivity and default parameters. Encoded ORFs were detected using the ORF finder tool available at the National Center for Biotechnology Information (NCBI)[2]. Conserved motifs were determined by aligning corresponding sequences using PROMALS3D (Pei and Grishin, 2014).

For phylogenetic analyses, multiple sequence alignments of totiviral CP and RdRp aa sequences were performed using PROMALS3D (Pei and Grishin, 2014), and gaps were removed from the alignments using trimAl v1.3 (strict mode) (Capella-Gutierrez et al., 2009). Maximum likelihood phylogenetic trees were inferred using the selected best fitting-model of PhyML 3 (Guindon et al., 2010). Nodes with less than 75% SH-like branch support were collapsed using TreeGraph 2 software (Stöver and Müller, 2010).

Purification of Virions and Protoplast Transfection

Fungal mycelium was grown on cellophane-covered PDA plates and 10 g of fungal mass was used for TkTV1 particles purification and transmission electron microscopic (TEM) visualization as previously described by Boine et al. (2012). TkTV1-free protoplasts were prepared from TkTV1-free isolates of *T. koningiopsis* (isolate TkF) and *C. rosea* (isolate CrF) using Glucanex and β-Glucuronidase as cell wall lytic enzymes (Sigma-Aldrich) as described by Shi-Wang et al. (2007) and Sun et al. (2017), respectively. For protoplast transfection, purified particles were passed through 0.45-μm syringe filters and used in PEG-mediated transfection tests of the previously prepared TkTV1-free protoplasts as described by Hillman et al. (2004). Transfected protoplasts were regenerated on regeneration medium for 4–5 days and 25 colonies for each fungus were randomly picked and transferred to PDA plates. DsRNA and total RNA were extracted as above and TkTV1 transmission was verified by RT-PCR amplification of an 879 bp-long fragment using specific primer pair TVF5 (5′-GTAAAGTAGGAGCCGTCC-3′) and TVR6 (5′-CTTCCAATTCGAGTGTTTCC-3′).

RESULTS AND DISCUSSION

With the advent of next-generation sequencing (NGS), mycovirus discovery from different sources has become more feasible (Ho and Tzanetakis, 2014). Mycoviruses from fungal material, environmental samples, insects, and other sources have been sequenced from dsRNA, total RNA and even siRNAs using NGS technologies (Al Rwahnih et al., 2011; Wu et al., 2012; Cook et al., 2013; Kraberger et al., 2013; Bruenn et al., 2015; Khalifa et al., 2016; Nerva et al., 2016). NGS platforms have been developed to produce nearly full-length reliable sequences that are comparable to those produced by conventional methods (Khalifa et al., 2016). In this study, NGS was utilized to sequence and identify a novel totivirus associated with two different fungal genera from dsRNA. The sequence was confirmed and the terminal sequences obtained using Sanger sequencing.

[1]http://www.bioinformatics.babraham.ac.uk/projects/fastqc/
[2]http://www.ncbi.nlm.nih.gov/projects/gorf

The sequence was deposited in GenBank with the accession number MK993478.

Fungal Identification and dsRNA Profiling

The nucleotide sequence of ITS region from isolates Mg10 and Mg06 shared the best match with publically available sequences of *T. koningiopsis* isolate TE26 (98.5% sequence identity; accession no. MH549097) and *C. rosea* isolate F6UP (98% sequence identity; accession no. MN252116), respectively.

Although nucleic acid bands of the same size do not necessarily have identical nucleotide sequences or represent the same virus, the banding patterns of dsRNAs purified from *T. koningiopsis* isolate Mg10 and *C. rosea* isolate Mg06 were nearly identical (**Figure 1B**). Both isolates contained two dsRNA segments that resisted digestions by DNase and RNase in high salt buffer, confirming their identity as dsRNAs. The estimated molecular weights of the two dsRNA segments were ∼5 kbp (dsRNA-L) and ∼3.5 kbp (dsRNA-S).

Sequencing of dsRNA-L Segments

Illumina sequencing resulted in 583,356 and 173,454 short reads from *T. koningiopsis* isolate Mg10 and *C. rosea* isolate Mg06, respectively. Short Illumina reads were trimmed and quality filtered prior to being assembled using the Geneious 11.0.3 *de novo* assembly tool set to medium sensitivity and default parameters. Assembly of filtered reads corresponding to *T. koningiopsis* isolate Mg10 and *C. rosea* isolate Mg06 dsRNAs resulted in 31 and 20 contigs, respectively (only four contigs from each isolate were longer than 1 kbp). The longest contig obtained from isolate Mg10 dataset was 4052 nt long (367,651 assembled reads) and shared nearly the same nucleotide sequence with the longest contig (4477 nt; 82,871 assembled reads) obtained from isolate Mg06. Specific DNA hybridization probes were designed and northern blotting analysis revealed that the sequences of the two contigs from both isolates correspond to dsRNA-L (**Figure 1B**). RACE-PCR and sequencing of dsRNA-L terminal sequences resulted in a full-length sequence of dsRNA-L.

Sequence Analysis of dsRNA-L

The complete Sanger sequencing confirmed sequence of dsRNA-L is 4712 nt long and contains two non-overlapping ORFs in reading frames 2 (ORF1) and 1 (ORF2) of its positive-sense strand, separated by a 248 nt long intergenic region, as revealed by ORF finder. Untranslated regions (UTRs) of 97 and 59 nt were detected at the 5′ and 3′ termini, respectively. ORF1 and ORF2 have the potential to code for 687 and 747 aa long proteins with predicted molecular weights of 77.652 and 85.114 kDa, respectively (**Figure 2A**). BLASTn search returned a single hit with 87% nt identity to a partial sequence of Snodland virus isolate UK1 (accession no. MF893257; E value: 0.0) associated with *Drosophila suzukii* (Medd et al., 2018). BLASTx searches of dsRNA-L nt sequence against NCBI databases revealed homologies to totiviruses and consequently, dsRNA-L from *T. koningiopsis* isolate Mg10 was tentatively named Trichoderma koningiopsis totivirus 1 (TkTV1/Mg10). The reason for proposing the TkTV1 name rather than Clonostachys rosea totivirus 1 (CrTV1/Mg06) is only because the dsRNA-L was detected and analyzed first in this isolate. It does not imply that the dsRNA has transmitted from *T. koningiopsis* to *C. rosea*. TkTv1/Mg06 genome shared the same length with that of TkTV1/Mg10 but differed in having five point mutations (99.89% sequence identity) at nt positions 84 (G to C; 5′-UTR), 1003 (C to T; ORF1), 1336 (G to A; ORF1), 1952 (G to C; ORF1), and 3507 (A to C; ORF2). Among the four substitutions located within the TkTV1 coding region, only one at nt position 1952 resulted in aa substitution, whereas the remaining three were silent.

The potential of TkTV1/Mg10 to code for two ORFs is typical for yeast totiviruses represented by Saccharomyces cerevisiae virus L-A (ScV-L-A) (Icho and Wickner, 1989; Kondo et al., 2016). ORF1 of TkTV1/Mg10 is 2064 nt long (nt positions 98-2161), starts at an AUG codon (nt positions 98-100) and terminates at an ochre (UAA) termination codon (nt positions 2159-2161). The length of ORF2 is 2244 nt, starting at nt positions 2410-4653 and it also terminates with a UAA codon, at nt positions 4651-4653 (**Figure 2A**).

Notably, the region preceding the stop codon of TkTV1/Mg10 ORF1 contains the three elements required to accomplish -1 ribosomal frameshifting in RNA viruses including totiviruses such as ScV-L-A (Dinman et al., 1991; **Figure 2B**). The first element is a slippery site, where frameshifting occurs, that consists of a shifty heptamer with the general sequence XXXYYYZ, where X represents A/G/C/U, Y represents A/U, and Z represents A/C/U (Bekaert and Rousset, 2005). The slippery site UGUUUUC was found at nt positions 2104-2110 of TkTv1/Mg10 genome. This corresponds to the slippery heptanucleotides found in ScV-L-A (GGGUUUA) (Brierley, 1995) and other related totiviruses, including *Xanthophyllomyces dendrorhous* viruses (GGAUUUU) (Baeza et al., 2012), *Puccinia striiformis* totiviruses (PsTVs) and red clover powdery mildew-associated totiviruses (RPaTVs; $GG^{G}/_{A}UUUU$) (Kondo et al., 2016; Zheng et al., 2017). The second element is a pseudoknot, downstream from the slippery site, that helps to pause translation and increase the rate of frameshifting (Rice et al., 1985). An H-type pseudoknot structure was detected at nt positions 2130-2154 of TkTV1/Mg10 genome (**Figure 2C**). The third element of the -1 frameshifting mechanism is a short spacer region between the slippery site and the pseudoknot, and is a 19 nt long stretch in TkTV1/Mg10. It was recently demonstrated that the presence of -1 ribosomal frameshifting elements does not necessarily lead to the expression of a fusion protein (Jamal et al., 2019). Although the expression of a CP-RdRp fusion protein by TkTV1 is yet to be confirmed experimentally, the presence of the -1 frameshifting signature in TkTV1 genome might induce the expression of an ORF1-ORF2 (CP-RdRp) fusion protein of 1518 aa with a molecular weight of 172.020 kDa. If this is the case, ORF2 devoid of any in-frame stop codons could possibly begin at nt positions 1990–1992 and the AUG start codon of ORF2 (nt positions 2410-2412) code for an internal methionine, resulting in a 172 nt long overlap between ORF1 and ORF2.

ORF1 and ORF2 both code for viral proteins identified as CP and RdRp, using BLASTp searches, respectively. ORF1 protein

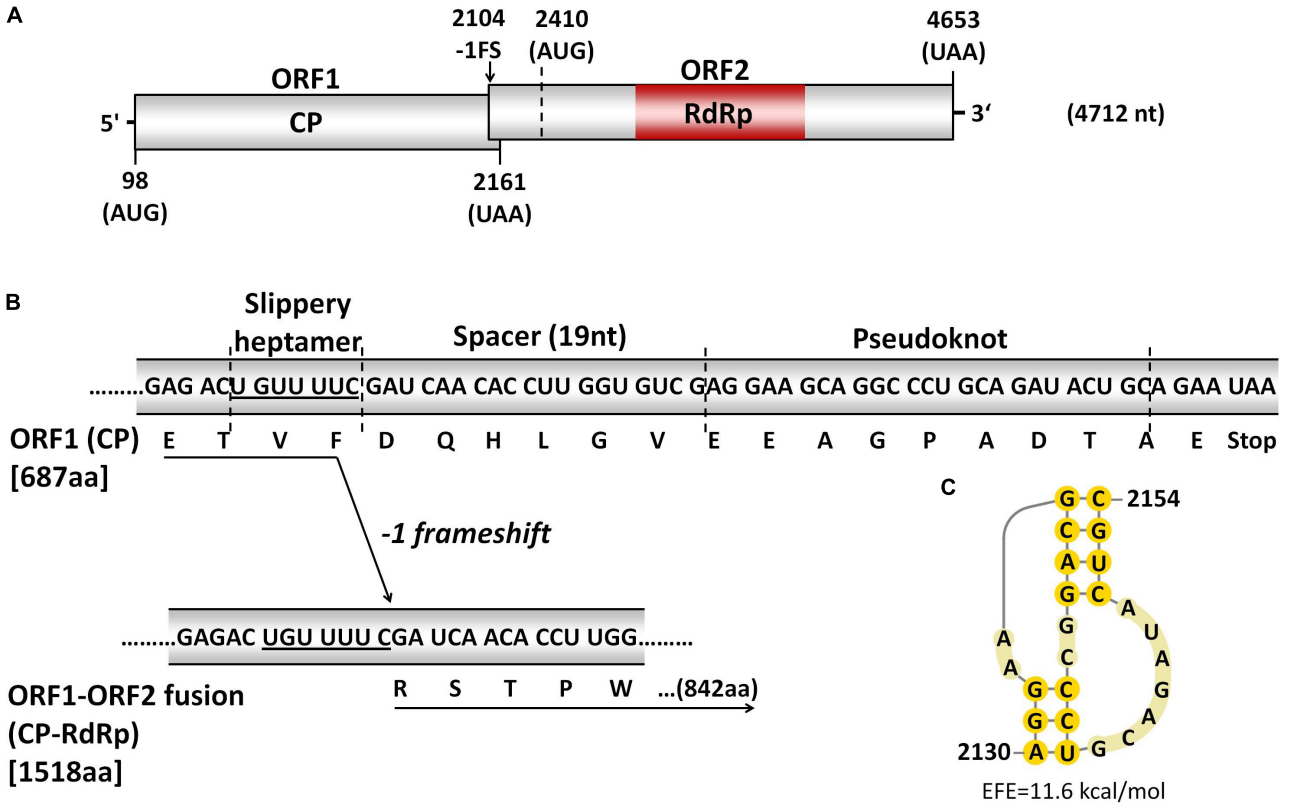

FIGURE 2 | (A) Schematic representation of dsRNA-L (TkTV1/Mg10; 4712 nts). The coding strand contains two overlapping open reading frames (ORFs), indicated by boxes, and is flanked by 5′- and 3′-untranslated regions (UTRs) indicated by short lines. The putative slippery site for -1 ribosomal frameshifting is indicated by the black arrow. **(B)** The three genetic elements involved in -1 ribosomal frameshifting mechanism to produce ORF1-ORF2 fusion protein. **(C)** The predicted H-type pseudoknot secondary structure downstream of the potential slippery heptamer and spacer. EFE (kcal/mol) indicates the estimated free energy.

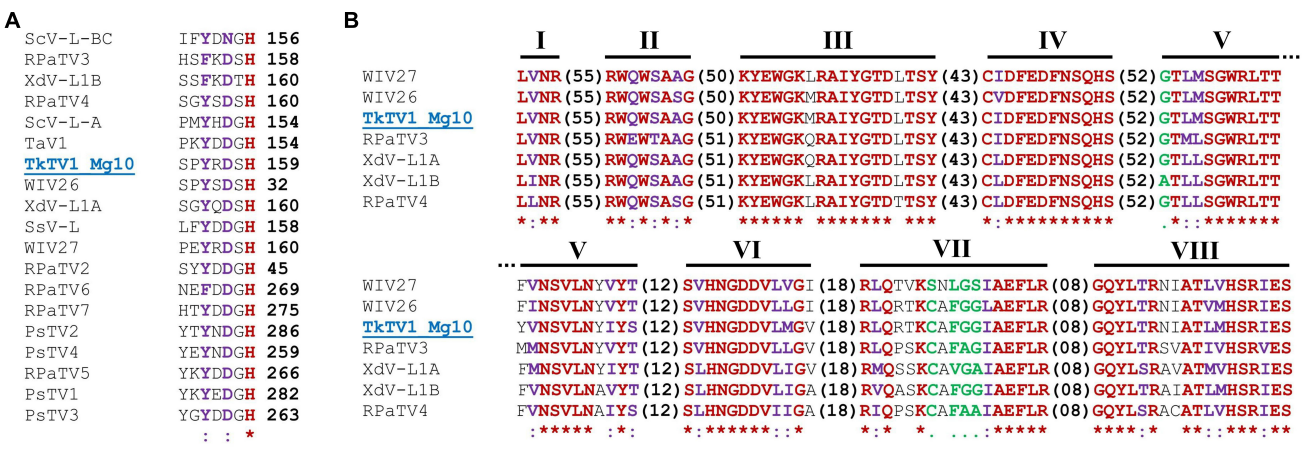

FIGURE 3 | (A) A region extracted from the multiple amino acid (aa) sequence alignment of TkTV1/Mg10 coat protein (CP) and those of other totiviruses showing the position of the Histidine (His) aa residue required for the cap-snatching mechanism of totiviral CPs. **(B)** Conserved aa sequence motifs (I–VIII) of RNA-dependent RNA polymerase (RdRp) of totiviruses (members of group I, subgroup C are shown). Virus notations are as in **Supplementary Table S1**. Identical residues are marked in red and indicated by asterisks "*". Higher and lower chemically similar residues are marked in purple and green and signified by colons ":" and dots ".", respectively.

shared aa sequence identities of 24–47% with hypothetical CPs of toti and toti-like viruses. TkTV1/Mg10 CP was most closely related to Wuhan insect virus 26 (WIV26; accession number YP_009342427, E-value 0.0, identity 47%), WIV27 (accession number YP_009342433, E-value 4e-156, identity 38%) and red clover powdery mildew-associated totivirus 4 (accession number

BAT62483, E-value 4e-131, identity 35%). Multiple aa sequence alignment of TkTV1/Mg10 CP and those of other totiviruses revealed the presence of the aa residue required for the cap-snatching mechanism of totiviral CPs. In TkTV1/Mg10, this is represented by His-159 (**Figure 3A**) which corresponds to His-154 of ScV-L-A (Fujimura and Esteban, 2011), His-156 of ScV-L-BC (Fujimura and Esteban, 2013), and related aa residues in RPaTVs (Kondo et al., 2016). The prediction of a CP gene in TkTV1/Mg10 suggests that its genome is encapsidated, as for other totiviruses.

ORF2 protein showed aa sequence identities ranging from 26 to 57% with hypothetical RdRps of toti and toti-like viruses. TkTV1/Mg10 RdRp shared the highest aa sequence identities with WIV26 (accession number YP_009342428, E-value 0.0, identity 57%), WIV27 (accession number YP_009342434, E-value 0.0, identity 55%) and Delisea pulchra totivirus IndA (accession number AMB17470, E-value 0.0, identity 48%). Searching the conserved domain database (CDD) and multiple RdRp alignment confirmed the presence of a conserved viral RdRp domain (RdRp_4; pfam02123) with the eight conserved motifs (I–VIII) characteristic of the RdRps in dsRNA viruses (Routhier and Bruenn, 1998), including totiviruses, in the predicted RdRp sequence of TkTV1/Mg10 (**Figure 3B**).

Identity of dsRNA-S

The remaining non-dsRNA-L-derived contigs were identified using BLASTx analysis with an E-value cut-off of 1×10^{-6}. A single short virus-like contig was identified from *C. rosea* and shared similarities with Ditton virus (AWA82278), a negative-strand virus associated with *D. Suzukii*. Unlike dsRNA-L, Sanger sequencing of dsRNA-S and BLASTx results showed that the nucleotide sequence of dsRNA-S from isolates Mg10 and Mg06 were not similar. An 834 nt long fragment of dsRNA-S-Mg10 shared 47% aa identity with RdRp of Magnaporthe oryzae ourmia-like virus 4 (MK507958), whereas the partial sequence obtained for dsRNA-S from *C. rosea* (1107 nt) shared 59% aa sequence identity with RdRp of Botrytis cinerea mitovirus 4 (NC_028474). This might indicate that isolates Mg10 and Mg06 contained dsRNA-S prior to dsRNA-L cross-transmission. The full-characterization of dsRNA-S was not included in this study and will be described elsewhere in future studies.

Phylogeny of TkTV1/Mg10

The current phylogeny status of *Totiviridae* classifies the family into five evolutionary lineages (genera), of which *Totivirus* is phylogenetically separated into two groups, I and II. Members of group I are further divided into four subgroups, A to D (Kondo et al., 2016). As shown in **Figure 4** and **Supplementary Figure S1**, phylogenetic analyses based on CP and RdRp multiple alignments of TkTV1/Mg10 and corresponding toti and toti-like sequences revealed that TkTV1/Mg10 is most closely related to, but distinct from, members of group I, sub-group C (I-C). The ML trees inferred based on RdRp and CP had similar topologies in which TkTV1/Mg10 clustered in a sub-clade with WIV26 and

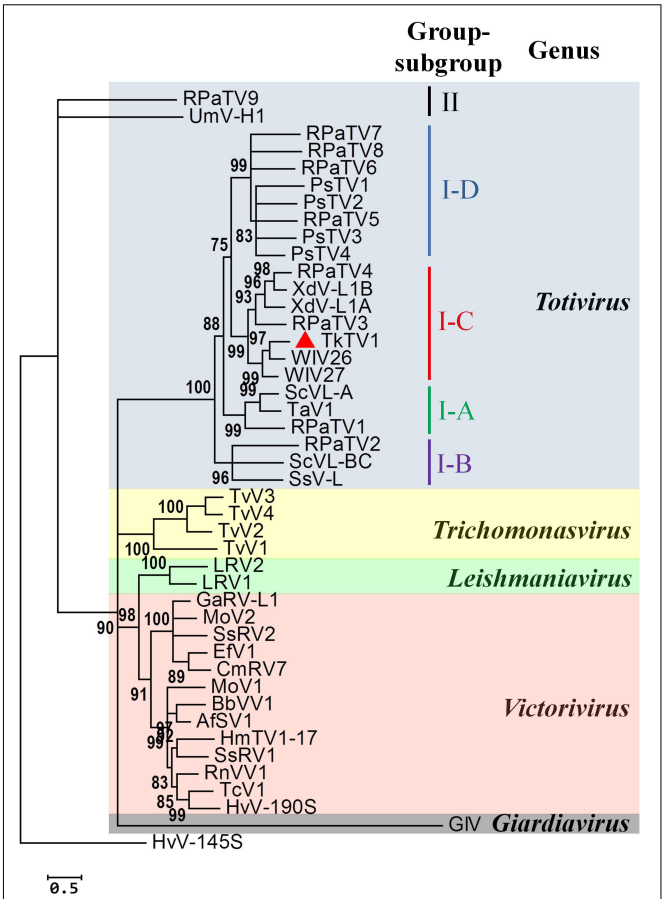

FIGURE 4 | Phylogenetic relationship between the RNA-dependent RNA polymerase (RdRp) of Trichoderma koningiopsis totivirus 1 (TkTV1/Mg10) and other selected *Totiviridae* members. The maximum likelihood tree was inferred using PhyML 3.0 (Guindon et al., 2010) with the LG + G + I + F as the best evolutionary model. The SH-like support values are indicated by numbers on the branches. Branches with <75% SH-like branch support have been collapsed using TreeGraph 2 software (Stöver and Müller, 2010). Virus notations are as in **Supplementary Table S1**.

WIV27 identified in flea and ants (Shi et al., 2016). Other members of sub-group C were isolated from a basidiomycetous fungus, *X. dendrorhous*, and the red clover powdery mildew ascomycete (Baeza et al., 2012; Kondo et al., 2016) suggesting possible horizontal virus transmission across different fungal phyla (Kondo et al., 2016). Moreover, it was suggested that uncharacterized totiviruses may infect a wide range of organisms across the different eukaryotic kingdoms such as fungi, plants, insects and red algae (Kondo et al., 2016), which is supported by the presence of closely related insect (WIV26 and WIV27) and fungal (TkTV1) totiviruses in a single sub-clade (**Figure 4**). As for Sclerotinia sclerotiorum hypovirulence-associated DNA virus 1 (SsHADV-1) which has the ability to infect a mycophagous insect that acts as transmission vector (Liu et al., 2016), transmission of TkTV1, WIV26, WIV27 and their ancestors may have been facilitated by mycophagous insects.

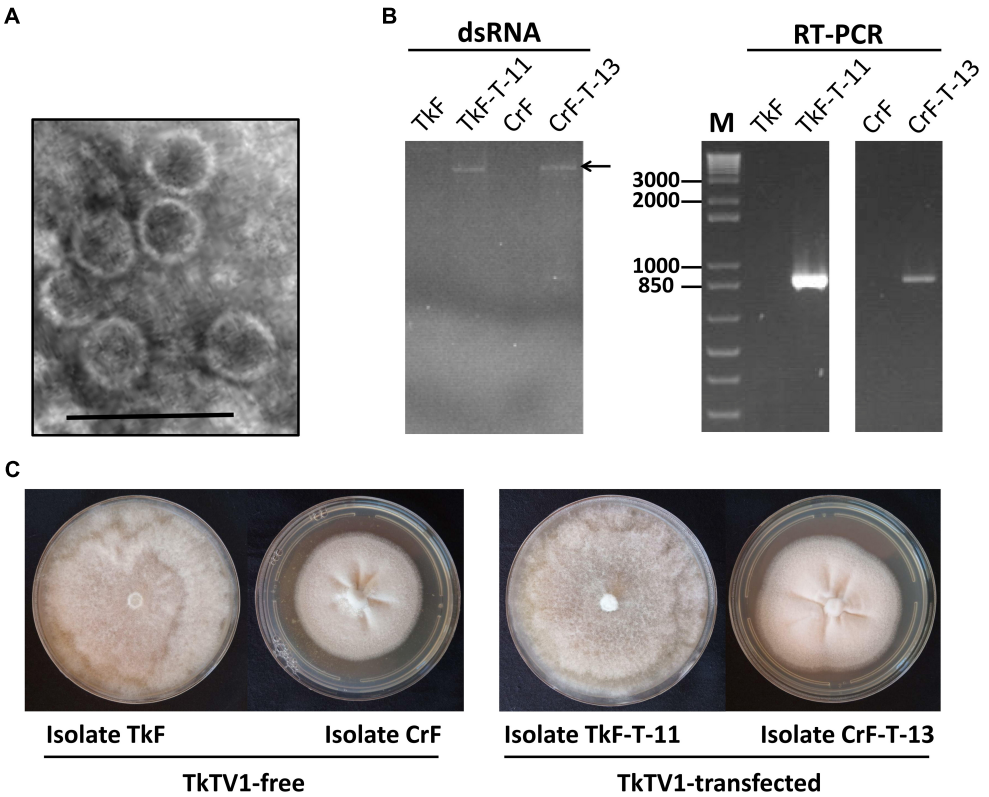

FIGURE 5 | (A) Electron micrograph of negatively stained purified particles of Trichoderma koningiopsis totivirus 1 (TkTV1:38–40 nm in diameter). The Scale bar denotes 100 nm. **(B)** Detection of TkTV1 in TkTV1-free and TkTV1-transfected isolates of *T. koningiopsis* and *Clonostachys rosea*, using dsRNA extraction and RT-PCR. **(C)** Colony morphology of TkTV1-free and TkTV1-transfected isolates of *T. koningiopsis* and *C. rosea* grown potato dextrose agar (PDA) for 7 days.

Infectivity of TkTV1 Particles Using Transfection Assay

Members of *Totiviridae* family have icosahedral virions that are 30–40 nm in diameter (Ghabrial et al., 2015). TkTV1 was purified and TEM examination showed that it has icosahedral virions of ∼38–40 nm in diameter (**Figure 5A**). TkTV1-free protoplasts of *T. koningiopsis* and *C. rosea* were transfected with TkTV1 virions purified from *T. Koningiopsis* isolate Mg10. Regenerated colonies of *T. koningiopsis* and *C. rosea* were nominated TkF-T-1 to -25 and CrF-T-1 to -25, respectively. Nine *T. koningiopsis* and two *C. rosea* colonies were tested positive for TkTV1 (**Figure 5B**) and showed identical colony morphology to those of original TkTV1-positive and TkTV1-free isolates (**Figure 5C**). Detection of TkTV1 in regenerated colonies confirms its ability to replicate in both fungal hosts.

Implication of TkTV1 Presence in Different Hosts

Although the external route of RNA mycovirus transmission is still lacking, several studies have shed light on possible higher transmission rates of RNA mycoviruses in nature compared with their transmission *in vitro* in laboratory experiments. For instance, Cryphonectria hypovirus 1 (CHV1) was found to transmit between different species of a *Cryphonectria* natural population (Liu et al., 2003). Moreover, *in situ* transmission experiments of CHV1 between virus-infected and virus-free incompatible types revealed that the natural ability of CHV1 transmission between vegetatively incompatible groups was underrated by the results obtained from using pairing-culture technique (Brusini and Robin, 2013). Sclerotinia sclerotiorum mycoreovirus 4 (SsMYRV4) infection was reported to suppress host non-self recognition and facilitate heterologous horizontal virus transmission between SsMYRV4-infected and -uninfected incompatible fungal individuals (Wu et al., 2017). Also, previous studies reported the presence of highly similar mycoviral sequences in different fungal hosts, suggesting possible mycovirus transmission between different fungi, e.g., the presence of 92.4% nt and 95.1% aa identical sequences in *Sclerotinia homoeocarpa* and *Ophiostoma novo-ulmi* (Deng et al., 2003). Moreover, Entoleuca hypovirus 1 (EnHV1) was reported to infect *Entoleuca* sp. and *Rosellinia necatrix* (Velasco et al., 2018), and Botrytis porri RNA virus 1 was discovered in *S. sclerotiorum* (Mu et al., 2018) suggesting intra- and interspecific virus transmission. The presence of nearly identical sequences represented by TkTV1 in two different fungal genera provides clear-cut supporting evidence to previous reports suggesting the existence of lateral mycovirus transmission across different fungi in nature. The nearly identical sequence of TkTV1 in *T. koningiopsis* and *C. rosea* indicates that this transmission event has happened very

recently in nature or probably while cultures were mixed prior to, or during, the isolation process.

DATA AVAILABILITY STATEMENT

TkTV1/Mg10 genome sequence is available in GenBank under the accession number MK993478.

AUTHOR CONTRIBUTIONS

Both authors secured the funding. MK undertook the research in consultation with RM and drafted the manuscript. RM revised the manuscript.

FUNDING

This research was funded by The New Zealand Institute for Plant and Food Research Limited, Auckland, New Zealand.

ACKNOWLEDGMENTS

The authors would like to thank Tracey Immanuel and Nicholas Tabi Amponsah for critically reviewing the manuscript prior to submission for publication.

SUPPLEMENTARY MATERIAL

The Supplementary Material for this article can be found online at: https://www.frontiersin.org/articles/10.3389/fmicb.2019.02318/full#supplementary-material

FIGURE S1 | Phylogenetic relationship between the coat protein (CP) of Trichoderma koningiopsis totivirus 1 (TkTV1/Mg10) and other selected *Totiviridae* members. The maximum likelihood tree was inferred using PhyML 3.0 (Guindon et al., 2010) with the RtREV + G + F as the best evolutionary model. The SH-like support values are indicated by numbers on the branches. Branches with <75% SH-like branch support have been collapsed using TreeGraph 2 software (Stöver and Müller, 2010). Virus notations are as in **Supplementary Table S1**.

TABLE S1 | Virus names and acronyms and GenBank accession numbers of proteins used to infer the phylogenetic trees.

REFERENCES

Al Rwahnih, M., Daubert, S., Urbez-Torres, J. R., Cordero, F., and Rowhani, A. (2011). Deep sequencing evidence from single grapevine plants reveals a virome dominated by mycoviruses. *Arch. Virol.* 156, 397–403. doi: 10.1007/s00705-010-0869-868

Baeza, M., Bravo, N., Sanhueza, M., Flores, O., Villarreal, P., and Cifuentes, V. (2012). Molecular characterization of totiviruses in Xanthophyllomyces dendrorhous. *Virol. J.* 9:140. doi: 10.1186/1743-422X-9-140

Bekaert, M., and Rousset, J. P. (2005). An extended signal involved in eukaryotic -1 frameshifting operates through modification of the E site tRNA. *Mol. Cell.* 17, 61–68. doi: 10.1016/j.molcel.2004.12.009

Boine, B., Kingston, R. L., and Pearson, M. N. (2012). Recombinant expression of the coat protein of Botrytis virus X and development of an immunofluorescence detection method to study its intracellular distribution in *Botrytis cinerea*. *J. Gen. Virol.* 93(Pt_11), 2502–2511. doi: 10.1099/vir.0.043869-43860

Brierley, I. (1995). Ribosomal frameshifting viral RNAs. *J. Gen. Virol.* 76(Pt 8), 1885–1892. doi: 10.1099/0022-1317-76-8-1885

Bruenn, J. A., Warner, B. E., and Yerramsetty, P. (2015). Widespread mitovirus sequences in plant genomes. *PeerJ* 3:e876. doi: 10.7717/peerj.876

Brusini, J., and Robin, C. (2013). Mycovirus transmission revisited by in situ pairings of vegetatively incompatible isolates of *Cryphonectria parasitica*. *J. Virol. Methods* 187, 435–442. doi: 10.1016/j.jviromet.2012.11.025

Capella-Gutierrez, S., Silla-Martinez, J. M., and Gabaldon, T. (2009). trimAl: a tool for automated alignment trimming in large-scale phylogenetic analyses. *Bioinformatics* 25, 1972–1973. doi: 10.1093/bioinformatics/btp348

Cook, S., Chung, B. Y., Bass, D., Moureau, G., Tang, S., McAlister, E., et al. (2013). Novel virus discovery and genome reconstruction from field RNA samples reveals highly divergent viruses in dipteran hosts. *PLoS One* 8:e80720. doi: 10.1371/journal.pone.0080720

Deng, F., Xu, R., and Boland, G. J. (2003). Hypovirulence-associated double-stranded RNA from Sclerotinia homoeocarpa is conspecific with ophiostoma novo-ulmi mitovirus 3a-Ld. *Phytopathology* 93, 1407–1414. doi: 10.1094/PHYTO.2003.93.11.1407

Dinman, J. D., Icho, T., and Wickner, R. B. (1991). A -1 ribosomal frameshift in a double-stranded RNA virus of yeast forms a gag-pol fusion protein. *Proc. Natl. Acad. Sci. U.S.A.* 88, 174–178. doi: 10.1073/pnas.88.1.174

Fujimura, T., and Esteban, R. (2011). Cap-snatching mechanism in yeast L-A double-stranded RNA virus. *Proc. Natl. Acad. Sci. U.S.A.* 108, 17667–17671. doi: 10.1073/pnas.1111900108

Fujimura, T., and Esteban, R. (2013). Cap snatching in yeast L-BC double-stranded RNA totivirus. *J. Biol. Chem.* 288, 23716–23724. doi: 10.1074/jbc.M113.490953

Ghabrial, S. A. (1994). New developments in fungal virology. *Adv. Virus Res.* 43, 303–388. doi: 10.1016/s0065-3527(08)60052-60054

Ghabrial, S. A. (2008). "Totiviruses," in *Encyclopedia of Virology*, 3rd Edn, eds B. W. J. Mahy, and M. H. V. Van Regenmortel, (Oxford: Elsevier), 163–174. doi: 10.1016/b978-012374410-4.00518-5

Ghabrial, S. A., Caston, J. R., Jiang, D., Nibert, M. L., and Suzuki, N. (2015). 50-plus years of fungal viruses. *Virology* 479-480, 356–368. doi: 10.1016/j.virol.2015.02.034

Ghabrial, S. A., and Suzuki, N. (2009). Viruses of plant pathogenic fungi. *Annu. Rev. Phytopathol.* 47, 353–384. doi: 10.1146/annurev-phyto-080508-081932

Goecks, J., Nekrutenko, A., and Taylor, J. (2010). Galaxy: a comprehensive approach for supporting accessible, reproducible, and transparent computational research in the life sciences. *Genome Biol.* 11:R86. doi: 10.1186/gb-2010-11-8-r86

Goodman, R. P., Ghabrial, S. A., Fichorova, R. N., and Nibert, M. L. (2011). Trichomonasvirus: a new genus of protozoan viruses in the family Totiviridae. *Arch. Virol.* 156, 171–179. doi: 10.1007/s00705-010-0832-838

Guindon, S., Dufayard, J. F., Lefort, V., Anisimova, M., Hordijk, W., and Gascuel, O. (2010). New algorithms and methods to estimate maximum-likelihood phylogenies: assessing the performance of PhyML 3.0. *Syst. Biol.* 59, 307–321. doi: 10.1093/sysbio/syq010

Hillman, B. I., Supyani, S., Kondo, H., and Suzuki, N. (2004). A reovirus of the fungus *Cryphonectria parasitica* that is infectious as particles and related to the Coltivirus genus of animal pathogens. *J. Virol.* 78, 892–898. doi: 10.1128/jvi.78.2.892-898.2004

Ho, T., and Tzanetakis, I. E. (2014). Development of a virus detection and discovery pipeline using next generation sequencing. *Virology* 471-473, 54–60. doi: 10.1016/j.virol.2014.09.019

Howitt, R. L. J., Beever, R. E., Pearson, M. N., and Forster, R. L. S. (1995). Presence of double-stranded RNA and virus-like particles in *Botrytis cinerea*. *Mycol. Res.* 99, 1472–1478. doi: 10.1016/s0953-7562(09)80795-80798

Icho, T., and Wickner, R. B. (1989). The double-stranded RNA genome of yeast virus L-A encodes its own putative RNA polymerase by fusing two open reading frames. *J. Biol. Chem.* 264, 6716–6723.

Jamal, A., Sato, Y., Shahi, S., Shamsi, W., Kondo, H., and Suzuki, N. (2019). Novel victorivirus from a Pakistani isolate of *Alternaria alternata* lacking a typical translational stop/restart sequence signature. *Viruses* 11:577. doi: 10.3390/v11060577

Karlsson, M., Durling, M. B., Choi, J., Kosawang, C., Lackner, G., Tzelepis, G. D., et al. (2015). Insights on the evolution of mycoparasitism from the genome of *Clonostachys rosea*. *Genome Biol. Evol.* 7, 465–480. doi: 10.1093/gbe/evu292

Kearse, M., Moir, R., Wilson, A., Stones-Havas, S., Cheung, M., Sturrock, S., et al. (2012). Geneious Basic: an integrated and extendable desktop software platform for the organization and analysis of sequence data. *Bioinformatics* 28, 1647–1649. doi: 10.1093/bioinformatics/bts199

Khalifa, M. E., and Pearson, M. N. (2013). Molecular characterization of three mitoviruses co-infecting a hypovirulent isolate of *Sclerotinia sclerotiorum* fungus. *Virology* 441, 22–30. doi: 10.1016/j.virol.2013.03.002

Khalifa, M. E., and Pearson, M. N. (2014). Molecular characterisation of an endornavirus infecting the phytopathogen Sclerotinia sclerotiorum. *Virus Res.* 189, 303–309. doi: 10.1016/j.virusres.2014.06.010

Khalifa, M. E., Varsani, A., Ganley, A. R. D., and Pearson, M. N. (2016). Comparison of Illumina de novo assembled and Sanger sequenced viral genomes: a case study for RNA viruses recovered from the plant pathogenic fungus *Sclerotinia sclerotiorum*. *Virus Res.* 219, 51–57. doi: 10.1016/j.virusres.2015.11.001

Kondo, H., Hisano, S., Chiba, S., Maruyama, K., Andika, I. B., Toyoda, K., et al. (2016). Sequence and phylogenetic analyses of novel totivirus-like double-stranded RNAs from field-collected powdery mildew fungi. *Virus Res.* 213, 353–364. doi: 10.1016/j.virusres.2015.11.015

Kraberger, S., Stainton, D., Dayaram, A., Zawar-Reza, P., Gomez, C., Harding, J. S., et al. (2013). Discovery of sclerotinia sclerotiorum hypovirulence-associated virus-1 in urban river sediments of Heathcote and Styx rivers in Christchurch city, New Zealand. *Genome Announc.* 1:e00559-13. doi: 10.1128/genomeA.00559-513

Lau, S. K. P., Lo, G. C. S., Chow, F. W. N., Fan, R. Y. Y., Cai, J. J., Yuen, K. Y., et al. (2018). Novel partitivirus enhances virulence of and causes aberrant gene expression in *Talaromyces marneffei*. *mBio* 9:e0947-18. doi: 10.1128/mBio.00947-918

Liu, S., Xie, J., Cheng, J., Li, B., Chen, T., Fu, Y., et al. (2016). Fungal DNA virus infects a mycophagous insect and utilizes it as a transmission vector. *Proc. Natl. Acad. Sci. U.S.A.* 113, 12803–12808. doi: 10.1073/pnas.1608013113

Liu, Y. C., Linder-Basso, D., Hillman, B., Kaneko, S., and Milgroom, M. (2003). Evidence for interspecies transmission of viruses in natural populations of filamentous fungi in the genus Cryphonectria. *Mol. Ecol.* 12, 1619–1628. doi: 10.1046/j.1365-294x.2003.01847.x

Medd, N. C., Fellous, S., Waldron, F. M., Xuereb, A., Nakai, M., Cross, J. V., et al. (2018). The virome of Drosophila suzukii, an invasive pest of soft fruit. *Virus Evol.* 4:vey009. doi: 10.1093/ve/vey009

Mu, F., Xie, J., Cheng, S., You, M. P., Barbetti, M. J., Jia, J., et al. (2018). Virome characterization of a collection of S. sclerotiorum from Australia. *Front. Microbiol.* 8:2540. doi: 10.3389/fmicb.2017.02540

Nerva, L., Ciuffo, M., Vallino, M., Margaria, P., Varese, G. C., Gnavi, G., et al. (2016). Multiple approaches for the detection and characterization of viral and plasmid symbionts from a collection of marine fungi. *Virus Res.* 219, 22–38. doi: 10.1016/j.virusres.2015.10.028

Nuss, D. L., and Koltin, Y. (1990). Significance of dsRNA genetic elements in plant pathogenic fungi. *Annu. Rev. Phytopathol.* 28, 37–58. doi: 10.1146/annurev.py.28.090190.000345

Pearson, M. N., Beever, R. E., Boine, B., and Arthur, K. (2009). Mycoviruses of filamentous fungi and their relevance to plant pathology. *Mol. Plant Pathol.* 10, 115–128. doi: 10.1111/j.1364-3703.2008.00503.x

Pei, J., and Grishin, N. V. (2014). PROMALS3D: multiple protein sequence alignment enhanced with evolutionary and three-dimensional structural information. *Methods Mol. Biol.* 1079, 263–271. doi: 10.1007/978-1-62703-646-7_17

Rice, N. R., Stephens, R. M., Burny, A., and Gilden, R. V. (1985). The gag and pol genes of bovine leukemia virus: nucleotide sequence and analysis. *Virology* 142, 357–377. doi: 10.1016/0042-6822(85)90344-90347

Roossinck, M. J., Saha, P., Wiley, G. B., Quan, J., White, J. D., Lai, H., et al. (2010). Ecogenomics: using massively parallel pyrosequencing to understand virus ecology. *Mol. Ecol.* 19(Suppl. 1), 81–88. doi: 10.1111/j.1365-294X.2009.04470.x

Routhier, E., and Bruenn, J. A. (1998). Functions of conserved motifs in the RNA-dependent RNA polymerase of a yeast double-stranded RNA virus. *J. Virol.* 72, 4427–4429.

Samuels, G. J., Dodd, S. L., Lu, B. S., Petrini, O., Schroers, H. J., and Druzhinina, I. S. (2006). The *Trichoderma koningii* aggregate species. *Stud. Mycol.* 56, 67–133. doi: 10.3114/sim.2006.56.03

Shi, M., Lin, X. D., Tian, J. H., Chen, L. J., Chen, X., Li, C. X., et al. (2016). Redefining the invertebrate RNA virosphere. *Nature* 540, 539–543. doi: 10.1038/nature20167

Shi-Wang, L., Zheng-Yi, W., and Ze-Jian, G. (2007). Isolation and transformation of Trichoderma viride protoplasts. *Chin. J. Agric. Biotechnol.* 1, 67–72. doi: 10.1079/cjb200417

Stöver, B. C., and Müller, K. F. (2010). TreeGraph 2: combining and visualizing evidence from different phylogenetic analyses. *BMC Bioinformatics* 11:7. doi: 10.1186/1471-2105-11-17

Sun, Z.-B., Sun, M.-H., Zhou, M., and Li, S.-D. (2017). Transformation of the endochitinase gene Chi67-1 in Clonostachys rosea 67-1 increases its biocontrol activity against *Sclerotinia sclerotiorum*. *AMB Express* 7:1. doi: 10.1186/s13568-016-0313-x

Sutton, J. C., Li, D.-W., Peng, G., Yu, H., Zhang, P., and Valdebenito-Sanhueza, R. M. (1997). Gliocladium Roseum a versatile adversary of *Botrytis cinerea* in crops. *Plant Dis.* 81, 316–328. doi: 10.1094/pdis.1997.81.4.316

Valverde, R. A., Nameth, S. T., and Jordan, R. L. (1990). Analysis of double-stranded RNA for plant virus diagnosis. *Plant Dis.* 74, 255–258. doi: 10.1094/pd-74-0255

Velasco, L., Arjona-Girona, I., Ariza-Fernandez, M. T., Cretazzo, E., and Lopez-Herrera, C. (2018). A novel Hypovirus species from Xylariaceae fungi infecting avocado. *Front. Microbiol.* 9:778. doi: 10.3389/fmicb.2018.00778

Warcup, J. H. (1950). The soil-plate method for isolation of fungi from soil. *Nature* 166, 117–118. doi: 10.1038/166117b0

White, T. J., Bruns, T., Lee, S., and Taylor, J. (1990). "Amplification and direct sequencing of fungal ribosomal RNA genes for phylogenetics," in *PCR Protocols: A Guide to Methods and Applications*, eds M. A. Innis, D. H. Gelfand, J. J. Sninsky, and T. J. White, (New York, NY: Academic Press), 315–322. doi: 10.1016/b978-0-12-372180-8.50042-1

Wickner, R. B., Ghabrial, S. A., Nibert, M. L., Patterson, J. L., and Wang, C. C. (2012). " Family Totiviridae," in *Virus Taxonomy: Classification and Nomenclature of Viruses: Ninth Report of the International Committee on Taxonomy of Viruses*, eds A. M. Q. King, M. J. Adams, E. B. Carstens, and E. J. Lefkowits, (London: Elsevier Academic Press), 639–650. doi: 10.1016/b978-0-12-384684-6.00052-5

Wu, K., Mouekouba, L. D. O., Zhang, L., Guan, X., Chen, X., Chen, H., et al. (2014). Analysis of Clonostachys rosea-induced resistance to tomato gray mold disease in tomato leaves. *PLoS One* 9:e102690. doi: 10.1371/journal.pone.0102690

Wu, S., Cheng, J., Fu, Y., Chen, T., Jiang, D., Ghabrial, S. A., et al. (2017). Virus-mediated suppression of host non-self recognition facilitates horizontal transmission of heterologous viruses. *PLoS Pathog.* 13:e1006234. doi: 10.1371/journal.ppat.1006234

Wu, Z., Ren, X., Yang, L., Hu, Y., Yang, J., He, G., et al. (2012). Virome analysis for identification of novel mammalian viruses in bat species from Chinese provinces. *J. Virol.* 86, 10999–11012. doi: 10.1128/JVI.01394-1312

Yun, S. H., Lee, S. H., So, K. K., Kim, J. M., and Kim, D. H. (2016). Incidence of diverse dsRNA mycoviruses in Trichoderma spp. causing green mold disease of shiitake *Lentinula edodes*. *FEMS Microbiol. Lett.* doi: 10.1093/femsle/fnw220 [Epub ahead of print].

Zheng, L., Lu, X., Liang, X., Jiang, S., Zhao, J., Zhan, G., et al. (2017). Molecular characterization of novel totivirus-like double-stranded RNAs from *Puccinia striiformis* f. sp. tritici, the causal agent of wheat stripe rust. *Front. Microbiol.* 8:1960. doi: 10.3389/fmicb.2017.01960

Conflict of Interest: The authors declare that the research was conducted in the absence of any commercial or financial relationships that could be construed as a potential conflict of interest.

Advantages of publishing in Frontiers

OPEN ACCESS
Articles are free to read for greatest visibility and readership

FAST PUBLICATION
Around 90 days from submission to decision

HIGH QUALITY PEER-REVIEW
Rigorous, collaborative, and constructive peer-review

TRANSPARENT PEER-REVIEW
Editors and reviewers acknowledged by name on published articles

Frontiers
Avenue du Tribunal-Fédéral 34
1005 Lausanne | Switzerland

Visit us: www.frontiersin.org
Contact us: info@frontiersin.org | +41 21 510 17 00

REPRODUCIBILITY OF RESEARCH
Support open data and methods to enhance research reproducibility

DIGITAL PUBLISHING
Articles designed for optimal readership across devices

FOLLOW US
@frontiersin

IMPACT METRICS
Advanced article metrics track visibility across digital media

EXTENSIVE PROMOTION
Marketing and promotion of impactful research

LOOP RESEARCH NETWORK
Our network increases your article's readership